UNIVERSIDAD DE SANTIAGO DE COMPOSTELA
DEPARTAMENTO DE BIOLOGÍA CELULAR Y ECOLOGÍA
ÁREA DE BIOLOGÍA CELULAR

Brain and retina regionalization in sharks: study based on the spatiotemporal expression pattern of Pax6 and other neurochemical markers.

MEMORIA

Que para optar al Grado de Doctor en Biología presenta

SUSANA FERREIRO GALVE

Santiago de Compostela, 2010

ISABEL RODRÍGUEZ-MOLDES REY, PROFESORA TITULAR DEL ÁREA DE BIOLOGÍA CELULAR Y EVA CANDAL SUÁREZ, INVESTIGADORA CONTRATADA (Programa Isidro Parga Pondal), DEL DEPARTAMENTO DE BIOLOGÍA CELULAR Y ECOLOGÍA DE LA UNIVERSIDAD DE SANTIAGO DE COMPOSTELA,

CERTIFICAN:

Que la presente memoria titulada "**Brain and retina regionalization in sharks: study based on the spatiotemporal expresion pattern of Pax6 and other neurochemical markers**", que para optar al Grado de Doctor en Biología presenta Dña. SUSANA FERREIRO GALVE, ha sido realizada bajo nuestra dirección. Y considerando que constituye trabajo de Tesis, autorizamos su presentación al Consejo de Departamento correspondiente.

Y para que así conste, expedimos el presente certificado en Santiago de Compostela, a 4 de febrero de 2010.

La Doctoranda Las Directoras de la Tesis

Fdo.:Susana Ferreiro Galve Fdo.: Isabel Rodríguez-Moldes Rey Fdo.: Eva Candal Suárez

La realización de esta Tesis Doctoral ha sido posible gracias a la financiación de los siguientes proyectos y actividades de investigación por parte del Ministerio de Educación y Ciencia y la Xunta de Galicia:

- Beca para la realización de estudios de 3º ciclo. Consellería de Educación e Ordenación Universitaria. Xunta de Galicia.
- Beca Predoctoral+Contrato de Trabajo en Prácticas. Programa de Recursos Humanos de Investigación del Plan Gallego de I+D+I. Consellería de Innovación, Industria e Comercio. Dirección Xeral de Investigación e Desenvolvemento. Xunta de Galicia.
- Estudio de la morfogénesis y regionalización del sistema nervioso central de peces elasmobranquios. Ministerio de Educación y Ciencia (BFU2004-03313) y Xunta de Galicia (INCENTIVO, PGIDIT05PXIC20003PN
- Mecanismos moleculares de la morfogénesis del ojo de peces cartilaginosos. Xunta de Galicia. PGIDIT06PXIB200065PR.
- Formación del patrón del encéfalo en condrictios (peces cartilaginosos). Ministerio de Educación y Ciencia (BFU2007-61154/BFI)
- Evolución dos patróns de desenvolvemento do sistema nervioso central de peixes gnatostomos. Xunta de Galicia. PGIDIT07PXIB200102PR
- Ayudas Generales de la Comunidad Autónoma para Grupos de Ivestigación Consolidados del sistema gallego de I+D+I. Dirección Xeral de I + D – Xunta de Galicia (INCITE09ENA200048ES)

Vorágine de prisas… y llegados a este punto, sin perder un ápice de emoción, el mas difícil todavía: el último folio en blanco, ese en el que escribir aparentes sinsentidos, tornarse cervantino o poeta para ¡Ahí es nada! expresar en palabras mi agradecimiento a todos aquellos: compañeros y profesores del Área, familia y amigos, que habéis participado de una forma u otra, o aun sin daros cuenta, en este proyecto porque sin vosotros, sin duda, el viaje habría sido diferente… A todos, gracias.

En especial, a la Dra. Isabel Rodríguez-Moldes por haberme ofrecido la oportunidad de llevar a cabo este trabajo; de empezar en este "mundillo" con aquellas misteriosas células coronadas; por el cambio de tercio y los tiburones. A la Dra. Eva Candal por unirse a este proyecto, y enriquecerlo. A Eva e Isa, por su confianza y entusiasmo; por su dirección y ayuda; por todo el trabajo compartido; y por las grandes dosis de contagioso optimismo; ingredientes imprescindibles para terminar esta Tesis. Muchas gracias a las dos.

Al Dr. Ramón Anadón, por su constante interés, sugerencias y buenos consejos.

Je remercie la participation de la Dra. Sylvie Mazan, je tiens à remercier Sylvie de m'avoir fait confiance et m'acueillir dans son labo à Orléans; ce qui m'a permis d'aprendre beaucoup. Un grand merci a mes compagnons de l'équipe développement et évolution des vertébrés, qui m'ont beaucoup appris au cours de mes stages, pour leur nombreux coups de main; spécialement à Claire et Arno, pour les discussions, les conseils; et surtout pour leur disponibilité et humour.

A mis compañeros de aventura del Área de Bioloxía Celular, con los que a lo largo de estos años he compartido peripecias dentro y fuera del batiburrillo de nuestro despacho; cafecicos, cháchara, cenas, excursiones, chistes malos, congresos, dudas y anécdotas "venenezas"… gracias a los que han prestado su tiempo y oídos a mis parrafadas convirtiéndose en amigos… gracias también por la generosa ayuda experimental… No puedo dejar de agradecer aquí a: Catalina, que me mantiene informada de las andanzas del resto de la diáspora, por sus primeras enseñanzas, y por su cariño; ya sabes que te echo de menos, y no solo por el poder de convocatoria cafetera con permiso del Dr. Quintela; como tampoco a Iria por contagiarme su entusiasmo; junto con Bego, gracias a las tres por toda la ayuda y complicidad desde mis comienzos; ni mucho menos a Belén y Raquel, grandes conversadoras y organizadoras de despedidas; a Eva y Pablo por esas charlas y "no consejos"… También quisiera agradecer en particular a mis compañeros del grupo "desenvolvemento do sistema nervioso de peixes óseos e cartilaxinosos" por su simpatía, colaboración y por su desinteresada ayuda en los últimos experimentos y búsqueda de gazapos.

A mi familia, por su interés por mi trabajo y su curiosidad por "esas cosas de tiburones". A mis padres por haberme brindado esta posibilidad; y a Juan Ma, mi hermano; a los tres por estar ahí y querer ayudar siempre. Sin olvidar tampoco a los turolenses, que no dejan de interesarse por mi, impacientes por saber para cuando esta Tesis.

A Ángel por más de 100 motivos; por ayudarme a terminar y continuar esta etapa; por hacer que todo parezca más fácil compartiendo la magia del trayecto. Gracias también por la portada, la asistencia técnica y por el trabajo de maquetación.

Como no, a los buenos amigos que encontré con la lluvia de Santiago aunque cada vez nos veamos menos, por animarme en eso tan incierto de la carrera científica, en especial a la tresena formada por Rocío, Yago y Rocío, que se preocupan por mi. También a los de las grandes vacaciones griegas, que se han interesado por este trabajo, aunque sepan tanto como se sabe del trabajo del señor C. Bing. Y a esa gente fantástica que con su compañía alegró tardes grises en la vieja Orléans… a los almuerzos hispanohablantes, las soirées internacionales de L'atelier y el chateaux le puy… sans eux, Orléans aurait été une histoire comme une autre.

En fin, GRACIAS por vuestra colaboración e interés, y por querer celebrar conmigo el final de esta pequeña empresa

A la memoria de Eusebio y Eulalia.

"El ingrediente más importante es la fascinación ejercida por las maravillas de los seres vivos. A la mayoría de los biólogos les dura toda la vida; jamás dejan de apasionarles los descubrimientos científicos, sean empíricos o teóricos, ni pierden la afición a buscar nuevas ideas, nuevos puntos de vista, nuevos organismos. Y muchos aspectos de la biología influyen directamente en nuestras circunstancias personales y en nuestro sistema de valores. Ser biólogo no es un trabajo; es elegir un modo de vida"

Así es la biología. Ernst Mayr.

Contents

General introduction 3

Rationale and aims 43

Chapter 1. Pax6 expression in the developing and mature brain of sharks 51

Chapter 2. Pax6 expression in the developing olfactory system of a shark: evidence of expression in peripheral cells 149

Chapter 3. The segmental organization of the developing shark brain based on neurochemical markers, with special attention to the prosencephalon 171

Chapter 4. Development of the Cerebellar Body in Sharks: Spatiotemporal Relations of Pax6-Expression, Cell Proliferation and Differentiation 187

Chapter 5. Pax6 expression in the developing and mature retina of sharks 207

Chapter 6. Patterns of cell proliferation in the developing retina of sharks 241

Cahpter 7. Early development of GABAergic cells of the retina in sharks. Comparison with patterns of Pax6 expression and proliferation 273

Chapter 8. Spatiotemporal organization of Calretinin immunoreactivity in the shark retina 311

Chapter 9. Spatiotemporal organization of TH and 5-HT immunoreactivity in the shark retina 335

Chapter 10. Spatiotemporal organization of Opsin-immunoreactive cells in the shark retina 369

Conclusions 391

Appendix a 397

Appendix b 399

Appendix c. resumen 403

GENERAL INTRODUCTION

MORPHOGENESIS OF THE CENTRAL NERVOUS SYSTEM

The early events that shape the vertebrate central nervous system (CNS) involve the emergence of vesicles, as well as transverse and longitudinal zones. Interestingly, the pattern of pioneer neurons and their axons is related to neural segmentation. Given that brain morphogenesis results from the establishment of neural cells and their connections, understanding early segmentation, neurogenesis and axonogenesis of the nervous system provides insight into the underlying pattern that gives rise to adult brain complexity (Kimmel, 1993).

Shortly after formation of the vertebrate neural tube, its most enlarged anterior portion bulges and a series of swellings form consecutively. The sequential appearance of three and finally five encephalic vesicles (i.e. transverse elements) along the anteroposterior vertebrate neural tube axis was first described by von Baer (1828). Two prominent external constrictions divide the brain into three main vesicles: hindbrain (or rhombencephalon), midbrain (or mesencephalon) and forebrain (or prosencephalon). The encephalic vesicles become progressively subdivided by constrictions along their length. These morphologically recognisable transverse neural tube elements or brain segments, caused by local intensifications in the cell proliferation rate (Nieuwenhuys 1998), were first denominated neuromeres by Orr (1887). A wide variety of experimental approaches have been used to identify neuromeres, based on morphological, gene expression and cell lineage restriction features (Puelles and Rubenstein, 1993, 2003; Lumsden 1990; Pritz 1999; Yoon et al. 2000; Redies et al. 2000; Larsen et al. 2001; Murakami et al. 2001). Neuromeres have been reported to share some of the following characteristics: they appear as protrusions separated by external constrictions; they also present internal ventricular ridges located at the centre of proliferation zones during early development, which later disappear as a result of a decrease in mitotic activity; they represent centres of cell proliferation, early cell differentiation and migration; in each neuromere stem progenitor cells and neuroblasts are radially orientated with respect to the ventricular surface; most neuromeres have fixed relations to structures of the head and peripheral nervous system, which can serve as reference points in comparative studies; the limits of the domains of expression of early regulatory genes often correspond to interneuromeric boundaries, and in some cases the boundaries restrict cell mixing between neuromeres (Larsen et al. 2001). Although the concept of neuromery involves

the idea of metamerism (repetition of transverse units with the same organization) and compartmentalization, only rhombomeres fit the criteria for being metameric (repetitive) segments, as they have glial intersegmental boundaries, and show segmental generation of comparable neuronal classes and axonal routing in each neuromere, as well as neuromere-specific cellular lineage restriction (Fraser et al. 1990). These features gave rise to the strictest definition of a neuromere as a neural compartment (Larsen et al. 2001), which has made extension of the neuromeric interpretation into the midbrain and forebrain difficult.

In addition to transverse elements, longitudinal zones are observed along the neural axis. The columnar model (His-Herrick-Kuhlenbeck) was postulated in contrast to the neuromeric one, and proposed that the basic organization of the developing vertebrate brain is based on four longitudinal zones or columns separated by ventricular sulci, which constitute morphological and functional entities. These longitudinal zones are particularly evident in the spinal cord and hindbrain, where the ventral and ventrolateral (together forming the basal plate), and the dorsolateral and dorsal (together forming the alar plate) columns are recognized. According the columnar model, the ventricular limits between these columns correspond to 3 ventricular sulci: the intermediate dorsal sulcus, the sulcus limitans of His and the intermediate ventral sulcus. The ventral column does not surpass the mesencephalon rostrally, and the dorsal column is limited to the rhombencephalon. However, how far these columns extend into the anteriormost portion of the neural axis is a matter of discussion (Nieuwenhuys et al., 1998).

On the basis of the expression patterns of regionalization genes, Puelles and Rubenstein (1993, 2003) proposed the so-called neuromeric/prosomeric model, which integrates the previous neuromeric and columnar models, providing a basic bauplan of the vertebrate brain. In general, this model recognizes the longitudinal axis flexure of the forebrain with respect to the midbrain and hindbrain, and defines transverse neuromeres and longitudinal zones along the anteroposterior and dorsoventral axes respectively. According to the authors, it should be regarded as a morphological instrument (paradigm), which has been shown to be useful for comparative neuroanatomical studies, in identifying homologous structures from the perspective of evolutionary developmental biology.

Autoradiographic studies (reviewed in Bayer and Altman 1995a,b; Rakic 2002a,b, 2003a,b) have revealed that the early neural tube walls consist of a pseudostratified proliferative

neuroepithelium, as previously proposed by Sauer (1935). At early stages of development, every cell in this neuroepithelium is proliferating and is attached to both the ventricular and pial surfaces. The cell nucleus migrates periodically from ventricle to pia (interkinetic nuclear migration) as it goes through the cell cycle, always going through mitosis and cell division close to the ventricle. Initially, these progenitor cells divide symmetrically to give off more proliferating cells, thus increasing the thickness of the neuroepithelium. Later, asymmetrical divisions of the proliferating neural cells will give rise to postmitotic neuroblasts, which migrate away from the ventricular zone (VZ) to form a second layer called the intermediate zone (IZ). The IZ becomes progressively thicker as more neuroblasts are added to it; moreover, postmitotic neuroblasts differentiate into neurons and glia in this layer. The neurons then make connections between each other and send axons to the pial surface, thereby creating a cell-poor marginal layer (MZ). A three-zone pattern can therefore be observed in the developing CNS, consisting of: a ventricular proliferating zone (VZ); a more peripheral intermediate zone (IZ) containing postmitotic neuroblasts and differentiating cells, and a marginal zone (MZ) consisting of the processes of differentiated cells. Modifications in this pattern due to cell migration, differential neuronal proliferation, and selective cell death are observed in the brain. The VZ zone is not uniform along the neural tube ventricular surface, but rather shows local differences in proliferation and migration dynamics. Apart from the VZ, other proliferating zones have been described in the adult vertebrate brain, and thus in mammals the external granular layer in the cerebellum, the subventricular zone in the telencephalic hemispheres, as well as the granular precursor cells in the hippocampus constitute secondary zones of neurogenesis that produce neurons after birth (reviewed in Sanes et al., 2006).

CHONDRICHTHYANS IN NEUROANATOMICAL, DEVELOPMENTAL AND EVOLUTIONARY STUDIES

Chondrichthyans (cartilaginous fishes) constitute a monophyletic group, an ancient lineage of the gnathostomous vertebrates characterized by having a cartilaginous endoskeleton, and placoid scales (dermal denticles) covering their body. This group includes two major radiations that diverged over 350 million years ago: Holocephala (chimaeras), whose upper jaw is fused to the skull (neurocranium) and is thus not articulated, and Elasmobranchs (including sharks, skates and rays), characterized by having articulated jaws (Fig. 1). Most sharks have a fusiform, streamlined body and are divided into two groups, squalimorphs (the most primitive group of extant sharks) and galeomorphs (which include most extant sharks), whereas a few sharks with flattened bodies, known as angel sharks, form the squantinomorphs group. Skates and rays with characteristic flattened bodies and large fused pectoral fins are grouped together as batoids.

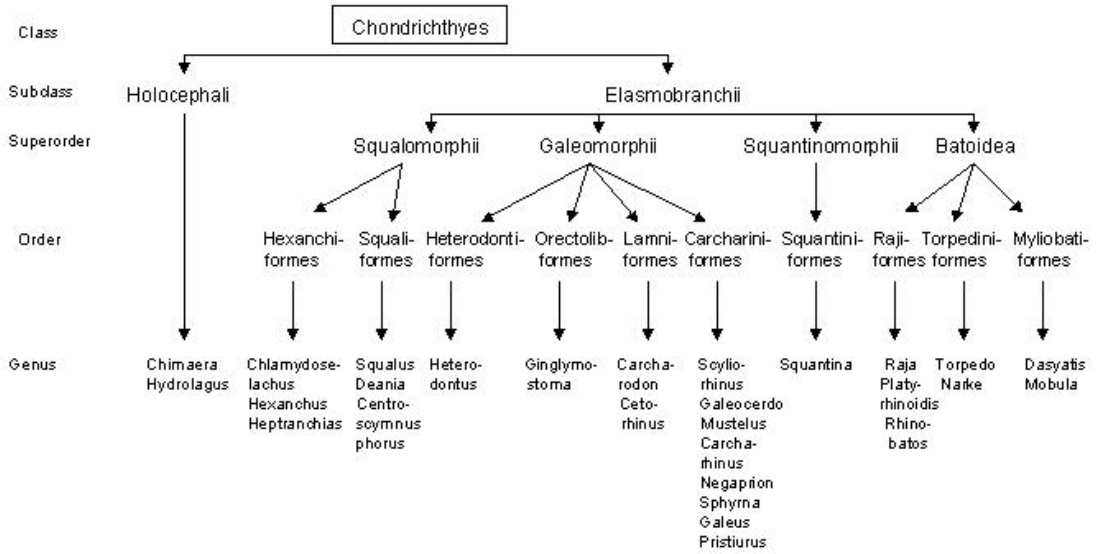

Figure 1. Classification of the cartilaginous fishes based on Compagno, 1977.

Recent molecular-phylogenetic studies based on sequencing of ribosomal RNA and mitochondrial DNA genes have revised shark phylogeny on the basis of morphological characters (Winchel et al., 2004), however interrelationships between living elasmobranchs are still a matter of debate.

Chondrichthyans are currently considered as the sister group to osteichtyans, i.e., the group of gnathostomes that gave rise to actynopterigians, (ray-finned fishes, which includes modern bony fish), and sarcopterygians (lobe-finned fishes and their derivatives, the tetrapods: amphibians and amniotes). This phylogenetic position as an out-group to all other living gnathostomes (Fig. 2A) makes chondrichthyans crucial in assessing the ancestral vertebrate condition of brain organization, because they provide a comparative reference for distinguishing between ancestral and derivative characteristics.

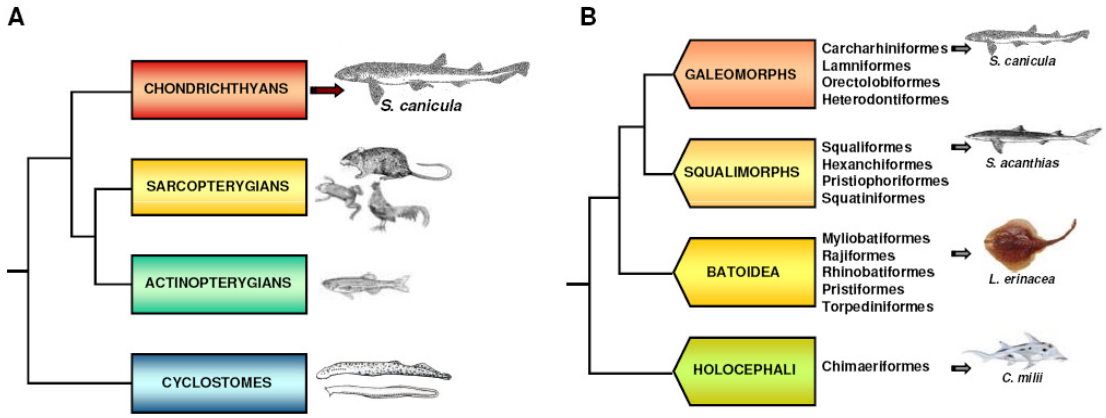

Figure 2. (A). Phylogenetic position of chondrichthyans among gnathostomes. Chondrichthyans constitute a sister-group to osteichthyans (sarcopterygian and actinopterygians). (B). Position of *S. canicula* within chondrichthyans. Elasmobranchs appear subdivided into three superorders; according to Maisey (1980), squantinomorphs and squalimorphs are grouped together, in contrast to previous classifications (Compagno, 1977). Taken from Coolen et al., 2009.

Despite the fact that chondrichthyans represent an ancient vertebrate radiation, they do not have primitive or unspecialized, but rather well-developed, large brains, comparable in size to those of birds and mammals of equivalent body weight. In contrast to other fish groups, such as the agnathans, ray-finned, and sarcopterygian fish they have relatively larger brains.

Among chondrichthyans, studies of brain organization in galeomorph sharks are especially critical, because these sharks have elaborated-type brains (Northcutt, 1978), similar to those of teleosts and amniotes, and are thus more likely to reveal homologies between chondrichthyans and other vertebrates. According to Northcutt (1978), elaborated shark brains are characterized by migration of the neuronal cell bodies away from the periventricular matrix during development and, as a consequence formation of more or less distinct cell groups. Whereas in laminar shark brains (squantinomorphs and squalomorphs sharks, as well as holocephala, see Fig. 1), most neurons remain periventricularly, i.e., close to where they were born. Northcutt's designations of laminar and elaborated brains was reviewed by Butler and Hodos (2005), who proposed the nomenclature Type I and Type II to designate laminar and elaborated brain organizations respectively.

In the last few years, most, if not all, developmental studies on elasmobranches have been carried out on a small shark belonging to the Family *Scyliorhinidae*, Genus Scyliorhinus, Order *Carchariniformes,* SuperOrder *Galeomorphii,* the lesser spotted dogfish or lesser spotted catshark, *Scyliorhinus canicula* (Fig. 2B), (for a review, see Coolen et al., 2009). Species of the family Scyliorhinidae are commonly referred to as catsharks, because they have elongated eyes with a cat-like appearance, however they are also called dogfish, the common name usually given to the Order *Squaliformes* (with *Squalus acanthias*, the spiny dogfish, as a representative species, Fig. 2B), which may cause confusion. There are several distinguishing features between these groups; catsharks have an anal fin, the first dorsal fin originates above or posterior to the pelvic fins level and the dorsal fins do not have spines. in contrast, dogfishes are characterized by a sharp spine along the leading edge of each dorsal fin, lack of an anal fin, the first dorsal fin originating well in front of the pelvic fins, and are generally stockier than catsharks.

For several reasons this species is a suitable candidate as a "model organism". *Scyliorhinus canicula* is easily reared in captivity and abundant embryonic material can be obtained throughout the year. The eggs are easily maintained under laboratory conditions until hatching, and the transparency of the egg shells makes it possible to obtain embryonic series. In fact, normal developmental series have been available since the work of Ballard et al. (1993).

Although many neuroanatomical studies have been carried out in different elasmobranch species, such as *Squalus acanthias*, much knowledge of the elasmobranch brain is essentially based on studies carried out in *S. canicula*, or more generally in *Scyliorhinus* spp., as their brain complexity makes comparison with teleosts and amniotes more straightforward. Thus, immunohistochemical studies have provided a great deal of information about the organization of different neuronal systems, such as the cholinergic (Anadón et al. 2000), catecholaminergic (Molist et al., 1993; Sueiro et al., 2003; Sueiro, 2003; Carrera et al., 2005; Carrera, 2008), serotoninergic (Yamanaka et al., 1990; Carrera et al., 2008b), GABAergic (Álvarez-Otero et al., 1995; Sueiro, 2003; Sueiro et al., 2004, 2007; Carrera et al. 2006, 2008a; Carrera, 2008) and some peptidergic systems (neuropeptide Y: Vallarino et al., 1988; Chiba and Honma 1992; substantia P: Rodríguez-Moldes et al., 1993; enkephalins: Vallarino et al., 1994, Sueiro, 2003; calcitonin gene-related peptide, CGRP: Molist et al., 1995; thyrotropin releasing hormone, TRH: Teijido et al., 2002; calbindin-D28k: Rodríguez-Moldes et al., 1990). Moreover, the fibre connection patterns in the chondrichthyan brain have also been investigated in *S. canicula* (reviewed in Smeets et al. 1983; Timerick et al., 1992; Mandado et al., 2001). Analysis of the gene expression pattern of several transcription factors involved in early brain regionalization *(Emx, Otx, and Pax6* genes*)* has been conducted in early embryos of *S. canicula* (Sauka-Splenger et al., 2001; Derobert et al., 2002a,b; Plouhinec et al., 2005). Furthermore, in the last few years, an ancient origin for morphogenetic processes, such as neuronal migration, has been suggested on the basis of the results of developmental studies in *S. canicula* (Carrera et al. 2008a). All of these studies indicate *S. canicula* as a valuable model for shedding light on the vertebrate brain organization.

GENERAL ANATOMY OF THE ELASMOBRANCH BRAIN.

Classical neuroanatomical studies have dealt with the elasmobranch brain (for a review see Smeets, 1998). The elasmobranch brain is large, well developed, and generally enclosed tightly by the *neurocranium* (Fig. 3). Although the brain anatomy is comparable among elasmobranch species, there are some differences in features such as the olfactory bulb insertion, length of the olfactory peduncles, and the degree of fusion between the medial walls of the telencephalic hemispheres/lobes.

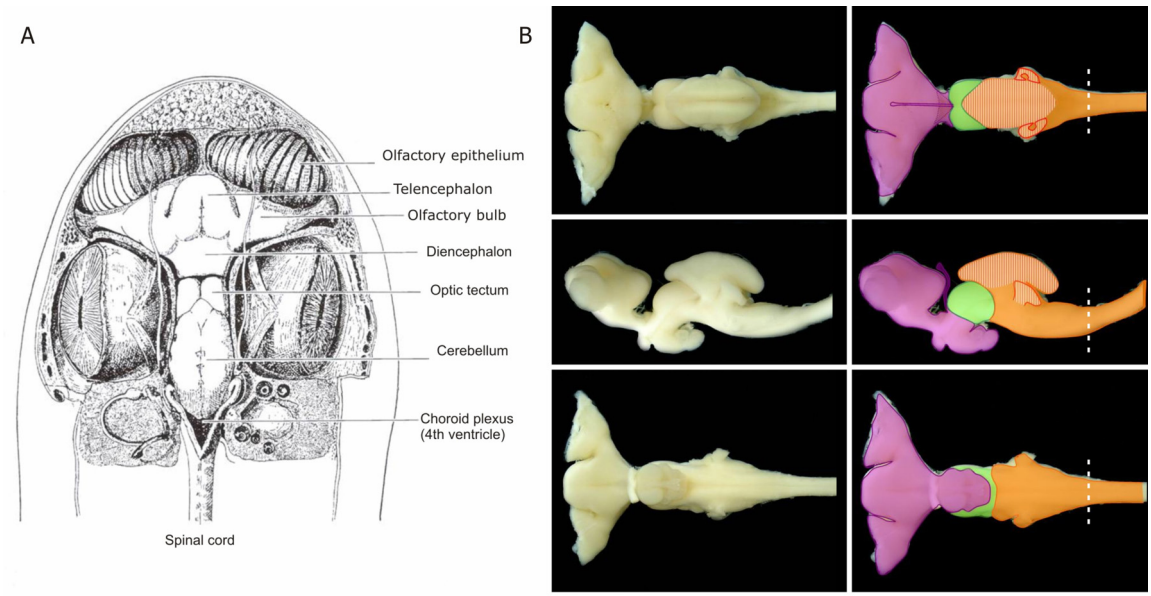

Figure 3. (A) Dorsal view of brain and sensory organs of a juvenile *Scyliorhinus canicula*, adapted from Storch and Welsch (2001). (B) From top to bottom, dorsal, lateral and ventral views of the brain of *S. canicula*. Right column shows, in orange, the extension of the rostral spinal cord and hindbrain (the dotted line marks the obex level), in green the midbrain, and in purple the forebrain.

Hindbrain

There is no clear boundary between the spinal cord and the hindbrain, but rather a transitional area, the obex. Rostrally the isthmus marks the boundary with the midbrain constituting the rostralmost hindbrain area. The hindbrain comprises the choroids plexus, the cerebellum, and the hindbrain tegmentum. The choroids plexus (caudally) and cerebellum (rostrally) derive from the alar plate, and are found enclosing the roof of the fourth ventricle. The hindbrain tegmentum is organized in longitudinal zones, and has a dual origin, since it consists of lateral walls derived from the alar plate, and medial walls derived from the basal plate, with the sulcus limitans of His as a landmark between both.

The tegmental alar plate (lateral walls) consists of two longitudinal sensory zones: the dorsal and dorsolateral areas. The dorsal area comprises the lateral line centres, which are unique to chondrichthyans: the dorsal (electroreceptive) and medial (mechanoreceptive) octavolateral nuclei, organized into two cellular columns covered by the cerebellar crest, contiguous rostrally with the molecular layer of the cerebellum. The dorsolateral area consists of the viscerosensory column or vagal lobe, which protrudes laterally into the ventricle and receives the afferent fibres of the facial (VII), glossopharyngeal (IX) and vagal (X) nerves (taste and visceral sensitivity); the somatosensory nucleus of the trigeminal nerve, and the nucleus octavomagnocellularis, which receives afferences from the octaval (VIII) nerve (hearing and vestibular senses).

The basal plate (medial tegmental walls) is divided into two longitudinal regions: the ventrolateral visceromotor area, which contains the motor nuclei of the trigeminal (V), VII, IX, and X nerves, and the ventral somatomotor area, which comprises the medial longitudinal fascicle, the main encephalospinal pathway in elasmobranchs; the neurons of the spinooccipital nerves (i.e., the, hypoglossal, XII, nerve homologues); the motoneurons of the abducens (VI) nerve; somatomotor nuclei as the inferior olive, which projects to the cerebellum, and the reticular formation - divided into superior and inferior groups, each containing both raphe and reticular groups. Large neurons of the reticular formation, reported to be cholinergic (Anadón et al., 2000), project to somatomotor centres in the spinal cord via medial longitudinal fascicle. Cells of the reticular formation also project to the cerebellum and optic tectum (Paul and Roberts, 1975; Smeets, 1982; Fiebig, 1988) and receive inputs from these regions as well as from the spinal cord and the telencephalon (Smeets and Timerick, 1981;

Smeets et al., 1983). The reticular formation contains abundant serotoninergic cells, which arise close to the floor plate and migrate to form raphe or reticular groups (Carrera et al., 2008b), as well as enkephalinergic, catecholaminergic and cholinergic cells (Stuesse and Cruce, 1992; Stuesse et al., 1990, 1991a,b, 1995; Vallarino et al., 1994; Anadón et al., 2000). Interestingly, although no rhombomeres are observed in the mature hindbrain, immunocytohistochemical studies have reported evidence of a segmental disposition in some motor nuclei (Anadón et al., 2000) and in serotoninergic cell groups of the reticular formation (Carrera et al., 2008b). At the isthmic tegmentum, the ventral area comprises the somatomotor nucleus of the trochlear (IV) nerve, and other nuclei not related to somatomotor function, such as the interpeduncular nucleus (which receives habenular afferences, and for which efferent connections are unknown), and the central grey, which projects to the cerebellum (Fiebig, 1988).

Cerebellum

The elasmobranch cerebellum consists of a large cerebellar body and a pair of ear-shaped auricular lobes closely related to the lateral line centres. Interestingly, the elasmobranch cerebellum contains the same kind of elements as the mammalian cerebellum - four types of neurons (Purkinje, granule, Golgi and stellate cells) - and exhibits the basic cerebellar circuitry typical of vertebrates (Nicholson and Llinás, 1969; Álvarez-Otero and Anadón, 1992, 1993). The cerebellar body originates as a dorsal evagination that extends rostrally over the midbrain and caudally over the fourth ventricle. Its basal part or peduncle is joined to the tectum by the *vellum medullare anterioris*. The cerebellar body presents a cortical structure that consists of four layers: the innermost granular layer arranged into two longitudinal columns (the paramedian granular eminences) that protrude into the ventricle (Nieuwenhuys, 1967a; Álvarez-Otero and Anadón, 1987), the fibre zone, the Purkinje cell and the molecular layers. The auricles are subdivided into upper/rostromedial and lower/caudolateral leaves. The upper leaves fuse medially covering the fourth ventricle and the lower leaves are joined to the lateral hindbrain walls constituting the octavolateral area (Larsell, 1967).

Midbrain

The midbrain comprises the optic tectum (alar plate), which consists of two well-developed bilateral lobes, and the midbrain tegmentum (basal plate), which is caudally continuous with the hindbrain tegmentum. The optic tectum is organized in at least five layers (Smeets et al 1983; Manso and Anadón, 1991a, b, 1993a), and is the primary centre for the perception of vision as its main input is from retinofugal fibres (Smeets, 1981, 1982). However, it also receives afferences from the dorsal pallium, diencephalon, hindbrain and spinal cord. The organizational pattern of elamobranch retinal projections show a high degree of complexity, comparable to that found in some actinopterygians and amniotes, and it is thought that evolution of the elasmobranch primary visual system occurred as a result of an increase in neuronal density of the projection zones rather than an increase in the number of projection zones themselves (Northcutt, 1979; Smeets et al., 1983; Repérant et al. 1986; Northcutt, 1990). The mesencephalic trigeminal (V) nucleus is periventricularly located in the optic tectum, and other nuclei derived from the midbrain alar plate that receive ascending auditory and lateral line inputs and that correspond to the *torus semicircularis* of other anamniotes, are located in the tegmentum. The midbrain tegmentum comprises several motor nuclei: medially, the nucleus of the oculomotor (III) nerve; also medially but more dorsally, the Edinger-Westphal nucleus, which is the origin of the cholinergic visceromotor fibres that course along nerve III to innervate the iris and ciliary body of the eye (Anadón et al., 2000), and two cell populations that are absent in teleost fish, the ventral tegmental area, and the substantia nigra, both of which contain catecholaminergic neurons (Meredith and Smeets, 1987; Carrera et al., 2005) and extend rostrally along the basal part of the caudal diencephalon.

Forebrain

The forebrain consists of the diencephalon (primary prosencephalon) and the secondary prosencephalon, which includes the hypothalamus, preoptic region and telencephalon.

Diencephalon

Although the limit between alar and basal territories in the diencephalon is not as evident as in the brainstem (i.e., hindbrain and midbrain), transverse boundaries are well recognized: dorsally a constriction at the posterior commisure level and ventrally the oculomotor nerve exit serve as landmarks that separate midbrain and forebrain. In the diencephalon, the limits between different nuclei are anatomically diffuse, and contain neurons of more uniform size than those of the brainstem.

The diencephalic alar plate comprises:

- the pretectum, containing the pretectal nucleus, which receives retinal fibres lateral to the posterior commisure, as well as the ventrally located subcommisural organ;
- the epithalamus, which consists of the pineal organ or epiphysis, a well-developed tubular structure that contains receptor, supporting and ganglion cells, some of them GABAergic as well as extensive GABAergic innervation (Carrera et al., 2006), and the habenula, which is markedly asymmetrical, with the left habenular ganglion larger than the right one (Smeets et al., 1983; Rodríguez-Moldes et al., 1990).
- the thalamus and the prethalamus, both of which have a medial part with densely arranged cells and a lateral part with larger scattered cells, constitute relay centres for ascending sensory pathways to the telencephalon. According to the prosomeric model, the thalamus (the former dorsal thalamus) and prethalamus (the former ventral thalamus), which are separated by the *zona limitans intrathalamica* (Puelles and Rubenstein, 1993, 2003; Larsen et al., 2001; Zelster et al., 2001), represent transverse divisions of the neural tube, likewise the pretectum.

The diencephalic basal plate comprises the synencephalic tegmentum, containing the medial longitudinal fascicle nucleus (Nflm), and numerous cathecolaminergic cells related to the rostral extension of the midbrain ventral tegmental area/substantia nigra, and the posterior tubercle, which also contains abundant catecholaminergic cells (Carrera et al., 2005; Carrera 2008).

Within the prosomeric model framework (Puelles and Rubenstein, 1993, 2003), the diencephalon consists of three prosomeres: p1, p2 and p3. All of which including an alar plate derived portion: the pretectum (p1); the thalamus, pineal organ and habenula (p2); and the prethalamus (p3); as well as a part derived from the basal plate: the synencephalon with the Nflm (p1), and the posterior tubercle (p3) (for further details see Chapter 4).

Hypothalamus

The walls of the infundibular recess, the ventrocaudal expansion of the third ventricle, give rise to the hypothalamus. Lateral expansion of the hypothalamic/infundibular walls gives rise to the inferior hypothalamic lobes, which have been associated with control of feeding behaviour. The hypothalamus is divided into the medial or tuberal region, closely related to the hypophysis, which contains the hypothalamic-hypophyseal tract, and the caudal or mammillary region, which comprises several circumventricular organs, such as the posterior recess organ, and the paraventricular organ, characterized by folded walls with cerebrospinal-fluid contacting catecholaminergic, serotoninergic, and peptidergic neurons (Rodríguez-Moldes and Anadón, 1987; Molist et al., 1993, 1995; Chiba et al., 2002; Carrera et al., 2005, 2008b), as well as caudally the *saccus vasculosus,* the function of which is still unknown (Sueiro et al., 2007).

Preoptic Area

Although embryologically and morphologically the preoptic area (the forebrain region bordering the preoptic recess) belongs to the telencephalon, functionally it is related to the hypophysis, and is thus considered as part of the hypothalamus. The preoptic area contains the magnocellular preoptic nucleus, the axons of which form the hypothalamus-hypophyseal tract which courses along the hypothalamic floor and ends in the neurointermediate lobe (i.e., the neurohypophysis/hypothalamic neural lobe, derived from the ventral infundibular walls, and the pars intermedia of the adenohypophysis/hypophysis together constitute the "classic" neurosecretory system), as well as aminergic and peptidergic cerebrospinal-fluid contacting

neurons that form the preoptic recess organ, a neurohemal structure located in the median eminence region of the hypothalamic floor (for a review see Smeets, 1998).

Telencephalon

As in agnathans and sarcopterygians, the chondrichthyan telencephalon develops by a morphogenetic process known as evagination (Fig. 4), which involves protrusion towards the outside and expansion of the lateral telencephalic walls, giving rise to formation of the telencephalic hemispheres (Northcutt and Braford, 1980; revised in Butler and Hodos, 2005).

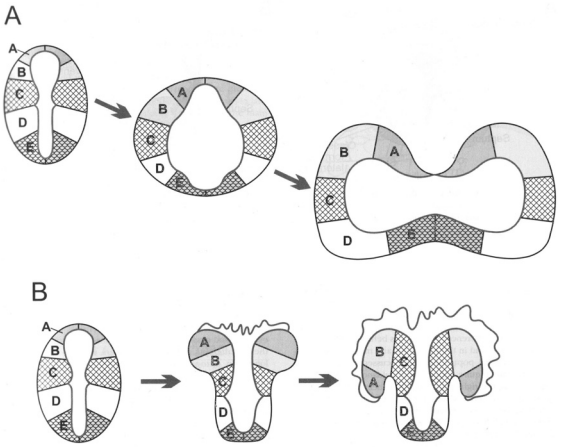

Figure 4. Drawing showing the possible morphogenetic processes that give rise to the telencephalon in different vertebrates: evagination (A, chondrichthyans and sarcopterygians) and eversion (B; actinopterygians). From Butler and Hodos, 2005.

The telencephalon comprises the telencephalic hemispheres - the medial walls of which are completely fused in *Scyliorhinus* - and the olfactory bulbs. The dorsal part of the telencephalon hemispheres, the pallium, consists of dorsal (characterized by a cortical organization), medial (considered equivalent to the amniote hippocampus) and lateral territories (which receive olfactory projections). A wide variety of cell types has been reported in the pallium of *S canicula* (Manso and Anadón, 1993b). The subpallium, ventral part of the telencephalic hemispheres, comprises a medial part that contains the septal nucleus, a lateral part that consists of the basal superficial area, the striatum, and the periventricular area, all of which are related to the basal ganglia of mammals. In elasmobranchs, several authors have proposed different neuronal groups as homologues of the striatum and pallidum (Reiner and Carraway, 1985; Northcutt et al., 1988; Northcutt, 1989; Medina y Reiner, 1995; Reiner et al., 1998; Smeets, 1998; Smeets et al., 2000), however homologies are difficult to assess, and more data about connections and development of the telencephalon are necessary. According to Smeets et al. (1983), the striatum of *S. canicula* consists of a group of cells in

the lateroventral telencephalic walls that form a protrusion in the ventricle. However, Northcutt et al. (1988) proposed the periventricular ventrolateral area as the homologue of the striatum in *Squalus*. The olfactory bulbs are large, well-developed structures that enclose extensions of the lateral ventricles (see Fig. 4), with a layered organization consisting of four layers: the primary olfactory fibres, the glomerular, the mitral cells, and the broad granular cells layers. Morphological and electrophysiological studies (Catois, 1901; Sterzi, 1909; Nieuwenhuys, 1967b; Andres, 1970; Brückmoser and Dieringer, 1973; Dryer and Graziadei, 1991, 1993, 1996) have revealed that Elasmobranchs present most of the neuronal elements found in the mammalian olfactory bulb, although there are some structural differences, such as a lack of basal dendrites in the mitral cell and a scarcity of periglomerular and granular cells. As in lampreys, granular cells have axons that contribute, together with those of the mitral cells, to form secondary olfactory fibres (Smeets, 1983; Dryer and Graziadei, 1996).

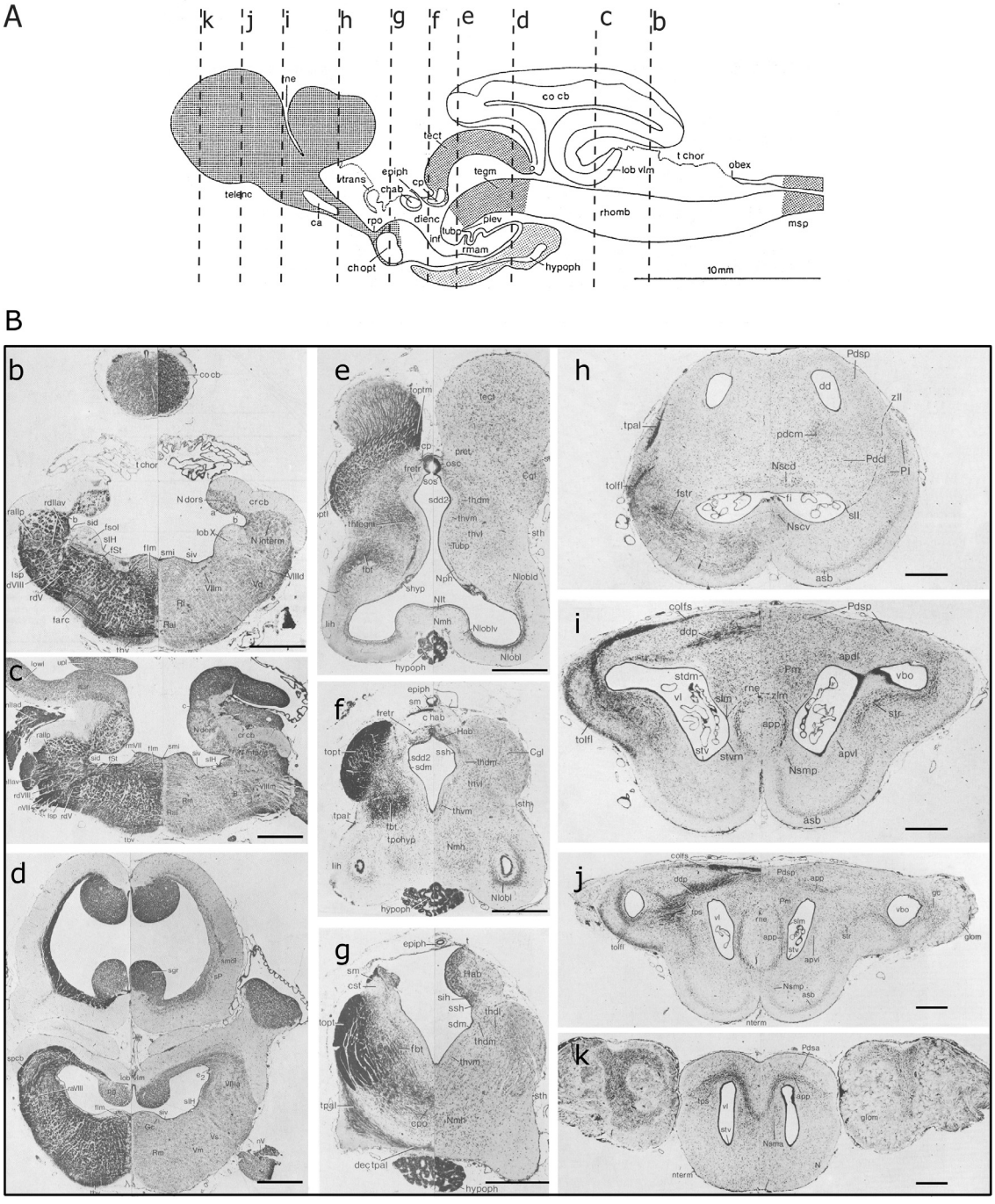

Figure 5. Overall anatomy of the *S. canicula* brain. **A.** Drawing showing a sagittal view of the adult *S. canicula* brain. **B.** Micrographs of transverse sections at the levels indicated in A. Scale bar: 1 mm. Taken from Smeets et al. (1983).

EYE MORPHOGENESIS AND GENERAL ANATOMY OF THE ELASMOBRANCH RETINA.

In elasmobranch species, vision, together with other sensory systems such as the lateral line, play important roles in predatory behaviour, habitat selection and reproductive behaviour (for a review, see Hart et al., 2006). Elasmobranchs have conspicuous eyes, generally positioned laterally on the head, thus providing some binocular overlap in the visual field.

As a highly accessible extension of the brain, the visual system is an excellent model for studying the development of brain organization. Eye morphogenesis from an undifferentiated neuroepithelium involves a complex hierarchy of inductive processes and intercellular interactions that lead to the formation of the retina, optic stalk and lens within the developing forebrain (reviewed in Saha et al., 1992). Inductive events during gastrulation establish the rostrocaudal and dorsoventral axes of the neural plate, and further specification results in localisation of the presumptive retinal fields to lateral regions of the rostral neural plate (Macdonald et al., 1995 and references therein). During neurulation, the optic vesicles evaginate from the forebrain and make contact with the overlying surface ectoderm, remaining attached to the forebrain via the optic stalks. The surface ectoderm in contact with the optic cups gives rise to the lens placodes. A transient period of close contact between the optic vesicle and the presumptive lens ectoderm, during which they exchange inductive signals, is critical for normal eye development (reviewed in Chow and Lang, 2001). The optic vesicles subsequently invaginate to form double-layered optic cups. In each optic cup, the surrounding neuroepithelium ultimately gives rise to the retinal pigment epithelium, optic stalk, and optic nerve myelinating sheet, while the inner layer gives rise to the optic nerve fibres and **neural retina** (Gilbert, 2003). The optic stalks decrease progressively in size (Schmidtt and Dowling, 1994) so that eventually only the optic nerve connects the eyes to the forebrain.

Initially, the neural retina is composed of undifferentiated multipotent progenitors (Sidman, 1961; Turner and Cepko, 1987; Wetts and Fraser, 1988; Turner et al., 1990) from which all retinal cell types derive. The retinal progenitor cells (RPC) undergo a final mitotic event, migrate toward the vitreal neural retina, and then undergo further migrations and establishment of synaptic connections, giving rise to the mature laminated retina. Development of the mature vertebrate retina therefore requires the differentiation and assembly of a network that comprises a certain number of cell types, namely, six major types

of neurons (ganglion, amacrine, bipolar, horizontal, cone photoreceptor and rod photoreceptor cells) and one type of macroglia (Müller cells), originated in a stereotyped sequence (reviewed in Cremisi et al., 2003).

Like in other vertebrates, the elasmobranch retina consists of two synaptic layers interspersed between three cellular layers. From the vitreal to scleral eye surfaces, the following layers are distinguished:

- the optic fibre layer, formed by ganglion cells axons coursing towards the optic nerve exit,
- the ganglion cell layer, which contains ganglion cell bodies, and some displaced amacrine cells,
- the inner plexiform layer, where the axons of bipolar and amacrine cells establish synapses with the ganglion cell dendrites,
- the inner nuclear layer, which contains amacrine, bipolar, horizontal and Müller glia, as well as cells and displaced ganglion cell bodies,
- the outer plexiform layer, which contains the dendrites of the horizontal and bipolar cells and synapses between photoreceptors and bipolar and horizontal cells occur,
- the outer nuclear layer, which consists of the photoreceptor cell bodies,
- the outer limiting membrane, which delimitates the outer portion of the outer nuclear layer, is made up of the junctions between the Müller glia cells and the photoreceptor cell segments,
- the photoreceptor layer, which comprises the outer segment of the photoreceptor cells that consists of membranous discs containing photopigments,
- the retinal pigment epithelium, which consists of a monolayer of unpigmented cells located below a reflecting *tapetum lucidum* (Nicol, 1961; Braeckevelt, 1994a,b), with scarce pigmented melanosome-containing cells at non-tapetal locations.

Several morphological and physiological studies have characterized the retinal circuitry and cell types in different elasmobranch species (Witkowsky and Stell, 1973a,b; Stell and Witkowsky, a,b; Toyoda et al., 1978; Bozzano and Collin, 2000), including photoreceptor cells (Stell, 1972; Gruber et al., 1991; Logiudice and Laird, 1994; Sillman et al., 1996).

Interestingly, several authors have investigated the topography of ganglion cells, and photoreceptors since it is thought that variations in these parameters are related to different visual requirements dependent on lifestyle and environment (Bozzano and Collin, 2000; Hart et al, 2006; Lisney and Collin, 2008; Litherland and Collin, 2008). However, developmental studies dealing with retinal morphogenesis are scarce (Fishelson and Baranes, 1999; Harahush et al., 2009). Similarly, studies of gene expression in elasmobranch retina are scarce, and only the expression of Otx genes has been investigated in *S. canicula* (Sauka-Spengler et al., 2001; Plouhinec et al., 2005).

Fish retina has been found to be useful for studying retinogenesis as it contains retinal stem cells, which give rise to all cell types throughout the entire life of the animal. The presence of a potential retinal stem cell population within mammalian (including human) retinas has recently been reported (Kubota et al., 2002; Ahmad et al., 2004; Amato et al., 2004; reviewed in Reh and Fischer, 2006), though these cells are quiescent *in vivo* (Reh and Fischer, 2006). It has also recently been discovered that adult avian retinas contain neural stem cells with the ability to self-renew and to differentiate into multiple phenotypic lineages (Kubota et al., 2002; Amato et al., 2004; Reh and Fischer, 2006), although the new retinal addition is more limited than in anamniotes. Indeed, in amphibians and fish, retinal stem cells are contained within the ciliary marginal zone (CMZ), a peripheral ring of undifferentiated cells located at the extreme perimeter of the retina. In the two-dimensional disc of the retina, the CMZ is seen as a wedge-shaped neuroepithelial germinal zone formed by the converging retinal laminae, which lies between the laminated retina and the ciliary epithelium. Interestingly, in amphibians and teleost (Harris and Perron, 1998; Raymond et al., 2006) the CMZ can be divided into several zones, from peripheral to central, which reflect the temporal sequence of retinal development, i.e., multipotent progenitors (deep stem cells) keep at the extreme periphery adjacent to the ciliary epithelium, proliferating retinoblasts are found slightly more centrally, and postmitotic but undifferentiated progenitors are located at the centre of the CMZ. This process must be precisely regulated in order to produce differentiated cells at specific times, and in appropriate types and numbers (De Melo et al., 2003; Philips et al., 2005). For temporal regulation, the switch from dividing progenitor to terminal division is controlled by general cell-cycle regulators (Ohnuma et al., 2002; Ohnuma and Harris, 2003). The conserved birth order of distinct types of neuronal and glial cells suggests that the timing of terminal division is somehow integrated with the process of cell-

type determination (Philips et al., 2005), although the mechanism for integrating timing and determination remains unclear. Moreover, the specific factors in the retina that couple determination to differentiation programs and regulate the timing of differentiation are not entirely known. However, a number of genes are expressed in optic tissues during the formation of the eye, and these may play regulatory roles (see below).

THE PAX6 GENE IS A KEY REGULATOR OF MULTIPLE ASPECTS OF DEVELOPMENT.

Genetic and molecular developmental studies have led to the identification of developmental regulatory genes, which are highly conserved among organisms as diverse as nematodes and humans. Most of these genes are grouped together in the homeobox superfamily because they share a conserved 180-base pair nucleotide sequence named homeo-box, which encodes a 60-amino acid DNA binding motif known as the homeodomain. Many of these homeobox genes codify for transcription factors essential for embryonic development, expression of which is finely regulated in time and space (Püschel et al., 1992; Duparc et al., 2007), and the high degree of conservation of which suggests that vertebrates share a common genetic program of development (Püschel et al., 1992; Callaerts et al., 1997). Among these, the Pax (paired box) gene family is characterized by a highly conserved 384-base pair DNA sequence, the paired box, which encodes a 128-aminoacid-long DNA binding domain (paired box domain) with six alpha helices, identified for the first time in *Drosophila* segmentation genes (for a review see Callaerts et al., 1997), as well as a complete or partial homeodomain. Several Pax genes have been identified, and grouped into four classes on the basis of sequence similarity and comparison of domain structure: class I includes Pax1, Pax9 and *Drosophila* Pox meso; class II comprises Pax2, Pax5, Pax8 and Drosophila Pox neuro; class III comprises Pax3, Pax7, and Drosophila gooseberry and paired, and class IV includes Pax4, Pax6 and *Drosophila* eyeless (Balczarek et al., 1997).

Pax6 is probably the best studied member of the Pax gene family because of its essential role in eye development; loss of Pax6 disrupts eye development in invertebrates such as *Drosophila*, (Quiring et al., 1994), and also in vertebrates (Hogan et al., 1986, 1988; Grindley et al., 1995) resulting in the small eye phenotype in mouse or aniridia disorders in humans. Moreover, misexpression of vertebrate Pax6 or its *Drosophila* homologue *eyeless* at

inappropriate positions induces ectopic eyes (Halder et al., 1995; Chow et al., 1999; Onuma et al., 2002)

Pax6 homologues have been identified in many of the Metazoa, including the nematode *Caenorhabditis elegans* (Chisholm and Horvitz, 1995; Zhang and Emmons, 1995), squid (Tomarev et al., 1997; Hartmann et al., 2003), ribbon worm (Loosli et al 1996), flatworm (Callaerts et al., 1999), sea urchin (Czerny and Busslinger 1995), ascidians (Glardon et al., 1997), *Drosophila* (Quiring et al., 1994; Czerny et al., 1999), *Amphioxus* (Glardon et al., 1998), lamprey (Murakami et al., 2001), zebrafish (Krauss et al., 1991; Püschel et al., 1992) *Xenopus* (Hirsch and Harris, 1997; Li et al., 1997), chick (Goulding et al., 1993; Li et al., 1994), quail (Martin et al., 1992), mouse (Walther and Gruss, 1991; Stoykova and Gruss, 1994), rat (Matsuo et al., 1993), human (Ton et al., 1991), and elasmobranchs (Derobert et al., 2002b).

The sequence of the Pax6 protein is highly conserved among these species, including its three functional domains: the paired box domain (PD; DNA-binding domain, located at the amino-terminus of the protein and characteristic of all members of the Pax gene family), the paired homeobox domain (HD; which is entirely present only in Pax6, Pax3 and Pax7, meanwhile the other vertebrate Pax genes show truncated HD), and the proline, serine and threonine-rich domain (PST-rich; at the carboxy-terminus of the Pax6 protein), which is variable except in vertebrates, echinoderms, and molluscs (Callaerts et al., 1997). Both the PD and the HD have been shown to bind DNA, whereas the PST domain functions in transcriptional activation (Tsonis and Fuentes, 2006; Osumi et al 2008 and references therein). Comparison of Pax6 proteins has revealed that human and rodent Pax6 proteins show 100% identity, and these show 96% identity with chick Pax6 protein and 93% identity with ostheichtyans (zebrafish), whereas elasmobranch (*S. canicula*) Pax6 protein displays 94% identity with osteichthyan Pax6. Moreover, the percentage similarity between mammalian and Drosophila Pax6 protein ranges between 80-90% (Callaerts et al., 1997; van Heyningen and Williamson, 2002; Manuel and Price, 2005).

Alternative splicing of the Pax6 transcript has been reported in mouse, humans, zebrafish, chick and quail (Glaser et al., 1992; Goulding et al., 1993; Püschel et al., 1992; Carriere et al., 1993; Walther and Gruss, 1991), suggesting that vertebrate Pax6 functions may be divided among alternative splice variants/or isoforms (Epstein et al., 1994; Haubst et al., 2004; Lakowski et al., 2007), since these isoforms have shown different DNA-binding specificity. Although different authors have reported more than three Pax6 isoforms (Carriere et al., 1993), the most frequent are the canonical Pax6 (which contains a PD, and HD), a paired-less isoform (only showing the HD), and isoform Pax6(5a), which presents a 14 amino acid insertion (exon 5a) in the PD, which modifies its DNA-binding properties (Haubst et al., 2004).

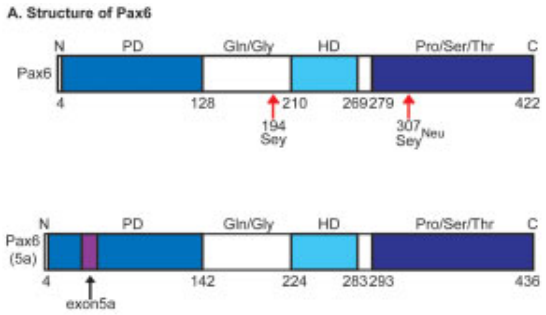

Figure 6. (A) Structure of the Pax6 gene showing the characteristics paired (PD) and homeo (HD) domains. Arrowheads indicate the mutation sites (deletion) resulting in truncated non-functional proteins responsible for the Sey phenotypes in mice (alleles Sey, and SeyNeu). (B). Structure of the Pax6(5a) isoform (originated by alternative splicing), which contains an insertion of 14-amino acid (exon 5a). Taken from Simpson and Price (2002).

Pax6 has been reported to be expressed in specific spatio-temporal patterns during development, and is thus thought to be upstream of gene networks involved in the development of the vertebrate and invertebrate (flies, squid and other species) central nervous systems (Callaerts et al., 1997; Kammermeier and Reichert 2001). The high degree of conservation of the sequence and structure of the Pax6 DNA-binding domains (Callaerts et al., 1997), together with similar spatiotemporal expression patterns among organisms, has suggested conservation of Pax6 functions. Thus, the expression pattern of Pax6 in the developing nervous system of both vertebrates (Stoykova and Gruss, 1994; Kawakami et al., 1997; Wullimann and Rink, 2001) and invertebrates (Drosophila: Callaerts et al., 2001; Kammermeier et al., 2001) suggests that similar mechanisms may be involved in the specification of spatial domains in the embryonic brain of vertebrates and invertebrates, as

well as in the eye (see above). Further evidence is provided by the fact that the Pax6 expression domains in the embryonic brain are progressively reduced to subsets of Pax6 cells in both vertebrates and invertebrates, such as *Drosophila* (Callaerts et al., 1997; Wulliman and Rink, 2001). In addition to conservation of sequence and function, Xu et al. (1999) have reported conservation at the level of Pax6 control, since regulatory regions of the mouse Pax6 are recognized by a Drosophila enhancer, and thus Pax6 expression induced in transgenic mice reproduces normal Pax6 expression.

Study of Pax6 mutant lines of mice and rat, conditional knockouts and transgenic studies have provided insight into the different roles of Pax6 in the developing central nervous system of vertebrates, which includes patterning (Stoykova et al., 1996; Callaerts et al., 1997; Mastick et al., 1997; Mastick and Andrews, 2001; Simpson and Price, 2002; Osumi et al., 1997; Stoykova et al., 2000; Takahashi and Osumi, 2002), neurogenesis (Osumi et al., 2008 and references therein) and neuronal differentiation, as well as roles in cell migration and axon growth (Schmahl et al., 1993; Caric et al., 1997; Talamillo et al., 2003, Kawano et al., 1999; Pratt et al., 2000; Hevner et al., 2002, Mastick et al., 1997; Vitalis et al., 2000; Osumi et al., 2008) (for further details see Chapter 1). Outside the brain, Pax6 is essential for the development of nasal structures (Hogan et al., 1986, 1988; Grindley et al., 1995), endocrine pancreas (St-Onge et al., 1997; Dohrmann et al., 2000), pituitary gland (Kioussi et al., 1999), lacrimal gland (Makarenkova et al., 2000) and the eye (see Chapter 5).

REFERENCES

Ahmad I, Das AV, James J, Bhattacharya S, Zhao X (2004). Neural stem cells in the mammalian eye: types and regulation. Semin Cell Dev Biol, 15: 53-62.

Álvarez-Otero R, Anadón R (1987). The cerebellum of the dogfish, *Scyliorhinus canicula*: a quantitative study. J Hirnforsch, 28: 133-137.

Álvarez-Otero R, Anadón R (1992). Golgi cells of the cerebellum of the dogfish, *Scyliorhinus canicula* (elasmobranchs): a Golgi and ultrastructural study. J Hirnforsch, 33: 321-327.

Álvarez-Otero R, Regueira SD, Anadón R (1993). New structural aspects of the synaptic contacts on Purkinje cells in an elasmobranch cerebellum. J Anat, 182: 13-21.

Álvarez-Otero R, Pérez SE, Rodríguez MA, Adrio F, Anadón R (1995). GABAergic neuronal circuits in the cerebellum of the dogfish *Scyliorhinus canicula* (Elasmobranchs): an immunocytochemical study. Neurosci Lett, 187:87-90.

Amato MA, Arnault E, Perron M (2004). Retinal stem cells in vertebrates: parallels and divergences. Int J Dev Biol, 48: 993-1001.

Anadón R, Molist P, Rodríguez-Moldes I, López JM, Quintela I, Cerviño MC, Barja P, González A (2000). Distribution of choline acetyltransferase immunoreactivity in the brain of an elasmobranch, the lesser spotted dogfish (*Scyliorhinus canicula*). J Comp Neurol, 420: 139-70.

Andres KH (1970). Anatomy and ultraestructure of the olfactory bulb in fish, amphibia, reptiles, birds and mammals. In: Ciba Foundation Symposium on Taste and Smell in Vertebrates (Wolstenholme GEW, Knight J, eds), pp. 177-194. Churchill Livingstone, London.

Balczarek KA, Lai ZC, Kumar S (1997). Evolution and functional diversification of the paired box (Rzx) DNA-binding domains. Mol Biol Evol, 14: 829-842.

Ballard W, Mellinger J, Lechenault H (1993). A series of normal stages for development of *Scyliorhinus canicula*, the lesser spotted dogfish (Chondrichthyes: *Scyliorhinidae*). J Exp Zool, 267: 318–336.

Bayer SA, Altman J (1995a). Neurogenesis and neuronal migration. In: The rat nervous systems (Paxinos GT, ed.) 2nd ed., pp. 1079-1098. Academic Press, San Diego.

Bayer SA, Altman J (1995b). Principles of Neurogenesis, neuronal migration and neural circuit formation. In: The rat nervous systems (Paxinos GT, ed.) 2nd ed., pp. 1041-1077. Academic Press, San Diego.

Bozzano A, Collin SP (2000). Retinal ganglion cell topography in elasmobranches. Brain Behav Evol, 55: 191-208

Braekevelt CR (1994a). Fine structure of the retinal pigment epithelium in the Port Jackson (*Heterodontus phillipi*). Anat Embryol, 190: 501-506.

Braekevelt CR (1994b). Retinal pigment epithelial fine structure in the short-tailed stingray (*Dasyatis brevicaudata*). Histol Histopathol, 9: 501-506.

Brückmoser P, Dieringer N (1973). Evoked potentials in the primary and secondary olfactory projection areas of the forebrain in elasmobranchia. J Comp Physiol, 87: 65-74.

Butler AB, Hodos W (2005). Vertebrate phylogeny and diversity in brain organization. In: Comparative vertebrate neuroanatomy: evolution and adaptation. 2nd ed., pp.73-91. John Wiley & Sons Inc, Hoboken, New Jersey.

Callaerts P, Halder G, Gehring WJ (1997). Pax6 in development and evolution. Annu Rev Neurosci, 20: 483–532.

Callaerts P, Munoz-Marmol AM, Glardon S, Castillo E, Sun H, Li WH, Gehring WJ, Salo E (1999). Isolation and expression of a Pax-6 gene in the regenerating and intact Planarian Dugesia(G)tigrina. Proc Natl Acad Sci USA, 96: 558-563.

Callaerts P, Leng S, Clements J, Benassayag C, Cribbs D, Kang YY, Walldorf U, Fischbach KF, Strauss R (2001). *Drosophila* Pax-6/*eyeless* is essential for normal adult brain structure and function. J Neurobiol, 46: 73-88.

Caric D, Gooday D, Hill RE, McConnell SK, Price DJ (1997). Determination of the migratory capacity of embryonic cortical cells lacking the transcription factor Pax-6. Development, 124: 5087-5096.

Carrera I (2008). Desarrollo de los sistemas gabaérgico y aminérgicos en el sistema nervioso central de peces cartilaginosos. Ph. D. Thesis. University of Santiago de Compostela.

Carrera I, Sueiro C, Molist P, Ferreiro S, Adrio F, Rodríguez MA, Anadón R, Rodríguez-Moldes I (2005). Temporal and spatial organization of tyrosine hydroxylase-immunoreactive cell groups in the embryonic brain of an elasmobranch, the lesser-spotted dogfish *Scyliorhinus canicula*. Brain Res Bull, 66: 541-545.

Carrera I, Sueiro C, Molist P, Holstein GR, Martinelli GP, Rodríguez-Moldes I, Anadón R (2006). GABAergic system of the pineal organ of an elasmobranch (*Scyliorhinus canicula*): a developmental immunocytochemical study. Cell Tissue Res, 323: 273-281.

Carrera I, Ferreiro-Galve S, Sueiro C, Anadón R Rodríguez-Moldes I, (2008a). Tangentially migrating GABAergic cells of subpallial origin invade massively the pallium in developing sharks. Brain Res Bull, 75: 405-409.

Carrera I, Molist P, Anadón R, Rodríguez-Moldes, I (2008b). Development of the serotoninergic system in the central nervous system of a shark, the lesser spotted dogfish *Scyliorhinus canicula*. J Comp Neurol, 511: 804-831.

Carriere C, Plaza S, Martin P, Quatannens B, Bailly M, Stehelin D, Saule S. (1993). Characterization of quail Pax-6 (Pax-QNR) proteins expressed in the neuroretina. Mol Cell Biol, 13: 7257-7266.

Catois EM (1901). Recherches sur l'histologie et l'anatomie microscopique de l'encéphale chez les poissons. Imprimerie L. Danel, Lille.

Chiba A, Honma Y (1992). Distribution of neuropeptide Y-like immunoreactivity in the brain and hypophysis of the cloudy dogfish, *Scyliorhinus torazame*. Cell Tissue Res, 268: 453-461.

Chiba A, Oka S, Saito E (2002). Ontogenetic changes in neuropeptide Y-immunoreactive cerebro spinal-fluid contacting neurons in the hypothalamus of the cloudy dogfish, *Scyliorhinus torazame* (*Elasmobranchii*). Neurosci Lett, 329: 301-304.

Chisholm AD, Horvitz HR (1995). Patterning of the *Caenorhabditis elegans* head region by the Pax-6 family member vab-3. Nature, 377: 52-55.

Chow RL, Altmann CR, Lang RA, Hemmati-Brivanlou A (1999). Pax6 induces ectopic eyes in a vertebrate. Development, 126: 4213–4222.

Chow RL, Lang RA (2001). Early eye development in vertebrates. Annu Rev Cell Dev Biol, 17: 255-296.

Compagno LJV (1977). Phyletic relationships of living sharks and rays. Am Zool, 17: 303-322.

Coolen M, Menuet A, Chassoux D, Compagnucci C, Henry S, Lévèque L, Da Silva C, Gavory F, Samain S, Wincker P, Thermes C, D'Aubenton-Carafa Y, Rodríguez-Moldes I, Naylor G, Depew M, Sourdaine P, Mazan S (2009). The dogfish *Scyliorhinus canicula*, a reference in jawed vertebrates. In: Emerging model organisms. A laboratory manual, vol. 1, pp 431-446. Cold Spring Harbour, New York.

Cremisi F, Philpott A, Ohnuma S (2003). Cell cycle and cell fate interactions in neural development. Curr Opin Neurobiol, 2003: 26-33.

Czerny T, Busslinger M (1995). DNA-binding and transactivation properties of Pax-6: three amino acids in the paired domain are responsible for the different sequence recognition of Pax-6 and BSAP (Pax-5). Mol Cell Biol, 15: 2858–2871.

Czerny T, Halder G, Kloter U, Souabni A, Gehring WJ, Busslinger M (1999). twin of eyeless, a second Pax-6 gene of Drosophila, acts upstream of eyeless in the control of eye development. Mol Cell, 3: 297-307.

De Melo J, Qiu X, Du G, Cristante L, Eisenstat DD (2003). Dlx1, Dlx2, Pax6, Brn3b, and Chx10 Homeobox gene expression defines the retinal ganglion and inner nuclear layers of the developing and adult mouse retina. J Comp Neurol, 461: 187-204.

Derobert Y, Plouhinec JL, Sauka-Spengler T, Le Mentec C, Baratte B, Jaillard D, Mazan S (2002a). Structure and expression of three Emx genes in the dogfish *Scyliorhinus canicula*: functional and evolutionary implications. Dev Biol, 247: 390-404.

Derobert Y, Baratte B, Lepage M, Mazan S (2002b). Pax6 expression patterns in *Lampetra fluviatilis* and *Scyliorhinus canicula* embryos suggest highly conserved roles in the early regionalization of the vertebrate brain. Brain Res Bull, 57: 277-280.

Dohrmann C, Gruss P, Lemaire L (2000). Pax genes and the differentiation of hormone-producing endocrine cells in the pancreas. Mech Dev, 92: 47-54.

Dryer L, Graziadei PPC (1991). Heterogeneity and compartmentalization in the olfactory bulb of elasmobranch fishes. Soc Neurosci Abstr, 17: 1017.

Dryer L, Graziadei PPC (1993). A pilot study on morphological compartmentalization and heterogeneity in the elasmobranch olfactory bulb. Anat Embryol, 188: 41-51.

Dryer L, Graziadei PPC (1996). Synaptology of the olfactory bulb of an elasmobranch fish, *Sphyrna* tiburo. Anat Embryol, 193: 101-114.

Duparc RH, Abdouh M, David J, Lépine M, Tétreault N, Bernier G (2007). Pax6 controls the proliferation rate of neuroepithelial progenitors from the mouse optic vesicle. Dev Biol, 301: 374-387.

Epstein JA, Glaser T, Cai J, Jepeal L, Walton DS, Maas RL (1994). Two independent and interactive DNA-binding subdomains of the Pax6 paired domain are regulated by alternative splicing. Genes Dev, 8: 2022-2034.

Fiebig E (1988). Connections of the corpus cerebelli in the thornback guitarfish, *Platyrhinoidis triseriata* (Elasmobranchii): a study with WGA-HRP and extracellular granule cell recording. J Comp Neurol, 268: 567-83.

Fishelson L, Baranes A (1999). Ocular development in the oman shark, *Iago omanensis* (Triakidae), Gulf of Aqaba, Red Sea. Anat Rec, 256: 389-402.

Fraser S, Keynes R, Lumsden AC (1990). Segmentation in the chick embryo hindbrain is defined by cell lineage restrictions. Nature, 344: 431-435.

Gilbert SF (2003). Development of the vertebrate eye. In: Developmental biology (Sinauer Associates Inc. Publishers, eds), pp. 413-414. Sunderland, Massachusetts, USA.

Glardon S, Callaerts P, Halder G, Gehring WJ (1997). Conservation of Pax-6 in a lower chordate, the ascidian Phallusia mammillata. Development, 124: 817-825.

Glardon S, Holland LZ, Gehring WJ, Holland ND (1998). Isolation and developmental expression of the amphioxus Pax-6 gene (AmphiPax-6): insights into eye and photoreceptor evolution. Development, 125:2701-27

Glaser T, Walton DS, Maas RL (1992). Genomic structure, evolutionary conservation and aniridia mutations in the human PAX6 gene. Nat Genet, 2: 232-239.

Goulding MD, Lumsden A, Gruss P (1993). Signals from the notochord and floor plate regulate the region-specific expression of two Pax genes in the developing spinal cord. Development, 117: 1001-1016.

Grindley JC, Davidson DR, Hill RE (1995). The role of Pax-6 in eye and nasal development. Development, 121: 1433-1442.

Gruber SH, Loew ER, McFarland WN (1991). Rod and cone pigments of the Atlantic guitarfish, *Rhinobatos lentiginosus* Garman. J Exp Zool Suppl, 5: 85-87.

Halder G, Callaerts P, Gehring WJ (1995). Induction of ectopic eyes by targeted expression of the eyeless gene in Drosophila. Science, 267: 1788–1792.

Harahush BK, Hart NS, Green K, Collin SP (2009). Retinal neurogenesis and ontogenetic changes in the visual system of the brown banded bamboo shark, Chiloscyllium *punctatum (Hemiscyllidae, Elasmobranchii)*. J Comp Neurol, 513: 83-97.

Harris WA, Perron M (1998). Molecular recapitulation: the growth of the vertebrate retina. Int J Dev Biol, 42: 299-304.

Hart SN, Lisney TJ, Collin SP (2006). Visual communication in elasmobranchs. In: Communication in Fishes (Ladich F, Collin SP, Moller P, Kapoor BG, eds), pp. 337–372. Science Publishers, Plymouth.

Hartmann B, Lee PN, Kang YY, Tomarev S, de Couet HG, Callaerts P (2003). Pax6 in the sepiolid squid Euprymna scolopes: evidence for a role in eye, sensory organ and brain development. Mech Dev, 120: 177-183.

Haubst N, Berger J, Radjendirane V, Graw J, Favor J, Saunders GF, Stoykova A, Götz M (2004). Molecular dissection of Pax6 function: the specific roles of the paired domain and homeodomain in brain development. Development, 131: 6131-6140.

Hevner RF, Miyasshita-Lin E, Rubenstein JL (2002). Cortical and thalamic axon pathfinding defects in Tbr1, Gbx2, and Pax6 mutant mice: evidence that cortical and thalamic axons interact and guide each other. J Comp Neurol, 447: 8-17.

Hirsch N, Harris WA (1997). Xenopus Pax-6 and retinal development. J Neurobiol, 32: 45-61.

Hogan BLM, Hirst EMA, Horsburgh G, Hetherington CM (1988). Small eye (Sey): a mouse model for the genetic analysis of craniofacial abnormalities. Development, 103: 115-119.

Hogan BLM, Horsburgh G, Cohen J, Hetherington, Fisher CM, Lyon MF (1986). Small eyes (Sey): a homozygous lethal mutation on chromosome 2 which affects the differentiation of both lens and nasal placodes in the mouse. J Embryol Exp, 97: 95-110.

Kammermeier L, Reichert H (2001). Common developmental genetic mechanisms for patterning invertebrate and vertebrate brains. Brain Res Bull, 55: 675-682.

Kammermeier L, Leemans R, Hirth F, Flister S, Wenger U, Walldorf U, Gehring WJ, Reichert H (2001). Differential expression and function of the Drosophila Pax6 genes eyeless and twin of eyeless in embryonic central nervous system development. Mech Dev, 103: 71-78.

Kawakami A, Kimura-Kawakami M, Nomura T, Fujisawa H (1997). Distributions of PAX6 and PAX7 proteins suggest their involvement in both early and late phases of chick brain development. Mech Dev, 66: 119-130.

Kawano H, Fukuda T, Kubo K, Horie M, Uyemura K, Takeuchi K, Osumi N, Eto K, Kawamura K (1999). Pax6 is required for thalamocortical pathway formation in the fetal rats. J Comp Neurol, 408: 147-160.

Kimmel CB (1993). Patterning the brain of the zebrafish embryo. Annu Rev Neurosci, 16: 707-732.

Kioussi C, O'Connell S, St-Onge L, Treier M, Gleiberman AS, Gruss P, Rosenfeld MG. (1999). Pax6 is essential for establishing ventral-dorsal cell boundaries in pituitary gland development. Proc Natl Acad Sci USA, 25: 14378-14382.

Krauss S, Johansen T, Korzhi V, Fjose A (1991). Expression of the zebrafish paired box gene pax[zf-b] during early neurogenesis. Development, 113: 1193-1206.

Kubota R, Hokoc JN, Moshiri A, McGuire G, Reh TA (2002). A comparative study of neurogenesis in the retinal ciliary marginal zone of homeothermic vertebrales. Brain Res Dev Brain Res, 134: 31-41.

Lakowski J, Majumder A, Lauderdale JD (2007). Mechanisms controlling Pax6 isoform expression in the retina have been conserved between teleosts and mammals. Dev Biol, 307: 498-520.

Larsell O (1967). In: The comparative anatomy and histology of the cerebellum from myxinoids through birds (Jansen J , ed). University of Minnesota Press, Minneapolis.

Larsen CW, Zelster LM, Lumsden A (2001). Boundary formation and compartition in the avian diencephalon. J Neurosci, 21: 4699–4711.

Li H, Tierney C, Wen L, Wu JY, Rao Y (1997). A single morphogenetic field gives rise to two retina primordia under the influence of the prechordal plate. Development, 124: 603-615.

Li HS, Yang JM, Jacobson RD, Pasko D, Sundin O (1994). Pax-6 is first expressed in a region of ectoderm anterior to the early neural plate: implications for stepwise determination of the lens. Dev Biol, 162: 181-194.

Lisney TJ, Collin SP (2008). Retinal ganglion cell distribution and spatial resolving power in elasmobranchs. Brain Behav Evol, 72: 59-77.

Litherland L, Collin SP (2008). Comparative visual function in elasmobranchs: spatial arrangement and ecological correlates of photoreceptor and ganglion cell distributions. Vis Neurosci, 25: 549-561.

Logiudice FT, Laird RJ (1994). Morphology and density distribution of cone photoreceptor in the retina of the Atlantic stingray, Dasyatis sabina. J Morphol, 221:277-289.

Loosli F, Kmita-Cunisse M, Gehring WJ (1996). Isolation of a *Pax-6* homolog from the ribbonworm *Lineus sanguineus. Proc Natl Acad Sci USA,* 92: 2658–26.63

Lumsden A (1990). The cellular basis of segmentation in the developing hindbrain. TINS, 13: 329-435.

Macdonald R, Barth KA, Xu Q, HolderN, Mikkola I, Wilson SW (1995). Midline signalling is required for Pax gene regulation and patterning of the eyes. Development, 121: 3267-3278.

Maisey JG (1980). An evaluation of jaw suspension in sharks. Am Mus Novit, 2706:1–17.

Makarenkova HP, Ito M, Govindarajan V, Faber SC, Sun L, McMahon G, Overbeek PA, Lang RA (2000). FGF10 is an inducer and Pax6 a competence factor for lacrimal gland development. Development, 127: 2563-2572.

Mandado M, Molist P, Anadón R, Yáñez J (2001). A DiI-tracing study of the neural connections of the pineal organ in two elasmobranchs (*Scyliorhinus canicula* and *Raja montagui*) suggests a pineal projection to the midbrain GnRH-immunoreactive nucleus. Cell Tissue Res, 303: 391-401.

Manso MJ, Anadón R (1991a). The optic tectum of the dogfish *Scyliorhinus canicula* L.: a Golgi study. J Comp Neurol, 307: 335-349.

Manso MJ, Anadón R (1991b). Specialized presynaptic dendrites in the stratum cellulare externum of the optic tectum of an elasmobranch, *Scyliorhinus canicula* L. Neurosci Lett, 129: 291-293.

Manso MJ, Anadón R (1993a). Distribution of types of neurons in the optic tectum of the small-spotted dogfish, *Scyliorhinus canicula* L. A Golgi study. Brain Behav Evol, 41: 82-87.

Manso MJ, Anadón R (1993b). Golgi study of the telencephalon of the small-spotted dogfish *Scyliorhinus canicula* L. J Comp Neurol, 333: 485-502.

Manuel M, Price DJ (2005). Role of Pax6 in forebrain regionalization. Brain Res Bull, 66:387-393.

Martin P, Carriere C, Dozier C, Quatannens B, Mirabel MA, Vandenbunder B, Stehelin D, Saule S (1992). Characterization of a paired box- and homeobox-containing quail gene (Pax-QNR) expressed in the neuroretina. Oncogene, 7: 1721-1728.

Mastick GS, Andrews GL (2001). Pax6 regulates the identity of embryonic diencephalic neurons. Mol Cell Neurosci, 17:190–207.

Mastick GS, Davis NM, Andrews L, Easter SS (1997). Pax6 functions in boundary formation and axon guidance in the embryonic mouse forebrain. Development, 124: 1985-1997.

Matsuo T, Osumi-Yamashita N, Noji S, Ohuchi H, Koyama E, Myokai F, Matsuo N, Taniguchi S, Doi H, Iseki S, et al. (1993). A mutation in the Pax-6 gene in rat small eye is associated with impaired migration of midbrain crest cells. Nat Genet, 3: 299-304.

Medina L, Reiner A (1995). Neurotransmitter organization and connectivity of the basal ganglia in vertebrates: implications for the evolution of basal ganglia. Brain Behav Evol, 46: 235-258.

Meredith GE, Smeets WJ (1987). Immunocytochemical analysis of the dopamine system in the forebrain and midbrain of *Raja radiata*: evidence for a substantia nigra and ventral tegmental area in cartilaginous fish. J Comp Neurol, 265: 530-548.

Molist P, Rodríguez-Moldes I, Anadón R (1993). Organization of catecholaminergic systems in the hypothalamus of two elasmobranch species, *Raja undulata* and *Scyliorhinus canicula*. A histofluorescence and immunohistochemical study. Brain Behav Evol, 41: 290-302.

Molist P, Rodríguez-Moldes I, Batten TF, Anadón R (1995). Distribution of calcitonin gene-related peptide-like immunoreactivity in the brain of the small-spotted dogfish, *Scyliorhinus canicula* L. J Comp Neurol, 352: 335-50.

Murakami Y, Ogasawara M, Sugahara F, Hirano S, Satoh N, Kuratani S (2001). Identification and expression of the lamprey Pax6 gene: evolutionary origin of the segmented brain of vertebrates. Development, 128: 3521–3531.

Nicholson C, Llinás R (1969). Inhibition of Purkinje cells in the cerebellum of elasmobranch fishes. Brain Res, 12: 477-81.

Nicol JAC (1961). The tapetum in *Scyliorhinus canicula*. J Mar Biol Ass UK, 41:271-277.

Nieuwenhuys R (1967a). Comparative anatomy of the cerebellum. Prog Brain Res, 25: 1-93.

Nieuwenhuys R (1967b). Comparative anatomy of olfactory centres and tracts. In: Progress in brain research (Zotterman Y, eds), vol 25, pp: 1-93. Elservier, Amsterdam.

Nieuwenhuys R (1998). Morphogenesis and general structure. In: The Central Nervous System of Vertebrates (Nieuwenhuys R, Ten Donkelaar HJ, and Nicholson C, eds.), pp: 159 -228. Springer-Verlag, Berlin.

Northcutt RG (1978). Brain organization in the cartilaginous fishes. In: Sensory biology of sharks, skates and rays (Hodgson ES, Mathewson RF, eds), pp: 117-19. Department of the Navy, Arlington VA, USA.

Northcutt RG (1979). The comparative anatomy of the nervous system and sense organs. In Hyman's comparative vertebrate anatomy (Wake MH, ed), pp: 615-769. Chicago University Press, Chicago.

Northcutt RG (1989). Brain variation and phylogenetic trends in elasmobranch fishes. J Exp Zool Suppl, 2: 83-100.

Northcutt RG (1990). Visual pathways in elasmobranchs: organization and phylogenetic implications. J Exp Zool Suppl, 5: 97-107.

Northcutt RG, Braford MR, (1980). New observations on the organization and evolution of the telencephalon of actinopterygian fishes. In: Comparative neurology of the telencephalon (Ebbesson S.O.E., ed), pp: 41-98. Plenum Press, New York.

Northcutt RG, Reiner A, Karten HJ (1988). Immunohistochemical study of the telencephalon of the spiny dogfish, *Squalus acanthias*. J Comp Neurol, 277: 250-267.

Ohnuma S, Harris WA (2003). Neurogenesis and the cell cycle. Neuron, 40: 199-208.

Ohnuma S, Hopper S, Wang KC, Philpott A, Harris WA (2002). Co-ordinating retinal histogenesis: early cell cycle exit enhances early cell fate determination in the Xenopus retina. Development, 129: 2435-2446.

Onuma Y, Takahashi S, Asashima M, Kurata S, Gehring WJ (2002). Conservation of Pax6 function and upstream activation by Notch signalling in eye development of frogs and flies. Proc Natl Acad Sci USA, 99: 2020–2025.

Orr HA (1887). Contributions to the embryology of the lizard. J Morphol, 1: 311-372.

Osumi N, Hirota A, Ohuchi H, Nakafuku M, Iimurao T, Kuratani S, Fujiwara M, Noji S, Eto K (1997). Pax6 is involved in the specification of hindbrain motor neuron subtype. Development, 124: 2961-2972.

Osumi N, Shinoara H, Numayama-Tsuruta K, Maekawa M (2008). Concise review: Pax6 transcription factor contributes to both embryonic and adult neurogenesis as a multifunctional regulator. Stem Cells, 26: 1663-1672.

Paul DH, Roberts BL (1975). Proceedings: Connexions between the cerebellum and the reticular formation in the dogfish *Scyliorhinus canicula.* J Physiol, 249: 62P-63P.

Philips GT, Stair CN, Lee HY, Wroblewski E, Berberoglu MA, Brown NL, Mastick GS (2005). Precocious retinal neurons: Pax6 controls timing of differentiation and determination of cell type. Dev Biol, 279: 308-321.

Plouhinec JL, Leconte L, Sauka-Spengler T, Bovolenta P, Mazan S, Saule S. (2005). Comparative analysis of gnathostome *Otx* gene expression patterns in the developing eye: implications for the functional evolution of the multigene family. Dev Biol, 278: 560-575.

Pratt T, Vitalis T, Warren N, Edgar JM, Mason JO, Price DJ (2000). A role for Pax6 in the normal development of dorsal thalamus and its cortical connections. Development, 127: 5167-5178.

Pritz MB (1999). Rhombomere development in a reptilian embryo. J Comp Neurol, 411: 317-326.

Puelles L, Rubenstein JLR (1993). Expression patterns of homeobox and other putative regulatory genes in the embryonic mouse forebrain suggest a neuromeric organization. TINS, 16: 472–479.

Puelles L, Rubenstein JLR (2003). Forebrain gene expression domains and the evolving prosomeric model. TINS, 26: 469-476.

Püschel AW, Gruss P, Westerfield M (1992). Sequence and expression pattern of pax-6 are highly conserved between zebrafish and mice. Development, 114: 643-651.

Quiring R, Walldorf U, Kloter U, Gehring WJ (1994). Homology of the eyeless gene of *Drosophila* to the Small eye gene in mice and Aniridia in humans. Science, 265: 785-789.

Rakic P (2002a). Pre- and post-developmental neurogenesis in primates. Clin Neurosc Res, 2: 29–39.

Rakic P (2002b). Evolving concepts of cortical radial glia and areal specification. In: Progress in Brain Research (Azmitia E et al, eds), vol 136, pp. 265-280. Elsevier, Amsterdam.

Rakic P (2003a). Elusive radial glia cells: historical and evolutionary perspective. Glia, 43: 19-32.

Rakic P (2003b). Developmental and evolutionary adaptations of cortical radial glia cells. Cereb Cortex, 13: 541-549.

Raymond PA, Barthel LK, Bernardos RL, Perkowski JJ (2006). Molecular characterization of retinal stem cells and their niches in adult zebrafish. BMC Dev Biol, 6: 36-53.

Redies C, Ast M, Nakagawa S, Takeichi M, Martínez-de-la-Torre M, Puelles L (2000). Morphologic fate of diencephalic prosomeres and their subdivisions revealed by mapping cadherin expression. J Comp Neurol, 421: 481-514.

Reh TA, Fischer AJ (2006). Retinal stem cells. Methods Enzymol, 419: 52-73.

Reiner A, Carraway RE (1985). Phylogenetic conservatism in the presence of a neurotensin-related hexapeptide in neurons of globus pallidus. Brain Res, 341: 365-371.

Reiner A, Medina L, Veenman CL (1998). Structural and functional evolution of the basal ganglia in vertebrates. Brain Res Rev 28: 235-285.

Repérant J, Miceli D, Rio JP, Peyrichoux J, Pierre J, Kirpitchnikova E (1986). The anatomical organization of retinal projections in the shark *Scyliorhinus canicula* with special reference to the evolution of the selachian primary visual system. Brain Res, 396: 227-248.

Rodríguez-Moldes I, Anadón R (1987). Aminergic neurons in the hypothalamus of the dogfish, *Scyliorhinus canicula* L. (Elasmobranch). A histofluorescence study. J Hirnforsch, 28: 685-693.

Rodríguez-Moldes I, Timmermans JP, Adriaensen D, De Groodt-Lasseel MH, Scheuermann, DW, Anadón R (1990). Immunohistochemical localization of calbindin-D28K in the brain of a cartilaginous fish, the dogfish (Scyliorhinus canicula L.). Acta Anat (Basel), 137: 293-302.

Rodríguez-Moldes I, Manso MJ, Becerra M, Molist P, Anadón R. (1993). Distribution of substance P-like immunoreactivity in the brain of the elasmobranch *Scyliorhinus canicula*. J Comp Neurol, 335: 228-244.

Saha MS, Servetnick M, Grainger RM (1992). Vertebrate eye development. Curr Opin Gen Dev, 2: 582-588.

Sanes DH, Reh TA, Harris WA (2006). Genesis and migration. In: Development of the nervous system (Sanes DH, Reh TA, Harris WA, ed). 2nd ed, pp. 29-55. Academic Press,

Sauer FC (1935). Mitosis in the neural tube. J Comp Neurol, 62: 37-405.

Sauka-Splenger T, Baratte B, Shi L, Mazan S (2001). Structure and expression of an Otx5-related gene in the dogfish *Scyliorhinus canicula*: evidence for a conserved role of Otx5 and Crx genes in the specification of photoreceptors. Dev Genes Evol, 211: 533-544.

Schmahl W, Knoedlseder M, Favor J, Davidson D (1993). Defects of neuronal migration and the pathogenesis of cortical malformations are associated with Small eye (Sey) in the mouse, a point mutation at the Pax-6-locus. Acta Neuropathol, 86: 126-135.

Schmitt EA, Dowling JE, (1994). Early eye morphogenesis in the zebrafish, *Brachydanio rerio*. J Comp Neurol, 344: 532-542.

Sidman RL. (1961). Histogenesis of mouse retina studied with thymidine-H3. In: Structure of the eye (Smelser GK, ed), pp. 487-506. Academic Press, New York.

Sillman AJ, Letsinger GA, Patel S, Loew ER, Klimley AP (1996). Visual pigments and photoreceptors in two species of shark, *Triakissemifasciata* and *Mustelus henlei*. J Exp Zool, 276: 1-10.

Simpson TI, Price DJ (2002). Pax6; a pleiotropic player in development. BioEssays, 24: 1041-1051.

Smeets WJAJ (1981). Efferent tectal pathways in two chondrichthyans, the shark *Scyliorhinus canicula* and the ray *Raja clavata*. J Comp Neurol, 195: 13-23.

Smeets WJAJ (1982). The afferent connections of the tectum mesencephali in two chondrichthyans, the shark Scyliorhinus canicula and the ray Raja clavata. J Comp Neurol, 205: 139-152.

Smeets WJAJ (1983). The secondary olfactory connections in two chondrichthyans, the shark *Scyliorhinus canicula* and the ray *Raja clavata.* J Comp Neurol, 218: 334-344.

Smeets WJAJ (1998). Cartilaginous fish. In: The Central Nervous System of Vertebrates (Nieuwenhuys R, Ten Donkelaar HJ, Nicholson C eds.), vol 1., pp 551-654. Springer-Verlag, Berlin.

Smeets WJAJ, Timerick SJ (1981). Cells of origin of pathways descending to the spinal cord in two chondrichthyans, the shark *Scyliorhinus canicula* and the ray *Raja clavata*. J Comp Neurol, 202: 473-491.

Smeets WJAJ , Nieuwenhuys R and Roberts BL (1983). The Central Nervous System of Cartilaginous Fishes: Structure and Functional Correlations. Springer-Verlag, Berlin.

Smeets WJ, Marín O, González A (2000). Evolution of the basal ganglia: new perspectives through a comparative approach. J Anat, 196: 501-517.

Stell WK. (1972). The structure and morphologic relations of rods and cones in the retina of the spiny dogfish, Squalus. Comp Biochem Physiol A Comp Physiol, 42: 141-151.

Stell WK, Witkovsky P (1973a). Retinal structure in the smooth dogfish, Mustelus canis: general description and light microscopy of giant ganglion cells. J Comp Neurol, 148: 1-31.

Stell WK, Witkovsky P (1973b). Retinal structure in the smooth dogfish, Mustelus canis: light microscopy of photoreceptor and horizontal cells. J Comp Neurol, 148: 33-45.

Sterzi, G. (1909). Il Sistema Nervoso Centrale dei Vertebrate. Pesci I. Selaci. Vol 2, Draghi, Padova.

St-Onge L, Sosa-Pineda B, Chowdhury K, Mansouri A, Gruss P (1997). Pax6 is required for differentiation of glucagon-producing alpha-cells in mouse pancreas. Nature, 387: 406-409.

Storch V, Welsch U (2001). Curso práctico de zoología de Kükenthal, pp: 399-410. Ariel Practicum, Barcelona.

Stoykova A, Gruss P (1994). Roles of Pax genes in developing and adult brain suggested by expression patterns. J Neurosci, 74: 1395-1412.

Stoykova A, Fritsch R, Walther C, Gruss P (1996). Forebrain patterning defects in Small eye mutant mice. Development, 122: 3453-3465.

Stoykova A, Treichel D, Hallonet M, Gruss P (2000). Pax6 modulates the dorsoventral patterning of the mammalian telencephalon. J Neurosci, 20: 8042-8050.

Stuesse SL, Cruce WL, Northcutt RG (1990). Distribution of tyrosine hydroxylase and serotonin-immunoreactive cells in the central nervous system of the thornback guitarfish, *Platyrhinoidis triseriata*. J Chem Neuroanat, 3: 45-58.

Stuesse SL, Cruce WLR, Northcutt RG (1991a). Localization of tyrosine hydroxylase, serotonine, and leu-enkephalin immunoreative cells in the brainstem of the horn shark, *Heterodontus francisci*. J Comp Neurol, 308: 277-292.

Stuesse SL, Cruce WLR, Northcutt RG (1991b). Serotoninergic and enkephalinergic neuron cell groups in the reticular formation of the bar ray and two skates. Brain Behav Evol, 38: 39-52.

Stuesse SL, Cruce WLR (1992). Distribution of tyrosine hydroxylase, serotonine, and leu-enkephalin immunoreative cells in the brainstem of a shark, *Squalus acanthias*. Brain Behav Evol, 39: 77-92.

Stuesse SL, Stuesse DC, Cruce WLR (1995). Raphe nuclei in three cartilaginous fishes, *Hydrolagus colliei, Heterodontus francisci*, and *Squalus acanthias*. J Comp Neurol, 358: 414-427.

Sueiro C (2003). Estudio inmunohistoquímico de los sistemas gabaérgicos del sistema nervioso central de peces elasmobranquios y su relación con sistemas catecolaminérgicos y peptidérgicos. Ph. D. Thesis. University of Santiago de Compostela.

Sueiro C, Carrera I, Rodríguez-Moldes I, Molist P, Anadón R (2003). Development of catecholaminergic systems in the spinal cord of the dogfish *Scyliorhinus canicula* (Elasmobranchs). Brain Res Dev Brain Res, 142: 141-50.

Sueiro C, Carrera I, Rodríguez-Moldes I, Anadón R (2004). Distribution and development of glutamic acid decarboxylase immunoreactivity in the spinal cord of the dogfish *Scyliorhinus canicula* (elasmobranchs). J Comp Neurol, 478: 189-206.

Sueiro C, Carrera I, Ferreiro-Galve S, Molist P, Adrio F, Anadón R, Rodríguez-Moldes I (2007). New insights on *saccus vasculosus* evolution: a developmental and immunohistochemical study in elasmobranchs. Brain Behav Evol, 70: 187-204.

Takahashi M, Osumi N (2002). Pax6 regulates specification of ventral neurone subtypes in the hindbrain by establishing progenitor domains. Development, 129: 1327-1338.

Talamillo A, Quinn JC, Collinson JM, Caric D, Price DJ, West JD, Hill RE (2003). Pax6 regulates regional development and neuronal migration in the cerebral cortex. Dev Biol, 255 :151-163.

Teijido O, Manso MJ, Anadón R (2002). Distribution of thyrotropin-releasing hormone immunoreactivity in the brain of the dogfish *Scyliorhinus canicula*. J Comp Neurol, 454: 65-81.

Timerick SJ, Roberts BL, Paul DH (1992). Brainstem neurons projecting to different levels of the spinal cord of the dogfish *Scyliorhinus canicula*. Brain Behav Evol, 39: 93-100.

Tomarev SI, Callaerts P, Kos L, Zinovieva R, Halder G, Gehring W, Piatigorsky J (1997). Squid Pax-6 and eye development. Proc Natl Acad Sci, 94: 2421-2426.

Ton CC, Hirvonen H, Miwa H, Weil MM, Monaghan P, Jordan T, van Heyningen V, Hastie ND, Meijers-Heijboer H, Drechsler M, et al. (1991). Positional cloning and characterization of a paired box- and homeobox-containing gene from the aniridia region. Cell, 67: 1059-1074.

Toyoda JI, Saito T, Kondo H (1978). Three types of horizontal cells in the stingray retina: their morphology and physiology. J Comp Neurol, 179: 569-579.

Turner DL, Cepko CL (1987). A common progenitor for neurons and glia persists in rat retina late in development. Nature, 328: 131-136.

Turner DL, Snyder EY, Cepko CL (1990). Lineage independent determination of cell type in the embryonic mouse retina. Neuron, 4: 833-845.

Tsonis PA, Fuentes EJ (2006). Focus on molecules: Pax6, the eye master. Exp Eye Res, 83: 233-234.

Vallarino M, Bucharles C, Facchinetti F, Vaudry H (1994). Immunocytochemical evidence for the presence of Met-enkephalin and Leu-enkephalin in distinct neurons in the brain of the elasmobranch fish *Scyliorhinus canicula*. J Comp Neurol, 347: 585-597.

Vallarino M, Danger JM; Fasolo A, Pelletier G, Sain-Pierre S, Vaudry H (1988). Distribution and characterization of neuropeptide Y in the brain of an elasmobranch fish. Brain Res, 448: 67-76.

van Heyningen V, Williamson KA (2002). Pax6 in sensory development. Human Mol Genetics, 10: 1161-1167

Vitalis T, Cases O, Engelkamp D, Verney C, Price DJ. (2000). Defects of tyrosine hydroxylase-immunoreactive neurons in the brains of mice lacking the transcription factor Pax6. J Neurosci, 20: 6501–6516.

von Baer KE (1828). Ueber Entwickelungs-Geschicte der Thiere. Königsberg-Bornträger.

Walther C, Gruss P (1991). Pax-6, a murine paired box gene, is expressed in the developing CNS. Development, 113: 1435-1449.

Wetts R, Fraser SE, (1988). Multipotent precursors can give rise to all major cell types of the frog retina. Science, 239: 1142-1145.

Winchel CJ, Martin AP, Mallatt J (2004). Phylogeny of elasmobranchs based on LSU and SSU ribosomal RNA genes. Molecular Phylogenetics and Evolution, 31: 214–224.

Witkovsky P, Stell WK (1973a). Retinal structure in the smooth dogfish *Mustelus canis*: electron microscopy of serially sectioned bipolar cell synaptic terminals. J Comp Neurol, 150: 147-167.

Witkovsky P, Stell WK (1973b). Retinal structure in the smooth dogfish, *Mustelus canis*: light microscopy of bipolar cells. J Comp Neurol, 148: 47-59.

Wullimann MF, Rink E (2001). Detailed immunohistology of Pax6 protein and tyrosine hydroxylase in the early zebrafish brain suggests role of Pax6 gene in development of dopaminergic diencephalic neurons. Dev Brain Res, 131:173-191.

Xu PX, Zhang X, Heaney S, Yoon A, Michelson AM, Maas RL (1999). Regulation of Pax6 expression is conserved between mice and flies. . Development, 126: 383-395.

Yamanaka S, Honma Y, Ueda S, Sano Y (1990). Immunohistochemical demonstration of serotonin neuron system in the central nervous system of the Japanese dogfish, *Scyliorhinus torazame* (Chondrichthyes). J Hirnforsch, 31: 385–397.

Yoon MS, Puelles L, Redies C (2000). Formation of cadherin-expressing brain nuclei in diencephalic alar plate divisions. J Comp Neurol, 421: 461–480.

Zelster LM, Larsen CL, Lumsden A (2001). A new developmental compartment in the forebrain regulated by Lunatic fringe. Nat Neurosci, 4: 683-684.

Zhang Y, Emmons SW (1995). Specification of sense-organ identity by a *Caenorhabditis elegans* Pax-6 homologue. Nature, 377: 55-59.

Rationale and aims

RATIONALE AND AIM OF THE THESIS

The neuromeric model, conceived as an instrument to explain early segmentation of the embryonic brain (Puelles and Rubenstein, 1993, 2003), has contributed greatly to characterizing the neural body plan in vertebrates, by the identification of brain segments in a variety of model organisms ranging from jawed to jawless vertebrates. Among the former (gnathostomes), brain segmentation has been extensively studied in osteichthyan derivatives, including tetrapods (by use of: *Xenopus* as amphibian model, Bachy et al., 2001; Brox et al., 2003, 2004; the chick as an avian model, Larsen et al., 2001; Bell et al., 2001; Puelles et al., 2000; Medina et al., 2005, and the mouse/rat as mammalian models, Puelles et al., 2000; Puelles and Rubenstein, 2003) and bony fishes (zebrafish as a teleostean model, Hauptmann and Gerster, 2000, 2002; Wullimann and Rink, 2001, and medaka, Alunni et al., 2004; Kage et al., 2004). However, similar studies in other fish groups are scarce, despite the wide diversity of this vertebrate group.

On the other hand, diverse structures in the central nervous system (CNS) such as the cerebellum and the retina have been shown to be useful models for understanding morphogenesis, as they correspond to layered structures in which development is completed at late embryonic stages or even after birth. The cerebellum of fishes is an ideal model for studying morphogenetic development as it contains a limited number of cell types organized in three well-defined cell layers. It therefore also contains discrete proliferation areas that produce new neurons throughout the entire lifespan of the animal; these neurons subsequently migrate to reach their final positions and settle in specific cell layers (Zupanc et al., 2006). Although the sequence of formation of the cerebellum and patterns of proliferation, migration and differentiation in the embryonic and adult cerebellum have been studied in teleosts (Pouwels, 1978; Wulliman and Knipp, 2000; Candal et al., 2005, Zupanc et al., 2006; Ishizawa et al., 2008; Bae et al., 2009), similar studies are lacking in cartilaginous fish. The fish retina is also a valuable model for morphogenetic studies because of: (1) the presence of a limited number of neuronal/glial types, which are organized in three well-defined layers, and (2) the existence of a cilliary marginal zone that contain retinal stem cells, and thus can produce all types of retina cells, thus enabling the retina to grow along the whole lifespan. The general patterns of proliferation, differentiation and lamination are currently well-known in some species of teleosts, mainly fast-growing species such as

zebrafish (Macdonald et al., 1995; Hu and Easter, 1999; Marcus et al., 1999; Li et al., 2000; Easter and Malicki, 2002; Wehman et al., 2005; Raymond et al., 2006), traditionally considered as representative of the gnathostome fish radiation. However, data on other fish groups are scarce.

Despite the importance of the ancient gnathostome radiation (represented by chondrichthyans) from an evolutionary perspective, studies on early brain regionalization and morphogenesis are scarce in this group. The key phylogenetic position of chondrichthyans as an out-group to osteichthyans makes them of particular interest for identifying the gnathostome ancestral condition and thus gaining insight into the evolution of vertebrate brain and retina development. Moreover, sharks appear to be particularly suitable for developmental studies because of the large size of the embryonic brain and their slow development, which facilitates detailed analysis of developmental processes potentially overlooked in rapidly developing vertebrate models.

The main **aim** of this thesis was to study the expression pattern of the highly conserved transcription factor Pax6 in the developing and mature CNS of representative species of the cartilaginous fish group, the lesser spotted dogfish *Scyliorhinus canicula* and the brown shyshark *Haploblefarus fuscus*, both of which belong to the shark family (*Scyliorhinidae*) and commonly referred to as catsharks.

In particular, we explored regionalization and morphogenesis in the brain (and rostral spinal cord) and retina by following the spatiotemporal pattern of Pax6 expression, and comparatively, that of some markers of neuronal differentiation previously used in a wide range of vertebrates to study organization of the CNS during development.

The thesis is structured in two parts: Section I (Chapters 1-4) concerns aspects related to the brain, and Section II (Chapters 5-10) concerns aspects related to retina.

In Section I, **Chapter 1** deals with the identification of transverse (AP) and longitudinal (DV) domains, by means of systematic analysis of the distribution of Pax6 protein and mRNA in the brain of developing and postembryonic sharks. **Chapter 2** contains a detailed description of Pax6 expression in the olfactory system. **Chapter 3** provides more accurate information about brain regionalization in sharks, by comparing Pax6 expression with that of several molecular markers of neuronal differentiation, such as glutamic acid decarboxylase

(GAD), calretinin (CR) and tyrosine hydroxylase (TH) by means of double and triple immunofluorescence techniques. **Chapter 4** includes an extensive immunohistochemical study of the proliferation, differentiation and migration patterns in the cerebellum by immunohistochemistry against proliferating cell nuclear antigen (PCNA), reelin (RELN), gamma-aminobutyric acid (GABA)/GAD, CR and TH.

The following chapters (Section II) include an extensive study of the patterns of cell proliferation, differentiation and migration in the shark retina, involving analysis of the pattern of Pax6 (**Chapter 5**), and its relation to the proliferation pattern (**Chapter 6**), and spatiotemporal distribution of differentiation markers such as GABA/GAD (**Chapter 7**), CR (**Chapter 8**), TH and serotonin (5-HT) (**Chapter 9**) and opsins (**Chapter 10**). The putative role of Pax6 in each of these morphogenetic processes in the retina is also analysed by *in situ* hybridization as well as by double and triple immunolabelling.

REFERENCES

Alunni A, Blin M, Deschet K, Bourrat F, Vernier P, Rétaux S (2004). Cloning and developmental expression patterns of Dlx2, Lhx7 and Lhx9 in the medaka fish (*Oryzias latipes*). Mech Dev, 121: 977-983.

Bachy I, Vernier P, Rétaux S (2001). The LIM-homeodomain gene family in the developing Xenopus brain: conservation and divergences with the mouse related to the evolution of the forebrain. J Neurosci, 21: 7620-7629.

Bae YK, Kani S, Shimizu T, Tanabe K, Nojima H, Kimura Y, Higashijima S, Hibi M (2009). Anatomy of zebrafish cerebellum and screen for mutations affecting its development. Dev Biol, 330: 406-426.

Bell E, Ensini M, Giuliano M, Lumsden A (2001). Dynamic domains of gene expression in the early avian forebrain. Dev Biol, 236: 76-88.

Brox A, Puelles L, Ferreiro B, Medina L (2003). Expression of genes GAD67 and Distal-less-4 in the forebrain of *Xenopus laevis* confirms a common pattern in tetrapods. J Comp Neurol, 461: 370-393.

Brox A, Puelles L, Ferreiro B, Medina L (2004). Expression of the genes Emx1, Tbr1 and Eomes (Tbr2) in the telencephalon of Xenopus laevis confirms the existence of a ventral pallial division in all tetrapods. J Comp Neurol, 474: 562-577.

Candal E, Anadón R, Bourrat F, Rodríguez-Moldes I (2005). Cell proliferation in the developing and adult hindbrain and midbrain of trout and medaka (teleosts): A segmental approach. Dev Brain Res, 160: 157-175.

Easter SS, Malicki JJ (2002). The zebrafish eye: developmental and genetic analysis. Results Probl Cell Differ, 40: 346-370.

Hauptmann G, Gerster T (2000). Regulatory gene expression patterns reveal transverse and longitudinal subdivisions of the embryonic zebrafish forebrain. Mech Dev, 91: 105–118.

Hauptmann G, Söll I, Gerster T (2002). The early embryonic zebrafish forebrain is subdivided into molecularly distinct transverse and longitudinal domains. Brain Res Bull, 57:371-375.

Hu M, Easter SS (1999). Retinal neurogenesis: the formation of the initial central patch of postmitotic cells. Dev Biol, 207: 309-321.

Ishizawa Y, Yasuda T, KAge T, Takashima S, Yoshimoto M, Yamamoto N, Maruyama K, Takeda H, Ito H (2008). Early development of the cerebellum in teleosts fishes: a study based on gene expression patterns and histology in the medaka embryo. Zoolog Sci, 25: 407-418.

Kage T, Takeda H, Yasuda T, Maruyama K, Yamamoto N, Yoshimoto M, Araki K, Inohaya K, Okamoto H, Yasumasu S, Watanabe K, Ito H, Ishikawa Y (2004). Morphogenesis and regionalization of the medaka embryonic brain. J Comp Neurol. 476: 219-239

Larsen CW, Zelster LM, Lumsden A (2001). Boundary formation and compartition in the avian diencephalon. J Neurosci, 21: 4699–4711.

Li Z, Hu M, Ochocinska MJ, Joseph NM, Easter SS (2001). Modulation of cell proliferation in the embryonic retina of zebrafish (*Danio rerio*). Dev Dyn, 219: 391-401.

Macdonald R, Barth KA, Xu Q, HolderN, Mikkola I, Wilson SW (1995). Midline signalling is required for Pax gene regulation and patterning of the eyes. Development, 121: 3267-3278.

Marcus RC, Delaney CL, Easter SS (1999). Neurogenesis in the visual system of embryonic and adult zebrafish (*Danio rerio*). Off. Vis Neurosci, 16: 417:424.

Medina L, Brox A, Legaz I, García-López M, Puelles L (2005). Expression patterns of developmental regulatory genes show comparable divisions in the telencephalon of Xenopus and mouse: insights into the evolution of the forebrain. Brain Res Bull, 66: 297-302.

Pouwels E (1978). On the development of the cerebellum of the trout, *Salmo gairdneri*. I. Patterns of cell migration. Anat Embryol, 152: 291-308.

Puelles L, Rubenstein JLR (1993). Expression patterns of homeobox and other putative regulatory genes in the embryonic mouse forebrain suggest a neuromeric organization. TINS, 16: 472–479.

Puelles L, Rubenstein JLR (2003). Forebrain gene expression domains and the evolving prosomeric model. TINS, 26: 469-476.

Puelles L, Kuwana E, Puelles E, Bulfone A, Shimamura K, Keleher J, Smiga S, Rubenstein JLR (2000). Pallial and subpallial derivatives in the embryonic chick and mouse telencephalon, traced by the expression of the genes Dlx-2, Emx-1, Nkx-2.1, Pax-6, and Tbr-1. J Comp Neurol, 424: 409-438.

Raymond PA, Barthel LK, Bernardos RL, Perkowski JJ (2006). Molecular characaterization of retinal stem cells and their niches in adult zebrafish. BMC Dev Biol, 6: 36-53.

Wehman AM; Staub W, Meyers JR, Raymond PA, Bzier H (2005). Genetic dissection of the zebrafish retinal stem-cell compartment. Dev Biol, 281: 53-65.

Wullimann MF, Knipp S (2000). Proliferation pattern changes in the zebrafish brain from embryonic through early postembryonic stages. Anat Embryol, 202: 385-400.

Wullimann MF, Rink E (2001). Detailed immunohistology of Pax6 protein and tyrosine hydroxylase in the early zebrafish brain suggests role of Pax6 gene in development of dopaminergic diencephalic neurons. Dev Brain Res, 131:173-191.

Zupanc GKH (2006). Neurogenesis and neuronal regeneration in the adult fish brain. J Comp Physiol A, 192:649–670.

CHAPTER 1.

PAX6 EXPRESSION IN THE DEVELOPING AND MATURE BRAIN OF SHARKS

INTRODUCTION

In the last 20 years, developmental biologists have mainly focused their studies on the early embryonic stages that distinguish fecundation from organogenesis. The most important result of such studies has been the characterization of a number of genes that regulate development and that act together to establish the general body plan. **Early brain regionalization** occurs during these stages, with the establishment of broad subdivisions. Later, most of these genetic markers are involved in the control of **late brain morphogenesis**, a complex process that determines the number of cells in each organ by controlling the proliferation of progenitor cells, their differentiation and their positioning in the mature brain.

Many years before studies of gene expression were feasible, morphological studies identified the main brain regions as early transverse vesicles in the neural tube, which were considered as the manifestation of the brain regionalization process that leads to neural tube partitioning and brain complexity. In addition to the transverse anteroposterior (AP) segments, a dorsoventral (DV) structural pattern composed of four longitudinal zones (roof, alar, basal and floor plates) can be observed in the brain.

Three different criteria have been used to identify the early brain boundaries: morphological, cellular sorting, and molecular criteria. The morphological criterion is founded on the idea that two adjacent neural areas that show differential growth reveal segregated morphogenetic properties and therefore may differ. Their boundary is the interface between the areas, usually marked by an external constriction and an internal ridge (Puelles et al., 1987; Larsen et al., 2001). However, these subdivisions are transient, and their status may change during development from explicit to covert (and vice-versa), and thus require experimental demonstration at given stages. Moreover, bulging varies across species and therefore is not strictly required for definition of neural segments (Puelles and Rubenstein, 1993, 2003). The cellular sorting criterion is based on the idea that cells of different proliferative units are segregated during early development (Trujillo et al., 2005). This is the result of differential proliferative rates, as well as various secondarily acquired properties of the neuroepithelial cells at the boundaries, i.e., once specified they show clonal restriction, gap-junctional isolation, differential expression of cell adhesion and matrix molecules (Puelles and Rubenstein, 1993, 2003), disruption of interkinetic cellular migration, increase in

extracellular space, and definition of a precocious marginal zone (Guthrie et al., 1991; Larsen et al., 2001). Later, these cytological features may be reinforced by growth of axons and radial glial differentiation (Neyt et al., 1997; Yoshida et al., 2000). Specification of these regions occurs prior to the cellular migration process and may explain migration of specific cellular phenotypes to relatively distant regions. The idea of clonal restriction was elegantly demonstrated by clonal labelling of rhombomeres in the developing chick embryos (Fraser et al., 1990), although not all boundaries in the diencephalon display this characteristic (Larsen et al., 2001). The molecular criterion is typically supported by the gene expression pattern. Identification of genes with distinct temporal and spatial gradients in the developing brain shows that there are intrinsic mechanisms controlling early brain regionalization, and that the pattern of gene expression is functionally relevant (Kudo et al., 2007). Many studies show that boundaries of gene expression patches not only coincide with those of brain subdivisions, but are often causally related. Moreover, differential molecular specification along the AP and DV axes is evolutionarily conserved (Pasini and Wilkinson, 2002), and thus allows earlier and more fundamental delimitation of brain segments than purely morphological methods.

Pax6 in early brain patterning and morphogenesis

The transcription factor Pax6 is one of the most widely studied developmental molecules in the nervous system, as it is a highly conserved transcription factor that is crucial for the development of brain, retina (see Chapter 5) and non-neural tissues such as the nasal organs (see Chapter 2), pituitary gland (Bentley et al., 1999; Kioussi et al., 1999), pancreas (Sander et al., 1997) and enteroendocrine cells (Schonhoff et al., 2004).

The Pax6 expression pattern has been widely analysed in the developing central nervous system (CNS) of many vertebrates, including mammals (human: Gérard et al., 1995; mouse: Walther and Gruss, 1991; Stoykova and Gruss, 1994; Puelles et al., 2000; rat: Matsuo et al., 1993; Kawano et al., 1999), birds (Kawakami et al., 1997; Bell et al., 2001), reptiles (Pritz and Ruan, 2009), amphibians (Bachy et al., 2002; Moreno et al., 2008), teleosts (medaka: Kage et al., 2004; zebrafish: Hauptmann and Gerster, 2000; Wullimann and Rink, 2001), cyclostomes (Murakami et al., 2001; Derobert et al., 2002; Osorio et al., 2005), elasmobranchs (Derobert et al., 2002). Interestingly, comparison between vertebrate groups has revealed a highly conserved pattern of expression in the embryonic brain, despite the marked differences in adult brain morphologies across vertebrate species (Wullimann and Mueller, 2004).

In addition, several studies have focussed on the role of Pax6 in brain regionalization and morphogenesis, including in the spinal cord and hindbrain, midbrain and forebrain, where it has been shown to be involved in the patterning of neuromeres, proliferation, neuronal differentiation, cell/neuronal migration and axon growth (Osumi et al., 1997; Ericson et al., 1997; Takahashi and Osumi, 2002; Bel-Vialar et al., 2007; Matsunaga et al., 2000; Manuel and Price, 2005 and references therein).

The first evidence of the role of Pax6 in brain regionalization emerged from the study of Pax6 null mutants. Among the different Pax6 mutations reported in mammals, loss-of-function Small eye (*Sey*) mutations include different and independent alterations in the Pax6 gene/locus, all of which result in premature stop codons giving rise to truncated non-functional Pax6 proteins and, ultimately, to similar phenotypes (Hill et al., 1991; Matsuo et al., 1993; Fujiwara et al., 1994; Grindley et al., 1995, 1997). Interestingly, heterozygotes showed similar brain phenotypes to their wildtype littermates, with minor brain alterations reported in mouse (Schmahl et al., 1993) and human (Sisodiya et al., 2001), and eye abnormalities such as microphthalmia (i.e., reduction in the eye size) reported in mice (Hill et al., 1991; Grindley et al., 1995) or aniridia disorders in human (reviewed by Prosser and van Heyningen, 1998). In contrast, homozygotes display important abnormalities in the brain (see below), lack eyes and nose, and die shortly after birth (Hill et al., 1991; Schmahl et al., 1993; Grindley et al., 1995, 1997; Warren and Price, 1997 Mastick et al., 1997; Stoykova et al., 1996, 2000) which had precluded analysis of Pax6 roles in late brain development. Several different alterations have been described in the homozygous *Sey* brain: the posterior commissure fails to develop properly, and there is rostral expansion of mesencephalic markers and loss of expression of pretectal markers (Grindley et al., 1997; Warren and Price, 1997; Mastick et al., 1997); the *zona limitans intrathalamica* appears wider than normal, and expresses prethalamic markers (Warren and Price, 1997); the *eminentia thalami* grows laterally instead of rostroventrally giving rise to an enlarged third ventricle (Stoykova et al., 1996); the dorsal telencephalon (pallium) appears ventralised, since it expresses Gsh2 (a transcription factor normally expressed in the subpallium), whereas the lateral ganglionic eminence (LGE, the dorsalmost portion of the subpallium) fails to differentiate, shows expression of more ventral markers (Stoykova et al., 2000; Toresson et al., 2000, Yun et al., 2001) and moreover later in development, shows defects in cerebral cortex lamination (Stoykova et al., 1996; 2000), and a reduction in rostrolateral and expansion of caudomedial areas, have been reported (Manuel

and Price, 2005, and references therein). Despite these alterations, several authors have considered that regionalization in *Sey* mutants roughly resembles that of wild types, as diencephalic prosomeres (pretectum, thalamus and prethalamus) were recognized, and expression of regulatory genes along the antero-posterior axis appeared to be relatively normal (Stoykova et al., 1996; Grindley et al., 1997; Warren and Price, 1997; Pratt et al., 2000).

On the other hand, besides loss-of-function studies classically performed with Pax6 null mutants, gain-of-function analysis has been performed by electroporation in chick embryos, and evidence has been found that this transcription factor participates in the establishment of the midbrain-forebrain boundary (Matsunaga et al., 2000). The development of new experimental approaches such as chimeras comprising both wildtype and mutant Pax6 cells (Talamillo et al., 2003; Quinn et al., 2007), transgenic mice (Scheld et al., 1993; Manuel et al., 2007) and conditional gene targeting, also known as conditional knockout (Piñon et al., 2008; Tuoc et al., 2009; Carney et al., 2009) has enabled further investigation of the roles of Pax6 in brain development within a normal context, and also examination of the roles of Pax6 in late brain development, previously precluded by the perinatal lethality of Pax6 null mutants.

Concurrent with its role in early brain patterning, Pax6 is essential for the production of new neurons from neural stem/progenitor cells (for a review, see Osumi et al., 2008), participating in regulating proliferation, specification and differentiation. Several studies have shown that levels of Pax6 are crucial for regulation of proliferation, as overexpression of this transcription factor produces underproliferation, whereas the lack of Pax6 induces overproliferation (Götz et al., 1998; Warren et al., 1999; Estivill-Torrus et al., 2002; Heins et al., 2002 Haubst et al., 2004; Manuel et al., 2007). Pax6 is not only crucial for maintaining neural stem/progenitor cells, and interestingly, can also promote neuronal differentiation and is involved in specification of neuronal subtypes in different CNS regions, including the spinal cord and hindbrain (Osumi et al., 1997; Takahashi and Osumi, 2002; Bel-Vialar et al., 2007) or the telencephalon, in which Pax6 participates in the specification of dorsal telencephalic progenitors (Kroll and O'Leary, 2005).

Pax6 is a binary player in embryonic neurogenesis, promoting cell division and cell differentiation in a highly context-dependent and complex manner in terms of different protein expression levels, different isoforms, different co-partners, different direct target

genes, and different indirect downstream effectors (Osumi et al., 2008; Sansom et al., 2009).

Additionally, Pax6 is thought to be involved in axon growth/pathfinding, as several studies have revealed similar defects in the trajectories of different forebrain tracts, such as the tract of the post-optic commissure in Pax6 mutants (for a review, see Simpson and Price, 2002; Nural and Mastick, 2004; Manuel and Price, 2005). Similarly, analysis of *Sey* mutants have found evidence of Pax6 involvement in neuronal migration (Talamillo et al., 2003 and references therein; Fink et al., 2006 and references therein).

A role for Pax6 in regulating apoptosis has been suggested on the basis of evidence from diverse studies in different tissues, including the central nervous system: in early embryos of *Xenopus*, Pax6 cell expression overlaps with apoptotic cells, at the neural fold stage (Hensey and Gaultier, 1998); the failure in nasal placode development in *Sey/Sey* mice has been attributed to abnormal apoptosis (Fukuda et al., 2000), and recently Berger et al. (2007), reported a possible role for Pax6 in regulating progenitor apoptosis in mammalian corticogenesis.

Pax6 is also expressed in the adult central nervous system (Stoykova and Gruss, 1994; Kawano et al., 1999; Yamasaki et al., 2001; Hack et al., 2005; Kohwi et al., 2005; Maekawa et al., 2005; Nacher et al., 2005), and several studies have dealt with the role of this developmental regulatory gene in adulthood, indicating a role for Pax6 in postnatal neurogenesis (Nacher et al., 2005; Maekawa et al., 2005; Osumi et al., 2008 and references therein) and in gliogenesis in mammals (Sakurai and Osumi, 2008), whereas the role of Pax6 in mature neurons (Kawano et al., 1999; Hack et al., 2005; Kohwi et al., 2005; Nacher et al., 2005) and astrocytes (Sakurai and Osumi, 2008) remains unclear.

Therefore, it appears that Pax6 is relevant in all cellular events: proliferation, differentiation, migration and even in apoptosis, which work together in the morphogenetic processes that construct the nervous system.

Although Pax6 expression has been reported in bony fishes such as the zebrafish (Wullimann and Rink, 2001) and the medaka (Kage et al., 2004), as well as in cyclostomes/agnathan fish (lamprey: Murakami et al, 2001; Derobert et al., 2002; Osorio et al., 2005), studies of Pax6 expression in cartilaginous fish are scarce. Despite the key

phylogenetic position of the latter group as regards gaining insight into evolution of the vertebrate brain, only Derobert et al. (2002) have described the expression pattern of Pax6 mRNA in *S. canicula* embryos from mid-gastrulation to embryonic stage 22.

In order to gain insight into the ancestral gnathostome pattern of Pax6 expression in the CNS and its potential involvement in brain regionalization and morphogenesis, we analysed the distribution of Pax6 protein and mRNA in the brain and rostral spinal cord of developing and postembryonic specimens of two species of sharks. For comparative purposes, we also studied the distribution of the signalling molecule sonic hedgehog (Shh) in some regions of the embryonic CNS.

In this work we provide a detailed description of the spatiotemporal dynamics/distribution of Pax6-expressing cells in the CNS of sharks comparable to that available for the mouse (Walther and Gruss 1991; Stoykova and Gruss, 1994) and zebrafish (Wullimann and Rink, 2001).

MATERIAL AND METHODS

Experimental animals

Embryos and juvenile specimens of *Scyliorhinus canicula* and the *Haploblepharus fuscus* were kindly provided by the Aquário Vasco da Gama and the Oceanário in Lisbon (Portugal), and by the Finisterrae Aquarium in A Coruña (Spain). Embryos of *S. canicula* were also acquired from the Station Biologique de Roscoff (France). Specimens were transported in tanks to the laboratory. Adult specimens were kindly provided by the Aquarium Finisterrae (A Coruña). Juveniles and adults were immediately sacrificed, while eggs from different broods were raised in tanks of fresh sea water under standard conditions of temperature (16-18°C) and 12:12 hours day/night cycle.

Staging of embryos

The embryonic stages of *S. canicula* were identified by external features according to Ballard et al. (1993), and similar features were considered in staging the *H. fuscus* embryos (See Table 1). The following embryonic stages were analysed: stage 22 (5 *S. canicula* –*S.c.* embryos), stage 23 (4 *S.c.* and 1), stage 24 (4 *S.c.* and 2 *H.f.* embryos), stage 25 (3 *S.c.* and 2

H. fuscus –*H.f.* embryos), stage 26 (3 *S.c.* and 1 *H.f.* embryos), stage 27 (3 *S.c.* embryos), stage 28 (3 *S.c.* and 2 *H.f.* embryos), stage 29 (4 *S.c.* and 3 *H.f.* embryos), stage 30 (2 *S.c.* and 3 *H.f.* embryos), stage 31 (7 *S.c.* and 7 *H.f.* embryos), stage 32 (6 *S.c.* and 6 *H.f.* embryos and stages 33-34 (prehatching; 3 *S.c.* and 8 *H.f.* embryos). Moreover, 5 juveniles (3 *S. c.* and 2 *H. f.*, total length from 10 to 14 cm) and 1 adult *S. canicula* (about 50 cm total length) were also analised.

Tissue preparation

Adequate measures were taken to minimize pain or discomfort to the animals. All procedures conformed to the guidelines established by the Spanish Royal Decree 223/1998 for animal experimentation and were approved by the ethics committee of the University of Santiago de Compostela. Embryos were anaesthetized with 0.05% tricaine methane sulphonate (MS-222; Sigma, St. Louis, MO) in seawater and separated from the yolk before fixation in 4% paraformaldehyde (4% PFA) in elasmobranch phosphate buffer (EPB: 0.1 M phosphate buffer (PB) containing 670 mM urea, pH 7.4) for 48-72 h depending on the stage. Alternatively, the embryos were fixed in Clark's solution (75% ethanol, 25% acetic acid) for 12-36 h depending on the stage of specimens. Prehatching, juvenile and adult specimens were deeply anaesthetized with MS-222, then perfused intracardially with elasmobranch Ringer's solution (1.7% NaCl, 0.024% KCl, 0.031% $CaCl_2$, 0.044% $MgCl_2$, 0.113% Na_2SO_4, 0.049% $NaCO_3H$, and 2.7% urea), followed by either 4% PFA or Clark's solution. Specimens fixed in Clark's solution were dehydrated and embedded in paraffin. Parallel series of sections (10-12 µm thick) were cut in sagittal, horizontal or transverse planes on a rotary microtome, and mounted on Superfrost Plus (Menzel-Glasser1) slides. Specimens fixed in 4% PFA were rinsed in PBS, cryoprotected with 30% sucrose in PB, embedded in OTC compound (Tissue Tek, Torrance, CA), and frozen with liquid nitrogen-cooled isopentane. Parallel series of sections (14–18 µm thick) were cut in sagittal or transverse planes on a cryostat, and mounted on Superfrost Plus (Menzel-Glasser1) slides. Alternatively, specimens for *in situ* hybridisation were rinsed in PBS-DEPC (PBS: 0.015M $Na_2HPO_412H_2O$; 0.13M NaCl; 0.014M KH_2PO4; 0.02M KCl; 0.1% Diethyl pyrocarbonate, Sigma), dehydrated with a series of methanol in PBS-DEPC and stored in 100% methanol at -20°C.

Pax6 and Shh immunohistochemistry

For heat induced epitope retrieval, sections were pre-treated with 0.01M citrate buffer pH 6.0 for 30 min at 95°C, and allowed to cool for at least 20-30 min at room temperature (RT). Sections were rinsed twice in 0.05 M Tris-buffered saline pH 7.4 (TBS) for 5 min each and residual avidin/biotin activity was removed by incubation with the avidin/biotin blocking kit (Vector, Burlingame, CA). Sections were then incubated either with a rabbit anti-Pax6 polyclonal antiserum (Covance, Emeryville, CA; diluted 1:400; or Chemicon, now Millipore, MO; diluted 1:400) or with a rabbit anti-Shh polyclonal antiserum (Santa Cruz Biotechnology Inc, CA; diluted 1:300) as primary antibodies, overnight at RT. Sections were then rinsed in TBS (two 10-min rinses) and treated with 10% H_2O_2 in phosphate buffered saline pH 7.4 (PBS) for 30 min at RT to block endogenous peroxidase activity. Sections were rinsed in TBS, incubated for 1 h at RT in biotinylated goat anti-rabbit IgG (Dako, Glostrup, Denmark; diluted 1:500), rinsed again in TBS (two 10-min rinses), and incubated in the preformed Avidin: Biotinylated enzyme Complex (ABC complex; Vector) for 30 min at RT. The immunoreaction was developed with 0.25 mg/ml diaminobenzidine (DAB) tetrahydrochloride (Sigma) in TBS pH 7.4 with 2.5 mg/ml nickel ammonium sulphate and 0.00075% H_2O_2 (blue precipitate), or with SIGMAFAST™ 3.3'-DAB tablets (brown precipitate) as indicated by the manufacturers. All dilutions were made with TBS containing 2% bovine serum albumin (BSA; Sigma), 15% normal goat serum (Dako) and 0.2% Triton X-100 (Sigma), and all incubations were carried out in a humid chamber. Finally, the sections were dehydrated, and coverslipped.

As negative controls, the primary, or secondary were omitted. No immunostaining was observed in these control sections. Moreover, to confirm the specificity of the Pax6 primary antibody, immunoreactivity was blocked by preadsorbing the primary antibody anti-Pax6 raised in rabbit (Covance, Emeryville, CA) with the antigenic peptide NB100-2913PEP (Novus Biologicals, Littleton, CO). The immunostaining was completely abolished in *S. canicula* sections treated with the primary antibodies at working dilution (5μg/mL), preadsorbed with the blocking peptide at a concentration of 10μg/mL at 4°C for 24 h.

The anti-Pax6 antibody from Covance was raised in rabbit against the peptide QVPGSEPDMSQYWPRLQ derived from the C-terminus of the mouse Pax6 protein, while the anti-Pax6 antibody from Chemicon (now Millipore) was raised against a synthetic peptide corresponding to the C-terminus of a human/mouse Pax6 protein. And the polyclonal anti-Shh

antibody (Santa Cruz Biotechnology Inc, CA) was raised in rabbit against the amino acids 41-200 of Shh human protein

Pax6 *in situ* hybridisation

A Pax6 cDNA fragment of 393 base pair (GenBank accession number: AF384972) previously isolated by Derobert et al. (2002) and kindly provided by Dr Mazan, was cloned into the pTZ19R plasmid. After linearization with EcoRI digestion, sense and antisense digoxygenin-UTP-labelled Pax6 RNA probes were synthesized directly by *in vitro* transcription, following standard procedures.

Whole-mount hybridisation was carried out as follows:

Embryos stored in 100% methanol at -20°C were rehydrated, permeabilised by proteinase K treatment (0.1mg/ml proteinase K, for 20-45 min depending on the embryonary stage), postfixed (4% PFA, 25% glutaraldehide 15-30 min depending on the embryonary stage), then rinsed in PBS-T DEPC (PBS DEPC with 1% tween-20), and incubated for 1h at 70° C in hybridisation mix: 50% de-ionized formamide, 1.3% SSC (Saline Sodium Citrate Buffer 20X: 3M NaCl, 0.3M Na-citrate, pH7), 5mM EDTA pH8, 0.2% Tween-20, 0.5% CHAPS (3-[(3-Cholamidopropyl)dimethylammonio]-1-propanesulphonate,Sigma) supplemented with 100µg/ml heparin and 50µg/ml tRNA, before adding the Sc*Pax6* probe that was incubated overnight at 70°C. The embryos were then rinsed in hybridisation mix at 70°C, treated with RNase A for 30min at 37°C, rinsed again in hybridisation mix at 55°C, rinsed in MABT (Maleic Acid Buffer: 0.1M maleic acid, 0.15M NaCl, 1% Tween-20):hybridisation mix (50:50) at 55°C, and finally in MABT at RT (three 10-min rinses). Then, embryos were incubated in blocking buffer (0.1M MABT, 20% decomplemented sheep serum, 2% blocking reagent for nucleic acid hybridisation and detection, Roche) for 3h at RT before addition of the alkaline phosphatase coupled anti-digoxygenin antibody (1:2000, Roche) overnight at 4°C. Finally, embryos were rinsed in MABT, and the reaction was developed in the presence of BM-Purple (Roche Applied Science, Mannheim, Germany), then embryos were rinsed in PBS, dehydrated through ethanol and butanol, embedded in paraffin and sectioned (10µm thick) on a rotary microtome. Sections were counterstained with nuclear fast red, dehydrated and coverslipped. Control sense probes did not lead to any detectable signal. The same probes has been previously used by

Derobert et al. (2002) to analyse Pax6 expression patterns in the developing brain (up to stage 22) of *S. canicula*.

Hybridisation on cryostat sections:

Cryostat sections were stored at -80°C and promptly processed as follows. After postfixation in PFA4%, sections were rinsed in PBS-T DEPC permeabilised with proteinase-K (5μg/ml proteinase-K, for 2 min), rinsed in PBS-T DEPC, post-fixed in PFA 4%, rinsed again in PBS-T DEPC, rinsed in NaCl 150mM, and incubated with hybridisation mix containing: 50% de-ionised formamide, 2xSSC (Saline Sodium Citrate Buffer 20X: 3M NaCl, 0,3M Na-citrate, pH 7), 5mM EDTA, 1% Denhardt's solution, 10% dextran sulphate, 10% CHAPS, 0,5mg/ml tRNA, 0,1mg/ml heparin for 1h at 65°C, before addition of the Pax6 sense or antisense probe. Hybridisation was carried out at 65°C. Posthybridisation washes were performed with SSC as follows: 1xSSC (10min), 1,5XSSC (10min) at 65°C; 2xSSC (two 20min-rinses) at 37°C. Sections were treated with RNase A (0.2μg/ml in 2xSSC, 30 minutes at 37°C), then rinsed in 2xSSC at RT (two 10min-rinses), in 0.2xSSC (two 20min-rinses) at 55°C, in MABT (three 10min-rinses) at RT, and then incubated 3h with blocking buffer at RT before addition of the alkaline phosphatase coupled anti-digoxygenin antibody (1:2000, Roche Applied Science) overnight at 4°C. After MABT rinses, colour reaction was performed in the presence of BM-Purple as described for whole-mounts (see above). Sections were then rinsed in PBS, postfixed with PFA 4%, and finally in H_2O, before being dehydrated and coverslipped. Control sense probes did not lead to any detectable signal.

Imaging

Photographs were taken with an Olympus DP71 colour digital camera, fitted to a Provis microscope (Olympus, Tokyo). Images acquired with the digital photo camera or with the confocal microscope were measured and optimized for brightness and contrast with Adobe Photoshop 7.0 (San Jose, CA), which was also used for plate photomontage and lettering.

RESULTS

General overview.

Pax6 expression during the early development *of S. canicula* (from mid-gastrulation to stage 22) has been investigated by Derobert et al. (2002) by *in situ* hybridisation (ISH) with a Pax6-specific probe for *S. canicula* (*ScPax6*). In this study, we performed ISH with the same *ScPax6* mRNA probe *S. canicula* between embryonic stage 22 and juveniles. We also applied immunohistochemistry (IHC) for Pax6 in embryos of *H. fuscus* and *S. canicula,* and obtained similar results in both species; in *S. canicula,* we obtained comparable results to those obtained by ISH. Thus, the ISH for the ScPax6 mRNA probe consistently validated the specificity of the antibodies we used. Although both techniques yielded identical results, IHC gave better cellular details, and enabled us to show the remarkably dynamic spatiotemporal distribution of Pax6 expressing cells (hereinafter, Pax6 cells) in the developing shark brain. The two polyclonal antibodies against Pax6 revealed a similar pattern of distribution of Pax6-immunoreactive cells, although the Chemicon (now Millipore) antibody labelled the blood vessel walls unspecifically.

Moreover, we have established a correspondence between the Table of normal developmental stages of *S. canicula*, according to Ballard et al. (1993), the embryo body size, and the three periods of brain development defined below. This was readily adapted to *H. fuscus*, as the first appearance of easily recognizable structures is the same in both species (see Table 1). Moreover, we have established a correspondence between the normal developmental stages of *S. canicula*, according to Ballard et al. (1993), their body size, and the three periods of brain development defined above (see Table 1). This was readily adapted to *H. fuscus*, as the first appearance of easily recognizable structures is the same in both species.

Although embryos of *H. fuscus* always had wider heads than those of *S. canicula*, there were no significant differences as regards the total body size of the embryos of each species. Indeed, although the relative timing of the formation of specific neural structures may vary greatly between species (at least in teleosts; Candal et al., 2005), no differences in the pattern of organogenesis of *S. canicula* and *H. fuscus* were observed throughout development. The only differences observed were in the degree of body pigmentation,

probably because of their different natural environments and distribution, i.e., *H. fuscus* (often found in superficial, rocky areas in the southeast Atlantic Ocean) is darker than *S. canicula* (found on sandy, coralline, algal, gravel or muddy bottoms at depths of a few meters in the northeast Atlantic Ocean).

According to Derobert et al. (2002), the earliest ScPax6 expression was detected at mid-gastrulation (stage 13 embryos) in the ectoderm layer at the anterior half of the head enlargement. From the end of neurulation (stage 17) to the stage 22 embryos, as well as in the broad anterior (forebrain) domain, *ScPax6* expression appeared in the posterior part of the head (hindbrain domain) and extended along the spinal cord (Derobert et al. 2002). In the present study we have observed that, from embryonic stage 22 onwards, Pax6 expression continued along the spinal cord and rhombencephalon to a far caudal isthmic level and the prosencephalon, but was absent from the mesencephalon and the presumptive metencephalon (Fig. 1). However, from stage 27, Pax6 cells were also observed in the basal mesencephalon and primordial cerebellum (Fig. 2). During most of the embryonic development, the overall distribution of Pax6 mRNA and protein was generally restricted to longitudinal and transverse domains (defined as areas where the majority of cells express Pax6), but from late embryos (stage 32), Pax6 cells mostly formed groups or clusters rather than domains (Fig. 2E). Outside the brain, Pax6 expression was observed in some brain-related structures such as the eye and optic stalk, the olfactory pit and olfactory epithelium, and Rathke's pouch and hypophysis (Figs. 1B,E-G, 2).

In cross sections, a dynamic spatiotemporal pattern of expression was observed in most Pax6 domains. The organization and location of Pax6 cells with respect to the ventricle was clearly related to the process of stratification of the neuroepithelial walls. The dynamic spatiotemporal distribution of Pax6 cells along the medio-lateral (ventricle-pial) axis may be clearly illustrated by the Pax6 expression in the prethalamus (ventral thalamus) domain throughout development (Fig. 3). During early developmental stages, when the neuroepithelial walls consists of a single layer of pseudostratified mitotically active cells, Pax6 cells were arranged radially occupying the entire extent of the ventricle-pial (Fig. 3A). Later, when the mantle zone formed lateral to the ventricular zone (VZ), most Pax6 cells appeared in the VZ but also in a subset of marginally located cells (arrows in Figs. 3B). Soon after, when an intermediate zone (IZ) was recognized between the VZ and the marginal zone (MZ), expression of Pax6 diminished in the VZ but was intense in some cells at the adjacent IZ and

in a lesser extent, externally closer to the pial surface, in the MZ (Figs. 3C-E). As development progressed, Pax6 expression in the VZ eventually disappeared, but did not disappear in the IZ and its derived subventricular and periventricular areas, where subsets of Pax6 cells remained visible even in postembryonic stages (Figs. 3F-H). These changes in the Pax6 expression during development, from ventricular to marginal cells, were first observed and were more evident at the basal boundaries of the Pax6 domains.

During development, the morphology of Pax6 cells, which can be inferred from the morphology of the immunolabelled nuclei, also differed depending on the position with respect to the ventricle: the ventricular and subventricularly located cells were fusiform and oriented radially with respect to the ventricle, while the externalmost cells were round, oval or piryform with the somata generally oriented tangentially (Fig. 3). As regards the spatiotemporal organization of Pax6 cells along the medio-lateral (ventricle-pial) axis, and also considering differences in cell shape, we have characterized three periods during the brain development of *S. canicula* and *H. fuscus* [1].

The **first period** comprised from stage 22 to stage 26 embryos and was characterized by the absence of layering in the walls of the developing brain, which consisted of a pseudostratified neuroepithelium that became progressively thicker during the period (Figs. 1;3A;4;5). Discrete Pax6 expression domains, each containing fusiform Pax6 nuclei that extended radially through the neuroepithelial walls, were observed at different levels along the antero-posterior axis. In these domains, Pax6 cells were loosely distributed and intermingled with some Pax6 negative cells. At the ventricular surface, Pax6 nuclei were more intensely immunostained and slightly more rounded in shape. Similarly, a few more intensely immunostained Pax6 nuclei were observed at the pial surface. This first period ends at stage 26, when some strongly expressing Pax6 cells, which became evident at late stage 25, were observed close to the pial surface in a barely visible mantle zone (arrow in Fig. 3A).

During the **second period** (from embryonic stages 27-31), the characteristic three-zone organization of the developing walls of the brain became progressively apparent (Figs. 2A-D;3B-E;6-15). Pax6 cells were observed at the same domains along the antero-posterior neuraxis as before, but as this second period proceeded, Pax6 cells were located at three

[1] Note that the three periods defined here during the development of the shark brain do not correspond to the periods that will be described for the retina (section II), as retina development takes place later on in embryonic development.

levels: in the VZ, in the IZ and in the MZ. In the VZ, round to elongate moderately immunostained Pax6 nuclei, similar to those described in the previous period, were observed. The morphology and organization of subventricular Pax6 cells resembled those located in the VZ but they were more intensely immunostained and located at different levels in the IZ. The scattered Pax6 cells observed in the MZ always showed intense immunostaining (Figs. 3B-E). The density of Pax6 cells and the intensity of Pax6 immunoreactivity decreased gradually in the VZ, meanwhile in the IZ and MZ both features increased throughout this second period. In contrast with the distribution of Pax6 cells observed along the mediolateral axis at the beginning of the period, at late stage 31 embryos there was a notable reduction in the density of Pax6 cells in the VZ and an increase in Pax6 cells in the IZ and MZ, which marked the end of this second period.

The **third period**, comprised from stage 32 embryos to hatching, was characterized by the marked reduction of Pax6 cells in the VZ and the well-defined groups or clusters of intensely stained Pax6 cells localised at different periventricular levels (Figs. 2E;3F-G;16-19). These clusters consisted of a discrete number of densely packed Pax6 cells, in contrast to the wider Pax6 domains observed earlier in development. Moreover, some Pax6 cells appeared to migrate away from the clusters extending into the outermost IZ or in the MZ. During this period, a few Pax6 cells were still observed at ventricular levels, especially in the telencephalic hemispheres. As the organization of Pax6 cell groups observed in postembryonic stages did not vary respect to these late embryos, we have considered the results in juveniles and adults within this period (Figs. 3H;17-19).

The distribution of Pax6 expressing cells along the anteroposterior and dorsoventral neural tube axes will be described in relation to these three periods.

First period: Pax6 cells in the neuroepithelial walls of the early regionalizing brain (Stages 22 to 26).

At these early embryonic stages, the brain walls were thin and enclosed a wide ventricle. During this period, Pax6 cells were observed in the neuroepithelial walls of the developing rhombencephalon and prosencephalon, but not in the alar and basal plates of the mesencephalon, in the isthmus or in the alar plate of the rostral rhombencephalon (primordial cerebellum or metencephalon).

In the **spinal cord,** Pax6 cells formed a continuous longitudinal column along the laterodorsal and lateroventral ventricular walls where the Pax6 cells were radially oriented (Figs. 4A-D). No labelling was observed in the roof and floor plates at any developmental stage (Fig. 4D). The labelling of adjacent sections with an antibody against the protein sonic hedgehog (Shh), used as marker of the floor plate, revealed that the region of the basal plate just adjacent to the floor plate did not contain Pax6 cells (compare Figs. 4D and E). Marked differences in the intensity of Pax6 labelling were observed along the dorsoventral axis since the laterodorsal Pax6 cells were much less intensely stained than those at the lateroventral walls (Fig. 4D).

The Pax6 domain of the spinal cord was continuous with that of the **rhombencephalon**, which also formed an uninterrupted column that extended rostrally to caudal isthmic levels (Figs. 4A,M). As in the spinal cord, Pax6 cells bordered the rhombencephalic ventricular walls except at the floor plate and the adjacent basal plate region (Figs. 4F,G,I,K), as deduced from the comparison of parallel sections immunostained with the anti-Shh (Figs. 4H,J). In these rhombencephalic walls, the most intensely labelled Pax6 cells occupied the lateroventral region. This region may coincide, at least partly, with the basal plate extension. In contrast, the Pax6 labelling in cells of the laterodorsal walls was less intense. Whether this laterodorsal walls correspond to the extension of the alar plate could not be determined with the handed markers. However, the rostral dorsalmost rhombencephalic levels that correspond to the cerebellar primordium (metencephalon), did no contain Pax6 cells (asterisk in Figs. 4A-C,K,L). Interestingly, the rhombencephalic distribution of Pax6 cells appeared to match different transverse segments or rhombomeres (r), which were observed as dorsal protrusions or swellings separated by small grooves along the antero-posterior axis (Fig. 4A-C,L,M). At least six rhombomeres (r1-r6) can be distinguished from early embryos by the differential extension of Pax6 cells along the mediolateral axis in each rhombomere and at the level of the inter-rhombomeric boundaries (Figs. 4A,C).

No Pax6 expression was observed in the alar (optic tectum) or basal (tegmentum) plates of the **mesencephalon**. The sharp limit between the caudal extension of Pax6-positive cells of the prosencephalic alar plate and the Pax6-negative of the mesencephalic alar plate marks the diencephalic–mesencephalic boundary (arrowhead in Fig. 5A).

The early **prosencephalon** (primary prosencephalon) subdivides into the diencephalon (caudal prosencephalon) and the secondary prosencephalon. We have framed the relative location of prosencephalic Pax6 cells within the segmental paradigm proposed by Puelles and Rubenstein (2003). Accordingly, the diencephalon is subdivided into three prosomeres (p1-p3), which contain the pretectum (p1); the thalamus and epithalamus, which includes the pineal organ and habenula (dorsal thalamus, p2); and the prethalamus (ventral thalamus, p3); and the secondary prosencephalon comprises the hypothalamus, the preoptic area and the telencephalon. In the diencephalon, Pax6 expression domains mainly occupied the alar plate. Pax6 cells were thus abundant in the pretectum, in the epithalamus including the primordial pineal organ and habenula, and in the prethalamus (ventral thalamus) (Figs. 5A-D,F-M). In the pretectal domain, a high density of Pax6 cells was observed from early embryonic stages (Figs. 5A-D,F-K). Pretectal Pax6 cells were intensely stained and radially oriented in the neuroepithelial walls (Figs. 5B-D). Interestingly, a few intensely immunostained Pax6 cells were observed at the ventral border of the pretectal Pax6 domain (arrows in Figs. 5C-D,F-J). From stage 25, they formed a band of intensely labelled cells arranged longitudinally along the synencephalon (Figs. 5A,F-J). This strip of Pax6 cells was separated from the densely packed Pax6 cells of the main part of the pretectal domain by a band of cells that showed very weak labelling (arrowhead in Figs. 5C,D,F-J). Comparison of adjacent sections labelled with the anti-Shh in order to identify the synencephalic basal plate (Fig. 5E), revealed that the ventral strip of pretectal Pax6 cells just bordered the dorsal extension of the Shh domain (compare Figs. 5D and E), suggesting that they may be related to the alar-basal boundary. The pineal organ, which is detectable from stage 22 embryos as a dorsal evagination in the diencephalic alar plate, showed Pax6 cells from these early stages (see Derobert et al., 2002). Later, this Pax6 domain was continuous with that of the pretectum (Fig. 5A,B,F-H,J). At the end of this period, the alar plate walls, just lateral and caudal to the pineal emergence, thickened to form the habenular primordium, which contained abundant densely arranged Pax6 cells in the thick VZ (Figs. 5A,J). In the thalamus, Pax6 expression was very faint during this period, which contrasts with the intense Pax6 expression in cells of the pretectal (caudally) and prethalamic (rostrally) domains (Figs. 5A,F,G,J,K). In the prethalamus, as in the pretectum, the more ventromedially located Pax6 cell formed a longitudinal strip of loosely arranged and strongly labelled cells, which contrasted with the weak expression in a just dorsal thin band of cells that was adjacent to the core of Pax6 cells of the prethalamus (white arrows in Figs. 5K-M). The continuity between the pretectal and

prethalamus longitudinal stripes of intensely expressing Pax6 cells was blurred because the near absence of Pax6 at the thalamus (Figs. 5A,F,G,J,K). In contrast, the strip of Pax6 cells in the prethalamus extended rostralwards to postchiasmatic levels (Figs. 5A,F,G,K) and, from stage 25, continued in the dorsal and dorsolateral walls of the preoptic area, probably representing the primordial eminentia thalami (Figs. 5F,K). This Pax6 domain also continued with the Pax6 cells of the dorsal part of the optic stalks (Figs. 5N,O). During this period, no Pax6 cells were observed in the hypothalamus or in the floor of the preoptic recess (Figs. 5A,F,H,K,L,N). Faint to moderately immunostained Pax6 cells were observed throughout the dorsal telencephalon (pallium), distributed from the ventricle to the pial surface contrasting with the ventral telencephalon (subpallium), which was devoid of Pax6 cells (Figs. 5A-C,F,L,N,O). Interestingly, some intensely immunostained cells were observed in the walls of the olfactory pit and grouped in its neighbours (Fig. 5C). The development of this Pax6 population and its relation to the development of the olfactory system will be considered in Chapter 2.

Second period: Pax6 cells in the layering walls of the late regionalizing brain (Stages 27 to 31).

At embryonic stages 27-28, the thickness of the neural walls increased, especially at the diencephalic and mesencephalic vesicles (compare Fig. 1A and Figs. 2A-D). The main changes in the gross morphology of the brain with respect to the previous period were the development of the cerebellar plate in the rhombencephalon and the saccus infundibuli in the hypothalamus, and the rostralward growth of the telencephalic hemispheres. In addition, at stage 31 the olfactory bulbs evaginated laterally from the telencephalic walls.

At the beginning of this period, **spinal cord** and **rhombencephalic** Pax6 cells showed a columnar organization similar to that observed at earlier stages, but with lower density of Pax6 cells at the level of the inter-rhombomere boundaries (Figs. 6A-C). The cross-sections revealed that, as in previous stages, the highest Pax6 expression was in the lateroventral walls, which exhibited Pax6 cells not only in the VZ but also subventricularly in the IZ (arrows in Figs. 6D-N). In comparison, the intensity of Pax6 staining in the laterodorsal and dorsal walls was barely reduced and restricted to the VZ which exhibited a slightly dorso (low)-ventral (high) gradient (Figs. 6D-L). At the time that the thickness of the rhombencephalic

walls increased by the formation of notable IZ and MZ, the alar plate expanded dorsomedially and protruded to form the primordial rhombic lips in which Pax6 expression was very faint and only observed in the VZ (Figs. 6M,N). At rostralmost levels, the primordial rhombic lips reached the midline giving rise to a narrow cerebellar plate (alar plate of r1), which also showed faint Pax6 expression restricted to VZ cells (Fig. 6O).

As development proceeded, the density of Pax6 cells and the intensity of labelling in the rhombencephalic VZ decreased greatly (compare Figs. 6A-C and 7A-C), but some expression persisted in ventricular cells of the dorsal aspect of the basal plate, especially at caudal levels (arrowheads in Figs. 7D-L), and in the alar plate (rhombic lips and cerebellar plate, Figs 7E-N). In parallel, the density and intensity of labelling of Pax6 in the IZ increased, especially at some levels where groups or clusters of loosely arranged Pax6 cells were recognizable, mostly in close apposition to the remaining Pax6 VZ domains. In particular, three strands of Pax6 cells appeared to emerge from the Pax6 VZ domain located at the dorsal basal plate. One extended radially along the tegmentum lining, which roughly corresponds to the alar-basal boundary (red arrows in Figs. 7D-I). We considered this boundary as being related to a slight depression in the ventricular surface, probably corresponding to the sulcus of His, which is fairly discernible at this stage of development, especially in the caudal rhombencephalon. Another strand emerged ventralwards extending along the caudal tegmentum, from a level not covered by the cerebellar plate to the caudal extension of the rhombic lip (green arrows in Figs. 7F-I). The third strand emerged medially lying dorsolaterally to the medial longitudinal fascicle at the rostral tegmental levels that were covered by the cerebellar plate (yellow arrows in Figs. 7I-L).

Late in this period, the rhombic lips formed conspicuous protrusions (Figs. 7D-I) that contained a moderate to high density of intensely labelled Pax6 cells located far from the VZ. Most of the rhombic lip Pax6 cells were arranged in a string that extended through the lateral walls and also medially, along the ventral border of the rhombic lip (open arrows in Figs. 7F-H). At some extension, this string of Pax6 cells continued more ventrally, lining the marginal walls of the alar plate, which roughly corresponded to its ventral aspect (black arrows in Figs. 7G-L). This lateral string of Pax6 cells extended all along the rhombencephalic tegmentum, mostly restricted to the alar plate, but at caudal levels some of them also reached the margin of the basal plate (black arrow in Fig. 7D,E).

The density of Pax6 cells and the intensity of expression in the cerebellar plate increased greatly during development and in addition to abundant Pax6 cells in the VZ, some Pax6 cells extended laterally in the external part of the IZ (Figs. 7L-N). The cerebellar development throughout this second period involved significant changes since the cerebellar plate gave raise to a dome-shaped cerebellar body and transversally widened caudal auricular lobe primordia. Moreover, the segregation between paramedian granular and lateral regions became visible in the cerebellar body as did some cortical layering. Pax6 cells were distributed in a thick dorsomedial VZ, but also externally in the MZ at the cerebellar body primordium (Figs. 7M,N; see also Chapter 4).

No Pax6 cells were detected in the **mesencephalic** alar plate (optic tectum) during this period. However, from early stage 27, Pax6 expression was observed in the mesencephalic tegmentum where a bilateral string of intensely labelled cells extended progressively along the longitudinal axis (Figs. 8A-I), probably in relation to the alar basal boundary. The earliest Pax6 cells in this domain occupied a rostral position just caudal to the ventral Pax6 string of the pretectal domain (Fig. 8A) but, as development proceeded, Pax6 was also expressed in more and more caudal cells (Figs. 8B-C) until they extended all along the length of the mesencephalic tegmentum (Figs. 2C-D). The number of Pax6 cells in the longitudinal string increased during development and they displayed similar organization to those of the ventral strand of the pretectal Pax6 domain. These intensely labelled mesencephalic Pax6 cells were fusiform and radially oriented at the intermediate level (Figs. 8D-F). Sagittal and horizontal views revealed that these longitudinally arranged Pax6 cells formed bilateral strings that arched following the mesencephalic flexures (Figs 8C,G-I). At the end of this period, the number of these Pax6 cells increased considerably, especially at the caudal mesencephalic tegmentum (Figs. 2B).

In the **diencephalon** (caudal prosencephalon), the density of subventricular (IZ) Pax6 cells increased greatly with respect to the previous stages, especially in the pretectum, habenula and prethalamus (Figs. 8A-C;G-I,9-11). The posterior commissure did not contain any Pax6 positive cells, which contrasted with the dense Pax6 population that mostly occupied the adjacent pretectum (Fig. 9A). As previously observed, pretectal Pax6 cells were intensely labelled and formed a very dense and extensive population. At the beginning of this period, Pax6 cells were radially oriented in the neuroepithelial walls (Figs. 9B), but soon after intensely labelled Pax6 cells were also observed laterally at the IZ and to a lesser extent in

the MZ (Figs. 9C-K). Later in this period, the density of these Pax6 cells decreased, mainly in the VZ but also in the IZ (Figs. 9L-P). The sharp limit between the Pax6 negative mesencephalic alar plate (optic tectum) and the caudal extension of the pretectal domain marked the diencephalic-mesencephalic boundary (Figs. 9J,K). At rostral pretectal levels, just adjacent to the fasciculus retroflexus, the density of Pax6 cells was lower than in the rest of the domain (Fig. 9J, see also Fig. 1 in Chapter 3). The longitudinal band of Pax6 cells ventral to the pretectal Pax6 domain, already detected by stage 25, now became more conspicuous and continued caudally with the rostralmost portion of the Pax6 domain of the basal mesencephalon (Figs. 9A,J-M). At the beginning of this period, the habenula continued to be organized as small symmetric thickenings of the alar plate just at the level of the pineal stalk basis, with abundant and densely packed Pax6 cells in the thick VZ, which was continuous with that of the pretectal domain (Figs. 9A,B, 10A,B). The size of the habenula increased markedly throughout this period, and the growth was proportional in both habenula, thus maintaining the symmetry until the end of this developmental period. Habenular growth was especially intense at distal levels because of the notable increase in thickness of the IZ and MZ (Figs. 9L-P;10C-H). Two habenular regions were distinguished from stage 29 onwards: a lateral and a medial region. The lateral/distal part was formed by a thick IZ and MZ without Pax6 cells and a much reduced VZ where Pax6 cells formed a very thin layer as development proceeded (Figs. 10C-H). In contrast, in the medial/proximal part, there was a population of densely packed Pax6 cells located at the thick VZ while other Pax6 cells formed a loose group in the well developed IZ, just adjacent to the VZ (Figs. 10D-H). The distribution of Pax6 cells in the habenula was rather symmetrical, although slight asymmetry was noted from caudal to rostral regions (Figs. 10B,C). During this period, the pineal organ was a tubular structure that grew lying against the external part of the dorsal telencephalon (Figs. 10A,D,E). It contained intensely immunostained Pax6 cells all along its length, which were continuous with that of the habenula and pretectal domains (Figs. 10D,E,H). No Pax6 cells were observed in the thalamus (dorsal thalamus) which contrasted with the dense and extensive conspicuous Pax6 population of the prethalamus (ventral thalamus) (Figs. 11A-H,L-N). During the first part of this period, the organization of the Pax6 cells in the prethalamus domain resembled that of the pretectum, firstly with Pax6 cells massively occupying the VZ to later extend also in subventricular and periventricular regions. Variations in the Pax6 expression from ventricular to marginal cells were especially evident in the basal boundaries of the domain (Figs. 11C-G,M,N). During this period, Pax6 cells of the prethalamus extended rostrally into the

eminentia thalami and ventrocaudally into the posterior tubercle (Figs. 11E-P). Immunolabelling of adjacent sections labelled with anti-Shh (Fig. 11Q) enabled identification of the *zona limitants intrathalamica* (zli), which formed a wedge between the thalamus and prethalamus.

In the secondary prosencephalon, new Pax6 cell groups appeared during this period, in particular in the hypothalamus, subpallium and olfactory bulb, which only developed during the second part of the period. In the hypothalamus and from embryonic stage 29, a few Pax6 cells were observed bordering the dorsal marginal walls of the inferior hypothalamic lobes, probably in relation to the extension of Pax6 cells between the prethalamic domain and the posterior tubercle (Figs. 11H-J,P). No Pax6 expression was observed in the basal hypothalamus (Figs. 11A,D-K,O,P), which contrasted with the immunolabelling against Shh at the same level (Figs. 11Q). The epithelium of the Rathke's pouch showed abundant Pax6 cells, although its medial portion, which was apposed against the floor of the hypothalamus, was devoid of labelled cells (Figs. 2A-D;11G).

At the beginning of this period, the distribution of Pax6 cells in the telencephalon remained as before, with abundant cells in the neuroepithelial walls of the pallium but no cells in the subpallium. However, at stage 28, although the overall distribution of Pax6 cell at medial and lateralmost telencephalic levels (Figs. 12A,B) was fairly similar to previous stages, some intensely labelled Pax6 cells extended along the marginal walls of the ventralmost pallium to the MZ of the subpallium (Figs. 12C-J). The level where these marginal Pax6 cells appeared to arise roughly corresponded to the pallial-subpallial boundary (dotted lines in Figs. 12C-J;13A-E). During stage 31, the development of the telencephalon gave rise to a mature-like morphology, with thickened telencephalic walls and reduced ventricles, and the caudal and lateral expansion of the pallial walls was notable (Fig. 14).

In the *subpallium*, the marginal Pax6 cells first appeared at its dorsal aspect (red arrows in Figs. 12C,D) but the number of these increased with development, and extended ventromedially and rostrocaudally along the marginal zone (red arrows in Figs. 12E-J;13A-D;14). These cells were absent from the most medial walls of the caudal subpallium (Figs. 13E;14A-G), where Shh immunoreactivity was observed (Figs. 13F). However, at rostral subpallial levels, where Shh expression was absent, these marginal subpallial Pax6 cells reached the midline and even continued along the dorsomedial extension of the subpallial walls

that will form the septum, which could be recognized at the end of this period separating the primordial telencephalic hemispheres (Figs. 14H-L). Pax6 cells also occupied the subpallial IZ where two groups were recognized in late stages during this period. One group formed a conspicuous cluster just adjacent to the dense band of mediolaterally oriented Pax6 cells, which probably corresponded to the pallial-subpallial boundary (dotted circle in Figs. 14A-H). The other was located laterodorsally but its extension and limits were poorly defined and appeared to be continuous with the marginal Pax6 strings (red asterisk in Figs. 14C-I).

The *pallium* contained abundant intensely labelled Pax6 cells densely packed in the VZ, but this ventricular population became notably thinner as development progressed, and labelled cells also appeared subventricularly, first in the IZ and later also in the MZ (Figs. 12C-J). These changes were first seen in the ventral aspect of the pallium but progressed following a ventrodorsal and a rostrocaudal direction, probably in relation to the expansion of the pallial walls along these axes. At the ventral aspect of the pallium, Pax6 cells in the VZ were faintly immunostained, unlike those in the IZ and MZ (arrowheads in Figs. 12C,D,G,I,J). Interestingly, the Pax6 marginal cells at these ventral pallial levels were continuous with those of the marginal subpallial walls (Figs. 12D-J; 13C,D). During stage 31, the pallial walls contained abundant Pax6 cells in the VZ and also subventricularly and periventricularly. Later in this period, a high density of Pax6 cells was observed in the primordial periventricular pallial area and also in the dorsalmost MZ, probably representing the superficial pallial area (Figs. 14I-L).

The primordial *olfactory bulbs* were roughly recognized before stage 31 as a marked discontinuity in the Pax6 cell distribution in the lateral part of the telencephalic hemispheres (Figs. 15A-C). From stage 31, the olfactory bulbs became evident (Figs. 14B-F;15D-F) and contained scattered and faintly labelled Pax6 cells (Figs. 14B-F;15D-F) in contrast with the abundant and intensely labelled Pax6 cells observed just dorsal to the olfactory bulbs, where they appeared to correspond to the lateral/ventral pallial borders (Figs. 14C-F;15D-F). Laterally, Pax6 cells were observed in the dorsal VZ and IZ but there were almost no Pax6 cells in the ventral portion close to the olfactory mucose (Figs 14B-F). Abundant Pax6 cells were observed throughout the olfactory epithelium, which show the characteristic folding as a result of nasal organ development by embryonic stage 28 (Ballard et al. 1993). As before, some Pax6 cells were located between the nasal organs and the olfactory bulbs (see Chapter 2).

Third period: Pax6 cells in the regionalized-"mature-like" embryonic brain. Comparison with postembryonic stages.

Development of the cerebellum and cerebellar-like structures (lateral line area) together with the expansion of pallial walls that started during stage 31, culminated during stage 32. From here onwards, the brain grew proportionally leading to a considerable increase in size but not development of new brain structures. Accordingly, the basic morphology of the mature brain was established at the beginning of this developmental period (stage 32).

During this last period, the distribution of Pax6 cells was qualitatively similar to that described at stage 31. Main differences were noted in the reduction in the density of Pax6 as the brain size increased, and in the near absence of ventricular Pax6 cells. Moreover, two new Pax6 cell groups were observed in the isthmus region from the beginning of this period. All the Pax6 populations observed at stage 32 were recognized in prehatching embryos (stages 33 and 34) and in juveniles and adults. We therefore consider the Pax6 distribution at stage 32 as representative of the Pax6 cell organization in the "mature" brain.

In the **rostral spinal cord** (and in the caudalmost rhombencephalon), no Pax6 cells were observed at dorsal (alar) levels. At the basal level, persistent faint Pax6 labelling was notable in the VZ (arrowhead in Fig. 16A-D) and in the group of marginal Pax6 cells (Figs. 16A-D), probably in relation to the string of Pax6 cells observed at the margin of the basal plate at the end of the previous period (compare with Fig. 7D).

All the Pax6 cell groups identified in the **rhombencephalic tegmentum** at stage 31 were also recognised from stage 32, except those in the VZ. Two Pax6 cell groups were observed: the Pax6 cell group roughly coincident with the alar-basal boundary (red arrows in Figs. 16E-J), and the Pax6 cell group oriented ventralwards, which appeared to be associated with the trigeminal descendent root (green arrows in Figs. 16H-J). The marginal dorsal Pax6 cell group occupied the viscerosensorial lobe (open arrows in Figs. 16E-J) but rostrally it extended laterally into both the alar and dorsal part of the basal plates (black arrows in Figs. 16K,L) splitting into two different Pax6 groups located laterally and oriented dorsoventrally. The outermost cells appeared to be related to the nerve fibres belonging to the VII/VIII craneal nerves, meanwhile the inner groups of cells extended along the course of the fibres of the trigeminal descendent root (Figs. 16K-L). These lateral groups with dorsoventrally oriented Pax6 cells were coincident with the Pax6 cluster dorsolateral to the medial longitudinal

fascicle, which extended from a level rostral to the VII/VIII nerve entry to the cerebellar peduncle (yellow arrows in Figs. 16K-L). Interestingly, two new Pax6 cell groups appeared in the rostralmost rhombencephalic tegmentum/isthmus region. Rostral to the group associated with the medial longitudinal fascicle and caudally to the IV nerve exit there was a new group of Pax6 cells located ventrally, surrounding the caudal interpeduncular nuclei (large white arrow in Fig. 16M). Moreover, a conspicuous group of Pax6 cells extended mediolaterally in the dorsalmost basal plate/central grey (small white arrows in Figs. 16M,N). The rostralmost Pax6 cells in this new group were located caudally to a small constriction in the tegmentum possibly corresponding to the mes-rhombencephalic boundary. At its rostral end, some Pax6 cells emerged dorsally from this Pax6 cluster and were observed associated with the IV nerve fibres. Caudally this group was reduced to some laterally located Pax6 cells. The same Pax6 cell clusters were observed in juveniles and even in adults, although the density of Pax6 cells was decreased markedly along the rhombencephalic tegmentum (Fig.17).

During the beginning of this period (late embryonic stages), changes in the rhombencephalon were particularly notable because of the development of the cerebellum and cerebellar-like structures as the octavolateral area and the cerebellar crest (Figs. 16H-K). By stage 32, the layering of the cerebellar body became evident and the auricles showed notable development. In the cerebellar body, Pax6 cells were observed in the VZ in the paramedian granular eminence primordium, and some Pax6 cell extended laterally and were scarce at lateral cerebellar body levels (Figs. 16K,L,M; see also Chapter 4). The cerebellar auricles showed abundant Pax6 cells in the granular layer up to the octavolateral area (Figs. 16H-K). No Pax6 cells were detected in the molecular layer or in the cerebellar crest (Figs. 16H-K). Later, segregation of the granular layer in the paramedian granular eminences was even more evident and well developed granular eminences extended longitudinally protruding into the cerebellar body ventricle. Growth and maturation of the cerebellum continued at postembryonic stages. In **juveniles** and adults, Pax6 cells were observed in the granular layer in the paramedian granular eminences, as well as in the auricular lobe (Figs. 17A-D,G,H).

During this third period, there were no changes in the Pax6 expression pattern in the **mesencephalon**. The bilateral Pax6 domain that extended along the dorsal part of the mesencephalic tegmentum was observed in late embryos (stages 32-34), **juveniles** (Figs. 18A,D,F) and even in **adults** (not shown). This group was not continuous with the rostral rhombencephalic Pax6 population first observed in stage 32 (see above), which was also

located at the dorsalmost basal plate, and probably are related to the alar-basal boundary. A region free of Pax6 cells, which probably corresponds to the mes-rhombencephalic boundary, was recognized between both groups (Figs. 18A,B).

In the **diencephalon,** the pattern of Pax6 cells distribution observed at stage 32 resembled that previously described in stage 31 embryos (Figs. 18A-E) and remained basically similar in juveniles (Fig. 18F) and in even in adults (Figs. 18G-J), although the cell density of Pax6 populations decreased considerably from juveniles to adults. This pattern included the presence of Pax6 cells in the pretectum, pineal organ, prethalamus (and its continuity in the eminentia thalami) and posterior tubercle, and in a loose strip that extended from the mesencephalon to the prethalamus, probably following the alar-basal boundary (white arrows in Figs. 18A,F). Some minor differences from previous periods were observed in relation to the Pax6 expression in the subcommissural organ (Fig. 18E), which was especially intense in adults (Figs. 18G,H), and in the habenula, which showed Pax6 cells in the ventricular zone of late embryos and juveniles (Figs. 18A,E,F) but only dispersed cells in central habenular regions of adults (Fig. 18I,J). At the beginning of the third period, the habenula continued growing laterally and rostralwards, and morphological asymmetry became evident since the left habenula was slightly larger than the right habenula.

There were no significant changes in the Pax6 expression pattern in the **secondary prosencephalon** of stage 32 in relation to the previous stage, except for the presence of some Pax6 cells in the basal hypothalamus (Figs. 18A,B) and in the preoptic area (Fig. 18D). From stage 32 onwards, the pattern of distribution of Pax6 cells did not vary in the hypothalamus and preoptic area (compare Figs. 18A and F) but from juveniles to adults the density of Pax6 cells decreased considerably (Figs. 18G-J). In the telencephalic hemispheres of stage 32 embryos, Pax6 cells were abundant in the pallium and moderate moderately abundant in the subpallium. In the *subpallium*, the distribution of Pax6 in stage 32 matched that described in late stage 31 (compare Figs. 14H and 19A). In juveniles (Figs. 19C,D), besides in the septum and the dorsal aspect of the striatum, Pax6 cells were located in the superficial basal area and, especially, dorsolaterally to this area forming a conspicuous group that was probably related to the Pax6 population observed in embryos at the pallial-subpallial boundary. The density of Pax6 cells in the telencephalic hemispheres decreased considerably from juvenile to adult stages (Figs. 19E,F), but the distribution of these cells was comparable to that of stage 32. In the *pallium*, three different regions were well recognized from stage

32, the dorsal, medial and lateral pallium. The medial pallial walls developed considerably and grew towards the ventricle forming two bilateral protrusions (Fig. 19A). The lateral pallium could be distinguished as the pallial region just adjacent to the olfactory bulbs (from which they appeared to emerge (Figs. 19A,B). The pallial wall that extended between the medial and lateral pallium represented the dorsal part of the pallium or dorsal pallium. At stage 32, the density of Pax6 cells was moderate to high in the three pallial regions but the density was considerably lower in juveniles and especially in adults (Figs. 19C-F). At stage 32, the density of Pax6 cells in the olfactory bulb increased (Figs. 18A,B), and continued to increase as development proceeded. Eventually, abundant Pax6 cells occupied the granular layer in the well-developed olfactory bulbs of juveniles (Figs. 19C,D) and the density of Pax6 cells appears to be lower in the adult olfactory bulb (Figs. 19E,F).

DISCUSSION

Pax6 spatiotemporal pattern in sharks: comparison with vertebrates.

Study of slow developing fish species, such as those used in the present work, has made it possible to observe fine-scale variations in the pattern of Pax6 expression during development. Sequential analysis (present study) has revealed that in early embryonic stages, Pax6 expression was confined to the rhombencephalon (excluding the metencephalon) and the prosencephalon, but later in development, the expression extended to all brain vesicles. The spatial pattern of Pax6 expression in sharks includes Pax6 cell groups in the rhombencephalic and mesencephalic tegmenti, cerebellum, pretectum, prethalamus and telencephalon (including both pallium and subpallium) and matches that reported in zebrafish (Hauptmann and Gerster 2000; Wullimann and Rink, 2001), medaka (Kage et al., 2004), *Xenopus* (Bachy et al., 2002; Moreno et al., 2008), chick (Kawakami et al 1997; Puelles et al., 2000; Bell et al. 2001) and mouse (Walther and Gruss, 1991; Stoykova and Gruss, 1994; Schubert et al., 1995 ; Puelles et al., 2000), and thus probably represents the basic pattern in gnathostomes.

We also noted that the broad areas showing Pax6 expression (domains) in early stages of shark development resolved to well-defined clusters of Pax6-expressing cells in the late ("mature-like") embryonic brain and that expression was even maintained in the postnatal brain (juveniles and adults). This dynamic pattern of Pax6 expression throughout brain

development has been well characterized in mammals (Walther and Gruss, 1991; Stoykova and Gruss, 1994; Puelles et al., 2000), and to a lesser extent in zebrafish and *Xenopus*, although most data refer to the forebrain (Wullimann and Rink, 2001; Moreno et al., 2008). The restriction of the large Pax6 expressing domains in the developing brain has been related to the role of Pax6 in the specification of spatial domains in the embryonic brain (Puelles and Rubenstein 1993). In addition, as in other vertebrates (Stoykova and Gruss, 1994; Kawakami et al., 1997; Wullimann and Rink, 2001; Nacher et al., 2005), Pax6 expression was observed in subsets of cells in the mature brain of sharks, supporting a role for Pax6 in the differentiation and/or maintenance of restricted populations of brain cells (Stoykova and Gruss, 1994; Callaerts et al., 1997). According to Walther and Gruss (1991), certain cell populations retain or reinitiate Pax6 expression after they undergo the final round of mitosis. In fact, Pax6 expression has been reported in mature neurons and astrocytes in the mammalian hippocampus (Nacher et al., 2005), in other telencephalic regions such as the olfactory bulb and septum, in certain diencephalic regions where Pax6 is involved in differentiation of the catecholaminergic neurons, and in some brainstem nuclei (Stoykova and Gruss, 1994; Vitalis et al., 2000). Although Pax6 appears to be involved in the maintenance of neuronal populations, its function remains unresolved.

Detailed comparison of sharks (present results), teleosts (Wullimann and Rink, 2001; Kage et al., 2004) and mouse (Walther and Gruss, 1991; Stoykova and Gruss, 1994) has yielded striking similarities, which provide support for homologies, and also minor differences. Of note we highlight:

- As observed in mouse and zebrafish, the rhombencephalic Pax6 domains in sharks appear to correspond to precerebellar nuclei.
- The diencephalic Pax6 domains observed in sharks are very similar to those described in other gnathostomes, allowing identification of prosencephalic segments (see Chapter 3).
- The Pax6 cells that extend from the shark prethalamic domain towards the posterior tubercle and inferior hypothalamic walls resemble those described in zebrafish but differ from the equivalent areas in mammals, in which no Pax6 cells have been observed.

- Pax6 cells observed in the shark pallium resemble those described in the developing telencephalon of mouse (Stoykova and Gruss, 1994; Götz et al., 1998; Englund et al., 2005) and teleosts (Wullimann and Rink, 2001; Kage et al., 2004).
- The progressive increase in Pax6 cells in the subpallium observed in the shark developing telencephalon also resembles that found in teleosts (Wullimann and Rink, 2001) and mouse embryos (Stoykova and Gruss, 1994; Puelles et al., 2000).

In summary, spatiotemporal patterns of Pax6 expression in sharks are strikingly similar to those described in other gnathostomes. Studies in lampreys (Murakami et al., 2001) revealed that the agnathan prosencephalon shows a rather similar pattern to that observed in gnathostomes, thus supporting the notion that the main Pax6 expressing prosencephalic domains appeared early in evolution of the vertebrate brain. In contrast, the spatiotemporal pattern of Pax6 expression in the agnathan mid and hindbrain, characterized by the delay in the rhombomere 4 and the absence of Pax6 cells in metencephalon and mesencephalon is different from that observed in gnathostomes, suggesting that it is less conserved among vertebrates.

Timing of the spatiotemporal pattern of Pax6 expression in the shark brain: a suitable tool for comparing the absolute chronology of development among vertebrates.

Taking into account the spatiotemporal organization of Pax6 cells along the ventricle-pial axis in *S. canicula* and *H. fuscus*, we have distinguished three periods in the brain development related to the histogenetic changes that the walls of the neural tube undergo during development (see Table 1). The *first* period is characterized by the location of abundant radially oriented Pax6 cells in the thin neuroepithelial neural walls of the prosencephalon and mielencephalon, while during the *second* period, stratification of the neural walls takes place, eventually establishing the characteristic three-layered pattern (ventricular, intermediate and marginal zone) of the neural walls; the Pax6 cells progressively occupy different layers, from ventricle to pia/marginal. During the *third* period, the cell populations mature, finally forming specific and definitive brain nuclei, some of which contain clusters of Pax6

We have made an attempt to establish a correspondence between these three developmental periods defined in the sharks and the timing of development of mouse, chick and zebrafish embryos (see Table 2). We have therefore taken into account the degree of

differentiation of the brain walls, as shown in different atlases of development and other publications (mouse: Kaufmann 1992; Schambra et al., 1992; chick: Bellairs and Osmond, 1998; zebrafish: Kimmel et al., 1995), and the patterns of Pax6 expression described in the developing brains (chick: Schubert and Lumsden, 2005; Ferrán et al., 2007; mouse: Walther and Gruss, 1991; Mastick et al., 1997; Smith-Fernandez et al., 1998; Kimura et al. 2005; zebrafish: Macdonald et al., 1994; Hauptmann and Gerster, 2000; Wullimann and Rink, 2001).

We have considered as landmark events:

- The formation of the three primary brain vesicles, which we have considered here as the beginning of an extended first period (characterized by the neuroepithelial organization of the brain walls, and defined from stage 22 to 26 according to our results). This event occurs at stage 17 in *S. canicula* (Ballard et al., 1993), at 33 hours *in ovo* in chick (end of stage HH9) (Hamburger and Hamilton, 1951; Bellairs and Osmond, 1998), at E8.5-9 (i.e., embryonic day, or days post conception, dpc) in mouse (Kaufmann, 1992) and at 16hpf (i.e., hours post-fertilization) in zebrafish (Kimmel et al., 1995).
- The onset of Pax6 expression in the mesencephalic tegmentum, which marks the beginning of the second period. This occurs at stage 26 in sharks (present results), at stage HH19 (i.e., 70 hours *in ovo*) in chick (Schubert and Lumsden, 2005) and at E10.5 in mouse (Mastick et al., 1997). In zebrafish, the onset of midbrain Pax6 expression may not be well established because of the rapid development of this species, and appears to occur at some time after 24hpf (Wullimann and Rink, 2001), corresponding to the first part of the second period.
- The emergence and growth of the limb buds in tetrapods (HH17 in chick, E9.5 in mouse) and of the fin rudiments in sharks (stage 24), which take place during the last part of the first developmental period, as in zebrafish (24hpf).

The proposed equivalences are supported by the following evidences:

- The pattern of Pax6 expression reported in the telencephalon and diencephalon of mouse embryos at E11.5-12.5 (Smith-Fernandez et al., 1998; Kimura et al., 2005) matches what we have observed in sharks at stages 28-29 (first half of the second period). Moreover, the pattern of Pax6 expression that we observed in the caudal

diencephalon of sharks at stages 25-26 (end of the first period) and stage 28 (second period) roughly resembles that of chick at stages HH17-18 and HH24-25, respectively (Ferrán et al., 2007).

- As we observed in sharks and also observed in mouse, Pax6 expression decreases in the VZ during the second period (from E11.5 according to Walther and Gruss, 1991), and at E15.5 (third period), most Pax6 expression occurs in postmitotic cells (not ventricular cells).

- Studies comparing gene expression patterns in chick and mouse embryos reported a correspondence between stages E10.5 of mouse and HH17 of chick (Nicotra et al., 2004) and between E13 of mouse and HH23/24 of chick (Puelles et al., 2000). We propose that these stages correspond, respectively, to the last part of the first period and to the first half of the second period. Because of the rapid development, it is difficult to find correspondence between the developmental stages of zebrafish and those of other model vertebrates. Despite this, Mueller et al. (2006) have proposed the existence of a "phylotypic stage" of brain development in vertebrates on the basis of correspondence of GABA cell patterns between postembryonic zebrafish stages at 2-3 days post-fertilization (according to our proposal, in the third period) and mouse embryos at stages E12.5-13.5 (in the second period). Comparison with the GABA cell patterns observed during the development of *S. canicula* (Carrera, 2008; Carrera et al., 2006; 2008), reveal that this phylotypic stage in sharks may correspond to the stage 28 (second period).

- Taking into account the high degree of conservation in early axons growth among vertebrates, development of the early tracts may also be considered as a type of landmark. In fact, the medial longitudinal fascicle (considered as the first longitudinal tract to appear in the developing brain) and the tract of the postoptic commisure follow similar pathways in mouse, chick and fish (Wilson et al., 1990; Ross et al., 1992; Easter et al., 1993; Mastick and Easter, 1996; Mastick et al 1997; Barreiro-Iglesias et al., 2008). These early tracts develop at HH14-HH17 in chick (Chédotal et al., 1995; Schubert and Lumsden, 2005), at E9.5-E10 in mouse (Easter et al., 1993, Mastick et al., 1997) and at 18-20hpf in zebrafish (Ross et al. 1992), which we propose as corresponding to the first period. In elasmobranchs, development of these early tracts also takes place during the first period as can be assumed from the study of

Kuratani and Horigome (2000) in a shark species (*Scyliorhinus torazame*). These authors reported that the medial longitudinal fascicle and the tract of the posterior commissure are first recognized in *S. torazame* embryos of 9.5 and 20 mm, respectively, which according to Ballard et al. (1993), may correspond to stages 22-23 and 24-25 of *S. canicula*. Moreover, it has been observed that in this species it has been observed that the GABAergic axons of the medial longitudinal fascicle can be discerned at stage 22, while those of the posterior commissure tract can be followed from stage 24 (Carrera et al., 2006; Carrera, 2008), thus showing that the establishment of the early tract scaffold takes place during the first period in this species.

Taking into account the embryonic lifespan in the different vertebrates (in *S. canicula*, around 175 days after laying, in contrast to 21 days for the chick, 19-21 days post conception for the mouse embryo, and 72 hours post-fertilization in zebrafish), we show that the first and second periods represent 8-15%, and 20-35% of the total, respectively in the three gnathostome groups, while the third period represents from 27.5-35% in mouse and zebrafish and from 56-65% in sharks and chick, suggesting differences in the rate of growth.

The correspondence (see Table 2) in the timing of vertebrate development according to the Pax6 expression and differentiation of the brain walls, requires further investigation, but constitutes a tentative approach to relating vertebrate embryonic development and gene expression patterns.

Pax6 roles in the developing brain

Since Pax6 expression in the developing CNS displays specific spatiotemporal patterns, Pax6 is thought to act upstream of gene networks involved in diverse functions such as brain patterning, neuronal migration and neural circuit formation (Osumi, 2001; Simpson and Price, 2002; Manuel and Price, 2005; Osumi et al, 2008). Multiple functions have been suggested for Pax6 on the basis of different molecular aspects, such as the existence of several isoforms of Pax6 that yield differences in expression levels, interactions between Pax6 and other transcription factors, and the downstream Pax6 targets (Osumi et al., 2008). For instance, the most common of the protein isoforms produced by the *Pax6* gene, i.e., Pax6 and Pax6 (5a), are generated by alternate splicing of exon5a. It has been suggested that these Pax6

isoforms may have different functions as the insertion of a 14 amino acid segment into the paired domain of the protein isoform Pax6(5a) appears to affect its DNA-binding and transactivation properties (reviewed by Simpson and Price, 2002; Osumi et al., 2008).

Study of mutant mice and rats has also provided some insight into the roles of Pax6 in development also comes from the study of mutant mice and rat. There are several mutant alleles of Pax6, the best studied of which are the Pax6Sey and Pax6Sey-Neu alleles, which have similar phenotypes and harbour mutations encoding premature stop codons that result in a truncated Pax6 protein. Homozygous mutants (*Sey/Sey*) lack eyes and nasal structures, present severe abnormalities in the brain and die at birth (Hogan et al., 1986; Hill et al., 1991; Matsuo et al., 1993; Fujiwara et al., 1994; Grindley et al., 1995, 1997; Stoykova et al., 1996; Osumi et al., 1997, 2008). Heterozygous Pax6 mutants display abnormalities in the eye, and although no apparent differences in gross brain anatomy are observed in comparison to wild-type littermates during embryonic and neonatal stages, some alterations have also been described (Hill et al., 1991; Matsuo et al., 1993; Stoykova et al., 1996; Osumi et al., 1997).

Studies on the spatiotemporal pattern of Pax6 expression in different vertebrate species have also shed some light on the role(s) of Pax6 in CNS morphogenesis. The results of some of such studies have led to the suggestion that Pax6 has a regulatory role in the development of the CNS and the eye (Walter and Gruss, 1991), in particular in controlling early and late brain regionalization (Derobert et al., 2002; Moreno et al., 2008), also that it is involved in the inhibition of subpallial cell migration into the pallium by the Pax6 migrating stream (Chapouton et al., 1999), and also participates in the development of some forebrain dopaminergic cells (Wullimann and Rink, 2001; Mastick and Andrews, 2001). The present results concerning the spatiotemporal distribution of Pax6 in sharks may indicate that besides playing a role in brain regionalization, Pax6 may act in regulating proliferation and neurogenesis. Moreover, the spatiotemporal distribution of Pax6 along the mediolateral axis is compatible with a role in axon guidance related to migratory streams; the colocalisation in some cells with TH and GAD at late embryonic stages and in juveniles (data not shown) suggests a role in neuronal differentiation/maturation. These roles are discussed in further detail below.

Pax6 in cell proliferation and neurogenesis

Several lines of evidence have led to the suggestion of a role for Pax6 in regulating proliferation. Pax6 expression has been observed early in development, in the neuroepithelial walls of the neural tube (Stoykova and Gruss, 1994), which consist of highly proliferating cells. The developing diencephalon of *Sey* mutant mice shows alterations in proliferation, although its regionalization roughly resembles that described in wild-type mice (Warren and Price, 1997). Similarly, in the developing mammalian cortex, altered levels of Pax6 affect proliferation but not regionalization (Manuel et al., 2007; Arai et al., 2005). Several loss and gain of function studies revealed that the lack of Pax6 results in overproliferation, meanwhile overexpression reduces proliferation in the developing cerebral cortex (Götz et al., 1998; Estivill-Torrus et al., 2002; Heins et al., 2002; Arai et al., 2005), retina (Duparc et al. 2007) and spinal cord (Bel-Vialar et al., 2007). In parallel, the production of neurons in the developing telencephalon is reduced in the absence of Pax6 (Warren et al., 1999; Fukuda et al., 2000; Estivill-Torrus et al., 2002), but overexpression of Pax6 in cultured cells derived from the developing cerebral cortex induces an increase in the number of neurons (Heins et al, 2002; Götz et al., 1998). Interestingly, loss of Pax6 function leads to precocious neuronal differentiation in the developing cerebral cortex (Caric et al., 1997; Quinn et al., 2007), spinal cord (Bel-Vialar et al., 2007), and retina (Philips et al., 2005). Recently, Quinn et al. (2007) showed that in the early developing cortex, Pax6 arrests precocious differentiation and thus prevents depletion of the progenitor pool by regulating the balance between proliferation and exit from the cell cycle. In accordance, Bel-Vialar et al. (2007) suggested that the level of Pax6 protein may be crucial for cell cycle exit and neuronal commitment, since in the developing spinal cord of chick and mouse the increase of the Pax6 level *directs* neuronal precursors to exit the cell cycle by way of Ngn2 activation (Scardigli et al., 2003). Bel-Vialar et al. (2007) also proposed a model in which the level of Pax6 would firstly control when a given progenitor will leave the cell cycle, and secondly when a selected precursor will differentiate. Similarly, Sansom et al., (2009) reported that Pax6 may regulate, in a dose-dependent manner, genes that promote self-renewal, intermediate progenitor genesis and neurogenesis and thus control the balance/*bias* between self-renewal and differentiation in neural stem cells.

The present results also indicate a role for Pax6 in regulating proliferation as the distribution of neuroepithelial Pax6 cells along the ventricle-pial axis in the shark brain during

the first (stages 22 to 26) and second (stages 27 to 31) developmental periods resembles that described in previous developmental studies involving BrdU-based experiments in mouse (Götz et al., 1998; Mastick and Andrews, 2001; Englund et al, 2005). Firstly, the intense round Pax6 nuclei observed close to the ventricular surface in sharks may correspond to mitotic cells, as several studies reported colocalisation of Pax6 and BrdU (Götz et al 1998; Mastick and Andrews, 2001), and also of Pax6 and phospho-histone-H3 (PH3), a marker for cells in the M phase of the cell cycle, which has been reported in the developing cerebral cortex VZ in the mouse (Englund et al., 2005). Secondly, the faint Pax6 cells in the VZ and IZ of the shark developing brain may correspond to neuroepithelial cells in the S-phase of the cell cycle, in accordance with the observations made by Englund et al. (2005), who reported colocalisation of BrdU and Pax6 in cells at the subventricular zone in the developing cortex of E14.5 mice. Although we did not inject the shark embryos with BrdU, double immunolabelling with PCNA (data not shown) revealed colocalisation of PCNA and PAX6, and the double immunolabelled cells located at the VZ displayed faint immunoreactivity to both markers (see also Chapter 6).

On the other hand, the intense Pax6 cells observed in the MZ of shark at the second developmental period roughly resemble early postmitotic/differentiating Pax6 neurons, as pointed out by Mastick and Andrews (2001). These authors reported Pax6 intensely labelled Pax6 cells in the incipient mantle layer in the developing mouse diencephalon at E10.5, when the first neurons differentiate, and identified them as early neurons on the basis of immunolabelling with neuronal specific markers such as βtubulin (TujI). They also observed faint Pax6-immunoreactive neuroepithelial cells in the ventricular zone, some of which were also labelled with TujI, indicating that some early Pax6 postmitotic neurons are intermingled with proliferating Pax6 cells (identified by BrdU immunolabelling) in the neuroepithelium. Moreover, as mentioned above, in sharks, faintly immunostained double-labelled Pax6/PCNA cells at the ventricular zone may be interpreted as early postmitotic neurons, as Pax6 expression is downregulated when differentiation begins (Englund et al., 2005; Bel-Vialar et al. 2007), in accordance with the fact that PCNA levels in cells leaving the cell cycle decrease only by about 30% within 24 h (Bravo and Macdonald-Bravo, 1987). Taking this into account, it is possible that some of the Pax6 cells in the shark VZ were early postmitotic cells, however further investigation is required to gain some insight into shark proliferation and neurogenesis.

In addition, Pax6 has been related to adult neurogenesis since low levels of expression were reported in the subgranular zone of the *dentate girus* in the hippocampus (Nacher et al. 2005; von Bohlen und Halbach, 2007) and in the subventricular zone of the lateral telencephalic ventricle (Hack et al., 2005; Kohwi et al., 2005), which are known to be neurogenic areas in the adult mammalian brain. Although several studies have dealt with neurogenesis and neuronal regeneration in the adult teleost fish brain (Zupanc, 2006), studies in elasmobranch fish are scarce. Only recently, Margotta (2007) reported the distribution of PCNA in the adult brain of an elasmobranch species, the electric ray *Torpedo marmorata*. Although we have shown colocalisation of PCNA and Pax6 in the granular eminences of the juvenile cerebellum of *S. canicula*, (see Chapter 4), our results on adult shark Pax6 expression are far from exhaustive, and further investigation is required to determine whether or not Pax6 is involved in neurogenesis in the adult elasmobranch fish brain.

Pax6 and the dorsoventral patterning of the brainstem

A revision of the classical concept that divides the hindbrain into alar sensory and basal motor longitudinal zones (based on morphological features, such as ventricular constrictions) considers that the longitudinal zones observed in the neural tube are specified by gradients of signalling molecules, which in turn control expression of the transcription factors responsible for neural patterning (for a review see Jessell and Sanes, 2000; Puelles et al., 2008). It has been proposed that in the hindbrain, the patterns of expression of Pax6, Pax7, Otp, Nkx2.2, cadherin-7 and cadherin-6B and Shh define molecular domains along the dorsoventral axis (for a review, see Ju et al., 2004). Pax6, like other transcription factors involved in regionalization of the developing CNS, may interpret gradients of morphogens and translate this information into dorsoventral patterning (Goulding et al., 1993; Ericson et al., 1997; Ju et al., 2004). In particular, Pax6 appears to play a role in the dorsoventral patterning of the hindbrain and spinal cord by regulating the specification of certain subtypes of ventral neurons (Osumi et al., 1997; Briscoe and Ericson, 1999; Briscoe et al., 2000; Takahashi and Osumi, 2002). This role appears to be mediated by Shh, as the graded signal of Shh that emerges from the floor plate represses Pax6 expression (Ericson et al., 1997). The present results provide anatomical evidence for a similar role for Pax6 in sharks. Firstly, the early expression of Pax6 in the shark hindbrain and spinal cord, with labelled cells at the VZ of the basal plate, except a small area abutting the floor plate, matches that

observed in amniotes (Takahashi and Osumi, 2002; Ju et al., 2004). In addition, there is a Pax6 negative area in the ventral basal plate of shark embryos abutting the floor plate, which is clearly identified in sharks by the Shh immunolabelling. In amniotes, this Pax6/Shh interface of the ventral basal plate corresponds to the Nkx2.2 positive domain that contains the progenitors that give rise to V3 interneurons in the spinal cord and visceral motor neurons in the anterior cervical spinal cord and hindbrain (Briscoe et al., 1999). The present findings suggest that the characteristics of the Pax6 expression through the early development of the hindbrain and spinal cord already present in cartilaginous fish are well conserved among vertebrates.

The revised vision of the classic longitudinal divisions of the CNS also proposes that the location of the alar and basal boundary is determined by the balance between gradients of morphogens and that this boundary does not necessarily coincide with the sulcus of His (Ju et al., 2004). The pattern of Pax6 expression during early development of the hindbrain in sharks is not compatible with a role in the patterning of the alar-basal boundary, since Pax6 cells extend throughout the alar plate and almost all of the basal plate. In contrast, the expression of another member of the Pax gene family, the Pax7 gene, whose ventral limit roughly coincides with the alar-basal boundary, has been directly related to specification of this limit (Ju et al., 2004). Unfortunately, we could not test whether the same occurs in sharks, as we did not obtain positive results with anti-Pax7 antibodies. However, later on in development (from the second developmental period), a relation between Pax6 and the alar-basal boundary can be inferred from the distribution of Pax6 cells in the hindbrain, in which we observed a longitudinal strip of Pax6 cells that extend mediolaterally along what roughly coincides with the alar-basal boundary. Similarly, from the second developmental period, the midbrain of the sharks contains longitudinal strips of Pax6 cells at the dorsalmost aspect of the basal plate, at the border between the tectum (alar plate) and tegmentum (basal plate), that appeared to be related to the alar-basal boundary. These Pax6 cells may correspond to the longitudinal strip of Pax6 cells described in the ventral midbrain of mouse and chick embryos, just dorsal to the oculomotor nucleus (Stoykova and Gruss, 1994; Schubert et al., 1995; Schubert and Lumsden, 2005; Ahsan et al., 2007), which has been related to the fate specification of neurons forming the early axon scaffold, such as those of the nucleus of the medial longitudinal fascicle (Schubert and Lumsden, 2005). This mesencephalic group is rostrally continuous with similar strips of Pax6 located just ventral to the pretectal

expression domain (p1). Likewise in the hindbrain, the comparison of Pax6 and Shh expressions in the caudal prosomere (p1) provides anatomical evidence to suggest a role for Pax6 in the dorsoventral regionalization of the synencephalon. Similar observations have been made in zebrafish in which it has been noted that the trajectory of the alar/basal boundary in the fore- and midbrain is outlined by the dorsal limits of Shh expression and the ventral borders of the pax- 6.1 domains (Hauptmann and Gester, 2000). On the other hand, as the ventral part of the pretectal Pax6 domain is closely associated with the boundaries of the first prosencephalic longitudinal tract (the tract of the postoptic commissure, tpoc) a role in axon guidance has been suggested for these ventral pretectal Pax6 cells (Mastick et al., 1997, see below).

Pax6 and neural migration

In addition to their role in patterning and cell-type specification, Pax6 have also been related to cell migration, in particular involving the precursors of cerebellar granule cells and precerebellar nuclei (Engelkamp et al., 1999; Yamasaki et al., 2001; Fink et al., 2006) and cortical neurons (Schmahl et al., 1993; Caric et al., 1997; Talamillo et al., 2003). In the present study, we show anatomical evidence of the existence of migrating Pax6 cells in the hindbrain as well as in the telencephalon (see later) of sharks.

In mouse, Pax6 is strongly expressed in the rhombic lips and in subsets of rhombic lip-derived cells (Engelkamp et al., 1999; Fink et al., 2006). These observations came from the sequential analysis of the Pax6 expression pattern in the normal and mutant mice at different gestational stages (Engelkamp et al., 1999; Fink et al., 2006). Two routes of migration have been described (Engelkamp et al., 1999): from the upper (rostral) rhombic lip, Pax6 cells migrate dorsally to cover the cerebellar primordium and give rise to the granule cells; and from the lower (caudal) rhombic lip Pax6 cells migrate ventrally along two migration streams, the anterior and posterior, to give rise to the different precerebellar nuclei. Although at present, functional studies with Pax6 in sharks are far from possible, the spatiotemporal analysis of Pax6 expression in the hindbrain has revealed that similar routes of migrating Pax6 exist in sharks. Pax6 cells observed in the early rhombic lips and in the granular layer of the developing and mature cerebellum of the sharks studied may form part of the dorsal/rostral migrating route followed by precursors of the cerebellar granule cells. On the

other hand, Pax6 cells observed more caudally migrating away from the alar plate (caudal rhombic lips) may give rise to precerebellar nuclei, as observed in the mouse (Engelkamp et al., 1999; Fink et al., 2006). The three strands of Pax6 cells that appear to emerge from the dorsal basal plate VZ: one radially oriented, another located ventralwards along the caudal tegmentum, and a third one located medially and associated with the medial longitudinal fascicle, may later give rise to reticular nuclei, as in the mouse (Stoykova and Gruss, 1994). This possibility is supported by the fact that later in development (third period), some streams of Pax6 cells are still observed in the rhombencephalic tegmentum, together with clusters of Pax6 cells that may correspond to reticular or precerebellar nuclei, such as the inferior olive. Walther and Gruss (1991) reported Pax6 expression in the mouse inferior olive, although no defects were observed in this precerebellar nucleus of Pax6 mutants in contrast to the alterations found in the migration of other precerebellar neurons (Engelkamp et al., 1999; Horie et al., 2003). It has also been suggested that in zebrafish, Pax6 may be related to the inferior olive nucleus (Wullimann and Rink, 2001). The present results in sharks also support this hypothesis.

The Pax6 cell groups that appear in the shark rostral hindbrain tegmentum (isthmic region) in the third period may therefore be related to rostral migrations of cells from the cerebellar external granular layer, which in turn derive from the rostral rhombic lips and strongly express Pax6, in parallel to the pattern described by Lin et al. (2001), who performed retroviral lineage and molecular marker analysis and reported migration of cells from the external granular layer into ventral regions of the rostral hindbrain tegmentum in the chick embryo, showing that some of them coexpressed Pax6 and markers of the locus coeruleus (such as the homeobox gene Phox2), and suggesting that this migration may also occur in other vertebrate species. Although in the present study we could not show clear evidence of the presence of Pax6 cell streams suggestive of cellular migration from the primordial external granular layer to ventral regions, this possibility should be investigated further to determine whether rostral rhombic lip/external granular layer Pax6-expressing derived cells migrate ventrally to give rise to rostral tegmental populations in the developing brain of the shark. It appears that the two shark Pax6 clusters described here may be related to the central grey and associated respectively with the interpeduncular nucleus, rather than with the locus coeruleus (Lin et al., 2001).

Pax6 and axon growth

It has been reported that early/initial tracts in fish and chick form along the borders of gene expression domains (Figdor and Stern, 1993; Macdonald et al., 1994; Chédotal et al., 1995). Macdonald et al. (1994) reported a correlation between the boundaries of expression domains of Pax6 and other genes and initial scaffold of tracts in zebrafish. These and other observations in amniotes have led some authors to propose that the borders of Pax6 domains may influence navigating axons differentially (Mastick and Easter, 1996; Mastick et al., 1997). Moreover, Pax6 is considered a general regulator of longitudinal tract formation in the forebrain, as interactions between the Pax6 gene and pioneer axons have been reported (Mastick et al., 1997; Nural and Mastick, 2004). However, it has been shown that in zebrafish only some pioneer axons course close to the Pax6 (and Shh) expression borders for a relative short portion of their pathway, meanwhile the later growing axons appeared to course closely apposed to the borders of some gene expression domains (Hjorth and Key, 2001).

Our observations in sharks are also compatible with a role for Pax6 in axon growth. In the early developing brain of the sharks studied, the borders of some Pax6 domains correspond to the trajectories of some longitudinal tracts such as the midbrain Pax6 cells, which, as suggested in amniotes (see above), may be related to the fate specification of neurons of the nucleus of the medial longitudinal fascicle (Schubert and Lumsden, 2005; Ahsan et al., 2007). Later on development, the cluster of Pax6 cells just dorsal to the medial longitudinal fascicle is also observed in the rhombencephalon. Taking into account that Pax6 expression in this brainstem longitudinal cluster remains after the formation of the medial longitudinal fascicle, roles for Pax6 other than regulation of longitudinal tract formation must be investigated.

Several studies have focused on the role of Pax6 in axon guidance in the forebrain longitudinal and transverse tracts, which show aberrant outgrowth or guidance defects in the absence of Pax6 (Mastick et al., 1997; Kawano et al., 1999; Pratt et al., 2000; Vitalis et al., 2000; Jones et al., 2002; Andrews and Mastick 2003). The alterations in thalamic/prethalamic territories found in the Pax6 homozygous mutants appear to be responsible for misguidance of longitudinal tracts (Pratt et al., 2000; Vitalis et al., 2000; Jones et al., 2002; Nural and Mastick 2004). Especially interesting are the alterations related to the posterior commissure tract, as in addition to a failure in development of this tract in Pax6 mutant mice, misspecification of the pretectum (p1) also occurs, causing a shift

to a mesencephalic identity. These observations suggest an important role for Pax6 in formation of the posterior commissure, but also in establishment of the forebrain-midbrain boundary (see also Chapter 3). Mastick et al., (1997) suggested that posterior commissure defects may be due to misspecification of the posterior commissure neurons, differentiation of which may be directly regulated by early Pax6 expression or indirectly by extrinsic signals from neighbouring Pax6 expressing cells. The present data suggest the participation of Pax6 in the formation of the posterior commissure in sharks, which can be followed from stage 24 (Carrera et al., 2006; Carrera, 2008), because the conspicuous Pax6 pretectal domain, observed from very early developmental stages, closely resembles that described in mouse (Mastick et al., 1997).

Regionalization of the shark telencephalon

There is much evidence indicating a role for Pax6 in regionalization of the vertebrate telencephalon, in particular dorsalizing the telencephalon. Firstly, Pax6 expression in the dorsal telencephalon (pallium) is observed from very early developmental stages (Walther and Gruss, 1991; Stoykova and Gruss, 1994; Stoykova et al., 1996, 2000). Secondly, Pax6 mutants show important alterations in telencephalic regionalization (Stoykova et al., 1996, 2000), including ectopic expression of genes normally expressed in the subpallium, which suggests that Pax6 represses expression of ventral regulatory genes (Toresson et al., 2000; Corbin et al. 2000). In fact, it has been proposed that some dorsoventral patterning mechanisms will be used at all axial levels of the CNS, so that the dorsoventral patterning of the telencephalon involves the same or very similar mechanisms to those described for the hindbrain and spinal cord (Stoykova et al., 2000; Yun et al., 2001). Thirdly, a conspicuous band of Pax6 cells has been observed along the pallial-subpallial boundary in different vertebrates (Stoykova et al., 2000; Puelles et al. 2000; Wullimann and Rink 2001; Bachy et al., 2002; Moreno et al., 2008). In fact, Pax6 has been used as a molecular marker to distinguish the telencephalic primordia flanking the pallial-subpallial boundary as it is strongly expressed in progenitors around this boundary (Yun et al., 2001; Stenman et al., 2003).

The present results in the shark brain also indicate a role for Pax6 in patterning the telencephalon, because: i) Pax6 is expressed in the dorsal telencephalon from early developmental stages (Derobert et al., 2002; present results); ii) expression of Pax6 differs

in the dorsal and ventral telencephalon, which allows identification of the limits and extension of pallial (dorsal) and subpallial (ventral) telencephalic subdivisions; and iii) the pallial-subpallial interface contains a band of mediolaterally oriented Pax6 cells that marks the putative pallial-subpallial boundary.

We also report the existence of scattered Pax6 cells that appear to emerge from the pallial-subpallial boundary towards subpallial regions from stage 28 onwards (close to the beginning of the second period). A stream of Pax6 cells emerging from the ventricular zone and coursing towards the marginal zone has been observed at the pallial-subpallial boundary of chick and mouse (Puelles et al., 2000). It has been considered that these migrating Pax6 cells are subpallial (Puelles et al., 2000) or that they represent a population of transitional cells between the pallial and subpallial compartments (Stenman et al., 2003). More recently, it has been shown that during mouse embryogenesis some cells of the lateral cortical stream, a population of cells migrating from the pallial-subpallial boundary (also called the corticostriatal border) to the basal telencephalon, express Pax6 (Carney et al., 2006, 2009). The present results in sharks also provide evidence to support the hypothesis of the pallial-subpallial boundary as the source of a migrating stream of Pax6 cells into the subpallium. This strongly suggests that ventrally migrating telencephalic cells may have appeared very early on in the vertebrate forebrain.

Interestingly, as the second developmental period in sharks proceeds, the putative pallial-subpallial boundary crosses two bilateral protrusions of the ventricular walls into the ventricle, which can be observed from stage 30. These prominences bear a striking resemblance to the mammalian lateral ganglionic eminences, and like these, may be the source of tangentially migrating GABAergic cells towards the pallium (Carrera et al., 2008) and that of migrating Pax6 cells towards the subpallium (present results).

In both shark species, several pallial subdivisions (dorsal, lateral and medial pallium) are well discerned from stage 32 onwards (third developmental period) and characteristically, all of them contain Pax6 cells at a rather homogeneous density, which precludes identification of their extension and the allocation of different pallial nuclei on the basis of Pax6 expression. Comparison with the expression pattern of other developmental genes and a detailed analysis of the Pax6 expression pattern are therefore necessary, but are outside the scope of this work.

The present results concerning the spatiotemporal dynamics of Pax6 expression in the shark telencephalon throughout the developmental periods considered in this study suggest remarkable conservation of the roles of Pax6 in telencephalic regionalization throughout vertebrate evolution.

REFERENCES

Ahsan M, Riley K, Schubert FR (2007). Molecular mechanisms in the formation of the medial longitudinal fascicle. J Anat, 211: 177–187.

Andrews GL, Mastick GS (2003). R-Cadherin Is a Pax6-Regulated, Growth-Promoting Cue for Pioneer Axons. J Neurosci, 23: 9873–9880.

Arai Y, Funatsu N, Numayama-Tsuruta K, Nomura T, Nakamura S, Osumi N (2005). Role of Fabp7, a Downstream Gene of Pax6, in the Maintenance of neuroepithelial cells during early embryonic development of the rat cortex. J Neuroscience, 25: 9752–9976.

Bachy I, Berthon J, Retaux S (2002). Defining pallial and subpallial divisions in the developing *Xenopus* forebrain. Mech Dev, 117: 163-172.

Ballard W, Mellinger J, Lechenault H (1993). A series of normal stages for development of *Scyliorhinus canicula*, the lesser spotted dogfish (*Chondrichthyes: Scyliorhinidae*). J Exp Zool, 267: 318–336.

Barreiro-Iglesias A, Villar-Cheda B, Abalo XM, Anadón R, Rodicio MC (2008). The early scaffold of axon tracts in the brain of a primitive vertebrate, the sea lamprey. Brain Res Bull, 75:42-52.

Bell E, Ensini M, Giuliano M, Lumsden A (2001). Dynamic domains of gene expression in the early avian forebrain. Dev Biol, 236: 76-88.

Bellairs R, Osmond M (1998). The atlas of chick development. London: Academic Press.

Bel-Vialar S, Medevielle F, Pituello F (2007). The on/off of Pax6 controls the tempo of neuronal differentiation in the developing spinal cord. Dev Biol, 305: 659-673.

Bentley CA, Zidehsarai MP, Grindley JC, Parlow AF, Barth-Hall S, Roberts VJ (1999). Pax6 is implicated in murine pituitary endocrine function. Endocrine, 10: 171-177.

Berger J, Berger S, Tuoc TC, D'Amelio M, Cecconi F, Gorski J, Jones KR, Gruss P, Stoykova A (2007). Conditional activation of Pax6 in the developing cortex of transgenic mice causes progenitor apoptosis. Development, 134: 1311-1322.

Bravo R, Macdonald-Bravo H (1987). Existence of two populations of cyclin/proliferating cell nuclear antigen during the cell cycle: association with DNA replication sites, J Cell Biol, 105:1549– 1554.

Briscoe J, Ericson J (1999). The specification of neuronal identity by graded sonic hedgehog signalling. Semin Cell Dev Biol, 10: 353-362.

Briscoe J, Sussel L, Serup P, Hartigan-O'Connor D, Jessell TM, Rubenstein JLR, Ericson J (1999). Homeobox gene Nkx2.2 and specification of neuronal identity by graded Sonic hedgehog signalling. Nature, 398: 622-627.

Briscoe J, Pierani A, Jessell TM, Ericson J (2000). A homeodomain protein code specifies progenitor cell identity and neuronal fate in the ventral neural tube. Cell, 101: 435–445.

Callaerts P, Halder G, Gehring WJ (1997). Pax6 in development and evolution. Annu Rev Neurosci, 20: 483–532

Candal E, Anadón R, Bourrat F, Rodríguez-Moldes I (2005). Cell proliferation in the developing and adult hindbrain and midbrain of trout and medaka (teleosts): A segmental approach. Dev Brain Res, 160: 157-175.

Caric D, Gooday D, Hill RE, McConnell SK, Price DJ (1997). Determination of the migratory capacity of embryonic cortical cells lacking the transcription factor Pax-6. Development, 124: 5087-5096.

Carney RSE, Alfonso TB, Cohen D, Dai H, Nery S, Stoica B, Slotkin J, Bregman BS, Fischell G, Corbin JG (2006). Cell migration along the Lateral Cortical Stream to the developing basal telencephalic limbic system. J Neurosci, 26: 11562-11574.

Carney RSE, Cocas LA, Hirata T, Mansfield K, Corbin JG (2009). Differential regulation of telencephalic pallial-subpallial boundary patterning by Pax6 and Gsh2. Cerebral Cortex, 19: 745-759.

Carrera I (2008). Desarrollo de los sistemas gabaérgico y aminérgicos en el sistema nervioso central de peces cartilaginosos. Ph. D. Thesis. University of Santiago de Compostela.

Carrera I, Sueiro C, Molist P, Holstein GR, Martinelli GP, Rodríguez-Moldes I, Anadón R (2006). GABAergic system of the pineal organ of an elasmobranch (*Scyliorhinus canicula*): a developmental immunocytochemical study. Cell Tissue Res, 323: 273-281.

Carrera I, Ferreiro-Galve S, Sueiro C, Anadón R Rodríguez-Moldes I, (2008). Tangentially migrating GABAergic cells of subpallial origin invade massively the pallium in developing sharks. Brain Res Bull, 75: 405-409.

Chapouton P, Gärtner A, Götz M (1999). The role of Pax6 in restricting cell migration between developing cortex and basal ganglia. Development, 126: 5569-5579.

Chédotal A, Pourquié O, Sotelo C (1995). Initial tract formation in the brain of the chick embryo: selective expression of the BEN/SC1/DM-GRASP cell adhesion molecule. Eur J Neurosci, 7: 198-212.

Corbin JG, Gaiano N, Machold RP, Langston A, Fishell G (2000). The Gsh2 homeodomain gene controls multiple aspects of telencephalic development. Development, 127: 5007-5020.

Derobert Y, Baratte B, Lepage M, Mazan S (2002). Pax6 expression patterns in *Lampetra fluviatilis* and *Scyliorhinus canicula* embryos suggest highly conserved roles in the early regionalization of the vertebrate brain. Brain Res Bull, 57: 277–280.

Duparc RH, Abdouh M, David J, Lépine M, Tétrault N, Bernier G (2007). Pax6 controls the proliferation rate of neuroepithelial progenitors from the mouse optic vesicle. Dev Biol, 301: 374-387.

Easter SS, Ross LS, Frankfurter A (1993). Initial tract formation in the mouse brain. J Neurosci, 13: 285-299.

Engelkamp D, Rashbass P, Seawright A, van Heyningen V (1999). Role of Pax6 in development of the cerebellar system. Development, 126: 3585-3596.

Englund C, Fink A, Lau C, Pham D, Daza RA, Bulfone A, Kowalczyk T, Hevner RF. (2005). Pax6, Tbr2, and Tbr1 are expressed sequentially by radial glia, intermediate progenitor cells, and postmitotic neurons in developing neocortex. J. Neurosci, 25: 247–251.

Ericson J, Rashbass P, Schedl A, Brenner-Morton S, Kawakami A, van Heyningen V, Jessell TM, Briscoe J (1997). Pax6 controls progenitor cell identity and neuronal fate in response to graded Shh signalling. Cell, 90: 169-180.

Estivill-Torrus G, Pearson H, van Heyningen V, Price DJ, Rashbass P. (2002). Pax6 is required to regulate the cell cycle and the rate of progression from symmetrical to asymmetrical division in mammalian cortical progenitors. Development, 129: 455–466.

Ferrán JL, Sanchez-Arones L, Sandoval JE, Puelles L (2007). A model for early regionalization in the chicken embryonic pretectum. J Comp Neurol, 505: 379–403.

Figdor MC, Stern CD (1993). Segmental organization of embryonic diencephalon. Nature, 363:630-634.

Fink AJ, Englund C, Daza RAM, Pham D, Lau C, Nivison M, Kowalczyk T, Hevner RF (2006). Development of the deep cerebellar nuclei: transcription factors and cell migration from the rhombic lip. J Neurosci, 26: 3066–3076.

Fraser S, Keynes R, Lumsden A (1990). Segmentation in the chick embryo hindbrain is defined by cell lineage restrictions. Nature, 344: 431-435.

Fujiwara M, Uchida T, Osumi-Yamashita N, Eto K (1994). Uchida rat (rSey): A new mutant rat with craniofacial abnormalities resembling those of the mouse Sey mutant. Differentiation, 57: 31–38.

Fukuda T, Kawano H, Osumi N, Eto K, Kawamura K (2000). Histogenesis of the cerebral cortex in rat fetuses with a mutation in the Pax-6 gene. Brain Res Dev Brain Res,120: 65-75.

Gérard M, Abitbol M, Delezoide AL, Dufier JL, Mallet J, Vekemans M. (1995). PAX-genes expression during human embryonic development, a preliminary report. C R Acad Sci III, 318: 57-66.

Götz M, Stoykova A, Gruss P (1998). Pax6 controls radial glia differentiation in the cerebral cortex. Neuron, 21: 1031-1044.

Goulding MD, Lumsden A, Gruss P (1993). Signals from the notochord and floor plate regulate the region-specific expression of two Pax genes in the developing spinal cord. Development, 117: 1001-1016.

Grindley JC, Davidson DR, Hill RE (1995). The role of Pax-6 in eye and nasal development. Development, 121: 1433-1442.

Grindley JC, Linda K, Hill RE, Ross A, Hogan BLM (1997). Disruption of PAX6 function in mice homozygous for the Pax6seylNeu mutation produces abnormalities in the early development and regionalization of the diencephalon. Mech Dev, 64: 111-126.

Gutrhie S, Butcher M, Lumsden A (1991). Patterns of cell division and interkinetic nuclear migration in the chick embryo hindbrain. J Neurobiol, 22: 742-754.

Hack MA, Saghatelyan A, de Chevigny A, Pfeifer A, Ashery-Padan R, Lledo PM, Götz M (2005). Neuronal fate determinants of adult olfactory bulb neurogenesis. Nat Neurosci, 8: 865–872.

Hamburger V, Hamilton HL (1951). A series of normal stages in the development of the chick embryo. J Morph, 88: 49–92.

Haubst N, Berger J, Radjendirane V, Graw J, Favor J, Saunders GF, Stoykova A, Götz M (2004). Molecular dissection of Pax6 function: the specific roles of the paired domain and homeodomain in brain development. Development, 131: 6131-6140.

Hauptmann G, Gerster T (2000). Regulatory gene expression patterns reveal transverse and longitudinal subdivisions of the embryonic zebrafish forebrain. Mech Dev, 91: 105–118.

Heins N, Malatesta P, Cecconi, F, Nakafuku M, Tucker KL, Hack MA, Chapouton P, Barde YA, Götz M (2002). Glial cells generate neurons: the role of the transcription factor Pax6. Nat Neurosci, 5: 308–315.

Hensey C, Gautier J (1998). Programmed cell death during Xenopus development: a spatio-temporal analysis. Dev Biol, 203: 36-48.

Hill RE, Favor J, Hogan BL, Ton C., Saunders GF, Hanson IM, Prosser J, Jordan T, Hastie ND, van Heyningen V (1991). Mouse small eye results from mutations in a paired-like homeobox-containing gene. Nature, 354: 522–525.

Hjorth JT, Key B (2001). Are pioneer axons guided by regulatory gene expression domains in the zebrafish forebrain? High-resolution analysis of the patterning of the zebrafish brain during axon tract formation. Dev Biol, 229: 271–286.

Hogan BL, Horsburgh G, Cohen J, Hetherington CM, Fisher G, Lyon MF (1986). Small eyes (Sey): a homozygous lethal mutation on chromosome 2 which affects the differentiation of both lens and nasal placodes in the mouse. J Embryol Exp Morphol, 97: 95–110.

Horie M, Sango K, Takeuchi K, Honma S, Osumi N, Kawamura K, Kawano H (2003). Subpial neuronal migration in the medulla oblongata of Pax-6-deficient rats. Eur J Neurosc, 17: 49–57.

Jessell TM, Sanes JR (2000). Induction and patterning of the nervous system. In: Principles of Neural Science. Kandel ER, Schwartz JH, Jessell TM (eds.). New York: Elsevier; pp 1019-1040.

Jones L, López-Bendito G, Gruss P, Stoykova A, Molnar Z (2002). Pax6 is required for the normal development of the forebrain axonal connections. Development, 129: 5041-5052.

Ju MJ, Aroca P, Luo J, Puelles L, Redies C (2004). Molecular profiling indicates avian branchiomotor nuclei invade the hindbrain alar plate. Neuroscience, 128: 785-796.

Kage T, Takeda H, Yasuda T, Maruyama K, Yamamoto N, Yoshimoto M, Araki K, Inohaya K, Okamoto H, Yasumasu S, Watanabe K, Ito H, Ishikawa Y (2004). Morphogenesis and regionalization of the medaka embryonic brain. J Comp Neurol. 476: 219-239.

Kaufmann MH (1992). The Atlas of Mouse Development. London: Academic Press.

Kawakami A, Kimura-Kawakami M, Nomura T, Fujisawa H (1997). Distributions of PAX6 and PAX7 proteins suggest their involvement in both early and late phases of chick brain development. Mech Dev, 66: 119-130.

Kawano H, Fukuda T, Kubo K, Horie M, Uyemura K, Takeuchi K, Osumi N, Eto K, Kawamura K (1999). Pax6 is required for thalamocortical pathway formation in the fetal rats. J Comp Neurol, 408: 147-160.

Kimmel CB, Ballard WW, Kimmel SR, Ullmann B, Schilling TF (1995). Stages of embryonic development of the zebrafish. Dev Dyn, 203: 253–310.

Kimura J, Suda Y, Kurokawa D, Hossain ZM, Nakamura M, Hara A, Aizawa S (2005). Emx2 and Pax6 function in cooperation with Otx2 and Otx1 to develop caudal forebrain primordium that includes future archipallium. J Neurosci, 25: 5097–5108.

Kioussi C, O'Connell S, St-Onge L et al. (1999). Pax6 is essential for establishing ventral-dorsal cell boundaries in pituitary gland development. PNAS, 96: 14378–14382.

Kudo LC, Karsten SL, Chen J, Levitt P, Geschwind DH (2007). Genetic analysis of anterior posterior expression gradients in the developing mammalian forebrain. Cereb Cortex, 17: 2108-2122.

Kuratani S, Horigome N (2000). Developmental morphology of branchiomeric nerves in a cat shark, Scyliorhinus *torazame*, with special reference to rhombomeres, cephalic mesoderm, and distribution patterns of cephalic crest cells. Zoolog Sci, 17: 893–909.

Kohwi M, Osumi N, Rubenstein JL, Alvarez-Buylla A (2005). Pax6 is required for making specific subpopulations of granule and periglomerular neurons in the olfactory bulb. J Neurosci, 25: 6997–7003.

Kroll TT, O'Leary DDM (2005). Ventralized dorsal telencephalic progenitors in Pax6 mutant mice generate GABA interneurons of a lateral ganglionic eminence fate. PNAS, 102: 7374–7379.

Larsen CW, Zelster LM, Lumsden A (2001). Boundary formation and compartition in the avian diencephalon. J Neurosci, 21: 4699–4711.

Lin JC, Cai L, Cepko CL (2001). The external granule layer of the developing chick cerebellum generates granule cells and cells of the isthmus and rostral hindbrain. J Neuroscience, 21: 159-168.

Macdonald R, Xu Q, Barth KA, Mikkola I, Holder N, Fjose A, Krauss S, Wilson SW (1994). Regulatory gene expression boundaries demarcate sites of neuronal differentiation in the embryonic zebrafish forebrain. Neuron 13: 1039-1053.

Maekawa M, Takashima N, Arai Y, Nomura T, Inokuchi K, Yuasa S, Osumi N (2005). Pax6 is required for production and maintenance of progenitor cells in postnatal hippocampal neurogenesis. Genes Cells, 10: 1001-1014.

Manuel M, Price DJ (2005). Role of Pax6 in forebrain regionalization. Brain Res Bull, 66:387-393.

Manuel M, Georgala PA, Carr CB, Chanas S, Kleinjan DA, Martynoga B, Mason JO, Moliner Mm, Pinson J, Pratt T, Quinn JC, Simpson IT, Tyas DA, van Heyningen V, West JD, Price DJ (2007). Controlled overexpression of Pax6 in vivo negatively autoregulates the Pax6 locus, causing cell-autonomous defects of late cortical progenitor proliferation with little effect on cortical arealization. Development, 134: 545-555.

Margotta V (2007). PCNA immunoreactivity revealing normal proliferative activity in the brain of an adult Elasmobranch, *Torpedo marmorata*. Ital J Anat Embryol, 112: 145-55.

Mastick GS, Easter SS (1996). Initial organization of neurons and tracts in the embryonic mouse fore- and midbrain. Dev Biol, 173: 79-94.

Mastick GS, Davis NM, Andrews L, Easter SS (1997). Pax6 functions in boundary formation and axon guidance in the embryonic mouse forebrain. Development, 124:1985-1997.

Mastick GS, Andrews GL (2001). Pax6 regulates the identity of embryonic diencephalic neurons. Mol Cell Neurosci, 17: 190–207.

Matsunaga E, Araki I, Nakamura H (2000). Pax6 defines the di-mesencephalic boundary by repressing En1 and Pax2. Development, 127: 2357-2365.

Matsuo T, Osumi-Yamashita N, Noji S, Ohuchi H, Koyama E, Myokai F, Matsuo N, Taniguchi S, Doi H, Iseki S, et al (1993). A mutation in the Pax-6 gene in rat small eye is associated with impaired migration of midbrain crest cells. Nat Genet, 3: 299-304.

Moreno N, Retaux S, González A (2008). Spatio-temporal expression of Pax6 in *Xenopus* forebrain. Brain Res, 1239: 92-99.

Mueller T, Vernier P, Wullimann MF (2006). A phylotypic stage in vertebrate brain development: GABA cell patterns in zebrafish compared with mouse. J Comp Neurol, 494: 620-634.

Murakami Y, Ogasawara M, Sugahara F, Hirano S, Satoh N, Kuratani S (2001). Identification and expression of the lamprey Pax6 gene: evolutionary origin of the segmented brain of vertebrates. Development, 128: 3521–3531.

Nacher J, Varea E, Blasco-Ibañez JM, Castillo-Gómez E, Crespo C, Martinez-Guijarro J, McEwen B (2005). Expression of the transcription factor Pax6 in the adult rat dentate gyrus. J Neurosci Res, 81: 753–761.

Neyt C, Welch M, Langston A, Kohtz J, Fishell G (1997). A short-range signal restricts cell movement between telencephalic proliferative zones. J Neurosci, 17: 9194-9203.

Nicotra A, Cicirata F, Martinez S (2004). Analysis of cCx39 expression pattern during chick development. Dev Brain Res, 148: 179-183.

Nural HF, Mastick GS (2004). Pax6 guides a relay of pioneer longitudinal axons in the embryonic mouse forebrain. J Comp Neurol, 479: 399-409.

Osorio J, Mazan S, Rétaux S (2005). Organisation of the lamprey (Lampetra fluviatilis) embryonic brain: Insights from LIM-homeodomain, Pax and hedgehog genes. Dev Biol, 288: 100-112.

Osumi N (2001). The role of Pax6 in brain patterning. Tohoku J Exp Med, 193: 163–174.

Osumi N, Hirota A, Ohuchi H, Nakafuku M, Iimurao T, Kuratani S, Fujiwara M, Noji S, Eto K (1997). Pax6 is involved in the specification of hindbrain motor neuron subtype. Development, 124: 2961-2972.

Osumi N, Shinoara H, Numayama-Tsuruta K, Maekawa M (2008). Concise review: Pax6 transcription factor contributes to both embryonic and adult neurogenesis as a multifunctional regulator. Stem Cells, 26: 1663-1672.

Pasini A, Wilkinson DG (2002). Stabilizing the regionalisation of the developing vertebrate central nervous system. Bioessays, 24: 427-438.

Philips GT, Stair CN, Young Lee H, Wroblewski E, Berberoglu MA, Brown NL, Mastick GS (2005). Precocious retinal neurons: Pax6 controls timing of differentiation and determination of cell type. Dev Biol, 279: 308–321.

Piñón MC, Tuoc TC, Ashery-Padan R, Molnar Z, Stoykova A (2008). Altered molecular regionalization and normal thalamocortical connections in cortex-specific Pax6 knock-out Mice. J Neurosci, 28: 8724–8734.

Pratt T, Vitalis T, Warren N, Edgar JM, Mason JO, Price DJ (2000). A role for Pax6 in the normal development of dorsal thalamus and its cortical connections. Development, 127: 5167-5178.

Pritz MB, Ruan YW (2009). PAX6 immunoreactivity in the diencephalon and midbrain of alligator during early development. Brain Behav Evol, 73: 1-15.

Prosser J, van Heyningen V (1998). Pax6 mutations reviewed. HUMAN MUTATION, 11: 93.108.

Puelles L, Rubenstein JLR (1993). Expression patterns of homeobox and other putative regulatory genes in the embryonic mouse forebrain suggest a neuromeric organization. TINS, 16: 472–479.

Puelles L, Rubenstein JLR (2003). Forebrain gene expression domains and the evolving prosomeric model. TRENDS in Neurosciences, 9: 469-476.

Puelles L, Amat JA, Martinez-de-la-Torre M (1987). Segment-related, mosaic neurogenetic pattern in the forebrain and mesencephalon of early chick embryos: I. Topography of AChE-positive neuroblasts up to stage HH18. J Comp Neurol, 266: 247–268.

Puelles L, Kuwana E, Puelles E, Bulfone A, Shimamura K, Keleher J, Smiga S, Rubenstein JLR (2000). Pallial and subpallial derivatives in the embryonic chick and mouse telencephalon, traced by the expression of the genes Dlx-2, Emx-1, Nkx-2.1, Pax-6, and Tbr-1. J Comp Neurol, 424: 409-438.

Puelles López L, Martínez-Pérez S, Martínez de la Torre M (2008). Neuroanatomía. Médica Panamericana, Buenos Aires, Madrid.

Quinn JC, Molinek M, Martynoga BS, Zaki PA, Faedo A, Bulfone A, Hevner RF, West JD, Price DJ (2007). Pax6 controls cerebral cortical cell number by regulating exit from the cell cycle and specifies cortical cell identity by cell autonomous mechanism. Dev Biol, 302: 50–65.

Ross LS, Parrett T, Easter SS (1992). Axonogenesis and morphogenesis in the embryonic zebrafish brain. J Neurosci, 71: 467-482.

Sakurai K, Osumi N (2008). The neurogenesis-controlling factor, Pax6, inhibits proliferation and promotes maturation in murine astrocytes. J Neurosci, 28: 4604-4612.

Sander M, Neubüser A, Kalamaras J, Ee HC, Martin GR, German MS (1997). Genetic analysis reveals that PAX6 is required for normal transcription of pancreatic hormone genes and islet development. Genes Dev, 11: 1662-1673.

Sansom SN, Griffiths D, Faedo A, Kleinjan DJ, Ruan Y, Smith J, van Heyningen V, Rubenstein JL, Livesey FJ (2009). The level of the transcription factor Pax6 is essential for controlling the balance between neural stem cell self-renewal and neurogenesis. PLoS Genet, 5: e1000511. doi:10.1371/journal.pgen.1000511.

Scardigli R, Baumer N, Gruss P, Guillemot F, Le Roux I (2003). Direct and concentration-dependent regulation of the proneural gene Neurogenin2 by Pax6. Development, 130: 3269–3281.

Schambra UB, Lauder JM, Silver J (eds.) (1992). Atlas of the Prenatal Mouse Brain. San Diego: Academic Press.

Schedl A, Ross A, Lee M, Engelkamp D, Rashbass P, van Heyningen V, Hastie ND (1993). Influence of PAX6 gene dosage on development: overexpression causes severe eye abnormalities. Cell, 86: 71-82.

Schmahl W, Knoedlseder M, Favor J, Davidson D (1993). Defects of neuronal migration and the pathogenesis of cortical malformations are associated with Small eye (Sey) in the mouse, a point mutation at the Pax-6-locus. Acta Neuropathol, 86: 126-135.

Schonhoff SE, Giel-Moloney M, Leiter AB (2004). Minireview: Development and differentiation of gut endocrine cells. Endocrinology, 145: 2639-2644.

Schubert FR, Fainso A, Gruenbaum Y, Gruss P (1995). Expression of the novel murine homeobox gene Sax1 in the developing nervous system. Mech Dev, 51: 99-114.

Schubert FR, Lumsden A (2005). Transcriptional control of early tract formation in the embryonic chick midbrain. Development, 132: 1785-1793.

Simpson TI, Price DJ (2002). Pax6; a pleiotropic player in development. BioEssays, 24: 1041-1051.

Sisodiya SM, Free SL, Williamson KA, Mitchell TN, Willis C, Stevens JM, Kendall BE, Shorvon SD, Hanson IM, Moore AT, van Heyningen V (2001). PAX6 haploinsufficiency causes cerebral malformation and olfactory dysfunction in humans. Nat Genet, 28: 214-216.

Smith-Fernandez A, Pieau C, Repérant J, Boncinelli E, Wassef M (1998). Expression of the Emx-1 and Dlx-1 homeobox genes define three molecularly distinct domains in the telencephalon of mouse, chick, turtle and frog embryos: implications for the evolution of telencephalic subdivisions in amniotes. Development, 125: 2099-2111.

Stenman J, Yu RT, Evans RM, Campbell K (2003). Tlx and Pax6 co-operate genetically to establish the pallio-subpallial boundary in the embryonic mouse telencephalon. Development 130:1113-1122.

Stoykova A, Gruss P (1994). Roles of Pax genes in developing and adult brain suggested by expression patterns. J Neurosci, 74: 1395-1412.

Stoykova A, Fritsch R, Walther C, Gruss P (1996). Forebrain patterning defects in small eye mutant mice. Development, 122: 3453–3465.

Stoykova A, Treichel D, Hallonet M, Gruss P (2000). Pax6 modulates the dorsoventral patterning of the mammalian telencephalon. J Neurosci, 20:8042-8050.

Takahashi M, Osumi N (2002). Pax6 regulates specification of ventral neurone subtypes in the hindbrain by establishing progenitor domains. Development, 129: 1327-1338.

Talamillo A, Quinn JC, Collinson JM, Caric D, Price DJ, West JD, Hill RE (2003). Pax6 regulates regional development and neuronal migration in the cerebral cortex. Dev Biol, 255:151-163.

Toresson, H., Potter, S.S., Campbell, K (2000). Genetic control of dorsal–ventral identity in the telencephalon: opposing roles for Pax6 and Gsh2. Development 127, 4361–4371.

Trujillo MC, Alonso A, Delgado AC, Damas C (2005). The rostral and caudal boundaries of the diencephalon. Brain Research Reviews, 49:202– 210.

Tuoc TC, Radyushkin K, Tonchev AB, Piñón MC, Ashery-Padan R, Molnar Z, Davidoff M, Stoykova A (2009). Selective cortical layering abnormalities and behavioral deficits in cortex-specific Pax6 Knock-Out Mice. J Neurosci, 29:8335-8349.

von Bohlen und Halbach O (2007). Immunohistological markers for staging neurogenesis in adult hippocampus. Cell Tissue Res, 329:409–420.

Vitalis T, Cases O, Engelkamp D, Verney C, Price DJ. (2000). Defects of tyrosine hydroxylase-immunoreactive neurons in the brains of mice lacking the transcription factor Pax6. J Neurosci, 20:6501–6516.

Walther C, Gruss P (1991). Pax-6, a murine paired box gene, is expressed in the developing CNS. Development, 113:1435-1449.

Warren N, Price DJ (1997). Roles of Pax-6 in murine diencephalic development. Development, 124:1573-1582.

Warren N, Caric D, Pratt T, Clausen JA, Asavaritikrai P, Mason JO, Hill RE, Price DJ (1999). The transcription factor, Pax6, is required for cell proliferation and differentiation in the developing cerebral cortex. Cerebral Cortex, 9:627-635.

Wilson SW, Ross LS, Parrett T, Easter SS (1990). The development of a simple scaffold of axon tracts in the brain of the embryonic zebrafish, *Brachydanio reri*o. Development 108, 121-145.

Wullimann MF, Rink E (2001). Detailed immunohistology of Pax6 protein and tyrosine hydroxylase in the early zebrafish brain suggests role of Pax6 gene in development of dopaminergic diencephalic neurons. Dev Brain Res, 131:173-191.

Wullimann MF, Mueller T (2004). Teleostean and Mammalian Forebrains Contrasted: Evidence from Genes to Behavior. J Comp Neurol, 475:143–162.

Yamasaki T, Kawaji K, Ono K, Bito H, Hirano T, Osumi N, Kengaku M (2001). Pax6 regulates granule cell polarization during parallel fibre formation in the developing cerebellum. Development, 128:3133-3144.

Yoshida M, Colman DR (2000). Glial-defined rhombomere boundaries in developing Xenopus hindbrain. J Comp Neurol, 424:47-57.

Yun K, Potter S, Rubenstein JLR (2001). Gsh2 and Pax6 play complementary roles in dorsoventral patterning of the mammalian telencephalon. Development 128:193-205.

Zupanc GKH (2006). Neurogenesis and neuronal regeneration in the adult fish brain. J Comp Physiol A, 192:649–670.

Table 1: Correspondence between the embryonic stages of *S. canicula*, described by Ballard et al. (1993) and *H. fuscus*, as regards external features, age (from "day 1", when they were laid naturally), body length and the developmental periods defined according to the pattern of Pax6 expression and progressive differentiation of the brain walls.

Stage	External features and landmark events	Age (days) at 16 °C	*Size of H.fuscus* (in mm)	*Size of S.canicula* (in mm)	
22	- Pharyngeal clefts C1, (the future spiracles) open	27-28	-	8-9	FIRST PERIOD
23	- Pharyngeal clefts C1, C2 and C3 open	28-30	10	9	
24	- First gill buds in clefts C2 and C3; mouth opening diamond-shaped	30-31,5	12	11.5-12.5	
25	- Pharyngeal clefts C5 open	31-38	13.5	12.5-15.5	
26	- Pharyngeal clefts C1-C6 open	37-42	17	16	
27	- Hatching gland begins to show; olfactory placodes wide open; mouth diamond shaped; buds of gill filaments	42-46	-	17-20	SECOND PERIOD
28	- Hatching gland developed; olfactory placodes closed; mouth is transverse oval; gill filaments clearly seen	46-51	22-24	21-23	
29	- Mouth as an arching line; incomplete circle of eye pigment; body: no pigment anywhere	49-53	25-33	23.5-30	
30	- No signs of rostral protrusion; eyes circled with black pigment	52-60	34-38	31-33	
31	- Rostrum as a detectable protrusion, that increases progressively in size; maximum development of gill filaments	60-92	39-46	34-40	
32	- Rostrum becomes prominent and angle to the body decreases; Pigment completely covers the eye; Body: pigments begins to appear	75-125	47-62	40-57	THIRD PERIOD
33	- Body: pigmentation increases; the external yolk sac is shrinking in size	115-155	68-82	68-78	
34	- the external yolk sac is practically empty - Hatching	145-175	83-96	78-82	
Juvenile			96	82	

Table 2. Correspondences in timing of development of different vertebrate embryos, according to the Pax6 expression patterns, the three development periods defined in the present study and some external features (see text for details).

		From fertilization to neurulation	FIRST PERIOD - Brain walls formed by a pseudo-stratified neuroepithelium - Pax6 expression restricted to prosencephalon and mielencephalon	SECOND PERIOD - Layering of the brain walls and development of periventricular formations - Pax6 expression extended to basal mesencephalon and metencephalon	THIRD PERIOD - Development of nuclei from layers of migrated cells - Pax6 expression maintained in cell clusters
CATSHARKS	Stages (from Ballard et al., 1993)	S1-S16	S17-S26	S27-S31	S32-S34
	Length of development (days) *-hatching after 175 days-*	17	25	35	98
	Percentage of development	10%	14%	20%	56%
	Main features	cleavage (S1-S7) gastrulation (S11-S14) neural folds closing (S16)	three primary brain vesicles visible (S17) dorsal and ventral finfolds (from S19) pectoral fin rudiments (S24) pharyngeal clefts C1-C6 open (S26)	gill filaments clearly seen (S28) eye ball circled with black pigment (S30) buds of the caudal scales begin to show (S30) rostrum as a detectable protrusion (S31)	skin pigmentation begins (S32) hatching (S34)
CHICK	Stages (from Hamburger and	HH1-HH8	HH9-HH18	HH19-HH30	HH31-HH45
	Length of development *-hatching 21 days after laying-*	28h	40h	100h (4d)	312h (13 d)
	Percentage of development	6%	8%	21%	65%
	Main features	neural folds meet at the level of the midbrain (HH8)	three primary brain vesicles visible (HH10) limb buds lifted off blastoderm (HH17) four visceral arches visible (HH18)	distinct eye pigment (HH22) feather germs start to be visible (HH30)	flight feathers conspicuous (HH36) mandible and maxillae cornified (opaque) (HH39) hatching (HH46)
MOUSE	Stages (embryonic day, E)	E0.5-E8.5	E8.5-E10.5	E10.5-E14.5	E14.5-Birth
	Length of development (days) -born at 20 days *post conception (dpc)*-	8,5	2	4,00	5,5
	Percentage of development	42.5%	10%	20%	27.5%
	Main features	early fusion of neural folds starts at 8dpc	three primary brain vesicles visible (9dpc) limb buds (9.5 dpc) four branchial pouches visibles (10.5 dpc)	distinct retina pigmentation (12 dpc) face takes "adult" features (13 dpc) hair follicles start to be distinguish (13.5-14 dpc)	extensive distribution of the hair follicles (15 dpc)
ZEBRAFISH	Stages	10hpf	12hpf-24hpf	24hpf-48hpf (pharyngula period)	48-78hpf (hatching period)
	Length of development (hours) *-hatching at 72 hours post fertilization (hpf)-*	10h	12h	24h	24h
	Percentage of development	14%	17%	33%	33%
	Main features	neural keel (10hpf)	optic vesicle (12hpf) brain vesicles visibles (16hpf) median finfold visible (24dpf) early pigmentation in retina and skin (24hpf)	distinct retina pigmentation (30hpf) shallow pectoral fin buds (30hpf)	gill slits and filament buds (72hpf)

Figure 1. Sagittal sections through the heads of *S. canicula* (A-E,G,H) and *H. fuscus* (F) embryos at indicated stages, showing the distribution of Pax6-expressing cells after immunolabelling with anti-Pax6 (B,C,F-H) and after *in situ* hybridisation for Pax6 mRNA and counterstaining with nuclear fast red (A,D,E). Scale bars: 250 μm (A,B,D,F); 500 μm (C,E,G,H). For abbreviations, see list in Appendix A.

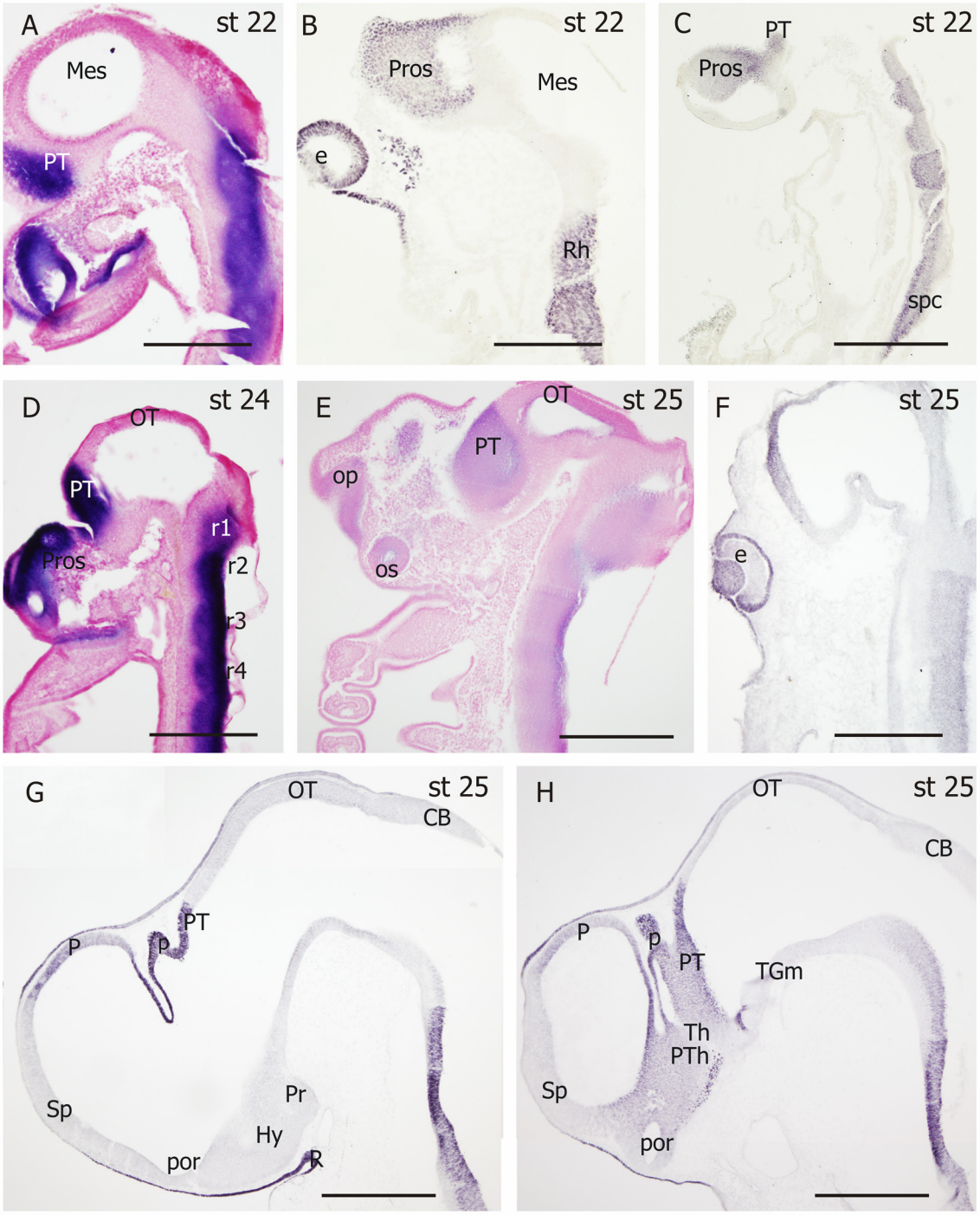
A
st 22
Mes
PT
B
st 22
Pros
Mes
e
Rh
C
PT
st 22
Pros
spc
D
st 24
OT
PT
Pros
r1
r2
r3
r4
E
OT
st 25
PT
op
os
F
st 25
e
G
OT
st 25
CB
PT
P
p
Sp
Pr
Hy
por
R
H
OT
st 25
CB
P
p
PT
TGm
Th
PTh
Sp
por

Figure 2. Sagittal sections through the heads (A-D) and brains (E) of *S. canicula* embryos at indicated stages, showing the distribution of Pax6-immunoreactivity. Anterior is left and dorsal is up. Arrows in A and D label the primordial cerebellum. Lines in D and E indicate the levels of the transverse sections in Figs. 9, 11 and 19, respectively. Scale bars: 500 μm. For abbreviations, see list in Appendix A.

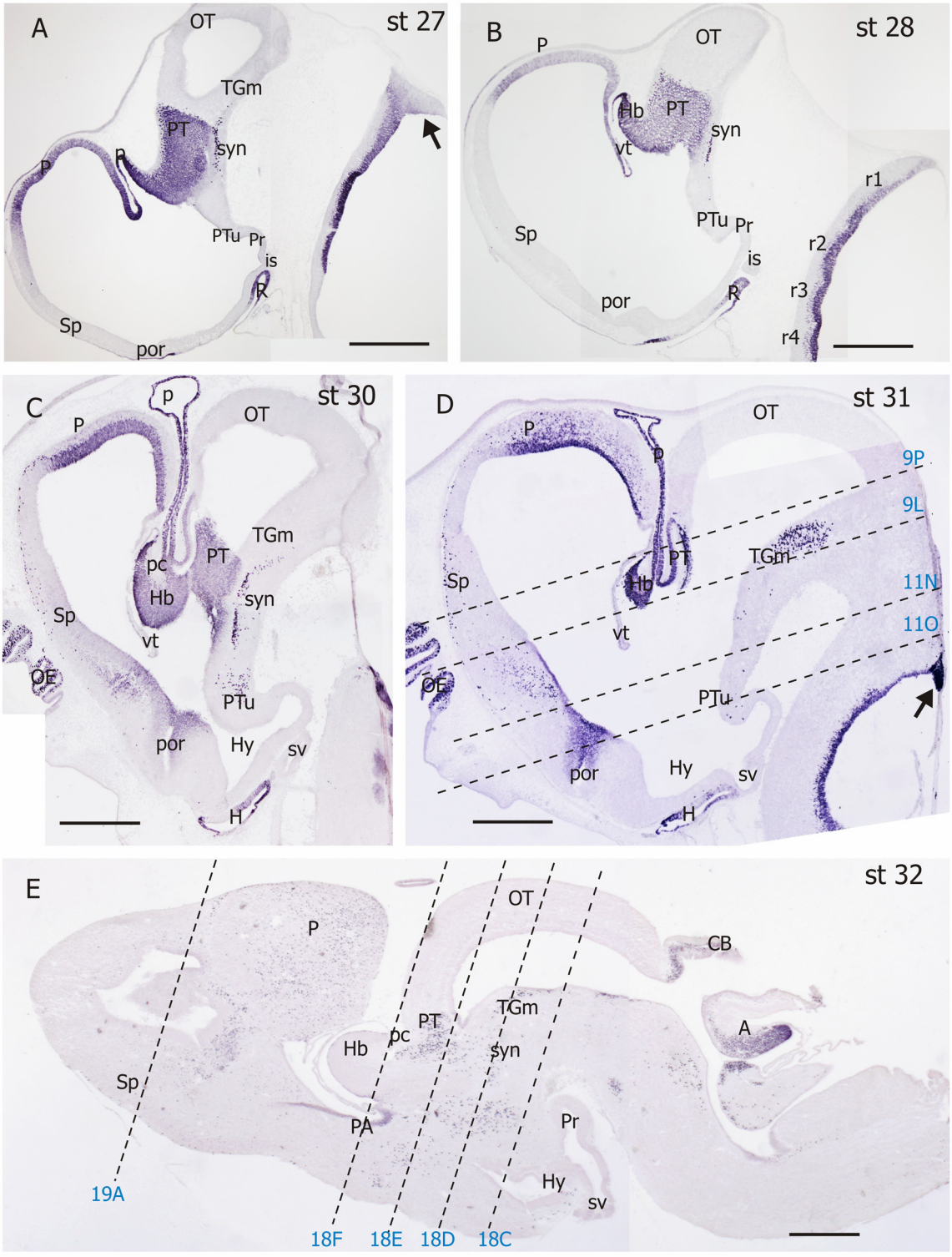
A
st 27
OT
TGm
PT
syn
P
R
PTu
Pr
is
R
Sp
por
B
st 28
P
OT
Hb
PT
syn
vt
r1
PTu
Pr
Sp
r2
is
r3
por
R
r4
C
st 30
p
P
OT
TGm
pc
PT
Hb
syn
Sp
vt
OE
PTu
por
Hy
sv
H
D
st 31
P
P
OT
9P
9L
PT
TGm
Sp
Hb
11N
vt
11O
OE
PTu
por
Hy
sv
H
E
st 32
P
OT
CB
TGm
PT
pc
A
Hb
syn
Sp
PA
Pr
Hy
sv
19A
18F
18E
18D
18C

Figure 3. Cross sections of the prethalamus (ventral thalamus) of embryos (A-G) and juvenile specimens (H) of *S canicula,* showing the mediolateral distribution of Pax6-immunoreactive cells throughout development and the progressive organization of the three-layered structure of the neural walls. Note the abundance of Pax6 neuroepithelial cells at early stages (A, B), the increase in density of these cells in the intermediate (IZ) and marginal (MZ) zones from early (arrows in A and B) to later stages (C-G), and their progressive absence from the ventricular (VZ) zone in later embryonic stages (F, G) and in juveniles (H). These figures are higher magnifications of the square areas outlined in Figures 5L (A) and 11A (B), 11F (C) and 18D (F). In A-E, ventral is up and dorsal is down. In F-H, dorsal is up and ventral down. Scale bars: 50 μm (A-D) 100 μm (E-H).

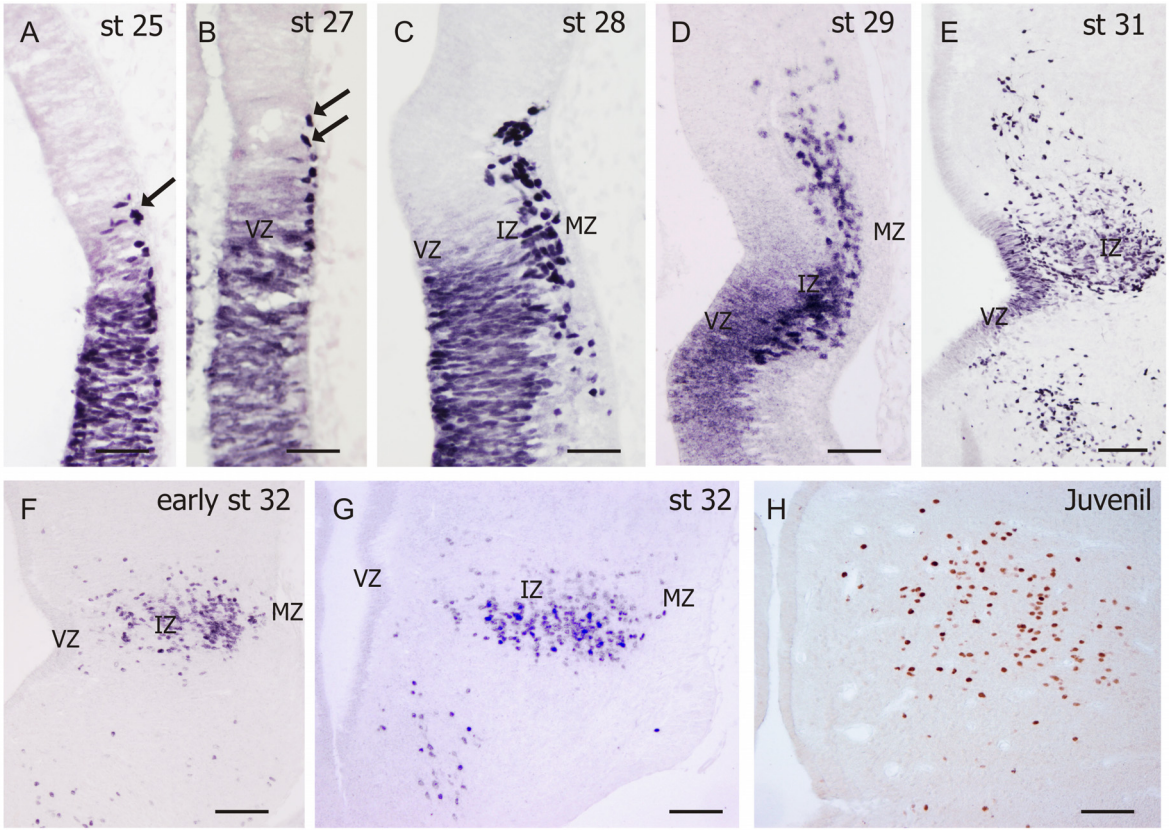
A
st 25
B
st 27
VZ
C
st 28
VZ
IZ
MZ
D
st 29
MZ
IZ
VZ
E
st 31
IZ
VZ
F
early st 32
VZ
IZ
MZ
G
st 32
VZ
IZ
MZ
H
Juvenil

Figure 4. Sagittal (A-C,L,M) and transverse sections (D-K) through the spinal cord (A-D,M) and rhombencephalon (A-C, F,G,K-M) of *S. canicula* after ISH for Pax6 mRNA (A,B), and after immunohistochemistry for Pax6 (C, D,F,G,I, K-M) and for Shh (E,H,J) at indicated stages, showing the distribution of Pax6 cells in relation to with the distribution of Shh. Note the Pax6 expression in the spinal cord and its continuity with the longitudinal domain of the rhombencephalon that extends up to caudal isthmic levels (A-C,K,L). The rhombomeres are well distinguished in A and C and their magnifications in B and L-M, respectively. Transverse sections through the spinal cord (D) and the rhombencephalon from caudal (F) to isthmic levels (K,L) show radially oriented Pax6 cells in the lateral ventricular walls. Note that the laterodorsal Pax6 cells are less intensely stained than the lateroventral Pax6 cells, and that the primordium of the cerebellum (alar plate of r1) shows no Pax6 cells (asterisk in A-C,K,L). Sections in E,H and J are adjacent to those in D,I and G and show the immunolabelling with anti-Shh in the floor plate (fp). Note the absence of Pax6 cells in the region just lateral to the floor plate (arrows in D, G-J). Insets in G,I and K show panoramic views of the corresponding whole transverse sections Arrowhead in D indicate the putative alar-basal boundary. Scale bars: 250 μm (A), 100 μm (C-M). For abbreviations, see list in Appendix A.

FIRST PERIOD: RHOMBENCEPHALON

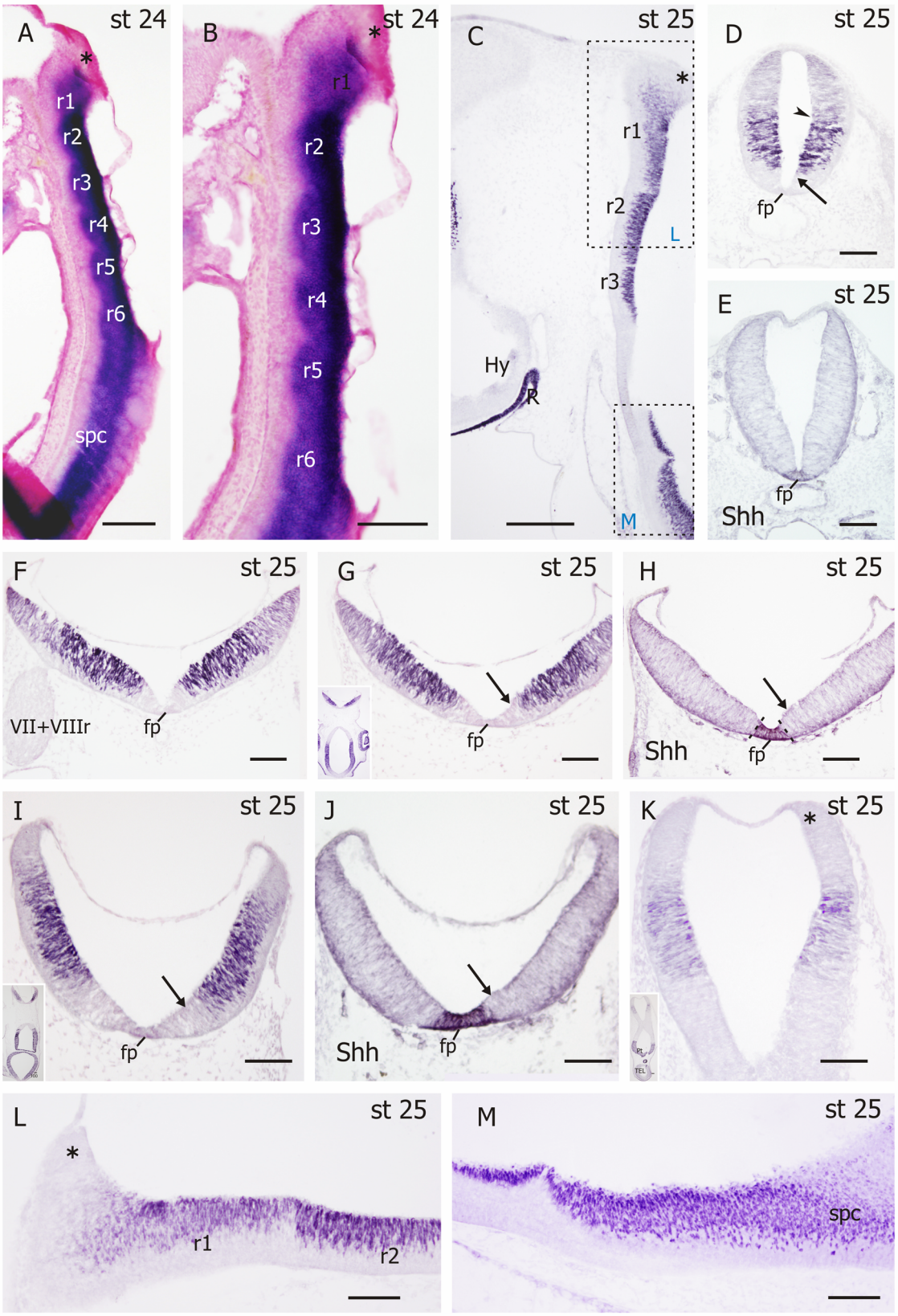

Figure 5. Sagittal (A,F-K) and cross (B-E,L-O) sections through the prosencephalon of *S. canicula* at indicated stages after immunohistochemistry for Pax6 (A-D, F,G,J-O), or Shh (E), and after ISH for Pax6 mRNA (H,I). **A**. Sagittal section at a lateral level to show the Pax6 expression in the diencephalon and telencephalon. Note the absence of immunoreactivity in the mesencephalon and the faint labelling in the thalamus. Arrowhead indicates the mesencephalon-diencephalon boundary. **B**. Cross section at the level indicated in Figure 5A showing Pax6 neuroepithelial cells in the pretectal and pallial Pax6 domains. Note also intense labelling in the pineal organ. Arrowhead indicates the mesencephalic-prosencephalic boundary. **C.** Cross section at the level indicated in Figure 5A showing Pax6 expression in the pretectal and pallial domains. Note the absence of labelling in the subpallium. Note also the presence of Pax6 cells close to the olfactory epithelium (white arrowhead). In **C-J** black arrow indicates a strip Pax6 cells ventral to the pretectal Pax6 domain, black arrowhead indicates the faint Pax6 labelling in between this stripe and the intensely labelled pretectal cells. **D-E**. Details of the square area outlined in C (D) and of the adjacent section immunolabelled for Shh (E), showing that the ventral limit of Pax6 expression abuts the dorsal limit of Shh immunolabelling. Note the weak Pax6 labelling in the band of cells that separates the ventral strip of intensely labelled cells (arrow) and the main pretectal domain (arrowhead). **F**. Sagittal section through the prosencephalon at stage 26 showing the telencephalic and diencephalic Pax6 domains. **G**. Detail of the square area outlined in F, showing the near absence of Pax6 expression in the thalamus. **H**. Sagittal section adjacent to G, showing similar distribution of the Pax6 mRNA. **I.** Detail of the square area outlined in H. **J.** Detail of the square area outlined in A. Note the Pax6 expression in the primordium of the habenula, (asterisk). **K**. Pax6 cells in the prethalamus and post-optic region. White arrows indicate the ventral extension of the prethalamic Pax6 cells. **L**. Cross section at the level indicated in Figure 5A, showing the rostral extension of the Pax6 prethalamic domain. Note the absence of Pax6 cells in the subpallium and in the hypothalamus. Abundant Pax6 cells are observed in the retina and also in the olfactory pit. **M**. Detail of the square area outlined in L, showing the distribution of Pax6 cells at the interface between the prethalamus and the posterior tubercle (basal plate of p3). White arrow in L,M indicates marginal Pax6 cells extending towards the posterior tubercle walls. **N**. Cross section at the level indicated in Figure 5A showing Pax6 cells in the optic stalk and Rathke's pouch. No Pax6 expression is observed in the subpallium and hypothalamus. **O.** Detail of a more ventral section to that in N showing Pax6 cells in the optic stalk, and in the preoptic region. Note that the level of sections N, O is close to the horizontal plane, and the ventral part of the preoptic recess is not visible. Scale bars: 250μm (A-C,F,H,K,L,N), 100 μm (D,E,G,I,J,M,O). For abbreviations, see list in Appendix A.

FIRST PERIOD: MES- and PROSENCEPHALON

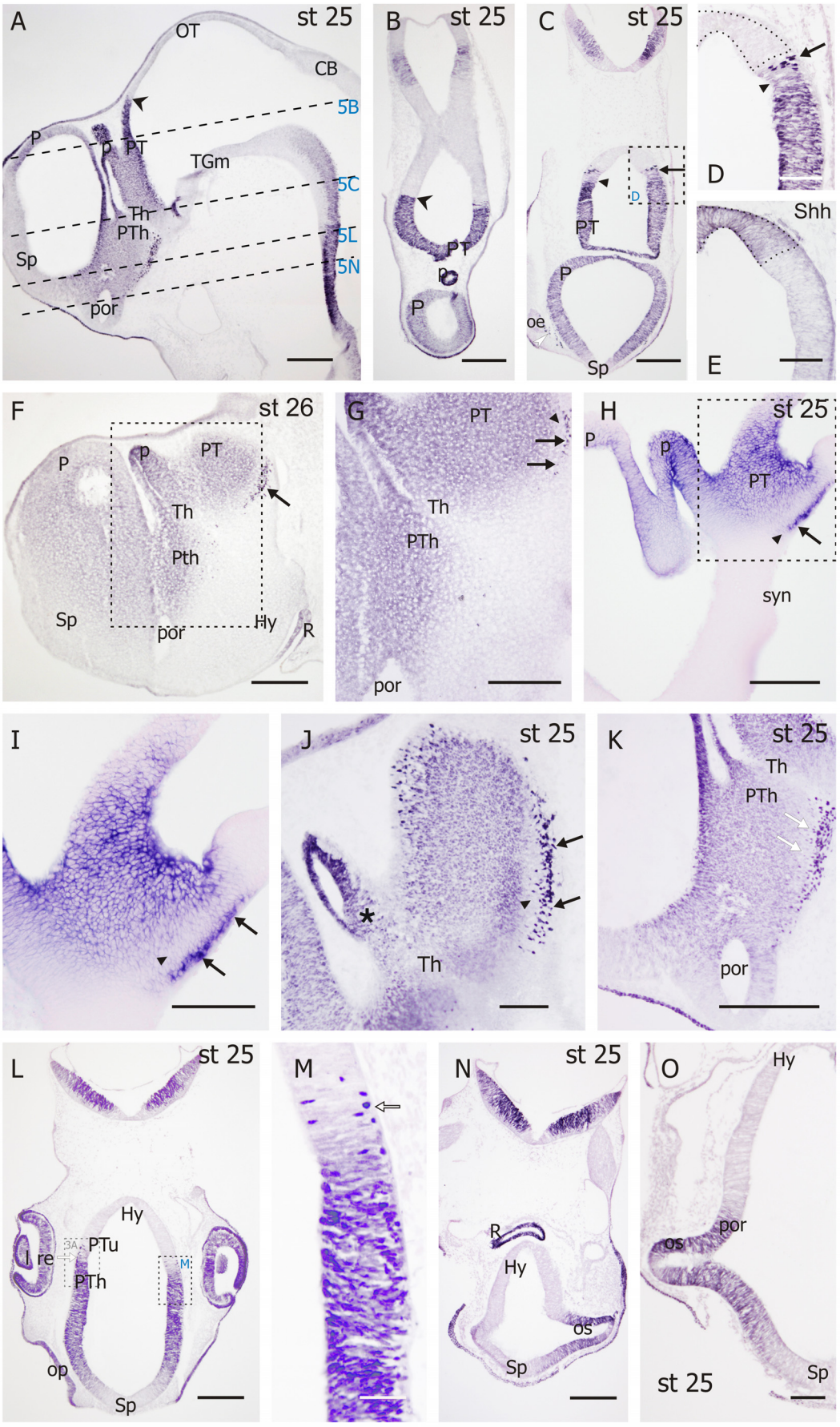

Figure 6. Sagittal (*A-C*) and transverse (D-*O*) sections through the spinal cord (B,D) and rhombencephalon (E-*O*) of *S. canicula* at indicated stages after Pax6 immunohistochemistry . **A**. Midsagittal section, showing the levels of transverse sections *G-O*. **B**. Detail of a section adjacent to *A* showing the spinal cord-rhombencephalic Pax6 domains. Note that the density of Pax6 cells is reduced at the inter-rhombomere boundaries (arrowheads). Arrows indicate Pax6 cells in the prospective IZ. ***C*.** Detail of stage 27 rhombencephalon to show Pax6 cells in the prospective IZ (arrows). **D**. Transverse section of the rostral spinal cord, showing differences in the intensity of labelling in the lateroventral (intense) and in the laterodorsal and dorsal (faint) walls. Arrows indicate Pax6 cells in the IZ. **E-*O***. Transverse sections from caudal (E) to rostral (*O*) rhombencephalon showing similar Pax6 distribution than in the spinal cord. Arrows label Pax6 cells in the IZ. Asterisks in **M** and **N** indicate Pax6 cells in the VZ of the primordial rhombic lips. Note in ***O*** the faint labelling in Pax6 cells at the VZ of the cerebellar plate. Scale bars: 250μm (*A*,B,*G-O*), 100μm (D-F), 50 μm (*C*). For abbreviations, see list in Appendix *A*.

EARLY SECOND PERIOD: RHOMBENCEPHALON

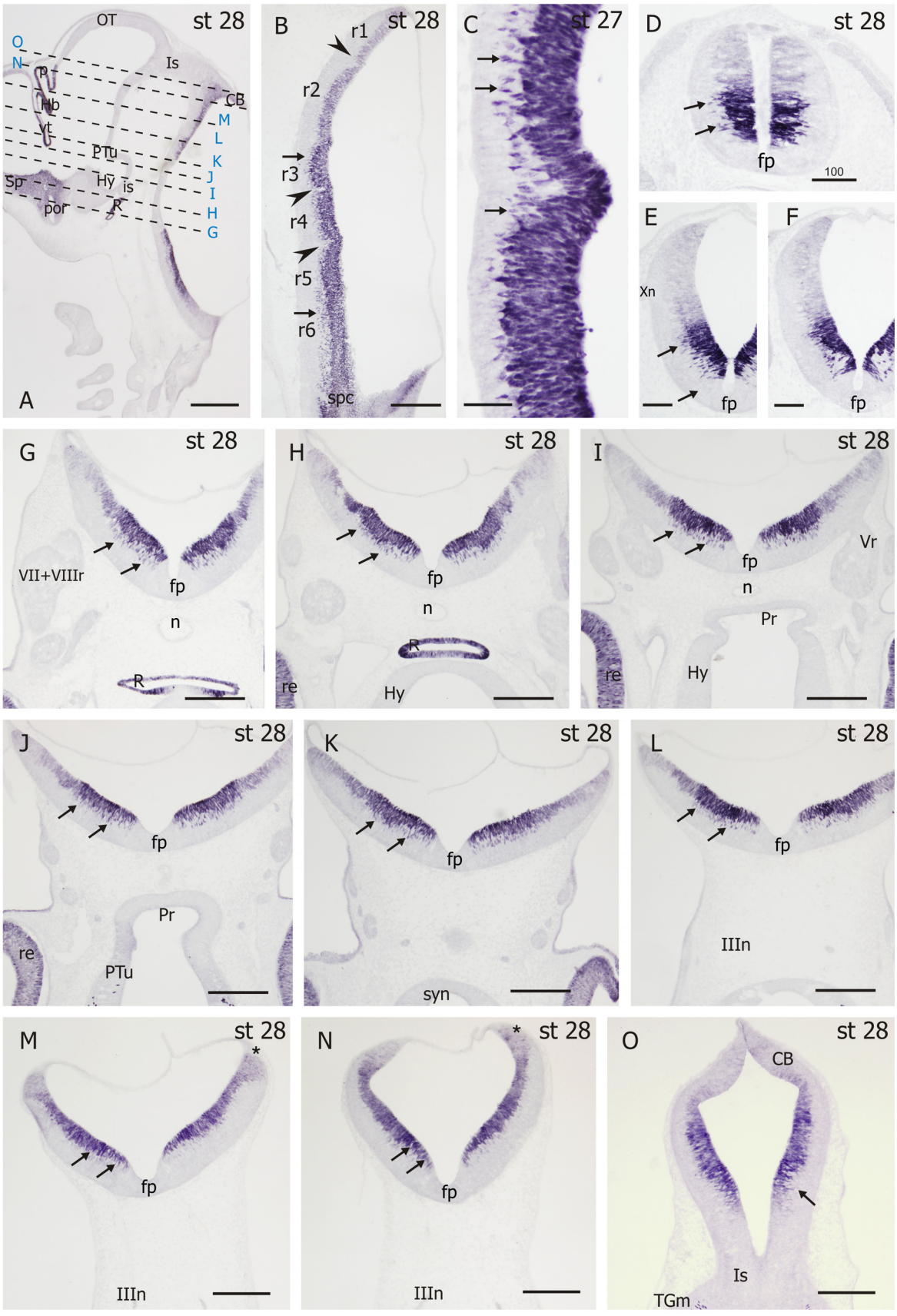

Figure 7. Sagittal (*A-C*,M,N) and transverse sections (D-L) through the *S. canicula* rhombencephalon at stage 31 after Pax6 immunohistochemistry. **A.** Panoramic view showing the lateral aspect of the rhombencephalon. The level of some transverse sections is indicated by dotted lines. **B,C**. Details of sagittal sections of the rhombencephalon at medial (B) and lateral (*C*) levels. Note abundant Pax6 cells in the tegmentum (in the VZ and IZ) and in the primordial cerebellar body. **D-L**. Transverse sections from caudal (D) to rostral (L) rhombencephalon, showing the three tegmental populations that appear to emerge from the Pax6 ventricular group at the dorsal basal plate (arrowheads): one that roughly lines the alar-basal boundary (red arrows); another that extends ventralwards in the caudal tegmentum (green arrows); and one located dorsolaterally to the medial longitudinal fascicle (yellow arrows). Open arrows in F-H indicate Pax6 cells at the rhombic lip ventral border. Black arrows in D-L indicate Pax6 cells in the marginal walls of the alar and basal plates. Note that at caudal rhombencephalic levels (D) these cells extend to the margin of the basal plate, and that at rostral levels (I-L) they appear to emerge from the Pax6 population of the rhombic lips. Red dotted lines in E-I indicate the putative alar-basal boundary. **M,N**. Details of the square areas outlined in B, showing the distribution of Pax6 cells at the rostral (M) and caudal (N) levels of the primordial cerebellar body. Note the abundant Pax6 cells in the VZ, which is thicker at caudal levels, and in the MZ (arrowheads). Scale bars: 500μm (*A*), 250 μm (B-N). For abbreviations, see list in Appendix A.

LATE SECOND PERIOD: RHOMBENCEPHALON

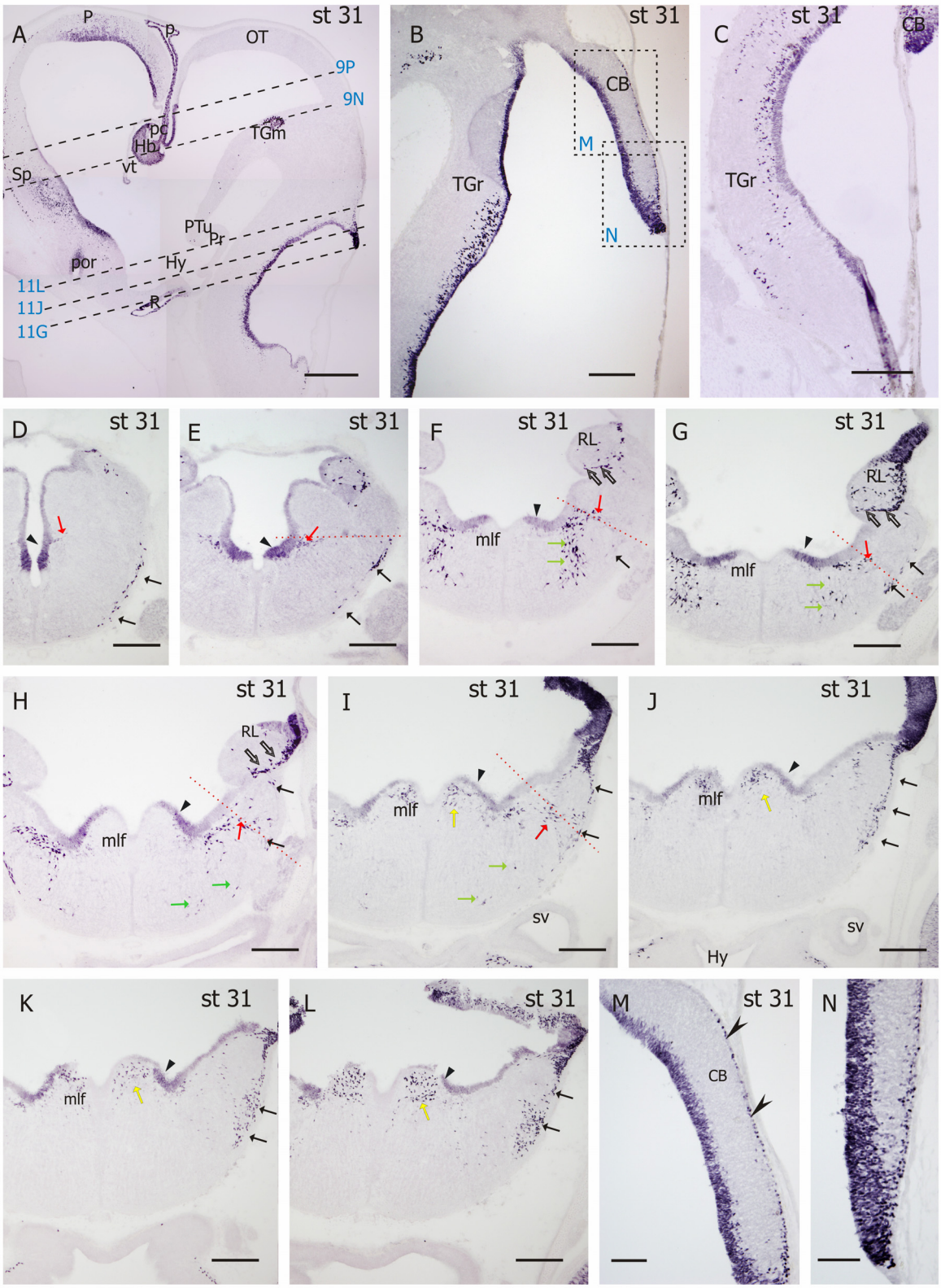

Figure 8. Sagittal (A-C, I) and cross (D-H) sections through the mesencephalon of *S. canicula* embryos at indicated stages after immunohistochemistry for Pax6. **A-C,I**. Pax6 cell group of the mesencephalic tegmentum (black arrows). First cells appear rostrally at S27 (A) to extent up to caudal levels as development proceeds (B,C). Note the continuity with the ventral Pax6 cell group of the synencephalon (white arrows). **D-F.** Details of the mesencephalic Pax6 cells from caudal (D) to rostral (F) levels. Note the intense immunostaining and radial orientation. Insets show panoramic views of the whole cross sections. **G,H**. Cross sections showing mesencephalic Pax6 cells (black arrows) forming bilateral strings that arch following the mesencephalic flexures. Line in I indicates the level of transverse section H. Scale bars: 500μm (insets in D-F), 250 μm (A-C, H,I), 100 μm (D-G). For abbreviations, see list in Appendix A.

SECOND PERIOD: MESENCEPHALON

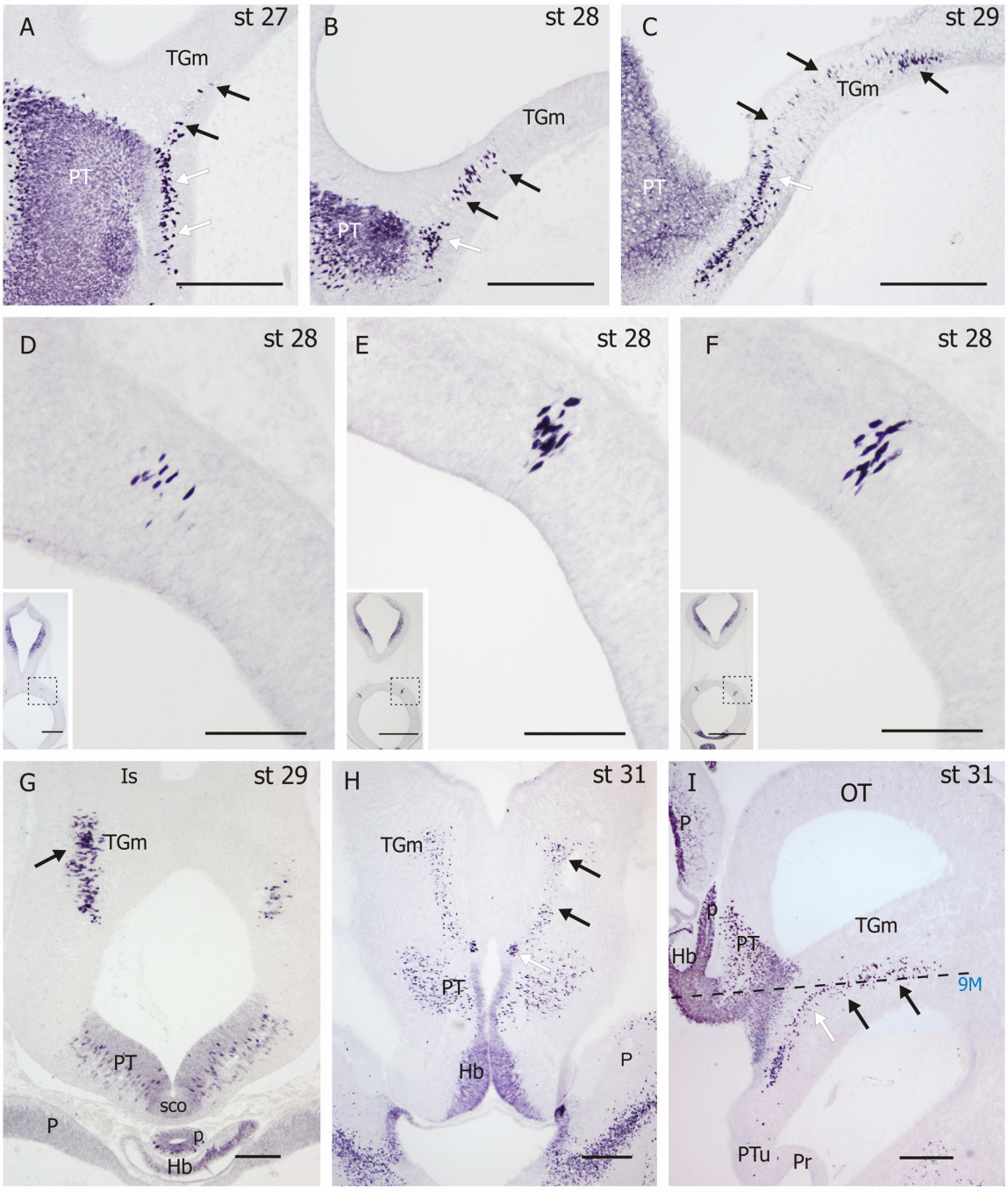

Figure 9. Sagittal (A,J,K) and transverse (B-I,L-P) sections through the prosencephalon of *S. canicula* at indicated stages after immunohistochemistry against Pax6. **A**. Sagittal section of stage 27 at a lateral level, showing the abundant Pax6 cells in the diencephalon and caudal telencephalon. White and black arrows label, respectively, the strip of Pax6 cells ventral to the prethalamus and pretectum. **B.** Cross section at the level indicated in A, showing the abundant Pax6 neuroepithelial cells in the pretectal and pallial Pax6 domains. Arrow indicates Pax6 cells in the mesencephalic tegmentum. Arrowhead indicates Pax6 cells between the olfactory pit and the telencephalon walls. **C-I**. Cross sections from caudal (C) to rostral (I), showing Pax6 expression in the pretectum. Arrows indicate the string of Pax6 cells ventral to the pretectal domain. Details of the organization of pretectal Pax6 are seen in D-F and H. **J,** Lateral sections of stage 29, showing Pax6 expression in the prosencephalon and the levels of the transverse sections in C-I. **K**. Sagittal section of stage 30 at a more medial level than J, indicating the transverse levels in L-P. **L-P.** Cross sections through the stage 31 diencephalon from caudal (L) to rostral (P) levels, showing the decrease in density of pretectal Pax6 cells relative to previous stages. Of note abundant Pax6 cells in the habenular VZ (M-P). Scale bars: 250μm (A,B,G,I-P), 100 μm (C-F, H). For abbreviations, see list in Appendix A.

SECOND PERIOD: CAUDAL PROSENCEPHALON

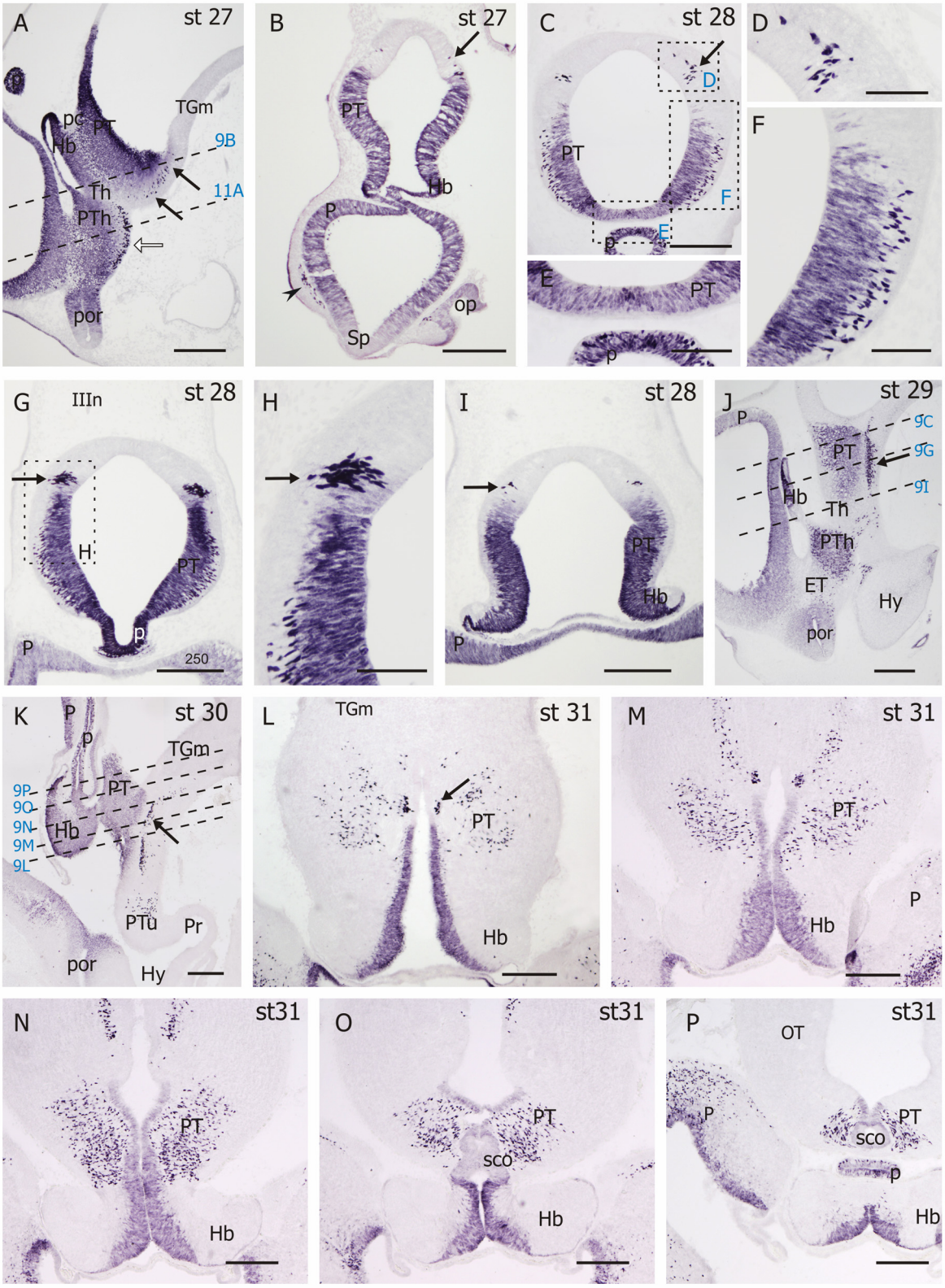

Figure 10. Sagittal (A,D-F) and transverse sections (B,C,G,H) through the *S. canicula* habenula after immunohistochemistry for Pax6. **A-B.** Sections showing Pax6 cells are abundant at rostral habenular levels (A) and in the VZ of the medial habenula (B). Arrowheads indicate Pax6 cells in the VZ in the lateral habenula. Note the continuity between the habenular and pretectal domains **C.** Cross section showing a slight asymmetric distribution of Pax6 cells, with the left habenula showing more Pax6 cells in the VZ of both the medial (arrows) and lateral regions (arrowheads) **D,E**. Sections showing the continuity between the habenula and pineal Pax6 domains at stage 30 (D) and 31 (E). Note the differences in the distribution of Pax6 cells in the pallium. **F-H.** Magnification of sections through the habenula, showing the abundant Pax6 cells in the VZ of the lateral habenula (arrowheads), and some loosely arranged Pax6 cells in the medial habenula IZ (arrows). Note the absence of Pax6 cells in the subcommissural organ (G), and abundant intensely immunostained cells in the pineal stalk (H). Panoramic views of G and H are seen in Figs. 9O and P. Scale bars: 250 μm (A,D,E-H), 100 μm (B,C). For abbreviations, see list in Appendix A.

SECOND PERIOD: CAUDAL PROSENCEPHALON

Habenula and Pineal Organ

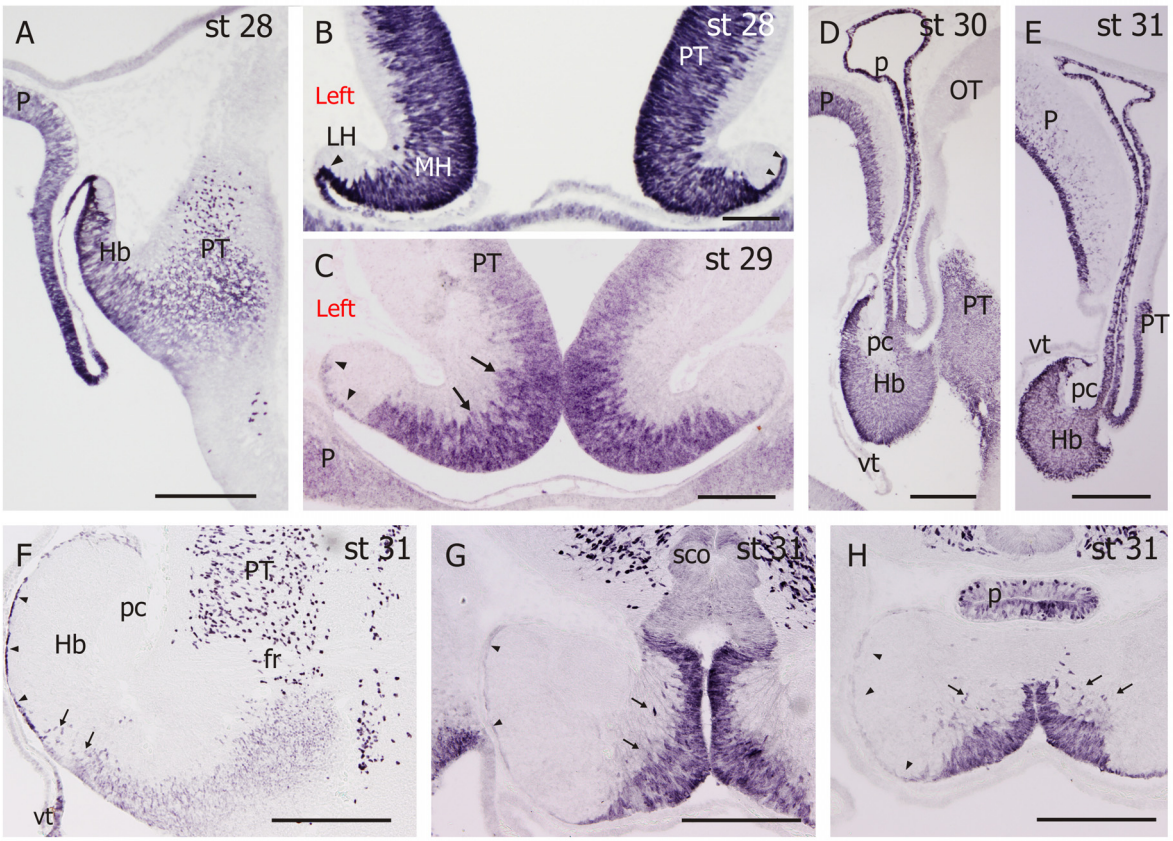

Figure 11. Sagittal (B,H-K,Q) and transverse (A,C-G,L-P) sections through the *S canicula* secondary prosencephalon at indicated embryonic stages after immunohistochemistry against Pax6 (A-P), and against Shh (Q). **A.** Abundant neuroepithelial Pax6 cells occupy the prethalamus. White arrow indicates marginal Pax6 cells at the interface with the posterior tubercle. Note the absence of Pax6 cells in the hypothalamus and subpallium. **B**. Parasagittal section through the prosencephalon showing the prethalamic Pax6 domain and its continuity through rostral (preoptic) and caudal (posterior tubercle) levels. Abundant and intensely labelled Pax6 cells are also seen in other diencephalic domains (pretectum and habenula). Note Pax6 expression in the dorsal portion of the optic stalk. White arrow indicates Pax6 cells in the ventral thalamus extending towards the preoptic area/posterior tubercle. Levels of cross sections C-G are also indicated by dotted lines. **C-F**. Cross sections through the rostral stage 28 diencephalon, showing the extension of the prethalamic Pax6 domain. White arrows indicate the ventral extension of prethalamic Pax6 cells towards the posterior tubercle. **G**. Pax6 cells in the preoptic area and optic stalk. Note the continuity with the rostral extension of the prethalamic group (white arrows). Intense Pax6 cells are also seen in the Rathke's pouch epithelium and retina. **H.** Panoramic view of the stage 29 diencephalon, showing the transverse level of figures 11L-O. **I**. Detail of squared area in H showing Pax6 cells in the prethalamus, and in the posterior tubercle bordering the inferior hypothalamic lobe walls (empty arrow), and extending to basal marginal regions (green arrows) . **J.** Adjacent section showing Pax6 cells in the posterior tubercle, bordering the dorsal wall of the inferior hypothalamic lobe (empty arrow) and extending to basal regions (green arrows). **K.** Section adjacent to J showing Pax6 cells in the ventral marginal walls of the posterior tubercle walls (green arrows). Note the absence of Pax6 cells in the hypothalamus. **L-P.** Transverse sections of the stage 31 rostral diencephalon from ventro-rostral (L) to dorso-caudal (P) levels. Pax6 cells are abundant in the VZ and IZ in the preoptic area (L, probably corresponding to the eminentia thalami), prethalamus (L,M) and in the posterior tubercle (M-O). Note Pax6 expression in the lateral walls of the preoptic recess and its continuity through the head of the optic stalk (O, P). Note in P a few Pax6 cells in the external walls of the hypothalamic lobes (open arrow?). **Q.** Sagittal section at the hypothalamus and rostral diencephalon of a stage 31 embryo showing Shh immunolabelling in the basal hypothalamus and in the zona limitans intrathalamica. In L-P, caudal is up and rostral down. Levels of cross sections N,O are indicated in Figure 2D. Scale bars: 250μm (A-I, L-R), 100μm (J,K). For abbreviations, see list in Appendix A.

SECOND PERIOD: CAUDAL PROSENCEPHALON and HYPOTHALAMUS

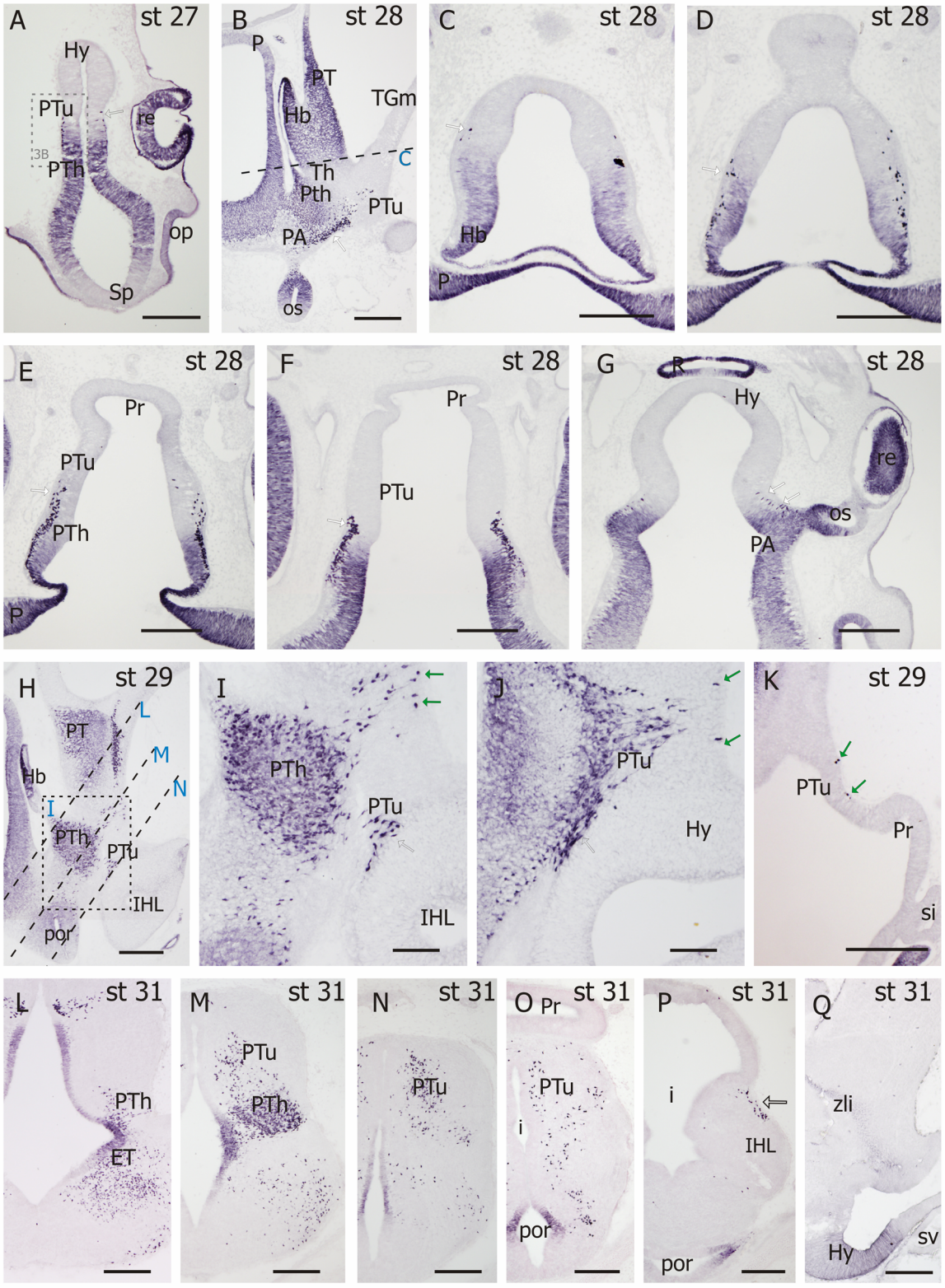

Figure 12. Sagittal (*A-C*, E-J) and transverse (D) sections through the *S. canicula* telencephalon at indicated embryonic stages after Pax6 immunohistochemistry. **A**. Midsagittal section showing Pax6 cells in the pallium and preoptic area. **B.** Lateral section showing the pallial Pax6 domain, as well as those in the diencephalon (prethalamus, habenula, pretectum). Of note, intensely immunostained Pax6 cells in the olfactory epithelium and in the dorsal walls of the optic stalk. Red arrows in **C-J** indicate Pax6 cells in the subpallial MZ. **C,D.** Magnifications showing the pallial-subpallial interface in sagittal (*C*) and transverse (D) sections. Arrowheads indicate the ventral portion of the pallium which contains weak labelled Pax6 cells except at marginal level. Of note intense Pax6 cells in the subpallial MZ (red arrows). Dotted red lines indicate the possible level of the pallial-subpallial boundary. **E-F**. Midsagittal (E) and lateral (F) sections showing differences in the Pax6 cell distribution in the pallium and subpallium at stage 30. **G.** Detail of the square area outlined in E, showing Pax6 cells in the pallial VZ, IZ and MZ. Note the weak labelling of Pax6 cells in the ventralmost pallium (arrowhead) and the continuity between the intense labelled Pax6 marginal cells of the ventral pallium and subpallium (red arrows). **H-I**. Midsagittal (H) and lateral (I) sections showing differences in the pallial and subpallial Pax6 cell distribution in the stage 31. Note the increased density of Pax6 cells in the pallial IZ with respect to previous stages. **J.** Detail of the square area outlined in H, showing the distribution of Pax6 cells at the pallial-subpallial boundary. Rostral is right and dorsal up in all the sagittal sections. Ventral is down and dorsal up in D. Scale bars: 250μm (*A*,B,E,F,H,I), 100 μm (*C*,D,*G*,J). For abbreviations, see list in Appendix *A*.

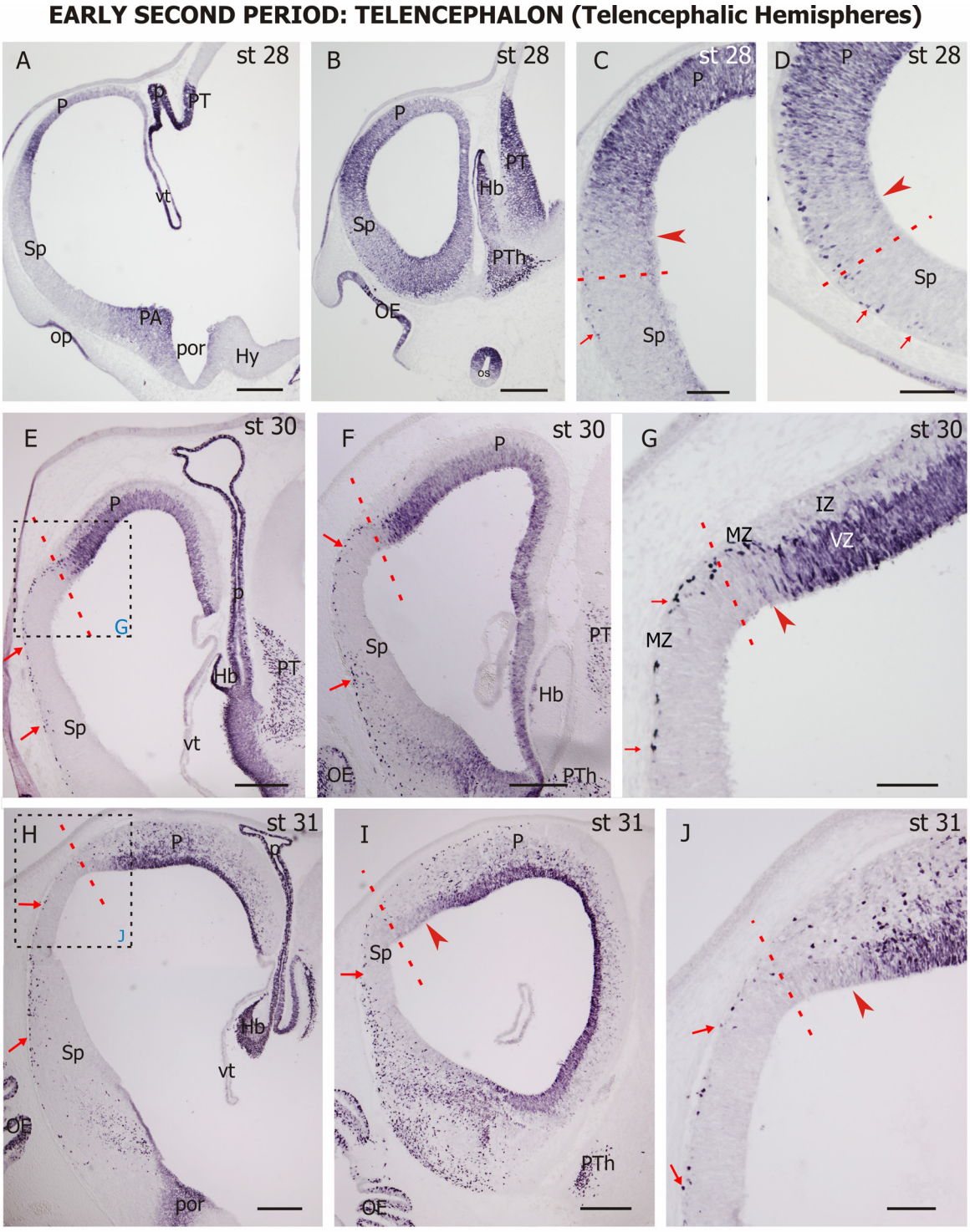
EARLY SECOND PERIOD: TELENCEPHALON (Telencephalic Hemispheres)
A
st 28
P
PT
vt
Sp
PA
op
por
Hy
B
st 28
P
PT
Hb
Sp
PTh
OE
os
C
st 28
P
Sp
D
P
st 28
Sp
E
st 30
P
G
Hb
PT
Sp
vt
F
st 30
P
PT
Sp
Hb
OE
PTh
G
st 30
IZ
MZ
VZ
MZ
H
st 31
P
J
Hb
Sp
vt
OE
por
I
st 31
P
Sp
PTh
OE
J
st 31

Figure 13. Sagittal sections through the telencephalon of *S canicula* at indicated stages after Pax6 immunohistochemistry (A,B,F), Pax6 *in situ* hybridisation (C,D) and after Shh immunohistochemistry (E). **A,B.** Adjacent sections at a lateral telencephalic level showing the similar distribution of Pax6 protein (A) and mRNA (B). **C,D.** Magnifications of the square areas outlined in A,B, showing Pax6 expression at the pallial-subpallial boundary. Arrows in A-D indicate subpallial Pax6 cells. **E,F**. Midsagittal sections showing the absence of Pax6 cells in the margin of the subpallial midline (E) where Shh is expressed (F). Note also Shh immunolabelling in the basal hypothalamus. Dotted black lines in E,F indicate the subpallial Shh domain. Dotted red lines indicate the pallial-subpallial boundary. Scale bars: 200μm. For abbreviations, see list in Appendix A.

SECOND PERIOD: TELENCEPHALON (Telencephalic hemispheres)

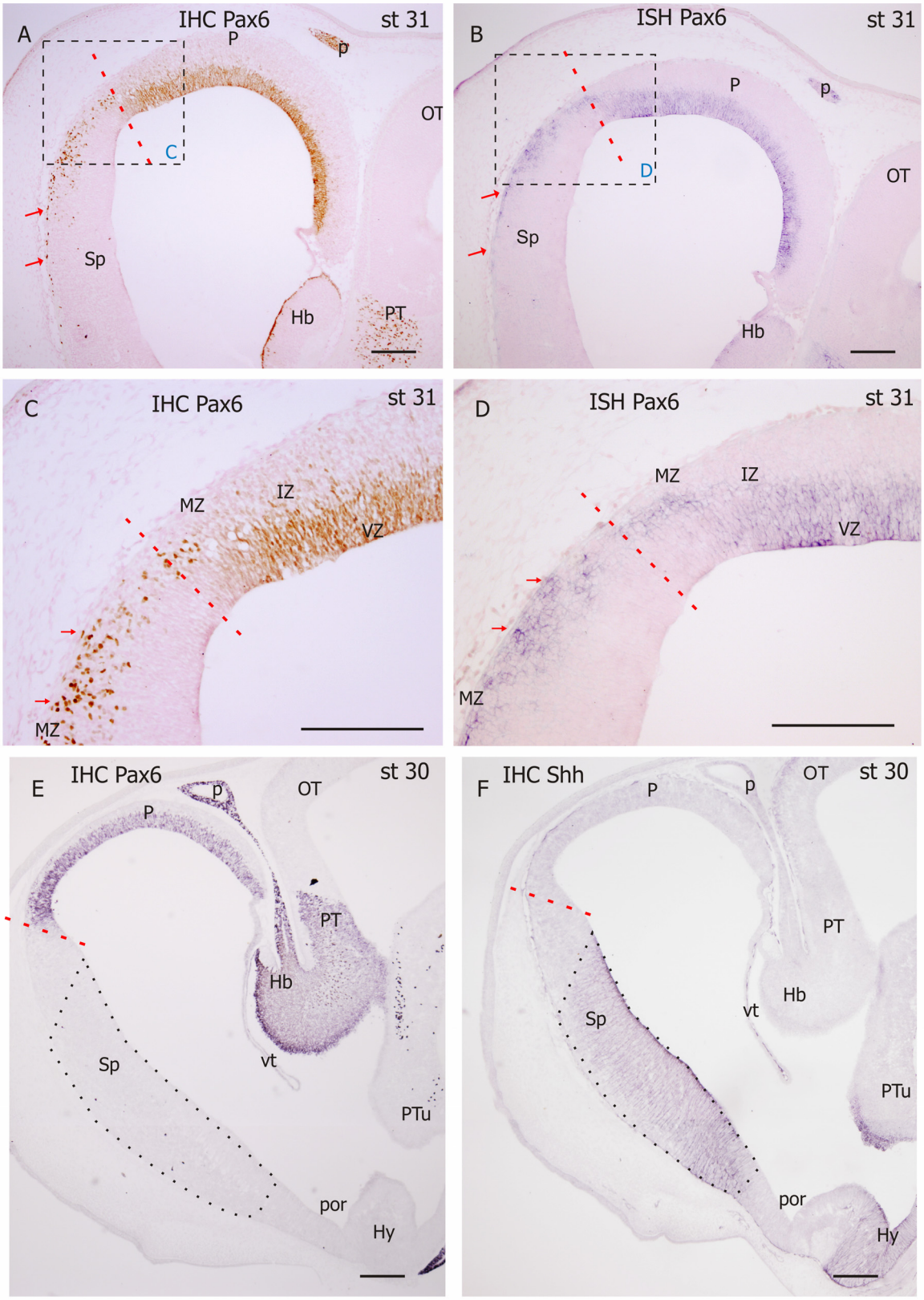

Figure 14. Transverse sections from the caudal (A) to rostral (L) levels of the *S. canicula* telencephalon at embryonic stage 31 after Pax6 immunohistochemistry. Dashed red lines indicate the possible pallial-subpallial boundary, and red arrows the string of Pax6 cells in the subpallial MZ. Dotted circles in A-H indicate a subpallial group of Pax6 cells just adjacent to the pallial-subpallial boundary. In C-I an asterisk indicates a laterodorsal group of Pax6 cells that appears to be continuous with the marginal stream of Pax6 cells (arrows). Of note abundant Pax6 cells in the primordial septal area (J,K), and in the periventricular pallial area (J-L). Note faint Pax6 cells in the olfactory bulbs in B-G. In F,G,J the brown labelling correspond to PCNA-immunopositive cells, see material and methods section in chapter 4. Scale bars: 250μm. For abbreviations see list in Appendix A.

LATE SECOND PERIOD: TELENCEPHALON (Telencephalic hemispheres)

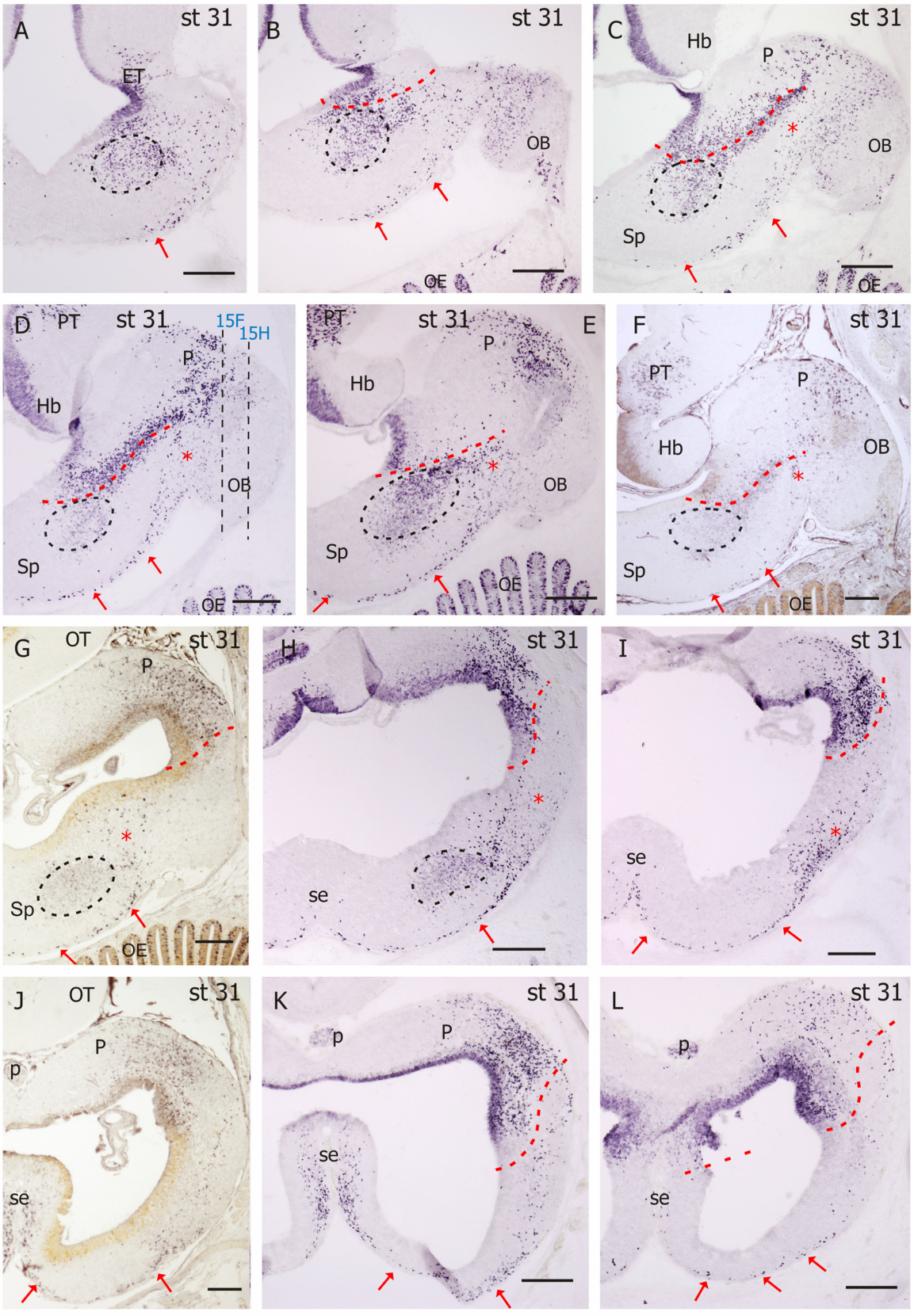

Figure 15. Parasagittal sections through the *S. canicula* telencephalon at indicated embryonic stages after Pax6 immunohistochemistry (*A*-D,F) and in situ hybridisation (E). Asterisk in B-E indicates the prospective/primordial olfactory bulb. Dotted red lines in B, D, E indicate the pallial-subpallial boundary. **A.** Lateral section through the telencephalon showing abundant Pax6 cells in the mostly neuroepithelial pallial walls. Note the proximity with to the primordial olfactory epithelium and the string of Pax6 cells that extend between the olfactory organ and the telencephalon (arrowheads). **B.** Lateral section at a level comparable to that in *A* but at stage 30 showing the incipient developing bulb (asterisk) in the region between the pallium and subpallium. ***C.*** Magnification of the square area outlined in B, showing the distribution of Pax6 cells. **D.** Section more lateral to that in D through the stage 31 telencephalon, showing the interface between the primordial olfactory bulb and the pallium **E.** Section parallel to D, showing the same distribution of the Pax6 mRNA. Dotted red lines in D,E indicate the pallial-subpallial boundary. **F.** Section through the developing olfactory bulb, showing abundant Pax6 cells dorsally, but scarce Pax6 cells ventrally (large arrowhead). Small arrowheads indicate Pax6 cells in between the olfactory organ and the telencephalic walls (see chapter 2). Level of transverse sections D-F is indicated in Fig. 14D. Scale bars: 250 μm (*A*, B,D-F), 100 μm (*C*). For abbreviations, see list.

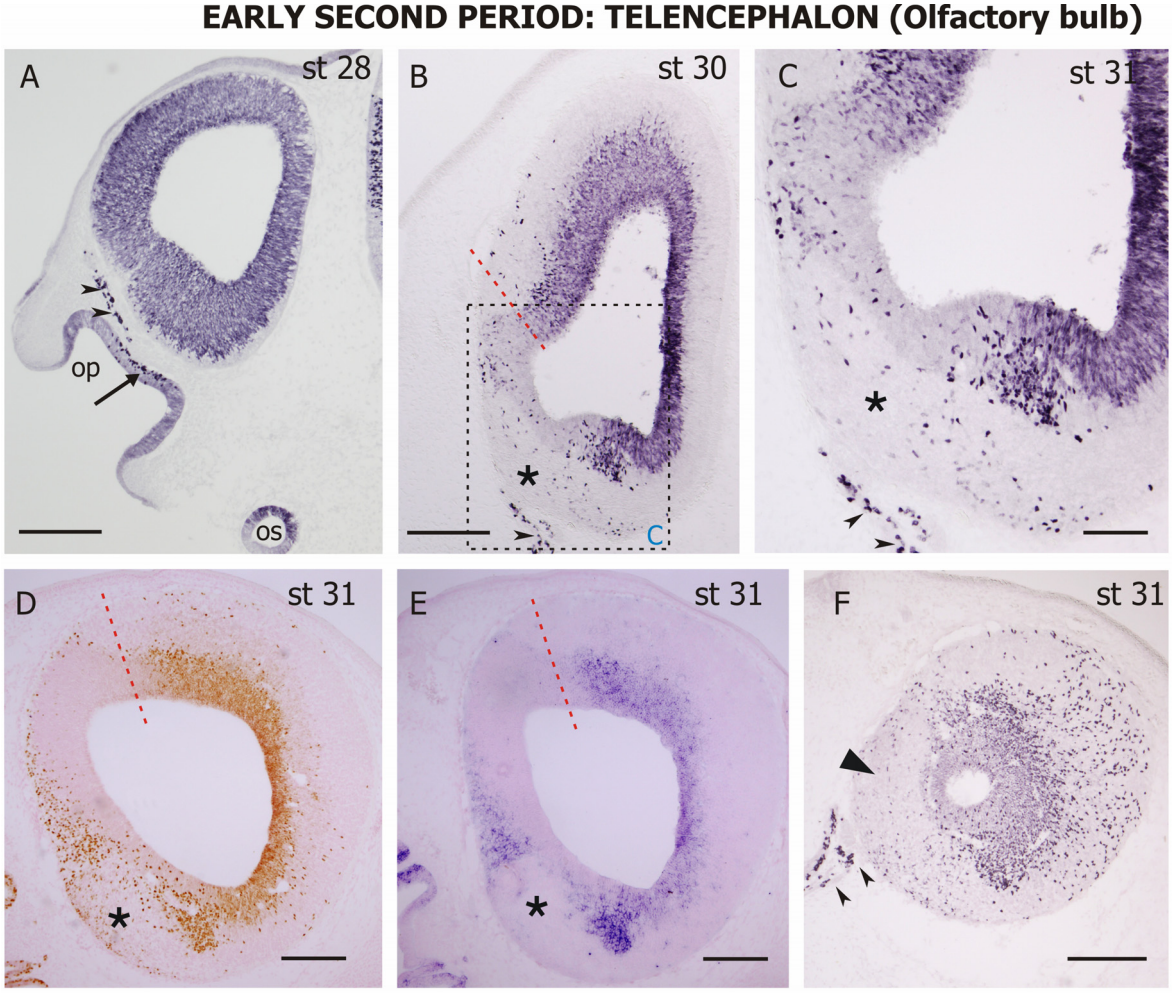
EARLY SECOND PERIOD: TELENCEPHALON (Olfactory bulb)
A
st 28
op
os
B
st 30
C
C
st 31
D
st 31
E
st 31
F
st 31

Figure 16. Transverse sections through the rostral spinal cord (A,B) and rhombencephalon from caudal (C) to rostral (N) levels of *S. canicula* embryos at stage 32 after IHC for Pax6. **A-D**. Panoramic views (A,C) and magnifications (B,D) of the rostral spinal cord (A,B) and caudal rhombencephalon (C,D) showing Pax6 cells in the VZ of the basal plate (arrowheads), and in the MZ extending to the basal plate (black arrows). **E-N**. Transverse sections showing different Pax6 cell populations: red arrows in E-J indicate the Pax6 cell group roughly lining the alar-basal boundary; green arrows in H-J indicate Pax6 cells extending ventralwards; yellow arrows in K,L indicate the Pax6 cell population dorsolateral to the medial longitudinal fascicle; open arrows indicate Pax6 cells in the medial walls of the viscerosensorial lobe (E-J) and black arrows indicate their rostral extension in the marginal walls of the alar and dorsal basal plates (K,L). White arrow in M indicates the Pax6 group surrounding the caudal interpeduncular nuclei. Small white arrows in M and N indicate the Pax6 cell group extending mediolaterally in the dorsalmost basal plate. Note abundant Pax6 cells in the cerebellar body and auricular lobe in F,H-N. Scale bars: 250 μm. For abbreviations, see list in Appendix A.

THIRD PERIOD: RHOMBENCEPHALON

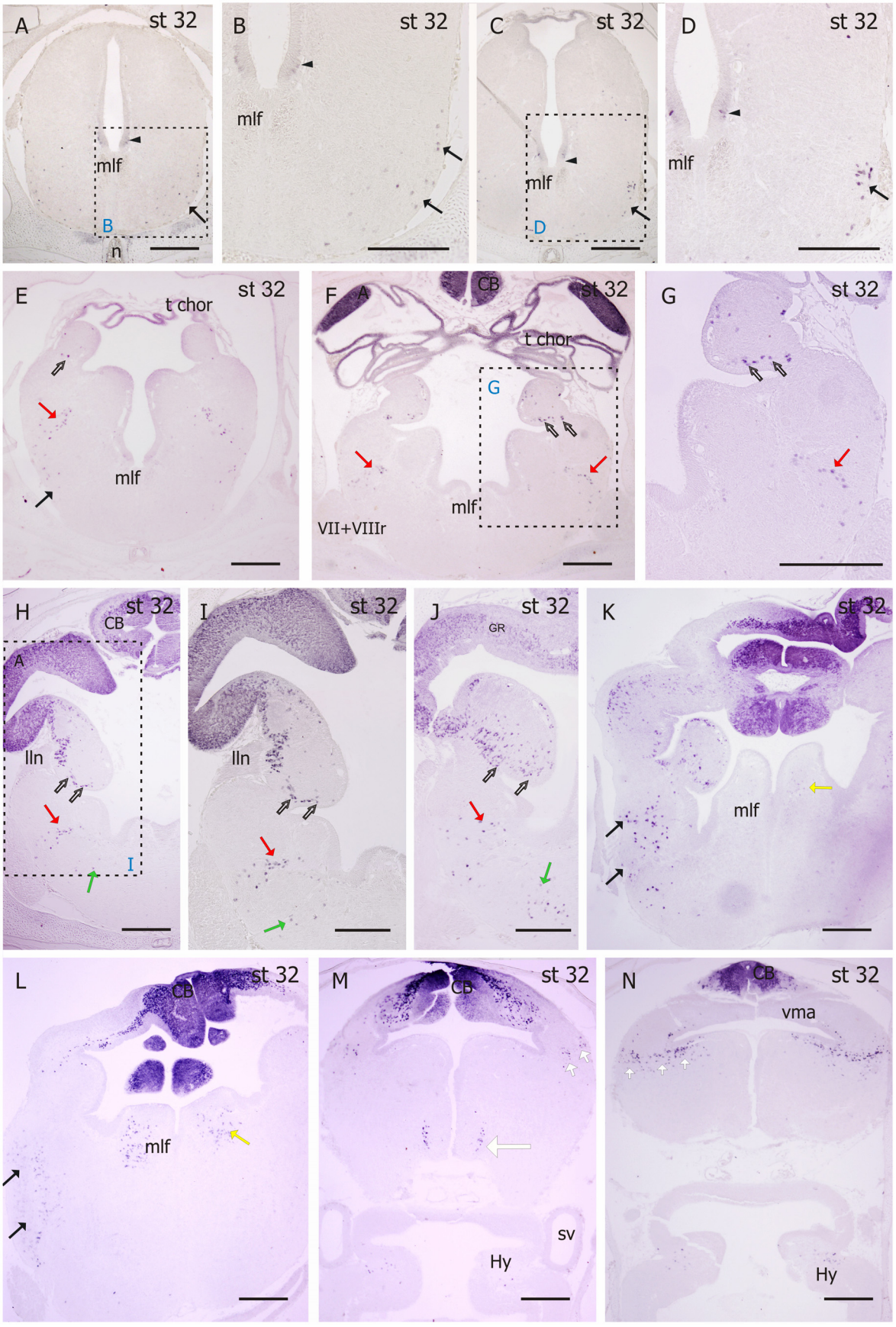

Figure 17. Sagittal (A,B) and transverse sections through the rhombencephalon of *S. canicula* at indicated stages after Pax6 immunohistochemistry. **A**. Panoramic view showing the lateral aspect of the juvenile rhombencephalon. Note the different Pax6 cell populations in the tegmentum, and the abundant Pax6 cells in the cerebellar granular layer. **B.** Detail of a sagittal section at a more medial level than A. Arrowheads indicate the Pax6 cell group at the central grey level. **C-D.** Transverse sections through the caudal rhombencephalon of juveniles, showing the tegmental Pax6 groups: roughly lining the alar-basal boundary (red arrows) and medial to the octavolateral lobe (open arrows). Black arrows indicate Pax6 cells in the marginal walls of the alar and dorsal basal plates. Note abundant Pax6 cells in the auricular granular layer. **E.** Pax6 cells in the adult rhombencephalic tegmentum, in the medial walls of the octavolateral lobe (open arrows). **F**. Magnification of the square area outlined in E. **G-I.** Transverse sections through the rostral juvenile rhombencephalon. In G, open arrows indicate Pax6 cells in the medial walls of the octavolateral lobe, black arrows indicate marginal Pax6 cells, and green arrows indicate Pax6 cells extending ventralwards. In H,I yellow arrow indicates the Pax6 group dorsolateral to the medial longitudinal fascicle and white arrow the Pax6 cell group surrounding the caudal interpeduncular nucleus in the rostralmost rhombencephalic tegmentum/isthmus region. Note the abundant Pax6 cells in the cerebellar paramedian eminences. Scale bars: 500 μm (A), 250 μm (B-E, G-I), 100 μm (F). For abbreviations, see list in Appendix A.

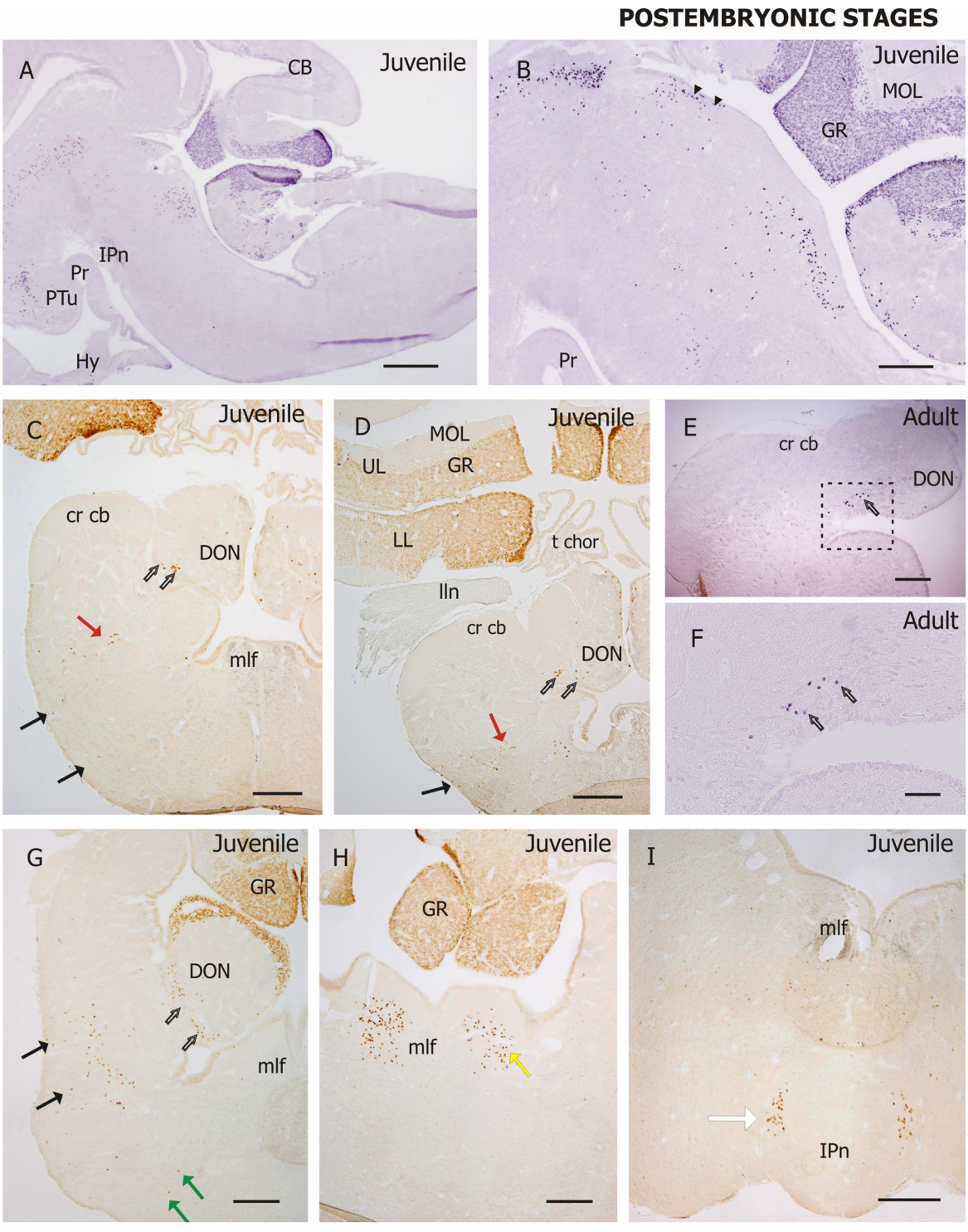
POSTEMBRYONIC STAGES
A
Juvenile
CB
IPn
Pr
PTu
Hy
B
Juvenile
MOL
GR
Pr
C
Juvenile
cr cb
DON
mlf
D
Juvenile
MOL
UL
GR
LL
t chor
lln
cr cb
DON
E
Adult
cr cb
DON
F
Adult
G
Juvenile
GR
DON
mlf
H
Juvenile
GR
mlf
I
Juvenile
mlf
IPn

Figure 18. Sagittal (A,F) and transverse (B-E,G-J) sections through the mesencephalon and prosencephalon of *S. canicula* after Pax6immunohistochemistry. **A,F.** Panoramic views of sagittal sections of the stage 32 (A) and juvenile (F) specimens, showing the permanence in the distribution of mesencephalic and prosencephalic Pax6 cell groups. Note the conspicuous Pax6 cell domains in the mesencephalic tegmentum, pretectum and prethalamus. White arrows indicate the stripe of Pax6 cells ventral to the pretectum. Lines in A indicate the level of transverse sections in C-F. **B.** Section through the basal prosencephalon and hypothalamus, showing scattered Pax6 cells in the dorsal walls of the inferior hypothalamic lobes, as well as in the hypophysis. Note the absence of Pax6 cells at this caudal mesencephalic level. **C.** Section through the mesencephalic tegmentum, showing the Pax6 cell group that extends along the putative alar-basal boundary. Note also Pax6 cells in the posterior tubercle. **D.** Section through the caudal prosencephalon, showing the conspicuous Pax6 populations in the pretectum and prethalamus. Note the contrast with the Pax6 immunonegative thalamus and the Pax6 cells extending into the preoptic area. **E**. Transverse section at rostral diencephalic levels, showing Pax6 cells in the VZ in the habenula, pineal and subcommisural organs, and in the eminentia thalami. Note also abundant Pax6 cells in the telencephalic regions next to the olfactory bulb. **F**. Panoramic view of the juvenile prosencephalon and mesencephalon (see above). Black arrows indicate Pax6 cells in the habenula. **G-J.** Transverse sections from caudal (G) to rostral (J) prosencephalon of adults, showing Pax6 cells in the prethalamus, pretectum and subcommissural organ (G,H), and in the habenula and pineal organ (I,J). H and J are magnifications of G and I, respectively. Scale bars: 500 μm. For abbreviations, see list in Appendix A.

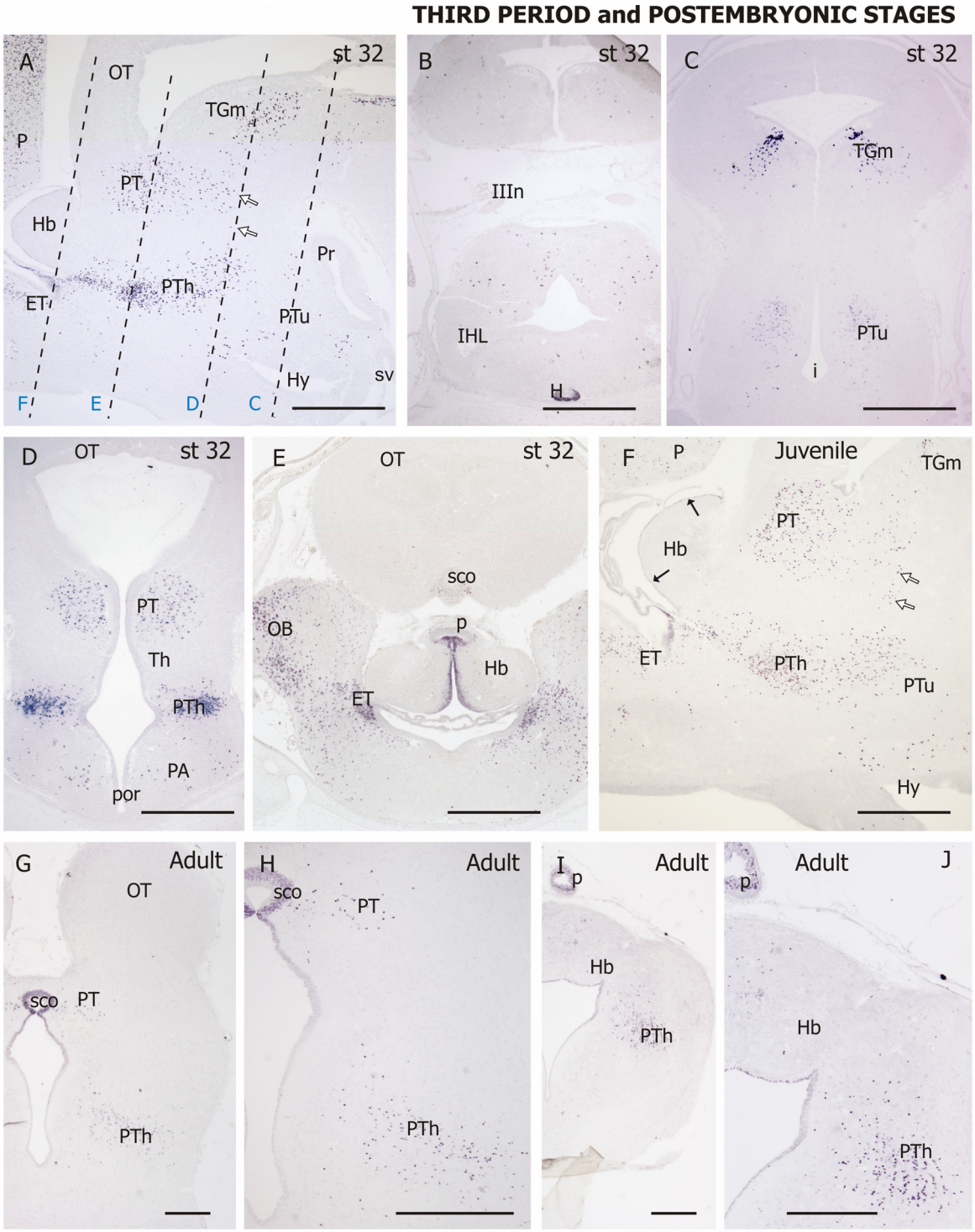
THIRD PERIOD and POSTEMBRYONIC STAGES
A
st 32
OT
TGm
P
PT
Hb
Pr
ET
PTh
PTu
Hy
sv
F
E
D
C
B
st 32
IIIn
IHL
H
C
st 32
TGm
PTu
i
D
OT
st 32
PT
Th
PTh
PA
por
E
OT
st 32
sco
OB
p
Hb
ET
F
P
Juvenile
TGm
PT
Hb
ET
PTh
PTu
Hy
G
Adult
OT
sco
PT
PTh
H
Adult
sco
PT
PTh
I
Adult
p
Hb
PTh
Adult
J
p
Hb
PTh

Fig 19. Transverse sections through the telencephalon of *S. canicula* at indicated stages after Pax6 immunohistochemistry. **A,B**. Panoramic view and detail of telencephalon, showing abundant Pax6 cells in the pallium dorsal, medial and lateral and scarce to moderate Pax6 cells in subpallial the marginal (arrows), dorsolateral (dotted lines), lateral (asterisk) and septal (se) areas. Note the intense labelling of the olfactory epithelium which contrasts with the less abundant Pax6 cells in the olfactory bulb. **C,D.** Panoramic view and detail of a section through the juvenile telencephalon at a level comparable to that of A. Note abundant Pax6 cells in the pallium, olfactory bulb, and in the subpallial lateral area and in the septum (se). The band of Pax6 cells associated with the pallial-subpallial boundary is not recognized. **E,F**. Panoramic and detail of a section through the adult telencephalon showing Pax6 cells in the dorsal pallium, striatum, and in the olfactory bulb. Scale bars: 500 μm. For abbreviations, see list in Appendix A.

THIRD PERIOD and POSTEMBRYONIC STAGES: TELENCEPHALON

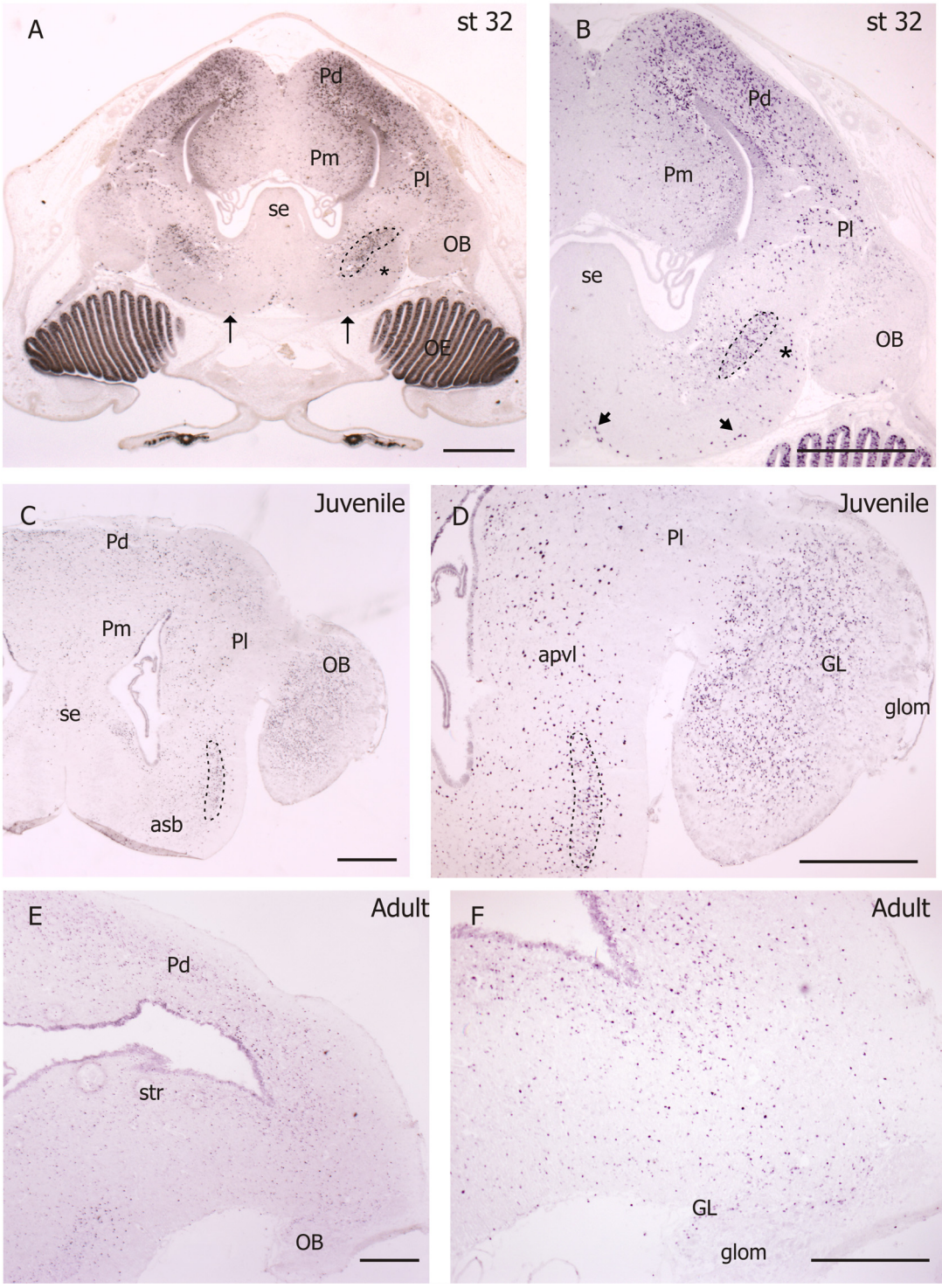

Chapter 2.

Pax6 expression in the developing olfactory system of a shark: evidence of expression in peripheral cells

INTRODUCTION

The primary olfactory system in vertebrates consists of a neuroepithelium (the olfactory epithelium) with receptor neurons (the olfactory receptor neurons) whose axons converge in the olfactory nerve and run to the telencephalic walls (olfactory bulbs). The olfactory epithelium develops from the olfactory placodes, which are thickenings of the head ectoderm that invaginate to form the nasal (olfactory) pit and the nasal organ, which eventually became folded to form the olfactory *lamellae* consisting of different types of sensory neurons and non-sensorial cells. First olfactory receptor neurons are derived from neuroblasts differentiating in the olfactory placodes, and from these early cells the olfactory axons extend to the primordial olfactory bulbs.

The olfactory system has been considered a good model for studying the role of Pax6 as it is expressed in its different components at different developmental stages. During development of the mouse, strong Pax6 expression is first observed in cells of the nasal placode and pit, and later in the developing olfactory epithelium and olfactory bulb (Walther and Gruss, 1991; Stoykova and Gruss, 1994; Grindley et al., 1995; Davis and Reed, 1996). Moreover, studies of Pax6 mutants such as *Small eye (Sey)* have revealed that Pax6 is necessary for normal development of the olfactory system, as homozygous mutant mice (*Sey/Sey*) fail to form nasal placodes and olfactory bulbs (Thieler et al., 1978; Hogan et al., 1986; Hill et al., 1991; Grindley et al., 1995; Jiménez et al., 2000) and in heterozygote mice (*Sey/+*) development of the main olfactory bulb, but not the olfactory epithelium, is dramatically altered (Dellovade et al., 1998). These findings have led to the suggestion that Pax6 plays pivotal roles during development of the olfactory system, and that it is involved in nasal placode induction, differentiation of the olfactory epithelium and development of the olfactory bulb (reviewed in Nomura et al., 2007). It is not clear whether these roles apply to other vertebrates because no similar studies have been carried out in other groups.

In cartilaginous fishes, the olfactory bulbs are well developed, as corresponds to animals with a highly developed sense of smell. Classic neuroanatomists considered that the entire shark telencephalon was involved in olfaction ("rhinencephalon"), but this idea was discounted after it was found that the olfactory information only reaches restricted regions of the telencephalon (Hofmann and Northcutt, 2008). The olfactory bulb of elasmobranchs has been considered an excellent model for the study of the olfactory network in fishes (Dryer and

Graziadei, 1993). In fact, structural and ultrastructural studies of the organization of the elasmobranch olfactory bulbs and olfactory epithelium are rather numerous (Theisen et al., 1986; Dryer and Graziadei, 1993, 1994a, 1996; Takami et al., 1994; Ferrando et al., 2006a,b, 2007a; Schluessel et al., 2008). In contrast, developmental studies are very scarce and mainly concerned with the olfactory epithelium (Fishelson and Baranes, 1997; Ferrando et al., 2007b) and olfactory placode, in which expression of some developmental genes has been reported (Sauka-Spengler et al., 2001; O'Neill et al., 2007).

In order to know how *Pax6* is involved in the development of the olfactory system in cartilaginous fishes, we studied the expression of Pax6 in the different components of the olfactory system (olfactory epithelium, olfactory nerve and olfactory bulb) in the lesser spotted catshark *Scyliorhinus canicula,* which is an important fish model in studies of vertebrate development (Coolen et al., 2009). We applied both *in situ* hybridisation and immunohistochemical techniques, the latter yielding the best cellular details. The results shed light on the development of the olfactory system in cartilaginous fish and provide evidence for highly conserved roles of Pax6 in the early and late development of the olfactory structures.

MATERIAL AND METHODS

Experimental animals

Embryos, juveniles and an adult specimen of *S. canicula* were obtained and processed as mentioned in Chapter 1. The following embryonic stages were analysed: stage 25 (4 embryos), stage 27 (3 embryos), stage 28 (3 embryos), stage 29 (4 embryos), stage 30 (4 embryos), stage 31 (7 embryos), and stage 32 (6 embryos). In addition, 3 juveniles (total length from 10 to 14 cm) and 1 adult (about 50 cm total length) were also used.

Tissue preparation

After fixation and sectioning tissue was processed either by immunohistochemistry with a polyclonal anti-Pax6 antibody (Covance, Emeryville, California) or by *in situ* hybridisation with a *ScPax6* probe (Derobert et al., 2002). For further details see material and methods section in Chapter 1.

RESULTS

Pax6 expression during early stages of the olfactory organ development.

In *S. canicula*, the olfactory placode becomes morphologically visible at stage 20 (Sauka-Spengler et al., 2001) and starts to invaginate to form the olfactory pit at stage 22 (O'Neill et al., 2007). These early embryonic stages were not examined in the present study. At stage 25, the earliest we analysed, the olfactory placode was further invaginated, already forming the olfactory pit, where faint Pax6-expression was observed (Figs. 1A). At this early stage, Pax6-expressing cells (hereafter, Pax6 cells) were sparse or formed small clusters at the more basal part of the olfactory pit epithelium (arrows in Fig. 1B). Interestingly, similar Pax6 cells were also observed at the periphery of the olfactory pit and formed a conspicuous string that extended between the pit and the external surface of the rostral forebrain (arrowheads in Fig. 1B). Similar Pax6 expression was also observed in subsequent stages, in which the olfactory pit became expanded to form a wide sac with smooth walls (Figs. 1C-E). The density of Pax6 cells in the olfactory epithelium increased at these stages, but the cells continued to be located at the more basal part (Figs. 1C-E). Streams of peripheral Pax6 cells continued to extend at some distance between the nasal epithelium and the forebrain, following the prospective olfactory nerve (arrowheads in Fig. 1D,F,G). Pax6 cells located basally in the olfactory pit and along the peripheral stream were similar in morphology, size and intensity of labelling, and differed from the moderately labelled Pax6 cells of the brain walls (Figs. 1B,D,F,G).

Pax6 expression in olfactory lamellae

The first folds of the olfactory epithelium occurred at stage 29 and the characteristic *lamellae* of the elasmobranch olfactory organ (Theisen et al., 1986; Takami et al., 1994) appeared progressively and became symmetrically organized with respect to a raphe (Fig. 2A). From here onwards, the surface area of the olfactory epithelium was increased greatly by the numerous primary *lamellae* arranged in parallel (Figs. 2B-F) and by the secondary folds of lamellae that were first observed at late stage 32 (Figs. 2G-I), and numerous in adults (Figs. 2J,K). During the first stages of formation of *lamellae*, Pax6 cells were observed at different levels of the epithelium among negative cells (Fig 2B) but later were more abundant and became intensely labelled in the basal part of the epithelium, although they also occupied

intermediate and even apical levels (Fig. 2F,H,I). Pax6 cells were also numerous in the olfactory epithelium of adults, and were mainly located at the basal part of the epithelium (Figs. 2J,K).

Pax6 expression in cells along the olfactory nerve

As the surface area of the olfactory epithelium increased due to the appearance of *lamellae*, the density of Pax6 cells located along the olfactory nerve also increased. These cells mainly formed longitudinal groups along the entire course of the nerve (Figs. 3A). Pax6 cells in the nerve showed similar characteristics to those of the olfactory epithelium and were observed as just adjacent to the *lamellae* as along the thin olfactory fascicles that exit from the *lamellae* (Fig. 3B), which suggests a similar origin. These Pax6 cells were observed even at distal nerve levels, just at the entrance of olfactory nerve bundles in the forebrain (Figs. 3C,D). At early stage 31, peripheral Pax6 cells were very scarce along the distal part of the olfactory tract (black arrowhead in Fig. 3E), and at the most external region of the primordial olfactory bulb (see below) where the olfactory fibres will form the early olfactory glomeruli (white arrowheads in Fig. 3E).

Pax6 expression in the olfactory bulb

At early stage 31, the primordial olfactory bulbs were recognizable as lateroventral protrusions of the primordial dorsal telencephalon (pallium). At this stage, no Pax6 cells were observed in inner regions of the olfactory bulb (primordial granular/mitral cell layers; asterisk in Fig. 3E), which contrasted with the abundant Pax6 cells observed just dorsally, in that appeared to correspond to the lateral/ventral pallium. Interestingly, at stage 32, when the main regions of the mature olfactory bulb become recognizable, some scattered and faintly labelled Pax6 cells appeared in the developing granular layer (Fig. 3F); the density of these cells increased as development proceeds. Eventually, numerous Pax6 cells occupied the granular layer in the well developed olfactory bulbs of juveniles (Fig. 3G) but their density was considerably reduced in adults (Fig. 3H). No Pax6 were observed in the glomerular layer of juveniles and adults (Figs. 3F-H).

DISCUSSION

In the present study we show that in sharks, as in other vertebrates, Pax6 is expressed in the developing olfactory epithelium and olfactory bulb. More interestingly, we show, for the first time, evidence for the existence of Pax6 cells along the course of olfactory nerve bundles.

The existence of Pax6-expressing cells in the developing olfactory epithelium appears to be a rather common feature in vertebrates. In mouse, Pax6 cells were reported in the developing olfactory epithelium, from the relative primitive olfactory pit stage (E10.5) to the adult-like nasal structure (E18.5) (Walther and Gruss, 1991; Stoykova and Gruss, 1994; Grindley et al., 1995). In *Xenopus*, Pax6 cells were also located in the olfactory placode of late embryos and in the olfactory epithelium of hatched larvae (Reiss and Burd, 1997; Franco et al., 2001). In zebrafish, scattered Pax6 cells were observed in the olfactory epithelium of 2-day old embryos, and remained at a lower density in postembryonic 5-day-old specimens (Wullimann and Rink, 2001). In the present study, we report Pax6 cells in the *S. canicula* olfactory epithelium, from its early development until adulthood, which strongly extends the relevance of this transcription factor in the adult olfactory system of gnathostomes. Probably, this is a highly conserved trait that appeared in evolution earlier than vertebrates as Pax6 expression was observed in the head surface ectoderm of the cephalochordate amphioxus from which primary sensory neurons develop (Glardon et al., 1998). These authors have related the expression of *AmphiPax6* in the anterior epidermis of embryos with the development of an olfactory epithelium.

Chimeric analysis in mice showed that functional Pax6 is absolutely required during the early stages of differentiation of the invaginating olfactory epithelium (Collinson et al., 2003). Likewise, the pattern of Pax6 expression we have observed in *S. canicula* during the olfactory pit stage, with a weak and homogeneous labelling in the primordial nasal epithelium suggests that Pax6 may be playing a role in the nasal placode invagination. Moreover, the appearance of scattered intensely labelled Pax6 in the early folds of the *S. canicula* olfactory epithelium and its increasing density concurrently with the formation of *lamellae* suggest a role of Pax6 in the differentiation of the nasal epithelium. In particular, Pax6 may be involved in the formation of new cells as, when lamellar development proceeded, Pax6 cells became restricted to the basal part of the epithelium, where the basal proliferating (stem) cells of

are located (Theisen et al., 1986). Also in mouse, the process of stratification of the olfactory epithelium has been related to the segregation of Pax6 cells to the basal and apical poles of the epithelium to form, respectively, basal and sustentacular (support) cells (Davis and Reed, 1996; Behrens et al., 2000). At difference with mice, as the *S. canicula* olfactory epithelium differentiates, Pax6 cells remain segregated only in the basal cell layer. Expression of Pax6 in most *S. canicula* basal cells, even in the adult olfactory epithelium, may be related to the possible involvement of Pax6 in the control of proliferation and differentiation, as suggested for the rat dentate gyrus and the retina (Maekawa et al., 2005; Hsieh and Yang, 2009).

Although Pax6-expressing cells are consistently present in the olfactory epithelium of other vertebrates, as far as we know there are no reports of the presence of Pax6 cells exiting the olfactory epithelium toward the mesenchyma, or coursing along the olfactory nerve of any vertebrate. The existence of cells originated in the olfactory neuroepithelium that migrate towards the forebrain during embryonic development is well known in mammals and other vertebrates (for a review, see Fornaro et al., 2001). At least four types of migratory olfactory placode-derived cells have been described in mouse: ensheathing (glial) cells, luteinizing hormone-releasing hormone (LHRH)-producing neurons, olfactory receptor neurons and dorsally migrating neurons that course through the mesenchyma and follow a path not associated with any fibre and involved in neocortical development (Valverde et al., 1993; De Carlos et al., 1995, 1996). Moreover, migrating neurons from the olfactory epithelium to the telencephalon were observed during early differentiation of the chick olfactory placode (Fornaro et al., 2001, 2003). In the present study, the early appearance of peripheral Pax6 cells appeared concurrently with early stages of olfactory nerve development, and they were especially evident during stage 30, just before development of the olfactory bulb (at stage 31). The presence of peripheral Pax6 cells from early developmental stages, concurrently with the presence of Pax6 cells in the olfactory pit/epithelium, and the similarities in morphology and intensity of labelling between them (peripheral and epithelial cells) are compatible with a placodal origin for these cells. These may be young (postmitotic) neurons similar to those observed migrating from the early olfactory epithelium towards the telencephalon in the chick (Fornaro et al., 2001, 2003). Moreover, the fact that Pax6 cells mainly formed strings on the nerve surface (see Figs. 3B,C) indicates that they may be involved in the development of the olfactory nerve. In fact,

the cells may correspond to the early olfactory receptor neurons that extend along the developing olfactory nerve after leaving the olfactory epithelium in the developing mouse (Valverde et al., 1993; De Carlos et al., 1996). As proposed for peripheral olfactory neurons in mammals (Valverde et al., 1993; De Carlos et al., 1996), peripheral Pax6 cells of *S. canicula* may also serve as "guidepost" cells for olfactory axons in their trajectory to the olfactory bulb. The possibility that these cells are glial in nature, and perhaps related to the olfactory ensheathing glia, which is active in guiding the olfactory fibres (Franssen et al., 2007) should be tested by future experimental studies. We considered less likely that peripheral Pax6 cells are related to the LHRH-secreting cells that migrate from the olfactory placode and enter the telencephalon via the *nervus terminalis*, as in mammals (Schwankel-Fukuda and Pfaff, 1989; Valverde et al., 1993; Pellier and Astic, 1994) because in *S. canicula*, as in most elasmobranchs, the *nervus terminalis* appeared to be completely isolated from the adjacent olfactory tract (Demski and Fields, 1988).

Formation of the olfactory bulbs has largely been considered as being induced by the contact between the developing axons of the olfactory receptor cells and the forebrain (revised in Dryer and Graziadei, 1994b; De Carlos et al., 1995). However, the observation of an olfactory bulb-like structure in the Pax6 homozygous-mutant mice (*Sey/Sey*), in which the olfactory epithelium and olfactory nerve are not developed (López-Mascaraque et al., 1998, Jiménez et al., 2000), has led to the suggestion that specification of the olfactory bulb is independent from contact with nasal placode neural structures (Jiménez et al., 2000) and that Pax6 may be required to determine the position where the olfactory bulb should form within the telencephalon (Nomura and Osumi, 2004). The results of the present study did not allow us to determine whether or not the olfactory fibres of *S. canicula* influence olfactory bulb development. However, we observed that the first sign of olfactory bulb differentiation, indicated by the lateroventral expansion of the forebrain at stage 31, occurs much after the arrival of early olfactory fibres to the forebrain, already observed with tracers at stage 29 (I. Rodríguez-Moldes, unpublished observations). Peripheral Pax6 cells are relatively abundant in embryos at stage 30, but almost absent in later embryos, while the first Pax6 cells are visible in the early developing olfactory bulb of stage 31 embryos and they increase in abundance with development. The absence of Pax6 cells in the incipient olfactory bulb and their abundance in the differentiating and differentiated olfactory bulb suggest that bulbar Pax6 cells arise in the forebrain and are not olfactory epithelium derivatives. This is

consistent with findings in mouse, as it has been reported that Pax6 cells of the olfactory bulb originate in the telencephalic hemispheres, even postnatally (Franco et al., 2001; Kowhi et al., 2005).

In conclusion, the present study reveals that sharks are good models for studying olfactory development in fish, and that Pax6 appears to play different roles during development of the olfactory epithelium, during organization of the olfactory nerve and during the differentiation of the olfactory bulb. In addition, Pax6 continues to play role/s in the differentiated olfactory epithelium and olfactory bulb.

REFERENCES

Behrens M, Venkatraman G, Gronostajski RM, Reed RR, Margolis FL (2000). NFI in the development of the olfactory neuroepithelium and the regulation of olfactory marker protein gene expression. Eur J Neurosci, 12: 1372-1384.

Collinson JM, Quinn JC, Hill RE, West JD (2003). The roles of Pax6 in the cornea, retina, and olfactory epithelium of the developing mouse embryo. Dev Biol, 255: 303-312.

Coolen M, Menuet A, Chassoux D, Compagnucci C, Henry S, Lévèque L, Da Silva C, Gavory F, Samain S, Wincker P, Thermes C, D'Aubenton-Carafa Y, Rodríguez-Moldes I, Naylor G, Depew M, Sourdaine P, Mazan S (2009). The dogfish *Scyliorhinus canicula*, a reference in jawed vertebrates. In: Emerging model organisms. A laboratory manual, vol. 1, pp 431-446 New York: Cold Spring Harbour.

Davis JA, Reed RR (1996). Role of Olf-1 and Pax-6 transcription factors in neurodevelopment. J Neurosci, 16: 5082-5094.

De Carlos JA, López-Mascaraque L, Valverde F (1995). The telencephalic vesicles are innervated by olfactory placode-derived cells: a possible mechanism to induce neocortical development. Neuroscience, 68: 1167-1178.

De Carlos JA, L6pez-Mascaraque L Valverde F (1996). Early olfactory fiber projections and cell migration into the rat telencephalon. Int. J. Devl Neuroscience, 14: 853-866.

Dellovade TL, Pfaff DW, Schwanzel-Fukuda M (1998). Olfactory bulb development is altered in small-eye (Sey) mice. J Comp Neurol, 402: 402-418.

Demski LS, Fields RD (1988). Dense-cored vesicle-containing components of the terminal nerve of sharks and rays. J Comp Neurol, 278: 604-614.

Derobert Y, Baratte B, Lepage M, Mazan S (2002). Pax6 expression patterns in *Lampetra fluviatilis* and *Scyliorhinus canicula* embryos suggest highly conserved roles in the early regionalization of the vertebrate brain. Brain Res Bull, 57: 277-280.

Dryer L, Graziadei PP (1993). A pilot study on morphological compartmentalization and heterogeneity in the elasmobranch olfactory bulb. Anat Embryol (Berl), 188: 41-51.

Dryer L, Graziadei PP (1994a). Mitral cell dendrites: a comparative approach. Anat Embryol (Berl), 189: 91-106.

Dryer L, Graziadei PP (1994b). Influence of the olfactory organ on brain development. Perspect Dev Neurobiol, 2: 163-174.

Dryer L, Graziadei PP (1996). Synaptology of the olfactory bulb of an elasmobranch fish, *Sphyrna tiburo*. Anat Embryol (Berl), 193: 101-114.

Ferrando S, Bottaro M, Gallus L, Girosi L, Vacchi M, Tagliafierro G (2006a). Na+/K+ATPase immunoreactivity in olfactory epithelium of small-spotted catshark *Scyliorhinus canicula* (Linnaeus, 1758): possible presence of ion exchanging cells? J Fish Biol 69 (Supl B):278-282.

Ferrando S, Bottaro M, Gallus L, Girosi L, Vacchi M, Tagliafierro G (2006b). Observation of crypt neuron-like cells in the olfactory epithelium of a cartilaginous fish. Neurosci Lett, 403: 280-282.

Ferrando S, Bottaro M, Gallus L, Girosi L, Vacchi M, Tagliafierro G. (2007a). First detection of olfactory marker protein (OMP) immunoreactivity in the olfactory epithelium of a cartilaginous fish. Neurosci Letters, 413: 173-176.

Ferrando S, Bottaro M, Pedemonte F, De Lorenzo S, Gallus L, Tagliafierro G (2007b). Appearance of crypt neurons in the olfactory epithelium of the skate *Raja clavata* during development. Anat Rec (Hoboken), 290: 1268-1272.

Fishelson L, Baranes A (1997). Ontogenesis and cytomorphology of the nasal olfactory organ in the oman shark, *Iago omanensis* (Triakidae), in the Gulf of Aqaba, Red Sea. Anat. Rec, 249: 409-421.

Fornaro M, Geuna S, Fasolo A, Giacobini-Robecchi MG (2001). Evidence of very early neuronal migration from the olfactory placode of the chick embryo. Neuroscience, 107: 191-197.

Fornaro M, Geuna S, Fasolo A, Giacobini-Robecchi MG (2003). HuC/D confocal imaging points to olfactory migratory cells as the first cell population that expresses a post-mitotic neuronal phenotype in the chick embryo. Neuroscience, 122: 123-128.

Franco MD, Pape MP, Swiergiel JJ, Burd GD (2001). Differential and overlapping expression patterns of X-dll3 and Pax-6 genes suggest distinct roles in olfactory system development of the African clawed frog *Xenopus l*æ*v*is. J Exp Biol, 204: 2049-2061.

Franssen EHP, de Bree FM, Verhaagen J (2007). Olfactory ensheathing glia: Their contribution to primary olfactory nervous system regeneration and their regenerative potential following transplantation into the injured spinal cord. Brain Res Rev, 56: 236-258.

Glardon S, Holland LZ, Gehring WJ, Holland ND (1998). Isolation and developmental expression of the amphioxus Pax-6 gene (AmphiPax-6): insights into eye and photoreceptor evolution. Development, 125: 2701-2710.

Grindley J C, Davidson DR, Hill RE (1995). The role of Pax-6 in eye and nasal development. Development, 121: 1433-1442

Hill RE, Favor J, Hogan BLM, Ton CCT, Saunders GF, Hanson IM, Prosser J, Jordan T, Hastie ND, Heyningen V (1991). Mouse small eye results from mutations in a paired-like homeobox-containing gene. Nature, 354: 522–525.

Hofmann MH, Northcutt RG (2008). Organization of major telencephalic pathways in an elasmobranch, the thornback ray *Platyrhinoidis triseriata*. Brain Behav Evol, 72: 307-325.

Hogan BLM, Horsburgh G, Cohen J, Hetherington CM, Fisher G, Lyon MF (1986). Small eyes (Sey): a homozygous lethal mutation on chromosome 2 which affects the differentiation of both lens and nasal placodes in the mouse. J Embryol, 97: 95-110.

Hsieh YW, Yang XJ (2009). Dynamic Pax6 expression during the neurogenic cell cycle influences proliferation and cell fate choices of retinal progenitors. Neural Dev, 4: 32-50.

Jiménez D, Garcia C, de Castro F, Chedotal A, Sotelo C, de Carlos JA, Valverde F López-Mascaraque L (2000). Evidence for intrinsic development of olfactory structures in Pax-6 mutant mice. J Comp Neurol, 428: 511-526.

Kohwi M, Osumi N, Rubenstein JL, Alvarez-Buylla A (2005). Pax6 is required for making specific subpopulations of granule and periglomerular neurons in the olfactory bulb. J Neurosci, 25: 6997-7003.

López-Mascaraque L, García C, Valverde F, de Carlos JA (1998). Central olfactory structures in Pax-6 mutant mice. Ann N Y Acad Sci, 855: 83-94.

Maekawa M, Takashima N, Arai Y, Nomura T, Inokuchi K, Yuasa S, Osumi N (2005). Pax6 is required for production and maintenance of progenitor cells in postnatal hippocampal neurogenesis. Genes Cells, 10: 1001-1014.

Nomura T, Osumi N (2004). Misrouting of mitral cell progenitors in the Pax6/small eye rat telencephalon. Development, 131: 787-796.

Nomura T, Haba H, Osumi N (2007). Role of a transcription factor Pax6 in the developing vertebrate olfactory system. Develop Growth Differ, 49: 683-690.

O'Neill P, McCole RB, Baker CVH (2007). A molecular analysis of neurogenic placode and cranial sensory ganglion development in the shark, *Scyliorhinus canicula*. Dev Biol, 304: 156-181.

Pellier V, Astic L (1994). Histochemical and immunocytochemical study of the migration of neurons from the rat olfactory placode. Cell Tissue Res, 275: 587-598.

Reiss JO, Burd GD (1997). Cellular and molecular interactions in the development of the *Xenopus* olfactory system. Sem Cell Dev Biol, 8: 171-179.

Sauka-Spengler T, Baratte B, Shi L, Mazan S (2001). Structure and expression of an Otx5-related gene in the dogfish *Scyliorhinus canicula*: evidence for a conserved role of Otx5 and Crx genes in the specification of photoreceptors. Dev Genes Evol, 211: 533-544.

Schluessel V, Bennett MB, Bleckmann H, Blomberg S, Collin SP (2008). Morphometric and ultrastructural comparison of the olfactory system in elasmobranchs: the significance of structure-function relationships based on phylogeny and ecology. J Morphol, 269: 1365-1386.

Schwanzel-Fukuda M, Pfaff DW (1989). Origin of luteinizing hormone-releasing hormone neurons. Nature, 338: 161-164.

Stoykova A, Gruss P (1994). Roles of Pax-genes in developing and adult brain as suggested by expression patterns. J Neurosci, 74: 1395-1412.

Takami S, Luer CA, Graziadei PPC (1994). Microscopic structure of the olfactory organ of the clearnose skate, *Raja eglanteria*, Anat Embryol, 190: 211-230.

Theisen B, Zeiske E, Breucker H (1986). Functional morphology of the olfactory organs in the spiny dogfish (*Squalus acanthias* L.) and the small-spotted catshark (*Scyliorhinus canicula* L.), Acta Zool. (Stockh.), 67: 73-86.

Thieler K, Varnum DS, Stevens LC (1978). Development of Dickie's small eye, a mutation in the house mouse. Anat Embryol, 155:81-86.

Valverde F, Heredia M, Santacana M (1993). Characterization of neuronal cell varieties migrating from the olfactory epithelium during prenatal development in the rat. Immunocytochemical study using antibodies against olfactory marker protein (OMP) and luteinizing hormone-releasing hormone (LH-RH). Dev Brain Res, 71: 209-220.

Walther C, Gruss P (1991). Pax-6, a murine paired box gene, is expressed in the developing CNS. Development, 113: 1435-1449.

Wullimann MF, Rink E (2001). Detailed immunohistology of Pax6 protein and tyrosine hydroxylase in the early zebrafish brain suggests role of Pax6 gene in development of dopaminergic diencephalic neurons. Dev Brain Res, 131: 173-179.

Figure 1. Parasagittal (A,D,G) and transverse sections (B,C,E,F) through the head of *S. canicula* embryos at early stages of the olfactory organ development (stages 25 to 28) after whole-mount *in situ* hybridisation (A) or immunohistochemistry for Pax6 (B-G). A. Sagittal section counterstained with nuclear fast red showing Pax6 expression in the olfactory pit, optic stalk and in several brain domains. B-G. Sections through the head of *S. canicula* embryos at stages 25 (B), 27 (C,D) and 28 (E-G) to show the distribution of Pax6 cells in the developing olfactory organ. Arrows point to intense Pax6 cells located in the distal olfactory epithelium (B, C, E) and arrowheads indicate a stream of peripheral Pax6 cells in between the olfactory pit and the rostral forebrain walls. Note differences in the intensity of immunolabelling between Pax6 cells in the brain walls (moderate) and in the olfactory epithelium and peripheral cell stream (intense). Scale bars 250μm (A, E), 100μm (C,D,G) 50 μm (B,F). For abbreviations, see list in Appendix A.

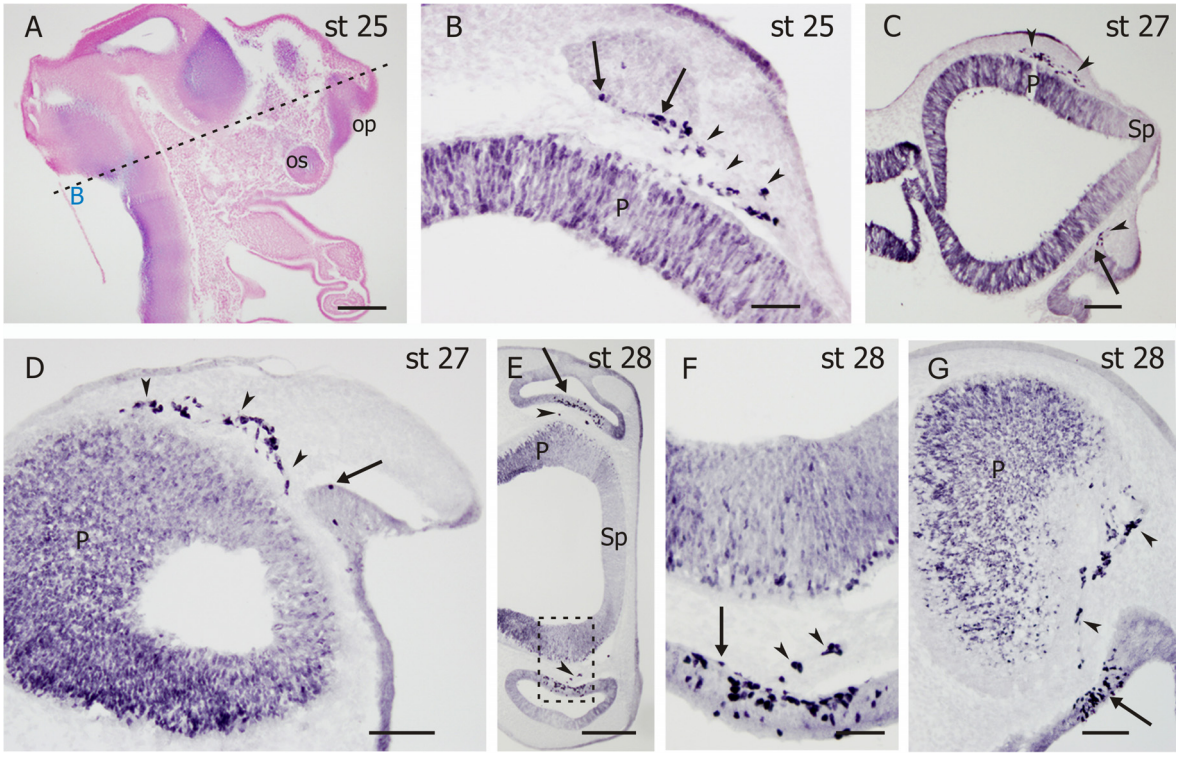
A
st 25
op
os
B
B
st 25
P
C
st 27
P
Sp
D
st 27
P
E
st 28
P
Sp
F
st 28
G
st 28
P

Figure 2. Parasagittal (A-D) and transverse (E-K) sections through the olfactory epithelium of *S. canicula* embryos (A-I) and adults (J,K) after Pax6 immunohistochemistry (A-C, E-K) and *in situ* hybridisation (D). A. Lateral section of a stage 29 embryo showing Pax6 cells in the neuroepithelial pallial walls, in the olfactory epithelium (arrows), which shows the early signs of folding, and in its periphery (arrowheads). B. Detail of the first lamellae of a stage 31 embryo to show its symmetric structure in relation to a central raphe (Ra). Epithelial Pax6 cells are scarce in the raphe but abundant at different levels of the lamellae (arrows). Arrowhead indicates peripheral Pax6 cells and empty arrows the Pax6 cells in the subpallial marginal walls. C,D. Adjacent lateral sections showing the similar distribution of Pax6 protein (C) and mRNA (D) in the olfactory epithelium and its periphery (arrowheads). Note scarce Pax6 cells in the prospective olfactory bulb (asterisk). E. Panoramic view of the olfactory epithelium of a stage 31 embryo folded into numerous *lamellae*. Note the incipient olfactory bulb with few Pax6 cells (white arrows). Empty arrows indicate subpallial marginal Pax6 cells. F. Detail of the squared area in E to show the distribution of Pax6 cells at different levels in the olfactory epithelium. Arrows point to intense Pax6 cells at basal level. G. Transverse section showing the mature-like nasal organ of a stage 32-embryo. Note the onset of secondary folding of the olfactory epithelium. H,I. Magnifications the squared areas in G. J. Section trough the adult nasal organ showing abundant basal Pax6 cells in the olfactory epithelium. Note the increased surface of the olfactory epithelium due to the secondary folding in the epithelium. K. Detail of the area squared in J to show the Pax6 cell distribution in the basal part of the adult olfactory epithelium. Scale bars 250μm (A,C-E,G,J), 100 μm (B,F,H,I,K). For abbreviations, see list in Appendix A.

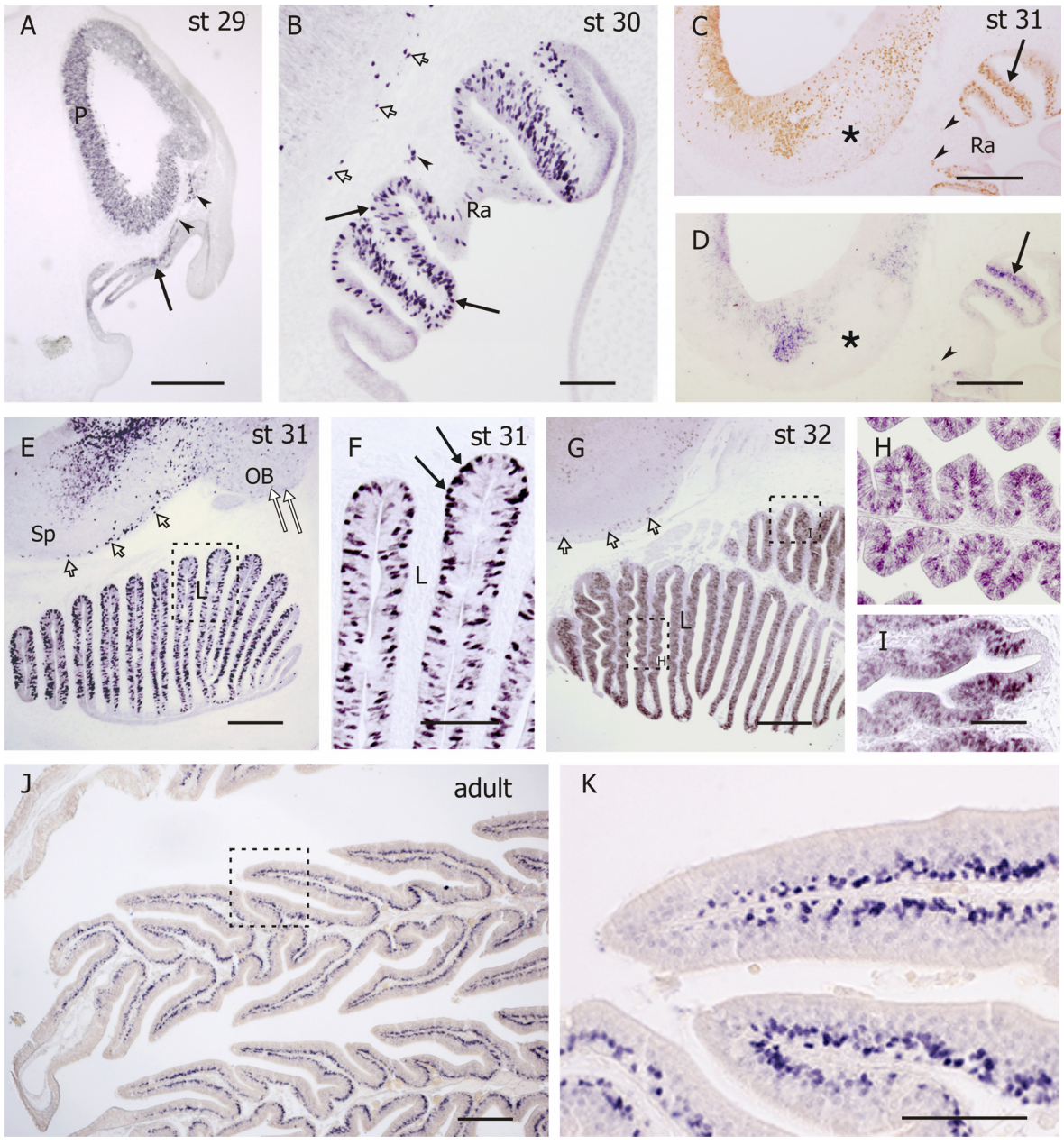
A
st 29
P
B
st 30
Ra
C
st 31
Ra
D
E
st 31
OB
Sp
L
F
st 31
L
G
st 32
L
H
H
I
J
adult
K

Figure 3. Parasagittal (A-D) and transverse (E-H) sections through the head of embryos (A-F), juveniles (G) and adults (H) of *S. canicula* after Pax6 immunohistochemistry to show the spatiotemporal distribution of Pax6 cells along the olfactory tract (A-F) and in the olfactory bulb (E-H). A-D. Lateral sections through the telencephalon and nasal organ of stage 30- embryos to show abundant peripheral Pax6 cells (arrowheads) apposed to fibres of the olfactory nerve (double arrows) from proximal (B) to distal (C, D) levels. Arrows in A and B point to Pax6 cells in the olfactory epithelium. E. Early stage 31-embryo to show some Pax6 cells associated with the olfactory tract (black arrowhead) and at the external region of the primordial olfactory bulb (white arrowheads). Note the absence of labelled cells in the inner part of the primordial olfactory bulb (asterisk). F. Transverse section of a stage 32-embryo to show scarce Pax6 in the primordial olfactory bulb (white arrows). Note also Pax6 cell in the *lamellae* (L) and its periphery (arrowheads). G, H. Transverse sections through the juvenile (G) and adult (H) olfactory bulb, to show the presence of Pax6 cells in the granular layer and its absence in the glomerular layer. Scale bars: 500μm (A), 200 μm (C,E,F), 100 μm (B,D,G,H). For abbreviations, see list in Appendix A.

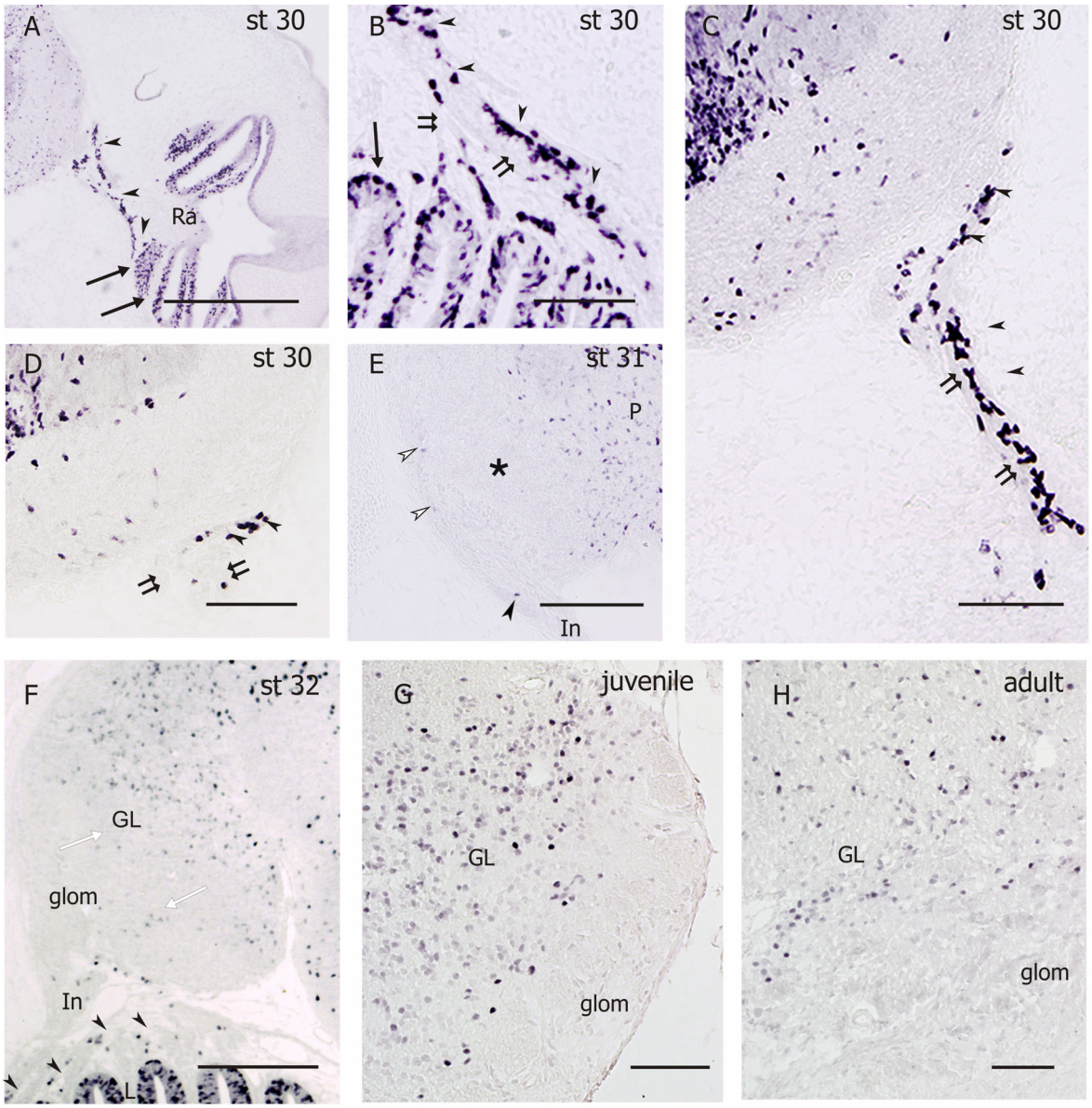
A
st 30
Ra
B
st 30
C
st 30
D
st 30
E
st 31
P
In
F
st 32
GL
glom
In
G
juvenile
GL
glom
H
adult
GL
glom

Chapter 3.

The segmental organization of the developing shark brain based on neurochemical markers, with special attention to the prosencephalon

INTRODUCTION

As indicated in previous chapters, the homeobox gene Pax6 encodes a highly conserved transcription factor, which plays multiple roles in early forebrain, and more generally in central nervous system patterning, including boundary formation, neuron specification and axon guidance (Stoykova and Gruss, 1994; Mastick et al., 1997; Osumi, 2001; Manuel and Price, 2005; Osumi et al., 2008). In order to gain insight into the ancestral gnathostome pattern, we have compared the Pax6 expression in the prosencephalon of developing and postembryonic sharks with that of some markers for neuronal differentiation such as glutamic acid decarboxylase (GAD), tyrosine hydroxylase (TH), and calretinin (CR), by using double and triple immunofluorescence techniques. By correlating the cytoarchitectonic limits with the specific location of these markers, we identified transverse and longitudinal boundaries and domains, which suggested a segmental pattern reminiscent of the one described in other vertebrates (Pombal and Puelles, 1999; Puelles and Rubenstein, 2003). These data provide an initial scheme of the developing shark brain, which will be further tested and refined using a broader range of genetic markers involved in patterning and differentiation, thus extending and supporting the data available in early *S. canicula* embryos (Derobert et al., 2002).

MATERIALS AND METHODS

Experimental animals

Embryos and juveniles of *S. canicula* and *H. fuscus* were obtained and processed as mentioned in Chapter 1. Embryos were staged according to Ballard et al. (1993), and the following embryonic stages were analysed: stage 25 (4 *S.c.* and 2 *H.f.* embryos), stage 26 (3 *S.c.* embryos), stage 27 (3 *S.c.* embryos), stage 28 (3 *S.c.* embryos and 2 shyshark embryos), stage 29 (4 *S.c.* embryos and 3 *H.f.* embryos), stage 30 (2 *S.c.* embryos and 3 *H.f.* embryos), stage 31 (7 *S.c.* and 7 *H.f.* embryos), stage 32 (6 *S.c.* and 6 *H.f.* embryos), and stages 33-34 (prehatching; 3 *S.c.* and 8 *H.f.* embryos). In addition to 5 juveniles (3 *S. canicula* and 2 *H. fuscus*, total length from 10 to 14 cm).

Tissue preparation

After fixation and sectioning, tissue was processed either by immunohistochemistry or by *in situ* hybridisation with a *ScPax6* probe (Derobert et al., 2002). For further details on tissue preparation see material and methods section in Chapter 1.

Immunohistochemistry

The following primary antibodies were used: a rabbit polyclonal anti-Pax6 antibody (Chemicon, now Millipore, Billerica, MA); a polyclonal sheep anti-GAD65/67 antiserum, kindly provided by Dr. E. Mugnaini; which details about origin and specificity have been published previously (MacLeod et al., 2006); a rabbit anti-CR antiserum (Swant, Bellizona, Switzerland) obtained in rabbit against recombinant human calretinin containing 6-his tag at the N-terminal; a monoclonal anti-Pax6 antiserum (Sigma, St. Louis, MO), raised against amino acids 1-223 of chick Pax6; and, a monoclonal anti-TH antiserum from Chemicon (now Millipore, Billerica, MA). For further details on the characterization of the anti-GAD, anti-CR, and anti-TH antibodies see material and method section in chapters 7, 8 and 10 respectively.

Single labelling

Briefly, after heat induced epitope retrieval, sections were rinsed in TBS, and then processed by the streptavidin/biotin method (for Pax6 and CR immunohistochemistry). The residual avidin/biotin activity was removed by incubation with the avidin/biotin blocking kit (Vector, Burlingam, CA), as indicated by the manufacturers and the endogenous peroxidase activity was blocked. As primary antibodies, sections were incubated overnight at RT with rabbit polyclonal anti-Pax6 (Chemicon; diluted 1:400), or with rabbit polyclonal anti-CR (Swant; diluted 1:500) antisera, then rinsed in TBS, incubated for 1h in biotinylated goat anti-rabbit IgG (Dako, Glostrup, Denmark; diluted 1:500), rinsed again in TBS, incubated for 30 min in the preformed avidin:biotinylated enzyme complex by using the Vectastain ABC system (Vector) and rinsed in TBS. Finally, the immunoreaction was developed, and then sections were dehydrated and coversliped. Negative controls performed by omitting the primary, or secondary antibodies showed no immunostaining. For further details, see material and methods section in Chapter 1.

Double and triple immunofluorescence

Double and triple immunofluorescence was performed on alternate series of sections, which were incubated overnight at RT with a cocktail of primary antibodies containing either: a) rabbit anti-Pax6 (Chemicon; 1:200), and anti-TH (Chemicon; 1:500) or anti-$GAD_{65/67}$ (Mugnaini's antibody; 1:25000); b) rabbit anti-Pax6 (Chemicon; 1:200), anti-TH (Chemicon; 1:500) and sheep anti-$GAD_{65/67}$ (Mugnaini's antibody; 1:25000); or c) rabbit anti-CR (Swant, 1:200), monoclonal anti-Pax6 (Sigma; 1:50) and anti-$GAD_{65/67}$, then rinsed in TBS and subsequently detected by using a mixture of the following secondary antibodies: Alexa Fluor 488 Goat-anti-Rabbit IgG and Alexa Fluor 546 Goat-anti-Mouse IgG or Alexa Fluor 488 Donkey-anti-Sheep IgG antibodies (Molecular Probes, The Netherlands; diluted 1:200) for double labelling, and Alexa Fluor 546 Goat-anti-Rabbit IgG antibodies (Molecular Probes; diluted 1:200), Alexa Fluor 488 Donkey-anti-Sheep IgG antibodies (Molecular Probes; diluted 1:200) and FluoProbes 642 Donkey-anti-Mouse IgG (FluoProbes, Interchim, France; diluted 1:100) for triple labelling. All dilutions were made with TBS containing 15% of the donkey, and rabbit normal sera and 0.2% of Triton X-100. All incubations were carried out in a humid chamber. Sections were rinsed in TBS for 30 min, then in distilled water (twice for 30 min), and finally mounted in Vectashield mounting medium for fluorescence (Vector). As negative controls, the primary or secondary antibodies were omitted. No immunostaining was observed in the control sections. Double and triple-labelled samples were studied with a spectral confocal laser scanning microscope TCS-SP2 (Leica, Wetzlar, Germany).

In situ hybridisation

Some series of sections were processed by *in situ* hybridisation with a digoxigenin-11 UTP-labelled *S. canicula* Pax6 probe (Derobert et al., 2002) according to standard procedures (see material and methods section in Chapter 1).

RESULTS

As shown in Chapter 1, we have used a systematic analysis of the distribution of Pax6 protein by immunohistochemistry and the Pax6 mRNA by *in situ* hybridisation, to identify transverse and longitudinal domains in the shark brain. Concerning the Pax6 distribution in relation to certain boundaries we briefly pointed that the alar/basal boundary along the mesencephalon and caudal diencephalon is related with a longitudinal stripe of Pax6-expressing cells (hereafter, Pax6 cells) extending from the mesencephalon to the prethalamus that is observed in embryos (Fig. 1A-C) and even in juveniles (see Chapter 1). The sharp limit between the caudal extension of prosencephalic Pax6 cells and the Pax6-negative mesencephalic alar plate (optic tectum) marks the diencephalic-mesencephalic boundary (Fig. 1A-C, see also Chapter 1).

Comparative analysis of the expression domains of Pax6, glutamic acid decarboxylase (GAD), calretinin (CR) and tyrosine hydroxylase (TH) and cytoarchitectonic analysis of the caudal diencephalon leads to the identification of three transverse segments, referred to as the prosomeres 1-3 (p1-p3), from caudal to rostral. Pax6 cells are conspicuous in alar domains corresponding to p1 and p3 (Fig. 1A-E). The synencephalon (p1) contains Pax6 and GABAergic cells in the alar plate (pretectum) and CR-ir and TH-ir cell groups in the basal plate (Fig. 1A-C). The pretectal domain is characterized by a GAD-ir cell population and by abundant GAD-ir fibres in the posterior commissure (Fig. 1A-C). The posterior commissure dorsally covers the pretectum, which can be subdivided into two transverse domains, a caudal one containing a conspicuous Pax6 cell group lateral to the posterior commissure, and a rostral one adjacent to the *fasciculus retroflexus*, lacking Pax6 cells (Fig. 1B,C). In the p1 basal plate, the large CR-ir cells of the nucleus of the medial longitudinal fascicle (Fig. 1C) lie dorsal to the synencephalic TH-ir cells of the rostral part of the ventral tegmental area (Fig. 1A-B). In p2, the thalamus (alar plate of p2) does not contain Pax6 cells at stage 29 (Fig. 1), although weak Pax6 cells are observed at earlier stages (stage 25, see Chapter 1). Pax6-ir can be observed in the habenula (Fig. 1A-C). Moreover, the thalamus exhibits a group of CR-ir cells (Fig. 1D,E) from stage 31 onwards. p3 contains a group of Pax6 cells that extends both into the alar (prethalamus) and basal regions (rostral posterior tubercle) from the ventricular region to the ventrolateral surface (Fig. 1A-D). This Pax6-ir group overlaps with the abundant TH-ir population of the posterior tubercle and the dorsal hypothalamus (Fig. 1A,B). The *fasciculus retroflexus* marks

the p1/p2 boundary (Fig. 1A-C) and a transverse band of GAD-ir cells and fibres (the reticular thalamic nucleus) forms a wedge between the alar regions of p3 (prethalamus) and p2 (thalamus) following the *zona limitans intrathalamica* (Fig. 1B,C).

The secondary prosencephalon comprises the telencephalon, the preoptic area and the hypothalamus (the rostral diencephalon). From stage 31 onwards, the hypothalamus contains abundant TH-ir and 5-HT-ir cells, and the TH-ir groups lie dorsal to the periventricular 5-HT-ir cell groups (Carrera 2008; Carrera et al., 2008a). CR-ir cells are also abundant in the hypothalamus (not shown). From stage 28 onwards, numerous GABA-expressing subpallial cells migrate progressively to pallial areas (Carrera et al., 2008b), but a dense band of mediolaterally oriented Pax6 cells follows the putative pallial/subpallial boundary (Fig. 2A-D, see also Chapter 1). From this band, scattered Pax6 cells mainly extend to pallial regions. In late embryos and juveniles, Pax6 cells are abundant in the pallium and sparse in the subpallium (see Chapter 1). From stage 32 onwards, CR-ir cells and fibres are very abundant in the pallium, which shows striking differences in CR-ir density among areas (Fig. 2E-I). The transverse and longitudinal boundaries and domains described here are schematically represented in Figure 3.

DISCUSSION

In this study, we have applied immunohistochemistry for Pax6 and several neuronal markers previously used to study brain organization in a wide range of vertebrates (Pax6: Wullimann and Rink, 2001; GAD/GABA: Ekström and Ohlin., 1995; Katarova et al., 2000; Mueller et al., 2006; CR: González et al., 2002; Milán and Puelles, 2000; Pombal and Puelles, 1999; TH: Puelles and Medina, 1994; Carrera et al., 2005; Carrera 2008). Double and triple immunolabelling with these markers gave more accurate regional information than single labelling, so that we could analyze the organization of the shark brain in detail, and identify prosomeric domains in the caudal diencephalon. Our results in developing sharks reveal that the distribution pattern of Pax6 cells highlight the presence of conserved longitudinal and transverse boundaries of the vertebrate brain, such as the alar-basal, diencephalic-mesencephalic and pallial-subpallial boundaries as well as some prosomeric domains. A conspicuous longitudinal stripe of Pax6 cells extends in the caudal diencephalon and mesencephalon along the alar-basal boundary. This stripe may be related to the sharp

boundary of the *Pax6* and *Pax7* expression at the *sulcus limitans* in the mouse mesencephalic tegmentum (Stoykova and Gruss, 1994). Pax6-expression demarcates the prosencephalic-mesencephalic boundary in early *S. canicula* embryos (Derobert et al., 2002). Our results support the proposed role for Pax6 in the formation of this boundary (Derobert et al., 2002; Matsunaga et al., 2000) and indicate that the sharp limit of the Pax6-expression is maintained in postembryonic stages, always at the caudal border of the posterior commissure. The relation of Pax6 to this transverse boundary appears to be common for vertebrates (Bachy et al., 2002; Derobert et al., 2002; Mastick et al., 1997; Matsunaga et al., 2000; Murakami et al., 2001; Puelles and Medina, 1994; Wullimann and Rink, 2001).

In the caudal diencephalon of sharks, combination of Pax6 expression with that of GAD, CR and TH allows to distinguish prosomeres p3 to p1. As observed in mice and zebrafish (Puelles and Rubenstein, 2003; Stoykova and Gruss, 1994; Wullimann and Rink, 2001) the alar plate of p3 contains the most extensive groups of Pax6 cells. Moreover, in sharks the alar plate of p1 contains a conspicuous Pax6 group ventral to the posterior commissure, as in mice and zebrafish (Stoykova and Gruss, 1994; Wullimann and Rink, 2001; present results). No Pax6 cells were observed in the thalamus of shark embryos from stage 27 onwards (see Chapter 1), unlike in early embryos of zebrafish (Hauptmann and Gerster, 2000; Wullimann and Rink, 2001) and lamprey (Murakami et al., 2001). However, in earlier shark embryos (Derobert et al., 2002; and stage 25/26, present results) the thalamus expresses Pax6, indicating that Pax6 expression is downregulated in p2 (present results). Similarly, in mouse embryos at E10.5, Pax6 cells become restricted to the prethalamus and the epithalamus whereas at early stages they are present in the thalamus as well (Pratt et al., 2000). This dynamic Pax6 pattern appears to play a role in the formation of the thalamocortical tract in mice, since it develops at the time of downregulation of Pax6 in the thalamus and is absent in the *Sey* (Pax6) mutant (Pratt et al., 2000). Calretinin is a suitable marker of the thalamus/p2 alar plate in tetrapods (González et al., 2002; Milán and Puelles, 2000) and also in lamprey (Pombal and Puelles, 1999). In shark embryos, CR-ir cell groups are also observed in the Pax6-negative domain of p2 alar plate (thalamus). CR is a late marker for this thalamic domain because CR-ir cells were not observed in embryos earlier than stage 31.

Just caudal to the Pax6-positive domain of the prethalamus (see Fig. 1A-C), GAD immunoreactivity reveals a conspicuous stripe of GAD-ir cells and fibres. This wedge-shaped stripe extends close to or in the boundary between p2 and p3, and is closely related to the

zona limitans intrathalamica (ZLI) (Carrera et al., 2006). A similar stripe of GABAergic cells is located in or close to the ZLI in mouse and zebrafish embryos (Katarova et al., 2000; Mueller et al., 2006).

Our present results reveal overlapping of Pax6-ir and TH-ir cell groups in the shark prethalamus/posterior tubercle, which coincides with that reported in zebrafish (Wullimann and Rink, 2001). However, in sharks they extend caudalwards to synencephalic and mesencephalic levels (Carrera et al., 2005; present results). With confocal microscopy we found that there are separate Pax6-expressing and TH-ir cell populations, which are intermingled in the prethalamus and posterior tubercle but adjacent in the synencephalon and mesencephalon, where Pax6 cells are located just dorsal and medial to TH-ir cells (Figs. 1A,B).

In the telencephalon of stage 28 shark embryos, Pax6- cells form a band along the pallial-subpallial boundary, and many cells are also located in the pallium, although migrated Pax6 cells can be observed in the subpallium. We have shown interesting differences in Pax6 expression between sharks and zebrafish. In zebrafish embryos (2dpf) (Wullimann and Rink, 2001), most Pax6-ir cells in the telencephalon were found along the pallial-subpallial boundary, but no Pax6 expression was found in the ventricular zone, unlike in sharks (present results) and in tetrapods (Bachy et al., 2002; Puelles et al., 2000). As for Pax6, the catecholaminergic cell organization in the elasmobranch telencephalon differs from teleosts. In sharks, a large pallial TH-ir population (Carrera et al., 2005; Carrera 2008) codistributes with that of Pax6 cells, while these catecholaminergic cells are absent in bony fishes.

It is accepted that Pax6 has a role in the dorsoventral patterning of the telencephalon (Bachy et al., 2002; Puelles et al., 2000). In sharks, Pax6 and GAD are good markers to distinguish ventral and dorsal telencephalic territories, the ventral telencephalon containing GABA-expressing cells at early stages of telencephalic development (Carrera et al., 2008b; Carrera 2008) and the dorsal telencephalon containing Pax6- and GABA-expressing cells at late stages (present results; Carrera, 2008; Carrera et al., 2008b). Also, CR appears useful for distinguishing pallial territories in late shark embryos.

REFERENCES

Bachy I, Berthon J, Retaux S (2002). Defining pallial and subpallial divisions in the developing *Xenopus* forebrain. Mech Dev 117:163-172.

Ballard W, Mellinger J, Lechenault H (1993). A series of normal stages for development of *Scyliorhinus canicula*, the lesser spotted dogfish (*Chondrichthyes: Scyliorhinidae*). J Exp Zool, 267:318–336.

Carrera I (2008). Desarrollo de los sistemas gabaérgico y aminérgicos en el sistema nervioso central de peces cartilaginosos. Ph. D. Thesis. University of Santiago de Compostela.

Carrera I, Sueiro C, Molist P, Ferreiro S, Adrio F, Rodríguez MA, Anadón R, Rodríguez-Moldes I (2005). Temporal and spatial organization of tyrosine hydroxylase-immunoreactive cell groups in the embryonic brain of an elasmobranch, the lesser-spotted dogfish *Scyliorhinus canicula*. Brain Res Bull, 66:541-545.

Carrera I, Sueiro C, Molist P, Holstein GR, Martinelli GP, Rodríguez-Moldes I, Anadón R (2006). GABAergic system of the pineal organ of an elasmobranch (*Scyliorhinus canicula*): a developmental immunocytochemical study. Cell Tissue Res 323:273-281.

Carrera I, Molist P, Anadón R, Rodríguez-Moldes, I (2008a). Development of the serotoninergic system in the central nervous system of a shark, the lesser spotted dogfish *Scyliorhinus canicula*. J Comp Neurol, 511:804-831.

Carrera I, Ferreiro-Galve S, Sueiro C, Anadón R Rodríguez-Moldes I, (2008b). Tangentially migrating GABAergic cells of subpallial origin invade massively the pallium in developing sharks. Brain Res Bull, 75:405-409.

Derobert Y, Baratte B, Lepage M, Mazan S (2002). Pax6 expression patterns in *Lampetra fluviatilis* and *Scyliorhinus canicula* embryos suggest highly conserved roles in the early regionalization of the vertebrate brain. Brain Res Bull, 57:277–280.

Ekström P, Ohlin LM (1995). Ontogeny of GABA-immunoreactive neurons in the central nervous system in a teleost, *Gasterosteus aculeatus* L. J Chem Neuroanat, 9:271-288.

González G, Puelles L, Medina L (2002). Organization of the mouse dorsal thalamus based on topology, calretinin immunostaining, and gene expression. Brain Res Bull, 57:439-442.

Hauptman G, Gerster T (2000). Regulatory gene expression patterns reveal transverse and longitudinal subdivisions of the embryonic zebrafish forebrain. Mech Dev, 91:105–118.

Katarova Z, Sekerková G, Prodan S, Mugnaini E, Szabó G (2000). Domain restricted expression of two glutamic acid decarboxylase genes in midgestation mouse embryos. J Comp Neurol, 424:607-627.

MacLeod KM, Soares D, Carr CE (2006). Interaural timing difference circuits in the auditory brainstem of the emu (*Dromaius novaehollandiae*). J Comp Neurol, 495: 185-201.

Manuel M, Price DJ (2005). Role of Pax6 in forebrain regionalization. Brain Res Bull, 66:387-393.

Mastick GS, Davis NM, Andrews L, Easter SS (1997). Pax6 functions in boundary formation and axon guidance in the embryonic mouse forebrain. Development, 124:1985-1997.

Matsunaga E, Araki I, Nakamura H (2000). Pax6 defines the di-mesencephalic boundary by repressing En1 and Pax2. Development, 127:2357-2365.

Milán FJ, Puelles L (2000). Patterns of calretinin, calbindin, and tyrosine-hydroxylase expression are consistent with the prosomeric map of the frog diencephalon. J Comp Neurol, 419:96-121.

Mueller T, Vernier P, Wullimann MF (2006). A phylotypic stage in vertebrate brain development: GABA cell patterns in zebrafish compared with mouse. J Comp Neurol, 494:620-634.

Murakami Y, Ogasawara M, Sugahara F, Hirano S, Satoh N, Kuratani S (2001). Identification and expression of the lamprey Pax6 gene: evolutionary origin of the segmented brain of vertebrates. Development, 128:3521–3531.

Osumi N (2001). The role of Pax6 in brain patterning. Tohoku J Exp Med, 193:163–174.

Osumi N, Shinoara H, Numayama-Tsuruta K, Maekawa M (2008). Concise review: Pax6 transcription factor contributes to both embryonic and adult neurogenesis as a multifunctional regulator. Stem Cells, 26:1663-1672.

Pombal MA, Puelles L (1999). Prosomeric map of the lamprey forebrain based on calretinin immunocytochemistry, Nissl stain, and ancillary markers. J Comp Neurol, 414:391-422.

Pratt T, Vitalis T, Warren N, Edgar JM, Mason JO, Price DJ (2000). A role for Pax6 in the normal development of dorsal thalamus and its cortical connections. Development, 127:5167-5178.

Puelles L, Rubenstein JLR (2003). Forebrain gene expression domains and the evolving prosomeric model. Trends Neurosci, 26:469-476.

Puelles L, Medina L (1994). Development of neurons expressing tyrosine hydroxylase and dopamine in the chicken brain: a comparative segmental analysis. In: Phylogeny and Development of Catecholamine Systems in the CNS of Vertebrates (Smeets WJAJ, Reiner A, eds) pp:103-133, Cambridge University Press, Cambridge.

Puelles L, Kuwana E, Puelles E, Bulfone A, Shimamura K, Keleher J, Smiga S, Rubenstein JLR (2000). Pallial and subpallial derivatives in the embryonic chick and mouse telencephalon, traced by the expression of the genes Dlx-2, Emx-1, Nkx-2.1, Pax-6, and Tbr-1. J Comp Neurol, 424:409-438.

Stoykova A, Gruss P (1994). Roles of Pax genes in developing and adult brain suggested by expression patterns. J Neurosci, 74:1395-1412.

Wullimann MF, Rink E (2001). Detailed immunohistology of Pax6 protein and tyrosine hydroxylase in the early zebrafish brain suggests role of Pax6 gene in development of dopaminergic diencephalic neurons. Dev Brain Res, 131:173-191.

Figure 1. Sagittal sections through the brain of embryos of *H. fuscus* at the indicated stages after triple labelled by immunofluorescence for Pax6/TH/GAD (A,B,E) and Pax6/CR/GAD (C-E). **A-C**. Sections at median (A) and paramedian (B-C) levels showing Pax6 domains in the pretectum and prethalamus. Note the column of Pax6-ir cells along the mesencephalon, and caudal prosencephalon related with the alar/basal boundary (arrows in A). B and C are adjacent sections. Note abundant GAD-ir fibres (green) in the posterior commissure (pc) Short arrow in C indicates cells CR-ir (red) of the nucleus of the longitudinal medial fascicle **D.** Detail of a parasagittal section of the caudal prosencephalon to show the CR-ir cell group of the thalamus adjacent to the Pax6 population of the prethalamus. Rostral is at left. **E.** Magnification of the squared area in D. Scale bars 100µm. For abbreviations, see list in Appendix A.

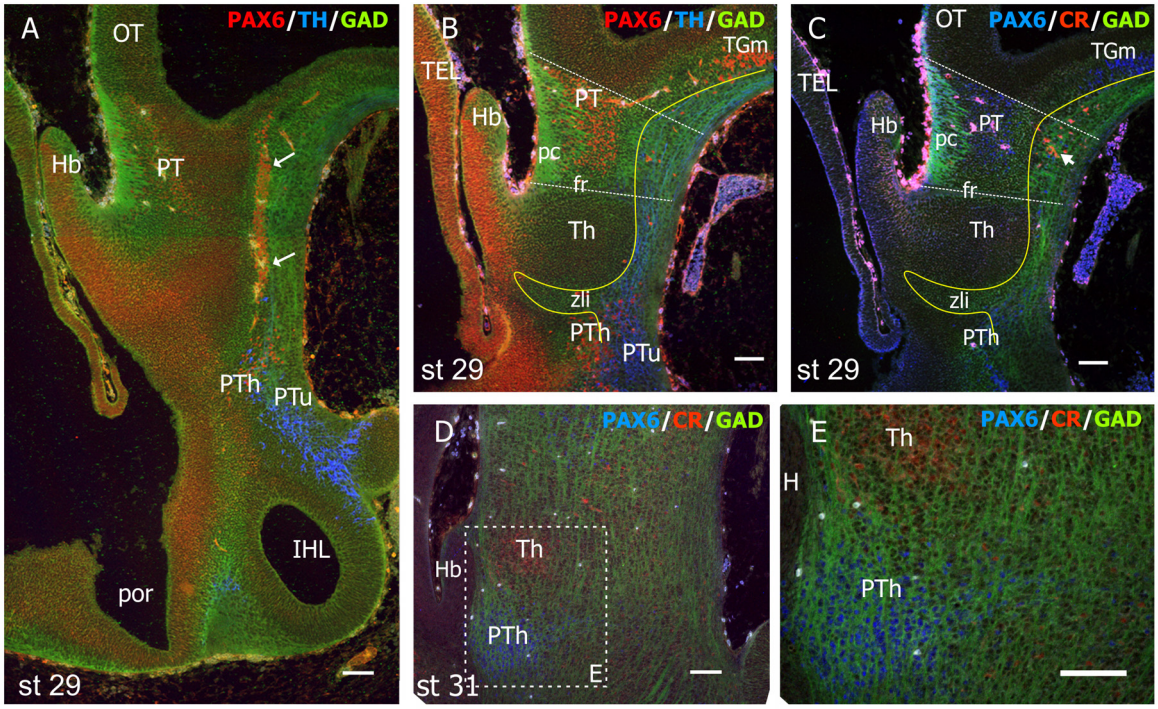

Figure 2. Transverse sections through the telencephalon of *S. canicula* (A-F/G) and *H. fuscus* (H-J) embryos after immunohistochemistry against Pax6 (A,C) or CR (E-I) or Pax6 in situ hybridisation (B,D). **A-D.** Transverse sections through the telencephalon of stages 31 (A,C) and 30 (B,D) showing abundant Pax6-expressing cells extending along the pallial-subpallial boundary (arrows). Arrowheads (A,C) indicate Pax6 cells in the MZ in the subpallium. **E-I.** Transverse sections through the telencephalon of stage 32 embryos showing differences in the distribution of CR-ir cells among various pallial and subpallial areas. F,H,I. Details of the areas squared in E and G to show CR-ir in the pallium (F,H) and subpallium (I). Scale bars 100µm. For abbreviations, see list in Appendix A.

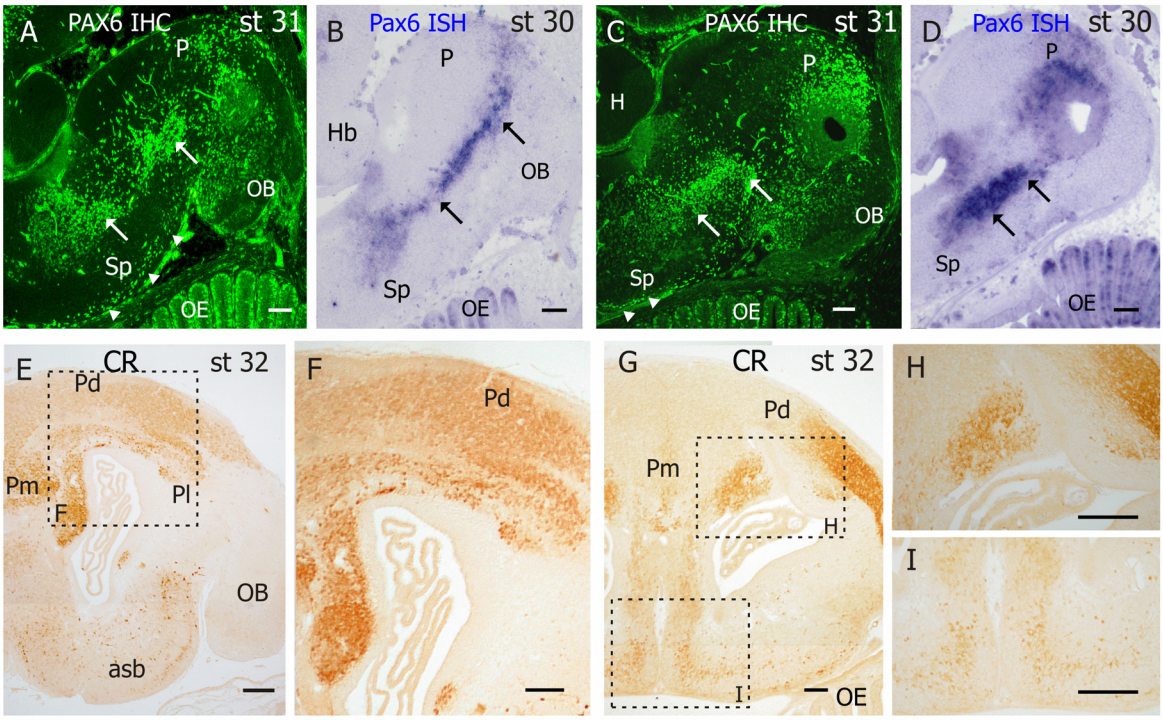

Figure 3. Schematic representation of a sagittal section of the stage 31-embryonic brain summarizing the transverse and longitudinal domains identified in the diencephalon. Red lines indicate the interprosomeric boundaries and the orange and red dotted lines the putative alar-basal and pallial-subpallial boundaries respectively. Scale bar 250µm. For abbreviations see list in Appendix A.

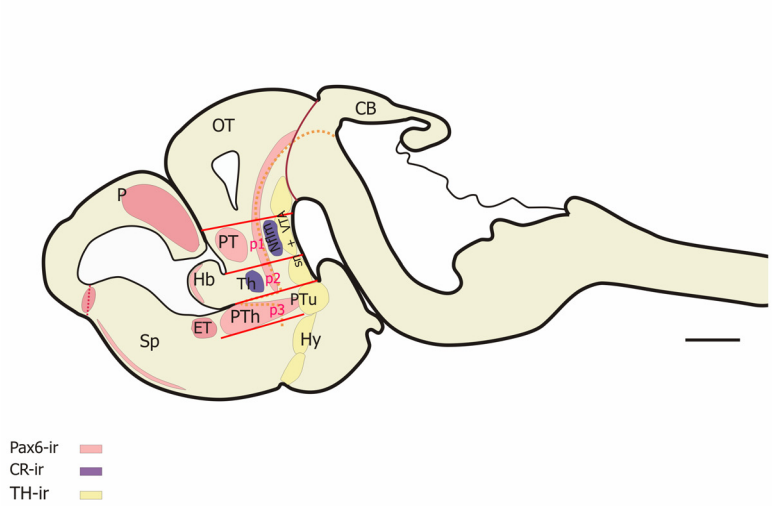

Chapter 4.

Development of the Cerebellar Body in Sharks: Spatiotemporal Relations of Pax6-Expression, Cell Proliferation and Differentiation

INTRODUCTION

The cerebellum is traditionally considered as an evolutionary innovation of jawed vertebrates or gnathostomes. This important neuroanatomical structure can thus be unambiguously recognized not only in osteichthyans, comprising bony fishes and tetrapods, but also chondrichthyans (or cartilaginous fishes), which represent an ancient gnathostome radiation. The latter have large cerebella with a hollow cerebellar body that exhibits striking segregation between granular regions (longitudinal granular eminences) and molecular /Purkinje cell layers, and a large caudal cerebellar region that forms paired ear-shaped auricular lobes. Ultrastructural and immunohistochemical studies on the adult cerebellum of a small shark, *S. canicula* , have revealed main cell types (Purkinje cells, Golgi cells, granule cells, stellate cells) that are similar to, but simpler than those of mammals (Álvarez-Otero et al., 1993, 1995; Sueiro et al., 1999). Jawless vertebrates, such as lampreys, do posses a cerebellar-like region, but Purkinje cells, granule cells and the cerebellar nuclei found in all jawed vertebrates are lacking. Systematic comparisons of the molecular and cellular mechanisms controlling hindbrain development between the major vertebrate taxa are important to identify gnathostome and cyclostome general characteristics and point to possible differences underlying this anatomical divergence. Among gnathostomes, these mechanisms have been extensively studied in model organisms, all belonging to osteichthyans. In contrast, analyses of cerebellar morphogenesis in cartilaginous fishes have been restricted to general histological methods (Larsell, 1967) and the cellular and molecular mechanisms of its development remain poorly known.

The absence of rhombic lip-derived cerebellar and precerebellar systems in lampreys has been related with the lack of Pax6 expression in the rhombic lip (Murakami et al., 2005). In the mouse, this transcription factor is expressed in rhombic lip-derived cells (granule cell precursors) during their migration from the external germinal layer (Engelkamp et al., 1999) and it appears involved in regulating granule cell polarization during parallel fibre formation (Yamasaki et al., 2001) and in the coordinated transition from proliferative precursor cells to fully differentiated cerebellar neurons (Swanson et al., 2005). Pax6 is also expressed in cerebellar granule cell precursors of the chick (Gilthorpe et al., 2002) and zebrafish (Wullimann and Rink, 2001). Whether this expression is an osteichthyan specific character or whether it is also conserved in cartilaginous fishes remains to be assessed. More generally,

studies in a representative of chondrichthyans are necessary to formally test whether the emergence of a true cerebellum in gnathostomes paralleled an early co-option of Pax6 in the rostral hindbrain in this lineage, as previously suggested (Murakami et al., 2005).

In order to address these points, we have first completed a study of the patterns of proliferation, migration and differentiation in the developing cerebellum of two shark species (*Scyliorhinus canicula* and *Haploblepharus fuscus*). This analysis was conducted by immunochemistry, using immunomarkers of proliferation (PCNA), migration/lamination (RELN) and early and late neuronal differentiation (GABA, GAD, CR). The extracellular matrix protein reelin (RELN), the calcium-binding protein calretinin (CR) and the inhibitory neurotransmitter GABA are all known to play important roles during cerebellar morphogenesis in mammals. We have then performed an exhaustive analysis of the organisation of Pax6 expressing cells using both *in situ* hybridisation and immunohistochemistry. Finally, we have taken advantage of double and triple immunolabelling to address the coexpression of Pax6 and markers of proliferation and differentiation. Systematic comparisons of the results with those reported in osteichthyan model organisms shed light on the ancestral pattern of cerebellum development in jawed vertebrates, thus highlighting the importance of developmental studies conducted in elasmobranchs.

MATERIALS AND METHODS

Experimental animals

Embryos, juveniles and adult specimen of *S. canicula* were obtained and processed as mentioned in Chapter 1. The following embryonic stages were analysed: stage 26 (3 embryos), stage 27 (3 embryos), stage 28 (3 embryos), stage 29 (4 embryos), stage 30 (4 embryos), stage 31 (7 embryos), and stage 32 (6 embryos). In addition, 3 juveniles (total length from 10 to 14 cm) and 1 adult (about 50 cm total length) was also used.

Tissue preparation

After fixation and sectioning (see material and methods section in Chapter 1 for futher details), tissue was processed either by immunohistochemistry for Pax6, CR, RELN, GAD and GABA (see below), or by *in situ* hybridisation with a *ScPax6* probe (Derobert et al., 2002).

For GABA immunohistochemistry, specimens where fixed by immersion (embryos) or perfusion (prehatching embryos, juveniles and adults) in 5% glutaraldehyde in EPB with 1% sodium metabisulphite added, and postfixed in the same fixative.

Immunohistochemistry

The following primary antibodies were used: monoclonal anti-Pax6 (Sigma, St Louis, MO), anti-PCNA (Sigma), and anti-RELN (Chemicon, now Millipore, Billerica MA) antisera; as well as polyclonal anti-Pax6 (Chemicon); anti-GAD65/67 (kindly provided by Dr. E. Mugnaini), anti-GABA (Affinity, Mamhead, UK), and anti-CR (Swant, Bellinzona, Switzerland) antisera. For a characterization of the polyclonal antibodies: anti-Pax6, anti-CR and anti-GAD see material and methods section in Chapter 3. The anti-GABA polyclonal antiserum (Affinity) was raised by immunizing albino rabbits with a GABA glutaraldehyde-bovine serum albumin complex. The anti-RELN monoclonal antiserum (Chemicon) was generated against recombinant reelin amino acids 40-189. The specificity of the RELN and CR antisera have been previously tested by western blot in dogfish and rat brain extracts (Candal et al., 2000; 2006; Graña et al., 2008).

Single labelling

Sections were processed by the PAP (for PCNA IHC) or ABC method for different immunocytochemical markers. First, sections were pre-treated for heat induced epitope retrieval, with 0.01M citrate buffer pH 6.0 for 30 min at 95°C, and allowed to cool for at least 20-30 min at room temperature (RT). Sections were rinsed in 0.05 M Tris-buffered saline containing 0.1% Tween-20 at pH 7.4 (TBS) for 5 min each, and endogenous biotin was blocked (except for PCNA IHC) by incubation with the avidin/biotin blocking kit (Vector, Burlingame, CA). Then sections were incubated with the primary antiserum overnight at RT. The following primary antibodies were used: rabbit polyclonal anti-Pax6 antiserum (Chemicon; diluted 1:400); rabbit polyclonal anti-CR antiserum (Swant; 1:500), rabbit polyclonal anti-

GABA antiserum (Affiniti, Manhead, UK; diluted 1:1000); sheep polyclonal anti-GAD65/67 antiserum (kindly provided by Dr. E. Mugnaini; diluted 1:5000); mouse monoclonal antibody anti-RELN (Sigma; diluted 1:300) and mouse monoclonal anti-PCNA antiserum (Sigma; diluted 1:500). The sections were then successively rinsed in TBS (two 10-min rinses), incubated in biotinylated goat anti-rabbit antiserum (Dako; 1:500), biotinylated rabbit anti-sheep antiserum (Dako; 1:200), biotinylated goat anti-mouse antiserum (Dako; 1:500), or goat anti mouse antiserum (Sigma; 1:30) for 1h at RT, rinsed in TBS (two 10-min rinses), and then incubated in either StreptABComplex/HRP (Dako) for 30 min or in mouse peroxidase-anti-peroxidase (PAP) complex (Sigma; 1:400) for 1h at RT. The immunoreaction was developed with SIGMAFAST™ 3.3'-DAB tablets (brown precipitate) as indicated by manufacturers. All dilutions were made with TBS containing 15% normal goat or sheep serum (Dako), 2% bovine serum albumin (BSA; Sigma), and 0.2% Triton X-100 (Sigma), and all incubations were carried out in a humid chamber. Of note that for GABA, all dilutions were made with TBS containing 1% sodium metabisulfite, and for RELN all dilutions contained 4% BSA. Finally, the sections were dehydrated, mounted and coverslipped, in some cases sections were counterstained with nuclear fast red.

Double labelling Pax6-PCNA

Sections were treated as described previously for Pax6 (Chemicon; diluted 1:400) immunohistochemistry, and the immunoreaction was developed with 0.25 mg/ml diaminobenzidine (DAB) tetrahydrochloride (Sigma) in TBS pH 7.4 with 2.5 mg/ml nickel ammonium sulphate and 0.00075% H_2O_2 (blue precipitate). Then, sections were rinsed in TBS (four 15-min rinses) and peroxidase activity was blocked again as above. After rinsing in TBS, sections were processed for PCNA immunohistochemistry as described above, and the immunoreaction was developed with SIGMAFAST™ 3.3'-DAB tablets (brown precipitate).

Double and triple immunofluorescence

Briefly, after heat induced epitope retrieval, sections were rinsed in TBS, and then incubated overnight at RT with a cocktail of primary antibodies containing either: a) rabbit anti-Pax6 (Chemicon; 1:200) and mouse anti-PCNA (Sigma; 1:200); or b) rabbit anti-CR (Swant, 1:200), monoclonal anti-Pax6 (Sigma; 1:50) and anti-$GAD_{65/67}$ (Mugnaini's antibody; 1:2500),

rinsed in TBS and subsequently detected by using a mixture of the following secondary antibodies: a) Alexa Fluor 546-labelled Goat-anti-Rabbit IgG and Alexa Fluor 488-labelled Goat-anti-Mouse IgG; or b) Alexa Fluor 546-labelled Goat-anti-Rabbit IgG antibodies (Molecular Probes; 1:200), Alexa Fluor 488-labelled Donkey-anti-Sheep IgG antibodies (Molecular Probes; 1:200) and FluoProbes 642-labelled Donkey-anti-Mouse IgG (FluoProbes, Interchim, France; 1:100). Immunofluorescent sections were photographed with a Spectral Confocal Laser Scanning Microscope (Leica TCS-SP2).

In situ hybridisation

In situ hybridisation was performed with a *ScPax6* probe on sections as described in material and methods section in Chapter 1.

RESULTS

The rhombencephalic alar plate exhibits paired rhombic lips that grow towards the dorsal midline in the rostral hindbrain, and at stages 28/29 have reached the midline to form a paired cerebellar plate, since both plates remain separated by a thick ependymal raphe. At stage 31, the cerebellar plate appeared in sagittal sections as an S-shaped lamina, with a rostral dome-shaped cerebellar body primordium and a transversally widened caudal auricular lobe primordium. The characteristic segregation between paramedian granular and lateral regions, as well as some cortical layering in the latter, became visible in the cerebellar body. In later developmental stages studied, regional segregation and layering of the cerebellar body became more apparent. These observations match with that described and illustrated by (Larsell, 1967) in elasmobranchs species (sharks and rays).

Stage 29.

The most caudal cerebellar plate region consisted of PCNA-immunoreactive (proliferating) cells. More rostrally, PCNA-immunoreactive cells were mostly observed in the thick ventricular zone (VZ), which was covered by a PCNA-negative layer (IZ) except near the midline (Fig. 1A). Interestingly, faint to moderate PCNA-ir cells extended over the IZ, forming a thin external germinal layer, which was more apparent caudally (arrows in Fig. 1A).

Pax6-expressing cells were abundant in the proliferating VZ, which was thicker toward the dorsal midline, and also some Pax6-ir extended laterally internal to the PCNA-ir cells of the external germinal layer (arrows in Fig. 1B). Faint Pax6-expressing cells were also observed migrating away the VZ in intermediate regions of the cerebellar plate (arrowhead in Fig. 1B). The cells of the midline medullary velum were PCNA-ir but Pax6 negative. GABA and its synthesizing enzyme GAD, which are reliable markers of some cerebellar neuronal populations (Takayama and Inoue, 2004), are expressed in cells that form a thick IZ band extended throughout most the cerebellar plate, probably mostly consisting of Purkinje cells (Figs. 1C, D; see also Carrera, 2008). Some GABAergic (differentiating) cells were also observed among cells of the VZ (arrow in Fig. 1D).

Stage 31.

Intense cell proliferation was maintained through the entire width of the caudal cerebellar plate (auricular lobe primordium), but rostrally (the cerebellar body primordium) PCNA-ir cells became concentrated in the thick dorsomedial VZ. The transition auricular lobe/cerebellar body was marked by the appearance of an IZ between the medial VZ and the wide proliferating caudal region, which gave also rise to a lateral thick IZ rostral to a small lateral ventricular recess. PCNA-ir cells were very scarce in and over the IZ (Fig. 1E), and the external germinal layer was no longer recognizable after stage 31. Pax6-ir cells showed a distribution similar to the intense PCNA-ir cells in the auricular lobe but at rostral levels most Pax6-ir cells occupied external IZ layers (Fig. 1F). In the cerebellar body primordium, Pax6-expressing cells were mostly located in or close to the thick dorsomedial VZ, which will originate the paramedian granular eminences (Figs. 1G, H). Three layers were distinguished in the lateral IZ of the cerebellar body of late stage-31 embryos (Fig. 1G) on the basis of the patterns of Pax6-, PCNA-, RELN- and CR-immunoreactivity (present results) and of the previously reported GABAergic pattern (Carrera, 2008): a thin transient band of GABA-ir cells (arrow in Fig. 1I) that lay below a layer of cerebellar afferents, that contains CR-ir fibres (Fig. 1G); a thick Purkinje cell layer mostly consisting of faint GABA-ir perikarya Purkinje cells; and a thin primordial molecular layer that contains densely grouped small highly GAD-ir cells (Fig. 1I). The primordial granular layer was broader close to the thick dorsomedial VZ and contained abundant Pax6 cells (Fig. 1G). RELN appears to be a key regulator of Purkinje cell migration through its expression by granule cells of the external

germinal layer and a subset of rhombic lip-derived cells (D'Arcangelo et al., 1995; Swanson et al., 2005; Fink et al., 2006). In the *S. canicula* stage 31 embryos, RELN-immunoreactivity was observed in small cells of the IZ and weak RELN immunoreactivity also appeared in a thin external band (arrows in Fig. 1J).

Stage 32.

PCNA immunoreactivity was maintained in the VZ especially at medial levels of the cerebellar body (Fig. 2A). Numerous Pax6-ir cells were observed adjacent to the medial VZ in the paramedian granular eminence primordium, and some Pax6-ir cells also extended as a thin wedge more laterally, but the lateral region of the cerebellar body was devoid of these cells (Fig. 2A). Most of these Pax6-positive cells probably represent granule cells. At later stages, the thickness of the medial granular layer increased notably to form the longitudinal granular eminences. CR, that is a consistent marker of some cerebellar neuronal populations (Bastianelly, 2003), is expressed in some CR-ir cells (stellate cells), firstly observed in an external position corresponding to the primordial molecular layer (Fig. 2B), and in abundant CR-ir fibres in the inner fibre layer (Fig. 2B). For comparison with the GAD-ir distribution at this stage, firstly described by Carrera (2008), see Fig. 2C.

Juveniles and adults.

A thick VZ facing the midline was maintained in the granular eminences of juveniles and adults (Figs.2D-I), where PCNA-ir cells were co-distributed with Pax6-ir cells, though colocalisation of these markers was not apparent (Fig. 2D). Expression of both Pax6 gene and protein was high in cerebellar granule cells of these sharks (Figs. 2D-G). Coinciding with that previously reported in adults (Sueiro, 2003), in juveniles GAD immunoreactivity was absent from the VZ of the granular eminences, weak in Purkinje cells, moderate in Golgi cells of the granular layer and in stellate cells of the molecular layer, and intense in Golgi cell terminals around *glomeruli* of the granular layer, in fibres of the molecular layer and in boutons contacting somata and dendrites of Purkinje cells (Figs. 2F, G). Numerous CR-ir stellate cells were observed in the molecular layer of juveniles and adults (Figs. 2F,G), and some Golgi cells showed moderate CR immunoreactivity. CR and GAD appears to colocalise in some stellate and Golgi cells (arrows in Fig. 2F). RELN immunoreactivity was also observed in a few cells of both

the granular and molecular layers in the adult (Sueiro et al., 1999). Other changes as regards stage 32 were the conspicuous growth and maturation of the molecular and granular layers.

DISCUSSION

In mammals, Pax6 is expressed in precursors of granule cells during their migration from the external germinal layer (Engelkamp et al., 1999), being involved in regulating granule cell polarization during parallel fibre formation (Yamasaki et al., 2001) and the coordinated transition from proliferative precursor cells to fully differentiated granular neurons (Swanson et al., 2005). Results in developing zebrafish showing Pax6-expression in external germinal layer and cerebellar granule cells (Wullimann and Rink, 2001) and present results in developing and adult sharks showing Pax6 expression in granule cells indicate that Pax6 is a general marker of this cerebellar cell type in gnathostomes.

Our study of the spatiotemporal distribution of proliferating and Pax6-expressing cells in the cerebellar body reveals two phases in the development of shark granule cells. During the *first phase*, some early granule (Pax6) cells appear to arise from two proliferation zones well recognized in the cerebellar body at stage 29: the VZ and the external germinal layer (see Fig. 1B). This interpretation is based on the observation of external Pax6 cells just internal to the band of proliferating cells of the external germinal layer (compare Figs. 1A and B), and inner (IZ) Pax6 cells apparently migrating from the VZ (see arrowhead in Fig. 1B). From stage 32 onwards (*second phase*), new Pax6 (granule) cells arise exclusively from the medial VZ because the external germinal layer is no longer recognized after stage 31, i.e. when most granule cells originate. These observations suggest two different mechanisms in the development of (Pax6-expressing) granule cells: some early granule cells arise from a transient external germinal layer but most of them originate in the VZ to migrate either radially (see arrowhead in Fig. 1B), or tangentially (most of the cerebellar body granule cells). During the *first phase*, Pax6 cells of these two origins appear to form a primordial granular layer of the cerebellar body that extends from medial to lateral, while during the *second phase,* there is a clear relation between the progressive restriction of the proliferative zone and the Pax6-expressing cells to the medial region of the cerebellar body, and the formation of the paramedian granular eminences.

By comparison with other elasmobranch cerebellar neurons, granule cells appear very late, as has been reported in mammals (Altman and Bayer, 1997). Likewise, a transient external germinal layer exists in sharks, but it differs in extension and origin because a caudal specialized region equivalent to the germinal trigone of mammals was not observed in the present work; this germinal trigone gives rise to the extensive external germinal layer that migrates massively and populates of granule cells the cerebellar cortex (Altman and Bayer, 1997).

As in teleosts (Ekström et al., 2001; Zupanc et al., 2005), proliferation in the cerebellum of sharks remains active through whole lifespan. However, differences can be noted in the location of proliferation zones in adults. In teleosts (Ekström et al., 2001; Zupanc et al., 2005), proliferating cells extend in a superficial band similar to the secondary matrix zone (external granular layer) observed during development (Pouwels, 1978; Wullimann and Knipp, 2000; Candal et al., 2005). In contrast, proliferative activity in adult sharks is not located in a secondary matrix zone (the external germinal layer) but in ventricular zones located medially in the granular eminences. This location is similar to that observed in amphibians. In *Xenopus*, although a proliferative external germinal layer is distinguished at larval stages (Wullimann and Rink, 2001), proliferating cells in the adult cerebellum are exclusively observed in the medial part of the granular layer (Raucci et al., 2006).

Granule cell precursors secrete RELN in mammals, which has been related with the regulation of migration of Purkinje cells (D'Arcangelo et al., 1995). A similar role for RELN has been suggested in zebrafish on the basis of its expression in granule cells and in the external germinal layer of postembryonic stages (Costagli et al., 2002). Our results showing RELN-ir cells in the cerebellar body suggest that RELN may have a similar role in sharks. However, unlike in zebrafish (Costagli et al., 2002), we have distinguished RELN immunoreactivity in the primordial and mature molecular layer.

Results obtained with CR and GAD (present results and Carrera, 2008) reinforce the hypothesis of the two phases in the shark cerebellar development because they reveal that the beginning of the *second phase* coincides with the organization and segregation of the three cerebellar layers. Our results also reveal that the expression of GABAergic markers in cerebellar cells occurs earlier than CR expression.

In conclusion, our results reveal that the patterns of cell proliferation and differentiation in the cerebellar body are rather similar between sharks and tetrapods. We therefore propose that the developing cerebellar body of cartilaginous fish may be a reliable model to infer ancestral, evolutionary conserved, developmental patterns through systematic comparisons with vertebrate model organisms. This in no way means that cerebellar development as a whole should be regarded as primitive in these species. Actually, the developmental patterns of auricles and cerebellar-like structures (lateral line area), which appear unique to chondrichthyans, may provide interesting examples of taxon-specific, highly specialized, derived patterns.

REFERENCES

Altman J, S.A. Bayer SA (1997). Development of the cerebellar system. CRC Press, Boca Raton, pp. 783.

Álvarez-Otero R, Díaz-Regueira S, Anadón R (1993). New structural aspects of the synaptic contacts on Purkinje cells in an elasmobranch cerebellum. J Anat, 182: 13-21.

Álvarez-Otero R, Pérez SE, Rodríguez MA, Adrio F, Anadón R (1995). GABAergic neuronal circuits in the cerebellum of the dogfish *Scyliorhinus canicula* (Elasmobranchs): an immunocytochemical study. Neurosci Lett, 187: 87-90.

Ballard WW, Mellinger J, Lechenault H (1993). A series on normal stages for development of *Scyliorhinus canicula*, the lesser-spotted dogfish (Chondrichthyes: Scyliorhinidae). J Exp Zool, 267: 318-336.

Bastianelli E (2003). Distribution of calcium-binding proteins in the cerebellum. Cerebellum, 2: 242-262.

Candal E, Anadón R, Bourrat F, Rodríguez-Moldes I (2005). Cell proliferation in the developing and adult hindbrain and midbrain of trout and medaka (teleosts): A segmental approach. Dev Brain Res, 160:157-175.

Candal E, Pérez-Costas E, Cerviño MC, Quintela I, Sueiro C, Meléndez-Ferro M, Barja P, Rodicio MC, Rodríguez-Moldes I, Anadón R, Caruncho HJ (2006). Different localization of reelin and reelin cleavage products. Soc Neurosci (abstr), 26: 59.

Carrera I (2008). Desarrollo de los sistemas gabaérgico y aminérgicos en el sistema nervioso central de peces cartilaginosos. Ph. D. Thesis. University of Santiago de Compostela.

Costagli A, Kapsimali M, Wilson SW, Mione M (2002). Conserved and divergent patterns of reelin expression in the zebrafish central nervous system. J Comp Neurol, 450: 73-93.

D'Arcangelo G, Miao GG, Chen S, Soares HD, Morgan JI, Curran T (1995). A protein related to extracellular matrix proteins deleted in the mouse mutant reeler. Nature, 374: 719-723.

Derobert Y, Baratte B, Lepage M, Mazan S (2002). Pax6 expression patterns in *Lampetra fluviatilis* and *Scyliorhinus canicula* embryos suggest highly conserved roles in the early regionalization of the vertebrate brain. Brain Res Bull, 57: 277-280.

Ekström P, Johnson CM, Ohlin LM (2001). Ventricular proliferation zones in the brain of an adult teleost fish and their relation to neuromeres and migration (secondary matrix) zones. J Comp Neurol, 436: 92-110.

Engelkamp D, Rashbass P, Seawright A, van Heyningen V (1999). Role of Pax6 in development of the cerebellar system. Development, 126: 3585-3596.

Fink AJ, Englund C, Daza DAM, Pham D, Lau C, Nivison M, Kowalczyk T,. Hevner RF (2006). Development of the deep cerebellar nuclei: transcription factors and cell migration from the rhombic lip. J Neurosci, 26: 3066-3076.

Gilthorpe JD, Papantoniou EK, Chédotal A, Lumsden A, WingateRJT (2002). The migration of cerebellar rhombic lip derivatives. Development, 129: 4719-4728.

Graña P, Anadón R, Yáñez J (2008). Immunocytochemical study of calretinin and calbindin D-28K expression in the retina of three cartilaginous fishes and a cladistian (*Polypterus*). Brain Res Bull, 75: 375-378.

Larsell O (1967). The comparative anatomy and histology of the cerebellum from myxinoids through birds. pp. 37-61. University of Minnesota Press, Minneapolis,

Murakami Y, Uchida K, Rijli FM, Kuratani S (2005). Evolution of the brain developmental plan: Insights from agnathans.Dev Biol, 280: 249-259.

Pouwels E (1978). On the development of the cerebellum of the trout, *Salmo gairdneri*. I. Patterns of cell migration. Anat Embryol, 152: 291-308.

Raucci F, Di Fiore MM, Pinelli C, D'Aniello B, Luongo L, Polese G, Rastogi RK (2006). Proliferative activity in the frog brain: A PCNA-immunohistochemistry analysis. J Chem Neuroanat, 32: 127-142.

Sueiro C (2003). Estudio inmunohistoquímico de los sistemas gabaérgicos del sistema nervioso central de peces elasmobranquios y su relación con sistemas catecolaminérgicos y peptidérgicos. Ph. D. Thesis. University of Santiago de Compostela.

Sueiro C, Rodríguez-Moldes I, Caruncho HJ, Sieghart W, Anadón R (1999). Estudio inmunocitoquímico de la distribución de subunidades del receptor $GABA_A$ en el cerebelo de un pez, la pintarroja (*Scyliorhinus canicula*). Rev Neurol, 30: 228.

Swanson DJ, Tong Y, Goldowitz D (2005). Disruption of cerebellar granule cell development in the Pax6 mutant, *Sey* mouse. Dev Brain Res, 160: 176-193.

Takayama C, Inoue Y (2004). Morphological development and maturation of the GABAergic synapses in the mouse cerebellar granular layer. Dev Brain Res, 150: 177-190.

Wullimann MF, Knipp S (2000). Proliferation pattern changes in the zebrafish brain from embryonic through early postembryonic stages. Anat Embryol, 202: 385-400.

Wullimann MF, Rink E (2001). Detailed immunohistology of Pax6 protein and tyrosine hydroxylase in the early zebrafish brain suggests role of Pax6 gene in development of dopaminergic diencephalic neurons. Dev Brain Res, 131: 173-179.

Wullimann MF, Rink E, Vernier P, Scholler G (2005). Secondary neurogenesis in the brain of the African clawed frog, *Xenopus laevis*, as revealed by PCNA, Delta-1, Neurogenin-Related-1, and NeuroD expression. J Comp Neurol, 489: 387–402.

Yamasaki T, Kawaji K, Ono K, Bito H, Hirano T, Osumi N, Kengaku K (2001). Pax6 regulates granule cell polarization during parallel fiber formation in the developing cerebellum. Development, 128: 3133-3144.

Zupanc GK, Hinsch K, Gage FH (2005). Proliferation, migration, neuronal, differentiation, and long-term survival of new cells in the adult zebrafish brain. J Comp Neurol, 488: 290-319.

Figure. 1. Transverse (A, B, D-I) and sagittal (C, J) sections through the cerebellum of *S. canicula* (C, D, I, J) and *H. fuscus* (A, B, E, F, H) at the embryonic stages indicated, showing the patterns of the different markers. **A-B.** Cerebellar plate with PCNA-ir (A) and Pax6-ir (B) cells in the VZ and in the external part of the IZ (arrows). Note Pax6-ir cells in the inner IZ (arrowhead in B). **C-D.** GABA-ir (C) and GAD-ir (D) cells occupy the IZ of the cerebellar body (CB). Note also GAD-ir cells radially oriented in the VZ (arrow in D). **E-F.** The IZ at the transition auricular lobe/cerebellar body contains very scarce PCNA-ir cells (E) but abundant Pax6-ir cells (arrows in F). **G.** Schematic drawing of the cerebellar body showing the location of primordial molecular, Purkinje cell and granular layers. **H.** Pax6-ir (red) and PCNA-ir (green) cells in the paramedian granular eminences. Arrows indicate unspecific labelling in blood vessels and epidermis. **I.** GABA immunoreactivity in the lateral part of the cerebellar body. Asterisk, layer of immunonegative cerebellar afferents fibres; Arrow, transient band of GABA-ir cells. **J:** Nuclear red counterstained section of the caudal cerebellar body showing RELN immunoreactivity in the IZ and primordial molecular layer (arrows). GR, granular layer; MOL, molecular layer; P, Purkinje cell layer; RhTg, rhombencephalic tegmentum; TO, optic tectum. Scale bars: 10 μm (J); 50 μm (A, H, I); 100 μm (B, D-F); 250 μm (C, G).

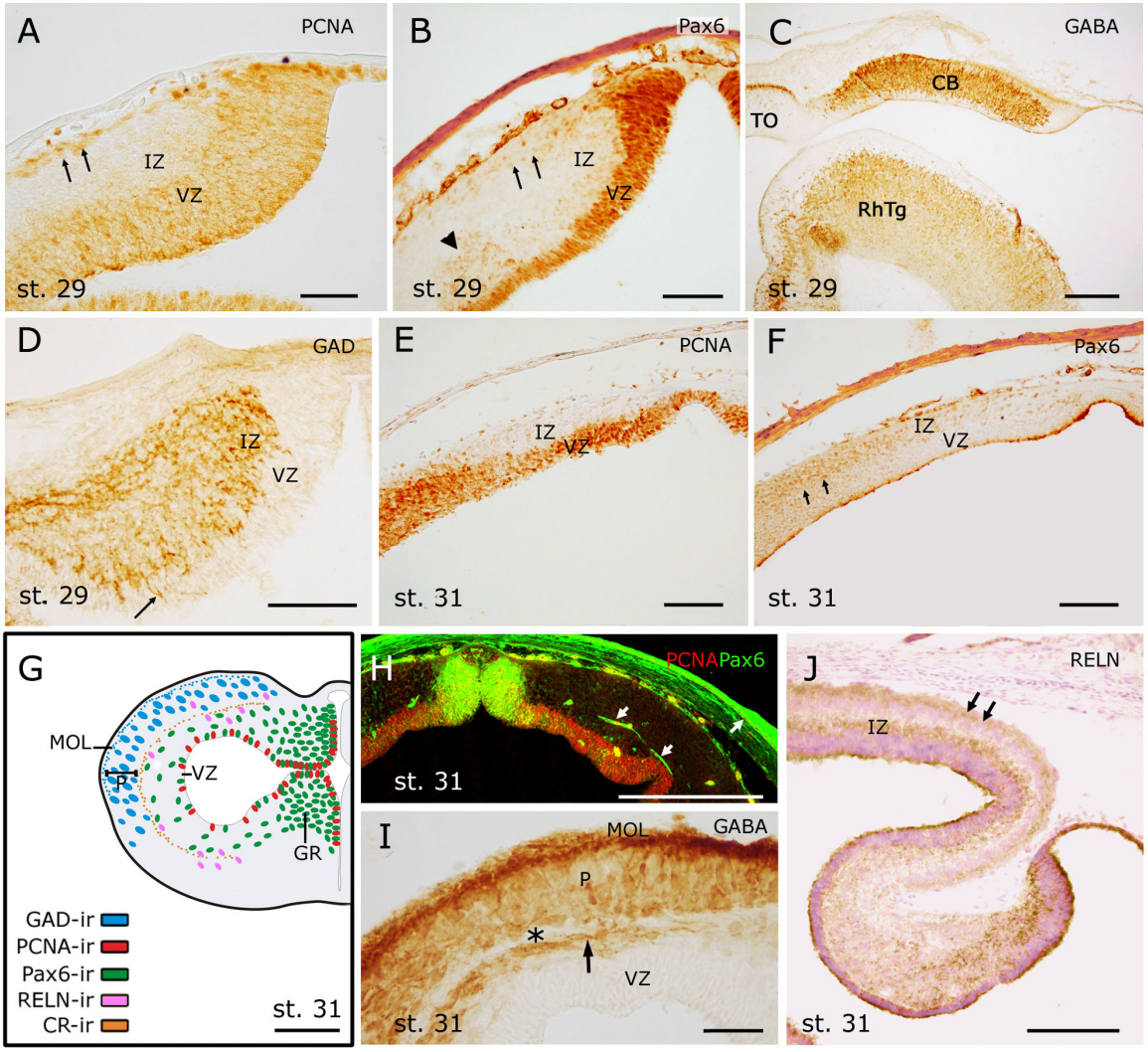
A
PCNA
IZ
VZ
st. 29
B
Pax6
IZ
VZ
st. 29
C
GABA
CB
TO
RhTg
st. 29
D
GAD
IZ
VZ
st. 29
E
PCNA
IZ
VZ
st. 31
F
Pax6
IZ
VZ
st. 31
G
MOL
P
VZ
GR
GAD-ir
PCNA-ir
Pax6-ir
RELN-ir
CR-ir
st. 31
H
PCNAPax6
st. 31
I
MOL
GABA
P
VZ
st. 31
J
RELN
IZ
st. 31

Figure 2. Transverse (A-D, F) and parasagittal (E) sections through the cerebellum of stage 32 embryos (A-C), and juveniles (D-F) of *S. canicula* (B,C, E,) and *H. fuscus* (A, D, F). **A.** Stage 32 showing abundant PCNA-ir (brown) and Pax6-expressing (blue) cells at paramedian levels of the cerebellar body but very scarce laterally. **B-C.** At stage 32, CR immunoreactivity (B) is found in some cells of the molecular layer (arrow) and in fibres of the inner fiber layer (asterisk), whereas largely different distribution of GAD immunoreactivity (C) is seen in the three cerebellar layers. **D**. In the VZ of the granular eminences, Pax6-ir cells (green) are among PCNA-ir cells (red). Note that cells are either PCNA-ir (large arrow) or Pax6-ir (short arrow). **E.** Section through the paramedian granular eminences labelled with the ScPax6 probe. **F.** Triple labelling shows the distribution of Pax6 (blue), GAD (green) and CR (red) in the cerebellar body. Arrows point to some CR/GAD-ir cells. **G.** Schematic drawing of a transverse section of the developed cerebellar body. For colour code, see figure 1G. Scale bars: 50 μm (D); 100 μm (A-C, E, F); 250 μm (G). For abbreviations, see Fig. 1 legend.

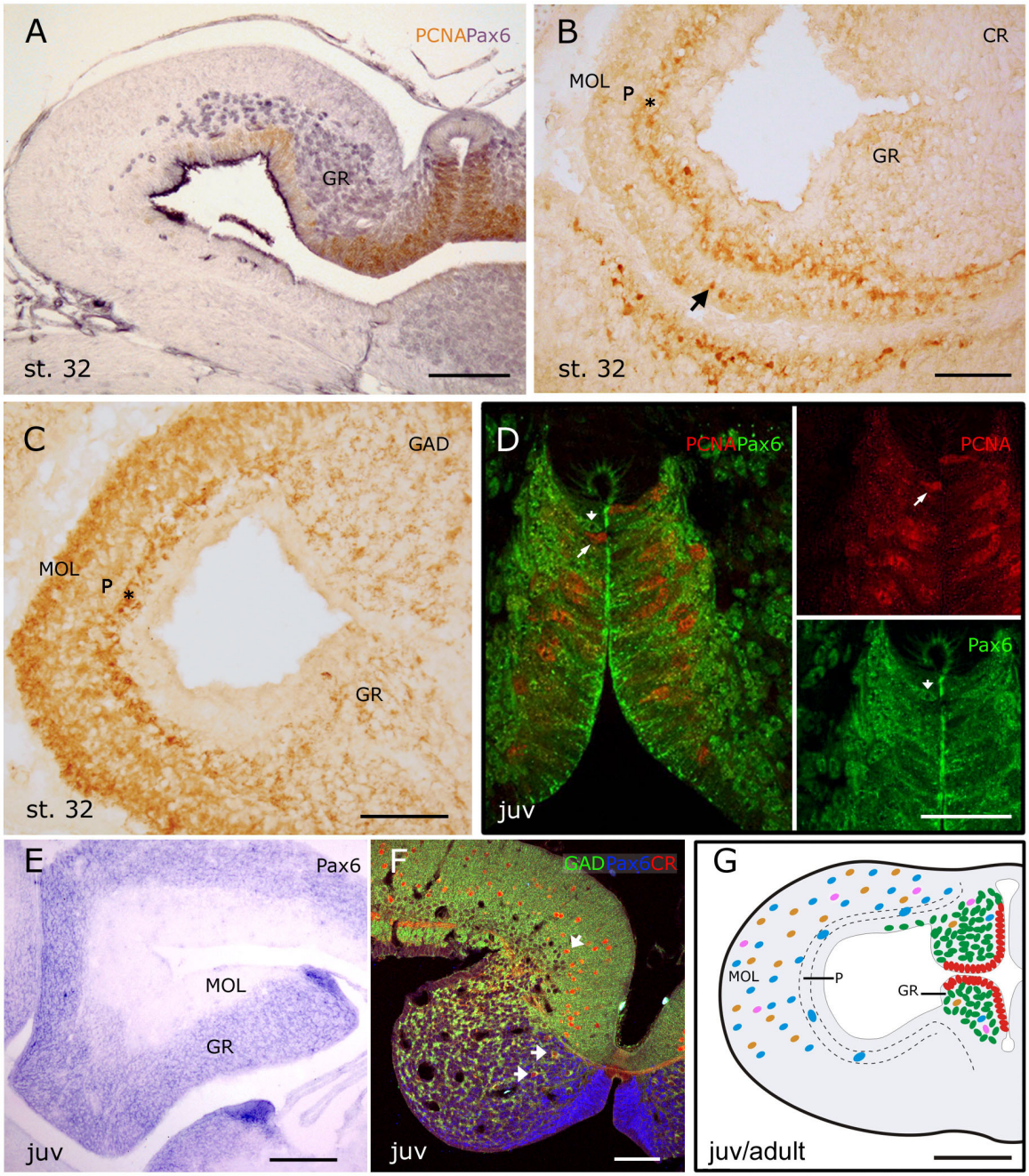
A
PCNAPax6
GR
st. 32
B
CR
MOL
P
*
GR
st. 32
C
GAD
MOL
P
*
GR
st. 32
D
PCNAPax6
PCNA
Pax6
juv
E
Pax6
MOL
GR
juv
F
GADPax6CR
juv
G
MOL
P
GR
juv/adult

Chapter 5.

Pax6 expression in the developing and mature retina of sharks

INTRODUCTION

The Pax6 gene is a key regulator of multiple aspects of eye development

Correct formation of eyes depends on specific interactions between neural and ectodermal tissues, coupled with temporally distinct gene expression, and a regulated sequence of signalling events. Retinogenesis is a multistep developmental process that requires differentiation and assembly of several different types of neurons and glia. This process must be precisely regulated to produce differentiated cells at specific times, and in appropriate types and numbers. Developmental processes are controlled by several morphogens and developmental control genes that are highly conserved among organisms as diverse as nematodes and humans, suggesting that vertebrates share a common genetic programme of development (Püschel et al., 1992). Most of these genes are members of multigene families that share conserved domains such as homeo-boxes, paired-boxes, zincfingers, and POU-boxes, expression of which is finely regulated in time and space (Püschel et al., 1992; de Melo et al., 2003; Duparc et al., 2007).

One such gene is the Pax6 (Paired box 6) transcription factor. From among a number of potential regulatory genes that are expressed in optic tissues during formation of the eye, Pax6 has been shown to be critical for development. In vertebrates, *Pax6* mRNA (and/or its encoded protein Pax6) it is first localised toward the end of gastrulation in the anterior neural plate. As neurulation proceeds, *Pax6* expression resolves to the head ectoderm (presumptive lens placode region before lens induction) as well as to the optic pit from which the optic vesicle evaginates (Walther and Gruss, 1991; Püschel et al., 1992; Li et al., 1994; Del Rio-Tsonis et al., 1995; Grindley et al., 1995; Hirsch and Harris, 1997; Li et al., 1997; Kamachi et al., 1998; Derobert et al., 2002). In various vertebrates (including zebrafish, urodeles, *Xenopus*, chick, mouse and human), *Pax6* is later expressed in the optic vesicle, the lens, the cornea, the iris, the retinal pigment epithelium and throughout the entire retinal progenitor population preceding differentiation within the neural retina (Krauss et al., 1991; Walther and Gruss, 1991; Püschel et al., 1992; Del Rio-Tsonis et al., 1995; Grindley et al. 1995; Macdonald et al., 1995; Belecky-Adams et al., 1997; Hirsch and Harris, 1997; Nishina et al., 1999; Ashery-Padan et al., 2000; Wullimann and Rink, 2001; de Melo et al., 2003; Arresta et al., 2005; Canto-Soler et al., 2008). In the mature eye, expression of Pax6 occurs in the corneal and lens epithelium and in the neural retina, where Pax6 become largely restricted to cells in

the ganglion cell layer (GCL) and inner part of the inner nuclear layer (INLi; Püschel et al., 1992; Del Rio-Tsonis et al., 1995; Macdonald et al., 1995; Hitchcock et al., 1996; Belecky-Adams et al., 1997; Hirsch and Harris, 1997; Nishina et al., 1999; Ashery-Padan et al., 2000; Wullimann and Rink, 2001; de Melo et al., 2003; Arresta et al., 2005; Edqvist et al., 2006; Alunni et al., 2007; González-Curto et al., 2007; Candal et al., 2008; Canto-Soler et al., 2008), and in some species (zebrafish, chick and mouse), also in the horizontal cell layer (HCL; Macdonald et al., 1995; Belecky-Adams et al. 1997; Wullimann and Rink, 2001; de Melo et al., 2003; Edqvist et al., 2006; Canto-Soler et al., 2008). This changing pattern of expression has led to the suggestion that Pax6 plays different roles during eye development (Macdonald and Wilson, 1997).

Early eye development is highly sensitive to levels of Pax6

Mutations in the *Pax6* gene of several phylogenetically distant species reflect the evolutionary requirement of the gene for eye development (Del Rio-Tsonis et al., 1995; Grindley et al., 1995; Macdonald et al., 1995; Hirsch and Harris, 1997; Chow et al., 1999; Ashery-Padan et al., 2000; Chow and Lang, 2001; Kondoh et al., 2004; Philips et al., 2005; Canto-Soler and Adler, 2006; Tsonis and Fuentes, 2006; Duparc et al., 2007).

Deletions in the *Pax6* gene are semi-dominant and most result in loss-of-function mutations (Grindley et al., 1995; Chow and Lang, 2001; Tsonis and Fuentes, 2006). In the heterozygous state, they underlie the *Small eye* (*Sey*) phenotype in mice (Hogan et al. 1986; Hill et al. 1991) and rats (Matsuo et al. 1993; Fujiwara et al., 1994), characterized by reduced eye size (microphthalmia) in conjunction with lens defects, cataractogenesis and iris hypoplasia. In humans, heterozygous mutations cause Peter's anomaly (Hanson et al., 1994) and the ocular syndrome aniridia, characterized by iris hypoplasia and corneal opacification (Ton et al. 1991; Glaser et al. 1992; Jordan et al. 1992; Hanson et al. 1993).

Flies carrying homozygous mutations in *eyeless* (*ey*, the Drosophila equivalent of *Pax6*) and homozygous mouse or rat (*Sey*) mutants are anophthalmic (one or both eyes are absent) with neonatal death occurring (Hogan et al. 1986; Matsuo et al. 1993; Quiring et al., 1994; Grindley et al. 1995). Optic vesicles evaginate from the brain in *Sey/Sey* mutants but fail to constrict proximally, which results in a persisting luminal optic stalk. These optic vesicles come into contact with the surface ectoderm (Grindley et al. 1995), but this contact is not maintained

and lens placode thickening does not occur (Hogan et al. 1986; Matsuo et al. 1993; Grindley et al. 1995). Eventually, a structure that resembles the optic cup forms, although there is no indication of differentiation in presumptive neural retina or retinal pigment epithelium (both layers appear identical), and finally the optic structures degenerate (Grindley et al. 1995). This indicates that the initiation of optic vesicle formation occurs in a Pax6-independent manner, although the maintenance and continued development of these structures, i.e., the transformation of the optic vesicle into a normal optic cup, must be Pax6 dependent (Chow et al., 1999; Philips et al., 2005; Canto-Soler and Adler, 2006).

Correct development of the eye is particularly sensitive to Pax6 dosage (Hirsch and Harris, 1997; Chow et al., 1999; Ashery-Padan et al., 2000; Canto-Soler and Adler, 2006), as has been illustrated by overexpression studies in which additional copies of the *Pax6* locus were introduced in transgenic mice (Schedl et al. 1996). These studies revealed that an excess of *Pax6* is detrimental to normal eye development as it can also result in anophthalmia (Schedl et al., 1996). Misexpression of *eyeless* or mouse *Pax6* (Halder et al. 1995), squid *Pax6* (Tomarev et al. 1997), and ascidian *Pax6* (Glardon et al. 1997) in *Drosophila* non-eye imaginal discs, all resulted in the formation of ectopic eyes. Likewise, misexpression of *Pax6* in *Xenopus* (Altmann et al., 1997) resulted in the formation of small ectopic eyes containing fully differentiated cells for lens as well as the retinal pigment epithelium, photoreceptor, Müller, ganglion and amacrine cells characteristic of retinal layers (Chow et al., 1999). Thus, Pax6 expression is sufficient to induce ectopic eyes with complete networks of differentiated retinal cell types, although in a tissue and stage-specific manner (Halder et al., 1995; Chow et al., 1999; Tsonis and Fuentes, 2006).

Studies in chimeric mice derived from *Sey/Sey* and wild-type cells (Quinn et al., 1996; Collinson et al., 2000), as well as Pax6-misexpressing explant experiments (Fujiwara et al., 1994; Altmann et al., 1997) and conditional knockouts (Ashery-Padan et al., 2000) also suggest a cell-autonomous requirement for *Pax6* in lens ectoderm for adequate lens placode development (see Collinson et al., 2000; Chow and Lang, 2001; Duparc et al., 2007). However, Pax6 expression in the prospective lens ectoderm, although probably sufficient to ensure the formation and invagination of a lens placode, may not by itself ensure further maturation of the lens (Canto-Soler and Adler, 2006). Indeed, when the optic vesicle becomes defective as a result of Pax6 downregulation in the neural epithelium, lens placode begins to form, but becomes arrested at the lens vesicle stage (Reza and Yasuda, 2004; Canto-Soler and Adler,

2006). Moreover, Pax6 was also shown to be the primary determinant of maintenance of contact with the lens epithelium (Collinson et al., 2000). Together these results suggest that normal early eye development requires Pax6 expression both in the lens ectoderm and in the optic vesicle, and that there is a critical stage at which Pax6 expression in the optic vesicle is required not only for optic vesicle development, but also for lens development (Canto-Soler and Adler, 2006).

These findings have led to the suggestion that pax6/eyeless may be a "master control gene of eye development in multi-cellular organisms" (Halder et al. 1995; Chow et al., 1999; Gehring and Kazuho, 1999; Gehring, 2002; Cartier et al., 2006; Duparc et al., 2007), and that at least some of the functions of Pax6 in eye development have been conserved from invertebrates to vertebrates (Chow et al., 1999). However, much evidence indicates a role for Pax6 as a major selector gene rather than a master regulator, since a number of other genes operate upstream of, or in parallel with Pax6 in the gene network controlling eye development (Hever et al., 2006). Nevertheless, expression of all the molecules that participate in the dorsoventral (D-V) patterning of the retina are delayed relative to that of Pax6, suggesting that Pax6 may act at the initial steps of the cascade leading to the D-V patterning of the retina (Gibson-Brown et al., 1998; Sakuta et al., 2001; Schulte et al., 1999; Trousse et al., 2001; Zhang and Yang, 2001; Canto-Soler et al., 2006). Indeed, Pax6 activity is required for the establishment and maintenance of dorsal and nasotemporal characteristics in the optic vesicle, the optic cup and the optic stalk (Baumer et al., 2002, 2003). Pax6 has also been shown to act during proximo-distal specification (Collinson et al., 2000).

Later distinct functions of Pax6 in retinal neurogenesis

Studies in animals carrying homozygous mutations for Pax6 demonstrated that the optic cup (if formed) degenerates in the absence of Pax6, and that the animals die before completing embryonic development (González-Curto et al., 2007), leading to the assumption that neurogenesis is either arrested or fails to initiate. This complex phenotype has obscured attempts to address the incidence of the gene in processes following the formation of the optic vesicle, such as formation of the retina (Grindley et al. 1995; Ashery-Padan et al., 2000; González-Curto et al., 2007). However, as depicted above, in wild type animals Pax6 expression is maintained throughout retinal development, including early expression in all

retinal progenitor cells, and, in the differentiating retina, continued expression in some differentiated neurons in three retinal layers (GCL, INLi, and HCL; see above), suggesting that Pax6 is also necessary to ensure subsequent aspects of eye development, including maintenance of multipotency and proliferation of retinal progenitors in order to generate all retinal cell types, and regulation of the timing of neuron differentiation in the retina.

Neuron differentiation in the elasmobranch retina

While it is generally accepted that the pattern of expression of Pax6 within the retina is evolutionary conserved, studies are lacking in key vertebrate groups such as cartilaginous fishes. The retina of elasmobranchs (sharks, skates and rays) offers unique opportunities to explore retinogenesis for three main reasons: 1) as all fish species studied so far, it is expected to contain retinal stem cells within the ciliary marginal zone (CMZ), a peripheral ring of undifferentiated neuroepithelial cells located between the laminated retina and the ciliary region; 2) contrary to fast-developing species usually used as models for developmental studies (all of them osteichthyans), the large size and slow development of elasmobranchs make them appropriate for detailed analysis of the dynamics of development; and 3) elasmobranchs have a key phylogenetic position as an out-group to osteichthyans (bony fishes), which makes them suitable for identifying ancestral features of gnathostomes and thus for obtaining knowledge about the evolution of retinogenesis in vertebrates. Several studies have tackled with topography, neurochemistry and synaptic connections of neurons in the adult retina of elasmobranchs. A general description of the adult eye of a hound shark (the smooth dogfish, *Mustelus canis*) has been provided by Stell and Witkovsky (1973a) and the same authors have also provided light microscopy descriptions of ganglion cells (Stell and Witkovsky, 1973a), bipolar cells (Witkovsky and Stell, 1973a), horizontal and photoreceptor cells (Stell and Witkovsky, 1973b), and an electron microscopy study of bipolar cell synaptic terminals (Witkovsky and Stell, 1973b). Visual pigments and photoreceptors have been further analysed in *M. canis* by *in situ* absorbance measurements and scanning electron microscopy, as well as in other species of hound sharks (leopard shark, *Triakis semifasciata*; Sillman et al., 1996). The topographical distribution of retinal cells within the GCL has been reported in elasmobranchs, including the cat shark *Scyliorhirnus canicula* (Bozzano and Collin, 2000). More phylogenetically distant selaceans have also been studied as regards the morphology and physiology of horizontal cells (Toyoda et al., 1978), density distribution of

cones (Logiudice and Laird, 1994), morphologic relations of rods and cones and their synaptic connections (Stell, 1972), and absorbance measurements of rod and cone pigments (Gruber et al., 1990).

However, the patterns of cell proliferation and neurochemical differentiation in the retina of these fishes have received little attention. The scarce studies on retinogenesis in elasmobranchs have revealed differences with teleosts as regards the order of retinal cell differentiation (Fishelson and Baranes, 1999; Harahush et al., 2009). We thus provide a detailed analysis of the time of appearance of each retinal layer in *S. canicula* and *H. fuscus*, on the basis of which we define three developmental periods in the retina. To make this study useful for further comparative studies on the retina of elasmobranchs, we also provide a correlation between these periods and the "normal stages of development" defined by Ballard et al. (1993).

To gain insight into retinal morphogenesis in sharks, we have analysed the spatial and temporal distribution of Pax6 during retinogenesis and in the mature retina of two shark species, the lesser spotted catshark *Scyliorhinus canicula* (currently considered as a model organism; Coolen et al., 2009) and the shyshark *Haploblepharus fuscus*. We show that Pax6 distribution is conserved in the mature eyes of other distantly related vertebrate species suggesting conservation of Pax6 function across the Vertebrata. In order to compare Pax6 expression and cell proliferation during retinal development, we used double immunohistochemistry with a marker of cell proliferation (proliferating cell nuclear antigen, PCNA; see Chapter 6). The relationship between Pax6 and different subsets of differentiated cells (identified by expressing glutamic acid decarboxylase (GAD, the gamma-aminobutyric acid synthesizing enzyme), calretinin (CR), tyrosine hydroxylase (TH; the rate-limiting enzyme of the catecholamine synthesis), serotonin (5-HT) and CERN922-opsin, will be investigated in the following Chapters.

MATERIAL AND METHODS

Experimental animals

Embryos and juvenile specimens of *S. canicula* and *H. fuscus* were kindly provided by the Aquário Vasco da Gama and the Oceanário in Lisbon (Portugal), the Aquarium Finisterrae in A Coruña (Spain). Adult specimens were also provided by the Aquarium Finisterrae. Additionally, embryos of *S. canicula* were supplied by the Station Biologique de Roscoff (France). Eggs from different broods and juveniles were raised in fresh sea water tanks in standard conditions of temperature (16-18°C) and 12:12 h day/night cycle.

Staging of embryos

The embryonic stages of *S. canicula* were identified by their external features following Ballard et al. (1993) and the same features were used for staging the *H. fuscus* embryos. The following embryonic stages were analysed: stage 26 (3 *S. canicula* embryos), stage 27 (3 *S. canicula* embryos), stage 28 (3 *S. canicula* and 2 *H. fuscus* embryos), stage 29 (4 *S. canicula* and 3 *H. fuscus* embryos), stage 30 (2 *S. canicula* and 3 *H. fuscus* embryos), stage 31 (7 *S. canicula* and 7 *H. fuscus* embryos), stage 32 (6 *S. canicula* and 6 *H. fuscus* embryos), and stages 33 and 34 (prehatching; 3 *S. canicula* and 8 *H. fuscus* embryos). Moreover, 5 juveniles (3 *S. canicula* and 2 *H. fuscus*, from 10 to 14 cm in total length) and 1 adult *S. canicula* (about 50 cm in total length) were also processed.

Tissue preparation

Adequate measures were taken to minimize pain or discomfort to the animals. All procedures conformed to the guidelines established by the Spanish Royal Decree 223/1998 for animal experimentation and were approved by the ethics committee of the University of Santiago. Embryos were anaesthetized with 0.05% tricaine methane sulphonate (MS-222; Sigma, St. Louis, MO) in seawater and separated from the yolk before fixation in 4% paraformaldehyde (PFA) in elasmobranch's phosphate buffer (0.1 M phosphate buffer (PB) containing 670 mM urea, pH 7.4) for 48-72 h or in Clark's solution (75% ethanol, 25% acetic acid) for 12-36 h. Prehatching, juvenile and adult specimens were deeply anaesthetized with MS-222 and then perfused intracardially with elasmobranch Ringer's solution (1.7% NaCl,

0.024% KCl, 0.031% CaCl2, 0.044% MgCl2, 0.113% Na2SO4, 0.049% NaCO3H, and 2.7% urea) followed by the appropriate fixative. Eyes of stage 32-34 embryos, juveniles and adults were dissected out and postfixed for 4 h in the corresponding fixative. Specimens fixed in 4% PFA were cryoprotected with 30% sucrose in PB, embedded in OTC compound (Tissue Tek, Torrance, CA), frozen with liquid nitrogen-cooled isopentane, and cut on a cryostat. Specimens fixed in Clark's solution were dehydrated, embedded in paraffin, and cut on a rotary microtome. Parallel series of cryostat sections (14–18 μm thick) and rotary microtome sections (10–12 μm thick) of specimens, cut in vertical planes along the dorsoventral or nasotemporal axis of the retina (transverse or sagittal planes with respect to the brain, respectively), were mounted on Superfrost Plus (Menzel-Glasser1) slides.

Antibody characterisation

The polyclonal antibodies to Pax6 were generated in rabbit (PRB-278P; Covance, Emeryville, California) and goat (NB100-2913; Novus Biologicals, Littleton, CO). The rabbit antibody was raised against the peptide QVPGSEPDMSQYWPRLQ derived from the C-terminus of the mouse Pax6 protein and subsequently purified on a Protein A Column. The goat Pax6 antibody was raised against the peptide EPDMSQYWPRLQC derived from the C-terminus of the human Pax6 protein and according the manufacturers it is expected to recognize both reported human isoforms (NP_000271.1 and NP_001595.2). The specificity of the immunoreaction in the retina and brain of *S. canicula* was tested in our laboratory by preadsorbing the primary antibodies with the antigenic peptide (NB100-2913PEP; Novus Biologicals, Littleton, CO) used for generation of the NB100-2913 antiserum. For both antibodies, the immunostaining was completely abolished in *S. canicula* sections treated with the primary antibodies at working dilution (5μg/mL) preadsorbed with the blocking peptide at a concentration of 10μg/mL at 4°C for 24 hours. Both antibodies label the same retinal cell types in *S. canicula* and *H. fuscus* (see Results section).

Pax6 immunohistochemistry

For heat induced epitope retrieval, sections were pretreated with 0.01M citrate buffer pH 6.0 for 30 min at 95°C, and allowed to cool for at least 20-30 minutes at room temperature (RT). Sections were rinsed twice in 0.05 M Tris-buffered saline pH 7.4 (TBS) for 5 min each,

and residual avidin/biotin activity was removed by incubation with the avidin/biotin blocking kit (Vector, Burlingame, CA), as indicated by the manufacturers. Sections were incubated overnight at RT with rabbit polyclonal anti-Pax6 (Covance, Princeton, NJ; diluted 1:400) or goat polyclonal anti-Pax6 (Novus Biologicals, Littleton, CO; diluted 1:200). Sections were then rinsed in TBS (two 10 min rinses) and endogenous peroxidase was blocked with 10% H_2O_2 in phosphate buffered saline pH 7.4 (PBS) for 30 min at RT. Sections were rinsed in TBS, incubated in biotinylated goat anti-rabbit IgG (Dako; 1:500) for 1 h at RT, rinsed again in TBS, and incubated in the preformed avidin:biotinylated enzyme complex by using the Vectstain ABC system (Vector Laboratories) for 30 min at RT. After two 10 min rinses in TBS, the immunoreaction was developed with 0.25 mg/ml diaminobenzidine (DAB) tetrahydrochloride (Sigma) in TBS pH 7.4 with 2.5 mg/ml nickel ammonium sulfate and 0.00075% H_2O_2 (blue precipitate), as indicated by manufacturers. All dilutions were made with TBS containing 2% bovine serum albumin (BSA; Sigma), 15% normal goat serum (Dako) and 0.2% Triton X-100 (Sigma), and all incubations were carried out in a humid chamber. Finally, the sections were dehydrated, mounted and coverslipped. Negative controls performed by omitting the primary, secondary or tertiary antibodies showed no immunostaining. Parallel sections were stained with haematoxylin-eosin to facilitate identification of retinal cells and layering. Photomicrographs were taken with an Olympus DP71 colour digital camera, fitted to a Provis photomicroscope (Olympus, Tokyo).

***Pax6 in situ* hybridisation**

A Pax6 cDNA fragment of 393 bp (GenBank accession number: AF384972), previously isolated by Derobert et al. (2002) and kindly provided by Dr Mazan, was cloned into the pTZ19R plasmid. After linearization by *Eco*RI digestion, sense and antisense digoxigenin-UTP labeled *Pax6* RNA probes (*ScPax6*) were synthesized directly by reverse transcription following standard procedures. In situ hybridisation on cryostat sections was performed using standard protocols. Briefly, sections were treated with 5μg/ml proteinase-K (Roche Applied Science, Mannheim, Germany) for 2 min at RT, hybridized with sense or antisense probes overnight at 65°C, and incubated with the alkaline phosphatase coupled anti-digoxygenin antibody (1:2,000; Roche Applied Science) overnight at 4°C. Finally, colour reaction was performed in the presence of BM-Purple (Roche Applied Science). Control sense probes did not lead to any detectable signal. The same probes has been previously used by Derobert et

al. (2002) to analyse *Pax6* expression patterns in the developing brain (up to stage 22) of *S. canicula*.

RESULTS

Growth pattern of the *S. canicula* / *H. fuscus* embryonic retina

Three developmental periods can be distinguished in the retina of the *S. canicula* and *H. fuscus* embryos as regards the growth pattern (Fig. 1). As both species showed similar timing of retinal development, only *S. canicula* sections are shown in the Figure. The *first developmental period*, between stages 26 and 29 (Figs. 1A, B), is characterized by the neuroepithelial appearance of the retina, the arrangement of cells in radial columns and by the absence of any regional differentiation or layering. The *second developmental period* (Figs. 1C, D) is recognizable by the progressive formation of layers in the central part of the retina from vitreal to scleral and from central to marginal. It begins in stage 30 embryos, with the appearance of a differentiating central region where the inner plexiform layer (IPL) becomes recognizable between the GCL and the inner nuclear layer (INL), coinciding with the appearance of a primordial optic fibre layer. This period ends at stage 32, when the outer plexiform layer (OPL) becomes recognizable in the central retina between the outer nuclear layer (ONL) and the INL. The formation of retinal layers allows defining the CMZ as a wedge-shaped neuroepithelial zone that lies between the laminated retina and the ciliary epithelium. A *transition zone* is distinguished between the not layered CMZ and the layered central retina (Fig. 1C). This *transition zone* is formed by an inner part where the IPL separates the GCL and INLi, and an outer neuroepithelial part in which the OPL is not observed. In the *third developmental period* (Figs. 1E-G), from stage 33 embryos up to hatching, the layering of the retina extends following a central-to-peripheral gradient to nearly the entire circumference of the retina. The two plexiform layers are easily distinguished thoroughly, except in the temporoventral retina (asterisk in Figs. 1C, E), where only the GCL, IPL and INL are distinguishable. The neuroepithelial organization of the CMZ of the neural retina (without any signs of layering; Fig. 1F), is also observed in the optic disc (OD in Fig. 1G), the region in the retina containing no photoreceptors, formed by the meeting of all the retinal ganglion cell axons as they enter the optic nerve. In summary, morphogenesis in the embryonic neural retina of the both shark species follows a vitreal-to-scleral progression of layering, each

layer containing specific cell types and shows central-to-peripheral sequence of differentiation, with central areas being more mature than peripheral areas. Between early juveniles and adults, the neural retina also increases in surface and decreases in thickness. Thickness diminution is particularly obvious in the adult INL.

We have established a correlation between the table of normal developmental stages of *S. canicula* according to Ballard et al. (1993), and their body size, extent of retinal morphogenesis and the developmental periods of the retina defined above (see Table 1). This was readily adapted to *H. fuscus*, as the first appearance of easily recognizable structures is the same in both species. Although embryos of *H. fuscus* always had wider heads than those of *S. canicula*, there were no significant differences as regards the total body size of the embryos of each species. Indeed, although the relative timing of the formation of specific neural structures may vary greatly between species (at least in teleosts; Candal et al., 2005a), no differences were observed concerning the pattern of organogenesis of *S. canicula* and *H. fuscus* throughout development. Moreover, the timing of retinal development was coincident in *S. canicula* and *H. fuscus*, that is, each retinal developmental period can be recognizable in both species at equivalent developmental stages (defined by landmark events other than body size; see Table 1). Differences were only observed regarding the degree of body pigmentation, probably due to their particular natural environments and different geographical distribution, i.e., *H. fuscus* (often found in shallow waters, associated to rocky areas in the southeast Atlantic) is darker than *S. canicula* (found in shallow waters, on sandy, coralline, algal, gravel or muddy bottoms on the northeast Atlantic).

Spatiotemporal pattern of Pax6 expression in the shark retina .

The two polyclonal anti-Pax6 antibodies (rabbit and goat; see Material and Methods) revealed a similar pattern of distribution of Pax6-immunorreactive cells within the retina of both shark species, although only results obtained with the rabbit anti-Pax6 antibody are shown in Figures. No differences between the two species were observed in the distribution of Pax6 immunoreactivity throughout the development and mature retina. Accordingly, the following description applies to both.

During the *first developmental period*, intense Pax6-immunoreactive (ir) cells were observed in the retinal pigment epithelium and the neuroepithelium (Fig. 2A). In the retinal

pigment epithelium, spatial differences in Pax6 expression were observed along the dorsoventral and nasotemporal axes of the retina (compare Figs. 2B, C). In addition, within the retinal neuroepithelium, Pax6 immunoreactivity was lacking in some cells of the ventral retina, close to the proximal edge of the optic fissure (a temporary gap in the ventral margin of the developing optic cup, located at the place where the optic nerve head will be found; Fig. 2C). In the lens, intense Pax6-ir cells were observed throughout the lens epithelium, but Pax6 immunoreactivity was pale in the nuclei of differentiating lens fibres (asterisk in Fig. 2B).

At the beginning of the *second developmental period*, the organization of Pax6 immunoreactivity in the most central (and most mature) part of the retina (Fig. 2D) varied with respect to that of the peripheral retina (Fig. 2E) and the retina bordering the recently formed optic nerve head (Fig. 2F). In the central retina, strongly Pax6-ir cells formed a thick band of densely grouped large round-shaped cells in the innermost region (prospective GCL; arrowheads in Fig. 2D), whereas more scattered elongated cells located mostly in the inner region of the prospective INLi (short arrows in Fig. 2D). At this stage a primordial IPL first appears, as noted by the presence of GAD-ir processes originated from early GAD-ir amacrine cells located in the INL (Ferreiro-Galve et al., 2008). Strongly Pax6-ir cells were also observed at outer levels throughout the neuroepithelium (Fig. 2D). Strongly Pax6-ir cells were not found in either the CMZ (Fig. 2E) or in the region bordering the optic nerve head (asterisks in Fig. 2F). Most Pax6-ir cells in the outer non-layered retina and at the CMZ showed pale immunoreactivity. Similar Pax6-ir cell populations were observed in the retina of stage 31 embryos (Fig. 2G-J), including intensely stained cells in the GCL, although cells at different levels in the INLi were far more numerous. Some intensely stained Pax6-ir cells were found within the IPL (arrow in Fig. 1H), and in the outer retina, which was unlayered. Most of the Pax6-ir cells found in the outer retina were pale stained and had a neuroepithelial appearance. Weak Pax6-ir cells were observed in the CMZ (Fig. 2I) as well as in the ventral (less mature) retina, located close to the optic nerve head (Fig. 2J). Similar distribution of Pax6-ir cells was observed in early stage 32 embryos (Figs. 2K, L), when retinal layering was completed in central regions with the appearance of the OPL between the outer part of the INL (INLo) and the prospective ONL. At this time, weakly stained Pax6-ir cells were arranged in a loose band at the primordial HCL (Fig. 2K, L). At the end of the *second developmental period* (late stage 32; Fig. 2M), the density of Pax6-ir cells decreased

in the INLo, whereas they were openly arranged in the HCL. Most strongly Pax6-ir cells were located in the INLi and GCL. Pax6-ir cells were observed in the lens epithelium (but not in lens fibres) throughout the entire developmental period (Figs. 2E, G, I, K, L).

During the *third developmental period*, the central retina showed strongly Pax6-ir cells in the GCL, IPL, INLi and HCL (Fig. 2N). Faint Pax6 labelling was also observed in some bipolar cells in the INLo (arrow in Fig. 2N). Very faint Pax6 immunoreactivity was found in the now much reduced CMZ, which showed no signs of layering (arrow in Fig. 2O). The thick *transition zone* (TZ in Fig. 2O) consisted of a layered inner part where the GCL and IPL were clearly appreciable, and a non-layered outer part (nl in Fig. 2O). At the *transition zone*, the organization of Pax6-ir cells resembled that observed in the central retina of stage 30 (compare with Fig. 2D), i.e., Pax6-ir neurons were observed in the GCL and INLi as well as throughout the outer non-layered neuroepithelium. The retina bordering the *transition zone* was similar to that found in the central retina at the end of the *second developmental period* (late stage 32, compare with Fig. 2M). The distribution of Pax6-ir cells in this peripheral region still differed from that found in the centralmost retina (compare with Fig. 2N). Therefore, the patterns of Pax6 immunoreactivity observed from the most-peripheral to the central retina successively recapitulated those found in the central retina from early to late development. The same gradient patterns of Pax6 immunoreactivity were observed in the margin of the retina of *juveniles* (Fig. 2P) and adults (not shown).

In situ hybridisation with Pax6 probes in *S. canicula*

In order to assess the Pax6 expression observed with immunohistochemistry, we have performed *in situ* hybridisation with the *ScPax6* mRNA probe at various developmental periods of the retina of *S. canicula* (Fig. 3B). These hybridisation results were comparable to those evidenced by immunohistochemistry, and therefore validate the specificity of the antibodies used here (compare Figs. 3A, 3B). Although immunohistochemistry and *in situ* hybridisation yielded similar results, the former method gave better cellular detail and was easily combined with other immunohistochemical markers. Accordingly, it was chosen to study the changing spatiotemporal expression of Pax6 in the developing shark retina.

DISCUSSION

Pax6 expression in the retinas of *S. canicula* and *H. fuscus*. Comparison with other vertebrates

We aimed to investigate the patterns of Pax6 expression in the retina of two shallow dwelling shark species. *S. canicula* is found in the Northeast Atlantic, in shallow sublittoral waters from a few metres commonly down to 100 m (around British Isles), and exceptionally to 400 m (Mediterranean). It lives at the bottom on sandy, coralline, algal, gravel or muddy substrata, though it may also be found in rocky areas. Spawning occurs in shallow water, often in sandy areas. *H. fuscus* is found in the Southeast Atlantic, and is locally common close inshore in shallow waters to depths of around 130 metres. It is reported to rest on the bottom during the day, associated to rocky reefs.

The spatiotemporal pattern of Pax6 immunoreactivity was analysed from embryonic stage 26 to adults, thus covering a time-course from the prelayered undifferentiated retina to when different cell types and retinal layers can be distinguished. The pattern of Pax6 immunoreactivity depicted in this study coincides with that revealed by *in situ* hybridisation, although the former allows enhanced histological preservation. This pattern consists in a strong Pax6 expression in most retinal cells throughout the early (non-layered) retina to turn into the sustained expression in discrete cell layers (mostly the GCL and INLi) as they become distinguishable.

This pattern observed in sharks is roughly coincident with those observed in the neuroepithelial and/or the mature retina of other vertebrate groups (teleosts: Püschel et al., 1992; Macdonald et al., 1995; Hitchcock et al., 1996; Wullimann and Rink, 2001; Alunni et al., 2007; Candal et al., 2008; amphibians: Del Rio-Tsonis et al., 1995; Hirsch and Harris, 1997; Arresta et al., 2005; chick: Belecky-Adams et al., 1997; Edqvist et al., 2006; Canto-Soler et al., 2008; mouse: Ashery-Padan et al., 2000; de Melo et al., 2003; González-Curto et al., 2007; human: Nishina et al., 1999; Stanescu et al., 2007). The presence in *S. canicula* (present results) of additional Pax6-expressing cells in the HCL coincides with that observed in the layered retina of zebrafish (Macdonald et al., 1995; Wullimann and Rink, 2001), chick (Belecky-Adams et al., 1997; Edqvist et al., 2006; Canto-Soler et al., 2008), and mouse (de Melo et al., 2003; González-Curto et al., 2007).

Of note, pale Pax6-expressing cells have been observed in the CMZ throughout the entire life of *S. canicula* and *H. fuscus*. Although Pax6 expression has been widely analysed in the layered retina of vertebrates (see above), the expression in the CMZ - or its equivalent retinal stem cell population in mammals - has received little attention, and few comments have been made regarding the presence of absence of Pax6-ir cells in this zone. Faint Pax6 expression in the CMZ has also been observed in the mature retina of some teleosts (Hitchcock et al., 1996; Alunni et al., 2007; Candal et al., 2008) and in the adult mouse (González-Curto et al., 2007). On the contrary, in *Xenopus*, the cells in the CMZ, which are undifferentiated and have the capacity to generate many retinal cell types, do not express Pax6 (Hirsch and Harris, 1997), an intriguing observation owing that multipotent mitotic neuroblasts in the early retinal development of *Xenopus* express this transcription factor abundantly.

Pax6 is expressed by retinal progenitors throughout development.

A remarkable amount of data has been collected as regards the role of Pax6 during early eye development (see Introduction), but comparatively little is known about its expression and role during retinogenesis. Strong Pax6 immunoreactivity has been observed in most cells during the *first developmental period,* as well as in a few cells within the outer non-layered (undifferentiated) retina during the *second developmental period*. Of note, coinciding with the beginning of retinal layering, most cells within the outer non-layered retina and at the CMZ show pale Pax6 immunoreactivity. The fading of Pax6 labelling in these cells could be due to changes in the shape and size of nuclei that occur during the differentiation process, i.e., Pax6 could be diluted in the larger nuclei of differentiating cells. The possibility must also be considered that changes in the amount of protein are related to Pax6 down-regulation during the neurogenic cell cycle, as have been reported in chick (Hsieh and Yang, 2009). The dynamic spatiotemporal pattern changes of Pax6 expression throughout shark retinogenesis suggests a shift in its role over time (see Fig. 4).

In the neuroblastic retina of sharks (Fig. 4A), Pax6 could play the same roles revealed by analyzing neurogenesis in the optic vesicle of mutant embryos: i.e., Pax6 could be necessary to specify a retinal (vs. non-retinal) neuron fate by coupling general neuron-inducing signals to specific retinal neurogenic programs (Philips et al., 2005), and also for the maintenance of an

undifferentiated state of retinal progenitors by promoting cell proliferation and/or inhibiting cell differentiation (Philips et al., 2005; Duparc et al., 2007; Osumi et al., 2008).

With the beginning of layering in the shark retina (Fig. 4B), Pax6 fading could be influencing neurogenesis by several overlapping mechanisms. First, recent immunocytochemistry and flow cytometry studies have evidenced that quantitative changes in Pax6 expression in the embryonic chick retina are correlated with changes in the mode of cell division (Hsieh and Yang, 2009). Thus, high levels of Pax6 are found in preneurogenic (uncommitted) progenitors, while low levels of Pax6 are observed in neurogenic (lineage-restricted) progenitors during the G1 and S phases of the cell cycle. These observations supported the hypothesis that Pax6 is required for the initiation of the specification programs that normally prompt the transition of subsets of progenitor cells from uncommitted to neurogenic, which then go through asymmetrical divisions towards different lineage-restricted fates (Marquardt et al., 2001; Hsieh and Yang, 2009). This could account for the diminution in the level of Pax6-expression observed in cells within the non-layered areas of the shark retina during the second developmental period (present results; see Fig. 4B). Second, Pax6 appears to be necessary for the multipotency of retinal progenitors to generate all cell types, as conditional loss of Pax6 in retinal progenitor cells at the peripheral and central retina of mouse leads to the exclusive generation of terminally differentiated amacrine cells (Ashery-Padan and Gruss, 2001; Marquardt et al., 2001; Oron-Karni et al., 2008). Third, Pax6 has been reported be necessary for maintain proliferation of retinal progenitors. Conditional Pax6 ablation in the peripheral retina of mouse caused underproliferation of retinal progenitor cells and resulted in retinas of reduced size (Marquardt et al., 2001). It has been additionally demonstrated that the maintenance of low levels of Pax6 is essential for sustaining cell proliferation of neurogenic progenitors, especially the reentry of S phase (Hsieh and Yang, 2009). The relation of strong and faint Pax6 expression with proliferation within the undifferentiated areas mentioned above has been thoroughly investigated in Chapter 6.

Pax6 is expressed in discrete populations of neurons in the layered retina.

The pattern of Pax6 immunoreactivity in layered shark retinas includes Pax6 expression in discrete cell types in the GCL, INLi and HCL (ganglion, amacrine and horizontal cells), and its absence in photoreceptors (ONL), bipolar cells and Müller cells (Fig. 4C). The restriction of Pax6 expression to discrete cell types suggests that Pax6 may induce *differentiation of particular cell types in a context dependent manner*, as has been previously proposed (Philips et al., 2005). Furthermore, regulation of Pax-6 expression controls the identity and differentiation potential of retinal pigment epithelium cells (see Gehring, 2002; Treisman, 2004; Tsonis and Fuentes, 2006). Pax6 is also able to induce retinal pigment epithelium transdifferentiation when overexpressed in chick eyes at embryonic stages that are normally not permissive for transdifferentiation (Spence et al., 2007). Moreover, Pax6 is expressed in the retina of adult elasmobranchs, suggesting a role for Pax6 in some mature neurons. That Pax6-expressing cells were present throughout the lifespan of the human retina has been attributed to roles for this gene after completion of eye morphogenesis (Stanescu et al., 2007). Interestingly, some genes controlling cell cycle exit during early development are also observed in mature regions of the central nervous system, suggesting differential roles for these molecules from development to adulthood (Candal et al., 2004, 2005b; Deyts et al., 2005).

In summary, the changing pattern of expression of Pax6 throughout retinal development in elasmobranchs (our observations) together with the results of functional analysis in other species (reviewed in Osumi et al., 2008), suggest that Pax6 acts as a binary player promoting cell proliferation or cell differentiation in a context dependent manner. Functional cross-talk between molecules coordinating cell cycle regulation and cell fate has been previously emphasized (Candal et al., 2005b), although the specific mechanisms in the retina that integrate both processes remain largely undefined.

REFERENCES

Altmann CR, Chow RL, Lang RA, Hemmati-Brivanlou A (1997). Lens induction by Pax-6 in *Xenopus laevis*. Dev Biol, 185: 119-123.

Alunni A, Menuet A, Candal E, Pénigault JB, Jeffery WR, Rétaux S (2007). Developmental mechanisms for retinal degeneration in the blind cavefish *Astyanax mexicanus*. J Comp Neurol, 505: 221-233.

Arresta E, Bernardini S, Bernardini E, Filoni S, Cannata SM (2005). Pigmented epithelium to retinal transdifferentiation and Pax6 expression in larval *Xenopus laevis*. J Exp Zoolog A Comp Exp Biol, 303: 958-67.

Ashery-Padan R, Gruss P (2001). Pax6 lights-up the way for eye development. Curr Opin Cell Biol, 13: 706-714.

Ashery-Padan R, Marquardt T, Zhou X, Gruss P (2000). Pax6 activity in the lens primordium is required for lens formation and for correct placement of a single retina in the eye. Genes Dev, 14: 2701-2711.

Ballard W, Mellinger J, Lechenault H (1993). A series of normal stages for development of *Scyliorhinus canicula*, the lesser spotted dogfish (Chondrichthyes: Scyliorhinidae). J Exp Zool, 267: 318-336.

Baumer N, Marquardt T, Stoykova A, Ashery-Padan R, Chowdhury K, Gruss P (2002). Pax6 is required for establishing nasotemporal and dorsal characteristics of the optic vesicle. Development, 129: 4535-4545.

Baumer N, Marquardt T, Stoykova A, Spieler D, Treichel D, Ashery-Padan R, Gruss P (2003). Retinal pigmented epithelium determination requires the redundant activities of Pax2 and Pax6. Development, 130: 2903-2915.

Belecky-Adams T, Tomarev S, Li HS, Ploder L, McInnes RR, Sundin O, Adler R (1997). Pax-6, Prox 1, and Chx10 homeobox gene expression correlates with phenotypic fate of retinal precursor cells. Invest Ophthalmol Vis Sci, 38: 1293-1303.

Bozzano A, Collin SP (2000). Retinal ganglion cell topography in elasmobranchs. Brain Behav Evol, 55: 191-208.

Candal E, Ferreiro-Galve S, Anadón R, Rodríguez-Moldes I (2008). Morphogenesis in the retina of a slow-developing teleost: emergence of the GABAergic system in relation to cell proliferation and differentiation. Brain Res, 1194: 21-27.

Candal E, Anadón R, Bourrat F, Rodríguez-Moldes I (2005a). Cell proliferation in the developing and adult hindbrain and midbrain of trout and medaka (teleosts): A segmental approach. Dev Brain Res, 160: 157-175.

Candal E, Nguyen V, Joly JS, Bourrat F (2005b). Expression domains suggest cell-cycle independent roles of growth-arrest molecules in the adult brain of the medaka, *Oryzias latipes*. Brain Res Bull, 66: 426-430.

Candal E, Thermes V, Joly JS, Bourrat F (2004). Medaka as a model system for the characterisation of cell cycle regulators: a functional analysis of Ol-Gadd45gamma during early embryogenesis. Mech Dev, 121: 945-958.

Canto-Soler MV, Adler R (2006). Optic cup and lens development requires Pax6 expression in the early optic vesicle during a narrow time window. Dev Biol, 294: 119-132.

Canto-Soler MV, Huang H, Romero MS, Adler R (2008). Transcription factors CTCF and Pax6 are segregated to different cell types during retinal cell differentiation. Dev Dyn, 237: 758-67.

Cartier L, Laforge T, Feki A, Arnaudeau S, Dubois-Dauphin M, Krause KH (2006). Pax6-induced alteration of cell fate: shape changes, expression of neuronal alpha tubulin, postmitotic phenotype, and cell migration. J Neurobiol, 66: 421-436.

Chow RL, Altmann CR, Lang RA, Hemmati-Brivanlou A (1999). Pax6 induces ectopic eyes in a vertebrate. Development, 126: 4213-4222.

Chow RL, Lang RA (2001). Early eye development in vertebrales. Annu Rev Cell Dev Biol, 17: 255-296.

Collinson JM, Hill RE, West JD (2000). Different roles for Pax6 in the optic vesicle and facial epithelium mediate early morphogenesis of the murine eye. Development, 127: 945-956.

Coolen M, Menuet A, Chassoux D, Compagnucci C, Henry S, Levèque L, Da Silva C, Savory F, Samain S, Wincker P, Thermes C, D'Aubenton-Carafa Y, Rodríguez-Moldes I, Naylor G, Depew M, Sourdaine P, Mazan S (2009). The dogfish *Scyliorhinus canicula*, a reference in jawed vertebrates. In: Emerging Model Organisms: a laboratory manual. pp. 431–446. Cold Spring Harbor, New York.

de Melo J, Qiu X, Du G, Cristante L, Eisenstat DD (2003). Dlx1, Dlx2, Pax6, Brn3b, and Chx10 homeobox gene expression defines the retinal ganglion and inner nuclear layers of the developing and adult mouse retina. J Comp Neurol, 461: 187-204.

Del Rio-Tsonis K, Washabaugh CH, Tsonis PA (1995). Expression of pax-6 during urodele eye development and lens regeneration. Proc Natl Acad Sci U S A, 92: 5092-5096.

Derobert Y, Baratte B, Lepage M, Mazan S (2002). Pax6 expression patterns in *Lampetra fluviatilis* and *Scyliorhinus canicula* embryos suggest highly conserved roles in the early regionalization of the vertebrate brain. Brain Res Bull, 57: 277-280.

Deyts C, Candal E, Joly JS, Bourrat F (2005). An automated *in situ* hybridization screen in the Medaka to identify unknown neural genes. Dev Dyn, 234: 698-708.

Duparc RH, Abdouh M, David J, Lépine M, Tétreault N, Bernier G (2007). Pax6 controls the proliferation rate of neuroepithelial progenitors from the mouse optic vesicle. Dev Biol, 301: 374-87.

Edqvist PH, Myers SM, Hallböök F (2006). Early identification of retinal subtypes in the developing, pre-laminated chick retina using the transcription factors Prox1, Lim1, Ap2alpha, Pax6, Isl1, Isl2, Lim3 and Chx10. Eur J Histochem, 50: 147-154.

Ferreiro-Galve S, Candal E, Carrera I, Anadón R, Rodríguez-Moldes I (2008). Early development of GABAergic cells of the retina in sharks: an immunohistochemical study with GABA and GAD antibodies. J Chem Neuroanat, 36: 6-16.

Fishelson L, Baranes A (1999). Ocular development in the oman shark, *Iago omanensis* (Triakidae), Gulf of Aqaba, Red Sea. Anat Rec, 256: 389-402.

Fujiwara M, Uchida T, Osumi-Yamashita N, Eto K (1994). Uchida rat (rSey): a new mutant rat with craniofacial abnormalities resembling those of the mouse Sey mutant. Differentiation, 57:31-38.

Gehring WJ (2002). The genetic control of eye development and its implications for the evolution of the various eye-types. Int J Dev Biol, 46: 65-73.

Gehring WJ, Kazuho I (1999). Pax6 mastering eye morphogenesis and eye evolution. Trends Genet, 15: 371-377.

Gibson-Brown JJ, S, I Agulnik SI, Papaioannou VE (1998). Expression of T-box genes Tbx2–Tbx5 during chick organogenesis. Mech Dev, 74: 165-169.

Glardon S, Callaerts P, Halder G, Gehring WJ (1997). Conservation of Pax-6 in a lower chordate, the ascidian *Phallusia mammillata*. Development, 124: 817-825.

Glaser T, Walton DS, Maas RL (1992). Genomic structure, evolutionary conservation and aniridia mutations in the human PAX6 gene. Nat Genet, 2: 232-239.

González-Curto G, Lara JM, Parrilla M, Aijón J, Velasco A (2007). Modifications of the retina neuronal populations of the heterozygous mutant small eye mouse, the Sey(Dey). Brain Res, 1127: 163-176.

Grindley JC, Davidson DR, Hill RE (1995). The role of Pax-6 in eye and nasal development. Development, 121: 1433-1442.

Gruber SH, Loew ER, McFarland WN (1990). Rod and cone pigments of the Atlantic guitarfish, *Rhinobatos lentiginosus Garman*. J Exp Zool Suppl, 5: 85-87.

Halder G, Callaerts P, Gehring WJ (1995). Induction of ectopic eyes by targeted expression of the eyeless gene in *Drosophila*. Science, 267: 1788-1792.

Hanson IM, Seawright A, Hardman K, Hodgson S, Zaletayev D, et al. (1993). PAX6 mutations in aniridia. Hum Mol Genet, 2: 915-20.

Hanson IM, Fletcher JM, Jordon T, Brown A, Taylor D, Adams RJ, Punnett HH, van Heyningen V (1994). Mutations at the PAX6 locus are found in heterogeneous anterior segment malformations including Peters' anomaly. Nature Genet, 6: 168-173.

Harahush BK, Hart NS, Green K, Collin SP (2009). Retinal neurogenesis and ontogenetic changes in the visual system of the brown banded bamboo shark, *Chiloscyllium punctatum* (Hemiscyllidae, Elasmobranchii). J Comp Neurol, 513: 83-97.

Hever AM, Williamson KA, van Heyningen V (2006). Developmental malformations of the eye: the role of PAX6, SOX2 and OTX2. Clin Genet, 69: 459-470.

Hill RE, Favor J, Hogan BL, Ton CC, Saunders GF, Hanson IM, Prosser J, Jordan T, Hastie ND, van Heyningen V (1991). Mouse small eye results from mutations in a paired-like homeoboxcontaining gene. Nature, 354:522-25. Erratum in: Nature. 1992 Feb 20;355(6362):750

Hirsch N, Harris WA (1997). Xenopus Pax-6 and retinal development. J Neurobiol, 32: 45-61.

Hitchcock PF, Macdonald RE, VanDeRyt JT, Wilson SW (1996). Antibodies against Pax6 immunostain amacrine and ganglion cells and neuronal progenitors, but not rod precursors, in the normal and regenerating retina of the goldfish. J Neurobiol, 29: 399-413.

Hogan BL, Horsburgh G, Cohen J, Hetherington CM, Fisher G, Lyon MF (1986). Small eyes (Sey): a homozygous lethal mutation on chromosome 2 which affects the differentiation of both lens and nasal placodes in the mouse. J Embryol Exp Morphol, 97:95-110.

Hsieh YW, Yang XJ (2009). Dynamic Pax6 expression during the neurogenic cell cycle influences proliferation and cell fate choices of retinal progenitors. Neural Dev, 4:32-50.

Jordan T, Hanson I, Zaletayev D, Hodgson S, Prosser J, Seawright A, Hastie N, van Heyningen V (1992). The human PAX6 gene is mutated in two patients with aniridia. Nat Genet, 1: 328-32.

Kamachi Y, Uchikawa M, Collignon J, Lovell-Badge R, Kondoh H (1998). Involvement of Sox1, 2 and 3 in the early and subsequent molecular events of lens induction. Development, 125: 2521–2532.

Kondoh H, Uchikawa M, Kamachi Y (2004). Interplay of Pax6 and SOX2 in lens development as a paradigm of genetic switch mechanisms for cell differentiation. Int J Dev Biol, 48: 819-827.

Krauss S, Johansen T, Korzh V, Moens U, Ericson JU, FJose A (1991). Zebrafish pax [zf-a]: a paired box-containing gene expressed in the neural tube. EMBO J, 10: 3609-3619.

Li HS, Tierney C, Wen L, Wu JY, Rao Y (1997). A single morphogenetic field gives rise to two retina primordia under the influence of the prechordal plate. Development, 124: 603-615.

Li HS, Yang JM, Jacobson RD, Pasko D, Sundin O (1994). Pax-6 is first expressed in a region of ectoderm anterior to the early neural plate: implication for stepwise-determination of the lens. Dev Biol, 162: 181-194.

Logiudice FT, Laird RJ (1994). Morphology and density distribution of cone photoreceptor in the retina of the Atlantic stingray, *Dasyatis sabina*. J Morph, 221: 277-289.

Macdonald R, Barth KA, Xu Q, Holder N, Mikkola I, Wilson SW (1995). Midline signalling is required for Pax gene regulation and patterning of the eyes. Development, 121: 3267-3278.

Macdonald R, Wilson SW (1997). Distribution of Pax6 protein during eye development suggests discrete roles in proliferative and differentiated visual cells. Dev Genes Evol, 206: 363-369.

Marquardt T, Ashery-Padan R, Andrejewski N, Scardigli R, Guillemot F, Gruss P (2001). Pax6 is required for the multipotent state of retinal progenitor cells. Cell, 105: 43-55.

Matsuo T, Osumi-Yamashita N, Noji S, Ohuchi H, Koyama E, et al. (1993). A mutation in the Pax-6 gene in rat small eye is associated with impaired migration of midbrain crest cells. Nat Genet, 3:299-304.

Nishina S, Kohsaka S, Yamaguchi Y, Handa H, Kawakami A, Fujisawa H, Azuma N (1999). PAX6 expression in the developing human eye. Br J Ophthalmol, 83: 723–727.

Oron-Karni V, Farhy C, Elgart M, Marquardt T, Remizova L, Yaron O, Xie Q, Cvekl A, Ashery-Padan R (2008). Dual requirement for Pax6 in retinal progenitor cells. Development, 135: 4037-4047.

Osumi N, Shinohara H, Numayama-Tsuruta K, Maekawa M (2008). Concise review: Pax6 transcription factor contributes to both embryonic and adult neurogenesis as a multifunctional regulator. Stem Cells, 26: 1663-1672.

Philips GT, Stair CN, Young Lee H, Wroblewski E, Berberoglu MA, Brown NL, Mastick GS (2005). Precocious retinal neurons: Pax6 controls timing of differentiation and determination of cell type. Dev Biol, 279: 308-321.

Püschel AW, Gruss P, Westerfield M (1992). Sequence and expression pattern of pax-6 are highly conserved between zebrafish and mice. Development, 114: 643-51.

Quinn JC, West JD, Hill RE (1996). Multiple functions for Pax6 in mouse eye and nasal development. Genes Dev, 10: 435-46.

Quiring R, Walldorf U, Kloter U, Gehring WJ (1994). Homology of the eyeless gene of *Drosophila* to the Small eye gene in mice and Aniridia in humans. Science, 265: 785-89.

Reza HM, Yasuda K (2004). The involvement of neural retina pax6 in lens fiber differentiation. Dev Neurosci, 26: 318-327.

Sakuta H, Suzuki R, Takahashi H, Kato A, Shintani T, Iemura S, Yamamoto TS, Ueno N, Noda M (2001). Ventroptin: a BMP-4 antagonist expressed in a double-gradient pattern in the retina. Science, 293: 111-115.

Schedl A, Ross A, Lee M, Engelkamp D, Rashbass P, van Heyningen V, Hastie ND (1996). Influence of PAX6 gene dosage on development: overexpression causes severe eye abnormalities. Cell, 86: 71-82.

Schulte D, Furukawa T, Peters MA, Kozak CA, Cepko CL (1999). Misexpression of the Emx-related homeobox genes cVax and mVax2 ventralizes the retina and perturbs the retinotectal map. Neuron, 24: 541-553.

Sillman AJ, Letsinger GA, Patel S, Loew ER, Klimley AP (1996). Visual pigments and photoreceptors in two species of shark, *Triakis semifasciata* and *Mustelus henlei*. J Exp Zool, 276 : 1-10.

Spence JR, Madhavan M, Aycinena JC, Del Rio-Tsonis K (2007). Retina regeneration in the chick embryo is not induced by spontaneous Mitf downregulation but requires FGF/FGFR/MEK/Erk dependent upregulation of Pax6. Mol Vis, 13: 57-65.

Stanescu D, Iseli HP, Schwerdtfeger K, Ittner LM, Remé CE, Hafezi F (2007). Continuous expression of the homeobox gene Pax6 in the ageing human retina. Eye, 21: 90-93.

Stell WK (1972). The structure and morphologic relations of rods and cones in the retina of the spiny dogfish, *Squalus*. Comp Biochem Physiol A Comp Physiol, 42: 141-151.

Stell WK, Witkovsky P (1973a). Retinal structure in the smooth dogfish, *Mustelus canis*: general description and light microscopy of giant ganglion cells. J Comp Neurol, 148:1-31.

Stell WK, Witkovsky P (1973b). Retinal structure in the smooth dogfish, *Mustelus canis*: light microscopy of photoreceptor and horizontal cells. J Comp Neurol, 148:33-45.

Tomarev SI, Callaerts P, Kos L, Zinovieva R, Halder G, Gehring W, Piatigorsky J (1997). Squid Pax-6 and eye development. Proc Natl Acad Sci USA, 94: 2421-2426.

Ton CC, Hirvonen H, Miwa H, Weil MM, Monaghan P, Jordan T, van Heyningen V, Hastie ND, Meijers-Heijboer H, Drechsler M, Royer-Pokora B, Collins F, Swaroop A, Strong LC, Saunders GF (1991). Positional cloning and characterization of a paired box- and homeobox- containing gene from the aniridia region. Cell, 67: 1059-1074.

Toyoda JI, Saito T, Kondo H (1978). Three types of horizontal cells in the stingray retina: their morphology and physiology. J Comp Neurol, 179: 569-579.

Treisman JE (2004). How to make an eye. Development, 131: 3823-3827.

Tsonis PA, Fuentes EJ (2006). Focus on molecules: Pax-6, the eye master. Exp Eye Res, 83: 233-234.

Trousse F, Esteve P, Bovolenta P (2001). Bmp4 mediates apoptotic cell death in the developing chick eye. J Neurosci, 21: 1292-1301.

Walther C, Gruss P (1991). Pax-6, a murine paired box gene, is expressed in the developing CNS. Development, 113: 1435-1449.

Witkovsky P, Stell WK (1973a). Retinal structure in the smooth dogfish, *Mustelus canis*: light microscopy of bipolar cells. J Comp Neurol, 148:47-59.

Witkovsky P, Stell WK (1973b). Retinal structure in the smooth dogfish *Mustelus canis*: electron microscopy of serially sectioned bipolar cell synaptic terminals. J Comp Neurol, 150:147-67.

Wullimann MF, Rink E (2001). Detailed immunohistology of Pax6 protein and tyrosine hydroxylase in the early zebrafish brain suggests role of Pax6 gene in development of dopaminergic diencephalic neurons. Brain Res Dev Brain Res, 131: 173-191.

Zhang XM, Yang XJ (2001). Temporal and spatial effects of Sonic hedgehog signaling in chick eye morphogenesis. Dev Biol, 233: 271–290.

Table 1. Correlation among developmental stages of brown shyshark (*H. fuscus*) and lesser spotted dogfish (*S. canicula*) accordingly with their external features as proposed by Ballard et al., 1993, and their age (from "day 1", when they were laid naturally), body size, extent of retinal morphogenesis and developmental period of the retina (see text for details).

Stage	External features and landmark events	Age at 16ºC (days)	H.fuscus size (in mm)	S. canicula size (in mm)	Retina morphogenesis
First development period					
26	Pharyngeal sets are open	37-42		16	Neuroepithelium No layers
27	Hatching gland begins to show Olfatory placodes wide open Mouth is diamong shaped Buds of gill filaments	42-46	21	17-20	Neuroepithelium No layers
28	Hatching gland developed Olfatory placodes closed Mouth is traverse oval Gill filaments clearly seen	46-51	22-24	21-23	Neuroepithelium No layers
29	Mouth as an arched line Incomplete circle of eye pigment Body: no pigment anyware	49-53	25-33	23.5-30	Neuroepithelium No layers
Second development period					
30	No signs of a rostal protrusion Eyes circled with black pigment	52-60	34-38	31-33	IPL between the GCL and the INL Organization of the ON fibres
Early 31	Rostrum as a detectable protrusion Yolk begins to be transferred to the internal sac	60-70	39-42	34-35	Progressive vitreal-to-scleral formation of layers
Late 31	Rostrum increases in size Maximum development of gill filaments	69-80	43-46	37-40	Progressive vitreal-to-scleral formation of layers
Early 32	Rostrum becomes prominent, decreasing its angle with the body Pigment completely covers eyes Body: pigment begins to appear	75-92	47-52	40-48	OPL between the INLo and the ONL
Middle 32	Body: pigment increases	92-110	53-62	49-57	Progressive vitreal-to-scleral formation of layers
Late 32	The external yolk sac has not yet decreased	110-125	63-67	58-67	Progressive vitreal-to-scleral formation of layers
Third development period					
33	The external yolk sac is shrinking in size	115-155	68-82	68-78	OPL reaches the entire circumference of the retina IPL in the temporoventral retina
34	The external yolk sac is practically empty Hatching	145-175	83-96	78-82	Progressive vitreal-to-scleral formation of layers in the temporoventral retina
Juvenile			97-	82-	Retinal size increases Retinal thickness decreases

Figure 1. Three developmental periods of the retina of *S. canicula* embryonic development. Schematic drawings (*A*, *C*, E) and vertical sections along the dorsoventral axis (B, D, F, *G*) through the retina and optic stalk/optic nerve of *S. canicula* embryos at the indicated stages. Boxed areas in *A*, *C* and E are shown at higher magnification in B, D and F-*G*, respectively. In B, D, F, the scleral side is up; in *G*, the scleral side is down. **A, B.** *First developmental period* characterized by the absence of retinal layers. **C, D.** *Second developmental period* showing organization of layers throughout the retina except in its temporoventral part (asterisk in *C*) which lacks vitreal-to-scleral differentiation. Arrows in D indicate the primordial OPL in the central retina of stage 32 embryos. **E-G.** *Third developmental period* showing the centre-to-peripheral extension of the OPL as well as the presence of a primordial IPL in the temporoventral retina (asterisk in E). Layering is never appreciated in the CMZ (F) and in the optic disc (*G*). For abbreviations, see list in Appendix B.

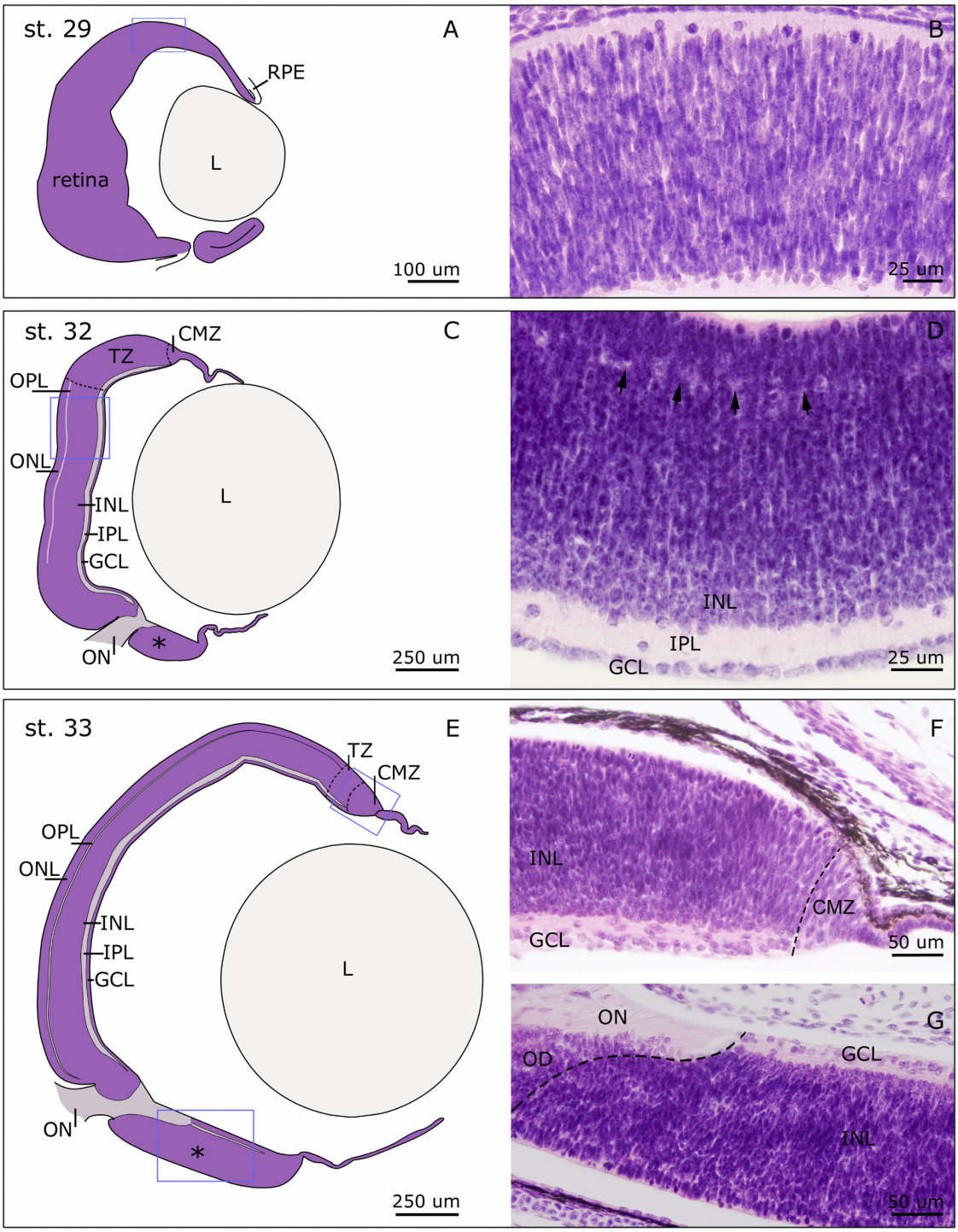
st. 29
A
RPE
retina
L
100 um
B
25 um
st. 32
C
CMZ
TZ
OPL
ONL
INL
IPL
GCL
L
ON
*
250 um
D
INL
IPL
GCL
25 um
st. 33
E
TZ
CMZ
OPL
ONL
INL
IPL
GCL
L
ON
*
250 um
F
INL
GCL
CMZ
50 um
G
ON
OD
GCL
INL
50 um

Figure 2. Patterns of Pax6 immunoreactivity in the retinas of *S. canicula* and *H. fuscus*. (*A-C*) Vertical sections along the horizontal axis of the retina of stage 28 *S. canicula*. **A.** Pax6 immunoreactivity is found in some cells of the retinal pigment epithelium and in most cells of the neuroepithelial neural retina. **B.** Pax6 immunoreactivity is found in cells of the lens epithelium but absent from lens fibres (asterisk). Arrows indicate Pax6-ir cells in the dorsonasal part of the retinal pigment epithelium. **C.** Pax6 immunoreactivity is absent from some cells close to the optic fissure. Arrows indicate Pax6-ir cells in the ventrotemporal part of the retinal pigment epithelium. **D-F.** Vertical sections along the dorsoventral axis of the retina of a stage 30 *S. canicula*. **D.** Detail of the central retina to show large round-shaped Pax6-ir cells in the GCL (arrowheads), as well as elongated Pax6-ir cells in the primordial INLi (short arrows) and in the outer nonlayered retina. **E.** Detail of the peripheral retina to show the absence of strongly Pax6-ir cells in the CMZ. Faint Pax6-ir cells are observed in the ciliary and lens epithelia. **F.** Detail to show the absence of intense Pax6-ir cells in the region bordering the optic nerve head (asterisks). **G-J.** Vertical sections along the dorsoventral axis of the retina of a stage 31 of *S. canicula* (G, H, J) and *H. fuscus* (I) to show intense Pax6-ir cells in the GCL, INLi (G, H), and in the IPL (arrow in H). Faint Pax6-ir cells are observed in the outer neuroepithelial retina (H) and in the lens epithelium **I.** Weak Pax6 immunoreactivity is observed in the CMZ (I) and in the region bordering the optic nerve head (J). **K-M.** Vertical sections along the dorsoventral axis the retina of a stage 32 of *H. fuscus* (K, L) and *S. canicula* (M), to show Pax6-ir cells arranged in a loose band at the primordial HCL. Pax6-ir cells are observed in the lens epithelium (K, L). **N, O.** Vertical sections along the dorsoventral axis of the retina of prehatching embryos of *H. fuscus.* **N.** In the central retina, Pax6-ir cells are mainly observed in the GCL, IPL and INLi. Faint Pax6-ir cells are also observed in the INLo (arrow) and in the HCL. **O.** Faint Pax6-ir cells are observed in the CMZ. The pattern of Pax6 immunoreactivity in the *transition zone* is similar to that found in the central retina at the beginning of the *second developmental period* (compare with D), and the pattern found central-wards in the region bordering the *transition zone* is similar to that found in the central retina at the end of the *second developmental period* (compare with N). **P.** Vertical section along the dorsoventral axis of the retina of a juvenile of *S. canicula*. The pattern of Pax6 immunoreactivity in the CMZ and the *transition zone* is similar to that found in prehatching embryos (compare with O). For abbreviations, see list in Appendix B.

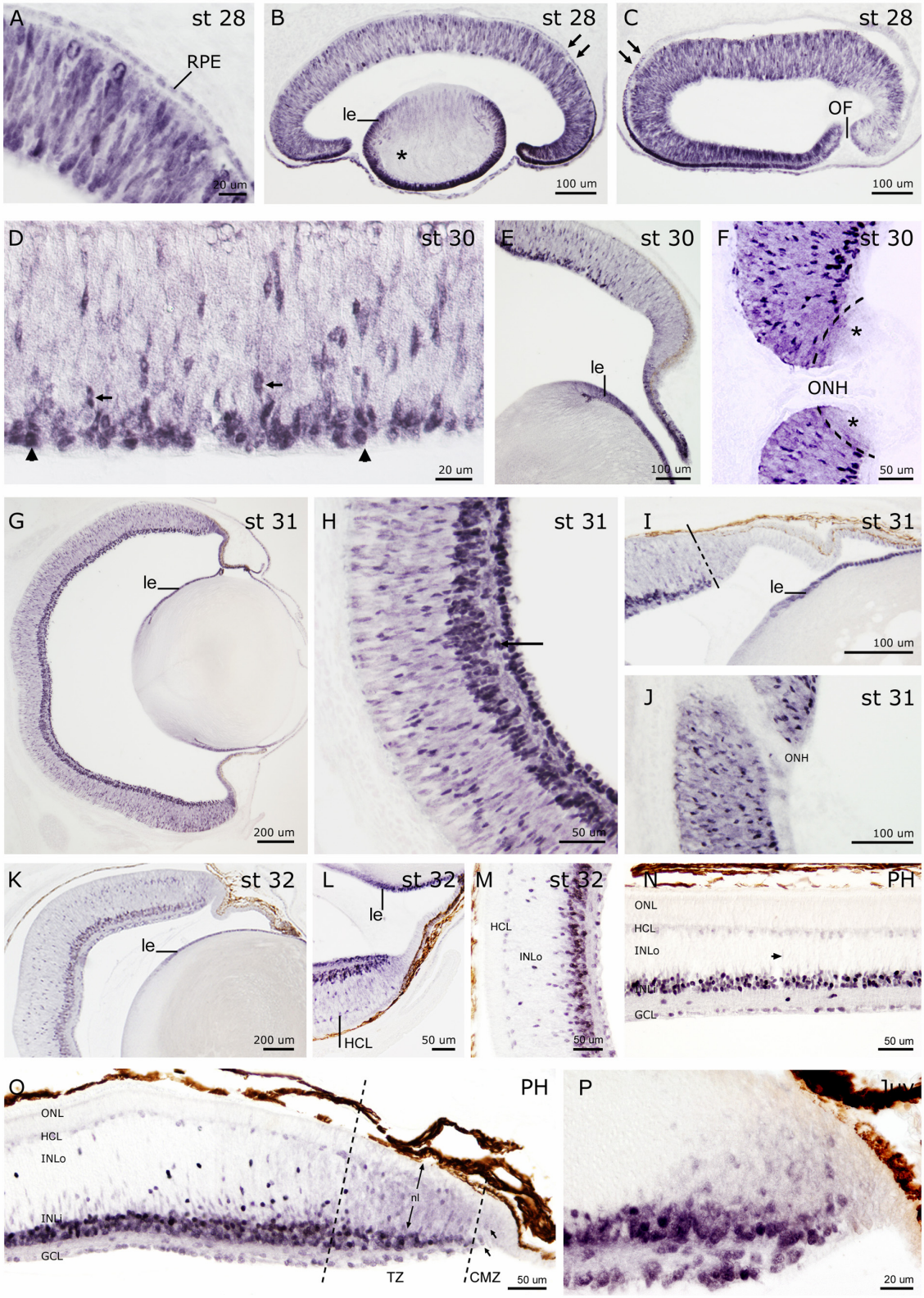
A
st 28
RPE
20 um
B
st 28
le
*
100 um
C
st 28
OF
100 um
D
st 30
20 um
E
st 30
le
100 um
F
st 30
*
ONH
*
50 um
G
st 31
le
200 um
H
st 31
50 um
I
st 31
le
100 um
J
st 31
ONH
100 um
K
st 32
le
200 um
L
st 32
le
HCL
50 um
M
st 32
HCL
INLo
50 um
N
PH
ONL
HCL
INLo
INL
GCL
50 um
O
PH
ONL
HCL
INLo
INL
GCL
nl
TZ
CMZ
50 um
P
20 um

Figure 3. Comparison of patterns of *ScPax6* and anti-Pax6 expression in the retina of S. canicula. **A.** Vertical section along the dorsoventral axis of the retina (transversal with respect to the brain) of a stage 32 of *S. canicula*, showing the distribution of Pax6-ir cells in the GCL, INLi, INLo (arrow) and HCL. **B.** Vertical section along the dorsoventral axis of the retina (transversal with respect to the brain) of a stage 32 of *S. canicula*, showing *ScPax6* expression in the GCL, INLi, in some cells of the INLo (arrow) and in the HCL. For abbreviations, see list in Appendix B.

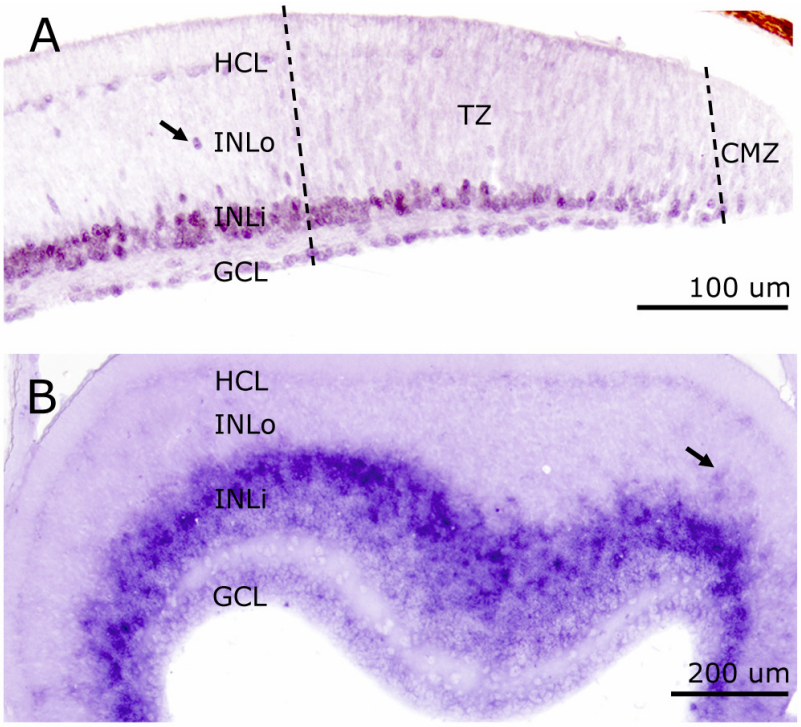

Figure 4. A model summarizing the changing pattern of Pax6 expression during retinogenesis. A. High levels of Pax6 expression are observed in neuroepithelial, (uncommitted) cells. **B.** Pax6 levels decay in committed progenitors with limited self-renewal, both in the outer non-layered retina and at the CMZ (not shown). **C.** In the layered retina, Pax6 expression is either up-regulated (GCL, INL, HCL) or abolished. For abbreviations, see list in Appendix B

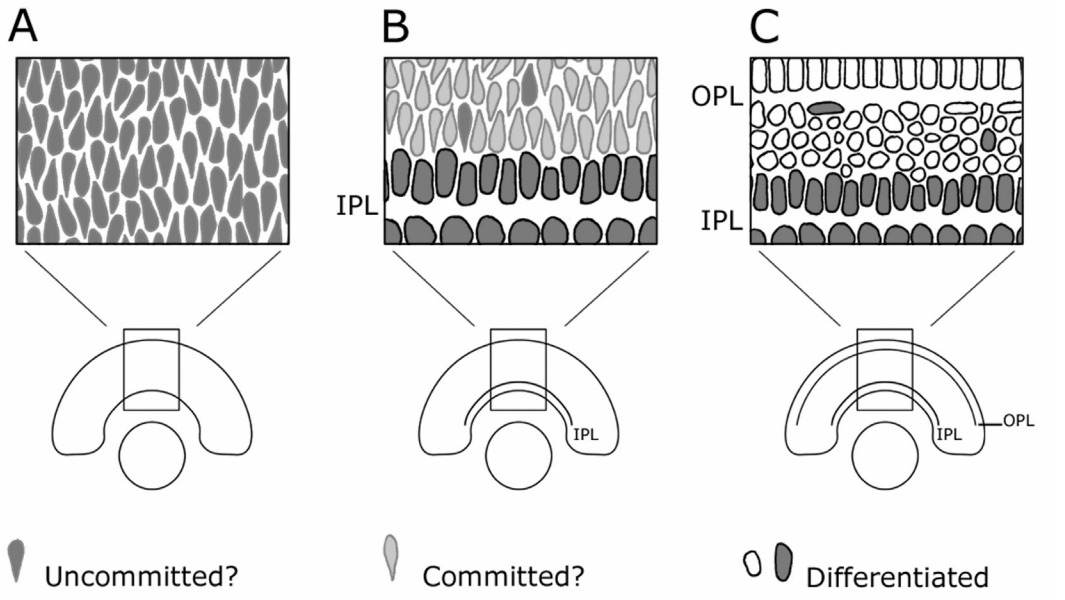

Chapter 6.

Patterns of cell proliferation in the developing retina of sharks

INTRODUCTION

In vertebrates, the retina develops from the highly proliferating pseudostratified neuroepithelium of the eye cup to a highly organized, layered structure. Retinal layering occurs after cell cycle withdrawal of neuronal precursor cells, and their subsequent migration to appropriate levels, where they become differentiated expressing the specific molecular markers and morphological characteristics of the cell type (Link et al., 2000; Candal et al., 2005c). The mature retina consists of two synaptic (plexiform) and three cellular (nuclear) layers that contain six major types of neurons: ganglion cells located mainly in the ganglion cell layer (GCL); amacrine, bipolar, horizontal cells in the inner nuclear layer (INL); rod and cone photoreceptor cell bodies in the outer nuclear layer (ONL), and one type of macroglia (Müller cells) (Link et al., 2000; Sivak and Sivak, 2000). Accordingly, development of the nervous system (and retina) has been schematically summarized as making the necessary functional cells, putting them in the right places, and connecting them appropriately (Galli-Resta, 2002).

On the basis of paleontological evidence, eyes are thought to have evolved independently in different organisms at least 40 times and possibly as many as 65 times, thus confirming their importance (reviewed in Fernald, 2004). Animals have evolved eyes with resolution, sensitivity and wavelength sensitivities to match their needs. Most of those adaptations are the result of developmental differences, as eyes are constructed during embryogenesis. Here, we focused our studies on the initial step towards retinogenesis, i.e., production of the necessary number of cells. The time course of cell proliferation in the developing and adult retina has received much attention in teleosts (Schmitt and Kunz, 1989; Mansour-Robaey and Pinganaud, 1990; Negishi et al., 1990; Hagedorn and Fernald, 1992; Negishi and Wagner, 1995; Kwan et al., 1996; Mack and Fernald, 1997; Julian et al., 1998; Hu and Easter, 1999; Marcus et al., 1999; Li et al., 2000; Cid et al., 2002; Candal et al., 2005a; Raymond et al., 2006; Alunni et al., 2007), which are modern representatives of the large radiation of ray-finned bony fishes. However, it is not known whether these observations are extensive to other groups of fishes.

We analysed cell proliferation in the developing retina of two small sharks that inhabit shallow waters (*Scyliorhinus canicula* and *Haploblepharus fuscus*), by examining the expression of the proliferating cell nuclear antigen (PCNA, a sububit of DNA polimerase), and of the phospho-histone-H3 (PH3). PCNA has been widely used as a proliferation marker both in the

retina and in the brain (revised in Candal et al., 2005a), as it can be detected in proliferating cells throughout the cell cycle except in the mitotic phase (M-phase). Its expression begins in late G1 phase, is maximal during the S phase and decreases from the S/G2 transition, the levels of PCNA being also low in resting cells (G0-phase). The use of PCNA as a proliferation marker has some advantages with respect to other assays to detect cell proliferation, including the use of DNA precursors such as tritiated thymidine (^{3}H-T) or nucleotide analogues such as bromodeoxyuridine to detect their incorporation into DNA (for a review, see Ortego et al., 1994). These DNA precursors are incorporated only during the S phase and, for slow-growing animals, require a long exposition to these substances for evaluating the results, which can affect their viability, while PCNA detects cycling cells without previous treatments of living specimens. Although PCNA immunohistochemistry (unlike the above mentioned methods) does not allow to study the dynamic evolution of cell populations, it labels basically the same cells and regions evidenced by the use of ^{3}H-T or BrdU as markers of proliferation (for a review, see Candal et al., 2005b). In addition, we examined the expression of PH3 currently used as a mitotic marker, since H3 phosphorylation is associated with chromosome condensation and dynamics during mitosis (Hendzel et al., 1997; McManus and Hendzel, 2006; Carney et al., 2007). The immunohistochemical detection of PCNA enables to distinguish between highly proliferating areas and areas containing recent or early postmitotic cells. Moreover, a temporal correspondence between the absence of PCNA immunoreactivity and the detection of differentiated cells has been reported (Negishi et al., 1990). Knowledge of the pattern of cell proliferation in the retina of elasmobranchs may contribute to improved comparative knowledge about the developmental processes associated with the vertebrate visual system.

As it has been suggested that the Pax6 transcription factor is involved in the maintenance of an undifferentiated (proliferative) state of retinal progenitors, as well as in the specification and differentiation of particular neuron fates in a context-dependent manner (see Chapter 5 for further details), we also performed double anti-Pax6/anti-PCNA immunohistochemistry studies. The results from these studies may help in exploring the relationships between Pax6 expression and cell proliferation throughout maturation, thus improving our knowledge of the functions of Pax6 in retinal development.

MATERIAL AND METHODS

Experimental animals

Embryos, juvenile and adult specimens of the lesser spotted dogfish (*S. canicula*) and the brown shyshark (*H. fuscus*) were obtained, transported to the laboratory and maintained as indicated in Chapter 5. The embryonic stages of *S. canicula* were identified by external features, following Ballard et al. (1993), and similar features were used for staging the *H. fuscus* embryos (see Table 1, this section). The following embryonic stages were analysed: stage 26 (1 *S. canicula* embryo), stage 28 (1 *H. fuscus* embryo), stage 29 (1 *S. canicula* embryo, and 1 *H. fuscus* embryo), stage 30 (1 *H. fuscus* embryo), stage 31 (3 *S. canicula* and 4 *H. fuscus* embryos), stage 32 (4 *S. canicula* and 2 *H. fuscus* embryos), and stages 33 and 34 (prehatching; 3 *S. canicula* and 4 *H. fuscus* embryos). 3 juveniles (2 *S. canicula* and 1 *H. fuscus*, from 10 to 14 cm in total lenght) and 1 adult *S. canicula* (about 50 cm total length) were also processed. Adults were sacrificed immediately after incoming to the lab.

Tissue preparation

Adequate measures were taken to minimize animal pain or discomfort. All procedures conformed to the guidelines established by the Spanish Royal Decree 223/1998 for animal experimentation and were approved by the ethics committee of the University of Santiago de Compostela. Tissue was prepared as indicated above (for details, see Chapter 5). Briefly, embryos were anaesthetized with 0.05% tricaine methane sulphonate (MS-222; Sigma, St. Louis, MO) in seawater and fixed either in 4% paraformaldehyde (PFA) in elasmobranch phosphate buffer for 48-72 h, or in Clark's solution for 12-36 h. Prehatching, juvenile and adult specimens were deeply anaesthetized with MS-222 and then perfused intracardially with elasmobranch Ringer's solution followed by the appropriate fixative. Eyes of stage 32-34 embryos, juveniles and adults were dissected out and postfixed for 4 hours in the corresponding fixative. Specimens fixed in 4% PFA were cryoprotected, embedded in OTC compound (Tissue Tek, Torrance, CA), and frozen with liquid nitrogen-cooled isopentane and cut on a cryostat. Specimens fixed in Clark's solution were dehydrated, embedded in paraffin and cut on a rotary microtome. Parallel series of cryostat (14–18 µm thick) and of rotary microtome (10–12 µm thick) sections of specimens cut in vertical planes along the dorsoventral

or nasotemporal axis of the retina (transverse or sagittal planes with respect to the brain, respectively) were mounted on Superfrost Plus (Menzel-Glasser1) slides.

Antibodies characterisation

The monoclonal anti-PCNA (P8825; Sigma, St. Louis, MO) is a mouse IgG2a isotype derived from the PC10 hybridoma produced by the fusion of mouse myeloma cells and splenocytes from a BALB/c mouse immunized with PCNA-Protein A fusion protein. According the manufacturer, from human to yeast the antibody recognizes a protein of 36 kDa corresponding to the acidic non-histone auxiliary protein of DNA polymerase, also known as polymerase delta accessory protein. This antibody specifically labels proliferating cells in the retina of sharks (Ferreiro-Galve et al., 2009), lampreys (Villar-Cheda et al., 2008) and teleosts (Candal et al., 2005a; Alunni et al., 2007).

The polyclonal anti-PH3 (Ser10; 06-570, Upstate-Millipore) was generated in rabbit against a KLH-conjugated peptide (ARKpSTGGKAPR KQLC) corresponding to amino acids 7-20 of human histone H3. According the manufacturer, the antibody detects mitotic cells in *Drosophila*, *Caenorhabditis elegans* and vertebrates (tested in zebrafish, *Xenopus* and human). For characterisation of the Pax6 antibody, see Chapter 5.

PCNA immunohistochemistry

For heat induced epitope retrieval, sections were pretreated with 0.01M citrate buffer pH 6.0 for 30 min at 95°C, and allowed to cool for at least 20-30 minutes at room temperature. Sections were rinsed twice in 0.05 M Tris-buffered saline containing 0.1% Tween-20 at pH 7.4 (TBS-T) for 5 min each, and then processed by the peroxidase-antiperoxidase (PAP) method with a mouse anti-PCNA monoclonal antiserum as primary antibody (Sigma; diluted 1:500), overnight at room temperature (RT). The sections were then rinsed in TBS-T (three 10-min rinses) and endogenous peroxidase was blocked with 10% H_2O_2 in phosphate buffered saline pH 7.4 (PBS) for 30 min at RT. Sections were rinsed in TBS-T, incubated in goat anti-mouse IgG (Sigma; 1:30) for 1 h at RT, rinsed again in TBS-T, and incubated in mouse PAP complex (Sigma; 1:500) for 30 min at RT. The immunoreaction was developed with SIGMA*FAST*™ 3,3'-Diaminobenzidine (DAB) tablets (Sigma), as indicated by the manufacturers. All dilutions were made with TBS-T containing 15% normal goat serum (Dako),

and all incubations were carried out in a humid chamber. Finally, the sections were dehydrated, mounted and coverslipped. In order to facilitate identification of retinal cells and layering parallel sections were stained with haematoxylin–eosin. As negative controls, the primary, secondary or tertiary antibodies were omitted. No immunostaining was observed in the control sections. Photographs were taken with an Olympus DP71 colour digital camera, fitted to a Provis microscope (Olympus, Tokyo).

PH3 immunohistochemistry

Sections were pretreated as above. Residual avidin/biotin activity was removed by incubation with the avidin/biotin blocking kit (Vector, Burlingame, CA). Sections were then incubated with the anti-PH3 (ser 10) rabbit polyclonal antiserum (Upstate BioTechonogy, diluted 1:400), overnight at RT. Sections were then rinsed in TBS (two 10-min rinses) and endogenous peroxidase was blocked as above. Sections were rinsed in TBS, incubated in biotinylated goat anti-rabbit IgG (Dako; 1:500) for 1 h at RT, rinsed again in TBS, and incubated in the preformed Avidin: Biotinylated enzyme Complex (ABC complex; Vector) for 30 min at RT. The immunoreaction was developed with SIGMA*FAST*™ 3,3'-Diaminobenzidine (DAB) tablets (Sigma). All dilutions were made with TBS containing 2% bovine serum albumin (BSA; Sigma), 15% normal goat serum (Dako) and 0.2% Triton X-100 (Sigma), and all incubations were carried out in a humid chamber. As negative controls, the primary or secondary were omitted. No immunostaining was observed in the control sections.

Quantification of PH3-immunoreactive cells

Quantification of PH3-immunoreactive (PH3-ir) cells was performed by counting all immunopositive cells of the neural retina on sections from *S. canicula* at stages 32 and 33. To avoid double cell counting, cells were counted in alternate serial sections. The number of sections in each serial set depended on eye size: 48 from stage 32; 56 sections from stage 33. The surface of each section was measured on digital microphotographs using ImageJ free software (http://rsb.info.nih.gov/ij/). Additionally, cells were counted separately in four different retinal zones (dorsal and ventral ciliary marginal zone, CMZ; dorsal and ventral *transition zone*) in 60 alternate serial sections of *S. canicula* at stage 32. The surface of these zones was measured as above. The rate of mitosis in each section and retinal zone was

expressed as the number of PH3-ir cells/mm^2. The mean number of PH3-ir cells/mm^2 and standard deviations in each set of observations were calculated. Statistical analyses were performed via two-tailed Student's t-test.

Double PCNA-PH3 immunofluorescence

Sections were pretreated for epitope retrieval as above, and then incubated with a cocktail of the anti-PCNA monoclonal mouse antiserum (Sigma, diluted 1:200) and anti-PH3 (ser 10) rabbit polyclonal antiserum (Upstate BioTechonogy, diluted 1:200), overnight at RT. The sections were then rinsed in TBS-T (two 10 min rinses) and endogenous peroxidase was blocked with 10% H_2O_2 in phosphate buffered saline pH 7.4 (PBS) for 30 min at RT. Secondary antibodies were used as follows: FluoProbes 546 Goat-anti-Mouse (Interchim, France; diluted 1:100) and Alexa Fluor 488 Goat-anti-Rabbit immunoglobulins (Molecular Probes, The Netherlands; diluted 1:200). All antibodies were diluted in Tris-buffered saline (TBS) containing 0.2% of Triton X-100 (Sigma) and 15% normal goat serum, and incubations were carried out in a humid chamber. Sections were rinsed in TBS for 30 min, then in distilled water (twice for 30 min), and allowed to dry for 2 hours at 37°C. Sections were mounted in MOWIOL 4-88 Reagent (Calbiochem, Merk KGaA, Darmstadt, Germany), allowed to dry for 30-60 min at 37°C. Double samples were studied with a spectral confocal laser scanning microscope TCS-SP2 (Leica, Wetzlar, Germany). Stack images were acquired separately from each laser channel with steps of 0.8 or 1μm along the z-axis and collapsed images were obtained from an average of 15 optical sections. Confocal stacks were acquired and processed with LITE software (Leica). As negative controls, the primary or secondary antibodies were omitted. No immunostaining was observed in the control sections.

Double Pax6-PCNA immunofluorescence

Sections were pretreated as above for epitope retrieval, rinsed twice in 0.05 M Tris-buffered saline containing 0.1% Tween-20 at pH 7.4 (TBS-T) for 5-min each, and then incubated with anti-Pax6 polyclonal rabbit antiserum (Covance, diluted 1:200) and anti-PCNA mouse monoclonal antiserum (Sigma, diluted 1:200), overnight at RT. The sections were then rinsed in TBS-T (two 10 min rinses) and endogenous peroxidase was blocked as above. Combinations of secondary antibodies were used as follows: (a) for stage 29 embryos, Alexa

Fluor 546 Donkey-anti-Rabbit immunoglobulins (Molecular Probes, The Netherlands; diluted 1:100) and Alexa Fluor 488 Donkey-anti-Mouse immunoglobulins (Molecular Probes, The Netherlands; diluted 1:100); (b) for stage 30 embryos onwards, Alexa Fluor 488 Goat-anti-Rabbit immunoglobulins (Molecular Probes, The Netherlands; diluted 1:200) and FluoProbes 546 Goat-anti-Mouse (Interchim, France; diluted 1:100). All dilutions were made with Tris-buffered saline (TBS) containing 0.2% of Triton X-100 (Sigma) and either 15% normal donkey serum (Dako) or 15% normal goat serum, depending on the combination of secondary antibodies. All incubations were carried out in a humid chamber. Sections were rinsed in TBS for 30 min, then in distilled water (twice for 30 min), and allowed to dry for 2 hours at 37°C. Sections were mounted in MOWIOL 4-88 Reagent (Calbiochem, Merk KGaA, Darmstadt, Germany), allowed to dry for 30-60 additional minutes at 37°C, and studied in a Leica spectral confocal laser scanning microscope (TCS-SP2) as indicated above. As negative controls, the primary or secondary antibodies were omitted. No immunostaining was observed in the control sections.

RESULTS

We showed previously that the timing of retinal development is similar in *S. canicula* and *H. fuscus* embryos, and that three developmental periods can be distinguished (see Chapter 5). The *first developmental period* (stages 26 to 29) is characterized by the neuroepithelial appearance of the retina and the absence of layering. The *second developmental period* (stages 30 to 32) is recognizable by: the progressive formation of the inner plexiform layer (IPL) between the GCL and INL, and of the outer plexiform layer (OPL) between the INL and the ONL; by the organization of a neuroepithelial zone adjacent to the ciliary epithelium (called ciliary marginal zone; CMZ); and by the presence of a *transition zone* between the not layered CMZ and the layered central retina. In the *third developmental period* (stages 33 to 34), layering progresses to nearly the entire circumference of the retina, that reaches the mature organization characteristic of postembryonic stages (juveniles and adults).

PCNA immunoreactivity

A schematic drawing indicating the dorsoventral and nasotemporal axis of the developing retina is shown in Fig. 1A. No between-species differences were observed in the spatial and temporal distribution of PCNA-immunoreactive (PCNA-ir) cells in the retina, so only the *H. fuscus* sections are shown in Figure 1.

During the *first developmental period*, the thick neuroepithelium of the retina was mostly formed by PCNA-ir cells. At the end of this period (stage 29) the density of PCNA-ir cells was high but some PCNA-negative cells appeared among proliferating cells in the inner region of the central retina, although regional differentiation or layering was not yet observable (Fig. 1B). Other eye structures such as the ciliary epithelium and the lens epithelium also contained abundant proliferating cells (not shown).

At the beginning of the *second developmental period* (stage 30) the primordial GCL was mostly formed of PCNA-negative cells. Some immunonegative cells were also observed in the innermost region of the neuroblastic layer, which represents the primordium of the inner part of the INL (INLi; Figs. 1C-E). The retina bordering the optic nerve head (asterisks in Fig. 1C) and the CMZ (Fig. 1E) exhibited only PCNA-ir cells, without any retinal layering. A similar distribution of PCNA-ir cells was observed at stage 31, but the area showing PCNA-negative cells has increased notably in surface, following a centre-to-peripheral sequence (compare Figs. 1C, 1F). As in previous stages, PCNA-ir cells were also observed in the ciliary epithelium (mostly in its inner non-pigmented layer) and in the lens epithelium (Fig. 1G). At stage 32, very few PCNA-ir cells were observed in the most central part of the retina, which now exhibits outer and INL (Fig. 1H). In the adjacent areas to this retinal region where the OPL is fairly evident, PCNA-ir cells were not observed in the GCL and INLi, but they were abundant in the outer part of the INL (INLo; Fig. 1I). Although most cells of the ONL of this region were PCNA-negative, some proliferating cells were observed in this layer, mostly located in its inner region near the primordial OPL and some close to the outer limiting membrane or in intermediate positions (Figs. 1H-K). The density of PCNA-ir cells in the INLo and ONL increased towards the *transition zone*, where the OPL was not yet evident (Figs. 1J, K). At this stage, the region bordering the optic nerve head (Fig. 1L) and the CMZ (Fig. 1M) showed closely packed PCNA-ir neuroepithelial cells. Interestingly, the density of PCNA-ir cells decreased significantly in the inner layer of the ciliary epithelium, which also showed

pigmentation in its outer layer, whereas PCNA immunoreactivity was still abundant in the lens epithelium (Fig. 1M).

At prehatching stages, the central retina contained very few, weakly PCNA-ir cells scattered in the INL and ONL and less frequently in the GCL and the IPL (Fig. 1N), and PCNA immunoreactivity was also observed in some cells of the retinal pigment epithelium (Fig. 1N). Most PCNA-ir cells were confined to the CMZ (Fig. 1O) and the retina bordering the optic nerve head (Fig. 1P). At the CMZ, numerous intensely PCNA-ir neuroepithelial cells extended from vitreal to scleral regions, without any sign of layering (Figs. 1O, P). A thick *transition zone* was observed between the CMZ and the clearly layered retina. In this *transition zone*, the inner (layered) part (in which the GCL and the IPL are clearly distinguished) contained very few weakly PCNA-ir cells, whereas the neuroblastic outer, non-layered part (nl in Figs. 1O, P), consisted of numerous PCNA-ir cells (Figs. 1O, P). In the *transition zone*, the organization of PCNA-ir cells resembled that observed in the central retina at stage 30 although the density of PCNA-ir cells in the neuroblastic region was clearly lower, and in the region just adjacent to the *transition zone* was similar to that found in the central retina of late stage 32 (compare Figs. 1H and 1P). Therefore, the patterns of proliferation observed from the CMZ to the central retina recapitulate the changes occurring in the central retina throughout development.

We investigated if the reduction in the number of PCNA-positive cells throughout development, especially obvious between stages 32 and 33, could be due to decreased mitotic activity. We used anti-PH3 as a mitotic marker, as it allows for quantification of the mitotic rate within a given area. The rate of mitosis in each section was calculated as the number of PH3-ir cells/mm^2. A significant reduction in the mean number of PH3-ir cells/mm^2 was found when comparing stages 32 and 33 (105.9 ± 40.4 cells/mm^2 *vs*. 42.1 ± 19.7 cells/mm^2, respectively; $p<0.000001$), which suggests that the reduction in the number of PCNA-positive cells results from decreased mitotic activity.

Comparison of PCNA and PH3 immunoreactivities in the peripheral retina

To further analyse the actual proliferation in remnant undifferentiated retinal areas, double immunofluorescence experiments were performed with anti-PCNA and anti-PH3 antibodies in prehatching embryos and juveniles. In prehatching embryos (Figs. 2A, B), mitotic

cells (PH3-ir) were found in the neuroepithelium close to the intraretinal cleft (i.e., the ventricular space located between the neural retina and the retinal pigment epithelium), mostly in the *transition zone* (Fig. 2B) and some in the CMZ (Fig. 2A). The same patterns were observed in juveniles (Fig. 2C). Since the *transition zone* appeared to be more active mitotically than the CMZ, we studied the mitotic rates of these particular zones in *S. canicula* retinal sections at late stage 32. The mean number of PH3-ir cells/mm^2 was found to be significantly higher in the *transition zone* than in the CMZ (402.2 ± 96.7 PH3-ir cells/mm^2 *vs.* 232.8 ± 140.8 PH3-ir cells/mm^2; $p<0.000001$).

Additionally, to know if there were significant differences in proliferation between the dorsal and ventral CMZs, or between the dorsal and ventral *transition zones*, we studied the mitotic rates of these four particular zones in *S. canicula* retinal sections at late stage 32. No statistically significant differences were found between (1) the mean area *per* section of the dorsal and ventral CMZs; (2) the mean area *per* section of the dorsal and ventral *transition zones*; (3) the mean number of cells/mm^2 of the dorsal and ventral CMZs (236.3 ± 172.4 cells/mm^2 *vs*. 228.4 ± 89.7 cells/mm^2); and (4) the mean number of cells/mm^2 of the dorsal and ventral *transition zones* (373.1 ± 94.3 cells/mm^2 *vs*. 439.2 ± 88.5 cells/mm^2).

Some proliferating cells in the retina express Pax6

During the *first developmental period*, most neuroepithelial cells were proliferating (they showed PCNA-ir nuclei) and some of them expressed Pax6 (Figs. 3A-E). At the end of this period differences began to appear between the inner part of the central retina, where innermost cells were PCNA negative but intensely Pax6-ir (arrows in Fig. 3A), and the outer part, where intensely (scarce) and weakly (abundant) labelled Pax6 neuroepithelial cells (open arrows in Fig. 3A) were scattered between the abundant PCNA-ir neuroepithelial cells. Only a few PCNA-ir cells in the central retina showed intense Pax6 labelling (arrow in Figs. 3B-D), which contrasts with the lens epithelium and the most peripheral retina (close to the ciliary epithelium) where most of cells were immunoreactive for both markers (Figs. 3A, E).

During the *second developmental period* (Figs. 3F-I), a sharp boundary was observed between the outermost Pax6-ir cells in the INLi and the PCNA-ir cells in the neuroblastic region, thus limiting the layered (inner) and the non-layered (neuroblastic, outer) retina (Figs. 3F, G). A moderate amount of intensely labelled Pax6 cells occurred among the abundant

PCNA-ir cells of the prospective INLo (Fig. 3F). Interestingly, PCNA labelling was very rarely found in these intensely Pax6-ir cells, and only in the peripheral retina (arrows in Fig. 3G). PCNA signal was more frequent in the weak Pax6-ir cells in the outer non-layered retina, in the CMZ and in the ciliary epithelium, where densities of PCNA-ir and Pax6-ir cells were similar (Fig. 3G). At the end of the *second developmental period*, PCNA-ir cells were still abundant in the outer half of the peripheral retina (Figs. 3H, I), whereas in the central part of the retina, they gradually disappeared from the prospective INLo and ONL (Fig. 3I). In parallel, abundant intensely labelled Pax6 cells occupied the inner layers (GCL and INLi) both in the central and peripheral retina, whereas they decreased in number in the INLo, especially in the central part (Fig. 3I).

During the *third developmental period* (stages 33 to hatching), the extension of the layered retina extended considerably as development progresses, following a central-to-peripheral gradient. In the peripheral retina (Fig. 3J), the CMZ contained abundant intensely PCNA-ir cells and very pale Pax6-ir cells, some of them colocalising for both substances (short arrows in Fig. 3J). In the *transition zone*, marked differences between the inner and outer parts were clearly observed when comparing the distribution of the different markers. The inner (layered) part contains strongly Pax6-ir (PCNA negative) cells in the GCL and INLi. The outer (neuroblastic) part contained some strongly labelled Pax6-ir among abundant PCNA-ir cells, with colocalisation rarely observed (large arrow in Fig. 3J). Therefore, patterns of PCNA/Pax6 immunoreactivity in the *transition zone* were highly reminiscent of those found in the central retina at the beginning of the *second developmental period* (stage 30). In the central retina (Figs. 3K, L), PCNA-ir cells were rarely found in the INLi (arrows in Fig. 3K) or GCL (arrow in Fig. 3L), or even in the INLo or ONL (arrowheads in Figs. 3K, L). In contrast, abundant intensely labelled Pax6 cells were still found in the INLi, although they decreased in number in the GCL. Thus, the spatial ordering of PCNA-ir and Pax6-ir cells in the *transition zone* showed the spatial sequence of proliferating, early postmitotic and differentiated cells from marginal-to-central and from vitreal-to-scleral axes.

DISCUSSION

Spatiotemporal distribution of PCNA and PH3 quantification in the retina of sharks

Since the timing of cell cycle exit is closely linked to cell fate specification in the developing retina, the immunohistochemical detection of proteins related to cell cycle control has frequently been used in developmental studies (reviewed in Candal et al., 2005a). We used PCNA as a marker for proliferating cells as it is expressed throughout the cell cycle: i.e., its expression begins in late G1 phase, is maximal during the S phase and decreases from the S/G2 transition towards mitosis. Since recent postmitotic cells may be weakly PCNA-labelled hours after leaving the cell cycle (Bravo and MacDonald-Bravo, 1987), the use of PCNA also allows to distinguish the areas of early differentiating cells (those weakly labelled). The advantages of the use of PCNA rather than other assays for detecting cell proliferation (i.e., direct counting of mitotic figures or the incorporation of DNA precursors) have previously been evaluated (Ortego et al., 1994; Candal et al., 2005a,b), although it does not enable study of the dynamic of cell proliferations.

Studies of the expression of diverse neurochemical markers of maturity in the retina of fishes reveal temporal coincidence between the loss of PCNA immunoreactivity and the expression of neurochemical markers for mature, postmitotic/differentiated retinal cells (Neghishi et al., 1990). The same holds true in *S. canicula* and *H. fuscus* retinas since decreasing levels and even the absence of PCNA were first observed in the central region of the GCL, where retinal ganglion cells are the first cell type to be born during vertebrate (including sharks) retinogenesis (Mu and Klein, 2004; Harahush et al., 2009). On the other hand, we used the PH3 antibody as a mitotic marker, which provides an accurate method for examining possible significant differences in the proliferation activities at different retinal regions, as it allows for quantification of the mitotic rate within a given area (Alunni et al., 2007).

The present findings as regards the spatiotemporal distribution of PCNA immunohistochemistry reveals that: (1) PCNA immunoreactivity was present in all neuroblasts until the end of the *first developmental period*, and was progressively lost in a vitreal-to-scleral and a centre-to-peripheral sequence that parallels cell and layer differentiation; (2) from juvenile stages onwards, PCNA immunoreactivity turned mostly confined to a ring of

dividing neuroblasts within the CMZ; (3) a *transition zone* was defined, which lies between the pure-proliferating CMZ and the central (layered) retina and contains many PCNA and PH3 positive cells in its scleral (unlayered) part; (4) PCNA-ir cells were not restricted to the peripheral growth zone but also appeared in the differentiated central area of the retina up to prehatching embryos: at the end of the *second developmental period*, large amounts of PCNA-positive cells were observed in the INLo and ONL, even within the layered retina, whereas PCNA decreased in this region during the *third developmental period*; (5) some PCNA-positive cells were also observed in the retinal pigment epithelium of prehatching embryos.

Drop in the number of PH3-ir cells we observe at the later stages of development suggest that reduction of PCNA-positive cells is the result of decreased mitotic activity. Moreover, our result correlates a loss of proliferating (PCNA and PH3 positive) cells with layering of the retina, which is indicative of cell maturation. Developmental patterns similar to those described here in sharks have been found in the retinas of other vertebrates, especially regarding the gradual loss of PCNA immunoreactivity in a spatiotemporal sequence that mirrors the gradient of maturation. It appears that this pattern of cell proliferation does not depend on the rate of growth, since the vitreal-to-scleral and centre-to-periphery loss of PCNA immunoreactivity in *S. canicula* is similar to that reported in goldfish (Neguishi et al., 1990), trout (Candal et al., 2005a), and even in rapid-growing species of teleosts such as *Haplochromis burtoni* (Hagedorn and Fernald 1992), medaka (Candal et al., 2002) and blind cavefish (Alunni et al., 2007).

Also similar is the presence in the adult retina of a peripheral growth zone containing stem cells. However, this proliferation region was not found after metamorphosis in the lamprey retina (Villar-Cheda et al., 2008), suggesting divergent developmental patters in retinas of agnathans and basal groups of gnathostomes.

PCNA in the *transition zone* between the proliferating marginal ciliary and the differentiated central zones

In sharks (present results) PCNA immunoreactivity becomes progressively confined to the peripheral retina during development. Indeed, high rates of mitosis (as shown by using the mitotic marker anti-PH3) have been found close to the subretinal space in the CMZ and the

transition zone, suggesting that PCNA-ir cells in these zones, especially in the latter, are not quiescent cells but rather actively proliferating cells. A proliferating CMZ has been previously described in teleosts, and new neurons are added to the retina from this region throughout life, so that peripheral regions become progressively more central as eye grows (Lyall, 1957; Neguishi et al., 1990; Candal et al., 2005a). Thus, the new neuron/glial cells originated in the CMZ are seamlessly incorporated into the existing retinal circuitry (Reh and Levine, 1988). The persistence of cells in the retina that exhibit all of the features of adult stem cells, i.e., self-renewal, multipotency, and the capacity to respond to injury by mitotic activation with the ability to regenerate differentiated tissues, has been reported in adult teleost fishes (revised in Raymond et al., 2006), as well as in amphibians, reptiles and chickens during their entire life (reviewed in Mitashov, 2001). However, to our knowledge, the presence of a prominent *transition zone* located between the CMZ and the central retina in adult fish such as that observed here has not previously been defined, although in the retina of the trout PCNA-ir cells have been reported to extend some distance in the INLi, INLo and ONL from the peripheral proliferating retina (Candal et al., 2005a). Raymond et al. (2006) subdivided the compact, narrow CMZ of the adult zebrafish retina into four anatomically different regions (peripheral, middle, central-inner and central-outer), and all contained PCNA-ir cells. The OPL separates the central-inner from the central-outer region. The GCL derives from the middle CMZ, whereas progenitors in central-inner CMZ form the INL, and the central-outer region produces photoreceptors of the ONL. The appearance of the *transition zone* of the shark retina is roughly coincident with the pattern described in the central zone of the zebrafish CMZ, although the *transition zone* in sharks is not split in two by the OPL and proliferation is much protracted in time (present results). Whereas in zebrafish these three zones are found in close spatial succession, in sharks the proliferation region that gives rise to the INL is the most protracted, extending centralward far beyond the ONL region containing PCNA-ir cells.

Sources of stem cells other than the proliferating peripheral retina

The presence of proliferating cells in the layered central area of the differentiated retina has been reported in several species of teleosts, such as killifish and goldfish (Neguishi et al., 1990), trout (Julian et al., 1998; Candal et al., 2005a), medaka (Candal, 2002), zebrafish (Raymond et al., 2006), and cavefish (Alunni et al., 2007). It has been suggested that these

clusters of proliferating cells within the differentiated retina are progenitors of the photoreceptor lineage (reviewed in Candal et al., 2005a), although following injury these clusters in the microenvironment around some Müller glia may function as multipotent retinal stem cells, in order to regenerate other types of retinal neurons (Raymond et al.,2006).

Temporal correlation of retinal layering with sustained PCNA immunoreactivity

Some significant differences with respect to those reported in teleosts can be observed as regards timing of loss of PCNA immunoreactivity with respect to layering. In sharks, the progressive loss of PCNA throughout the retina occurs once layering is complete. Accordingly, numerous PCNA-ir cells are found in the growing retina, even within areas that show clear evidence of layering, i.e., where differentiating cells have started to form synapses in the plexiform layers. The opposite is observed in trout, since the loss of PCNA immunoreactivity precedes layering, i.e., the central retina of late embryos is devoid of PCNA-ir cells before it becomes layered. Interestingly, in trout, PCNA-ir cells reappear secondarily in this region at hatching, once layering is complete. However, they are scattered and scarce in number (Candal et al., 2005a). The longer period of neurogenesis observed in sharks (present results) relative to that reported in teleosts analysed so far, may be related to a greater number of cells and larger eye at maturity.

PCNA in the retinal pigment epithelium

PCNA immunoreactivity has also been detected in cells of the retinal pigment epithelium of sharks (present results). The highly specialised retinal pigment epithelium plays a key role in regulating retinal development (Raymond and Jackson, 2001; Martínez-Morales et al., 2004; Giménez et al., 2005). Moreover, retinal pigment epithelium-derived cells display several properties of neural progenitor cells: (i) neural progenitor identity, based on the expression of markers used to identify neural stem and progenitor cells; (ii) proliferation with limited self-renewal; (iii) and differentiation into neuronal and glial cells based on the expression of differentiation markers (Reh and Levine, 1998; Seaberg and Van der Kooy, 2003). In some tetrapod species the retinal pigment epithelium is capable of transdifferentiation and generation of new neurons under certain conditions (Kaldarar-Pedotti, 1979; Anderson et al., 1981; Reh and Nagy, 1987; Reh and Levine, 1998; Fischer and Reh, 2001; Engelhardt et al.,

2005; Mitsuda et al., 2005, although complete retinal regeneration in adult animals occurs only in certain urodele amphibians (Del Río-Tsonis and Tsonis, 2003). The presence of a proliferation marker in cells of the shark retinal pigment epithelium thus suggests that these cells may have similar properties.

In *S. canicula*, the cells of the retinal pigment epithelium are unpigmented, located below a reflecting *tapetum lucidum* (Nicol, 1961), and this characteristic facilitates the observation of PCNA expression in retinal pigment epithelium cells. To our knowledge, the presence of proliferating non-pigmented cells in the retinal pigment epithelium has previously been described in urodeles, larval anurans, amphibians, embryonic and postnatal chickens and mice, but not in fishes. In *S. canicula* and *H. fuscus*, these cells can be observed long after massive proliferation ceases in the subjacent neural retina. The absence of pigment could be related with the proliferation activity in some retinal pigment epithelium cells. In fact, in albinos and in transgenic mice with pigment-free areas, an increase in retinal pigment epithelium cell proliferative activity and extended periods of mitosis during early post-natal stages has been reported (Berman and Payne, 1985; Ershov and Stroeva, 1989; Webster and Rowe, 1991; Ilia and Jeffery, 1996, 2000). Moreover, in early stages of frog, birds and mammals development, removal of the retina induces proliferation of the retinal pigment epithelium, creating a second layer of retinal pigment epithelium cells that lose pigmentation and rebuild a new retina in a sequence similar to that observed during development (Reh and Nagy, 1987; Mitsuda et al., 2005).

Pax6 versus proliferation in the undifferentiated retina of sharks

Strong Pax6 immunoreactivity has been observed in most cells during the *first developmental period,* as well as in a few cells within the outer non-layered (undifferentiated) retina during the *second developmental period* (see Chapter 5). Coinciding with the beginning of retinal layering, most cells within the outer non-layered retina and at the CMZ show pale Pax6 immunoreactivity. The fading of Pax6 labelling in most cells within the outer non-layered retina and at the CMZ could be related to Pax6 down-regulation as subsets of progenitor cells go from uncommitted to neurogenic, lineage-restricted fates (Hsieh and Yang, 2009). Moreover, in these lineage-restricted progenitors, the maintenance of low levels of Pax6 appears to be essential for sustaining cell proliferation, especially the reentry of S phase

(Hsieh and Yang, 2009; see discussion in Chapter 5). We therefore aimed to investigate the relation of strong and faint Pax6 expression with proliferation within the undifferentiated areas mentioned above. Colocalisation for strong Pax6-ir and PCNA-ir cells has been rarely found, while weak Pax-6 ir cells colocalise abundantly with PCNA-ir cells, especially in the CMZ. Of note, the presence of maximal levels of PCNA during the S phase (Bravo and MacDonald-Bravo, 1987) coincides with the absence of high levels of Pax6 at this phase (Hsieh and Yang, 2009), which could explain the scarce number of intense Pax6/PCNA-ir cells observed in both *S. canicula* and *H. fuscus* from the *second developmental period* onwards. Proliferating-Pax6-ir cells have been also observed in the ciliary epithelium and in the retinal margin in teleosts (Hitchcock et al., 1996; Otteson et al., 2001; Faillace et al., 2002) and chicken (Fischer and Reh, 2000), an expression that was maintained in adults.

Taken together, our present results suggest that proliferating, pale Pax6-ir cells within the outer non-layered retina and within the CMZ could represent retinal progenitors that had come into the neurogenic state, maintain their multipotency and will reenter the cell cycle.

Pax6 versus proliferation in the mature retina of sharks

The pattern of Pax6 immunoreactivity in mature shark retinas includes Pax6 expression in ganglion, amacrine and horizontal cells in the GCL, INLi and horizontal cell layer (HCL), and its absence in photoreceptors (ONL), bipolar cells and Müller cells (see Chapter 5). PCNA-positive cells are found within the layered retina of *S. canicula* and *H. fuscus* until the end of the *third developmental period* (current observations). Since Pax6 is expressed in areas of the mature retina long after they have exited the cell cycle, double-labelling experiments were performed in order to determine whether Pax6-ir cells in the layered retina coincide with PCNA-ir observed in these regions during development, which could be indicative of a role for Pax6 in the maintenance of proliferation of retinal progenitors. Alternatively, Pax6 immunoreactivity may be associated with postmitotic cells, suggesting a different role for these cells in the mature retina.

These experiments revealed complementary patterns of expression, and colocalisation of Pax6 and PCNA was rarely demonstrated. Very low levels of colocalisation have been also reported in teleosts, and less than 0.5% of all proliferating cells in the mature INL of the goldfish retina were Pax6-positive (Faillace et al., 2002). Since none of these cells were

labelled with markers of differentiated amacrine or bipolar cells, they have been interpreted as retinal stem cells that give rise to Pax6-negative fusiform cells (Otteson et al., 2001).

In summary, in sharks (present results), most Pax6-ir cells in the layered retina were PCNA-negative, suggesting that in the mature retina, Pax6 plays roles other than maintenance of multipotent progenitor cells (see discussion in Chapter 5).

REFERENCES

Alunni A, Menuet A, Candal E, Pénigault JB, Jeffery WR, Rétaux S (2007). Developmental mechanisms for retinal degeneration in the blind cavefish *Astyanax mexicanus*. J Comp Neurol, 505: 221-233.

Anderson DH, Stern WH, Fisher SK, Erickson PA, Borgula GA (1981). The onset of pigment epithelial proliferation after retinal detachment. Invest Ophthalmol Vis Sci, 21: 10-16.

Ballard W, Mellinger J, Lechenault H (1993). A series of normal stages for development of *Scyliorhinus canicula*, the lesser spotted dogfish (Chondrichthyes: Scyliorhinidae). J Exp Zool, 267: 318-336.

Berman NEJ, Payne BR (1985). An exuberant retinocollicular pathway in Siamese kittens: effects of abnormal activity on its maturation. Brain Res Dev Brain Res, 22: 197-209.

Bravo R, MacDonald-Bravo H (1987). Existence of two populations of cyclin/proliferating cell nuclear antigen during the cell cycle: association with DNA replication sites. J Cell Biol, 105: 1549-1554.

Candal E (2002). Proliferation and cell death in the brain and retina of teleosts: relation to Ol-KIP and Reelin expression. Ph. D. Thesis, Santiago de Compostela.

Candal E, Anadón R, DeGrip WJ, Rodríguez-Moldes I (2005a). Patterns of cell proliferation and cell death in the developing retina and optic tectum of the brown trout. Dev Brain Res, 154: 101-119.

Candal E, Anadón R, Bourrat F, Rodríguez-Moldes I (2005b). Cell proliferation in the developing and adult hindbrain and midbrain of trout and medaka (teleosts): A segmental approach. Dev Brain Res, 160: 157-175.

Candal E, Caruncho HJ, Sueiro C, Anadón R, Rodríguez-Moldes I (2005c). Reelin expression in the retina and optic tectum of developing common brown trout. Dev Brain Res, 154: 187-197.

Carney RS, Bystron I, López-Bendito G, Molnár Z (2007). Comparative analysis of extra-ventricular mitoses at early stages of cortical development in rat and human. Brain Struct Funct, 212: 37-54.

Cid E, Velasco A, Ciudad J, Orfao A, Aijón J, Lara JM (2002). Quantitative evaluation of the distribution of proliferating cells in the adult retina in three cyprinid species. Cell Tissue Res, 308: 47-59.

Del Rio-Tsonis K, Tsonis PA (2003). Eye regeneration at the molecular age. Dev Dyn, 226: 211-224.

Engelhardt M, Bogdahn U, Aigner L (2005). Adult retinal pigment epithelium cells express neural progenitor properties and the neuronal precursor protein doublecortin. Brain Res, 1040: 98-111.

Ershov AV, Stroeva OG (1989). Post-natal pattern of cell proliferation in retinal pigment epithelium of mice studied with tritiated thymidine autoradiography. Cell Differ Dev, 28: 173-177.

Faillace MP, Julian D, Korenbrot JI (2002). Mitotic activation of proliferative cells in the inner nuclear layer of the mature fish retina: regulatory signals and molecular markers. J Comp Neurol, 451: 127-141.

Fernald RD (2004). Evolving eyes. Int J Dev Biol, 48: 701-715.

Ferreiro-Galve S, Rodríguez-Moldes I, Candal E (2009). Patterns of cell proliferation and rod photoreceptor differentiation in shark retinas. J Chem Neuroanat, 39: 1-14.

Fischer AJ, Reh TA (2001). Transdifferentiation of pigmented epithelial cells: a source of retinal stem cells? Dev Neurosci, 23: 268-276.

Galli-Resta L (2002). Putting neurons in the right places: local interactions in the genesis of retinal architecture. Trends Neurosci, 25: 638-643.

Giménez E, Lavado A, Jeffery G, Montoliu L (2005). Regional abnormalities in retinal development are associated with local ocular hypopigmentation. J Comp Neurol, 485: 338-347.

Hagedorn M, Fernald RD (1992). Retinal growth and cell addition during embryogenesis in the teleost *Haplochromis burtoni*. J Comp Neurol, 321: 193-208.

Harahush BK, Hart NS, Green K, Collin SP (2009). Retinal neurogenesis and ontogenetic changes in the visual system of the brown banded bamboo shark, *Chiloscyllium punctatum* (Hemiscyllidae, Elasmobranchii). J Comp Neurol, 513: 83-97.

Hendzel MJ, Wei Y, Mancini MA, Van Hooser A, Ranalli T, Brinkley BR, Bazett-Jones DP, Allis CD (1997). Mitosis-specific phosphorylation of histone H3 initiates primarily within pericentromeric heterochromatin during G2 and spreads in an ordered fashion coincident with mitotic chromosome condensation. Chromosoma, 106: 348-60.

Hitchcock PF, Macdonald RE, VanDeRyt JT, Wilson SW (1996). Antibodies against Pax6 immunostain amacrine and ganglion cells and neuronal progenitors, but not rod precursors, in the normal and regenerating retina of the goldfish. J Neurobiol, 29: 399-413.

Hsieh YW, Yang XJ (2009). Dynamic Pax6 expression during the neurogenic cell cycle influences proliferation and cell fate choices of retinal progenitors. Neural Dev, 4:32-50.

Hu M, Easter Jr SS (1999). Retinal neurogenesis: the formation of the initial central patch of postmitotic cells. Dev Biol, 207: 309-321.

Ilia M, Jeffery G (1996). Delayed neurogenesis in the albino retina: evidence of a role for melanin in regulating the pace of cell generation. Brain Res Dev Brain Res, 95: 176-183.

Ilia M, Jeffery G (2000). Retinal cell addition and rod production depend on early stages of ocular melanin synthesis. J Comp Neurol, 420: 437-444.

Julian D, Ennis K, Korenbrot JI (1998). Birth and fate of proliferative cells in the inner nuclear layer of the mature fish retina. J Comp Neurol, 394: 271-282.

Kaldarar-Pedotti S (1979). Mitotic activity of the pigment epithelium during embryonic and postembryonic development. Adv Ophthalmol, 39: 37-58.

Kwan JW, Lee MJ, Mack AF, Chiu JF, Fernald RD (1996). Nonuniform distribution of cell proliferation in the adult teleost retina. Brain Res, 712: 40-44.

Li Z, Hu M, Ochosinska MJ, Joseph NM, Easter Jr SS (2000). Modulation of cell proliferation in the embryonic retina of Zebrafish (*Danio rerio*). Dev Brain Dyn, 219: 391-401.

Link BA, Fadool JM, Malicki J, Dowling JE (2000). The zebrafish young mutation acts non-cell-autonomously to uncouple differentiation from specification for all retinal cells. Development, 127: 2177-2188.

Lyall AH (1957). The growth of the trout retina. Q J Microsc Sci, 98: 101-110.

Mack AF, Fernald RD (1990). Cell movement and cell cycle dynamics in the retina of the adult teleost *Haplochromis burtoni*. J Comp Neurol, 388: 435-443.

Mansour-Robaey S, Pinganaud G (1990). Quantitative and morphological study of cell proliferation during morphogenesis in the trout visual system. J Hirnforsch, 31: 495-504.

Marcus RC, Delaney CL, Easter SS Jr (1999). Neurogenesis in the visual system of embryonic and adult zebrafish (*Danio rerio*). Vis Neurosci, 16: 417-424.

Martínez-Morales JR, Rodrigo I, Bovolenta P (2004). Eye development: a view from the retina pigmented epithelium. Bioessays, 26: 766-777.

McManus KJ, Hendzel MJ (2006). The relationship between histone H3 phosphorylation and acetylation throughout the mammalian cell cycle. Biochem Cell Biol, 84: 640-657.

Mitashov VI (2001). Multipotent and stem cells in the developing, definitive, and regenerating vertebrate eye. Izv Akad Nauk Ser Biol, 6: 717-727.

Mitsuda S, Yoshii C, Ikegami Y, Araki M (2005). Tissue interaction between the retinal pigment epithelium and the choroid triggers retinal regeneration of the newt *Cynops pyrrhogaster*. Dev Biol, 280: 122-132.

Mu X, Klein WH (2004). A gene regulatory hierarchy for retinal ganglion cell specification and differentiation. Semin Cell Dev Biol, 15: 115-123.

Negishi K, Teranishi T, Karkhanis A, Stell WK (1990). Emergence and development of immunoreactive cells in teleostean retinas during the perinatal period. Dev Brain Res, 55: 127-137.

Negishi K, Wagner HJ (1995). Differentiation of photoreceptors, glia and neurons in the retina of the cichlid fish *Aequidens pulcher*: an immunocytochemical study. Dev Brain Res, 89: 87-102.

Nicol JAC (1961). The tapetum in *Scyliorhinus canicula*. J Mar Biol As s UK, 41: 271-277.

Ortego LS, Hawkins WE, Walker WW, Kroi RM, Benson WH (1994). Detection of proliferating cell nuclear antigen in tissues of three small fish species. Biotech. Histochem, 69: 317-323.

Otteson DC, D'Costa AR, Hitchcock PF (2001). Putative stem cells and the lineage of rod photoreceptors in the mature retina of the goldfish. Dev Biol, 232: 62-76.

Raymond PA, Barthel LK, Bernardos RL, Perkowski JJ (2006). Molecular characterization of retinal stem cells and their niches in adult zebrafish. BMC Dev Biol, 6: 36-52.

Raymond SM, Jackson IJ (1995). The retinal pigmented epithelium is required for development and maintenance of the mouse neural retina. Curr Biol, 5: 1286-1295.

Reh TA, Levine EM (1998). Multipotential stem cells and progenitors in the vertebrate retina J Neurobiol, 36: 206-220.

Reh TA, Nagy T (1987). A possible role for the vascular membrane in retinal regeneration in Rana catesbienna tadpoles. Dev Biol, 122: 471-482.

Schmitt E, Kunz YW (1989). Retinal morphogenesis in the rainbow trout, *Salmo gairdneri*. Brain Behav Evol, 34: 48-64.

Seaberg RM, van der Kooy D (2003). Stem and progenitor cells: the premature desertion of rigorous definitions. Trends Neurosci, 26: 125-131.

Sivak B, Sivak J (2000). Vertebrate eye development and refractive function: an overview. In: Vertebrate eye development (Fini ME, ed), pp 1–14. Springer, Berlin, Heidelberg, New York.

Villar-Cheda B, Abalo XM, Villar-Cerviño V, Barreiro-Iglesias A, Anadón R, Rodicio MC (2008). Late proliferation and photoreceptor differentiation in the transforming lamprey retina. Brain Res, 1201: 60-67.

Webster ME, Rowe MH (1991). Disruption of developmental timing in the albino rat retina. J Comp Neurol, 307: 460-474.

Figure 1. Patterns of cell proliferation in the developing retina of *H. fuscus*. A. Schematic drawing of a lateral view of the head at stage 27 (after Ballard et al., 1993) showing the dorsoventral and nasotemporal axis of the developing retina. **B.** Vertical section along the dorsoventral axis of a stage 29 retina. Arrows indicate a layer of PCNA immunonegative cells in the inner region of the central retina. **C-E.** Vertical sections along the dorsoventral axis of a stage 30 retina. **C.** Asterisks indicate the region neighbouring the optic nerve. **D.** Detail of the anterior figure to show PCNA immunonegative cells in the GCL and also in the INLi. **E.** Detail of the peripheral region showing the abundance of PCNA-ir cells in the CMZ, even at inner levels. **F, G.** Vertical sections along the dorsoventral axis of a stage 31 retina. **F.** The area containing PCNA immunonegative cells extends towards the periphery. **G.** PCNA-ir cells are observed throughout the CMZ, the non-pigmented ciliary epithelium (ce) and the lens epithelium (arrows). **H-M.** Vertical sections along the nasotemporal axis from the most central (H) to the most peripheral (L and M) retina of a stage 32 embryo. **H.** The central retina shows a scarce number of PCNA-ir cells. Arrows point to the OPL located between the INLo and the ONL. **I.** Peripheral section of the retina with respect to that shown in H, showing abundant PCNA-ir cells in the INLo and throughout the ONL. Arrows indicate the OPL. **J, K.** Sections through the *transition zone* of the retina (peripheral with respect to that shown in I), showing increased numbers of PCNA-ir cells. Note the absence of the OPL in the *transition zone* of the retina (right margin in K). **L.** Abundant PCNA-ir cells are present in the region bordering the optic nerve. **M.** PCNA immunonegative cells are abundant in the ciliary epithelium but absent from the CMZ. Arrows indicate PCNA-ir cells in the lens epithelium. **N-P.** Vertical sections along the dorsoventral axis of the retina of prehatching embryos. **N.** The central retina contains very few PCNA-ir cells which were located in the ONL, INL, GCL and even in the IPL (arrows). Arrowheads indicate PCNA immunoreactivity in some non-pigmented cells of the retinal pigment epithelium. **O.** PCNA immunoreactivity is mostly confined to the CMZ, where it is observed in cells from vitreal to scleral. Abundant PCNA-ir cells are also observed in the non-layered outer part of the *transition zone* (nl), which contrasts with the scarcity of PCNA-ir cells in its layered inner part (l). Small arrows indicate the presence of the OPL in the adjacent central zone of the retina. **P.** Detail of the region bordering the optic nerve head showing PCNA-ir cells throughout the neuroepithelial retina (asterisk). Note the abundance of PCNA-ir cells in the non-layered outer part of the *transition zone* (nl), while they are absent from the inner layered

part (l). Small arrows indicate the OPL in the adjacent central zone. For abbreviations, see list in Appendix B.

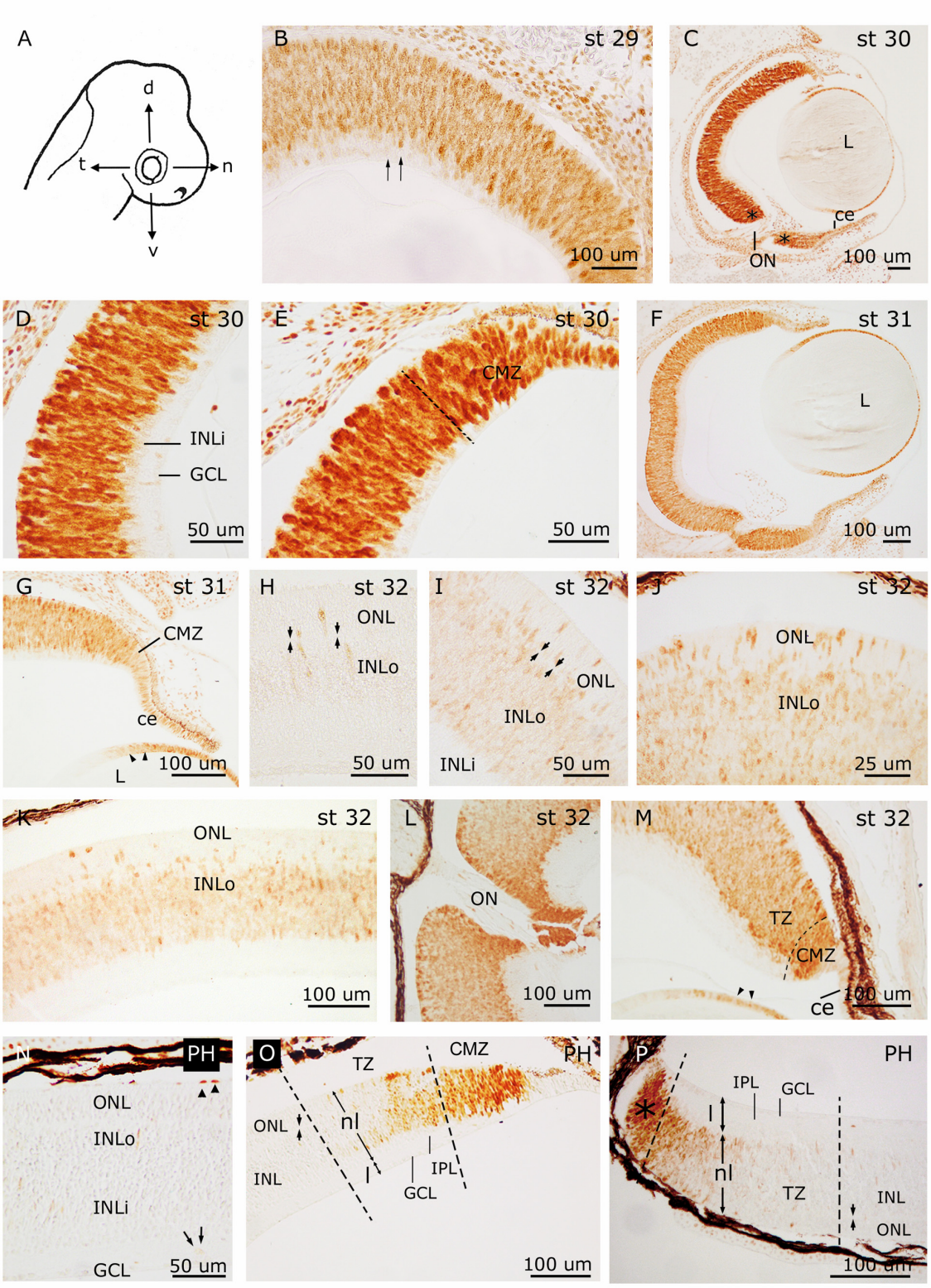

Figure 2. PCNA and PH3 immunoreactivities in the peripheral late developing retina. A-C. Vertical sections along the dorsoventral axis of the retina of prehatching (PH) embryos of *S. canicula* (A,B) and juveniles (Juv) of *H. fuscus* (C). PH3-ir cells (mitotic; green) are abundant close to the subretinal space in the CMZ (A) and the *transition zone* (B,C). Mitotic (PH3-positive) cells are absent from subventricular areas, which in turn showed abundant PCNA-ir cells (red). For abbreviations, see list in Appendix B.

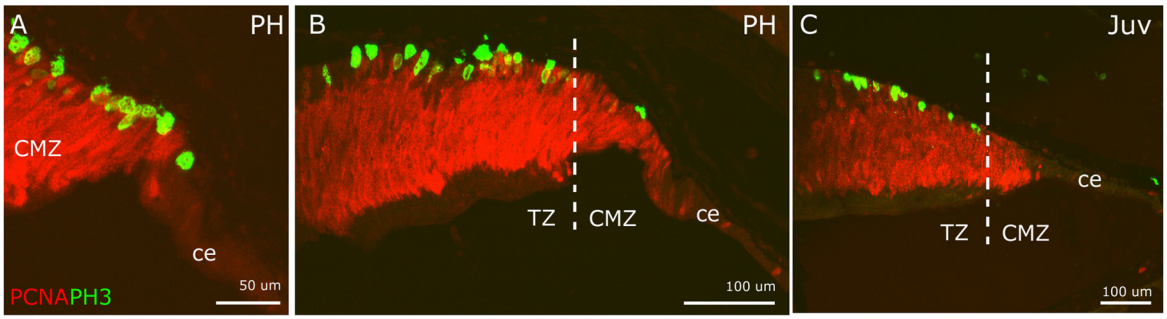
A
PH
CMZ
ce
PCNAPH3
50 um
B
PH
TZ
CMZ
ce
100 um
C
Juv
ce
TZ
CMZ
100 um

Figure 3. Comparison of spatiotemporal patterns of PCNA and Pax6 in the *S. canicula* / *H. fuscus* retinas. A-E. Vertical sections along the dorsoventral axis of the retina (transversal with respect to the brain) of a stage 29 of *S. canicula*. **A.** Section to show differences between the inner and the outer part of the neuroepithelial retina. The inner retina shows high numbers of PCNA-negative cells that are Pax6-ir (small arrows). In the outer retina, Pax6-ir neuroepithelial cells (open arrows) are observed among high numbers of PCNA-ir cells. The inset shows single optical sections (1-µm-thick) of the area squared in A, to show that most pale Pax6-ir cells in the lens epithelium and marginal zone of the retina are also PCNA-ir. **B-D.** Detail of the central retina to show a scarce number of strongly Pax6-ir/PCNA-ir cells (arrow). **E.** High numbers of double labelled cells (arrows) are found in the peripheral retina. The inset shows single optical sections (1-µm-thick) of the area squared in E. **F-G.** Vertical sections along the dorsoventral axis of the retina of a stage 31 of *H. fuscus*. A sharp limit exists between the inner (layered) and the outer (non-layered) retina. In the inner retina (mostly composed of Pax6-ir cells; green), few PCNA-ir cells are observed. In the outer retina, some Pax6-ir cells are found among abundant PCNA-ir cells, and colocalisation is observed only in the peripheral retina (arrows in G). **H-I.** Vertical sections along the dorsoventral axis of the retina of a stage 32 of *H. fuscus*. (H) Detail of the peripheral retina where moderate numbers of Pax6-ir cells are observed in the outer retina. **I.** Section to show decreased numbers of Pax6-ir cells in prospective INLo and ONL of the central with respect to that found in the peripheral retina. **J-L.** Vertical sections along the dorsoventral axis of the retina of a prehatching embryo of *S. canicula*. **J.** Detail of the peripheral retina to show colocalising PCNA/Pax6-ir cells in the CMZ (small arrows). Colocalisation is rarely found in the *transition zone* (arrow), where patterns of PCNA and Pax6 immunoreactivities are reminiscent of those found in the central retina at the beginning of the *second developmental period*. **K, L.** Details of the central retina to show some PCNA-ir cells in the INLo (arrowheads in K, L), INLi (arrows in K) and GCL (arrow in L). For abbreviations, see list in Appendix B.

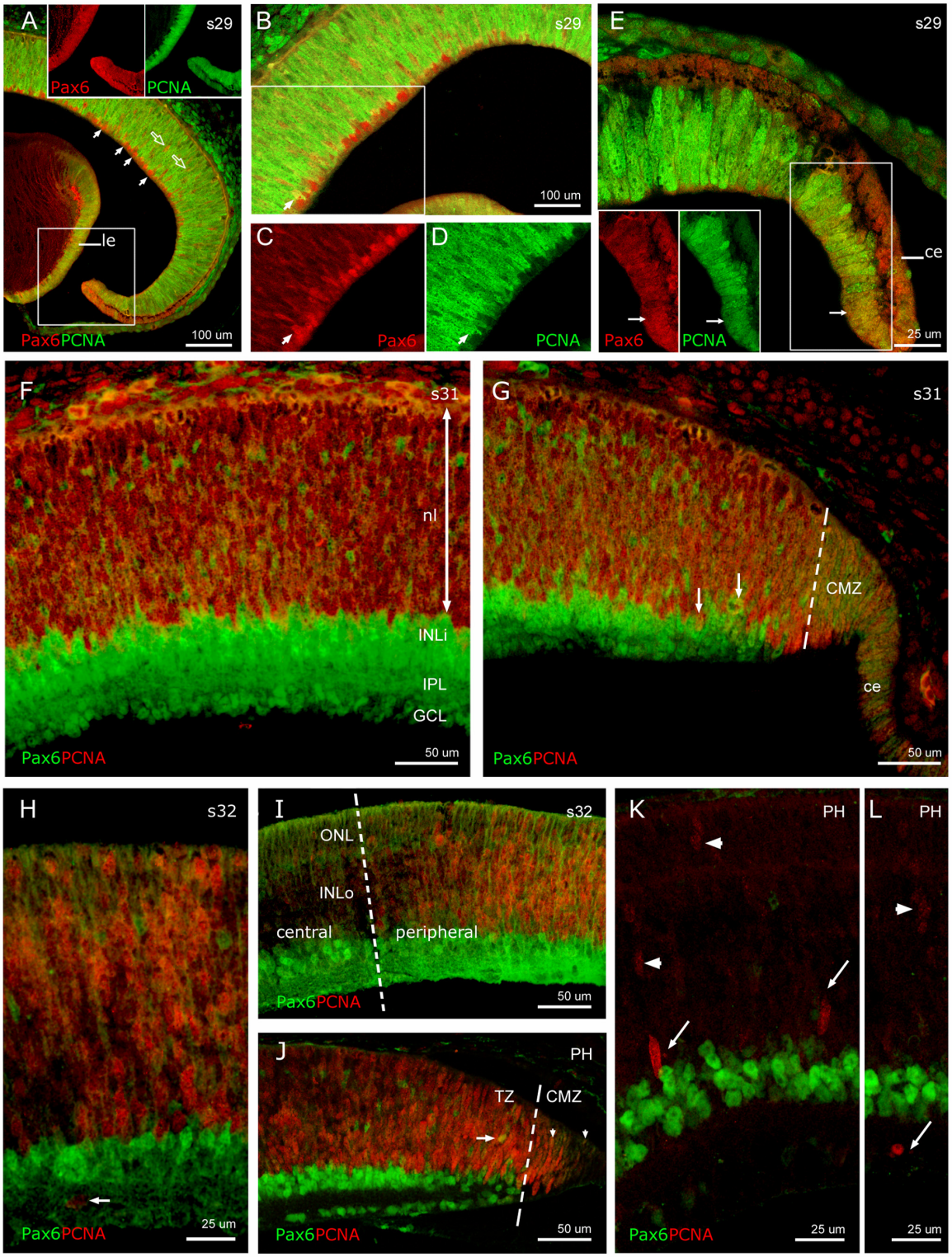
A
s29
Pax6
PCNA
le
Pax6PCNA
100 um
B
s29
100 um
C
Pax6
D
PCNA
E
s29
ce
Pax6
PCNA
25 um
F
s31
nl
INLi
IPL
GCL
Pax6PCNA
50 um
G
s31
CMZ
ce
Pax6PCNA
50 um
H
s32
Pax6PCNA
25 um
I
s32
ONL
INLo
central
peripheral
Pax6PCNA
50 um
J
PH
TZ
CMZ
Pax6PCNA
50 um
K
PH
Pax6PCNA
25 um
L
PH
25 um

Chapter 7.

Early development of GABAergic cells of the retina in sharks. Comparison with patterns of Pax6 expression and proliferation

INTRODUCTION

Gamma-aminobutyric acid (GABA) is the main inhibitory neurotransmitter that participates in the encoding of sensory information in the vertebrate retina. It is thought that GABA plays a neurotransmitter role in interneurons involved in lateral pathways (amacrine cells, horizontal cells and interplexiform cells; for a review see Kalloniatis and Tomisich, 1999), although recently it has been proposed that in horizontal cells GABA also acts as a neuromodulator (Kreitzer et al., 2003, 2007). GABA and its synthesizing enzyme glutamic acid decarboxylase (GAD) have been localised in amacrine cells in all vertebrates, but their presence in horizontal, interplexiform and ganglion cells is dependent on the species, the GAD isoform or the developmental stage. Knowledge of the GABAergic cells of the retina of elasmobranchs is based on results of GABA and GAD immunohistochemical studies (Brandon 1985; Brunken et al., 1986; Agardh et al., 1987), which have revealed the presence of GABAergic amacrine cells and, in some species, GABAergic horizontal and/or interplexiform cells. GABAergic horizontal cells have been reported in species of *Raja* (Agardh et al., 1987), whereas GABAergic interplexiform cells sending distal processes were reported in *Raja erinacea* and *Mustelus* (Brunken et al., 1986). In contrast with other vertebrates, no GABAergic cells were reported in the ganglion cell layer (GCL) of elasmobranchs. Two GABA transporters have been cloned in a skate and were shown to be located in horizontal and Müller cells (Malchow and Andersen, 2001; Birnbaum et al., 2005). The presence of GABA receptors and their responses to GABA have also been studied in some retinal cells of a skate (Malchow et al., 1989; Malchow and Ripps, 1990; Qian et al., 1996, 1997, 2001).

Other roles besides neurotransmission have been attributed to GABA in the retina, because it is one of the neuroactive substances that appears earlier during retinogenesis, prior to synaptogenesis. It has been proposed that GABA acts in the developing retina as a neurotrophic or signalling factor, promoting synaptogenesis, growth and differentiation of neurons (Versaux-Botteri et al., 1994; Sandell et al., 1994; Buznikov et al., 1996; Wang et al., 2007). However, the onset of the expression of GABA in retinal cells differs among vertebrates (Hokoç et al., 1990; Versaux-Botteri et al., 1994; Sandell et al., 1994; Negishi and Wagner, 1995; Hagedorn et al., 1998; Yamasaki et al., 1999; Nguyen and Grzywacz, 2000). Moreover, GABA has been implicated in the development and maturation of the outer retina because of its transient expression in horizontal cells (Schnitzer and Rusoff, 1984; Redburn and Madtes, 1987; Versaux-Botteri et al., 1989; Messersmith and Redburn , 1992, 1993; Pow

et al., 1994; Fletcher and Kalloniatis, 1997; Yamasaki et al., 1999; Dkhissi et al., 2001; Loeliger and Rees, 2005).

Studies on the development of retinal GABAergic cells have been carried out in some tetrapods (Yamasaki et al., 1999; Nguyen and Grzywacz, 2000; Dkhissi et al., 2001; Calaza et al., 2003; Loeliger and Rees, 2005), a few teleosts (Sandell et al., 1994; Negishi and Wagner, 1995; Hagedorn et al., 1998) and the sea lamprey (Anadón et al., 1998; Meléndez-Ferro et al., 2002; Villar-Cerviño et al., 2006). These studies revealed marked differences between agnathans and teleosts in the development of this neuronal system. Accordingly, the developmental pattern of the GABAergic cells in retinas of teleosts might not be representative of the early basic plan in jawed vertebrates. Cartilaginous fishes (Chondrichthyes) are the sister group of jawed vertebrates with a bony skeleton (Teleostomi) - which include land vertebrates - and thus are especially appropriate for out-group cladistic analysis. Moreover, the elasmobranch retina appears especially suitable for developmental studies because of its large size and slow development, which would facilitate detailed analysis (see Chapter 5). However, nothing is known about the neurochemical development of the elasmobranch retina, and the scarce data on its morphogenesis are derived from light microscopic studies with conventional staining methods (Yew, 1982) or from ultrastructural studies (Fishelson and Baranes, 1999). On the other hand, the pattern of expression of some developmental genes in the eye has been reported in very early stages of *Scyliorhinus canicula* (Sauka-Spengler et al., 2001; Plouhinec et al., 2005).

The main aim of the present study was to analyse how the GABAergic cells develop in the retina of elasmobranchs, using immunohistochemistry with antibodies raised against two GABAergic markers, GABA and GAD. We studied the spatiotemporal pattern of retinal structures in embryos, juveniles and adults of the lesser spotted dogfish (*S. canicula;* Scyliorhinidae), a species that has been largely used as model for neuroanatomical studies. For comparative purpose, we have also analyzed in parallel another member of the family Scyliorhinidae, the brown shyshark (*Haploblepharus fuscus).* This study revealed for the first time that the development of GABAergic neurons in the retina in these elasmobranchs is remarkably unlike that of teleosts as regards their very early appearance, before any layering was settled in the retinal neuroepithelium. Moreover, the presence of GABAergic cells in the GCL and of GABAergic fibres in the optic fibre layer and optic nerve, as well as

the transient expression of GABAergic markers in the horizontal cell layer (HCL), are firstly reported in elasmobranchs.

As first GABAergic cells were observed in early (non-differentiated) retina, a further aim of this work was to compare the spatiotemporal distribution of retina GABA-synthesizing cells with that of cells expressing Pax6, a key eye-patterning transcription factor that functions during retinogenesis to maintain pluripotency and proliferation of retinal progenitors to generate all retinal cell types (see Chapter 5). We further compared the expression of GAD and Pax6 with that of reliable markers of cell proliferation, such as the proliferating cell nuclear antigen (PCNA; see Chapter 6).

MATERIAL AND METHODS

Experimental animals

Embryos and juvenile specimens of *S. canicula* and *H. fuscus* were kindly provided by the "Aquário Vasco da Gama" and "Oceanário" in Lisbon (Portugal) and the Aquarium Finisterrae in A Coruña (Spain). The embryonic stages of *S. canicula* were identified by external features following Ballard et al. (1993) and similar features were considered in staging the *H. fuscus* embryos (See table 1 in Chapter 5). The following embryonic stages were analysed: stage 24 (with diamond-shaped mouth and four pair of pharyngeal clefts open; 2 *S. canicula* embryos), stage 25 (1 *S. canicula* embryo), stage 26 (3 *S. canicula* embryos), stage 27 (2 *S. canicula* embryos), stage 28 (2 *S. canicula* embryos), stage 29 (3 *S. canicula* and 2 *H. fuscus* embryos), stage 30 (3 *S. canicula* embryos), stage 31 (4 *S. canicula* and 2 *H. fuscus* embryos), stage 32 (3 *S. canicula* and 2 *H. fuscus* embryos) and stages 33-34 (prehatching; 6 *S. canicula* and 1 *H. fuscus* embryos). Moreover, 4 juveniles (2 *S. canicula* and 2 *H. fuscus*, total length about 12 cm) and 4 adult *S. canicula* (about 50 cm total length) were also used.

Tissue preparation

Embryos were anaesthetized with 0.05% tricaine methane sulphonate (MS-222; Sigma, St. Louis, MO) in seawater and separated from the yolk before fixation. Prehatching, juvenile and adult specimens were deeply anaesthetized with MS-222 and then perfused intracardially with elasmobranch Ringer's solution (1.7% NaCl, 0.024% KCl, 0.031% CaCl2, 0.044% MgCl2,

0.113% Na2SO4, 0.049% NaCO3H, and 2.7% urea) followed by the appropriate fixative. The eyes were dissected out and immersed in the same fixative for 4 h. Adequate measures were taken to minimize pain or discomfort. All procedures conformed to the guidelines established by the Spanish Royal Decree 223/1998 for animal experimentation and were approved by the ethics committee of the University of Santiago de Compostela.

For GAD immunohistochemistry, embryos (*S. canicula*: stages 24 to 34, one to three specimens of each stage; *H. fuscus*: stages 29, 31, 32, 33-34, one or two specimens of each stage), juveniles (1 *S. canicula* and 2 *H. fuscus*) and adults (2 *S. canicula*) were fixed in 4% paraformaldehyde in elasmobranch phosphate buffer (EPB: 0.1M phosphate buffer containing 670mM urea, pH 7.4). For GABA immunohistochemistry, specimens were fixed by immersion (embryos) or perfusion (prehatching embryos, juveniles and adults) in 5% glutaraldehyde in EPB with 1% sodium metabisulphite added, and postfixed in the same fixative.

Heads of embryos and eyes of juveniles and adults were postfixed for 4 h, cryoprotected with 30% sucrose in PB, embedded in OTC compound (Tissue Tek, Torrance, CA), and frozen with liquid nitrogen-cooled isopentane. Parallel series of sections (14-18 μm thick) were cut in sagittal or transverse planes on a cryostat, and mounted on Superfrost Plus (Menzel-Glasser®) slides.

Antibody characterisation

The sheep polyclonal antiserum to GAD65/67 (GAD 1440) was a gift from Dr. Mugnaini, and initially produced in the National Institutes of Health, Bethesda, MD from a source developed by Drs. Irwin J. Kopin, Wolfgand Oertel, Donald E. Schmechel, and Marcel Tappaz (Oertel et al., 1981), with methodological contributions from the laboratory of Enrico Mugnaini (University of Connecticut, Storrs). Details about the origin and specificity of the GAD 1440 antibody have been previously published (MacLeod et al., 2006). Additional controls for specificity of this antiserum in *S. canicula* and rat brain protein extracts were previously performed by Western blot (Sueiro et al., 2004); similar 65 and 67 kDa bands were observed in *S. canicula* and rat lanes, indicating that the antibody recognized both isoforms of GAD in *S. canicula*. The same antiserum has been used in invertebrates and different vertebrate groups, including fishes (Mugnaini et al., 1984; Carr et al., 1989; Kaufman et al., 1991; Martin et al., 1998; Maler and Mugnaini, 1994; Spiro et al., 1999; Siegler et al., 2001; MacLeod et al.,

2006). For characterisation of antibodies against Pax6 and PCNA see Chapters 5 and 6, respectively.

GAD immunohistochemistry

Sections were pretreated with H_2O_2 to eliminate endogenous peroxidase, rinsed twice in 0.05M Trizma-buffered saline containing 0.1% Tween-20 at pH 7.4 (TBS-T) (10-min each) before being processed by the ABC method with a sheep anti-$GAD_{65/67}$ polyclonal antiserum (1440-4) as primary antibody (kindly provided by Dr. E. Mugnaini; dilution 1:50,000) raised against GAD partially purified from rat brain synaptosomes (Oertel et al., 1981). The sections were then rinsed in TBS-T (two 10-min rinses), incubated in biotinylated rabbit anti-sheep antiserum (Dako; 1:200) for 1 hour, rinsed in TBS-T, and incubated in StreptABComplex/HRP (Dako) for 30 min. The endogenous biotin was blocked before incubation with a biotin blocking system (Dako). The immunoreaction was developed with 0.005% diaminobenzidine (DAB; Sigma) and 0.003% H_2O_2. All dilutions were made with TBS-T containing 15% rabbit preimmune serum (Chemicon), and all incubations were carried out in a humid chamber at room temperature (RT). Finally, the sections were dehydrated, mounted and coverslipped. Parallel sections were stained with haematoxylin-eosin to facilitate identification of retinal cells and layering. As negative controls, the primary, secondary or tertiary antibodies were omitted. No immunostaining was observed in these control sections. Details about the specificity of this antibody have been previously published (MacLeod et al., 2006). Additional controls for specificity of this antiserum in *S. canicula* and rat brain protein extracts were previously performed by Western blot (Sueiro et al., 2004); similar 65 and 67 kDa bands were observed in *S. canicula* and rat lanes, indicating that the antibody recognized both isoforms of GAD in *S. canicula*.

GABA immunohistochemistry

GABA immunohistochemistry was performed on sections of *S. canicula* retinas: embryos (stages 26, 28, 29, 30, 31, 32, 1 specimen of each), juvenile (1 specimen) and adults (2 specimens). The endogenous peroxidase was eliminated as above and sections were then processed by the PAP method, with a rabbit anti-GABA polyclonal antiserum raised by immunizing albino rabbits with a GABA-glutaraldehyde-bovine serum albumin complex

(Affiniti, Mamhead, UK; diluted 1:1000) as the primary antibody. Goat anti-rabbit IgG (Dako; 1:100) and rabbit PAP complex (Sigma, 1:500) were used as secondary and tertiary antibodies respectively. All dilutions were made with TBS-T containing 15% goat serum and 1% sodium metabisulphite. The immunoreaction was developed as above and the sections dehydrated and coverslipped accordingly. Negative controls were performed as above. No immunostaining was observed in control sections. The specificity of the anti-GABA antiserum has been characterised by ELISA by the supplier against conjugates with BSA-glutaraldehyde. The distribution of labelling with this polyclonal rabbit anti-GABA antibody in the *S. canicula* retina was similar to that observed for GAD immunoreactivity, and resembled that described in other vertebrates (see below). Moreover, the same antibody was previously used for demonstrating the GABAergic neurons in *S. canicula* central nervous system (Sueiro et al., 2004, 2007), as well as in retinas of lampreys (Meléndez-Ferro et al., 2002) and teleosts (Candal et al., 2008).

Double and triple immunofluorescence

For heat induced epitope retrieval, sections of early embryos (stages 29 and 31), prehatching embryos (stages 33 and 34) and juveniles were pretreated with 0.01M citrate buffer pH 6.0 for 30 min at 95°C, and allowed to cool for 30 min at RT. Sections were rinsed twice in 0.05 M Tris-buffered saline containing 0.1% Tween-20 at pH 7.4 (TBS-T) for 5 min each, and then incubated with combinations of the following primary antibodies, overnight at RT: anti-$GAD_{65/67}$ sheep polyclonal antiserum (provided by Dr. E. Mugnaini; dilution 1:30,000), anti-Pax6 polyclonal rabbit antiserum (Covance, diluted 1:200), anti-PCNA mouse monoclonal antiserum, (Sigma, diluted 1:200). The sections were then rinsed in TBS-T (two 10-min rinses). Secondary antibodies were used as follows: Alexa Fluor 488 Donkey-anti-Sheep IgG antibodies (Molecular Probes, The Netherlands; diluted 1:200), TRITC-conjugated Swine-anti-Rabbit immunoglobulins (Dako, Denmark; diluted: 1:20), and FluoProbes 642 Donkey-anti-Mouse (Interchim, France; diluted 1:100). All dilutions were made with Tris-buffered saline (TBS) containing 0.2% of Triton X-100 (Sigma) and 15% of donkey and swine normal serum. All incubations were carried out in a humid chamber. Sections were rinsed in TBS for 30 min, then in distilled water (twice for 30 min), and allowed to dry for 2 h at 37°C. Sections were mounted in MOWIOL 4-88 Reagent (Calbiochem, Merk KGaA, Darmstadt, Germany), allowed

to dry for 30-60 min at 37°C, and observed in a Leica Spectral Confocal Laser Scanning Microscope (TCS-SP2).

RESULTS

Three developmental periods can be distinguished in the retina as regards its growth pattern (see Chapter 5). The *first developmental period* (stages 26 to 29) is characterised by the absence of layering; the *second developmental period* (stages 30 to 32) is recognizable by the progressive layering of the central part of the retina, by the organization of a neuroepithelial zone adjacent to the ciliary epithelium (called ciliary marginal zone; CMZ), and by the presence of a *transition zone* between the not layered CMZ and the layered central retina; in the *third developmental period* (stages 33 to 34), the retina reaches the mature organization characteristic of postembryonic stages. Of note, this mature organization can be already observed in the most central retina from stage 32 onwards.

No differences were observed in the distribution of GAD immunoreactivity through the developing and mature retina of either species. Moreover, both GAD and GABA antibodies revealed the same pattern of immunoreactive (ir) cells in the embryonic retina of *S. canicula* (*H. fuscus* was not processed for GABA). In the following, we will describe the retina of both sharks together and to use the term GABAergic to refer to GAD- and GABA-ir structures.

The first GABAergic retinal cells were observed at stage 26. In these embryos the retina showed a neuroepithelial appearance, without any layering. A few weakly GABAergic spindle-shaped cells were observed in central areas (Fig. 1A). Similar neuroepithelial organization was observed at later stages (stages 27-28), but the number and staining intensity of spindle-shaped GABAergic neuroblastic cells increased notably from vitreal to scleral (Fig. 1B) and from the centre to the periphery. These GABAergic neuroblastic cells were located in the neural retina mainly near its vitreal or scleral surfaces, although somata were also observed in intermediate positions (Fig. 1B). Radial processes of these GABAergic cells coursed toward the inner and outer limiting membranes (Fig. 1C). At early stage 29, GABAergic cells were observed in almost the retina, excepting its marginal regions, and most GABAergic somata were located in the inner third of the neuroepithelium at central levels (Figs. 1D-F). At these levels, some GABAergic perikarya were triangular and showed radial and lateral processes

(arrow in Fig. 1F). At late stage 29, the spatial segregation of GABAergic cells into inner and outer regions was clearly observed (Fig. 1G). A loose band of GABAergic cells of multipolar or irregular appearance was distributed throughout the outer half of the neural retina, without forming any conspicuous row of somata (Fig. 1G). These cells extended processes in various directions, some reaching the primordial outer limiting membrane. Most GABAergic cells of the inner retina formed a thick band of rather densely grouped cells, with their somata at different levels and with some processes coursing among them (Figs. 1G, H). A few GABAergic cells also appeared between the two GABAergic cell bands (Fig. 1G). At early stage 29, the optic stalk was formed by a neuroepithelial tube surrounding a central cavity (Fig. 1I), but at late stage 29 this cavity became obliterated by accumulation of large cells and fibre fascicles, forming the optic nerve primordium (Figs. 1J-L). At this stage, GABAergic fibres were seen in small bundles mostly coursing in the periphery of the optic nerve all along its course, at its proximal (Fig. 1J), intermediate (Fig. 1K), and even distalmost part, at the level of the optic chiasm (Fig. 1L).

At stage 30, the organization of GABAergic structures in the peripheral retina (the marginal zone adjacent to the ciliary retina) resembled that observed in the central retina of earlier stages. Similar organization was observed in the retina bordering the optic nerve head (Figs. 2A, B). In the central retina, most GABAergic cells were located in the inner nuclear layer (INL). These cells were identified as amacrine cells because of their tall pyriform perikarya that gave rise to an inner process that ramified in the now conspicuous inner plexiform layer (IPL) (Fig. 2C). A few GABAergic cells were observed internally to the IPL, forming part of the prospective GCL (Fig. 2C). GABAergic fibres were seen in the optic fibre layer and the optic nerve head (Fig. 2A). In the outer two-thirds of the retina, a layered organization was hardly recognizable, but GABAergic cells of multipolar appearance were arranged in a loose band (primordial HCL) between the outer part of the INL (INLo) and the prospective outer nuclear layer (ONL). At stage 31, GABAergic horizontal cells formed a conspicuous but loose thin layer, whereas the band of GABAergic amacrine cells in the INL was thicker (Figs. 2D, E). Occasional varicose GABAergic fibres were seen coursing radially and horizontally through the INL externally to the somata of amacrine cells (Figs. 2D, F). Some large GABAergic cells were seen in the GCL (Fig. 2E) while abundant beaded GABAergic fibres coursed in the optic fibre layer (Figs. 2D-G), optic nerve head (Fig. 2H) and optic nerve (Figs. 2H, I). At this stage, some weakly GABAergic spindle-shaped cells were observed in the

boundary between the neural and the ciliary retina (Fig. 2J), which also showed isolated GABAergic fibres that coursed radially or obliquely in the marginal neuroepithelium (Fig. 2K).

At stage 32, the retinal layering was completed at central regions with the appearance of photoreceptor segments in the retinal cleft. From this stage to hatching (stage 34), retinal layering progresses from centre to periphery, and the organization of GABAergic structures along this axis recapitulates the events observed in the central retina at earlier stages (Fig. 3A). GABA/GAD immunoreactivity was found in subpopulations of cells in the HCL, INL and GCL, and in numerous processes of the IPL and in fibres coursing in the optic fibre layer and optic nerve (Figs. 3B-I). Processes of the GABAergic cells of the INL coursed to a well-developed IPL that showed a layered appearance because GABAergic innervation was denser in the sublayers 1, 3 and 5 than in the sublayers 2 and 4 (Figs. 3B, D). Some thin beaded GABAergic fibres were observed coursing radially in the INL (Fig. 3E). GABAergic horizontal cells became flattened and formed a conspicuous but faintly immunoreactive cell layer, and their processes extended horizontally forming a network (Figs. 3B, E, F). GABA/GAD immunoreactivity was moderate in some cells in the GCL (Figs. 3B, C). Beaded fibres that coursed in the optic nerve head showed occasional thick swellings (Fig. 3G). GABAergic cells of neuroblastic appearance were observed in the retina region neighbour to the optic nerve head (Fig. 3H), and in the peripheral retina, where some thin beaded GABAergic fibres also coursed radially just between the neural and the ciliary retina (Fig. 3I).

In juveniles and adults, the thickness of the INL has decreased considerably with respect to prehatching embryos. The layered organization of GABAergic structures in the retina extended very peripherally, with GABAergic processes of the IPL just reaching the limit with the ciliary retina (Fig. 4A). GABA and GAD immunoreactivity was moderate in GABAergic cells of the HCL in the peripheral retina but very weak in those of more central regions (Figs. 4A-D). Some GABAergic fibres were observed coursing radially in the INLo (Figs. 4B, D, E). Most GABAergic cells were observed in the INL, but some GABAergic cells were also noticed in the GCL (Figs. 4C-E). Abundant GABAergic fibres coursed in the optic fibre layer and optic nerve head (Figs. 4B-F).

Pax6 co-localised with GAD in non-proliferating retina cells

During the early stage 29, the distribution of GAD-ir cells was similar to that of intense Pax6-ir cells (Figs. 5A, B). GAD-ir cells were found scattered throughout the neuroepithelial retina (squared area in Fig. 5B), excepting peripheral regions (Fig. 5A) and close to the optic fissure (asterisk in Fig. 5B). Double immunofluorescence revealed that some GAD-ir cells also showed Pax6 immunoreactivity (arrows in Fig. 5B'). At the end of the *first developmental period,* no layering was further appreciable in the centralmost retina but differences started to be noted between its inner part, where most of Pax6- and GAD-ir somata were located, and the outer part, that resembled to the retina of previous stages, with Pax6- and/or GAD-ir neuroepithelial cells among the abundant proliferating neuroepithelial cells showing PCNA immunoreactivity (Fig. 5C). Triple immunofluorescence showed that GAD and Pax6 colocalised in some cells (white arrows in Fig. 5C'), while others contained both Pax6 and PCNA (open arrows in Fig. 5C'). However, double labelled cells for GAD and PCNA were not observed. Accordingly, triple colocalisation was neither observed throughout the early developing shark retina.

During the s*econd developmental period,* the distribution of Pax6-ir cells parallels that of GAD in the INL and HCL: abundant Pax6-ir were mostly occupying the GCL and inner part of the INL (INLi) while their number decreased in the outer retina (Fig. 5D). Double labelling GAD/Pax6 revealed that some Pax6-ir cells in the INLi and most of the horizontal cells (arrows in Fig. 5D) were labelled with both immunomarkers, although immunoreactivities were located in different cell regions: GAD immunoreactivity was distributed in the cytoplasm and processes while Pax6 immunoreactivity was located in nuclei (nucleoli were Pax6 immunonegative). Cells showing single immunoreactivity to one or another marker were also observed.

Comparable results were found in prehatching embryos *(third developmental period*) and juveniles (Figs. 5E-I). In the central retina, some cells were either GAD-ir or Pax6-ir, while others were labelled for both markers (Figs. 5F, H). In the peripheral retina (Fig. 5I), triple immunolabelling allowed to better show the *transition zone* formed by the inner (layered) part that contained GAD-positive, Pax6-positive, and PCNA negative cells in the primordial GCL and INLi, and the outer (unlayered) part that contained some intensely labelled Pax6 cells among abundant PCNA-positive cells. The distribution of these markers in the region adjacent

to the *transition zone* was similar to that found in the central layered retina at the end of the *second developmental period*, as GAD-ir and Pax6-ir cells were additionally arranged in the HCL.

DISCUSSION

Comparison of GABA and GAD expressions in the shark retina

In birds and mammals, the delayed onset of GAD expression with respect to that of GABA has led to the suggestion that in early developmental stages GABAergic retinal cells may synthesize GABA through a biochemical pathway that involves putrescine as a GABA precursor instead glutamate (Hokoç et al., 1990; Yamasaki et al., 1999). In the present work we showed that the earliest GAD signal was detected at the same stage that displayed GABA-ir cells (stage 26 embryos), thus suggesting that synthesis by GAD is the source for GABA contained in cells of the developing shark retina, although uptake of GABA synthesized and/or released by other nerve cells via GABA transporters and/or gap junctional contacts could also be possible.

As both antisera against GAD used in this study recognized the two GAD isoforms in the *S. canicula* brain (Sueiro et al., 2004), we consider plausible that in the two shark species it is labelling retinal cells containing both isoforms. GAD67 could be less abundant than GAD65 as it has been suggested for the *S. canicula* brain (Sueiro et al., 2004) but whether a dynamic expression of both isoforms occurs during shark retina development as it has been evidenced in rat (Dkhissi et al., 2001) could not be determined in the present study.

GABA and GAD location in developing and mature retina

GABA and GAD immunoreactivities were absent from retina of embryos prior to the stage 26, which contrasts with the abundance of GABA-ir and GAD-ir cells in the brain at earlier stages (Carrera et al., 2006). Strikingly, the onset of GABA and GAD expression in the retina occurred when it was just a neuroepithelium without any apparent layering. In embryos from stages 26 to 29, the retina is a single neuroblastic layer containing some GABA/GAD-ir neuroblastic cells. In embryos from stage 30 to 32, GABA/GAD-ir cells become organized in bands that will eventually form part of the HCL, INL and GCL, whereas GABAergic cells with

neuroblastic appearance diminish in number. From stage 32 onwards, the mature organization of the GABAergic cells can be distinguished in the central retina, where GABA/GAD-ir cells form subpopulations in the HCL, INL and GCL. As development proceeds, the retina layering progresses following a centre-to-periphery direction and the organization of GABAergic structures along this axis recapitulates what occurred in the central retina at earlier stages.

Stages 26-29: GABA/GAD in the neuroblastic retina

The first GABA and GAD-ir cells in the retina of both shark species were neuroblastic cells scattered among the neuroepithelial cells of stage 26 embryos. Neuroblastic GABAergic retinal cells have not been reported in other fish groups, but they were observed in the developing turtle and chick retinas before subdivision into nuclear or plexiform layers becomes apparent (Hokoç et al., 1990; Versaux-Botteri et al., 1994; Nguyen and Grzywacz, 2000). GABA is among the first neurotransmitters produced by the vertebrate retina (Messersmith and Redburn, 1993; Mitchell and Redburn, 1996), probably acting as a neurotrophic or signalling factor, promoting differentiation of neurons (Versaux-Botteri et al., 1994; Sandell et al., 1994; Buznikov et al., 1996). Moreover, in amphibians it has been demonstrated that some neuroblasts present in the neural plate and the neural fold acquire the ability to express the GABA phenotype during the early events of neurogenesis (Pituello et al., 1989). The early development of GABAergic neurons observed in the present study indicates that GABA may play a relevant role in shark retina development. In contrast with present observations in sharks, in teleosts the first appearance of GABAergic cells coincides with the onset of retinal layering (Sandell et al., 1994; Neguishi and Wagner, 1995; Hagedorn et al., 1998; Candal et al., 2008) and in lampreys with the completion of metamorphosis, which occurs several years after hatching when the image-forming circuitry matures (Villar-Cerviño et al., 2006), despite a layered organization can be observed in the central retina of larvae (Anadón at al., 1998).

At the end of this period, the spatial organization of GABA/GAD expressing cells in the shark retina reveals the dynamic sequence of events that lead to the transformation of GABAergic neuroblastic cells in morphologically recognizable horizontal and amacrine cells, and GABAergic cells of the GCL: some neuroblastic GABA/GAD-ir cells of the inner third of the retina appeared to have detached their apical process and showed lateral processes,

which can be interpreted as a very early sign of cell segregation. Then, the somata of GABA/GAD-ir cells appeared mainly located at two levels forming outer and inner rows, the incipient HCL and INL/GCL GABAergic cells, respectively. The labelled cells observed between these two rows perhaps represent migrating neuroblasts. Concurrently with cell maturation, the first GABA/GAD-ir fibres appeared in the optic stalk, which transforms during stage 29 (by changes in cell shape and size and growth of fibre fascicle), in the optic nerve.

Stages 30-32: GABA/GAD in cells of the layering retina

During this period, the outer row contains presumptive GABA/GAD-ir horizontal cells undergoing first steps of differentiation, and the inner row shows the first signs of subdivision by the presence of some GABA/GAD-ir processes (the incipient IPL) separating the GABAergic cells of the primordial INL and the GCL. Thus, the beginning of GABA synthesis in shark retinal cells precedes the beginning of retinal layering/cytodifferentiation in the central regions, in contrasts with the progression observed in other vertebrates. In teleosts, GABA appeared in horizontal cells after retinal layering (Sandell et al. 1994; Candal et al., 2008), coinciding in time and position with the onset of photoreceptor (rod) differentiation (Hagedorn et al., 1998; Candal et al., 2008). In rat, early GABA and GAD67 labelling in horizontal cells was detected after GABA labelling was observed in primordial amacrine cells (Yamasaki et al., 1999; Dkhissi et al., 2001). Also in guinea pig, GABA labelling in horizontal cells follows that of amacrine and ganglion cells for several days (Loeliger and Rees, 2005). Our results suggest a developmental role for GABA during differentiation of photoreceptors, prior to the establishment of any synaptic connections between photoreceptors and horizontal cells, where it could act as neurotransmitter. GABA may act as a signal for early events in the differentiation of the outer retina, perhaps promoting the events that stimulate the initiation and maintenance of photoreceptor differentiation.

Stage 32 onwards: GABA/GAD in cells of the "mature" retina

The location of GABA and GAD immunoreactivities in the INL and IPL of the mature retina (central retina of stage 32 embryos and the entire retina from stage 33 onwards) coincides with that previously reported in other elasmobranch species (Brandon, 1985; Brunken et al., 1986; Agardh, 1987). However, GABAergic horizontal cells appeared to be

present only in some *Raja* species (Brunken et al., 1986; Agardh et al., 1987), although we have shown them in the shark retina from early stages of differentiation to maturity. We also showed that the intensity of labelling in the HCL markedly decreased from late embryos to adults, especially in the central retina, contrary to that reported in teleosts, where GABA labelling in horizontal cells was faint in the developing retina and intense in the mature retina (Brandon 1985; Osborne et al. 1986; Sandell et al., 1994; Hagedorn et al., 1998; Studholme and Yazulla, 1997; Connaughton et al., 1999; Marc and Cameron, 2001; Mack et al., 2003; Candal et al., 2008). It has been suggested in teleosts that the GABA microenvironment at the level of horizontal cells may provide a stop signal to migration and stimulate differentiation of the new rods that are continuously added in the central retina (Mack et al., 2003). In amniotes, the number of GABA-containing horizontal cells or the levels of GABA and/or GAD_{67} were higher in embryonic than in mature retinas (Versaux-Botteri et al., 1989; Lake, 1994; Pow et al., 1994; Fletcher and Kalloniatis, 1997; Yamasaki et al., 1999; Dkhissi et al., 2001; Calaza et al., 2003), as seen in sharks. In mammals, it has been suggested that the transient synthesis of GABA in horizontal cells may be involved in development and maturation of the outer retina, in promoting outgrowth of neurites or in maintaining the normal pattern of cone location and synaptogenesis (Messersmith and Redburn, 1993; Dkhissi et al., 2001; Loeliger and Rees, 2005). The present study only characterizes as GABAergic one of the different types of horizontal cells described in elasmobranchs (Stell and Witkowsky, 1973; Toyoda et al., 1978; Malchow et al., 1990), which could correspond to the cells type H1 of *Mustelus* (Stell and Witkowsky, 1973) and *Dasyatis* (Toyoda et al., 1978), characterised by their cuboid shape and location in the external first row of horizontal cells. In elasmobranchs, the relation between H1 type and photoreceptors varies between species: in *Dasyatis,* H1 cells contact both with rods and cones (Toyoda et al., 1978) while in *Mustelus* they contact with rods (Stell and Witkowsky, 1973). Both *S. canicula* and *H. fuscus* appear to contain a low number of cones (personal observations) but if the GABAergic horizontal cells observed in these species contact with rods or cones could not be determined.

GABAergic cells have not been observed in the GCL of adult lampreys (Villar-Cerviño et al., 2006), but they have been described in gnathostomes (Brandon, 1985; Yazulla et al., 1986; Osborne et al., 1986; Agardh et al., 1987; Yang and Yazulla, 1988; Caruso et al., 1989; Hurd and Eldred, 1989; Grünert and Wässle, 1990; Sandell et al., 1994; Bennis et al., 2003; Loeliger and Rees, 005), including elasmobranchs (present results). This suggests that these cells may

have appeared in the common ancestors of Teleostomi and Chondrichthyes. However, whether or not these GCL GABAergic cells are ganglion cells and/or displaced amacrine cells (*axon-less cells with cell bodies in the GCL*) is controversial. In some species, GCL GABAergic cells have been identified as ganglion cells on the basis of the presence of GABA- and GAD67-ir axons in the optic fibre layer and optic nerve (Yu et al., 1988; Caruso et al., 1989; Sandell et al., 1994; Pow et al., 1994; Versaux-Botteri et al., 1994; Nguyen and Grzywacz, 2000; Dkhissi et al., 2001). Moreover, in a few species the ganglionic nature of these GABAergic cells has been demonstrated by combining tract-tracing and immunohistochemistry (Lugo-García and Blanco, 1991; Gábriel et al., 1992). Some authors explain the presence of GABA in ganglion cells by heterologous gap junction coupling between ganglion cells and conventional GABAergic amacrine cells (Marc and Jones, 2002). Other authors considered them as displaced amacrine cells because of their labelling with antibodies against GAD67 but not against GAD65 isoform (Brandon and Criswell, 1995), their smaller cell bodies and intense GABA staining (Kalloniatis and Tomisich, 1999), or because the absence of GABA immunoreactivity in the optic nerve (Osborne et al., 1986; Connaughton et al., 1999; Marc and Cameron 2001; Marc and Liu, 2000). More puzzling are results in teleosts. In adult zebrafish, GABA immunoreactivity was observed in cells of the GCL (considered as displaced amacrine cells) but not in fibres of the optic nerve (Connaughton et al., 1999; Marc and Liu, 2000; Marc and Cameron, 2001), whereas GAD67 immunoreactivity was shown in fibres of the optic nerve head but not in cells in the GCL (Yazulla and Studholme, 2001). Our results in sharks reveal GABA/GAD-ir cells in the primordial GCL from the onset of retinal layering, as well as numerous GABAergic axons in the optic fibre layer and optic nerve, which were traced to the optic chiasm. Although GABAergic cells of the shark GCL may correspond to displaced amacrine cells, the possibility that some of them were actually ganglion cells is strongly suggested by their size, larger than the amacrine cells of the INL, and by the presence of GABAergic axons in the optic fibre layer and optic nerve. Although the density of these cells decreases from juveniles to adults, as that of other cells of the inner retina, they are present in the GCL throughout development and in adults, which indicates that GABA synthesis in these GCL cells (and in optic nerve fibres) is not transient, unlike that reported in zebrafish (Sandell et al., 1994) and rabbit (Pow et al., 1994). The possibility that some cells labelled with the GABAergic markers in the shark retina were astrocytes, as reported in the developing optic nerve of rat with glial fibrillary acidic protein (GFAP) and GABA immunohistochemistry (Ochi et al., 1993), appears less probable because in the developing and mature retina of *S. canicula* and *H. fuscus* GFAP

immunohistochemistry specifically labelled Müller cells whose location and appearance was markedly different from that the GABAergic GCL cells or other GABAergic retinal cells (personal observations).

The presence of GABA-/GAD-ir beaded fibres and neuroblastic cells in the marginal retina from stage 31 embryos onwards is intriguing. These GABAergic cells may represent neuroblasts formed during late embryonic and postembryonic stages in the marginal proliferating area, which is present in the shark retina (personal observations), as in teleosts, amphibians and chick (for revision, see Kubota et al., 2002). The marginal GABAergic fibres, extending from the inner to the outer retina just at the boundary between the layered and the non-layered regions, may be playing signalling roles on cells of the marginal-proliferating areas and on GABA-expressing neuroblastic cells. As far as we know, similar GABAergic cell and fibres have not been reported in the marginal retina of vertebrates. However, axons of large unipolar glucagon-expressing neurons (bullwhip cells) projecting toward the circumferential marginal proliferating zone have been described in the avian retina (Fischer et al., 2005, 2007). This special retinal cell type appears to be involved in the regulation of the proliferation of progenitors of the marginal retina (Fischer et al., 2005, 2007). More studies will be necessary to know if there is any relationship of these cells with those giving rise to the marginal GABAergic fibres observed in the present work, but its presence in sharks is suggestive that GABA may be involved in the control of cell proliferation and/or differentiation in the marginal retina. Evidences for an anti-proliferative effect, probably regulating cell-cycle exit, cell-cycle length, and cell differentiation, have been reported for GABA in the developing retina (Martins and Pearson, 2007).

Possible retinofugal GABAergic projections in sharks

We observed GABAergic fibres in the optic stalk/optic nerve, optic nerve head and optic fibre layer of embryos and postembryonic specimens of both sharks studied. In the optic stalk, the earliest GABAergic fibres appeared at late stage 29, coinciding with the onset of segregation of GABAergic cells in the inner retina. Thus, the invasion of the optic stalk by GABAergic fibres appears to coincide with the differentiation of GCL cells and the formation of retinal ganglion axons. These GABAergic fibres perhaps are playing a role in the formation of the optic nerve. In fact, it has been shown that GABA may act *in vivo* to stimulate

outgrowth of *Xenopus* retinal ganglion cell axons along the optic tract (Ferguson and McFarlane, 2002). The observation of GABAergic fibres in the optic nerve and optic fibre layer of embryos and postembryonic specimens of sharks is compatible with the existence of a GABAergic retinofugal projection, although demonstration of this possibility needs further experiments. The existence of a GABAergic retinofugal projection has been demonstrated in tetrapods (Lugo-García and Blanco, 1991; Gábriel et al., 1992; Versaux-Botteri et al., 1994; Wilson et al., 1996) and, although transient, in a teleost (Sandell et al., 1994), but not in lampreys.

Alternatively, the GABAergic fibres observed in the optic nerve of sharks might correspond to retinopetal fibres. However, the existence of a GABAergic retinopetal projection has only been demonstrated in lampreys (Rio et al., 1993), where these fibres were the only GABAergic structures present in the retina of larval lampreys (Anadón et al., 1998; Meléndez-Ferro et al., 2002). Although retinopetal projections are present in a number of vertebrates (for revision see Repérant et al., 2006), only in lampreys some of these fibres are GABAergic, which might represent a fundamental difference between agnathans and gnathostomes. Whereas studies of the visual system of *S. canicula* have reported a number of retinofugal projections to target nuclei in the diencephalon and mesencephalon (Repérant et al., 1986), the existence of a retinopetal projection has not been reported yet with tract-tracing methods in elasmobranchs. The possibility that some GABA/GAD-ir fibres of the optic stalk/optic nerve of sharks actually represent centrifugal fibres cannot be ruled out without further experimental studies.

GABAergic cells coexpress Pax6 immunoreactivity in the retina of elasmobranchs

The continued expression of Pax6 in different layers of the differentiating retina suggests that, besides being involved in the maintenance of retinal stem cells, it could have additional roles in cell type specification (see Chapter 5). Indeed, it has been suggested that different combinations of transcription factors play important roles in determining the phenotypic (structural and functional) differences between different subtypes of cells (Fischer et al., 2007). We found here that some GABAergic cells coexpress Pax6 not only in neuroepithelial regions of the retina, but also in postmitotic (PCNA-negative) amacrine and horizontal cells as they differentiate in the layered retina. In the chick retina, Pax6

colocalised with GABA in subsets of differentiated amacrine cells (Fischer et al., 2006) and horizontal cells (Fischer et al., 2007). Indeed, all conventional glucagon-expressing amacrine cells in the chicken retina were Pax6-ir and strongly GABA-ir (Fischer et al., 2006), while Pax6 immunoreactivity was also found in some double labelled calretinin/GABA horizontal cells (Fischer et al., 2007). However, the involvement of Pax6 in the development of the GABAergic system of the retina remains undefined. Noteworthy, a number of Pax6-ir cells are immunonegative for GAD/GABA, wich indicates that the presence of Pax6 is not sufficient for directing cells towards a GABAergic fate. Conversely, some postmitotic GAD-ir cells lack Pax6, wich indicates that Pax6 alone is dispensable for the acquisition and/or maintenance of this phenotype. In this regards, functional analyses in the retina of *Xenopus* have shown that increasing Pax6 at early eye field stages does not affect the GABAergic phenotype (Zaghloul and Moody, 2007), and that conditional ablation of Pax6 in the peripheral retina of mouse does not modify the proportion of GABAergic amacrine cells (Marquardt et al., 2001).

REFERENCES

Agardh E, Bruun A, Ehinger B, Ekström P, Van Veen T, and Wu JY (1987). Gamma-aminobutyric acid- and glutamic acid decarboxylase-immunoreactive neurons in the retina of different vertebrates. J Comp Neurol, 258: 622-630.

Anadón R, Meléndez-Ferro M, Pérez-Costas E, Pombal MA, Rodicio MC (1998). Centrifugal fibers are the only GABAergic structures of the retina of the larval sea lamprey: an immunocytochemical study. Brain Res. 782, 297-302.

Ballard WW, Mellinger J, Lechenault H (1993). A series on normal stages for development of *Scyliorhinus canicula*, the lesser-spotted dogfish (Chondrichthyes: Scyliorhinidae). J Exp Zool, 267: 318-336.

Bennis M, Versaux-Botteri C, Repérant J, Armengol JA, Ward R (2003). γ-Aminobutyric acid-synthesizing cells in the retina of the chameleon *Chamaeleo chameleon*. J Neurosc Res, 73: 410-415.

Birnbaum AD, Rohde SK, Qian H, Al-Ubaidi MR, Caldwell JH, Malchow RP (2005). Cloning, immunolocalization, and functional expression of a GABA transporter from the retina of the skate. Vis Neurosci, 22: 211-223.

Brandon C (1985). Retinal GABA neurons: localization in vertebrate species using an antiserum to rabbit brain glutamate decarboxylase. Brain Res, 344: 286-295.

Brandon C, Criswell MH (1995). Displaced starburst amacrine cells of the rabbit retina contain the 67-kDa isoform, but not the 65-kDa isoform, of glutamate decarboxylase. Vis Neurosci, 12: 1053-1061.

Brunken WJ, Witkovsky P, Karten HJ (1986). Retinal neurochemistry of three elasmobranch species: an immunohistochemical approach. J Comp Neurol, 243: 1-12.

Buznikov GA, Shmukler YB, Lauder JM (1996). From oocyte to neuron: Do neurotransmitters function in the same way throughout development?. Cell Mol Neurobiol, 16: 537-559.

Calaza KC, de Mello MCF, de Mello FG, Gardino PF (2003). Local differences in GABA release induced by excitatory amino acids during retina development: selective activation of NMDA receptors by aspartate in the inner retina. Neurochem Res, 28: 1475-1485.

Candal E, Ferreiro-Galve S, Anadón R, Rodríguez-Moldes I (2008). Morphogenesis in the retina of a slow-developing teleost: Emergence of the GABAergic system in relation to cell proliferation and differentiation. Brain Res, 119: 21-27.

Carr CE, Fujita I, Konishi M (1989). Distribution of GABAergic neurons and terminals in the auditory system of the barn owl. J Comp Neurol, 286:190-207.

Carrera I, Sueiro C, Molist P, Holstein GR, Martinelli GP, Rodríguez-Moldes I, Anadón R (2006). GABAergic system of the pineal organ of an elasmobranch (*Scyliorhinus canicula*): a developmental immunocytochemical study. Cell Tissue Res, 323: 273-281.

Caruso DM, Owczarzak MT, Goebel DJ, Hazlett JC, Pourcho RG (1989). GABA-immunoreactivity in ganglion cells of the rat retina. Brain Res, 476: 129-134.

Connaughton VP, Behar TN, Liu WLS, Massey SC (1999). Immunocytochemical localization of inhibitory and excitatory neurotransmitters in the zebrafish retina. Vis Neurosci, 16: 483-490.

Dkhissi O, Julien JF, Wasowicz M, Dalil-Thiney N, Nguyen-Legros J, Versaux-Botteri C (2001). Differential expression of GAD65 and GAD67 during the development of the rat retina. Brain Res, 919: 242-249.

Ferguson SC, McFarlane S (2002). GABA and development of the *Xenopus* optic projection. J Neurobiol, 51: 272-284.

Fischer AJ, Omar G, Walton NA, Verrill TA, Unson CG (2005). Glucagon-expressing neurons within the retina regulate the proliferation of neural progenitors in the circumferential marginal zone of the avian eye. J Neurosci, 25: 10157-10166.

Fischer AJ, Skorupa D, Schonberg DL, Walton NA (2006). Characterization of glucagon-expressing neurons in the chicken retina. J Comp Neurol, 496: 479-494.

Fischer AJ, Stanke JJ, Ghai K, Scott M, Omar G (2007). Development of bullwhip neurons in the embryonic chicken retina. J Comp Neurol, 503: 538-549.

Fishelson L, Baranes A (1999). Ocular development in the Oman shark, *Iago omanensis* (Triakidae), Gulf of Aqaba, Red Sea. Anat Rec, 256: 389-402.

Fletcher EL, Kalloniatis M (1997). Localisation of amino acid neurotransmitters during postnatal development of the rat retina. J Comp Neurol, 380: 449-471.

Gábriel R, Straznicky C, Wye-Dvorak J (1992). GABA-like immunoreactive neurons in the retina of *Bufo marinus*: Evidence for the presence of GABAcontaining ganglion cells. Brain Res, 571: 175-179.

Grünert U, Wässle H (1990). GABA-like immunoreactivity in the macaque monkey retina: a light and electron microscopic study. J Comp Neurol, 297: 509-524.

Hagedorn M, Mack AF, Evans B, Fernald RD (1998). The embryogenesis of rod photoreceptors in the teleost fish retina, *Haplochromis burtoni*. Brain Res Dev Brain Res, 108: 217-227.

Hokoç JN, Ventura AL, Gardino PF, De Mello FG (1990). Developmental immunoreactivity for GABA and GAD in the avian retina: possible alternative pathway for GABA synthesis. Brain Res, 532: 197-202.

Hurd LB, Eldred WD (1989). Localization of GABA- and GAD-like immunoreactivity in the turtle retina. Vis Neurosci, 3: 9-20.

Kalloniatis M, Tomisich G (1999). Amino acid neurochemistry of the vertebrate retina. Progr Ret Eye Res, 18: 811-866.

Kaufman DL, Houser CR, Tobin AJ (1991). Two forms of the gammaaminobutyric acid synthetic enzyme glutamate decarboxylase have distinct intraneuronal distributions and cofactor interactions. J Neurochem, 56: 720-723.

Kreitzer MA, Andersen KA, Malchow RP (2003). Glutamate modulation of GABA transport in retinal horizontal cells of the skate. J Physiol, 546: 717-731.

Kreitzer MA, Collis LP, Molina AJ, Smith PJ, Malchow RP (2007). Modulation of extracellular proton fluxes from retinal horizontal cells of the catfish by depolarization and glutamate. J Gen Physiol, 130: 169-182.

Kroll TT, O'Leary DD (2005). Ventralized dorsal telencephalic progenitors in Pax6 mutant mice generate GABA interneurons of a lateral ganglionic eminence fate. Proc Natl Acad Sci U S A, 102: 7374-7379.

Kubota R, Hokoç JN, Moshiri A, McGuire C, Reh TA (2002). A comparative study of neurogenesis in the retinal ciliary marginal zone of homeothermic vertebrates. Dev Brain Res, 134: 31–41.

Lake N (1994). Taurine and GABA in the rat retina during postnatal development. Vis Neurosci, 11: 253-260.

Loeliger M, Rees S (2005). Immunocytochemical development of the guinea pig retina. Exp Eye Res, 80: 9-21.

Lugo-García N, Blanco RE (1991). Localization of GAD-like and GABA-like immunoreactivity in ground squirrel retina. Retrograde labeling demonstrates GAD-positive ganglion cells. Brain Res, 564: 19-26.

Mack AF, Papanikolaou D, Lillo C (2003). Investigation of the migration path for new rod photoreceptors in the adult cichlid fish retina. Exp Neurol, 184: 90-96.

MacLeod KM, Soares D, Carr CE (2006). Interaural timing difference circuits in the auditory brainstem of the emu (*Dromaius novaehollandiae*). J Comp Neurol, 495: 185-201.

Malchow RP, Andersen KA (2001). GABA transporter function in the horizontal cells of the skate. Prog Brain Res, 131: 267-275.

Malchow RP, Ripps H (1990). Effects of gamma-aminobutyric acid on skate retinal horizontal cells: evidence for an electrogenic uptake mechanism. Proc Natl Acad Sci USA, 87: 8945-8949.

Malchow RP, Qian HH, Ripps H (1989). Gamma-Aminobutyric acid (GABA)-induced currents of skate Müller (glial) cells are mediated by neuronal-like $GABA_A$ receptors. Proc Natl Acad Sci USA, 86: 4326-4330.

Malchow RP, Qian HH, Ripps H, Dowling JE (1990). Structural and functional properties of two types of horizontal cell in the skate retina. J Gen Physiol, 95: 177-198.

Maler L, Mugnaini E (1994). Correlating gamma-aminobutyric acidergic circuits and sensory function in the electrosensory lateral line lobe of a gymnotiform fish. J

Comp Neurol, 345: 224-252.

Marc RE, Cameron D (2001). A molecular phenotype atlas of the zebrafish retina. J Neurocytol, 30: 593-654.

Marc RE, Liu WLS (2000). Fundamental GABAergic amacrine cell circuitries in the retina: nested feedback, concatenated inhibition, and axosomatic synapses. J Comp Neurol, 425: 560-582.

Marc RE, Jones BW (2002). Molecular phenotyping of retinal ganglion cells. J Neurosci, 22: 413-427.

Marquardt T, Ashery-Padan R, Andrejewski N, Scardigli R, Guillemot F, Gruss P. (2001). Pax6 is required for the multipotent state of retinal progenitor cells. Cell 105:43-55.

Martin SC, Heinrich G, Sandell JH (1998). Sequence and expression of glutamic acid decarboxylase isoforms in the developing zebrafish. J Comp Neurol, 396: 253-266.

Martins RAP, Pearson RA (2007). Control of cell proliferation by neurotransmitters in the developing vertebrate retina, Brain Res., doi:10.1016/j.brainres.2007.04.076

Meléndez-Ferro M, Villar-Cheda B, Abalo XM, Pérez-Costas E, Rodríguez-Muñoz R, de Grip WJ, Yáñez J, Rodicio MC, Anadón R (2002). Early development of the retina and pineal complex in the sea lamprey: comparative immunocytochemical study. J Comp Neurol, 442: 250-265.

Messersmith EK, Redburn DA (1992). Gamma-aminobutyric acid immunoreactivity in multiple cell types of the developing rabbit retina. Vis Neurosci, 8: 201-211.

Messersmith EK, Redburn DA (1993). The role of GABA during development of the outer retina in the rabbit. Neurochem Res, 18: 463-470.

Mitchell CK, Redburn DA (1996). GABA and GABA-A receptors are maximally expressed in association with cone synaptogenesis in neonatal rabbit retina. Dev Brain Res, 95: 63–71.

Mugnaini E, Oertel WH, Wouterlood FF (1984). Immunocytochemical localization of GABA neurons and dopamine neurons in the rat main and accessory bulbs. Neurosci Lett, 47: 221-226.

Negishi K, Wagner HJ (1995). Differentiation of photoreceptors, glia, and neurons in the retina of the cichlid fish *Aequidens pulcher*: an immunocytochemical study. Dev Brain Res, 89: 87-102.

Nguyen LT, Grzywacz NM (2000). Colocalization of choline acetyltransferase and γ-aminobutyric acid in the developing and adult turtle retinas. J Comp Neurol, 420: 527-538.

Ochi S, Lim JY, Rand MN, During MJ, Sakatani K, Kocsis JD (1993). Transient presence of GABA in astrocytes of the developing optic nerve. Glia 9: 188-198.

Oertel WH, Schmechel DE, Tappaz ML, Kopin IJ (1981). Production of a specific antiserum to rat brain glutamic acid decarboxylase by injection of an antigen-antibody complex. Neuroscience 6: 2689-2700.

Osborne NN, Patel S, Beaton DW, Neuhoff V (1986). GABA neurones in retinas of different species and their postnatal development *in situ* and in culture in the rabbit retina. Cell Tissue Res, 243: 117-123.

Pituello F, Kan P, Geffard M, Duprat AM (1989). Initial GABAergic expression in embryonic amphibian neuroblasts after neural induction. Int J Dev Biol, 33: 445-453.

Plouhinec JL, Leconte L, Sauka-Spengler T, Bovolenta P, Mazan S, Saule S (2005). Comparative analysis of gnathostome Otx gene expression patterns in the developing eye: implications for the functional evolution of the multigene family. Dev Biol, 278: 560-575.

Pow DV, Crook DK, Wong RO (1994). Early appearance and transient expression of putative amino acid neurotransmitters and related molecules in the developing rabbit retina: an immunocytochemical study. Vis Neurosci, 11: 1115-1134.

Qian H, Malchow RP, Chappell RL, Ripps H (1996). Zinc enhances ionic currents induced in skate Müller (glial) cells by the inhibitory neurotransmitter GABA. Proc Proc R Soc Lond B, 263: 791-796.

Qian H, Li L, Chappell RL, Ripps H (1997). GABA receptors of bipolar cells from the skate retina: actions of zinc on GABA-mediated membrane currents. J Neurophysiol, 78: 2402-2412.

Qian H, Ripps H, Schuette E, Chappell RL (2001). Responses of small- and large-field bipolar cells to GABA and glycine. Brain Res, 893: 273-277.

Redburn DA, Madtes P (1987). GABA - Its role and development in the retina. In: Osborne, N.N., Chader, G.J. (Eds.), Progress and Retinal Research. Vol. 6. Pergamon Press, Oxford, pp. 69–84.

Repérant J, Miceli D, Rio JP, Peyrichoux J, Pierre J, Kirpitchnikova E (1986). The anatomical organization of retinal projections in the shark *Scyliorhinus canicula* with special reference to the evolution of the selachian primary visual system. Brain Res, 396: 227-248.

Repérant J, Ward R, Miceli D, Rio JP, Médina M, Kenigfest NB, Vesselkin NP (2006). The centrifugal visual system of vertebrates: A comparative analysis of its functional anatomical organization. Brain Res Rev, 52: 1-57.

Rio JP, Vesselkin NP, Kirpitchnikova E, Kenigfest NB, Versaux-Botteri C, Repérant J (1993). Presumptive GABAergic centrifugal input to the lamprey retina: a double-labeling study with axonal tracing and GABA immunocytochemistry. Brain Res, 600: 9-19.

Sandell JH, Martin SC, Heinrich G (1994). The development of GABA immunoreactivity in the retina of the zebrafish (*Brachydanio rerio*). J Comp Neurol, 345: 596-601.

Sauka-Spengler T, Baratte B, Shi L, Mazan S (2001). Structure and expression of an Otx5-related gene in the dogfish *Scyliorhinus canicula*: evidence for a conserved role of Otx5 and Crx genes in the specification of photoreceptors. Dev Genes Evol, 211, 533-544.

Schnitzer J, Rusoff AC (1984). Horizontal cells of the mouse retina contain glutamic acid decarboxylase-like immunoreactivity during early developmental stage. J Neurosci, 4: 2498-2955.

Siegler MV, Pankhaniya RR, Jia XX (2001). Pattern of expression of engrailed in relation to gamma-aminobutyric acid immunoreactivity in the central nervous system of the adult grasshopper. J Comp Neurol, 440 :85-96.

Spiro JE, Dalva MB, Mooney R (1999). Long-range inhibition within the zebra finch song nucleus RA can coordinate the firing of multiple projection neurons. J Neurophysiol, 81:3007-3020.

Stell WK, Witkovsky P (1973). Retinal structure in the smooth dogfish, Mustelus canis: light microscopy of photoreceptor and horizontal cells. J Comp Neurol, 148: 33-45.

Studholme KM, Yazulla S (1997). 3H-adenosine uptake selectively labels rod horizontal cells in goldfish retina. Vis. Neurosci, 14: 207-212.

Sueiro C, Carrera I, Molist P, Rodríguez-Moldes I, Anadón R (2004). Distribution and development of glutamic acid decarboxylase (GAD)-immunoreactivity in the spinal cord of the dogfish *Scyliorhinus canicula* (Elasmobranchs). J Comp Neurol, 478: 189-206.

Sueiro C, Carrera I, Ferreiro S, Molist P, Adrio F, Anadón R, Rodríguez-Moldes I (2007). New insights on saccus vasculosus evolution: A developmental and immunohistochemical study in elasmobranchs. Brain Behav Evol, 70: 187–204.

Toyoda JI, Saito T, Kondo H (1978). Three types of horizontal cells in the stingray retina: their morphology and physiology. J Comp Neurol, 179: 569-579.

Versaux-Botteri C, Pochet R, Nguyen-Legros J (1989). Immunohistochemical localization of GABA-containing neurons during postnatal development of the rat retina. Invest Ophthalmol Vis Sci, 30: 652-659.

Versaux-Botteri C, Hergueta S, Pieau C, Wasowicz M, Dalil-Thiney N, Nguyen-Legros J (1994). Early development of GABA-like immunoreactive cells in the retina of turtle embryos. Dev Brain Res, 83: 125-131.

Villar-Cerviño V, Abalo XM, Villar-Cheda B, Meléndez-Ferro M, Pérez-Costas E, Holstein GR, Martinelli GP, Rodicio MC, Anadón R (2006). Presence of glutamate, glycine, and gamma-aminobutyric acid in the retina of the larval sea lamprey: comparative immunohistochemical study of classical neurotransmitters in larval and postmetamorphic retinas. J Comp Neurol, 499: 810-827.

Wang CT, Blankenship AG, Anishchenko A, Elstrott J, Fikhman M, Nakanishi S, Feller MB (2007). GABA(A) receptor-mediated signaling alters the structure of spontaneous activity in the developing retina. J Neurosci, 27, 9130-9140.

Wilson JR, Cowey A, Somogy P (1996). GABA immunopositive axons in the optic nerve and optic tract of macaque monkeys. Vision Res, 36: 1357-1363.

Yamasaki EN, Barbosa VD, de Mello FG, Hokoç JN (1999). GABAergic system in the developing mammalian retina: dual sources of GABA at early stages of postnatal development. Int J Dev Neurosci, 17: 201-213.

Yang CY, Yazulla S (1988). Localization of putative GABAergic neurons in the larval tiger salamander retina by immunocytochemical and autoradiographic methods. J Comp Neurol, 277: 96-108.

Yazulla S, Studholme KM, Wu JY (1986). Comparative distribution of 3H-GABA uptake and GAD immunoreactivity in goldfish retinal amacrine cells: A double- label analysis. J Comp Neurol, 244: 149-162.

Yazulla S, Studholme KM (2001). Neurochemical anatomy of the zebrafish retina as determined by immunocytochemistry. J Neurocytol, 30: 551-592.

Yew DT (1982). Development of the eyes in Agnatha and Chondrichthyes (Elasmobranchia). Anat Anz Jena 151: 231-239.

Yu BC, Watt CB, Lam DM, Fry KR (1988). GABAergic ganglion cells in the rabbit retina. Brain Res, 439: 376-382.

Zaghloul NA, Moody SA (2007). Changes in Rx1 and Pax6 activity at eye field stages differentially alter the production of amacrine neurotransmitter subtypes in *Xenopus*. Mol Vis, 13: 86-95.

Figure 1. Sections through the retina and optic stalk/nerve of *S. canicula* embryos of stages 26 to 29 immunostained for GAD (A-F, I) and GABA (G, H, J-L). **A**. Central retina at stage 26 showing some weak GAD-ir cells (arrowheads). **B, C**. Central retina at stage 27 showing abundant GAD-ir neuroblastic cells with somata at different levels (arrowheads in B). Note their bipolar shape and the radial extension of their prolongations (C). **D-F**. Peripheral (D) and central retina (E,F) of an early stage 29. Note the peripheral extension of GAD-ir neuroblastic cells (D) and the high density of somata at inner levels of the central retina (arrows in E) where some cells extend lateral processes (arrow in F). **G**. Central retina of a late stage 29 embryo showing the segregation of GABA-ir cells in outer (O) and inner (I) regions. Note the highest density of cells in the inner region and immunolabelled cells, probably migrating, at intermediate levels (arrowhead). **H**. Detail of the inner region of the central retina in a late stage 29 showing GABAergic somata at different levels (small arrowheads). The largest arrowhead points to an outer located cell extending its process among the other labelled cells. **I**. Transverse section of the optic stalk in an early stage 29 at a level close to the retina, which appears tangentially sectioned. Note the absence of labelling in the optic stalk, which shows a tubular appearance (asterisk) and the presence of some GAD-ir cells at outer retinal levels (arrowheads). **J**. Transverse section of the optic stalk in a late stage 29 embryo at a very proximal level. Note the solid appearance of the stalk and the presence of some GABA-ir fibres coursing externally (arrowheads). Abundant GABAergic cells can be seen in the peripheral retina, which showed similar organization to that of the central retina at early stage 29 (compared with E). **K**. Transverse section of the optic stalk/nerve at a level intermediate between the retina and brain. Note GABA-ir fibres mostly coursing peripherally among immunonegative fibre fascicles and rounded cells (arrow). L. Detail of the chiasm region of a sagittal section of the brain in late stage 29 to show some GABA-ir fibres (arrowheads) in the distal part of the optic nerve (transversally sectioned). Labelled cells and fibres can also be seen in the ventral preoptic region (arrow). The asterisk marks the preoptic recess. Rostral is to the left. Scale bars: 25 μm (C, F), 50 μm (A, B, H-L), 100 μm (D, E, G). For abbreviations, see list in Appendix B.

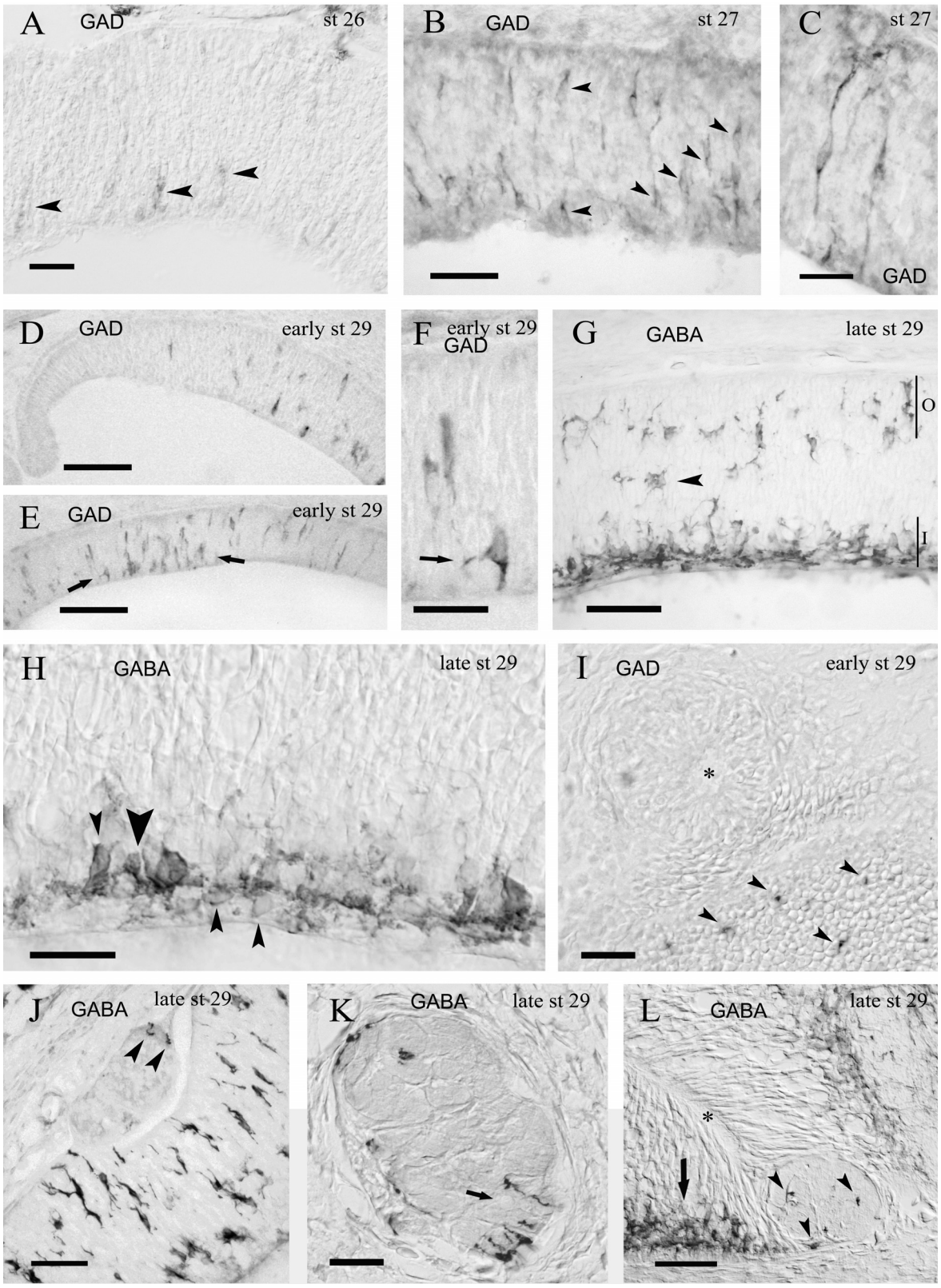
A GAD st 26
B GAD st 27
C st 27 GAD
D GAD early st 29
E GAD early st 29
F early st 29 GAD
G GABA late st 29
O
I
H GABA late st 29
I GAD early st 29
*
J GABA late st 29
K GABA late st 29
L GABA late st 29
*

Figure 2. Sections through the retina and optic nerve of embryos of stages 30 to 31 of *S. canicula* (A-D, F-K) and *H. fuscus* (E), immunostained for GAD (A-C, E, G) and GABA (D, F, H-K). **A**. Retina of stage 30 embryo sectioned at the level of the optic nerve head showing that the organization of GAD-ir cells matches that of central retina at previous stages. Note the abundant GAD-ir fibres in the optic fibre layer (arrowheads) and optic nerve head. **B**. Detail of the same retina sectioned more laterally. Note the neuroblastic appearance of the most marginal GAD-ir cells (arrow). **C**. Central retina at stage 30 showing abundant pyriform GAD-ir cells (large arrowheads) in the inner retina extending their basal processes horizontally to form the primordial IPL. Note also some GAD-ir cells inner to this primordial IPL (arrow), and the outer row of faint GAD-ir cells (small arrowheads). **D**. Central retina at stage 31 showing GABA-ir cells organized in a row in the HCL and in several rows in the INL. Note the incipient layered pattern of the IPL as well as abundant GABA-ir fibres in the optic fibre layer that appears tangentially sectioned (arrowheads). Note also some faint labelled fibres externally to the INL GABA-ir cells (arrow). **E.** Detail of the inner retina at central levels to show a GAD-ir cell in the GCL (arrow) and fibres in the optic fibre layer (arrowhead). **F-G**. Details of the central retina at stage 31 labelled with the GABA (F) and GAD (G) antibodies to show that the organization of GABA-ir and GAD-ir structures matches. Note that processes of GABAergic amacrine cells (thick arrows) contribute to the IPL. In the optic fibre layer, GABAergic fibres appeared circumferentially oriented (arrowheads). Note also a beaded GABA-ir fibre coursing circumferentially in the INL, externally to the GABA-ir amacrine cell rows (small arrows in F). **H**. Retina at stage 31 at the level of the optic nerve exit. Note GABA-ir structures in the inner part of the retina (arrowheads) and GABA-ir fibres in the optic nerve head and coursing in its proximal part (asterisk). **I.** Detail of a longitudinal section of the optic nerve of the same specimen at a level between the retina and brain showing abundant GABA-ir fibres. **J,K**. Marginal retina of stage 31 embryos showing GABA-ir neuroblastic cells (J) and beaded fibres (K) at the limit with the ciliary retina (dotted lines). For abbreviations, see list. Scale bars: 25 μm (E-G, J,-K), 50 μm (B, C, H, I), 100 μm (A, D). For abbreviations, see list in Appendix B.

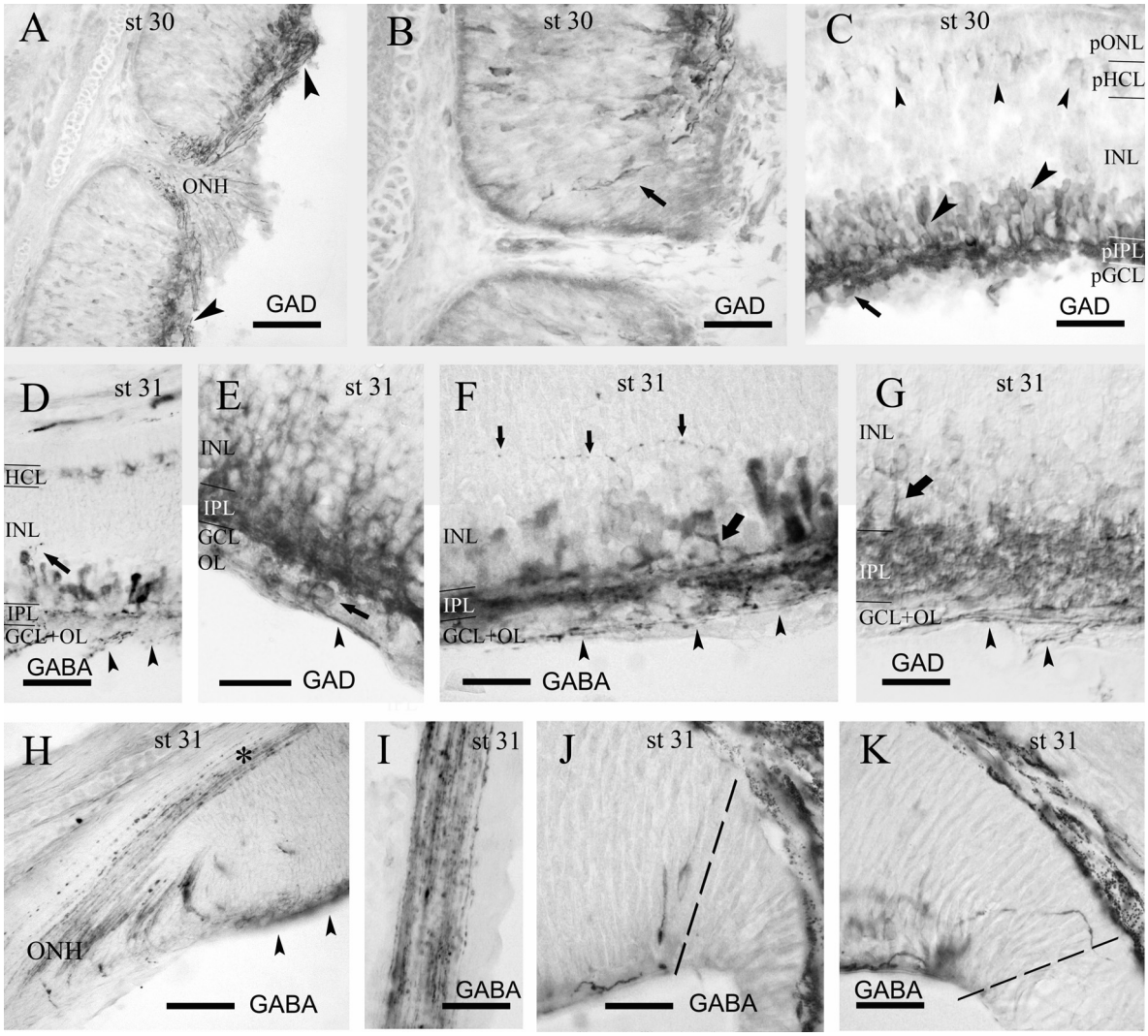
A
st 30
ONH
GAD
B
st 30
GAD
C
st 30
pONL
pHCL
INL
pIPL
pGCL
GAD
D
st 31
HCL
INL
IPL
GCL+OL
GABA
E
st 31
INL
IPL
GCL
OL
GAD
F
st 31
INL
IPL
GCL+OL
GABA
G
st 31
INL
IPL
GCL+OL
GAD
H
st 31
*
ONH
GABA
I
st 31
GABA
J
st 31
GABA
K
st 31
GABA

Figure 3. Sections through the retina of embryos of stages 32-34 of *S. canicula* (A, B, D-F, H, I) and *H. fuscus* (**C**, G) immunostained for GAD. **A**. Peripheral retina of a stage 32 embryo showing the contrast between the layered organization of GAD-ir structures in the "mature" (central) retina and the non-layered appearance in the *transition zone* (TZ). **B-F**. Central retina of embryos of stages 33 (B,C) and 34 (D-F) showing the "mature" organization of GABAergic structures. GAD-immunoreactivity is observed in cells of the INL (B-F), HCL (B,E,F) and GCL (arrows in B,C). Note also GAD-ir fibres in the optic fibre layer (arrowhead in C) and INL (arrowheads in E), the three-layered organization of GAD-ir neuropil in the IPL (B,D) and the processes of GABA-ir cells of the HCL (arrow in F). **G**. Optic nerve head of a stage 32 embryo showing GAD-ir fibres with swellings (arrows). **H.** Retina of a stage 33 embryo adjacent to the optic nerve head showing the organization of GAD-ir structures similar to that of the central retina of earlier stages (compare with Fig. 2C). **I**. Marginal zone of the retina in a stage 33 embryo to show GAD-ir fibres crossing radially at the ciliary margin. Arrowhead in I indicates GAD immunoreactivity in the optic fibre layer. For abbreviations, see list. Scale bars: 25 μm (C), 50 μm (B,D-G, I), 100 μm (A, H). For abbreviations, see list in Appendix B.

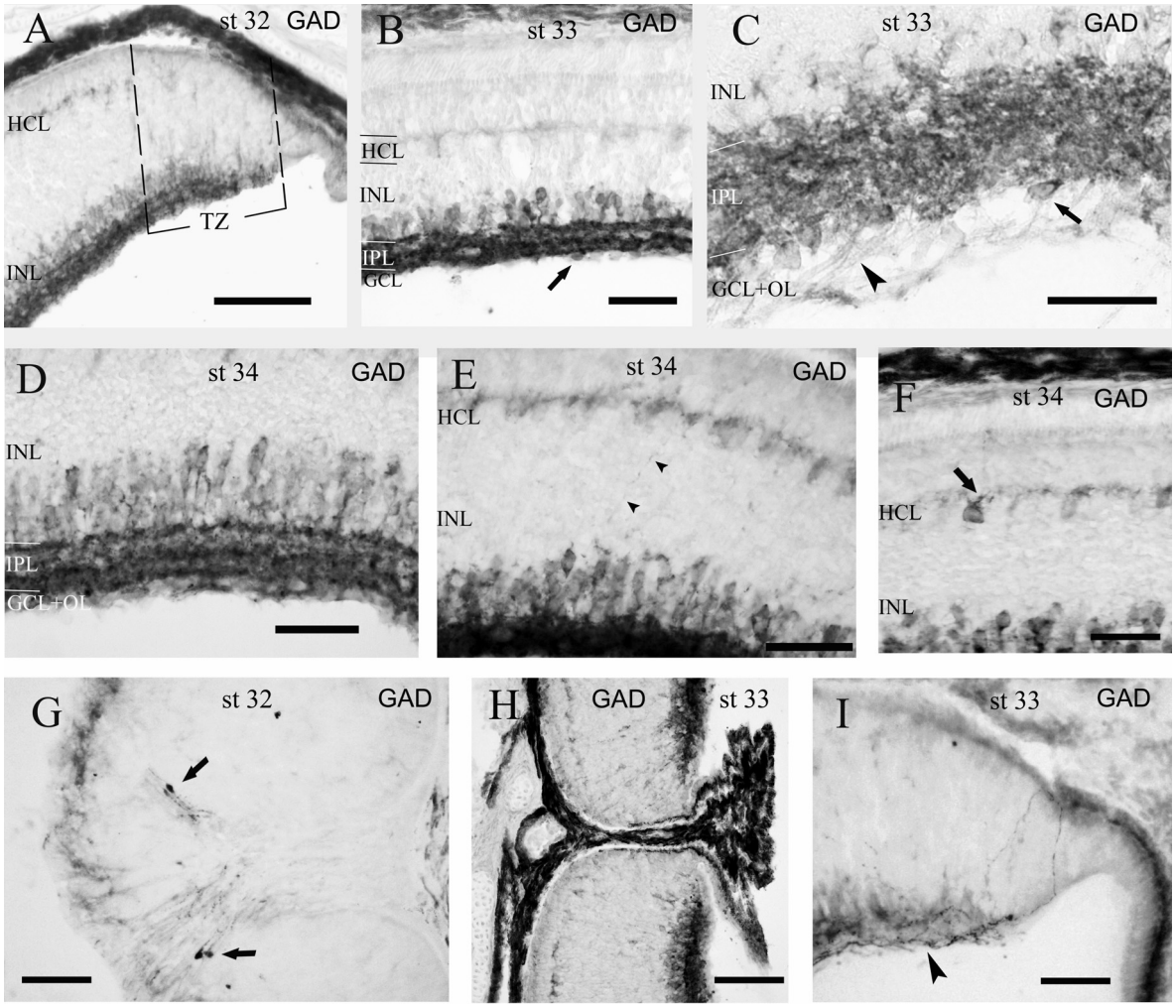
A
st 32
GAD
HCL
TZ
INL
B
st 33
GAD
HCL
INL
IPL
GCL
C
st 33
GAD
INL
IPL
GCL+OL
D
st 34
GAD
INL
IPL
GCL+OL
E
st 34
GAD
HCL
INL
F
st 34
GAD
HCL
INL
G
st 32
GAD
H
GAD
st 33
I
st 33
GAD

Figure 4. Sections through the retina of adults *S. canicula* immunostained for GABA. **A**. Marginal retina. GABA immunoreactivity is observed in cells of the HCL (arrowheads). Note a GABA-ir marginal fibre (arrows). **B-E**. Central retina showing GABA-ir cells in the INL (B-E) and GCL (large arrowheads in C,D,E), and GABA-ir fibres in the INLo (arrows in B, D, E). E is a detail of D. Small arrowheads in B-E indicate GABA immunoreactivity in the optic fibre layer. **F**. Section showing GABA-ir fibres in the optic nerve head and optic nerve. Note also GABA-ir cells in the INL (arrows) and GABA-ir processes in the IPL (asterisk). For abbreviations, see list. Scale bars: 25 μm (E), 50 μm (A-D,F). For abbreviations, see list in Appendix B.

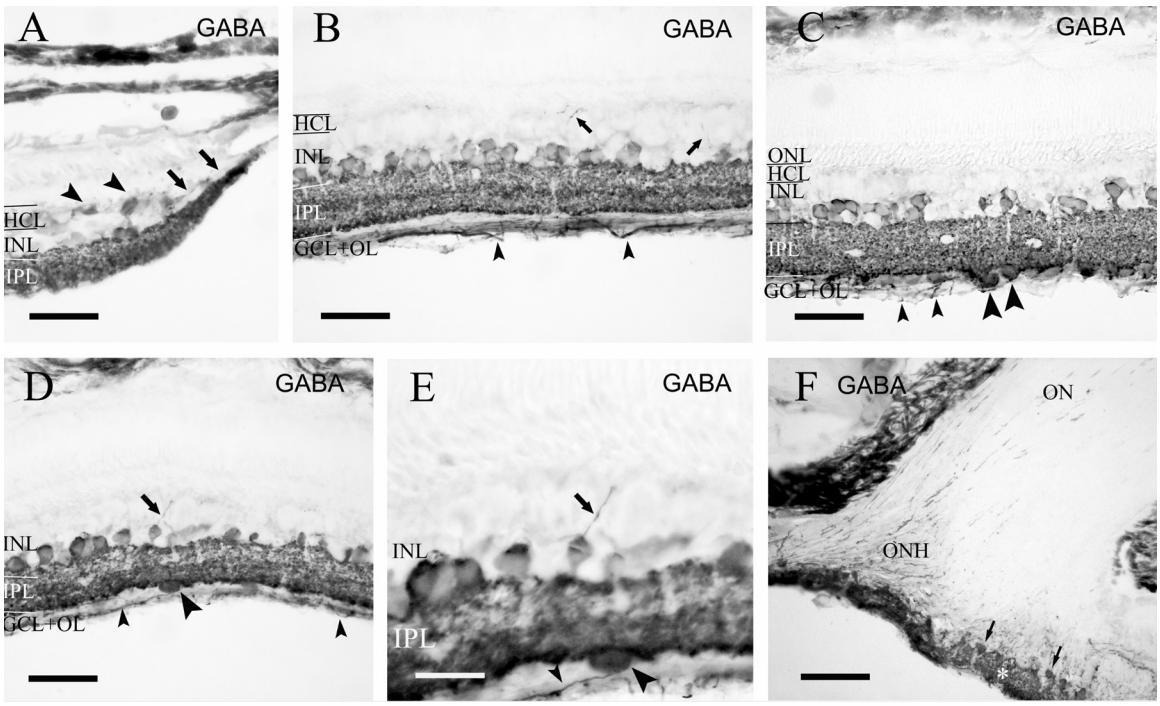
A
GABA
HCL
INL
IPL
B
GABA
HCL
INL
IPL
GCL+OL
C
GABA
ONL
HCL
INL
IPL
GCL+OL
D
GABA
INL
IPL
GCL+OL
E
GABA
INL
IPL
F
GABA
ON
ONH

Figure 5. Comparison of spatiotemporal patterns of GAD, PCNA and Pax6 in the *S. canicula* / *H. fuscus* retinas. A-C, Vertical sections along the dorsoventral axis of the retina (transversal with respect to the brain) of an early stage 29 of *S. canicula* (A-B') and a late stage 29 of *H. fuscus* (C, C'). A, GAD-ir and Pax6-ir cells are found throughout the neuroepithelial retina, although the peripheral zone contains only faint Pax6-ir cells. B, GAD-ir cells are absent from the region bordering the optic fissure (asterisk). B', Detail of the region squared in B to show that some GAD-ir cells are also Pax6-ir (arrows). C, Detail of the central retina with triple immunolabelling as indicated in C'. C', Detail of the area squared in C to show that some cells are either double GAD/Pax6-ir (white arrows), or double Pax6/PCNA-ir (open arrows). Double GAD/PCNA-ir cells are never observed. **D**, Vertical section along the dorsoventral axis of the retina of a stage 31 of *H. fuscus*, to show codistribution of GAD and Pax6 immunoreactivities in some cells of the GCL, INLi and HCL (white arrows). Of note, GAD immunoreactivity is found in cytoplasm and cell processes while Pax6 immunoreactivity is in the nuclei. **E, F**, Vertical sections along the dorsoventral axis of the retina of prehatching embryos of *H. fuscus.* E, Note the presence of a beaded GABA-ir fibre coursing circumferentially in the INL, externally to the GABA-ir amacrine cell rows (small arrows) and the presence of faint Pax6-ir cells in the INLo (large arrow) and HCL (open arrow). F, Detail of the central retina to show cells that are either GAD-ir (green arrows) or Pax6-ir (red arrows). Other cells are double GAD/PAx6-ir (white arrows). **G-I**, Vertical sections along the dorsoventral axis of the central (G, H) and the peripheral (I) retina of juveniles of *H. fuscus.* G, PCNA is absent form the central retina, while patterns of GAD and Pax6 resemble those of prehatching embryos. H, Detail to show cells that are GAD-ir (green arrows), Pax6-ir (red arrows) or double GAD/PAx6-ir (white arrows). I, The CMZ is mostly composed of PCNA-ir cells. The organization of GAD, Pax6 and PCNA in the *transition zone* resembles that of the central retina when layering begins (compare with C). Centralwards, in the region bordering the *transition zone*, GAD-ir and Pax6-ir cells are found in the GCL, INLi and also in the HCL (arrows). For abbreviations, see list in Appendix B.

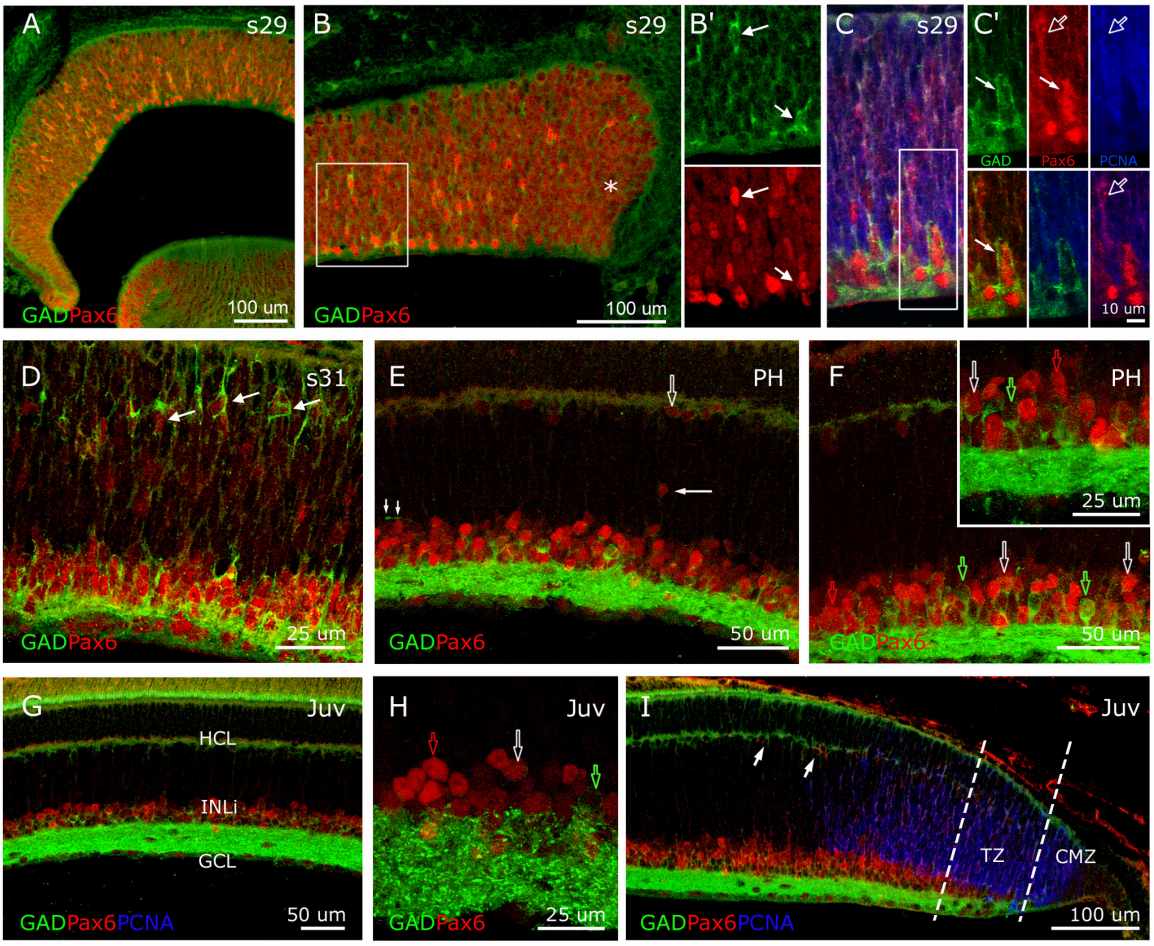
A
s29
GADPax6
100 um
B
s29
GADPax6
100 um
B'
C
s29
C'
GAD
Pax6
PCNA
10 um
D
s31
GADPax6
25 um
E
PH
GADPax6
50 um
F
PH
25 um
GADPax6
50 um
G
Juv
HCL
INLi
GCL
GADPax6PCNA
50 um
H
Juv
GADPax6
25 um
I
Juv
TZ
CMZ
GADPax6PCNA
100 um

Chapter 8.

Spatiotemporal organization of Calretinin immunoreactivity in the shark retina

INTRODUCTION

Neurogenesis entails a multi-step process consisting of proliferation, differentiation, migration, targeting, and synaptic integration that concludes with formation of a postmitotic functionally integrated new neuron. During specific time-frames of neurogenesis, various markers are expressed that correlate with the differentiation steps along the pathway from early progenitor cells to newly generated postmitotic neurons. Several markers have been widely used for the investigation of neurogenesis in the brain, including the EF-hand family of calcium-binding proteins (CBPs), consisting of proteins with high affinity for calcium ions. Among the many CBPs in the nervous system, calretinin (CR), together with parvalbumin and calbindin-D28K, are particularly striking in their abundance and in the specificity of their distribution since each of them labels different cell populations distributed throughout the entire nervous system (Weruaga et al., 2000). In the brain of vertebrates, these CBPs have been shown to be involved in the regulation of important processes such as calcium transients, specific neurone excitability, neurotransmitter release and synaptic plasticity (Arai et al., 1991; Andressen et al., 1993; Schurmans et al., 1997; Schiffmann et al., 1999; Schwaller et al., 2002; Gall et al., 2003). However, it is not yet known whether they play a triggering role or merely act as buffers to modulate intracellular calcium concentrations, thus protecting against excitotoxicity caused by an increased release of neurotransmitters (Lohmann and Friauf, 1996; Baimbridge et al., 1992; Diop et al., 1996; Vogt-Weisenhorn et al., 1996; Weruaga et al., 2000). Although their physiological function in the adult or immature brain is not fully understood (Baimbridge et al., 1992, Chiquet et al., 2005; Hendrickson et al., 2007; Morona et al., 2008), they are largely used as valuable markers of neuronal subpopulations in anatomical and developmental studies (Rogers, 1987; Baimbridge et al., 1992; Arai et al., 1991; Andressen et al., 1993; Arai et al., 1993; Nemoto et al., 1999; Díaz-Regueira and Anadón, 2000; Schwaller et al., 2002; Castro et al., 2003).

As pointed in the Introduction, the fish retina offers a model in which events related to neurogenesis can be studied. For this, it is essential to precisely characterise its chemoarchitecture and cell typology. Immunohistochemical techniques for localising CR have been extensively used to study cell morphology in the retina of a wide range of vertebrates, including: jawless fish (Dalil-Thiney et al., 1994; Villar-Cheda et al. 2006); actinopterigyans (cladistian: Graña et al., 2008; chondrosteans: Huesa et al. 2002; teleosts: Doldán et al. 1999;

Weruaga et al., 2000; García-Crespo and Vecino, 2004; Candal et al., 2008); amphibians (Pasteels et al., 1990; Gábriel et al. 1998; Deng et al., 2001; Morona et al., 2008); reptiles (Bennis et al. 2005); birds (Pasteels et al., 1990; Ellis et al. 1991), and mammals (Pasteels et al. 1990; Wässle et al., 1995; Goebel and Pourcho 1997; Völgyi et al., 1997; Jeon and Jeon, 1998; Massey and Mills, 1999; Mills and Massey, 1999; Nag and Wadhwa, 1999; Jeon et al., 2001; Cuenca et al., 2002; Hwang et al., 2005). Recently, the distribution of immunoreactivity to CR has been comparatively studied in the mature retina (though not during development) of several elasmobranch species (Graña et al., 2008). Considered together, these studies reveal that the expression of CR in ganglion and amacrine cells as well as its absence from photoreceptors is rather general, whereas CR expression in bipolar and horizontal cells is species dependent. Thus, CR appears to be a good marker for at least some types of differentiated ganglion and amacrine cells.

The aim of this work was to establish the pattern of distribution of the CR in the developing retina of two elasmobranch species while providing comparative data for other vertebrate species. We chose to study CR as this protein is located throughout the cytosol and thin dendritic processes in various subpopulations of mature retinal neurons, which facilitates study of neuronal shapes. We performed double-immunofluoresence experiments to analyse the expression of CR in relation to proliferation and differentiation during retinogenesis. For that, we compare the expression patterns of CR and proliferating cell nuclear antigen (PCNA; see also Chapter 6), which has been largely used as a proliferation marker. We also analyse the relationship between the expression patterns of CR and Pax6, a transcription factor that functions during retinogenesis to maintain pluripotency and proliferation of retinal progenitors to generate all retinal cell types (see Chapter 5). Finally, we characterise the subpopulations of CR-expressing cells with respect to those containing glutamic acid decarboxylase (GAD) in the maturing retina (see Chapter 7).

MATERIAL AND METHODS

Experimental animals

Embryos, juvenile and adult specimens of the lesser spotted dogfish (*Scyliorhinus canicula*) and the brown shyshark (*Haploblepharus fuscus*) were obtained, transported to the laboratory and maintained as indicated before (Chapter 5). The embryonic stages of *S. canicula* and *H. fuscus* embryos were identified by external features, according to Ballard et al. (1993). The following embryonic stages were analysed: stage 29 (1 *S. canicula* embryo and 1 *S. canicula* embryo), stage 31 (3 *S. canicula* and 2 *H. fuscus* embryos), stage 32 (4 *S. canicula* and 3 *H. fuscus* embryos), and stages 33-34 (prehatching; 7 *S. canicula* and 1 *H. fuscus* embryos). Moreover, 3 juveniles (2 *S. canicula* and 1 *H. fuscus*, from 10 to 14 cm in total length) and 1 adult *S. canicula* (about 50 cm in total length; provided by a local fisherman) were also processed. Adults were sacrificed immediately after incoming to the lab.

Tissue preparation

Tissue was prepared as indicated in Chapter 5. Briefly, embryos were anaesthetized with 0.05% tricaine methane sulphonate (MS-222; Sigma, St. Louis, MO) in seawater and fixed either in 4% paraformaldehyde (PFA) in elasmobranch phosphate buffer for 48-72 h or in Clark's solution for 12-36 h. Prehatching, juvenile and adult specimens were deeply anaesthetized with MS-222 and then perfused intracardially with elasmobranch Ringer's solution followed by the appropriate fixative. Eyes of stage 32-34 embryos, juveniles and adults were dissected out and postfixed for 4 h in the corresponding fixative. Specimens fixed in 4% PFA were cryoprotected, embedded in OTC compound (Tissue Tek, Torrance, CA), and frozen with liquid nitrogen-cooled isopentane. Specimens fixed in Clark's solution were dehydrated and embedded in paraffin. Parallel series of cryostat sections (14–18 µm thick) and of rotary microtome sections (10-12 µm thick) were cut in vertical planes along the dorsoventral or nasotemporal axis of the retina (transverse or sagittal planes with respect to the brain, respectively), and mounted on Superfrost Plus (Menzel-Glasser1) slides.

Antibody characterisation

The polyclonal antibody against CR from Swant (Bellinzona, Switzerland; code 7699/3H) was produced in rabbits by immunization with recombinant human CR containing a 6-his tag at the N-terminal. According to the manufacturers, 1) this antiserum does not cross-react with calbindin D-28k or other known calcium binding-proteins, as determined by immunoblots and by its distribution in the brain; 2) The antibody 7699/3H labels a subpopulation of neurons in the normal brain with high efficiency, but does not stain the brain of CR knock-out mice; 3) it recognizes a protein of approximately 59-61 kDa by Western blot. In addition, this antibody was characterised previously by western blotting in brain extracts of three cartilaginous fishes, which were run in parallel with a rat brain extract (Graña et al., 2008). In blots of *S. canicula* and other two elasmobranchs it stained a single protein band of the same molecular weight (29 kD) as the band stained in rat (Graña et al., 2008). This antibody has been widely used for immunohistochemistry to label specific cell populations in the retina of chondrosteans (Huesa et al., 2002), agnathans (Villar-Cheda et al., 2006), amphibians (Morona et al., 2008) and cartilaginous fishes (Graña et al., 2008). For characterisation of Pax6, PCNA and GAD antibodies, see Chapters 5-7.

CR immunohistochemistry

For heat induced epitope retrieval, sections were pretreated with 0.01M citrate buffer pH 6.0 for 30 min at 95°C, and allowed to cool for 30 minutes at room temperature (RT). Sections were rinsed in 0.05 M Tris-buffered saline pH 7.4 (TBS) for 5 min, and residual avidin/biotin activity was removed by incubation with the avidin/biotin blocking kit (Vector, Burlingame, CA), as indicated by the manufacturers. Sections were then incubated with a rabbit anti-CR polyclonal antiserum as primary antibody (Swant, Bellinzona, Switzerland; diluted 1:500), overnight at RT. Sections were then rinsed in TBS (two 15-min rinses) and endogenous peroxidase was blocked with 10% H_2O_2 in TBS for 30 min at RT. Sections were rinsed in TBS (three 10-min rinses), incubated in biotinylated goat anti-rabbit IgG (Dako; 1:500) for 1 h at RT, rinsed again in TBS, and incubated in the preformed avidin:biotinylated enzyme complex (ABC complex; Vector) for 30 min at RT. After two 10-min rinses in TBS, the immunoreaction was developed with either 0.25 mg/ml diaminobenzidine (DAB) tetrahydrochloride (Sigma) in TBS pH 7.4 with 2.5 mg/ml nickel ammonium sulphate and 0.00075% H_2O_2, or with SIGMAFAST™ 3,3'-Diaminobenzidine (DAB) tablets as indicated by

the manufacturers. All dilutions were made with TBS containing 15% normal goat serum (Dako) and 0.2% Triton X-100 (Sigma), and all incubations were carried out in a humid chamber. Finally, the sections were dehydrated, mounted and coverslipped. As negative controls, the primary, secondary or tertiary antibodies were omitted. No immunostaining was observed in these control sections. Photographs were taken with an Olympus DP71 colour digital camera, fitted to a Provis microscope (Olympus, Tokyo).

Double immunofluorescence for CR-PCNA antibodies

For double immunofluorescence, sections were pretreated with 0.01M citrate buffer pH 6.0 for 30 min at 95°C for heat induced epitope retrieval, and allowed to cool for 30 min at RT. Sections were rinsed twice in 0.05 M Tris-buffered saline containing 0.1% Tween-20 at pH 7.4 (TBS-T) for 5 min each, and then incubated with primary antibodies (anti-CR polyclonal rabbit antiserum, Swant, diluted 1:250; anti-PCNA mouse monoclonal antiserum, Sigma, diluted 1:200), overnight at RT. The sections were then rinsed in TBS-T (two 10-min rinses) and endogenous peroxidase was blocked with 10% H_2O_2 in phosphate buffered saline pH 7.4 (PBS) for 30 min at RT. Secondary antibodies were used as follows: Alexa Fluor 488 Goat-anti-Rabbit immunoglobulins (Molecular Probes, The Netherlands; diluted 1:200) and FluoProbes 546 Goat-anti-Mouse (Interchim, France; diluted 1:100). All dilutions were made with Tris-buffered saline (TBS) containing 0.2% of Triton X-100 (Sigma) and 15% normal goat serum. All incubations were carried out in a humid chamber. Sections were rinsed in TBS for 30 min, then in distilled water (twice for 30 min), and allowed to dry for 2 h at 37°C. Sections were mounted in MOWIOL 4-88 Reagent (Calbiochem, Merk KGaA, Darmstadt, Germany), allowed to dry for 30-60 minutes at 37°C, and observed in a Leica Spectral Confocal Laser Scanning Microscope (TCS-SP2). As negative controls, the primary or secondary antibodies were omitted. No immunostaining was observed in the control sections.

Double CR-Pax6 immunofluorescence

Sections were pretreated for epitope retrieval (see above), rinsed twice in 0.05 M Tris-buffered saline containing 0.1% Tween-20 at pH 7.4 (TBS-T) for 5-min each, and then incubated with primary antibodies (anti-CR polyclonal rabbit antiserum, Swant, diluted 1:200; anti-Pax6 goat polyclonal antiserum, Novus Biologicals, diluted 1:100), overnight at RT. The

sections were then rinsed in TBS-T (two 10-min rinses) and endogenous peroxidase was blocked as above. Secondary antibodies were used as follows: Swine-anti-Rabbit 546 (Dako; diluted 1:100), and Alexa Fluor 488 Donkey-anti-Sheep immunoglobulins (Molecular Probes, The Netherlands; diluted 1:100). All dilutions were made with Tris-buffered saline (TBS) containing 0.2% of Triton X-100 (Sigma), 15% normal swine serum and 15% normal donkey serum (Dako). All incubations were carried out in a humid chamber. Sections were treated as above before observation in a Leica Spectral Confocal Laser Scanning Microscope (TCS-SP2). As negative controls, the primary or secondary antibodies were omitted. No immunostaining was observed in the control sections.

Double CR-GAD immunofluorescence

Sections were pretreated for epitope retrieval (see above), rinsed twice in 0.05 M Tris-buffered saline containing 0.1% Tween-20 at pH 7.4 (TBS-T) for 5-min each, and then incubated with primary antibodies (anti-CR polyclonal rabbit antiserum, Swant, diluted 1:200; sheep anti-GAD65/67 polyclonal antiserum 1440-4, kindly provided by Dr. E.Mugnaini; diluted 1:20,000), overnight at RT. The sections were then rinsed in TBS-T (two 10-min rinses) and endogenous peroxidase was blocked as above. Secondary antibodies were used as follows: Swine-anti-Rabbit 546 (Dako; diluted 1:100), and Alexa Fluor 488 Donkey-anti-Sheep immunoglobulins (Molecular Probes, The Netherlands; diluted 1:100). All dilutions were made with Tris-buffered saline (TBS) containing 0.2% of Triton X-100 (Sigma), 15% normal swine serum and 15% normal donkey serum (Dako). All incubations were carried out in a humid chamber. Sections were treated as above before observation in a Leica Spectral Confocal Laser Scanning Microscope (TCS-SP2). As negative controls, the primary or secondary antibodies were omitted. No immunostaining was observed in the control sections.

RESULTS

Three developmental periods have been described in the retina of sharks as regards its growth pattern (for details of the spatiotemporal sequence of formation of retinal layers see Chapter 5). The *first developmental period* (stages 26 to 29) refers to the neuroepithelial retina; the *second developmental period* (stages 30 to 32) refers to the layering retina; the

third developmental period (stages 33 to 34) shows the mature organization characteristic of postembryonic stages.

CR immunoreactivity in the developing retina

Immunoreactivity to CR was first detected in the retina of embryos of *S. canicula* and *H. fuscus* during the *second developmental period* (early stage 32). Between-species differences in the appearance of CR-immunoreactive (-ir) cells and fibres were not observed, and patterns of CR immunoreactivity were similar in both species. CR immunoreactivity was first detected in the retina of embryos at early stage 32 (Figs. 1A-F). In both species the earliest CR-ir cells appeared in the central retina (Figs. 1A, D). Here, CR-ir cells were mainly located in the ganglion cell layer (GCL) and inner part of the inner nuclear layer (INLi), although some large and intensely stained CR-ir cells also appeared in the primordial IPL (Figs. 1B, E). Some weakly CR-ir cells showing triangular or ovoid somata were also observed in the horizontal cell layer (HCL; open arrows in Figs. 1A, D). A few CR-ir processes were observed in the IPL (small arrows in Figs. 1B, E), whereas very few CR-ir fibres were observed at the head of the optic nerve (not shown). No CR-ir cells were observed in the periphery of the retina (Figs. 1C, F), although in *H. fuscus* faint labelling was consistently observed in radial fibrous-like structures at the marginal retina (see Fig. 1F). As development progresses, the CR-ir cells and processes extended from centre-to-periphery, except in the non-layered temporoventral retina, which was devoid of CR immunoreactivity (asterisk in Fig. 1G). During this period, the density of CR-ir processes increased greatly in the IPL (mainly in sublayers 2 and 4/5), and CR-ir fibres were numerous in the optic fibre layer and in the optic nerve (Fig. 1G).

At the beginning of the *third developmental period* (stage 33), the density of CR-ir cells and fibres increased greatly in the central retina. CR-ir cells in the GCL were strongly stained and showed large, round uniformly labelled soma and branched processes (dendrites) directed to the IPL, whereas thin smooth axons coursed through the optic fibre layer (small arrowheads in Fig. 1H). Some large, strongly stained CR-ir cells with bipolar morphology were observed within the IPL (white arrowhead in Fig. 1H), among abundant CR-ir processes that showed a layered distribution in sublayers 2 and 4/5. These cells extended their thick processes within the IPL coursing tangentially along it. On the basis of their morphology, CR-ir neurons detected in the INLi correspond to two classes of cells: (1) large, rounded strongly

labelled cells, fairly similar to those observed in the GCL, which may therefore represent displaced ganglion cells (large arrowheads in Fig. 1H), and (2) smaller and less strongly labelled cells that also occupy the innermost row of cells of the INLi, which may represent amacrine cells (black arrow in Fig. 1H). The processes of both types of cell reach the IPL. In the HCL, the density of CR-ir horizontal cells increased notably as regards former stages (open arrows in Fig. 1H). At the peripheral retina (Fig. 1I), the organization of CR-ir structures resembled that observed in the central retina at earlier stages. As development progresses, the density of CR-ir cells (putative displaced ganglion and amacrine cells) in the INLi decreased with respect to that observed in previous developmental stages (Fig. 1J, K). The density of CR-ir cells in the HCL was lower in the central retina (Fig. 1K) and these cells were absent from the peripheral retina (Fig. 1L). The patterns of CR immunoreactivity were observed in the retina of juveniles (Figs. 1M, N) and adults (Fig. 1O) were similar to those observed in the *third developmental period*, although the CR immunoreactivity highly decreased in the HCL in the central retina.

Some CR-ir cells express Pax6 but not GAD.

CR was first seen in the GCL and INLi of stage 32 embryos, coinciding with the absence of PCNA immunoreactivity in most cells within these layers. However, CR-ir cells were also present in the HCL, which still contained abundant PCNA-ir cells. To know whether CR immunoreactivity occurs exclusively in postmitotic (PCNA-negative) cells, we performed double CR-PCNA immunofluorescence in stage 32 embryos, when PCNA was scarce in the central retina but still abundant in the outer part of the INL (INLo), including the HCL, and in the outer nuclear layer (ONL) of the peripheral retina (Fig. 2A). As expected, CR immunoreactivity (arrowheads in Fig. 2A) was never found in the few PCNA-ir cells still present in the GCL and INLi (large arrows in Fig. 2A), or even in PCNA-ir cells of the population present at the level of the HCL. CR immunoreactivity was also observed in radial fibrous-like structures that surround PCNA-ir neuroblastic cells at the marginal retina.

From stage 32 onwards, CR was found to codistribute with Pax6 in the GCL, INLi and HCL. Double immunofluorescence showed that CR-ir and Pax6-ir cells within the INLi and HCL formed separate populations, while some cells in the GCL were immunoreactive for both

markers (Figs. 2B, B'). Cells exclusively immunoreactive for Pax6 or CR were also seen in the GCL (green and red arrows, respectively, in Figs. 2B, B').

Similar patterns of CR and GAD immunoreactivity were observed in the mature retina of elasmobranchs, as both were expressed in subpopulations of cells in the GCL, INLi and HCL, as well as in fibres in the optic nerve, optic fibre layer, inner plexiform layer (IPL) and HCL. Double immunofluorescence (Figs. 2C-E) showed that strongly CR-ir cells (arrowheads in Fig. 2C-E) and faintly GAD-ir cells (arrows in Fig. 2C-E) in the GCL and INLi were separate populations, and colocalisation was not clearly demonstrated. Some cells in the HCL also expressed either CR (open arrowhead in Fig. 2C) or GAD (not shown). Indeed their processes spread in different IPL sublayers, and colocalisation of CR and GAD could not be demonstrated in processes of the HCL (Fig. 2C) or in the optic fibre layer (open arrow in Fig. 2E).

DISCUSSION

CR as a marker for retinal neurons

In the retina, CR is expressed in well-defined neuron types in a broad range of vertebrates from agnathans (Villar-Cheda et al., 2006) to mammals (revised in Morona et al., 2008), including elasmobranchs (Graña et al., 2008). The presence of this protein in ganglion cells and some amacrine cells has been extensively reported but this expression in bipolar, horizontal and photoreceptors cells appears to be species dependent, even among elasmobranchs (Graña et al., 2008). In the developing retina of sharks (present results), CR-ir cells were found in the GCL, within the IPL, in the INLi and in the HCL. CR-ir fibres were observed in the optic nerve, optic fibre layer, IPL and also in the outer plexiform layer (OPL). In the adult retina of *S. canicula*, subpopulations of CR-ir cells have been reported in the GCL (considered ganglion cells), in the INLi (displaced ganglion cells and amacrine cells) and in the HCL (horizontal cells).

CR-ir cells in the GCL of both developing and mature retina of *S. canicula* and *H. fuscus* (present results) were tentatively identified as (ordinary) ganglion cells by the presence of numerous CR-ir axons running in the optic fibre layer and optic nerve, and also because of their location and size (larger than most cells of the INLi). These features correspond to

those of the ordinary giant ganglion cells described in the smooth dogfish (*Mustelus canis;* Stell and Witkovsky, 1973). Two classes of CR-ir cells were found in the INLi of sharks (present results) on the basis of their morphology and intensity of immunolabelling: large, rounded strongly labelled cells that may correspond to displaced ganglion or Dogiel's cells (with perikarya in the amacrine cell layer) described by Stell and Witkovsky (1973); and small and faintly CR-ir cells that have been interpreted as amacrine cells. The presence of CR-ir subpopulations of ganglion and amacrine cells appears to be a conserved trait in vertebrates. To our knowledge, expression of CR has been reported in the GCL and inner nuclear layer (INL) of the developing and/or mature retina of all vertebrates studied so far (for references, see introduction). In these species, CR-ir cells in the GCL and INL were mostly interpreted as ganglion and amacrine cells, respectively, although displaced ganglion cells were reported in the INL of lamprey (Villar-Cheda et al., 2006) and sturgeon (Huesa et al., 2002). Moreover, displaced amacrine cells were also described in the GCL of the chamaleon (Bennis et al., 2005) and in the developing and mature retina of humans (Nag and Wadhwa, 1999). Interestingly, we also report large CR-ir cells in the IPL of embryonic and mature retina of sharks, which may correspond to the intermediate giant ganglion cells defined by Stell and Witkovsky (1973) in the smooth dogfish, which present both their perikarya and dendrites within the IPL. The presence of CR-ir ganglion cells within the IPL has also been reported in the mature retina of *S. canicula* and other elasmobranchs (Graña et al., 2008) and also in lamprey (Villar-Cheda et al., 2006) and sturgeon (Huesa et al., 2002). CR-ir cells in the IPL have been reported in other species and either have not been identified (turbot: Doldán et al., 1999; trout: Candal et al., 2008; human: Nag and Wadhwa, 1999), or have been interpreted as amacrine cells (chameleon: Bennis et al., 2005; rabbit: Völgyi et al., 1997; Massey and Mills, 1999).

CR-ir cells were also observed in the HCL of developing and the mature) retina of sharks (present results), their location and morphology coinciding with H1 type (first-row or external) horizontal cells. Interestingly, transient expression of CR in the HCL of the developing human retina has been reported by Nag and Wadhwa (1999), who suggested a role for CR in maturation of horizontal cells. The presence of CR in horizontal cells is not an evolutionary conserved feature, but rather is highly dependent on species. Indeed, CR-ir horizontal cells were found in the mature retina of sea lamprey (Villar-Cheda et al., 2006), turbot (Doldán et al., 1999), trout (Candal et al., 2008), *S. canicula* and skate (Graña et al.,

2008), Iberian green frog (Morona et al., 2008), salamander (Deng et al., 2001), chameleon (Bennis et al., 2005), chick (Ellis et al., 1991), cat and dog (Jeon and Jeon, 1998), pig (Jeon et al., 2001) and human (Nag and Wadhwa, 1999), although absent from the river lamprey (Dalil-Thiney et al., 1994), zebrafish (García-Crespo and Vecino, 2004), sturgeon (Huesa et al., 2002), bichir and electric ray (Graña et al., 2008), edible frog (Gábriel et al., 1998), and rabbit (Völgyi et al., 1997; Jeon and Jeon, 1998; Massey and Mills, 1999). Differences have even been observed between related species of jawless fish (Dalil-Thiney et al., 1994; Villar-Cheda et al., 2006) and amphibians (Gábriel et al., 1998; Morona et al., 2008), although the significance of these variations is unclear.

As with horizontal cells, the presence of CR in bipolar cells is species dependent. CR-ir bipolar cells have not been observed in the developing or mature retina of sharks (present results and Graña et al., 2008), unlike for most fish species studied so far, in which bipolar or bipolar-like cells have been found in the INLo (Doldán et al., 1999; Weruaga et al., 2000; Huesa et al., 2002; Dalil-Thiney et al., 1994; García-Crespo and Vecino, 2004; Villar-Cheda et al., 2006; Candal et al., 2008), or even displaced to the ONL (bichir: Graña et al., 2008). Although bipolar cells have been described in birds (Ellis et al., 1991; Pasteels et al., 1990), amphibians (Gábriel et al., 1998; Deng et al., 2001; Morona et al., 2008) and reptiles (Bennis et al., 2005), their presence in mammals is highly dependent on the species studied (Goebel and Pourcho; 1997; Völgyi et al., 1997; Jeon and Jeon, 1998; Massey and Mills, 1999; Mills and Massey, 1999; Nag and Wadhwa, 1999; Jeon et al., 2001; Cuenca et al., 2002; Hwang et al., 2005).

The observed absence of CR in photoreceptors in sharks (present results) is also a fairly conserved feature in vertebrates, though CR-ir cones were occasionally found in some mammals (Pasteels et al., 1990; Goebel and Pourcho, 1997; Völgyi et al., 1997; Nag and Wadhwa, 1999).

In summary, our results (together with the aforementioned results) confirm that the presence of CR immunoreactivity in subclasses of cells within the GCL and INL is a conserved character of vertebrate retinas. Moreover, CR immunoreactivity was not found in proliferating cells (present results), suggesting that CR can be reliably used as a marker for at least some types of differentiated ganglion and amacrine cells.

Roles of CR during retinogenesis

Calcium binding proteins (CBPs) act as buffers and are therefore the major factors determining the kinetics of fluctuations in intracellular calcium ions (Mojumder et al., 2008). CR, a major EF-hand (E-helix-loop-F-helix-hand) CBP in the retina, is therefore an important buffer of cytosolic free Ca^{2+} in neurons, and may also serve as a Ca^{2+}-dependent regulator of enzymes and ion channels. It is known that CR interacts with cytoskeletal components and basic helix–loop–helix transcription factors (Araki et al., 2000; Bambridge et al., 1992; Polans et al., 1996; Rogers, 1987; Schäfer and Heizmann, 1996; Mojumder et al., 2008). Previous studies have shown that CR plays an important role in neuroprotection and resistance to excitotoxic injury (Leuba et al., 1998; D'Orlando et al., 2002).

However, the function of CR during retinogenesis is not well understood. Analysis of the spatiotemporal distribution of CR in the developing retina of sharks performed here may help in understanding the possible involvement of CR in some aspects of retinal morphogenesis. In the adult retina of *S. canicula*, subpopulations of CR-ir cells have been reported in the GCL, in the INL and in the HCL. Our present work provides evidence that this pattern of CR-ir cell distribution is settled in the developing retina of both *S. canicula* and *H. fuscus* from the early stage 32 onwards, when the GCL and the INLi can be clearly distinguished by the presence of an IPL that has largely extended from the central to the peripheral retina. Moreover, the onset of CR expression coincides with the establishment of the first synapses within the OPL in the central part of the retina. Studies in bony fishes have also reported that the appearance of CR in the retina occurs along with the establishment of the early laminar organization (Doldán et al., 1999; García-Crespo and Vecino, 2004; Candal et al., 2008).

Following development, the spatiotemporal detection of CR-ir cells shows a centre-to-periphery gradient coincident with the progression of the retinal maturation, i.e., the pattern of CR-immunoreactivity observed in the peripheral retina resembles that found in the central retina at earlier stages. Indeed, developmental studies in different vertebrates have shown that CR expression is associated with morphological differentiation of neurons (Ellis et al., 1991; Nag and Wadhwa, 1999; Doldán et al., 1999; García-Crespo and Vecino, 2004; Candal et al., 2008). In sharks (present results), CR expression is first observed in the GCL of the central retina nearly one month after most cells in the GCL became postmitotic (see also

Chapter 6). Double immunohistochemistry also revealed that CR was never present in the few PCNA-ir cells found in this layer during this developmental period. Thus, it appears that CR is not expressed in early postmitotic (but undifferentiated cells), but rather in mature neurons several days after their commitment to a definitive cell phenotype. It has been reported that CR is involved in the development and maturation of human ganglion and amacrine cells (Nag and Wadhwa, 1999). García-Crespo and Vecino (2004) have reported that CR expression in bony fishes is associated with ganglion cell differentiation, which is in line with present results.

Because of its transient expression in horizontal cells (present results), CR may also be involved in the maturation of the outer retina. CR-ir horizontal cells were first detected in the central retina, concurrently with the observation of first postmitotic (PCNA-negative) cells in the ONL. Indeed, a correlation between the CR expression in the retina of different vertebrates and the dominance of one photoreceptor type has been reported. Rod dominant retinas possess ganglion cells, amacrine cells and horizontal CR-positive cells (Hamano et al., 1990). In the turbot retina (Doldán et al., 1999), rod differentiation starts at metamorphosis, when CR labelling extends to horizontal cells. Further investigation should be carried out to determine whether CR expression in horizontal cells in the retina of sharks (present results) temporally coincides with functional maturation of rods (see Chapter 10). Although it has been reported that CR may be involved in aspects such as phototransduction, light adaptation and photoreceptor motility (Morona et al., 2008), the heterogeneity of CR immunoreactivity in horizontal and bipolar cell populations among vertebrates suggests that the function of CR in visual information processing is unclear.

Pax6 is expressed in subsets of GAD-ir and CR-ir cells

CR in sharks has been found to codistribute with GAD-ir cells in the GCL, INLi and HCL of the mature retina. Despite this spatial coincidence, colocalisation has not been demonstrated in any of these layers, suggesting that CR and GABA must play matching, but somewhat different, roles in the development and maturation of the retina. However, this is not a conserved feature in vertebrates as CR/GABA colocalisation has been described in the GCL of teleosts (Candal et al., 2008), and in both the INL and GCL of the *Xenopus* retina (Gábriel et al., 1998).

Some cells in the GCL have been found to colocalise for both CR and Pax6, and could be interpreted as displaced amacrine cells in basis of their morphology (see above). Accordingly, in the retina of mouse, Stewart et al. (2005) have defined a subpopulation of displaced cholinergic amacrine cells characterised by coexpressing Pax6, CR and *Runx1*, a mammalian transcription factor that plays critical roles in regulating the differentiation of diverse cell types. Therefore, in sharks, the presence of Pax6 together with that of CR within the GCL could be useful for the identification of displaced amacrine cells.

REFERENCES

Arai M, Arai R, Sasamoto K, Kani K, Maeda T, Deura A, Jacobowitz DM (1993). Appearance of calretinin-immunoreactive neurons in the upper layers of the rat superior colliculus after eye enucleation. Brain Res, 613 : 341-346.

Arai R, Winsky L, Arai M, Jacobowitz DM (1991). Immunohistochemical localization of calretinin in the rat hindbrain. J Comp Neurol, 310: 21-44.

Araki C M, Hamassaki Britto DE (2000). Calretinin colocalizes with the NMDA receptor subunit NR1 in cholinergic amacrine cells of the rat retina. Brain Res, 869: 220-224.

Andressen C, Blümcke I, Celio MR (1993). Calcium-binding proteins: selective markers of nerve cells. Cell Tissue Res, 271: 181-208.

Baimbridge KG, Celio MR, Rogers JH (1992). Calcium-binding proteins in the nervous system. Trends Neurosci, 15: 303-308.

Ballard W, Mellinger J, Lechenault H (1993). A series of normal stages for development of *Scyliorhinus canicula*, the lesser spotted dogfish (Chondrichthyes: Scyliorhinidae). J Exp Zool, 267: 318-336.

Bennis M, Versaux-Botteri C, Repérant J, Armengol JA (2005). Calbindin, calretinin and parvalbumin immunoreactivity in the retina of the chameleon (*Chamaeleo chamaeleon*). Brain Behav Evol, 65: 177-187.

Candal E, Ferreiro-Galve S, Anadón R, Rodríguez-Moldes I (2008). Morphogenesis in the retina of a slow-developing teleost: emergence of the GABAergic system in relation to cell proliferation and differentiation. Brain Res, 1194: 21-27.

Castro A, Becerra M, Manso MJ, Anadón R (2003). Distribution and development of calretinin-like immunoreactivity in the telencephalon of the brown trout, *Salmo trutta fario*. J Comp Neurol, 467: 254-269.

Chiquet C, Dkhissi-Benyahya O, Cooper HM (2005). Calcium-binding protein distribution in the retina of strepsirhine and haplorhine primates, Brain Res Bull, 68: 185-194.

Cuenca N, Deng P, Linberg KA, Lewis GP, Fisher SK, Kolb H (2002). The neurons of the ground squirrel retina as revealed by immunostains for calcium binding proteins and neurotransmitters. J Neurocytol, 31: 649-666.

Dalil-Thiney N, Pochet R, Versaux-Botteri C, Vesselkin N, Repérant J, Nguyen-Legros J (1994). Immunohistochemical localization of calbindin-D28K and calretinin in the lamprey retina. J Comp Neurol, 340: 140-147.

Deng P, Cuenca N, Doerr T, Pow DV, Miller R, Kolb H (2001). Localization of neurotransmitters and calcium binding proteins to neurons of salamander and mudpuppy retinas. Vision Res, 41: 1771-1783.

Díaz-Regueira S, Anadón R (2000). Calretinin expression in specific neuronal systems in the brain of an advanced teleost, the gray mullet (*Chelon labrosus*). J Comp Neurol, 426: 81-105.

Diop AG, Dussarte C, Barthe D, Hugon J (1996). Neuroprotective properties of calretinin against the HIV-1gp120 toxicity. Neurosci Res Commun, 18: 107-113.

Doldán MJ, Prego B, De Miguel E (1999). Immunochemical localization of calretinin in the retina of the turbot (Psetta maxima) during development. J Comp Neurol, 406: 425-432.

D'Orlando C, Celio MR, Schwaller B (2002). Calretinin and calbindin D-28k, but not parvalbumin protect against glutamateinduced delayed excitotoxicity in transfected N18-RE 105 neuroblastoma-retina hybrids cells. Brain Res, 945: 181-190.

Ellis JH, Richards DE, Rogers JH (1991). Calretinin and calbindin in the retina of the developing chick. Cell Tissue Res, 264: 197-208.

Gábriel R, Volgyi B, Pollak E (1998). Calretinin-immunoreactive elements in the retina and optic tectum of the frog, *Rana esculenta*. Brain Res, 782: 53-62.

Gall D, Roussel C, Susa I, D'Angelo E, Rossi P, Bearzatto B, Galas MC, Blum D, Schurmans S, Schiffmann SN (2003). Altered neuronal excitability in cerebellar granule cells of mice lacking calretinin. J Neurosci, 23: 9320-9327.

García-Crespo D, Vecino E (2004). Differential expression of calretinin in the developing and regenerating zebrafish visual system. Histol Histopathol, 19: 1193-1199.

Goebel DJ, Pourcho RG (1997). Calretinin in the cat retina: colocalizations with other calcium-binding proteins, GABA and glycine. Vis Neurosci, 14: 311-322.

Graña P, Anadón R, Yáñez J (2008). Immunocytochemical study of calretinin and calbindin D-28K expression in the retina of three cartilaginous fishes and a cladistian (*Polypterus*). Brain Res Bull, 75: 375-378.

Hendrickson A, Yan YH, Erickson A, Possin D, Pow D (2007). Expression patterns of calretinin, calbindin and parvalbumin and their colocalization in neurons during development of *Macaca* monkey retina. Exp Eye Res, 85: 587-601.

Huesa G, Yáñez J, Anadón R (2002). Calbindin and calretinin immunoreactivities in the retina of a chondrostean, *Acipenser baeri*. Cell Tissue Res, 309: 355-360.

Hwang IK, Yoo KY, Kim DS, Jung JY, Shin MC, Seo K, Kim KS, Kang TC, Won MH (2005). Comparative study on calretinin immunoreactivity in gerbil and rat retina. Anat Histol Embryol, 34: 129-131.

Jeon MH, Jeon CJ (1998). Immunocytochemical localization of calretinin containing neurons in retina from rabbit, cat, and dog. Neurosci Res, 32: 75-84.

Jeon YK, Kim SY, Jeon CJ (2001). Morphology of calretinin and tyrosine hydroxylase-immunoreactive neurons in the pig retina. Mol Cells, 11: 250-256.

Leuba G, Kraftsik R, Saini K (1998). Quantitative distribution of parvalbumin, calretinin, and calbindin D28K immunoreactive neurons in the visual cortex of normal and Alzheimer cases. Exp Neurol, 152: 278-291.

Lohmann C, Friauf E (1996). Distribution of the calcium-binding proteins parvalbumin and calretinin in the auditory brainstem of adult and developing rats. J Comp Neurol, 367: 90-109.

Massey SC, Mills SL (1999). Antibody to calretinin stains AII amacrine cells in the rabbit retina: double-label and confocal analyses. J Comp Neurol, 411: 3-18.

Mills SL, Massey SC (1999). AII amacrine cells limit scotopic acuity in central macaque retina: A confocal analysis of calretinin labeling. J Comp Neurol, 411: 19-34.

Mojumder DK, Wensel TG, Frishman LJ (2008). Subcellular compartmentalization of two calcium binding proteins, calretinin and calbindin-28 kDa, in ganglion and amacrine cells of the rat retina. Mol Vis, 14: 1600-1613.

Morona R, Moreno N, Lopez JM, Muñoz M, Domínguez L, González A (2008). Calbindin-D28k and calretinin as markers of retinal neurons in the anuran amphibian *Rana perezi*. Brain Res Bull, 75: 379-383.

Nag TC, Wadhwa S (1999). Developmental expression of calretinin immunoreactivity in the human retina and a comparison with two other EF-hand calcium binding proteins. Neuroscience, 91: 41-50.

Nemoto C, Hida T, Arai R (1999). Calretinin and calbindin-D28k in dopaminergic neurons of the rat midbrain: a triple-labeling immunohistochemical study. Brain Res, 846: 129-36.

Pasteels B, Rogers J, Blachier F, Pochet R (1990). Calbindin and calretinin localization in retina from different species. Vis Neurosci, 5: 1-16.

Polans A, Baehr W, Palczewski K (1996). Turned on by Ca^{2+}! The physiology and pathology of Ca^{2+}-binding proteins in the retina. Trends Neurosci, 19: 547–554.

Rogers JH (1987). Calretinin: a gene for a novel calcium-binding protein expressed principally in neurons. J Cell Biol, 105: 1343-1353.

Schäfer BW, Heizmann CW (1996). The S100 family of EF-hand calcium-binding proteins: functions and pathology. Trends Biochem Sci, 21: 134-140.

Schiffmann SN, Cheron G, Lohof A, d'Alcantara P, Meyer M, Parmentier M, Schurmans S (1999). Impaired motor coordination and Purkinje cell excitability in mice lacking calretinin. Proc Natl Acad Sci USA, 96: 5257-5262.

Schurmans S, Schiffmann SN, Gurden H, Lemaire M, Lipp HP, Schwam V, Pochet R, Imperato A, Böhme GA, Parmentier M (1997). Impaired long-term potentiation induction in dentate gyrus of calretinindeficient mice. Proc Natl Acad Sci USA, 94: 10415-10420.

Schwaller B, Meyer M, Schiffmann S (2002). "New" functions for "old" proteins: the role of the calcium-binding proteins calbindin D-28k, calretinin and parvalbumin, in cerebellar physiology. Studies with knockout mice. Cerebellum, 1: 241-258.

Stell WK, Witkovsky P (1973). Retinal structure in the smooth dogfish, *Mustelus canis*: general description and light microscopy of giant ganglion cells. J Comp Neurol, 148: 1-31.

Stewart L, Potok MA, Camper SA, Stifano S (2005). Runx1 expression defines a subpopulation of displaced amacrine cells in the developing mouse retina. J Neurochem, 94: 1739-1745.

Villar-Cheda B, Abalo XM, Anadón R, Rodicio MC (2006). Calbindin and calretinin immunoreactivity in the retina of adult and larval sea lamprey. Brain Res, 1068: 118-130.

Vogt-Weisenhorn DM, Weruaga-Prieto E, Celio MR (1996). Calretinin-immunoreactivity in organotypic cultures of the rat cerebral cortex: effects of serum deprivation. Exp Brain Res, 108: 101-112.

Völgyi B, Pollak E, Buzas P, Garbriel R (1997). Calretinin in neurochemically well-defined cell populations of rabbit retina. Brain Res, 763: 79-86.

Wässle H, Grünert U, Chun MH, Boycott BB (1995). The rod pathway of the macaque monkey retina: identification of AII-amacrine cells with antibodies against calretinin. J Comp Neurol, 361: 537-551.

Weruaga E, Velasco A, Briñón JG, Arévalo R, Aijón J, Alonso JR (2000). Distribution of the calcium-binding proteins parvalbumin, calbindin D-28k and calretinin in the retina of two teleosts. J Chem Neuroanat, 19: 1-15.

Figure 1. Patterns of CR immunoreactivity in the *S. canicula* / *H. fuscus* retinas. A-E, Vertical sections along the dorsoventral axis of the retina (transversal with respect to the brain) of early stages 32 of *S. canicula* (A-C) and *H. fuscus* (D-F). The earliest CR-ir cells appear in the central retina (A, B, D, E). CR-ir cells are observed in the GCL (arrowheads), the INLi (arrows), the IPL (white arrows) and HCL (open arrows). A few CR-ir processes are observed in the IPL (small arrows). CR-ir cells were not observed in the peripheral retina (C, F), but radial fibrous-like immunoreactivity is observed in the marginal retina of *H. fuscus* (asterisk in F). **G**, Vertical section along the dorsoventral axis of the retina of a late stage 32 of *S. canicula*. CR-ir cells are abundant in the layered retina, but not in the temporoventral retina (non-layered; asterisk). CR-ir fibres are abundant in the optic fibre layer (short arrow) and the optic nerve. Note CR-ir processes in the IPL (large arrows). **H, I**, Vertical sections along the nasotemporal axis of the retina (sagittal with respect to the brain) of a stage 33 of *S. canicula*. H, The density of CR-ir cells and processes increases in the central retina. Several types of cells are observed: large, rounded GCL cells (small arrowheads); large, bipolar cells within the IPL (white arrowhead); large, rounded INLi cells (large arrowheads); small INLi cells (arrow); and HCL cells (white arrows). I, Detail of the peripheral retina. The organization of CR-ir cells and processes is similar to that of the central retina at earlier stages (compare with D). **J-L**, Vertical sections along the dorsoventral axis of the retina of a stage 34 of *H. fuscus*. Details of the region bordering the optic nerve (J), the central retina (K) and the peripheral retina (L), to show a decreased density of INLi cells. CR-ir horizontal cells are present in the central retina (open arrows in K) but they lack from the peripheral retina. Arrows in L indicate CR-ir processes in the peripheral retina. **M, N**, Vertical sections along the dorsoventral axis of the retina of a juvenile *H. fuscus*. Detail of the central (M) and the peripheral (N) retina, to show that the pattern of CR immunoreactivity is similar to that found in earlier developmental stages. Of note, the number of CR-ir cells highly decreases in the HCL (compare with H; notation of arrows and arrowheads is the same as in H). (O) Vertical section along the dorsoventral axis of the retina of an adult of *S. canicula* to shown that the pattern of CR immunoreactivity is similar to that found in juveniles. For abbreviations, see list in Appendix B.

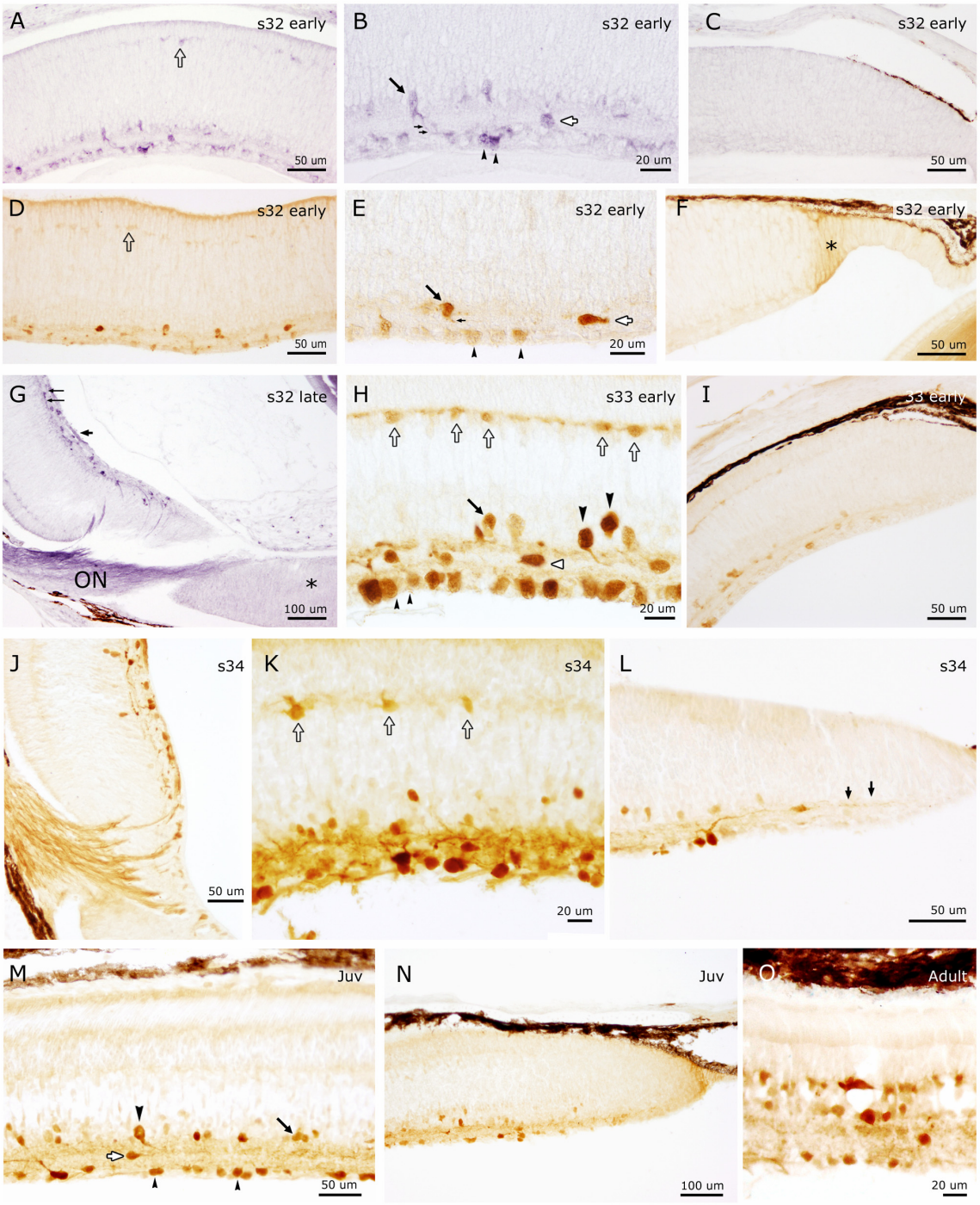
A
s32 early
50 um
B
s32 early
20 um
C
s32 early
50 um
D
s32 early
50 um
E
s32 early
20 um
F
s32 early
50 um
G
s32 late
ON
100 um
H
s33 early
20 um
I
50 um
J
s34
50 um
K
s34
20 um
L
s34
50 um
M
Juv
50 um
N
Juv
100 um
O
Adult
20 um

Figure 2. Comparison of spatiotemporal patterns of CR, PCNA, Pax6 and GAD immunoreactivities in the *H. fuscus* and *S. canicula* retina. **A**, Vertical sections along the dorsoventral axis of the retina of *H. fuscus* (transversal with respect to the brain) of a stage 32 embryo. The presence of CR-ir cells in the GCL and INLi (small and large arrowhead, respectively) coincides with a decrease in the number of PCNA-ir cells in these layers (large arrows). CR-ir cells are also found in the HCL (open arrow) among abundant PCNA-ir cells, but colocalisation was not evidenced in this layer. Note the presence of radial fibrous-like CR-ir structures at the marginal retina (asterisk). **B, B'**, Vertical sections along the dorsoventral axis of the retina of *S. canicula* (transversal with respect to the brain) of a prehatching embryo. B' is a detail of a 1-µm-thick optical section of the confocal z-series showed in B. Pax6-ir and CR-ir cells codistribute in the same cell layers, and some cells in the GCL express both markers (white open arrow in B'). Cells exclusively Pax6-ir (green arrow) or CR-ir (red arrow) are indicated. Some pale Pax6-ir cells are observed in close apposition to CR-ir cells in the HCL. **C-E**, Vertical sections along the dorsoventral axis of the retina of *H. fuscus* prehatching embryos. Double immunofluorescence reveals that strongly CR-ir cells (red) in the GCL and INLi (small and large arrowheads, respectively) are not GAD-ir (large arrows). Colocalisation was not evidenced in cells of the HCL (open arrow in C) or in fibres in the optic fibre layer (open arrow in E). Note the presence of CR-ir cells within the IPL (short arrows in D). For abbreviations, see list in Appendix B.

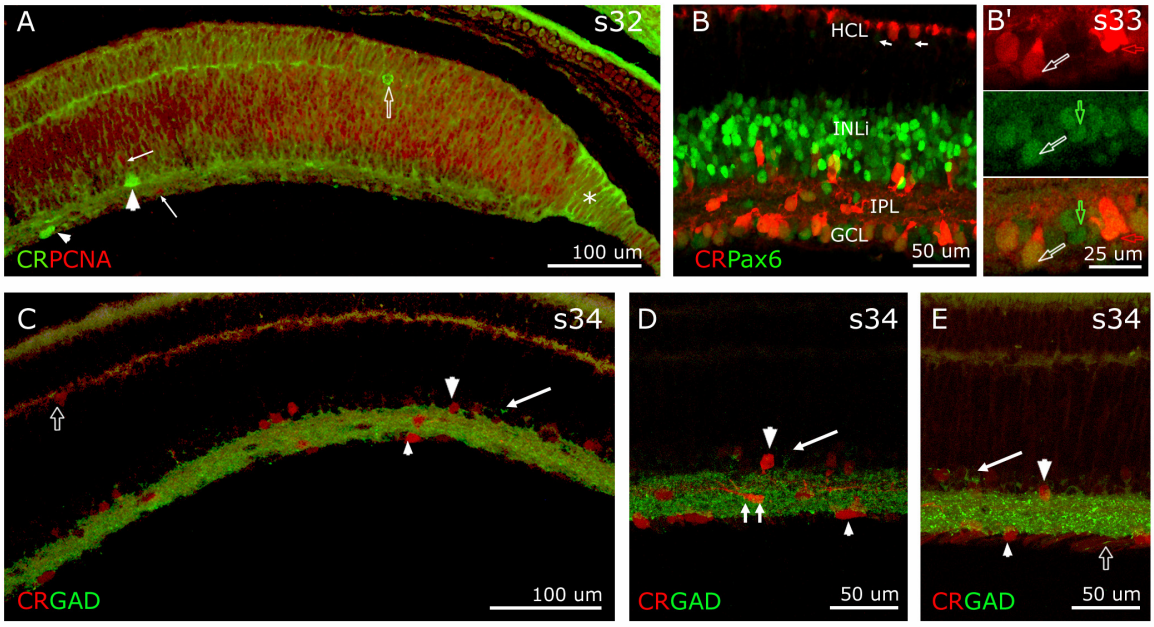

Chapter 9.

Spatiotemporal organization of TH and 5-HT immunoreactivity in the shark retina

INTRODUCTION

Biogenic amines such as dopamine, noradrenaline, adrenaline (catecholamines) and serotonin (indolamine) have been detected in some cell bodies at very early stages of differentiation. These neurochemical markers may be useful for distinguishing neurochemically differentiated cells from differentiating cells. Dopamine and serotonin (5-HT) occur at high concentrations in the retina of all vertebrates studied, where they play a role as neurotransmitters or neuromodulators. In particular, dopamine is believed to control increased signal transmission in cone rather than rod circuits (reviewed in Witkovsky, 2004), while 5-HT is involved in lateral inhibition and promotes the responses of bipolar cells to photoreceptor inputs (Brunken et al., 1993). Antibodies directed against the enzyme tyrosine hydroxylase (TH), which catalyzes the rate-limiting step in catecholamine synthesis, have largely been used as markers of catecholaminergic neurons. As noradrenaline and adrenaline have been detected in small quantities in the retina (Ehinger and Steinbusch, 1985), it is generally accepted that TH-immunoreactive (ir) cells in the retina are dopaminergic. The distribution of TH-ir structures in the mature retina has been analysed in a wide variety of fish species, including cartilaginous fish (chondrichthyans: Brunken et al., 1986; Frölich et al., 1995), as well as agnathans (De Miguel and Wagner, 1990; Yañez and Anadón, 1994; Dalil-Thiney et al., 1996; Abalo et al., 2008), and bony fish (Negishi et al., 1985; Yazulla and Zucker, 1988; Van Haesendonck et al., 1993; Wagner and Behrens, 1993; Becerra et al., 1994; Osborne et al., 1984; Frölich et al., 1995; Negishi and Wagner, 1997; Arenzana et al., 2006). These studies have revealed that in fish, as in tetrapods, the TH antibody is a reliable marker of a subpopulation of amacrine cells, although diverse densities of TH-ir interplexiform cells have also been reported. On the other hand, antibodies directed against 5-HT have mainly been used to study the serotonergic system in the mature retina of different vertebrates, including elasmobranchs (mammals: Osborne et al., 1982; Wilhelm et al., 1993; Lima and Urbina, 1998; birds: Wilhelm et al., 1993; reptiles: Osborne et al., 1982; Weiler and Schütte, 1985; Weiler and Ammermüller, 1986; Wilhelm et al., 1993; amphibians: Osborne et al., 1982; Gläsener et al., 1988; Schütte and Witkovsky, 1990; Zhu and Straznicky, 1990; Liu and Debski, 1993; Wilhelm et al., 1993; bony fish: Osborne et al., 1982; Marc et al., 1988; Hayashi et al., 1986; Wilhelm et al., 1993; Jaffe et al., 1987; Lima and Urbina, 1998; cartilaginous fish: Ritchie and Leonard, 1983; Brunken et al., 1986; Schlemermeyer and Chappell, 1996; agnathans: Versaux-Botteri et al., 1991). These studies have shown 5-HT to be a reliable

marker of 5-HT synthesizing amacrine cells, although 5-HT accumulating amacrine and/or bipolar cells have also been found. Differentiation of 5-HT amacrine cells has been related to the processing of visual information, as the development of these cells occurs concomitantly with the establishment of synaptic contacts (Fosser et al., 2005). In addition, there is evidence that dopamine is used as a developmental signal in the embryonic retina (Reis et al., 2007). Although ontogenetic studies are essential to establish how these neurotransmitters may influence the development of the retina, such studies are scarce as regards tetrapods (amphibians: Sarthy et al., 1981; Osborne et al., 1984; Zhu and Straznicky, 1991; Zhu and Straznicky, 1992; Liu and Debski, 1993; González et al., 1995; Dünker, 1997; Huang and Moody, 1998; Dünker, 1999; chick: Chung et al., 1975; Kato et al., 1984; Osborne et al., 1984; Kagami et al., 1991; Gardino et al., 1993; Ríos et al., 1997; Dos Santos and Gardino, 1998; mammals: Kato et al., 1980; Lam et al. 1981; Osborne et al., 1984; Osborne and Patel., 1984; Parkinson and Rando, 1984; Parkinson et al., 1985; Evans and Battelle, 1987; Mitrofanis et al., 1988; Martin-Martinelli et al., 1989; Mitrofanis et al., 1989; Wulle and Schnitzer, 1989; Mitrofanis and Finlay, 1990; Wang et al., 1990; Yew et al., 1991; Casini and Brecha, 1992; Mitrofanis et al., 1992; Versaux-Bottery, 1992; Jotwani et al., 1994; Witkovsky et al., 2005), bony fish (Osborne et al., 1984; Negishi et al., 1990; Becerra et al., 1994; Negishi and Wagner, 1995; Arenzana et al., 2006; Candal et al., 2008) and agnathans (Villar-Cerviño et al., 2006; Abalo et al., 2008), and are totally lacking for cartilaginous fish.

In the present study, we analysed for the first time the TH and 5-HT expression patterns in the retina of *Scyliorhinus canicula* and *Haploblepharus fuscus* throughout a wide range of stages of development from early embryos to adults, comparing the patterns with those already described for fish and other vertebrates. We focused on developmental aspects of the dopaminergic and serotonergic phenotype, emphasizing its relation to spatiotemporal patterns of retinal maturation described in relation to the expression of Pax6 (a transcription factor with essential roles during retinogenesis; see Chapter 5). In addition, we carried out double immunofluorescence studies to provide a more complete neurochemical characterisation of retinal neurons immunolabelled for TH and/or 5-HT, and with respect to subpopulations of amacrine cells characterised by expressing glutamic acid decarboxylase (GAD; see Chapter 7) and calretinin (CR; see Chapter 8).

MATERIAL AND METHODS

Experimental animals

Embryos, juveniles and adult specimens of the lesser spotted dogfish (S. *canicula*) and the brown shyshark (*H. fuscus*) were provided by the Aquário Vasco da Gama and the Oceanário in Lisbon (Portugal), the Aquarium Finisterrae in A Coruña (Spain). Embryos of *S. canicula* were additionally acquired from the Station Biologique de Roscoff (France). Specimens were transported to the laboratory and maintained as described (see Chapter 5). The embryonic stages of *S. canicula* were identified by external features according to Ballard et al. (1993) and similar features were considered in staging the *H. fuscus* embryos. For TH immunohistochemistry, we analysed the following embryonic stages: stage 26 (4 *S. canicula* embryos), stage 27 (4 *S. canicula* embryos), stage 28 (2 *S. canicula* embryos), stage 29 (2 *S. canicula* and 1 *H. fuscus* embryos), stage 30 (4 *S. canicula* and 1 *H. fuscus* embryos), stage 31 (2 *S. canicula* embryos), stage 32 (4 *S. canicula* embryos), and stages 33-34 (prehatching: 8 *H. fuscus* embryos). Moreover, 7 juveniles (1 *S. canicula* and 6 *H. fuscus*, from 10 to 14 cm in total length) and 1 adult *S. canicula* (about 50 cm in total length) were also processed. For 5-HT immunohistochemistry, the following embryonic stages were used: stage 26 (2 *S. canicula* embryos), stage 27 (2 *S. canicula* embryos), stage 28 (1 *S. canicula* embryos), stage 29 (1 *H. fuscus* embryos), stage 30 (3 *S. canicula* and 1 *H. fuscus* embryos), stage 31 (2 *S. canicula* and 1 *H. fuscus* embryos), stage 32 (3 *H. fuscus* embryos), and stages 33-34 (prehatching: 7 *H. fuscus* embryos). In addition, 6 juveniles (1 *S. canicula* and 5 *H. fuscus*, from 10 to 14 cm in total length) and 1 adult *S. canicula* (about 50 cm total length) were also used.

Tissue preparation

Adequate measures were taken to minimize pain or discomfort. All procedures conformed to the guidelines established by the Spanish Royal Decree 223/1998 for animal experimentation and were approved by the ethics committee of the University of Santiago de Compostela. Embryos were anaesthetized and separated from the yolk before fixation in 4% paraformaldehyde (PFA) in elasmobranch phosphate buffer for 48-72 h depending on the stage as described in Chapter 5. Prehatching, juvenile and adult specimens were deeply anaesthetized and then perfused intracardially with elasmobranch Ringer's solution (1.7% NaCl, 0.024% KCl, 0.031% CaCl2, 0.044% MgCl2, 0.113% Na2SO4, 0.049% NaCO3H, and 2.7%

urea) followed by the appropriate fixative. Eyes of stage 32-34 embryos, juveniles and adults were dissected out and postfixed for 4 h in 4% PFA. Specimens were cryoprotected with 30% sucrose in phosphate buffer, embedded in OTC compound (Tissue Tek, Torrance, CA), and frozen with liquid nitrogen-cooled isopentane. Parallel series of sections (14–18 µm thick) were cut on a cryostat along the dorsoventral or nasotemporal axis of the retina (transverse or sagittal planes with respect to the brain, respectively), and mounted on Superfrost Plus (Menzel-Glasser1) slides.

Antibody characterisation

The mouse monoclonal antiserum against TH from Chemicon (now Millipore, Billerica, MA) was obtained by using as immunogen TH purified from PC12 cells. According to the data sheet, 1) it recognizes an epitope on the outside of the regulatory N-terminus; 2) it does not react on Western blots with dopamine-beta-hydroxylase, phenylalanine hydroxylase, trytophan hydroxylase, dehydropteridine reductase, sepiapterin reductase or phenethanolamine-N-methyl transferase, 3) it recognizes a protein of approximately 59-61 kDa by Western blot. In addition, the antiserum gives a single band of 56-60 kDa when tested on Western blot of *S. canicula* brain extracts (Iván Carrera, personal communication). It stains specifically dopaminergic amacrine cells in the retina of mouse and rat (Witkowsky et al., 2008).

The polyclonal antiserum to 5-HT from rabbit was obtained by Diasorin/Immunostar (Hudson, WI; previously IncStar, Stillwater, MN) by using as immunogen 5-HT coupled to bovine serum albumin (BSA) with paraformaldehyde. The specificity of the Immunostar 5-HT antiserum was tested by the manufacturer using standard immunohistochemical methods. According to the data sheet, 1) the antiserum demonstrates significant labelling of rat hypothalamus, raphe nuclei, and spinal cord using indirect immunofluorescence and biotin/avidin–horseradish peroxidase (HRP) techniques; 2) the antiserum diluted 1/20,000 does not react with 5 µg, 10 µg, and 25 µg amounts of 5-hydroxytryptophan, 5-hydroxyindole-3-acetic acid, and dopamine using the BSA/HRP labelling method; and 3) the pretreatment of the diluted antiserum with 25 µg of 5-HT coupled to BSA completely eliminated the staining. In addition, the specificity of the immunoreaction in *S. canicula* was tested by Carrera et al. (2008) by preadsorbing the primary antibody with the 5-HT-BSA conjugate used for

generation of the antiserum. The immunolabelling was completely abolished in *S. canicula* sections treated with the primary antibody at working dilution preadsorbed with the 5-HT-BSA conjugated at a concentration of 10μg/mL at 4°C for 24 hours. The antiserum has previously been tested in several nonmammalian species, including fishes, and shows no crossreaction with other monoamines (Stuesse and Cruce, 1992; Marín et al., 1998; Adrio et al., 1999; Antri et al., 2006; Abalo et al., 2007). For characterisation of Pax6, GAD and CR antibodies, see Chapters 5, 7 and 8, respectively.

TH immunohistochemistry

For heat induced epitope retrieval, sections were pretreated with 0.01M citrate buffer pH 6.0 for 30 min at 95°C, and allowed to cool for 20-30 minutes at room temperature (RT). Sections were rinsed twice in 0.05 M Tris-buffered saline at pH 7.4 (TBS) for 5 min each, and then processed by the peroxidase-antiperoxidase (PAP) method with a mouse anti-TH monoclonal antiserum as primary antibody (Chemicon; diluted 1:1000), overnight at RT. The sections were then rinsed in TBS (two 15-min rinses) and endogenous peroxidase was blocked with 10% H_2O_2 in phosphate buffered saline pH 7.4 (PBS) for 30 min at RT. Sections were rinsed in TBS, incubated in goat anti-mouse IgG (Dako; 1:50) for 1 h at RT, rinsed again in TBS, and incubated in mouse PAP complex (Dako; 1:400) for 30 min at RT. The immunoreaction was developed with SIGMAFAST™ 3,3'-Diaminobenzidine (DAB) tablets, as indicated by the manufacturers. All dilutions were made with TBS containing 15% normal goat serum (Dako) and 0.1% Tween-20, and all incubations were carried out in a humid chamber. Finally, the sections were dehydrated, mounted and coverslipped. As negative controls, the primary, secondary or tertiary antibodies were omitted. No immunostaining was observed in the control sections. Photographs were taken with an Olympus DP71 colour digital camera, fitted to a Provis microscope (Olympus, Tokyo).

5-HT immunohistochemistry

Sections were pretreated as above for heat induced epitope retrieval, rinsed in 0.05 M Tris-buffered saline pH 7.4 (TBS) for 5 min, and incubated with a rabbit anti-5-HT polyclonal antiserum as primary antibody (IncStar, Stillwater, MN; diluted 1:5000), overnight at RT. Sections were treated as above but using goat anti-rabbit IgG (Dako; 1:100) and rabbit PAP

complex (Dako; 1:100) as secondary and tertiary antibodies. The specificity of the 5-HT antiserum has been previously tested by preabsorbing the primary antibody with the 5-HT-BSA conjugate used for generation of the antiserum, which completely abolished the immunolabelling (Carrera et al., 2008). Negative controls performed by omitting the primary, secondary or tertiary antibodies showed no immunostaining.

Double immuofluorescence

Sections were pretreated as above for epitope retrieval, and allowed to cool for 20-30 minutes at room temperature. Sections were rinsed twice in 0.05 M Tris-buffered saline containing 0.1% Tween-20 at pH 7.4 (TBS-T) for 5 min each, and then incubated with combinations of the following primary antibodies, overnight at RT: anti-TH mouse monoclonal antiserum (Chemicon; diluted 1:500), anti-5-HT swine polyclonal antiserum (IncStar, Stillwater, MN; diluted 1:2500), anti-Pax6 polyclonal rabbit antiserum (Covance, diluted 1:200), anti-GAD65/67 sheep polyclonal antiserum (kindly provided by Dr. E.Mugnaini; dilution 1:30,000), and anti-CR polyclonal rabbit antiserum (Swant, diluted 1:250). The sections were then rinsed in TBS-T (two 10-min rinses). Secondary antibodies were used as follows: for TH-5-HT immunofluorescence, FluoProbes 546 Goat-anti-Mouse (Interchim, France; diluted 1:100) and TRITC-conjugated Swine-anti-Rabbit immunoglobulins (Dako, Denmark; diluted: 1:20); for TH-Pax6 immunofluorescence, FluoProbes 546 Goat-anti-Mouse (Interchim, France; diluted 1:100) and Alexa Fluor 488 Goat-anti-Rabbit immunoglobulins (Molecular Probes, The Netherlands; diluted 1:200); for TH-GAD65/67 immunofluorescence, FluoProbes 546 Goat-anti-Mouse (Interchim, France; diluted 1:100) and Alexa Fluor 488 Donkey-anti-Sheep IgG antibodies (Molecular Probes, The Netherlands; diluted 1:200); for TH-CR immunofluorescence, FluoProbes 546 Goat-anti-Mouse (Interchim, France; diluted 1:100) and Alexa Fluor 488 Goat-anti-Rabbit immunoglobulins (Molecular Probes, The Netherlands; diluted 1:200); for 5-HT-Pax6 immunofluorescence, FluoProbes 546 Goat-anti-Mouse (Interchim, France; diluted 1:100) and Alexa Fluor 488 Goat-anti-Rabbit immunoglobulins (Molecular Probes, The Netherlands; diluted 1:200). All dilutions were made with Tris-buffered saline (TBS) containing 0.2% of Triton X-100 (Sigma) and 15% of the appropriate normal serum. All incubations were carried out in a humid chamber. Sections were rinsed in TBS for 30 min, then in distilled water (twice for 30 min), and allowed to dry for 2 h at 37°C. Sections were mounted in MOWIOL 4-88 Reagent (Calbiochem, Merk KGaA; Darmstadt,

Germany), allowed to dry for 30-60 minutes at 37°C, and observed in a Leica Spectral Confocal Laser Scanning Microscope (TCS-SP2).

RESULTS

Three developmental periods have been described in the retina of sharks as regards its growth pattern (for details of the spatiotemporal sequence of formation of retinal layers see Chapter 5). The *first developmental period* (stages 26 to 29) refers to the neuroepithelial retina; the *second developmental period* (stages 30 to 32) refers to the layering retina; the *third developmental period* (stages 33 to 34) shows the mature organization characteristic of postembryonic stages.

Immunoreactivity to TH in the developing retina

During the *first developmental period*, immunoreactivity to TH was not observed in the retina of the sharks studied. TH-ir cells were first detected in the inner part of the inner nuclear layer (INLi; amacrine cells) during the last part of the *second developmental period* (at middle stage 32). These amacrine cells showed differences in size and shape (Figs. 1A, B) and TH immunoreactivity was mostly concentrated at the periphery of somata. Processes from these cells coursed to the inner plexiform layer (IPL). In *H. fuscus*, but not in *S. canicula*, TH-ir cells appeared in the horizontal cell layer (HCL) during this developmental period (Figs. 1C, D).

During the *third developmental period*, the number of TH-ir cells increased in the INLi (Fig. 1E) and, in *H. fuscus*, in the HCL. Perikarya were round, oval or pear-shaped and showed small variation in size (Figs. 1F, G). Smooth processes coursed to the IPL and were mainly distributed in sublayers 1 and 3. Generally, processes were more stained that the perikarya (Figs. 1F, G). TH immunoreactivity was not homogeneously distributed in the retina. Differences were observed regarding distribution of TH-ir cells and processes, since they extended in the dorsal half of the retina along the nasotemporal axis (Fig. 1E), and were restricted to the peripheral retina in the temporal pole. In both species, TH-ir radial processes were never observed in the outer part of the inner nuclear layer (INLo).

In juveniles, the density of TH-ir amacrine cells in the INLi decreased greatly (Figs. 1H, I). As in previous developmental stages, they showed some slight variations in shape and size. Most cells showed a monopolar or bipolar appearance and formed a loose network of varicose processes extending throughout the entire circumference of the retina, mainly distributed in sublayers 1 and 3 and in a less extent in sublayer 5 (Figs. 1H-K). The spatiotemporal pattern of TH immunoreactivity did not change with respect to that described in earlier stages of development, i.e., TH-ir cells were consistently observed in the dorsal half of the retina, although in the nasotemporal axis, the more temporal the section considered, the more restricted the area in which TH-ir cells and processes were observed. In juvenile *H. fuscus*, TH-ir cells were still observed in the HCL but became restricted to the peripheral retina (compare Figs. 1H and 1I). In both species, TH-ir radial processes connecting the two plexiform layers were never observed in the INLo.

Immunoreactivity to 5-HT in the developing retina

No differences between the two shark species were observed in the distribution of 5-HT immunoreactivity in the developing and mature retinas.

As for TH, 5-HT-ir cells were first detected at the end of the *second developmental period* (stage 32) in the layered region of the retina. Some strongly stained 5-HT-ir perikarya were observed in the INLi, mostly close to the IPL, although some cells occupied the second or third tier of perikarya in the inner nuclear layer (INL; Fig. 2A). The cells were oval-shaped and uniformly labelled. Cell processes were very thin and pale (Fig. 2B). At stage 32, 5-HT-ir cells were more abundant in the nasal and temporal poles of the retina, and some 5-HT-ir rounded cells were observed in the ventral and dorsal parts of the retina (Fig. 2C). In contrast, in those regions where the IPL had not yet formed, 5-HT immunoreactivity was not detected in any cell body. Some 5-HT-ir fibres were observed in the distal portion of the optic nerve and in the optic chiasm but not in the optic nerve head or proximal levels of the optic nerve (Fig. 2C).

In prehatching embryos, the central retina showed strongly stained 5-HT-ir amacrine cells in the INLi (Fig. 2D) but these cells were absent in the peripheral retina. The 5-HT-ir perikarya were oval or round and their varicose processes formed a thin network in the sublayers 1 and 3 of the IPL (Fig. 2E). No 5-HT-ir cells were observed in the ganglion cell

layer (GCL). Long 5-HT-ir varicose fibres were observed coursing in the optic fibre layer (Fig. 2F) and the optic nerve (Fig. 2G).

In juveniles, 5-HT-ir amacrine cells were observed in the INLi along the differentiated retina but not in the marginal growing zone (Fig. 2H). 5-HT-ir cells were rounded or oval, and showed slight variations in size (Figs. 2I-K). Processes from 5-TH-ir cells branched in the IPL forming varicose processes distributed loosely in sublayers 1 and 3 that reached the marginal growing zone of the retina (Figs. 2I-K). 5-HT-ir fibres were also observed in the optic fibre layer (Fig. 2K) and optic nerve (not shown).

TH-ir and 5-HT-ir cells form separate populations, and 5-HT co-express Pax6.

Double labelling experiments with TH and 5-HT antibodies were performed in order to further characterise the subpopulations of catecholaminergic and serotonergic amacrine cells in the retina of prehatching embryos and juveniles. In prehatching embryos, TH-ir and 5-HT-ir amacrine cells formed separate populations in the INLi (Figs. 3A, B). Processes of these cells codistributed in the IPL but showed different appearance (Figs. 3A, B). Similar patterns of these amacrine cells were found in juveniles, and colocalisation of TH and 5-HT immunoreactivities was not observed in perikarya or processes (Fig. 3C). TH-ir and 5-HT-ir cells were occasionally close to each other (Fig. 3C).

To further characterise the populations of TH-ir cells in different retinal layers, the patterns of TH immunoreactivity in prehatching embryos and juveniles were compared with those of the other immunomarkers used in this work by means of double immunofluorescence. This analysis revealed that TH-ir amacrine cells were codistributed in the INL with Pax6-ir (Figs. 3D-F), GAD-ir (Fig. 3G) and CR-ir cells (Figs. 3H, I). In *H. fuscus*, TH-ir horizontal cells codistributed with GAD-ir and CR-ir horizontal cells in the HCL (not shown). However, colocalisation of TH and these substances was not observed in cells or processes of any layer (Figs. 3D-I).

Codistribution of 5-HT and Pax6 immunoreactivities was also studied. Interestingly, all strong 5-HT-ir amacrine cells in the INLi were found to be Pax6-ir cells (Figs. 3J, K), while pale 5-HT-ir cells were Pax6-immunonegative (Figs. 3J, L).

DISCUSSION

Antibodies raised against TH and 5-HT have revealed the presence of catecholaminergic and serotonergic amacrine cells in retinas of vertebrates, including elasmobranchs (Ritchie and Leonard, 1983; Brunken et al., 1986; Frölich et al., 1995; Schlemermeyer and Chappell, 1996). In the present study we extend these observations to other two shark species and, most important, we first report the development of these populations. The onset of TH and 5-HT expression in specific populations of amacrine cells in the INLi of both sharks coincides with the layering of the retina, which occurs in the central retina of stage 32 embryos (late *second developmental period*), and progressed until hatching from central to periphery

TH as marker of dopaminergic cells in the differentiated (layered) retina of *S. canicula* and *H. fuscus*

TH immunoreactivity in *S. canicula* and *H. fuscus* was first detected in cells and processes in the INLi and IPL, respectively. The density of TH-ir cells in the INL increased as layering progressed in prehatching embryos, but decreased from juveniles onwards, once layering was achieved in the whole retina. This decrease is opposite to the pattern observed in trout, in which dopaminergic cells increased in number throughout the fry and juvenile stages, and reached about 20% of the total number found in adults (Becerra et al., 1994). In *H. fuscus* (but not in *S. canicula*), TH immunoreactivity was observed in horizontal cells and in a plexus in the HCL in the same developmental period as in the INLi and IPL (stage 32). In other fish such as the trout, in which a dopaminergic plexus was described in the HCL, it appears later (in juveniles) than in the INL, where it was already observed in embryos (Becerra et al., 1994).

The morphology and distribution of dopaminergic cells has been investigated in agnathan, bony and cartilaginous fishes (see references below). In lampreys (De Miguel and Wagner, 1990; Yañez and Anadón, 1994) and teleosts (Osborne et al., 1984), TH-immunoreactivity has been associated with specific populations of amacrine cells. In the rainbow trout, TH-ir cell bodies were detected in the INLi, which showed radially oriented, thick dendrite processes running to the IPL, and tangential processes showing a number of varicosities (Wagner and Behrens, 1993; Becerra et al., 1994). However, some differences were observed with respect

to the patterns found in sharks (present observations), since in trout, a small number of TH-ir cells (12-17 per retina) have been reported to be displaced to the GCL. Despite the two sublayers found in sharks (present results), three levels of stratification have been detected in the IPL of trout (Wagner and Behrens, 1993).

In the retina of fish, a third type of TH-ir cells has been defined in addition to amacrine and displaced amacrine cells, i.e. the interplexiform cells, which have an amacrine-like somata on the INL and processes ramifying in both the IPL and outer plexiform layer (OPL) (Gallego, 1971; Van Haesendonck et al., 1993). The presence of TH-immunoreactive (-ir) processes in both the IPL and OPL has been demonstrated in the lamprey (De Miguel and Wagner, 1990; Dalil-Thiney et al., 1996), their external processes being in close contact with horizontal cell processes and photoreceptor terminals. Same patterns were found in most bony fishes, where thinner axonal processes run to the HCL and input to horizontal cells, but not to photoreceptors (Wagner and Behrens, 1993; Becerra et al., 1994). In *S. canicula* and *H. fuscus*, TH-ir cells of the INLi were amacrine cells, as found in *Raja*, *Mustelus* or *Squalus* (Brunken et al., 1986) and unlike that observed in the retina of teleosts, which possess dopaminergic interplexiform cells exhibiting processes contacting the OPL (Wagner and Behrens, 1993; Becerra et al., 1994). The observation of TH-ir processes in both the IPL and OPL of the shark *Scyliorhinus leviatus* and the ray *Dalatias licha* has been related to the presence of interplexiform cells in these species, despite the absence of sclerally-directed TH-ir processes (Frölich et al., 1995). As in cartilaginous fish, different results have been obtained regarding the densities of TH-ir interplexiform cells in bony fish species. In goldfish the dopamine system is predominantly composed of interplexiform cells (Yazulla and Zucker, 1988), but low densities of these cells have been found in trout and zebrafish (Wagner and Behrens, 1993; Becerra et al., 1994; Arenzana et al., 2006), and the cells were absent from carp (Negishi et al., 1985). Variable densities of interplexiform cells have also been reported in a number of species of tetrapods (mammals: Dowling et al., 1980; Oyster et al., 1985; Ryan and Hendrickson, 1987; Lugo-García and Blanco, 1993; Negishi et al., 1995; Jeon et al., 2001, among others; amphibians: Schütte and Witkovsky, 1991; reptiles: Lanuza et al., 1996; birds: Dkhissi et al., 1993), which may reflect differences in function (Smeets and González, 2000).

5-HT as marker of serotonergic cells in the differentiated (layered) retina of *S. canicula* and *H. fuscus*

The morphology and distribution of 5-HT-ir neurons were demonstrated in the retina of developing and adult shark by using an antibody against 5-HT. No differences were observed in the distribution of 5-HT immunoreactivity throughout the developing retina of the two species. 5-HT immunoreactivity was first detected in the INLi at the end of the *second developmental period*, only in regions where the IPL can be distinguished, their numbers and localisations roughly coinciding with those observed in adults (see above). From prehatching embryos onwards processes from 5-HT-ir cells generated a network of thin varicose processes in the IPL, which extended from the central to the peripheral retina, a pattern that is coincident with that observed in the mature retina. Although density analyses were not performed in the present study, we observed that the total number of 5-HT-ir cells decreased in the retina from prehatching embryos onwards. The density of 5-HT-ir cells also decreases in the adult retina of some amphibians (Zhu and Straznicky, 1992; Dünker, 1999), although in frog, an increase in both the proportion and the staining intensity of these cells as the animal matures has been reported (Liu and Debski, 1993). Variations in the density of 5-HT-ir cells during retinal maturation have not been analysed in other vertebrates, making further comparisons difficult. It has been suggested that in the embryonic retina, 5-HT may play a developmental role in neurogenesis, affecting the development and subsequent differentiation of cells and neuronal pathways (Meier et al., 1991), although the reason why 5-HT decreases in cells throughout development remains unclear.

In the mature retina of both *S. canicula* and *H. fuscus*, 5-HT immunoreactivity was found in cells throughout the INLi, suggesting the presence of a population of 5-HT containing amacrine cells in these species. Like TH-ir cells, they showed slight differences in size and shape, their processes mainly running in two sublayers within the IPL to the ciliary marginal zone (the wedge-shaped neuroepithelial zone that lies between the laminated retina and the ciliary epithelium; see Chapters 5-7). Amacrine cells containing 5-HT have also been described in other elasmobranch species (Ritchie and Leonard, 1983; Brunken et al., 1986), in agnathans (Versaux-Botteri et al., 1991), teleosts (Osborne et al., 1982; Hayashi et al., 1986; Jaffe et al., 1987; Marc et al., 1988; Wilhelm et al., 1993; Lima and Urbina, 1998), amphibians (Osborne et al., 1982; Gläsener et al., 1988; Schütte and Witkovsky, 1990; Zhu and Straznicky, 1990; Liu and Debski, 1993; Wilhelm et al., 1993; Dünker et al., 1999), reptiles

(Osborne et al., 1982; Witkovsky et al., 1984; Weiler ans Schütte, 1985; Weiler and Ammermüller, 1986; Wilhelm et al., 1993), chick (Osborne, 1982; Wilhelm et al., 1993; Ríos et al., 1997) and some mammals (Osborne et al., 1982), although not in mouse or rat (Mikkelsen, 1988; Lima and Urbina, 1998).

Several types of 5-HT-ir cells other than INL-located amacrine cells have been described in vertebrates on the basis of the soma sizes, density, location of the somata, and the arrangement of their processes within the IPL. However, patterns of 5-HT-associated neurons differ across or even within species as a result of problems in discriminating true serotonergic neurons from a larger set of 5-HT accumulating cells, especially when using formaldehyde-induced fluorescence (FIF) methods that involve preloading retinas with high levels of indole-like ligands, or autoradiography methods after uptake of ^{3}H-5-HT (Marc et al., 1988 and references therein). The use of 5-HT immunocytochemical staining has been alternatively or additionally used to analyse the morphology and distribution of other 5-HT-containing cell types, apart from the generally accepted amacrine cells. Thus, some 5-HT-ir cells are thought to be displaced amacrine cells in the GCL of elasmobranchs and amphibians (Brunken et al., 1986; Zhu and Straznicky, 1990) and in the IPL of lampreys (Versaux-Botteri et al., 1991). Some 5-HT-ir ganglion cells have been described in lampreys, amphibians and reptiles (Weiler and Schütte, 1985; Weiler and Ammermüller, 1986; Versaux-Botteri et al., 1991; Liu and Debski, 1993; Dünker, 1999). In addition, 5-HT -containing bipolar cells have been found in the retina of the skate (Schlemermeyer and Chappell, 1996), goldfish (Marc et al., 1998), amphibians (Schütte and Witkovsky, 1990; Dünker, 1999), turtle (Wilhelm et al., 1993; Witkovsky et al., 1984; Weiler and Schütte, 1985) and chick (Wilhelm et al., 1993; Ríos et al., 1997). These bipolar cells were not observed in *S. canicula* and *H. fuscus*. However, the use of double labelling with anti-5-HT and anti-phenylalanine hydroxylase antibodies (the latter recognizing one of the synthesizing enzymes for 5-HT) has revealed that, although most 5-HT-ir amacrine cells in the non-mammalian retina are the source of endogenous 5-HT, some 5-HT-ir amacrine and bipolar cells only accumulate 5-HT (Wilhelm et al., 1993). As the aim of the present study was to establish the ontogeny of this neurotransmitter and its possible involvement in the development of the retina, it has not been ascertained here if some 5-HT-ir amacrine cells found in *S. canicula* and *H. fuscus* are 5-HT-accumulating but not 5-HT-synthesizing neurons. Nevertheless, immunohistochemical labelling of these neurons

still constitutes a powerful method of selective marking, enabling further investigation into their participation in retinal circuitry.

Importantly, 5-HT-ir fibres were observed in the optic fibre layer and optic nerve of *S. canicula* and *H. fuscus* (present results; Carrera et al., 2008). In adult elasmobranchs, 5-HT-ir fibres were observed in the optic nerve of the stingray (Ritchie and Leonard, 1983), and in the optic fibre layer (but not in the optic nerve) of other elasmobranchs (*Raja*, *Mustelus* and *Squalus*; Brunken et al., 1986), although the origin of these fibres has not been established. 5-HT-ir fibres were also detected in the optic nerve of the mouse (Mikkelsen, 1988), although 5-HT-ir neurons have not been demonstrated in mouse or rat retina (Osborne et al., 1982), suggesting that they are retinopetal fibres. As further evidence of this, serotonergic retinopetal fibres have been described in the optic nerve of goldfish and rat (Lima and Urbina, 1998). On the contrary, 5-HT-ir centrifugal fibres have been described in frog (Schütte and Witkovsky, 1990), and ganglion cells have been reported to project to the tectum of turtle (Weiler and Ammermüller, 1986) and frog (Liu and Debsky, 1995). Study of serotonergic projections in *S. canicula* and *H. fuscus* retinas may be of interest in understanding the functional role of 5-HT in the retina of elasmobranchs.

Regional differences in densities of TH-ir and 5-HT neurons throughout the retina

Although no regional differences were detected regarding the distribution of CR-ir cells throughout the *S. canicula* and *H. fuscus* retina (Chapter 8), the distribution of TH-ir cells was found to be non-homogeneous. Following the nasotemporal axis, TH-ir cells were detected throughout the dorsal half of the nasal retina, and became progressively restricted to the dorsal periphery in the temporal retina. On the contrary, TH-ir processes, which were confined to the dorsal half of the retina in all embryonic stages, extended in juveniles throughout the entire circumference of the retina. Differences in size and shape of dopaminergic cells have been reported in teleosts (Negishi et al., 1996), and depend on regional differences in density and distribution, respectively. However, the regional differences regarding densities of TH-ir cells were not spatially coincident with those observed here. In the teleost *Thamnoconus* (Negishi et al., 1996), the highest densities correspond to the temporal, nasal and peripheral margin areas of the retina, areas of intermediate density were found in a horizontal streaked band located between the temporal

and nasal retina, whereas the lowest densities were located dorsally or ventrally to this horizontal band.

The 5-HT-ir cell densities were slightly lower at the peripheral than in the central retina of sharks (present results), as also found in amphibians (Zhu and Straznicky, 1990). However, 5-HT-ir cells were evenly distributed throughout the retina, contrary to observations in *Xenopus*, where highest densities of serotonergic amacrines occur in the posterolateral quadrant, and large portions of the anteromedial quadrant lack 5-HT-like immunoreactivity (Shütte and Witkovsky, 1990).

TH/5-HT density ratios in pure-rod retinas

In fish, a close correlation has been reported between the density ratio of dopaminergic to serotonergic cells in the inner retina and the rod-to-cone ratio. This means that the TH/5-HT density ratio is high (1.9-2.7) in fish with cone densities roughly equalling rod densities, decreases as rods dominate cone numbers, and is low (0.2-0.4) in deep-sea fish with pure rod retinas (Negishi and Wagner, 1997). We found that the TH/5-HT density ratios in *S. canicula* and *H. fuscus* were low (0.27 and 0.23 per section, respectively; results not shown), which may be indicative of a pure-rod retina in both species (see also discussion in Chapter 10). Moreover, it has been reported that in fish, the differentiation of dopaminergic cells into amacrine or interplexiform cells is correlated with the absence or presence of cones, respectively, so that in pure-rod retina, they occur as amacrine cells, while in mixed rod/cone retina, they occur as interplexiform cells (Fröhlich et al., 1995). Since such differentiation does not depend on the evolutionary classification of a given species, but rather is correlated with the occurrence of rods and/or cones, this may account for general differences observed among species of teleost fish, and particularly for the absence of interplexiform cells in the retina of *S. canicula* and *H. fuscus*.

Roles of dopamine and 5-HT in the developing retina

As discussed above, some retinas have a single catecholamine system containing only amacrine cells, whereas others also contain catecholaminergic displaced amacrine, interplexiform and even horizontal cells. This heterogeneity of the catecholaminergic system implies that dopamine may not have a single physiological role in the retina (Oyster et al.,

1985). It has been suggested that possible functions of dopamine in all-rod retinas, which may not require retinomotor adaptation, may include neuromodulation in the IPL for the sensitization of the rod pathway, the shaping of biological rhythms, and the control of eye growth (Fröhlich et al., 1995). Present results in the growing shark eye are more consistent with neural roles for dopamine rather than with developmental roles, since the onset of TH immunoreactivity follows that of opsin immunoreactivity (i.e., the probable onset of visual function; see Chapter 10) and decreases greatly once networks of fibres have been established in the mature retina. However, the existence of catecholaminergic horizontal cells in *H. fuscus* reveals intriguing differences between closely-related sharks, possibly indicating differences as regards the use of dopamine by the retina.

The similar sublaminar location of serotonergic with respect to dopaminergic phenotypes observed here suggests that similar roles in development may account for 5-HT with respect to dopamine in the retina of *S. canicula* and *H. fuscus*. Accordingly, 5-HT has been suggested to play a developmental role in neurogenesis by affecting the differentiation of cells and neuronal pathways (Meier et al., 1991). In this regards, the temporal correspondence between synaptogenesis in the OPL and development of the serotonergic network in the IPL, together with the stratified organization of fibres, is consistent with previous suggestions that the topographical arrangement of 5-HT-ir amacrine cells during development may depend on neural interactions (Linden, 1992; Ríos et al., 1997), and may be related to the generation and establishment of retinal fields (Ríos et al., 1997). It has also been suggested that 5-HT-amacrine cells may play a role in the process of lateral inhibition and in the establishment of antagonistic ON/OFF retinal fields in the retina (Brunken et al., 1993; Ríos et al., 1997). The presence of 5-HT-accumulating OFF bipolar cells in the all-rod retina of skate has lead to the suggestion that it contains an OFF bipolar cell pathway in addition to the classical ON rod pathway (Schlemermeyer and Chappell, 1996). However, 5-HT-ir bipolar cells have not been observed in *S. canicula* or *H. fuscus* retinas.

Coexpression but not colocalisation of dopamine and other neural markers

Both the absence of proliferation (see Chapter 6) and the emergence of abundant CR-ir, GAD-ir and Pax-6-ir cells in the INLi precede the appearance of TH-ir cells in the same layer at stage 32. In *H. fuscus*, TH-ir cells were also found in the HCL, together with CR-ir and

GABA/GAD-ir cells. Since this combination of populations persisted in the INLi and HCL, we checked whether colocalisation of TH and other markers existed in immunostained *S. canicula* and *H. fuscus* sections, which may indicate a functional role of GAD and/or Pax6 in the development of some dopaminergic cells. The present observations with a double-labelling approach demonstrate that TH-ir cells and processes do form a separate population from the CR-ir, 5-HT-ir, GAD-ir, Pax6-ir and GAD/Pax6-ir cells. Colocalisation of GABA and TH has been also analyzed in the retina of various vertebrate species to determine whether the coexistence of GABA and dopamine reported earlier in mammals is common to other vertebrates. It has been reported that GABA-ir cells constitute a separate population from TH-ir cells in fish and amphibians, whilst in reptiles, birds and mammals, all dopaminergic cells are also GABA-like-ir (Wulle and Wagner, 1990 and references therein). Instead, in the retina of sharks (present results), single Pax6-ir cells were located close but separately from TH-ir cells. Similar observations have been reported in zebrafish brain in regions where Pax6 and TH cells were mixed, which leaded to the suggestion that the former have an inductive action on prospective TH cells (Wullimann and Rink, 2001).

As described for TH immunoreactivity, the appearance of 5-HT immunoreactivity in the INLi at stage 32 ensures the emergence of CR-ir, GAD-ir and Pax-6-ir cells in the same cell layer. In sharks, Pax6 was found in most 5-HT-ir amacrine cells in the INLi (present results). Of note, a correlation was found between the intensity of both markers, as Pax6 was only found in cells with strong 5-HT immunoreactivity. To our knowledge, this is the first report of Pax6 expression by serotonergic amacrine cells.

REFERENCES

Abalo XM, Villar-Cerviño V, Villar-Cheda B, Anadón R, Rodicio MC (2008). Neurochemical differentiation of horizontal and amacrine cells during transformation of the sea lamprey retina. J Chem Neuroanat, 35: 225-232.

Abalo XM, Villar-Cheda B, Meléndez-Ferro M, Pérez-Costas E, Anadón R, Rodicio MC (2007). Development of the serotonergic system in the central nervous system of the sea lamprey. J Chem Neuroanat, 34: 29-46.

Adrio F, Anadón R, Rodríguez-Moldes I (1999). Distribution of serotonin (5HT)-immunoreactive structures in the central nervous system of two chondrostean species (*Acipenser baeri* and *Huso huso*). J Comp Neurol, 407: 333-348.

Antri M, Cyr A, Auclair F, Dubuc R (2006). Ontogeny of 5-HT neurons in the brainstem of the lamprey, *Petromyzon marinus*. J Comp Neurol, 495: 788-800.

Arenzana FJ, Arévalo R, Sánchez-González R, Clemente D, Aijón J, Porteros A (2006). Tyrosine hydroxylase immunoreactivity in the developing visual pathway of the zebrafish. Anat Embryol, 211: 323-234.

Ballard W, Mellinger J, Lechenault H (1993). A series of normal stages for development of *Scyliorhinus canicula*, the lesser spotted dogfish (Chondrichthyes: Scyliorhinidae). J Exp Zool, 267: 318-336.

Becerra M, Manso MJ, Rodríguez-Moldes MI, Anadón R (1994). The structure and development of dopaminergic interplexiform cells in the retina of the brown trout, *Salmo trutta fario*: a tyrosine hydroxylase immunocytochemical study. J Anat, 185: 377-385.

Brunken WJ, Jin XT, Pis Lopez AM (1993). The properties of the serotoninergic system in the retina. Prog Retinal Eye Res, 12: 75-99.

Brunken WJ, Witkovsky P, Karten HJ (1986). Retinal neurochemistry of three elasmobranch species: an immunohistochemical approach. J Comp Neurol, 243: 1-12.

Candal E, Ferreiro-Galve S, Anadón R, Rodríguez-Moldes I (2008). Morphogenesis in the retina of a slow-developing teleost: emergence of the GABAergic system in relation to cell proliferation and differentiation. Brain Res, 1194: 21-27.

Carrera I, Molist P, Anadón R, Rodríguez-Moldes I (2008). Development of the serotoninergic system in the central nervous system of a shark, the lesser spotted dogfish *Scyliorhinus canicula*. J Comp Neurol, 511: 804-831.

Casini G, Brecha NC (1992). Postnatal development of tyrosine hydroxylase immunoreactive amacrine cells in the rabbit retina: I. Morphological characterization. J Comp Neurol, 326: 283-301.

Chung SH, Stirling RV, Gaze RM (1975). The structural and functional development of the retina in larval *Xenopus*. J Embryol Exp Morphol, 33: 915-940.

Dalil-Thiney N, Versaux-Botteri C, Nguyen-Legros J (1996). Electron microscopic demonstration of tyrosine hydroxylase-immunoreactive interplexiform cells in the lamprey retina. Neurosci Lett, 207: 159-162.

De Miguel E, Wagner HJ (1990). Tyrosine hydroxylase immunoreactive interplexiform cells in the lamprey retina. Neurosci Lett, 113: 151-155.

Dkhissi O, Dalil-Thiney N, Versaux-Botteri C, Chanut E, Repérant J, Nguyen-Legros J (1993). Dopaminergic interplexiform cells in the retina of pigmented and hypopigmented quails (*Coturnix coturnix japonica*). Ophthalmic Res, 25: 280-288.

Dos Santos RM, Gardino PF (1998). Differential distribution of a second type of tyrosine hydroxylase immunoreactive amacrine cell in the chick retina. J Neurocytol, 27: 33-43.

Dowling JE, Ehinger B, Florén I (1980). Fluorescence and electron microscopical observations on the amine-accumulatingneurons of the cebus monkey retina. J Comp Neurol, 192: 665-685.

Dünker N (1997). Development and organization of the retinal dopaminergic system of *Ichthyophis kohtaoensis* (Amphibia; Gymnophiona). Cell Tissue Res, 289: 265-274.

Dünker N (1999). Serotonergic neurons and processes in the adult and developing retina of *Ichthyophis kohtaoensis* (Amphibia; Gymnophiona). Anat Embryol, 199: 35-43.

Ehinger B, Steinbusch HW (1985). Quantitation and immunohistochemistry of catecholamines in the posterior segment of the eye. Histochemistry, 82: 435-439.

Evans JA, Battelle BA (1987). Histogenesis of dopaminecontaining neurons in the rat retina. Exp Eye Res, 44: 407-414.

Fosser NS, Brusco A, Ríos H (2005). Darkness induced neuroplastic changes in the serotoninergic system of the chick retina. Dev Brain Res, 160: 211-218.

Fröhlich E, Negishi K, Wagner HJ (1995). The occurrence of dopaminergic interplexiform cells correlates with the presence of cones in the retinae of fish. Vis Neurosci, 12: 359-369.

Gallego A (1971). Cellules interplexiformes en la retina de gato. Archivos de la Sociedad española de oftalmología Madrid, 31: 299-304.

Gardino PF, dos Santos RM, Hokoc JN (1993). Histogenesis and topographical distribution of tyrosine hydroxylase immunoreactive amacrine cells in the developing chick retina. Dev Brain Res, 72: 226-236.

Gläsener G, Schmidt C, Himstedt W (1988). Two populations of serotonin-immunoreactive neurons in the frog (*Rana esculenta*) retina. Neurosci Lett, 84: 251-254.

González A, Marín O, Smeets WJ (1995). Development of catecholamine systems in the central nervous system of the newt *Pleurodeles waltlii* as revealed by tyrosine hydroxylase immunohistochemistry. J Comp Neurol, 360: 33-48.

Hayashi T, Hirose G, Kawata M, Sano Y (1986). Cytological features of serotonin-containing neurons and their processes in the retina of the carp (Cyprinus carpio). An immunohistochemical study using flat-mount preparations. Histochemistry, 84: 423-425.

Huang S, Moody SA (1998). Dual expression of GABA or serotonin and dopamine in *Xenopus* amacrine cells is transient and may be regulated by laminar cues. Vis Neurosci, 15: 969-977.

Jaffe EH, Urbina M, Ayala C, Chemello ME (1987). Serotonin containing neurons in the retina of the teleost *Eugerres plumieri*.Vision Res, 27: 2015-2026.

Jeon YK, Kim SY, Jeon CJ (2001). Morphology of calretinin and tyrosine hydroxylase-immunoreactive neurons in the pig retina. Mol Cells, 11: 250-256.

Jotwani G, Itoh K, Wadhwa S (1994). Immunohistochemical localization of tyrosine hydroxylase, substance P, neuropeptide-Y and leucine-enkephalin in developing human retinal amacrine cells. Brain Res Dev Brain Res, 77: 285-289.

Kagami H, Sakai H, Uryu H, Kaneda T, Sakanara M (1991). Development of tyrosine hydroxylase-like immunoreactive structures in the chick retina: three-dimensional analysis. J Comp Neurol, 308: 356-370.

Kato S, Nakamura T, Negishi K (1980). Postnatal development of dopaminergic cells in the rat retina. J Comp Neurol, 191: 27-36.

Kato S, Negishi K, Teranishi T (1984). Embryonic development of monoaminergic neurons in the chick retina. J Comp Neurol, 224: 437-444.

Lam DM, Fung SC, Kong YC (1981). Postnatal development of dopaminergic neurons in the rabbit retina. J Neurosci, 1: 1117-1132.

Lanuza E, Martínez-Marcos A, Font C, Martínez-García F (1996). Catecholaminergic interplexiform cells in the retina of lizards. Vision Res, 36: 1349-1355.

Lima L, Urbina M (1998). Serotonergic projections to the retina of rat and goldfish. Neurochem Int, 32: 133-141.

Linden R (1992). Dendritic competition: a principle of retinal development. In: The visual system: From Genesis to Maturity (Lent R, ed.), pp. 86-103. Birkhäuser Boston, Boston, Basel, Berlin.

Liu Q, Debski EA (1993). Serotonin-like immunoreactivity in the adult and developing retina of the leopard frog *Rana pipiens*. J Comp Neurol, 338: 391-404.

Liu Q, Debski EA (1995). Origins of serotonin-like immunoreactivity in the optic tectum of *Rana pipiens*. J Comp Neurol, 352: 280-296.

Lugo-García N, Blanco RE (1993). Morphology and distribution of dopaminergic neurons in the ground squirrel retina. P R Health Sci J, 12: 143-146.

Marc RE, Liu WL, Scholz K, Muller JF (1988). Serotonergic and serotonin-accumulating neurons in the goldfish retina. J Neurosci, 8: 3427-3450.

Marín O, Smeets WJ, González A (1998). Basal ganglia organization in amphibians: chemoarchitecture. J Comp Neurol, 392: 285-312.

Martin-Martinelli E, Simon A, Vigni A, Nguyen-Legros J (1989). Postnatal development of tyrosine-hydroxylase-immunoreactive cells in the rat retina. Morphology and distribution. Dev Neurosci, 11: 11-25.

Meier E, Hertz L, Schousboe A (1991). Neurotransmitters as developmental signals. Neurochem Int, 19: 1-15.

Mikkelsen JD (1988). The presence of serotonin-immunoreactive nerve fibers in the optic nerve of the mouse. Neurosci Lett, 94: 253-258.

Mitrofanis J, Finlay BL (1990). Developmental changes in distribution of retinal catecholaminergic neurones in hamsters and gerbils. J Comp Neurol, 292: 480-494.

Mitrofanis J, Maslim J, Stone J (1988). Catecholaminergic and cholinergic neurones in the developing retina in the rat. J Comp Neurol, 276: 343-359.

Mitrofanis J, Maslim J, Stone J (1989). Ontogeny of catecholaminergic and choline cell distribution in the cat's retina. J Comp Neurol, 289: 228-246.

Mitrofanis J, Robinson SR, Ashwell K (1992). Development of catecholaminergic, indoleamine-accumulating and NADPHdiaphorase amacrine cells in rabbit retinae. J Comp Neurol, 319: 560-585.

Negishi K, Teranishi T, Karkhanis A, Stell WK (1990). Emergence and development of immunoreactive cells in teleost retinas during the perinatal period. Dev Brain Res, 55: 127-137.

Negishi K, Teranishi T, Kato S (1985). Retinal growth in carp of the same age: density and number of dopamine neurons. Brain Res, 350: 125-131.

Negishi K, Wagner HJ (1995). Differentiation of photoreceptors, glia, and neurons in the retina of the cichlid fish Aequidens pulcher; an immunocytochemical study. Brain Res Dev Brain Res, 89: 87-102.

Negishi K, Wagner HJ (1997). Density ratio of dopaminergic versus serotonergic cells correlates with cone-to-rod ratio in teleost retinas. Neurosci Lett, 225: 37-40.

Negishi K, Yamane Y, Yoshimoto M, Ito H (1996). Density distribution of dopaminergic neurons in the retina of a marine teleost, *Thamnoconus (Navodon) modestus*. Nippon Ika Daigaku Zasshi, 63: 343-348.

Osborne NN, Nesselhut T, Nicholas DA, Patel S, Cuello AC (1982). Serotonin-containing neurones in vertebrate retinas. J Neurochem, 39: 1519-1528.

Osborne NN, Patel S (1984). Postnatal development of serotonin-accumulating neurones in the rabbit retina and an immunohistochemical analysis of the uptake and release of serotonin. Exp Eye Res, 38: 611-620.

Osborne NN, Patel S, Vigny A (1984). Dopaminergic neurones in various retinas and the postnatal development of tyrosine-hydroxylase immunoreactivity in the rabbit retina. Histochemistry, 80: 389-393.

Oyster CW, Takahashi ES, Cilluffo M, Brecha NC (1985). Morphology and distribution of tyrosine hydroxylase-like immunoreactive neurons in the cat retina. Proc Nat Acad Sci USA, 82: 6335-6339.

Parkinson D and Rando RR (1984). Ontogenesis of dopaminergic neurons in the post-natal rabbit retina: pre- and post-synaptic elements. Brain Res, 315: 207-217.

Parkinson D, Spira A, Wyse JP, Patten M (1985). The ontogenesis of the dopaminergic cell in the pre- and post-natal guinea-pig retina. Int J Dev Neurosci, 3: 157-167.

Reis RA, Ventura AL, Kubrusly RC, de Mello MC, de Mello FG (2007). Dopaminergic signaling in the developing retina. Brain Res Rev, 54: 181-188.

Ríos H, Brusco A, Pecci Saavedra J (1997). Development of serotoninergic chick retinal neurons. Int J Dev Neurosci, 15: 729-738.

Ritchie TC, Leonard RB (1983). Immunocytochemical demonstration of serotonergic neurons and processes in the retina and optic nerve of the stingray, *Dasyatis sabina*. Brain Res, 267: 352-356.

Ryan MK, Hendrickson AE (1987). Interplexiform cells in macaque monkey retina. Exp Eye Res, 45: 57-66.

Sarthy PV, RaybornME, Hollyfield JG, Lam DMK (1981). The emergence, localization and maturation of neurotransmitter systems during development of the retina in *Xenopus laevis*. III. Dopamine. J Comp Neurol, 195: 595-602.

Schlemermeyer E, Chappell RL (1996). Two classes of bipolar cell in the retina of the skate *Raja erinacea*. J Neurocytol, 25: 625-635.

Schütte M, Witkovsky P (1990). Serotonin-like immunoreactivity in the retina of the clawed frog *Xenopus laevis*. J Neurocytol, 19: 504-518.

Schütte M, Witkovsky P (1991). Dopaminergic interplexiform cells and centrifugal fibres in the *Xenopus* retina. J Neurocitol, 20: 195-207.

Smeets WJ, González A (2000). Catecholamine systems in the brain of vertebrates: new perspectives through a comparative approach. Brain Res Brain Res Rev, 33: 308-379.

Stuesse SL, Cruce WL (1992). Distribution of tyrosine hydroxylase, serotonin, and leu-enkephalin immunoreactive cells in the brainstem of a shark, *Squalus acanthias*. Brain Behav Evol, 39: 77-92.

Van Haesendonck E, Marc RE, Missotten L (1993). New aspects of dopaminergic interplexiform cell organization in the goldfish retina. J Comp Neurol, 333: 503-518.

Versaux-Botteri C, Dalil N, Kenigfest N, Reperant J, Vesselkin N, Nguyen-Legros J (1991). Immunohistochemical localization of retinal serotonin cells in the lamprey (*Lampetra fluviatilis*).Vis Neurosci, 7: 171-177.

Versaux-Botteri C, Verney C, Zecevic N, Nguyen-Legros J (1992). Early appearance of tyrosine hydroxylase immunoreactivity In the retina of human embryos. Dev Brain Res, 69: 283-287.

Villar-Cerviño V, Abalo XM, Villar-Cheda B, Meléndez-Ferro M, Pérez-Costas E, Holstein GR, Martinelli GP, Rodicio MC, Anadón R (2006). Presence of glutamate, glycine, and gamma-aminobutyric acid in the retina of the larval sea lamprey: comparative immunohistochemical study of classical neurotransmitters in larval and postmetamorphic retinas. J Comp Neurol, 499: 810-827.

Wagner HJ, Behrens UD (1993). Microanatomy of the dopaminergic system in the rainbow trout retina. Vis Res, 33: 1345-1358.

Wang HH, Cuenca N, Kolb H (1990). Development of morphological types and distribution patterns of amacrine cells immunoreactive to tyrosine hydroxylase in the cat retina. Vis Neurosci, 4: 159-175.

Weiler R, Ammermüller J (1986). Immunocytochemical localization of serotonin in intracellularly analyzed and dye-injected ganglion cells of the turtle retina. Neurosci Lett, 72: 147-152.

Weiler R, Schütte M (1985). Morphological and pharmacological analysis of putative serotonergic bipolar and amacrine cells in the retina of a turtle, *Pseudemys scripta elegans*. Cell Tissue Res, 241: 373-382.

Wilhelm M, Zhu B, Gábriel R, Straznicky C (1993). Immunocytochemical identification of serotonin-synthesizing neurons in the vertebrate retina: a comparative study. Exp Eye Res, 56: 231-240.

Witkovsky P (2004). Dopamine and retinal function. Doc Ophthalmol, 108: 17-40.

Witkovsky P, Arango-Gonzalez B, Haycock JW, Kohler K (2005). Rat retinal dopaminergic neurons: differential maturation of somatodendritic and axonal compartments. J Comp Neurol, 481: 352-362.

Witkovsky P, Eldred W, Karten HJ (1984). Catecholamine- and indoleamine-containing neurons in the turtle retina. J Comp Neurol, 228: 217-225.

Witkovsky P, Gábriel R, Krizaj D (2008). Anatomical and neurochemical characterization of dopaminergic interplexiform processes in mouse and rat retinas. J Comp Neurol, 510:158–174

Wulle I, Schnitzer J (1989). Distribution and morphology of tyrosine hydroxylase-immunoreactive neurons in the developing mouse retina. Dev Brain Res 48: 59-72.

Wulle I, Wagner HJ (1990). GABA and tyrosine hydroxylase immunocytochemistry reveal different patterns of colocalization in retinal neurons of various vertebrates. J Comp Neurol, 296:173-178.

Wullimann MF, Rink E (2001). Detailed immunohistology of Pax6 protein and tyrosine hydroxylase in the early zebrafish brain suggests role of Pax6 gene in development of dopaminergic diencephalic neurons. Brain Res Dev Brain Res, 131: 173-191.

Yáñez J, Anadón R (1994). Are the dopaminergic cells of the lamprey retina interplexiform cells? Neurosci Lett, 165: 63-66.

Yazulla S, Zucker CL (1988). Synaptic organization of dopaminergic interplexiform cells in the goldfish retina.Vis Neurosci, 1: 13-29.

Yew DT, Luo CB, Zheng DR, Guan YL, Tsang D, Stadlin A (1991). Immunohistochemical localization of substance P, enkephalin and serotonin in the developing human retina. J Hirnforsch, 32: 61-67.

Zhu BS, Straznicky C (1990). Morphology and distribution of serotonin-like immunoreactive amacrine cells in the retina of *Bufo marinus*. Vis Neurosci, 5: 371-378.

Zhu BS, Straznicky C (1991). Morphology and retinal distribution of tyrosine hydroxylase-like immunoreactive amacrine cells in the retina of developing Xenopus laevis. Anat Embryol, 184: 33-45.

Zhu BS, Straznicky C (1992). Large serotonin-like immunoreactive amacrine cells in the retina of developing *Xenopus laevis*. Brain Res Dev Brain Res, 69: 109-116.

Figure 1. Pattern of TH immunoreactivity in developing retinas of *S. canicula* and *H. fuscus*. A-D, Vertical sections along the dorsoventral axis of the retina (transversal to the head) of a stage 32 of *S. canicula* (A, B) and of *H. fuscus* (C, D), to show pale TH immunoreactivity in some INLi cells. Arrows in A indicate processes coursing to the IPL. In *H. fuscus*, a conspicuous layer of TH-ir cells is also observed in the HCL (arrows in D). D is a detail of the area boxed in C. **E-G**, Vertical sections along the dorsoventral axis of the retina of prehatching embryos of *S. canicula* (E) and *H. fuscus* (F, G). E, Section to show the increase in numbers of TH-ir amacrine cells and processes per section with respect to previous stages. Note that TH-ir cells are absent in the HCL. F-G, Details of TH-ir amacrine cells in the INLi, to show cell processes distributed in IPL sublayers 1 and 3 (arrows). **H-K**, Vertical sections along the dorsoventral axis of the retina of two juvenile *H. fuscus*. H, Detail of the central retina to show decreased numbers of TH-ir cells in the INLi and HCL. Processes in the IPL are organized in sublayers 1, 3 and 5. I, Detail of the peripheral retina to show that TH-ir cells are still abundant in the HCL of this region (arrows). J-K, Details of TH-ir amacrine cells in the INL to show their processes extending in the IPL (arrows). For abbreviations, see list in Appendix B.

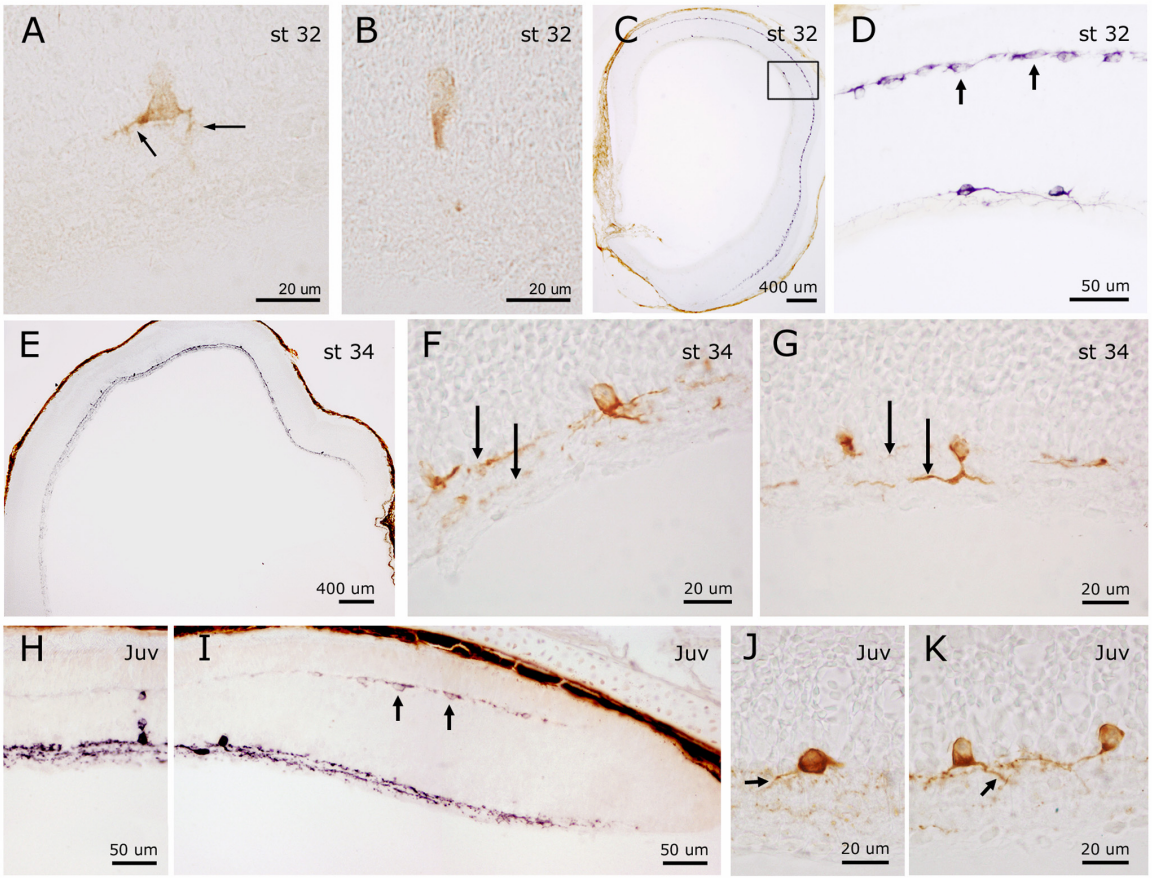
A
st 32
20 um
B
st 32
20 um
C
st 32
400 um
D
st 32
50 um
E
st 34
400 um
F
st 34
20 um
G
st 34
20 um
H
Juv
50 um
I
Juv
50 um
J
Juv
20 um
K
Juv
20 um

Figure 2. Pattern of 5-HT immunoreactivity in developing retinas of *S. canicula* and *H. fuscus*. A-C, Vertical sections along the dorsoventral axis of the retina (transversal with respect to the brain) of a stage 32 of *H. fuscus* (A, B) and of *S. canicula* (C). A, B, Details to show some 5-HT-ir labelled cells, located at several levels within the INL. C, Section to show 5-HT immunoreactivity in the proximal portion of the optic nerve (arrows). Sparse 5-HT-ir cells are found throughout the INLi (arrowheads). **D-G**, Vertical sections of the retina of prehatching embryos of *S. canicula* (D) and *H. fuscus* (E-G). D, Section to show that 5-HT-ir cells do not reach the most peripheral retina. E, 5-HT-ir cell processes branching in sublayers 1 and 3 of the IPL (arrows). F, 5-HT-ir fibres are observed in the optic fibre layer (arrow). G, Detail of the optic nerve showing 5-HT-ir fibres. **H-K**, Vertical sections along the dorsoventral axis of the retina of a juvenile of *H. fuscus*. H, Section to show 5-HT-ir cells in INL, and their absence form the HCL. (I-K) Detail of uniformly labelled 5-HT-ir amacrine cells in the INL, and their processes directed to the IPL. 5-HT-ir fibres are also present in the optic fibres layer (arrows in K). For abbreviations, see list in Appendix B.

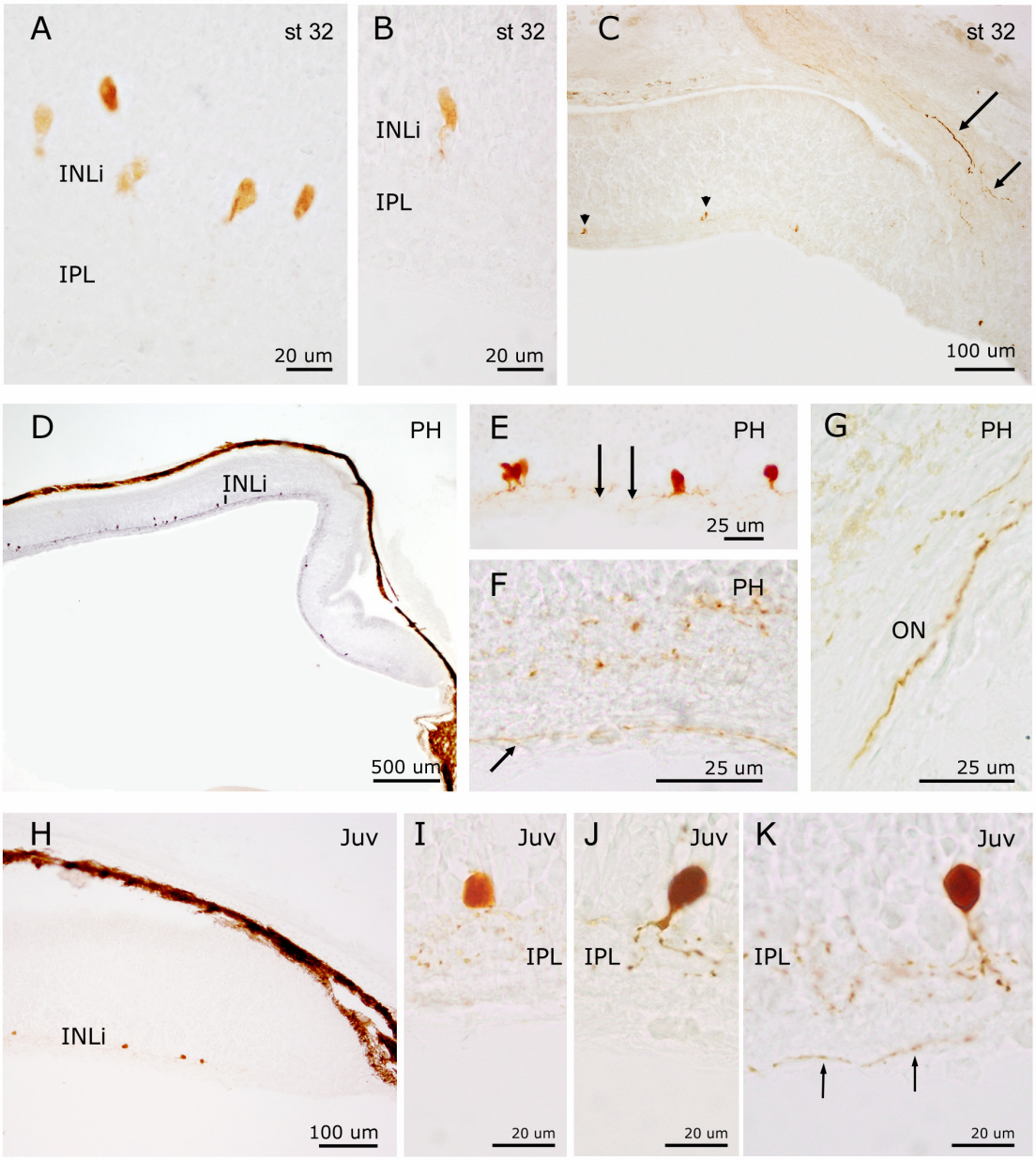
A
st 32
INLi
IPL
20 um
B
st 32
INLi
IPL
20 um
C
st 32
100 um
D
PH
INLi
500 um
E
PH
25 um
F
PH
25 um
G
PH
ON
25 um
H
Juv
INLi
100 um
I
Juv
IPL
20 um
J
Juv
IPL
20 um
K
Juv
IPL
20 um

Figure 3. Comparison of patterns of TH, 5-HT, Pax6, GAD and CR in the retinas of *S. canicula* and *H. fuscus*. A, B, Double TH/5-HT immunofluorescence in vertical sections along the dorsoventral axis of the retina (transversal with respect to the brain) of prehatching embryos of *H. fuscus* (A) and *S. canicula* (B). TH-ir and 5-HT-ir amacrine cells located in the INLi represent separate populations, and their processes intermingled in IPL sublayers 1 and 3. Note the presence of TH-ir horizontal cells in the HCL of *H. fuscus* (white arrows in A), which is in contrast with its absence in *S. canicula* (B). **C**, Double TH/5-HT immunofluorescence in a vertical section along the dorsoventral axis of the retina of a juvenile *H. fuscus*. Detail of TH-ir and 5-HT-ir amacrine cells and their processes, which are distributed in the INLi and IPL, respectively. **D-F**, Double TH/Pax6 immunofluorescence in vertical sections along the dorsoventral axis of the retina of prehatching embryos (D, E) and juveniles (F) of *H. fuscus.* TH-ir and Pax6-ir cells are codistributed in the INLi and HCL (arrows in D, E), and Pax6-ir cells are also observed in the GCL (arrowheads in D, E, F). **G**, Double TH/GAD immunofluorescence in a vertical section of the retina of juvenile *H. fuscus*, to show GAD-ir and TH-ir amacrine cells and processes in the INLi and IPL respectively, although they represent different populations. **H, I**, Double TH/CR immunofluorescence in vertical sections of the retinas of prehatching *S. canicula* (H) and juvenile *H. fuscus* (I). TH-ir and CR-ir cells are codistributed in the INL and their processes spread in different sublayers of the IPL. CR-ir cells are additionally found in the GCL (arrowheads in H) and HCL (arrows in H). TH-ir horizontal cells are found in the peripheral retina of juveniles of *H. fuscus* (arrows in I). **J-L**, Double immunofluorescence 5-HT/Pax6 in vertical sections along the dorsoventral axis of the retina of prehatching embryos of *S. canicula*. K and L are details of two single optical sections (1-µm-thick) of the same specimen. White open arrows indicate 5-HT/Pax6 double-labelled cells. Red open arrows indicate pale 5-HT-ir cells that lack Pax6 immunoreactivity. Small arrows indicate strong Pax6-ir cells. Arrowheads indicate Pax6 immunonegative cells. For abbreviations, see list in Appendix B.

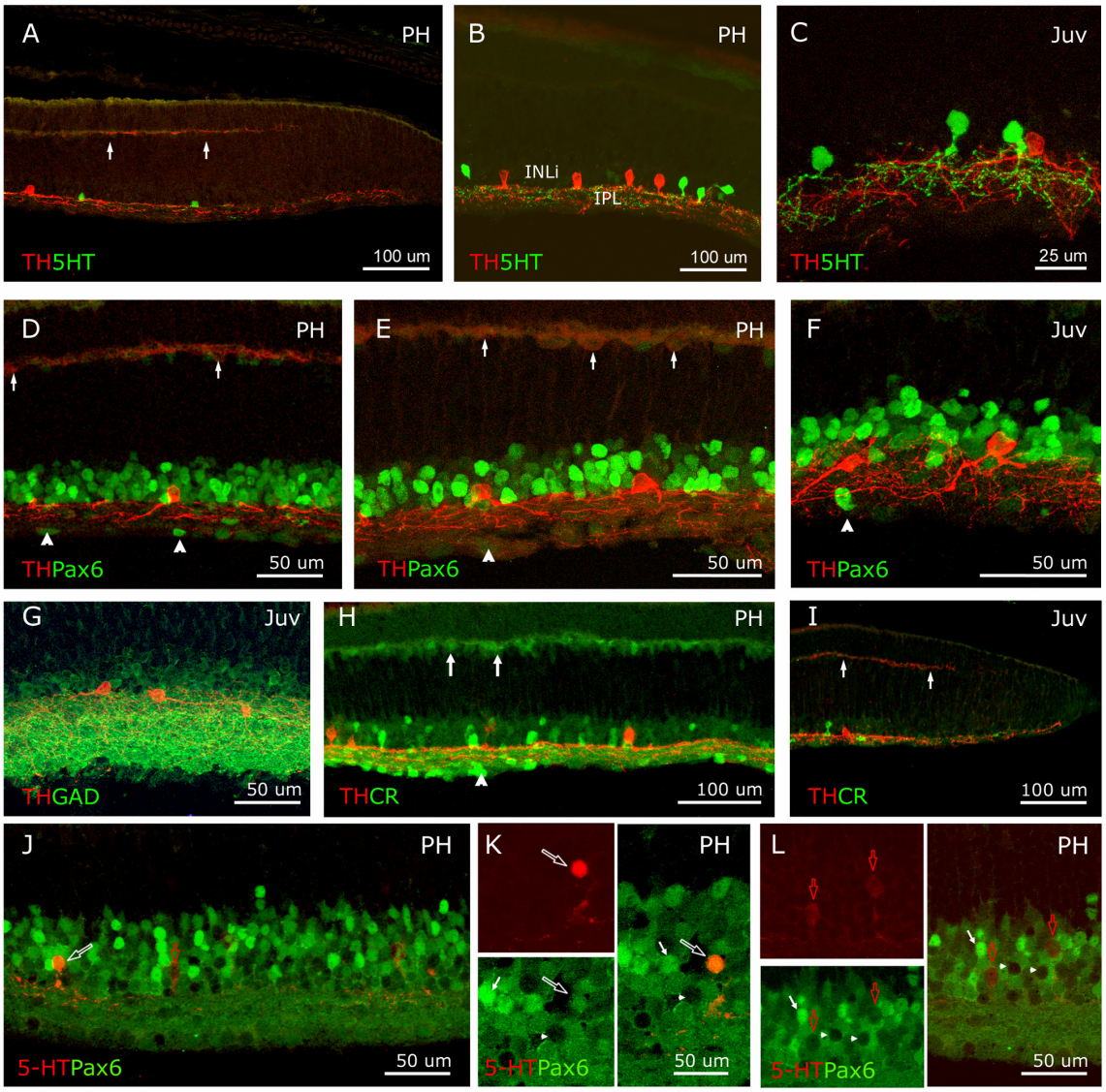
A
PH
TH5HT
100 um
B
PH
INLi
IPL
TH5HT
100 um
C
Juv
TH5HT
25 um
D
PH
THPax6
50 um
E
PH
THPax6
50 um
F
Juv
THPax6
50 um
G
Juv
THGAD
50 um
H
PH
THCR
100 um
I
Juv
THCR
100 um
J
PH
5-HTPax6
50 um
K
PH
5-HTPax6
50 um
L
PH
5-HTPax6
50 um

Chapter 10.

Spatiotemporal organization of Opsin-immunoreactive cells in the shark retina

INTRODUCTION

As stated in previous chapters, the early developing retina is composed of a single sheet of proliferative, apparently equivalent, neuroepithelial progenitors. These cells gradually withdraw from the cell cycle (see Chapter 6) and migrate to particular locations within the developing retina, where they become differentiated by the expression of specific molecular markers and morphological characteristics of the cell type (see Chapters 7-9). One clue to understanding the process of retinal cell diversification is provided by the order in which distinct classes of neurons and glia appear during development.

During development of the vertebrate retina, postmitotic cells in the outer neuroblastic layer differentiate to form two types of photoreceptors: rods and cones. Among retinal cell types, photoreceptors have been often used in studies of cell differentiation, because they are relatively abundant and can be readily identified morphologically and with cell type-specific molecular markers. Rods and cones contain visual pigments that are composed of a protein (opsin) linked to a chromophore. Opsins are extremely well characterised in terms of their structure and function (Nathans, 1987; Nickle and Robinson, 2007; Bowmaker, 2008) and are invaluable markers of the different types and subtypes of photoreceptors. Opsins are members of an extensive family of G-protein-linked membrane receptors. Comparative studies across all major vertebrate groups have established that in addition to the rod class of pigment (RH1, a middle-wave class of pigment sensitive in the green part of the spectrum at about 500 nm), there are four spectrally distinct classes of cone pigments encoded by different opsin gene families: a rhodopsin-like, middle-wave class (RH2, sensitive in the green spectral region); two short wavelength sensitive classes (SWS1 and SWS2, sensitive in the violet/ultraviolet and in the blue/violet respectively); and a long-to-middle wave class (LWS, maximally sensitive in the red/green). Each class operates within a given range of maximal absorbance, though there is some overlap in absorbance between classes (for a review, see Bowmaker et al., 2008). As a general rule, the RH1 class is restricted to rod photoreceptors, and the RH2, SWS1, SWS2, and LWS classes are restricted to the cone photoreceptors. While this generalization normally holds true, it is not absolute, as RH1 opsins have been reported to be expressed in cones in the retina of chameleon, red/green opsins have been found in rods in the retina of gecko, and blue/violet opsins are expressed in both rod and cone photoreceptors in the retina of salamander (reviewed in Nickle and Robinson, 2007).

The sequence of expression of rod and cone opsins during development varies among the species examined. In some fishes (goldfish: Stenkamp et al., 1996, 1997; and zebrafish: Raymond et al., 1995; Schmitt et al., 1999), chick (Bruhn and Cepko, 1996; Adler et al., 2001; Raymond and Barthel, 2004; Takechi and Kawamura, 2005) and some mammals (Szél et al., 1993; Bumsted et al., 1995; Seiler and Aramant, 1994; Dorn et al., 1995; Bumsted et al., 1997), rod-type opsins are expressed first, followed by cone-type opsins, although the time lag differs between species. On the contrary, in salmonids (Cheng et al., 2007) and some mammals (Bumsted et al., 1997; Szél et al., 1994; Xiao and Hendrickson, 2000; O'Brien et al., 2004; Chen et al., 2005), violet/blue opsin appears first and is then followed by rhodopsin and green and/or red opsin. Interestingly, in the retina of monkey, rods (which are the first to express opsins) are found more peripherally than red-type cones (Bumsted et al., 1997), suggesting that the sequence in which photoreceptors are born does not necessarily correlate with the sequence in which opsins are expressed (Bumsted et al., 1997; Schmitt et al., 1999).

Over 40 species of elasmobranch have been investigated for their photoreceptor system. Ultrastructural studies performed in the developing retina of the shark *Chiloscyllium punctatum* have revealed that photoreceptors are the last retinal cells to differentiate (Harahush et al., 2009), although the time of expression of visual pigments (opsins) is not known. The phylogenetic position of elasmobranchs (sharks, skates and rays), radiating early from the main gnathostome lineage (about 400 million years ago), implies that they have the potential to retain all four vertebrate cone opsin classes. Indeed, it is now clear that most elasmobranchs possess at least one class of cone in the retina (Gruber et al., 1963; Gruber and Cohen, 1978, 1985; Cohen, 1990; Gruber et al., 1991; Sillman et al., 1996; Hart et al., 2004, 2006; Theiss et al., 2007; Harahush et al., 2009) and some species of rays might have trichromatic colour vision (Govardovskii and Lychakov, 1977; Hart et al., 2004; Theiss et al., 2007; Bowmaker, 2008). However, other species may have pure rod retinas (Govardovskii and Lychakov, 1977; Dowling and Ripps, 1970; Dowling and Ripps, 1991; Ripps and Dowling, 1991; Bozzano et al., 2001; Bozzano, 2004), and in two species of *Raja*, the rods function at both scotopic and photopic levels (Dowling and Ripps, 1991; Ripps and Dowling, 1991), which indicates that rods are the only photoreceptor common to all elasmobranchs. To our knowledge, the photoreceptor system has not been investigated in *H. fuscus*, and the presence of cones in the genus *Scyliorhinus* is controversial, as *Scyliorhinus spp*. has been classically reported to posses cones (Neumayer, 1897; see also Gruber and Cohen, 1985;

Theiss et al., 2007; Davies et al., 2009), while *S. canicula* has been defined as a pure-rod species (Bozzano et al., 2001; Gačić et al., 2007).

In this study we examined the temporal and spatial pattern of photoreceptor genesis and specification during embryogenesis and postembryonic development in two species of elasmobranch, which display extended periods of retinal development. For this, we used an anti-rod opsin antibody (CERN 922; gifted by Dr. W. J. de Grip), been found useful to label early developing photoreceptors in the retina of agnathans (Meléndez-Ferro et al., 2002; Villar Cheda et al., 2008) and teleost fishes (Candal et al., 2005).. We also performed double colorimetric immunodetection for rod-opsins and proliferating cell nuclear antigen (PCNA) antibodies (see Chapter 6) in order to examine the spatiotemporal sequence of photoreceptor differentiation in relation to cell cycle exit (PCNA-immunonegativity).

MATERIAL AND METHODS

Experimental animals

Embryos, juvenile and adult specimens of the lesser spotted dogfish (*Scyliorhinus canicula*) and the brown shyshark (*Haploblepharus fuscus*) were obtained and maintained as described in Chapter 5. The embryonic stages of *S. canicula* were identified by external features following Ballard et al. (1993) and similar features were considered in staging the *H. fuscus* embryos. The following embryonic stages were analysed: stage 31 (2 *H. fuscus* embryos), stage 32 (3 *S. canicula* and 3 *H. fuscus* embryos), stages 33-34 (prehatching; 1 *S. canicula* and 2 *H. fuscus* embryos), 2 juveniles (1 *S. canicula* and 1 *H. fuscus*, from 10 to 14 cm in total length) and 1 adult *S. canicula* (about 50 cm total length) were also processed.

Tissue preparation

Tissue was prepared as indicated in Chapter 5. Briefly, embryos were anaesthetized with 0.05% tricaine methane sulphonate (MS-222; Sigma, St. Louis, MO) in seawater and fixed either in 4% paraformaldehyde (PFA) in elasmobranch phosphate buffer for 48-72 h or in Clark's solution for 12-36 h. Prehatching, juvenile and adult specimens were deeply anaesthetized with MS-222 and then perfused intracardially with elasmobranch Ringer's solution followed by the appropriate fixative. Eyes of stage 32-34 embryos, juveniles and

adults were dissected out and postfixed for 4 h in the corresponding fixative. Specimens fixed in 4% PFA were cryoprotected, embedded in OTC compound (Tissue Tek, Torrance, CA), frozen with liquid nitrogen-cooled isopentane, and cut on a cryostat. Specimens fixed in Clark's solution were dehydrated and embedded in paraffin and cut on a rotary microtome. Parallel series of cryostat (14–18 µm thick) and of rotary microtome (10-12 µm thick) sections of specimens cut along the dorsoventral or nasotemporal axis of the retina (transverse or sagittal with respect to the brain, respectively), were mounted on Superfrost Plus (Menzel-Glasser1) slides.

Opsin immunohistochemistry

Sections were pretreated with 0.01M citrate buffer pH 6.0 for 30 min at 95°C for heat induced epitope retrieval, and allowed to cool for 30 minutes at room temperature (RT). Sections were rinsed twice in 0.05M Tris-buffered saline pH 7.4 (TBS) for 10 min each and residual avidin/biotin activity was removed by incubation with the avidin/biotin blocking kit (Vector, Burlingame, CA). Sections were then incubated with a rabbit anti-opsin polyclonal antiserum (CERN-922, gifted by Dr. W. J. de Grip; dilution 1:1000), overnight at RT. Sections were then rinsed in TBS (two 10-min rinses) and endogenous peroxidase was blocked with 10% H_2O_2 in phosphate buffered saline pH 7.4 (PBS) for 30 min at RT. Sections were rinsed in TBS, incubated in biotinylated goat anti-rabbit IgG (Dako; 1:500) for 1 h at RT, rinsed in TBS, and incubated in the preformed avidin:biotinylated HRP complex (ABC complex; Vector) for 30 min at RT. The immunoreaction was revealed with either 0.25 mg/ml diaminobenzidine (DAB) tetrahydrochloride (Sigma) in TBS pH 7.4 with 2.5 mg/ml nickel ammonium sulfate and 0.00075% H_2O_2, or with SIGMAFAST™ 3,3'-Diaminobenzidine (DAB) tablets as indicated by the manufacturers. All dilutions were made with TBS containing 15% normal goat serum (Dako) and 0.2% Triton X-100 (Sigma), and all incubations were carried out in a humid chamber. Finally, the sections were dehydrated, mounted and coverslipped. To facilitate identification of retinal cells and layering, sections were counterstained with haematoxylin-eosin. As negative controls, the primary, secondary or tertiary antibodies were omitted. No immunostaining was observed in the control sections.

In order to investigate the presence of cones in the shark retina, some sections were incubated with commercial rabbit polyclonal antibodies raised against red/green-cone and

blue-cone opsins (Chemicon AB5405 and AB5407, respectively; dilution 1:250). The procedure followed for cone opsin immunohistochemistry was the same as per rod opsin. As positive controls for cone opsin antibodies, some sections of retinas of young *Acipenser baeri* (Siberian sturgeon, chondrostean) and *Salmo trutta fario* (brown trout, teleost) were submitted to the same immunocytochemical procedure.

Two-colour immunostaining of Opsin and PCNA

Sections were treated as described in the previous section for rod opsin immunohistochemistry but the immunoreaction was developed with SIGMAFAST™ 3,3'-Diaminobenzidine (DAB) tablets as indicated by the manufacturers. Then, the sections were rinsed in TBS-T (four 15-min rinses) and endogenous peroxidase was blocked again as above. After rinsing in TBS-T, sections were processed for PCNA immunohistochemistry as described above (PCNA-immunohistochemistry section) but this second immunoreaction was developed with 0.25 mg/ml diaminobenzidine (DAB) tetrahydrochloride (Sigma) in TBS pH 7.4 with 2.5 mg/ml nickel ammonium sulphate and 0.00075% H_2O_2. All dilutions were made with TBS containing 15% normal goat serum (Dako), and all incubations were carried out in a humid chamber. Finally, the sections were dehydrated, mounted and coverslipped. Photographs were taken with an Olympus DP71 colour digital camera, fitted to a Provis photomicroscope (Olympus, Tokyo).

RESULTS

Opsin immunoreactivity

Of the three anti-opsin antibodies employed here, only the anti-rod opsin revealed the presence of immunoreactive (-ir) cells in the shark retina, either developing or posthatching.

Although rod opsin immunoreactivity was observed in the two species during the *second developmental period*, slight between-species differences were noted in the time of appearance of rod opsin-ir cells. In S. *canicula,* first rod opsin-ir photoreceptors were observed at early stage 32 (Fig. 1A), whereas in *H. fuscus* they were not detected before mid-stage 32 (Fig. 1B). In both species, the first labelled photoreceptors showed rod opsin immunoreactivity in perikarya and inner processes and appeared in the centrodorsal region of

the outer nuclear layer (ONL) scattered among the numerous rod opsin-negative ONL cells (compare Figs. 1A, B). At mid-stage 32 in *S. canicula*, a small patch of rod opsin-ir photoreceptors was observed along the nasotemporal axis in the centrodorsal retina (Fig. 1C). The outer plexiform layer (OPL) extended far away the patch of rod opsin-ir cells (arrows in Fig. 1D) towards the region showing mitotic cells (see Figs. 1C, D'). At late stage 32, the region containing rod opsin-ir photoreceptors in *S. canicula* has increased notably in extension and cell density (Fig. 1E). The photoreceptor segments protrude in the subretinal space in the most mature central part of the retina, which shows scarce rod opsin-negative perikarya located among the numerous labelled cells (arrows in Fig. 1F). Rod opsin-ir photoreceptors showed narrow inner segments, elongated cylindrical outer segments and small nuclei. Interestingly, we also observed a few labelled perikarya in the ganglion cell layer (GCL; arrowhead in Fig. 1E), and outer part of the inner nuclear layer (INLo; arrowheads in Fig. 1F), where these rod opsin-ir cells showed an outer process directed to the ONL and one or more inner short processes in the inner nuclear layer (INL). Appearance of the most peripheral photoreceptors (elongated and pear-shaped perikarya located at several levels in the ONL) resembled that of the immature central retina of early stages (Fig. 1G). A similar pattern of rod opsin immunoreactivity was observed in *H. fuscus* in the same developmental period (data not shown).

In prehatching embryos of *H. fuscus* (Figs. 1H, I) and *S. canicula* (Figs. 1J, K), rod opsin-ir photoreceptors were observed along the retina, except the ciliary marginal zone (CMZ, the wedge-shaped neuroepithelial zone that lies between the laminated retina and the ciliary epithelium; Fig. 1J). As in previous stages, the most peripheral rod opsin-ir photoreceptors lacked photoreceptor segments (Figs. 1I, J). The anti-rod opsin antibody labelled the perikarya, inner and outer segments of most photoreceptors. In addition, labelled cells were also observed in the INLo extending long processes in the inner part of the INL (INLi) and GCL (Figs. 1H, J, K). These cells were more frequent in the central retina (Fig. 1K), but a few also appeared peripheral regions where they showed short inner processes (Fig. 1J).

The same patterns of distribution of rod opsin-ir photoreceptors were found in juveniles (Fig. 1L) and adults (Fig. 1M), but labelled cells were not observed in the INL of the adult *S. canicula*.

Comparison of spatiotemporal patterns of PCNA and rod opsin immunoreactivities

During the *first developmental period*, most cells were proliferating and no retinal cells expressed rod opsin immunoreactivity. During the *second developmental period*, PCNA immunoreactivity disappeared progressively from the outer retina, and rod opsin-ir photoreceptors extended in the ONL towards the periphery, coinciding with the loss of PCNA immunoreactivity in this layer (compare Figs. 2A and B). In order to further compare the relation between the exit of the proliferation cycle and the appearance of rod opsin immunoreactivity in differentiating photoreceptors we performed two-colour immunohistochemistry against PCNA and rod opsin in late stage 32 embryos. No double rod opsin/PCNA immunolabelled cells were found in the central or the peripheral retina (Fig. 2C) where the density of rod opsin-ir cells decreased while PCNA-ir cells were still abundant, and these proliferating cells and rod opsin-ir differentiating photoreceptors were found side by side. Similar patterns were found after stage 32 (*third developmental period*; Figs. 2D-G). At these later stages, PCNA-ir cells were mostly confined to the CMZ (Fig. 2D) and the region around the optic nerve head (Fig. 2E), and decreased in density at some distance. Rod opsin immunoreactivity was observed throughout the ONL (and also in a few cells in the GCL and INLo; arrowheads in Fig. 2E), but was absent from the CMZ, which showed a high density of intensely PCNA-ir cells. In the *transition zone,* rod opsin-ir cells did not extend to the pure-neuroblastic region, which in contrast contained a high density of PCNA-ir cells (Figs. 2F, G). Some cells in the prospective ONL of the *transition zone* were neither labelled with PCNA nor opsin antibodies (arrows in Figs. 2F, G).

DISCUSSION

Photoreceptor differentiation in relation to retinal cell proliferation

Early differentiation of photoreceptors was analysed in the shark retina by immunohistochemical detection of opsin expression with the CERN922, an antibody raised against cow rod opsin, combining it with immunohistochemical detection of PCNA. The results confirm that the antibody used is a good marker of early photoreceptor differentiation, which became opsin-ir much before the appearance of photoreceptor inner and outer segments. Moreover, rod opsin-ir cells were never labelled with cell cycle markers such as PCNA, indicating that these cells are postmitotic.

Rod opsin immunoreactivity was observed in both shark species during the stage 32 (*second developmental period)*, when the OPL begins to be recognizable in the central retina. Minor differences were noted regarding the chronology of appearance of the first rod opsin-ir cells in *S. canicula* and *H. fuscus*, which were observed slightly earlier in the former than in the latter. However, it greatly differs from that described with electron microscopy in a close related species with a similar timetable of development (Harahush et al., 2007), where photoreceptor differentiation was only observed in the last quarter of the total embryonic period (Harahush et al., 2009) by the presence of photoreceptor segments. The rod opsin immunodetection used in this work reveals early events of the photoreceptor differentiation that precede the formation of photoreceptor inner and outer segments, thus allowing a better characterisation of this process. The expression of opsin mRNA prior to the appearance of photoreceptor outer segments has been previously reported in salmonids (Cheng et al., 2007).

The anti-rod opsin antibody labelled most of the ONL perikarya in both shark species. The finding of opsin immunostaining in perikarya and processes the ONL has also been reported with the same antibody in larval lamprey photoreceptors (Villar-Cheda et al., 2008) and in rods of juvenile trout (Candal et al., 2005). The finding that most of the ONL cells are rod opsin-positive is consistent with other lines of evidence indicating that most photoreceptors in sharks are rods (Nicol, 1961; Hart et al., 2004; Harahush et al., 2009). In *S. canicula*, electroretinographic spectral sensitivity data revealed the presence of a single rod photopigment, and that the λmax value of this rod visual pigment was also quite usual for fishes living in shallow to moderately deep water (Bozzano et al., 2001; Gačić et al., 2007). As a possible relationship between visual pigment absorption and depth distribution has been quoted (Gačić et al., 2007), similar absorption data could be found in *H. fuscus*, that also inhabits shallow waters (see Chapter 5). In both *S. canicula* and *H. fuscus* embryos, rod opsin-ir perikarya were mainly located at several levels in the ONL along with PCNA-ir cells (see Fig. 2C). This is consistent with the location reported for the rod lineage in teleosts (Mack and Fernald, 1997; Henderson and Fernald, 2004; Candal et al., 2005; Nelson et al., 2008; Cheng et al., 2009). Moreover, sharks possess calretinin (CR)-ir ganglion, amacrine and horizontal cells (see Chapter 8), a pattern found in rod-dominant retinas of different vertebrate species (Hamano et al., 1990). Moreover, functional maturation of photoreceptors in sharks is temporally concurrent with the beginning of CR expression in horizontal cells, coincidently

with that observed in turbot (Doldán et al., 1999) where rod differentiation starts when CR labelling extends to horizontal cells.

Rod-opsin immunonegative cells in the ONL of elasmobranchs

The eyes of elasmobranchs were traditionally assumed to have all-rod retinas. However, while a few species are reported to be cone free (see introduction), the majority of over 40 species investigated so far have duplex retinas, with the proportion of cones and rods varying greatly between species (Hart et al., 2006; Harahush et al., 2009). Although no quantitative analysis was performed in the present study, opsin-ir cells vastly populate the ONL, suggesting that cones, if present, are scarce. However, as cones in the retina of different elasmobranchs are often obscured by the surrounding rods, and their outer segments are easily detached during tissue preparation (Hart et al., 2004), we aimed to know if the presence of cones had been underestimated. Examination of all tangential retinal sections after anti-rod-opsin immunohistochemistry have not revealed any particular spatial arrangement (commonly found in teleost fishes; Candal et al., 2005; Adler and Raymond, 2008) that could be reflecting the presence of different photoreceptor subtypes. Moreover, no cone-opsin-ir cells were found in *S. canicula* and *H. fuscus* by means of immunohistochemistry with commercially available antibodies against red/green-cone and blue-cone opsins (rabbit polyclonal Chemicon AB5405 and AB5407, respectively), while the anti-red/green-cone opsin labelled cone-like photoreceptors in *Acipenser baeri* (chondrostean) and *Salmo trutta fario* (teleost) (results not shown). These lines of evidence suggest that *S. canicula* and *H. fuscus* retinas are cone-free. Present results are in agreement with previous works reporting *S. canicula* as a pure-rod species with a single rod visual pigment in the basis of electroretinographic spectral sensitivity data (Bozzano et al., 2001; Gačić et al., 2007), although they disagree with an early histological study that described cones in the retina of *Scyliorhinus spp*. (Neumayer, 1897). This discrepancy could be conciliated if considering the different techniques employed. Indeed, in two cone-free species of *Raja* (Dowling and Ripps, 1991; Ripps and Dowling, 1991), some small cells with cone-shaped outer segments were seen occasionally despite only one spectrally distinct visual pigment was found; these cone-shaped cells were interpreted as recently differentiated rods that were being incorporated into the photoreceptor layer.

PCNA/rod opsin negative cells in the shark retina (present results) could be alternatively interpreted as mitotic cells, as PCNA is not expressed during the M-phase of the cell cycle. Indeed, high numbers of mitotic cells (identified by means of anti-phospho-histone-H3 immunocitochemistry) have been observed in the peripheral retina at locations that coincide with those showing PCNA/rod opsin negative cells (see Chapter 6). However, the possibility that these cells are postmitotic but not overtly differentiated rod progenitors cannot be ruled out.

Ectopic opsin-like cells in the INL of elasmobranchs

Interestingly, we have shown that in *S. canicula* and *H. fuscus*, the anti-opsin antibody labels cells in the GCL and in the outermost part of the INLo from late stage 32 to early juveniles, whereas labelled cells are absent in adult fishes. These ectopic rod-opsin-like-ir cells show a bipolar morphology with processes directed to the ONL and the GCL. Opsin-like-ir cells that express several phenotypic properties characteristic of rods, have previously been noted in the INL of the developing rat retina (Barnstable, 1982; Araki et al., 1988). More recently, a few rhodopsin-positive profiles were observed in the INL and the prospective GCL of developing rats (Günhan-Agar et al., 2000; Günhan et al., 2003). As in sharks (present results), ectopic rod opsin expression in the rat is transient. These opsin-like cells were apparent in the presumptive GCL as early as P0, but 1 week after birth they were present only in the INL, and in mature rats none were found outside the photoreceptor layer. It has been suggested that these cells may either degenerate or undergo phenotypic conversion during subsequent maturation of the retina (Araki et al., 1988). Indeed, these opsin-like cells were interpreted as a contingent of photoreceptors that fail to recognize a signal to stop migrating when they arrive at the photoreceptor layer, and that their early elimination from the GCL and later from the INL probably reflects the failure of these cells to form functional synapses in inappropriate retinal layers (Günhan et al., 2003).

REFERENCES

Adler R, Raymond P (2008). Have we achieved a unified model of photoreceptor cell fate specification in vertebrates? Brain Res, 1192: 134–150.

Adler R, Tamres A, Bradford RL, Belecky-Adams TL (2001). Microenvironmental regulation of visual pigment expression in the chick retina. Dev Biol, 236: 454-464.

Araki M, Hanihara T, Saito T (1988). Histochemical observations on unique rod-like cells in the developing retina of the normal rat. J Neurocytol, 17: 179-188.

Ballard W, Mellinger J, Lechenault H (1993). A series of normal stages for development of *Scyliorhinus canicula*, the lesser spotted dogfish (Chondrichthyes: Scyliorhinidae). J Exp Zool, 267: 318-336.

Barnstable CJ (1982). Immunological studies of the retina. In: Neuroimmunology (Brockes J, ed), pp 183-214. New York: Plenum.

Bowmaker JK (2008). Evolution of vertebrate visual pigments. Vision Res, 48: 2022-2041.

Bozzano A (2004). Retinal specialisations in the dogfish *Centroscymnus coelolepis* from the Mediterranean deep-sea. Sci Mar, 68: 185-195.

Bozzano A, Murgia R, Vallerga S, Hirano J, Archer S (2001). The photoreceptor system in the retina of two dogfishes, *Scyliorhinus canicula* and *Galeus melastomus*: possible relationship with depth distribution and predatory lifestyle. J Fish Biol, 59: 1258-1278.

Bruhn SL, and Cepko CL (1996). Development of the pattern of photoreceptors in the chick retina. J Neurosci, 16: 1430-1439.

Bumsted K, Jasoni C, Szél A, Hendrickson A (1997). Spatial and temporal expression of cone opsins during monkey retinal development. J Comp Neurol, 378: 117-134.

Bumsted KM, Jasoni CL, Hendrickson AE (1995). Expression of blue and red opsin mRNA in the adult and fetal primate retina. Soc Neurosci Abstr, 21: 314.

Candal E, Anadón R, DeGrip WJ, Rodríguez-Moldes I (2005). Patterns of cell proliferation and cell death in the developing retina and optic tectum of the brown trout. Brain Res Dev Brain Res, 154: 101-19.

Chen J, Rattner A, Nathans J (2005). The rod photoreceptor-specific nuclear receptor Nr2e3 represses transcription of multiple conespecific genes. J Neurosci, 25: 118-129.

Cheng CL, Gan KJ, Flamarique IN (2007). The ultraviolet opsin is the first opsin expressed during retinal development of salmonid fishes. Invest Ophthalmol Vis Sci, 48: 866-73.

Cheng CL, Gan KJ, Flamarique IN (2009). Thyroid hormone induces a time-dependent opsin switch in the retina of salmonid fishes. Invest Ophthalmol Vis Sci, 50: 3024-3032.

Cohen JL (1990). Vision in elasmobranchs. In: The visual system of fish (Douglas RH and Djamgoz MBA, eds), pp. 465-490. London: Chapman and Hall.

Davies WL, Carvalho LS, Tay BH, et al. (2009). Into the blue: gene duplication and loss underlie color vision adaptations in a deep-sea chimaera, the elephant shark *Callorhinchus mili*. Genome Res, 19: 415–426.

Doldán MJ, Prego B, De Miguel-Villegas E (1999). Immunochemical localization of calretinin in the retina of the turbot (*Psetta maxima*) during development. J comp Neurol, 406: 425-432.

Dorn EM, Hendrickson L, Hendrickson AE (1995). The appearance of rod opsin during monkey retinal development. Invest Ophthalmol Vis Sci, 36: 2634-2651.

Dowling JE and Ripps H (1970). Visual adaptation in the retina of the skate. J Gen Physiol, 56: 491-520.

Dowling JE and Ripps H (1991). On the duplex nature of the skate retina. J Exp Zool, S5: 55-65.

Gačić Z, Damjanović I, Mićković B, Hegediš A, Nikćević M (2007). Spectral sensivity of the dogfish shark (*Scyliorhinus canicula*). Fish Phisiol Biochem, 33: 21-27.

Govardovskii VI and Lychakov LV (1977). Photoreceptors and visual pigments of Black Sea elasmobranchs. Zhurnal Evolyutsionnoi Biokhimij l Fiziologii, 13: 162-166.

Gruber SH, Cohen JL (1978). Visual system of the elasmobranchd: state of the art 1960–1975. In: Hodgson, E.S., Mathewson, R.F. (Eds.), Sensory Biology of Sharks, Skates ad Rays. ONR, Dept. Navy, Arlignton, Virginia.

Gruber SH, Cohen JL (1985). Visual system of the white shark, Carcharodon carcharias, with emphasis on retinal structure. Mem. Southern California Acad Sci, 9: 61–72.

Gruber SH, Hamasaki DI, Bridges CD (1963). Cones in the retina of the lemon shark (*Negaprion brevirostris*). Vision Res, 3: 397–399.

Gruber SH, Loew ER, McFarland WN (1991). Rod and cone pigments of the Atlantic guitarfish, *Rhinobatos lentiginosus garman*. J Exp Zool, S5: 85-87.

Günhan E, van der List D, Chalupa LM (2003). Ectopic photoreceptors and cone bipolar cells in the developing and mature retina. J Neurosci, 23: 1383-1389.

Günhan-Agar E, Kahn D, Chalupa LM (2000). Segregation of on and off bipolar cell axonal arbors in the absence of retinal ganglion cells. J Neurosci, 20: 306-314.

Hamano H, Kiyama H, Emson PC, Manabe R, Nakauchi M, Tohyama M (1990). Localization of two calcium-binding proteins, calbindin (D28KD) and parvalbumin (12KD), in the vertebrate retina. J Comp Neurol, 302: 417-424.

Harahush BK, Fischer ABP, Collin SP (2007). Captive breeding and embryonic development of Chiloscyllium punctatum Muller & Henle, 1838 (Elasmobranchii: Hemiscyllidae). J Fish Biol, 71: 1007-1022.

Harahush BK, Hart NS, Green K, Collin SP (2009). Retinal neurogenesis and ontogenetic changes in the visual system of the brown banded bamboo shark, Chiloscyllium punctatum (Hemiscyllidae, Elasmobranchii). J Comp Neurol, 513: 83-97.

Hart NS, Lisney TJ, Collin SP (2006). Visual communication in elasmobranchs. In: Fish communication (Ladich F, Collin SP, Moller P, Kapoor BG, eds), pp 337-392. Science Publishers, Inc., Enfield.

Hart NS, Lisney TJ, Marshall NJ, Collin SP (2004). Multiple cone visual pigments and the potential for trichromatic colour vision in two species of elasmobranch. J Exp Biol, 207: 4587-4594.

Henderson RG and Fernald RD (2004). Timing and location of rhodopsin expression in newly born rod photoreceptors in the adult teleost retina. Dev Brain Res, 151: 193-197.

Mack AF and Fernald RD (1997). Cell movement and cell cycle dynamics in the retina of the adult teleost *Haplochromis burtoni*. J Comp Neurol, 388: 435-443.

Meléndez-Ferro M, Villar-Cheda B, Manoel Abalo X, Pérez-Costas E, Rodríguez-Muñoz R, de Grip WJ, Yánez J, Rodicio MC, Anadón R (2002). Early development of the retina and pineal complex in the sea lamprey: comparative immunocytochemical study. J Comp Neurol, 442: 250-265.

Nathans J, Thomas D, Hogness DS (1986). Molecular genetics of human color vision: the genes encoding blue, green, and red pigments. Science, 232: 193-202.

Nelson NL, Frey RA, Wardwell SL, Stenkamp DL (2008). The developmental sequence of gene expression within the rod photoreceptor lineage in embryonic zebrafish. Dev Dyn, 237: 2903-2917.

Neumayer L (1897). Der feinere Bau der Salachier Retina. Archiv Mikroskopishes Anat, 48: 83–111.

Nickle B and Robinson PR (2007). The opsins of the vertebrate retina: insights from structural, biochemical, and evolutionary studies. Cell Mol Life Sci, 64: 2917-2932.

Nicol JAC (1961). The tapetum in *Scyliorhinus canicula*. J Mar Biol As s UK, 41: 271-277.

O'Brien KMB, Cheng H, Jiang Y, Schulte D, Swaroop A, Hendrickson AE (2004). Expression of photoreceptor-specific nuclear receptor Nr2e3 in rod photoreceptors of fetal human retina. Invest Ophthalmol Vis Sci, 45: 2807-2812.

Raymond PA, Barthel LK (2004). A moving wave patterns the cone photoreceptor mosaic array in the zebrafish retina. Int J Dev Biol, 48: 935-945.

Raymond PA, Barthel LK, Curran GA (1995). Developmental patterning of rod and cone photoreceptors in embryonic zebrafish. J Comp Neurol, 359: 537-555.

Ripps H and Dowling JE (1991). Structural features and adaptive properties of photoreceptors in the skate retina. J Exp Zool, S5: 46-54.

Schmitt EA, Hyatt GA, Dowling JE (1999). Erratum: Temporal and spatial patterns of opsin gene expression in the zebrafish (*Danio rerio*): corrections with additions. Vis Neurosci, 16: 601–605.

Seiler MJ and Aramant RB (1994). Photoreceptor and glial markers in human embryonic retina and in human embryonic retinal transplants to rat retina. Dev Brain Res, 80: 81-95.

Sillman AJ, Letsinger GA, Patel S, Loew ER, Klimley AP (1996). Visual pigments and photoreceptors in two species of shark, *Triakis semifasciata* and *Mustelus henlei*. J Exp Zool, 276: 1-10.

Stenkamp DL, Barthel LK, Raymond PA (1997). Spatiotemporal coordination of rod and cone photoreceptor differentiation in goldfish retina. J Comp Neurol, 382: 272-84.

Stenkamp DL, Hisatomi O, Barthel LK, Tokunaga F, Raymond PA (1996). Temporal expression of rod and cone opsins in embryonic goldfish retina predicts the spatial organization of the cone mosaic. Invest Ophthalm Vis Sci, 37: 363-376.

Szél A, van Veen T, Röhlich P (1994). Retinal cone differentiation. Nature, 370: 336.

Szél A., Rohlich P, Mieziewska K, Aguirre G, van Veen T (1993). Spatial and temporal differences between the expression of short- and middle-wave sensitive cone pigments in the mouse retina: a developmental study. J Comp Neurol, 331: 564-577.

Takechi M, Kawamura S (2005). Temporal and spatial changes in the expression pattern of multiple red and green subtype opsin genes during zebrafish development. J Exp Biol, 208: 1337-1345.

Theiss SM, Lisney TJ, Collin SP, Hart NS (2007). Colour vision and visual ecology of the blue-spotted maskray, *Dasyatis kuhlii* Muller and Henle, 1814. J Comp Physiol, 193: 67-79.

Villar-Cheda B, Abalo XM, Villar-Cerviño V, Barreiro-Iglesias A, Anadón R, Rodicio MC (2008). Late proliferation and photoreceptor differentiation in the transforming lamprey retina. Brain Res, 1201: 60-67.

Xiao M, Hendrickson A (2000). Spatial and temporal expression of short, long/medium, or both opsins in human fetal cones. J Comp Neurol, 425: 545-559.

Figure 1. Patterns of rod opsin-immunoreactivity in the developing and mature retina of *S. canicula* and *H. fuscus*. A. Vertical sections along the dorsoventral axis of the retina of an early stage 32 embryo of *S. canicula* showing first rod opsin-ir cells in the centrodorsal part of the ONL. **B.** First rod opsin-ir cells in the retina of a middle stage 32 embryo of *H. fuscus*. **C.** Vertical section along the dorsoventral axis of the retina of a middle stage 32 embryos of *S. canicula* showing a small patch of opsin-ir cells in the centrodorsal part of the retina (large boxed area). **D.** Detail of the large boxed area in C showing the centroperipheral extension of the OPL. **D'.** Detail of the small boxed area in C corresponding to the peripheral retina (which lacks OPL) to show abundant mitotic cells. **E-G.** Vertical sections along the dorsoventral axis of the retina of a late stage 32 embryo of *S. canicula*. **E.** Rod opsin-ir cells are found to extend in the ONL towards the peripheral retina. Some rod opsin-ir perikarya are observed in the GCL (arrowhead). **F.** In the central retina, abundant rod opsin-ir perikarya are located at various levels within the ONL. Thin opsin-ir inner segments are also observed. A scarce number of opsin-immunonegative cells are noted in the ONL (arrows). Note also some bipolar-like rod opsin-ir cells in the INLo (arrowheads). **G.** The density of rod opsin-ir cells decreases towards the peripheral retina. The most peripheral rod opsin-ir cells (open arrow) show immunoreactivity in perikarya and inner processes, which resemble those of immature opsin-ir cells of early stage 32 (compare with A). **H, I.** Vertical sections along the dorsoventral axis of the retina of prehatching embryos of *H. fuscus*. **H.** Cell perikarya and elongated outer segments show rod opsin immunoreactivity. Note also the outer limiting membrane (arrow). Bipolar-like rod opsin-ir cells are also observed in the INLo (arrowhead). **I.** Outer segments are not observed in peripheral rod opsin-ir cells. **J, K.** Vertical sections along the dorsoventral axis of prehatching embryos of *S. canicula*. **J.** The density of rod opsin-ir cells decreases towards the peripheral retina and are absent from the CMZ, while some rod opsin-ir cells are observed in the INLo (arrowhead). **K.** Detail of a vertical section along the dorsoventral axis of the retina showing bipolar-like opsin-ir cells with perikarya located in the INL and radial processes extending to the outer and inner retina. **L.** Vertical sections along the dorsoventral axis of the retina of a juvenile of *H. fuscus.* As in previous stages, nuclei of opsin-ir perikarya are found at several levels within the ONL. **M.** Vertical section along the dorsoventral axis of the retina of an adult of *S. canicula.* Opsin-ir perikarya (arrows) and elongated outer segments (arrowheads) are observed. For abbreviations, see list in Appendix B.

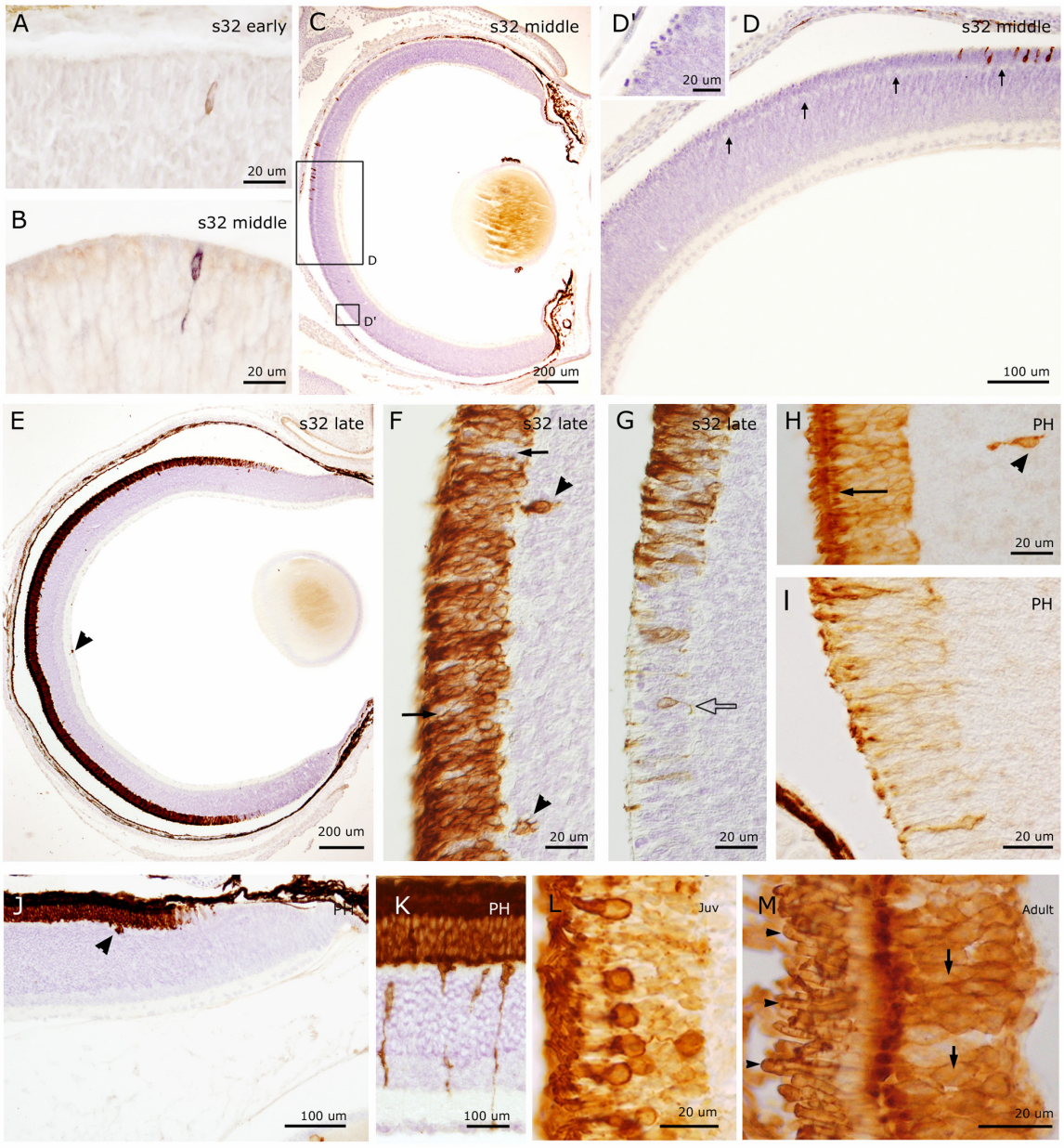
A
s32 early
20 um
B
s32 middle
20 um
C
s32 middle
D
D'
200 um
D'
20 um
D
s32 middle
100 um
E
s32 late
200 um
F
s32 late
20 um
G
s32 late
20 um
H
PH
20 um
I
PH
20 um
J
PH
100 um
K
PH
100 um
L
Juv
20 um
M
Adult
20 um

Figure 2. Comparison of spatiotemporal patterns of PCNA and opsin immunoreactivities in retina of *S. canicula* and *H. fuscus*. A, B. Parallel vertical sections along the dorsoventral axis of the retina of late stage 32 embryos of *S. canicula* showing the band of rod opsin-ir cells in the ONL extending towards the peripheral retina (A), which coincides with the absence of PCNA-ir cells in this ONL region (B). **C.** Detail of a double immunolabelled section showing rod opsin-ir (brown) and PCNA-ir (blue) cells in the area boxed in A-B. In the peripheral retina (right part of the image) no double opsin/PCNA labelling is observed in spite that PCNA-ir cells and opsin-ir cells appeared side-by-side. **D-G.** Vertical sections along the dorsoventral axis of the retina of juveniles of *H. fuscus* (D, E) and *S. canicula* (F, G). Rod opsin-ir cells are present in the ONL but absent from the outer non-layered retina of the *transition zone* (D, F and G), from the CMZ (D), and from the optic disc (E), which, in turn, contain PCNA-ir cells. Arrowheads in E indicate some rod opsin-ir cells in the GCL and INLo. Some cells in the ONL are neither labelled with PCNA nor rod opsin antibodies (arrows in F and G). For abbreviations, see list in Appendix B.

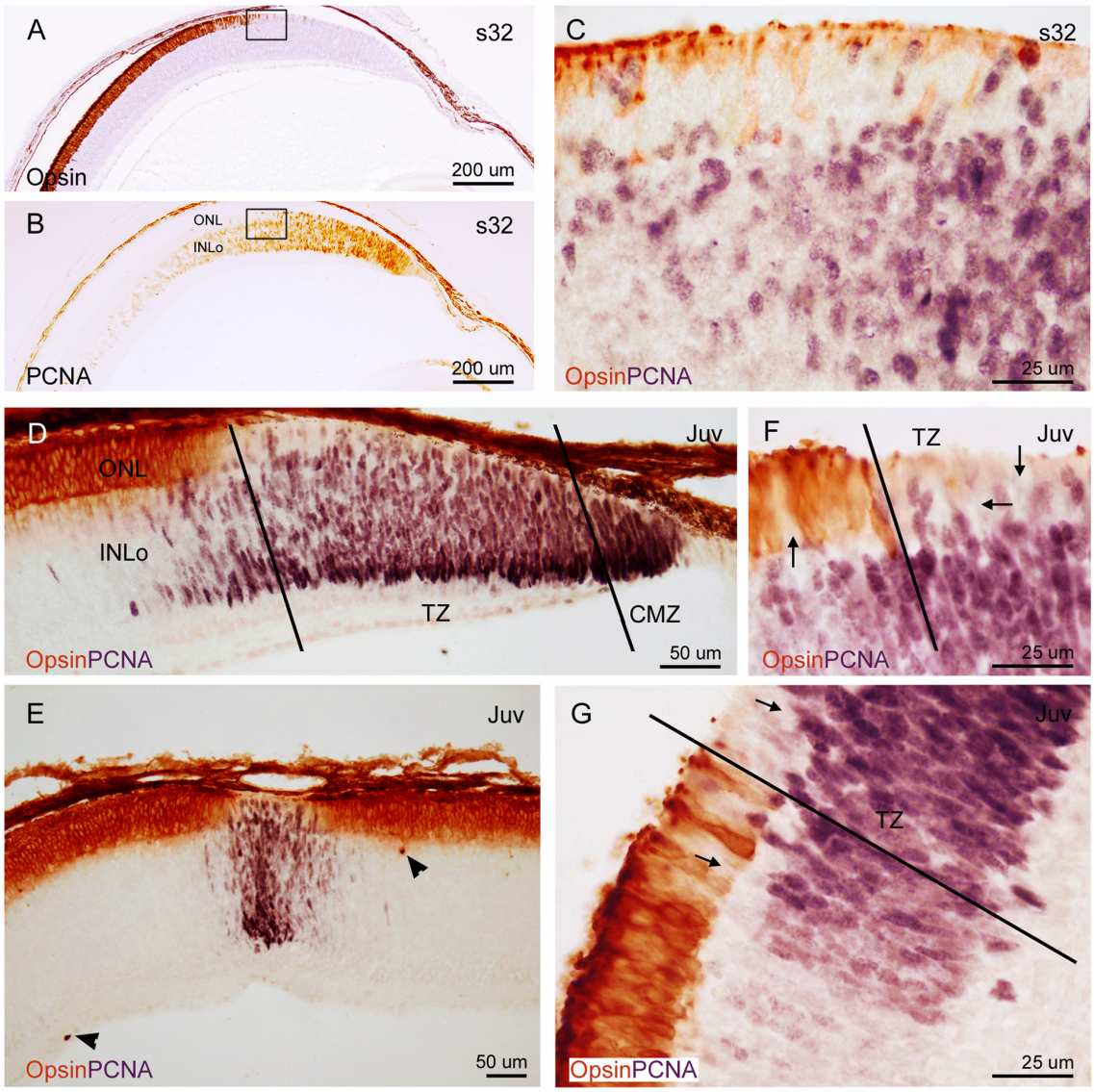
A
s32
Opsin
200 um
B
ONL
INLo
s32
PCNA
200 um
C
s32
OpsinPCNA
25 um
D
Juv
ONL
INLo
TZ
CMZ
OpsinPCNA
50 um
F
TZ
Juv
OpsinPCNA
25 um
E
Juv
OpsinPCNA
50 um
G
Juv
TZ
OpsinPCNA
25 um

Conclusions

1- Three developmental periods can be recognized in shark brain and retina on the basis of the Pax6 spatiotemporal patterns and the progressive layering of the neural walls; a first period consisting of neuroepithelial cells, a second period of layering and a third period of maturation, although timing is shifted in the retina with respect to the brain. Noteworthy, these periods constitute a useful framework for further comparative studies in vertebrate development as they can be unequivocally identified in different vertebrates.

2- The spatiotemporal progression of the Pax6 expression (protein and mRNA) in the developing brain of sharks studied reveals many similarities to those in other vertebrates, which supports the existence of an evolutionary conserved pattern. The recognition of this pattern makes the Pax6 distribution in the developing brain one of the most useful tools for comparative studies, especially in the search for homologies.

3- The distribution pattern of Pax6 cells in sharks, especially when compared with the distribution of markers as TH, GAD, CR and Shh, highlights the presence of longitudinal and transverse boundaries, such as the alar-basal, diencephalic-mesencephalic and pallial-subpallial boundaries, and provides accurate regional information about prosomeric domains.

4- In sharks, likewise in other vertebrates, Pax6 represents a good marker of dorsal telencephalic territories and of the pallial-subpallial border. Interestingly, we show evidence of a string of Pax6 cells in certain subpallial territories that appear to migrate tangentially from pallial territories adjacent to the pallial-subpallial boundary.

5- Our study about the olfactory system reveals that Pax6 may play pivotal roles during the development of the shark olfactory epithelium and bulb, as in other vertebrates. We show for the first time a transitory population of Pax6 cells along the olfactory nerve which suggests Pax6 is also involved in the development of olfactory fibres.

6- Proliferation and differentiation patterns revealed in sharks during the development of the cerebellar body with Pax6, PCNA, RELN, GAD/GABA, and CR have shown remarkable similarities with those of the cerebella of tetrapods, thus showing the importance of elasmobranch models to reconstruct the evolutionary developmental history of the vertebrate cerebellum.

7- This study will contribute to gain knowledge about the degree of evolutionary conservation of Pax6 expression during retinogenesis and in the mature retina. The present results may help to explore Pax6 involvement in timing cell type specification and cell identity within the retina. The time course of Pax6 expression in relation to the patterns of cells proliferation and differentiation in the shark retina suggests a shift in the role of Pax6 over time. Thus, Pax6 may be involved in the maintenance of the proliferative stage in retinoblasts and in the regulation of the differentiation of particular cell types as layering progresses from the vitreal to the scleral retina. In addition, the persistence of Pax6 expression in cells of the adult retina of sharks indicates a possible role in the ageing eye.

8- PCNA immunoreactivity was present in all neuroblasts until the end of the first developmental period and it was progressively lost in a vitreal-to-scleral and a central-to-peripheral sequence, that parallels cell and layer differentiation, similarly to that observed in teleosts. Likewise, PCNA labelling persists in the shark CMZ along the whole lifespan. At difference with teleosts, the progressive loss of PCNA throughout the retina in sharks occurs once layering is completed.

9- The study of the spatiotemporal distribution of GABAergic cells has revealed that, at difference to teleosts, GABA is synthesized in the shark retina before the differentiation of retinal layers, suggesting that GABA plays a developmental role in the early developing retina of sharks.

10- Spatiotemporal detection of differentiation markers shows a centre-to-periphery gradient coincident with the progression of the retinal maturation, i.e., their patterns in the peripheral retina resembles that found in the central retina at earlier stages.

11- Several lines of evidence indicate that most photoreceptors in sharks are rods: the anti-rod opsin labels most of the postmitotic perikarya in ONL; sharks have CR-ir ganglion, amacrine and horizontal cells and a low TH/5-HT density ratio, a pattern found in rod-dominant retinas of different vertebrate species.

12- Pax6 colocalize with CR in some cells of the GCL, with 5-HT and GAD in amacrine cells of the INLi and with GAD in cells of the HCL. A number of Pax6-ir cells are immunonegative for these markers, which indicates that the presence of Pax6 is not sufficient for directing cells towards one of these specific fates. Conversely, some postmitotic (PCNA-negative) cells lack Pax6, which indicates that Pax6 alone is dispensable for the acquisition and/or maintenance of CR-ir, 5-HT-ir and GAD-ir phenotypes.

13-.Our results highlight the importance of studies on developing elasmobranchs as they contribute to infer the ancestral condition of brain organization in gnathostomes. Moreover, in this study we provide evidences that sharks are especially suitable to describe the dynamics of brain and retina development, as their lengthened growth and the large size of the embryonic brain allow disclosing fine details of developmental processes.

APPENDIXES

ABBREVIATIONS LIST

A	cerebellar auricle
Apvl	anterior periventricular area
asb	superficial basal area
CB	cerebellum
cr cb	cerebellar crest
E	eye
DON	dorsal octavolateral nucleus
ET	eminentia thalami
fp	floor plate
fr	fasciculus retroflexus
GL	granular layer
glom	glomerular layer
GR	cerebellar granular layer
H	hypophysis
Hb	habenula
HL	hypothalamic lobe
Hy	hypothalamus
Ipn	interpeduncular nucleus
i	infundibulum
IHL	inferior hypothalamic lobes
In	olfactory nerve
is	infundibular sac
Is	isthmus
lln	lateral line nerve
IZ	intermediate zone
IIIn	oculomotor nerve
L	lamellae
LC	locus coeruleus
LH	lateral nucleus of the habenula
LL	lower cerebellar auricular leaf
Mes	mesencephalon
MH	medial nucleus of the habenula
MZ	marginal zone
mlf	medial longitudinal fascicle
MOL	cerebellar molecular layer
n	notochord
Nflm	nucleus of the medial longitudinal fascicle
OB	olfactory bulb
OE	olfactory epithelium
op	olfactory pit
os	optic stalk
OT	optic tectum
P	pallium
p	pineal organ
PA	preoptic area
pc	posterior commissure
Pd	dorsal pallium
por	preoptic recess
Pl	lateral pallium
Pm	medial pallium
Pr	posterior recess
Pros	prosencephalon
PT	pretectum
PTh	prethalamus (ventral thalamus)
PTu	posterior tubercle
R	Rathke's pouch

Ra	raphe
re	retina
Rh	rhombencephalon
RL	rhombic lip
r1-r6	rhombomeres 1-6
sco	subcommisural organ
se	septum
sn	substantia nigra
Sp	subpallium
spc	spinal cord
str	striatum
sv	saccus vasculosus
syn	synencephalon
t chor	tela choroidea
TEL	telencephalon
TGm	mesencephalic tegmentum
TGr	rhombencephalic tegmentum
Th	thalamus (dorsal thalamus)
UL	upper cerebellar auricular leaf
vma	vellum medularis anterioris
Vr	trigeminal nerve root
VII+VIIIr	octaval and facial nerve roots
vt	velum transversum
VTA	ventral tegmental area
VZ	ventricular zone
Xr	vagal nerve root
zli	zona limitans intrathalamica

ABBREVIATIONS LIST

ce	ciliary epithelium
CMZ	ciliary marginal zone
d	dorsal retina
GCL	ganglion cell layer
HCL	horizontal cell layer
I	neuroblastic retina, inner layer
INL	inner nuclear layer
INLi	inner part of the INL
INLo	outer part of the INL
IPL	inner plexiform layer
Juv	juvenil
L	lens
l	layered part of the TZ
le	lens epithelium
n	nasal retina
nl	non-layered part of the TZ
O	neuroblastic retina, outer layer
OD	optic disc
OF	optic fissure
OL	optic fibre layer
ON	optic nerve
ONH	optic nerve head
ONL	outer nuclear layer
OPL	outer plexiform layer
pGCL	primordial GCL
PH	prehatching
pHCL	primordial HCL
pIPL	primordial IPL
pONL	primordial ONL
RPE	retinal pigmented epithelium
t	temporal retina
TZ	transition zone
v	ventral retina

Appendix C

Resumen

REGIONALIZACIÓN DEL ENCÉFALO Y LA RETINA DE TIBURONES: ESTUDIO BASADO EN LOS PATRONES ESPACIOTEMPORALES DE EXPRESIÓN DE PAX6 Y DE OTROS MARCADORES NEUROQUÍMICOS.

INTRODUCCIÓN

Durante las etapas tempranas del desarrollo se establece la **regionalización** temprana del sistema nervioso central, es decir se establecen las grandes subdivisiones del encéfalo. Mas tarde, tiene lugar la **morfogénesis** del SNC, un proceso complejo que depende de la regulación espacio-temporal de procesos como la proliferación, la diferenciación celular y el establecimiento de los diferentes tipos celulares en su posición definitiva.

Los peces cartilaginosos o condríctios, que incluyen los tiburones y rayas (elasmobranquios) y las quimeras (holocefalos), constituyen un grupo monofilético que surgió temprano en la historia evolutiva de vertebrados con mandíbulas (gnatóstomos), y se han utilizado como referencia para diferenciar entre características ancestrales y derivadas en vertebrados. En particular, en los últimos años la pintaroja, *Scyliorhinus canicula*, se ha propuesto como organismo modelo para estudios de desarrollo [Coolen et al., Emerging Model Organisms, (2009):431]. Se trata de un pequeño tiburón perteneciente al superorden Galeomorphii, caracterizado por cerebros con organización elaborada [Butler AB, Hodos W, Comparative vertebrate neuroanatomy (2005)] comparable a la de peces óseos (teleósteos) y amniotas.

Diversos autores han estudiado la organización del sistema nervioso central (SNC) de vertebrados tanto en ciclóstomos como en vertebrados mandibulados, (incluyendo peces óseos y tetrápodos). Sin embargo, y a pesar de la gran diversidad existente dentro del grupo de peces, la mayoría de estudios se han centrado en los peces óseos (teleósteos), considerándose al pez cebra como modelo representativo del grupo.

Por otro lado, diversas estructuras del SNC tales como el cerebelo y la retina, han sido consideradas como sistemas modelo para el estudio de la morfogénesis dado que constituyen estructuras laminadas que se desarrollan completamente en etapas tardías del desarrollo embrionario, o incluso tras el nacimiento. Tanto el cerebelo como la retina de peces han demostrado ser valiosos modelos para estudios de desarrollo, puesto que contienen un número limitado de tipos celulares que se encuentran organizados en capas bien definidas, y además

presentan áreas de proliferación capaces de producir nuevas neuronas durante toda la vida del animal. Aunque la secuencia de formación del cerebelo, así como los patrones de proliferación, migración y diferenciación celular durante el desarrollo embrionario han sido estudiados en peces óseos, no existen estudios similares en peces cartilaginosos. Por otro lado, aunque los patrones generales de proliferación, diferenciación y laminación de la retina son actualmente bien conocidos en algunas especies de peces óseos, principalmente en especies de desarrollo rápido tales como el pez cebra, apenas existen datos en otros grupos de peces.

El factor de transcripción Pax6 es un gen regulador del desarrollo, que ha sido ampliamente estudiado tanto en vertebrados como en invertebrados debido a su papel fundamental en el desarrollo del ojo. Además, los patrones espacio-temporales de expresión de Pax6 observados durante el desarrollo en distintos organismos, han llevado a pensar que puede controlar cascadas de genes implicadas en el desarrollo del sistema nervioso central (SNC).

La primera parte de esta memoria está dedicada al análisis de la regionalización y morfogénesis del encéfalo de tiburones. En el Capítulo 1 realizamos un análisis exhaustivo de la distribución de la proteína Pax6 y de su ARNm en el cerebro en desarrollo, así como en etapas post-embrionarias, identificando dominios transversales y longitudinales. El Capítulo 2 contiene una descripción detallada de la expresión de Pax6 en el sistema olfatorio de tiburones. En el Capítulo 3 proporcionamos información mas detallada sobre la regionalización del cerebro de tiburones, al comparar los patrones de expresión de Pax6 con distintos marcadores de diferenciación neuronal tales como las enzimas de síntesis de neurotransmisores: decarboxilasa del ácido glutámico (GAD) y tirosina hidroxilasa (TH), o la proteína calretinina (CR), mediante técnicas de inmunofluorescencia. El Capítulo 4 incluye un estudio inmunohistoquímico de los patrones de proliferación, diferenciación y migración, es decir de la morfogénesis del cerebelo de tiburones mediante un conocido marcador de proliferación, el antígeno nuclear de proliferación celular (PCNA), la proteína reelina (RELN), GAD y TH.

La segunda parte incluye un detallado estudio de los procesos de retinogénesis en tiburones (Capítulos 5-10) incluyendo el estudio de los patrones de proliferación, diferenciación y migración celular, mediante el análisis del patrón de expresión de Pax6 (Capítulo 5), su relación con el patrón de proliferación (Capítulo 6), y con la distribución espacio-temporal de marcadores de diferenciación tales como GABA/GAD (Capítulo 7), CR

(Capítulo 8), serotonina (5-HT) y TH (Capítulo 9) y opsina-CERN922 (Capítulo 10). El posible papel de Pax6 en la morfogénesis de la retina ha sido analizado mediante técnicas inmunohistoquímicas y de hibridación *in situ*. Las posibles interacciones entre Pax6 y los marcadores de proliferación y diferenciación se han estudiado mediante técnicas de doble y triple inmunofluorescencia.

CAPÍTULO 1. Expresión de Pax6 en el cerebro maduro y en desarrollo de tiburones.

Aunque el patrón de expresión de Pax6 ha sido descrito en peces óseos y ciclóstomos, no existen datos en elasmobranquios, excepto por el trabajo de Derobert et al. [*Brain Res Bull*, 57(2002):277] que describe el patrón de expresión de Pax6 hasta el estadio embrionario 22 mediante hibridación *in situ*. Nuestros resultados incluyen una detallada descripción del patrón espacio-temporal de expresión de Pax6 en tiburones durante el desarrollo, pero también en etapas post-embrionarias, proporcionando así información comparable a la disponible en ratón [Stoykova y Gruss, *J Neurosci*, 74(1994):1395] y pez cebra [Wullimann y Rink, *Brain Res Bull*, 57(2002):363].

En este capitulo hemos aplicado técnicas inmunohistoquímicas con anticuerpos anti-Pax6, así como hibridación *in situ* (ISH) con una sonda especifica para *S. canícula* (*ScPax6).* Con ambas técnicas obtuvimos resultados similares en *S. canicula*, y por tanto los resultados de ISH validan la especificidad de los anticuerpos anti-Pax6 empleados. Sin embargo, las técnicas imunohistoquímicas, nos ha proporcionado una mayor resolución a nivel histológico, permitiendo una descripción detallada de la dinámica espacio-temporal de la distribución de células que expresan Pax6 (células Pax6). No hemos observado diferencias en la expresión de Pax6 entre las dos especies analizadas. Además en algunas regiones del SNC, hemos estudiado la distribución de la proteína de señalización sonic hedgehog (Shh) con fines comparativos.

En este trabajo hemos analizado embriones desde el estadio 22, en los que hemos observado expresión de Pax6 en la medula espinal, que se continúa en el rombencéfalo hasta el nivel del istmo, así como en el prosencéfalo. Sin embargo, a partir del estadio 27 encontramos expresión de Pax6 en el tegmento mesencefálico y en el primordio del cerebelo (metencéfalo). Durante gran parte del desarrollo, Pax6 se expresa en amplios dominios, pero en estadios embrionarios tardíos (desde el estadio 32) Pax6 se observa en grupos de células discretos y bien definidos. Además observamos expresión de Pax6 en algunas estructuras relacionadas

con el cerebro como son: el ojo y tallo óptico, las fosas nasales y epitelio olfatorio, la bolsa de Rathke y la hipófisis.

Considerando la organización de las células Pax6 con respecto al ventrículo y al proceso de estratificación de las paredes del cerebro hemos establecido los siguientes periodos: A) el primer periodo, que comprende los estadios 22-26, se caracteriza por la ausencia de laminación en las paredes del cerebro en desarrollo que consisten en un neuroepitelio pseudoestratificado, que presenta dominios Pax6 con células Pax6 neuroepiteliales extendiéndose desde la superficie pial a la ventricular a ciertos niveles a lo largo del eje antero-posterior; B) el segundo periodo, que incluye los estadios 27 a 31, se caracteriza por la progresiva laminación de las paredes del encéfalo, y por la presencia de células Pax6 en la zona ventricular (VZ), intermedia (IZ) y marginal (MZ); C) el tercer periodo engloba los estadios embrionarios tardíos (desde el estadio 32 hasta la eclosión), y se caracteriza porque el encéfalo alcanza un grado de organización comparable a la del encéfalo maduro, observándose distintos grupos de células Pax6 que se mantienen en etapas post-embrionarias (en juveniles, e incluso en adultos). La distribución de células que expresan Pax6 (células Pax6) a lo largo de los ejes antero-posterior y dorsoventral del tubo neural se ha descrito en relación con estos tres periodos:

- Primer periodo (estadios 22-26): en esta etapa temprana, las pareces cerebrales son delgadas y engloban amplias cavidades ventriculares, este periodo está caracterizado por la presencia de células Pax6 en las paredes neuroepitelialies del rombencéfalo y prosencéfalo, pero no en el mesencéfalo, istmo ni en la placa alar del rombencéfalo más rostral, es decir, en el primordio del cerebelo o metencéfalo.
- Segundo período (estadios 27-31): durante este periodo el grosor de las paredes del cerebro aumenta notablemente, en especial en el diencéfalo y mesencéfalo. Se desarrolla la placa cerebelosa en el rombencéfalo más rostral, la cual dará lugar mas tarde al cerebelo; el saco infundibular en el hipotálamo; los hemisferios telencefálicos crecen rostralmente; y en el estadio 31, los bulbos olfatorios se desarrollan como evaginaciones laterales de las paredes del telencéfalo. A partir del estadio 27, observamos células Pax6 en el tegmento mesencefálico, que forman una hilera continua con las células Pax6 observadas en el diencefalo, y que hemos relacionado con el posible límite alar-basal. En el primordio del cerebelo desde el estadio 28/29

encontramos abundantes células Pax6. En el telencéfalo, la presencia de una banda de expresión de Pax6 a nivel del límite pallial-subpallial, a partir de la cual parecen emerger células Pax6 hacia el subpalio, observándose numerosas células Pax6 en la MZ subpalial al final de este periodo.

- Tercer período (estadios 32-eclosión): el desarrollo del cerebelo, así como la expansión de las paredes paliales alcanzan su máximo desarrollo durante el estadio 32. A partir de esta etapa, el cerebro aumenta considerablemente de tamaño pero no se desarrollan nuevas estructuras. Los grupos de células Pax6 observados en embriones tardíos (pre-eclosión) se mantienen en etapas post-embrionarias, así observamos grupos Pax6 en el rombencéfalo, tegmento mesencefálico, pretecho, pretálamo (tálamo ventral), y numerosas células Pax6 en el telencéfalo.

Además, en este trabajo se discuten las posibles funciones que el factor de transcripción Pax6 puede desempeñar durante el desarrollo embrionario de tiburones, a la luz de las evidencias anatómicas proporcionadas por nuestros resultados y los datos proporcionados por estudios funcionales en otros vertebrados. Entre ellos, hemos considerado el papel de Pax6 en la regionalización del telencéfalo, puesto que: Pax6 se expresa desde estadios tempranos en el telencéfalo y de forma diferencial (siendo abundante en la región dorsal o palio, y estando ausente de la región ventral o subpalio); el límite pallial-subpallial parece coincidir con una banda de expresión de Pax6. Además, células Pax6 emergen de la zona de transición palio-subpalial y se observan en el subpalio. En pollo y en ratón también se han observado células Pax6 que emergen de la VZ en la región del limite palial-subpalial y se dirigen hacia la MZ, que se han interpretado como células paliales [Puelles et al., *J Comp Neurol* 424(2000):409] que migran hacia el subpalio o como una población de células de transición entre el palio y el subpalio [Stenmann et al., *J Neurosci* 74(2003):1395]. Además, en ratón se ha identificado una ruta de migración (LCS, lateral cortical stream), que se origina en la región del límite palial-subpalial. Nuestros resultados en tiburones proporcionan evidencias a favor de esta hipótesis de que el límite pallial-subpalial puede ser la fuente de una corriente migratoria de células Pax6 hacia el subpalio, sugiriendo que los fenómenos de migración celular en el telencéfalo podrían haber surgido muy temprano durante la evolución del prosencéfalo. Por otro lado, distintas divisiones del palio (palio dorsal, medial y lateral) pueden reconocerse desde el estadio 32 en adelante (tercer periodo); todas ellas contienen células Pax6 con una

distribución bastante homogénea que dificulta la identificación de su extensión concreta o la localización de núcleos paliales en función de la expresión de Pax6. Para ello será necesario el análisis del patrón de expresión de otros genes reguladores del desarrollo. Por otro lado, la restricción de los amplios dominios Pax6 a grupos de células más reducidos y la persistencia de células Pax6 en el cerebro adulto también se han observado en otros vertebrados y se han relacionado con un papel de Pax6 en la regionalización en el desarrollo, y con la diferenciación y/o mantenimiento de poblaciones celulares/neuronales respectivamente.

La comparación de nuestros resultados con los patrones de expresión de Pax6 descritos en pez cebra y en ratón han evidenciado asombrosas similitudes: los dominios Pax6 rombencefálicos en tiburón parecen corresponder con núcleos precerebelosos; los dominios diencefálicos son semejantes a los descritos en otros gnatostomos y nos han permitido identificar segmentos transversales o prosómeros (más en detalle en el Capítulo 2); células Pax6 se extienden desde el dominio pretalámico hacia el tubérculo posterior al igual que en pez cebra; por último, la distribución de células Pax6 en la VZ en el palio se asemeja al patrón observado en ratón, mientras que las células Pax6 marginales en el subpalio de tiburones recuerdan a las descritas tanto en ratón como en el pez cebra. En definitiva nuestros datos sugieren una notable conservación de la funciones de Pax6 en la regionalización del telencéfalo a lo largo de la evolución de los vertebrados.

CAPÍTULO 2. Expresión de Pax6 en el sistema olfatorio de tiburones en desarrollo.

En vertebrados, el sistema olfatorio maduro consiste en un epitelio olfatorio que contiene neuronas receptoras, cuyos axones forman el nervio olfatorio que cursa hasta el bulbo olfatorio (telencéfalo). El epitelio olfatorio deriva de las placodas olfatorias cuya invaginación y posterior plegamiento da lugar a las lamelas del órgano nasal, donde se encuentran los distintos tipos celulares del epitelio olfatorio.

La expresión de Pax6 en el epitelio olfatorio de ratón en desarrollo se ha relacionado con un posible papel en el control de la especificación, migración y diferenciación neuronal. Además, su expresión en el bulbo olfatorio maduro y en desarrollo ha llevado a sugerir que Pax6 puede jugar un papel en la diferenciación/producción de diferentes subtipos de interneuronas. Estas cuestiones no han sido abordadas en grupos de vertebrados basales, y por tanto se desconoce si estas funciones de Pax6 en el desarrollo del sistema olfatorio han

sido conservadas en el curso de la evolución, por ello consideramos clave el estudio en peces elasmobranquios. Los peces cartilaginosos presentan bulbos olfatorios bien desarrollados, y han sido utilizados como sistemas modelo para el estudio de los circuitos olfatorios en peces. Sin embargo los estudios sobre el desarrollo son escasos y se han centrado en el epitelio y en la placoda olfatoria.

Nuestros resultados en *S. canicula* aplicando técnicas inmunohistoquímicas y de hibridación *in situ,* muestran abundantes células Pax6 en el epitelio olfatorio, no solo durante su desarrollo sino también en el adulto. Mientras que en estadios muy tempranos de su desarrollo el bulbo olfatorio no muestra células Pax6, más tarde se observan abundantes células Pax6 en la capa granular, incluso en ejemplares adultos.

Además hemos evidenciado células Pax6 periféricas que forman hileras y se encuentran asociadas a las fibras olfatorias, y que podrían ejercer un papel importante durante las etapas tempranas del desarrollo del nervio olfatorio. Estas células parecen expresar Pax6 de manera transitoria puesto que se observan desde estadios tempranos, cuando se produce la invaginación de la placoda olfatoria, hasta el comienzo del desarrollo del bulbo olfatorio. Además, estas células Pax6 parecen derivar del epitelio olfatorio dado que presentan morfología e intensidad de marcaje similares a las células Pax6 observadas en el epitelio. En resumen, estos datos nos sugieren que durante el desarrollo del sistema olfatorio de tiburones, Pax6 podría estar implicado en la diferenciación del epitelio y del bulbo olfatorio, pero también podría guiar a las fibras olfatorias en desarrollo hacia el telencéfalo.

CAPÍTULO 3. Organización segmentaria del cerebro en desarrollo de tiburones basado en marcadores neuroquímicos: estudio centrado en el prosencéfalo.

A pesar de que la regionalización del cerebro ha sido estudiada en gran número de vertebrados, no existen estudios previos en peces elasmobranquios. Nuestros resultados proporcionan una primera aproximación al patrón segmentario del cerebro de tiburón durante el desarrollo embrionario basado en el patrón de expresión de Pax6 comparado con la distribución de otros marcadores neuroquímicos tales como CR, TH y GAD. La correlación de límites citoarquitectonicos con la distribución de estos marcadores nos ha permitido identificar límites transversales, longitudinales y dominios de expresión que sugieren un patrón similar al descrito en otros vertebrados.

Por un lado, el contraste entre la ausencia de Pax6 en el techo óptico y la fuerte expresión en el pretecho, nos permite identificar el límite mesencéfalo-prosencéfalo desde etapas tempranas del desarrollo. Además, hemos considerado la banda de células Pax6 que se extiende desde el tegmento mesencéfalico hasta el diencéfalo, como posible límite alar-basal. En el telencéfalo, la banda mediolateral Pax6 parece localizada en la región de transición entre el palio y subpalio, sirviendo así como marcador/indicador del limite pallial-subpallial.

Por último, en el diencéfalo hemos identificado claramente los prosómeros 1-3 descritos en el modelo prosomérico [Puelles y Rubenstein, *TINS* 26(2003):469]. Así, la porción alar de los prosómeros p1 (pretecho) y p3 (pretálamo o tálamo ventral) se caracteriza por presentar poblaciones conspicuas de células Pax6 durante el desarrollo que se mantiene en etapas post-embrionarias. Por el contrario, parte de la porción alar de p2 (tálamo o tálamo dorsal) presenta expresión de Pax6 transitoria, puesto que solo expresa Pax6 en etapas tempranas del desarrollo, mientras que en etapas tardías, presenta una población de células CR-inmunoreactiva (CR-ir). Por el contrario, la habenula y el órgano pineal, que también forman parte de la porción alar de p2, presentan expresión de Pax6 a lo largo de todo el desarrollo embrionario. La placa basal de p1 se caracteriza por una población CR-ir que corresponde con el núcleo del fascículo longitudinal medial, mientras que en p3 células Pax6 se extienden desde lo alar a lo basal ocupando las paredes del tubérculo posterior (porción basal de p3). Hemos identificado además el límite entre p3/p2 que parece corresponder con el curso del fascículo retroflexo, mientras que el limite p2/p1 vendría marcado por una cuña de fibras GAD-inmunoreactivas previamente identificadas como la posible *zona limitans* intratalámica.

En conjunto, estos datos constituyen un esquema inicial, que deberá ser completado en posteriores estudios ampliando el rango de marcadores genéticos implicados en el establecimiento del patrón básico del encéfalo de vertebrados.

CAPÍTULO 4. Desarrollo del cuerpo cerebeloso en tiburones: comparación de los patrones espacio-temporales de expresión de Pax6, y marcadores de proliferación y diferenciación.

El cerebelo de peces cartilaginosos se caracteriza por presentar un cuerpo cerebeloso bien desarrollado que se extiende rostralmente sobre el techo óptico, y dos estructuras con forma de oreja denominadas aurículas, que se localizan caudalmente. El cuerpo cerebeloso se caracteriza por la segregación entre las regiones granulares, que se encuentran formando las eminencias granulares a nivel medial, y las capas molecular y de células de Purkinje, que se disponen a niveles laterales. Estudios ultraestructurales e inmunohistoquímicos en el cerebelo adulto de *S. canicula* han mostrado los distintos tipos celulares que contiene (células de Purkinje, de Golgi, células grano, células estrelladas) evidenciado que son similares a los descritos en mamíferos, aunque más simples.

En este trabajo hemos estudiado los patrones de proliferación y diferenciación celular, así como la organización/regionalización del cuerpo cerebeloso de embriones y juveniles de *S. canicula* y *H. fuscus* mediante inmunohistoquímica (IHC) en ambas especies, y mediante ISH para *ScPax6 en S. canicula.*

Hemos observado que la placa cerebelosa, que da lugar al cerebelo, se forma en torno al estadio 28/29 debido a la fusión en la línea media de los labios rómbicos, estructuras pares derivadas de la placa alar del rombencéfalo. En el estadio 31, la placa cerebelosa en sección sagital se observa como una lámina en forma de ese, en la que podemos diferenciar el primordio del cuerpo cerebeloso, del primordio del lóbulo auricular ensanchado transversalmente a nivel caudal. La segregación entre las regiones mediales granulares y laterales, así como cierto grado de laminación en estas últimas, comienzan a ser aparentes en el cuerpo cerebeloso a partir de este estadio del desarrollo embrionario y se hace patente en el estadio 32, cuando comienzan a observarse células CR-ir, probablemente células estrelladas, en el primordio de la capa molecular. Nuestros resultados revelan dos fases en el desarrollo del cerebelo: en la primera, las células grano que expresan Pax6 se originan en dos zonas de proliferación en el cuerpo cerebeloso, la zona ventricular y la capa germinal externa, una zona secundaria de proliferación transitoria; más tarde (a partir del estadio 32) estas células Pax6 (células grano) se originan únicamente en la zona ventricular medial, y se acumulan en las eminencias granulares. Además, el comienzo de la segunda fase coincide con la organización de

las tres capas del cerebelo. La zona de proliferación que se observa a nivel medial en embriones tardíos permanece activa en etapas post-embrionarias, e incluso en ejemplares adultos.

Nuestros resultados evidencian semejanzas en los patrones de proliferación y diferenciación observados en el desarrollo del cuerpo cerebeloso de tiburones y del cerebelo de tetrápodos, mostrando la importancia de los elasmobranquios como modelo para reconstruir la historia evolutiva del desarrollo del cerebelo.

CAPÍTULO 5. Expresión de Pax6 en la retina madura y en desarrollo de tiburones

Como ya hemos mencionado previamente, la retina es considerada como un valioso sistema modelo para estudios de desarrollo. Brevemente, la retina consta de seis tipos celulares (células ganglionares, amacrinas, bipolares, horizontales, fotorreceptores, y células de Müller), que se organizan en las siguientes capas del interior (vitreal) al exterior (escleral): capa de fibras del nervio óptico, de células ganglionares (GCL), plexiforme interna (IPL), nuclear interna (INL), plexiforme externa (OPL), de células horizontales (HCL), nuclear externa (ONL), y el epitelio pigmentario retiniano (RPE).

Hemos estudiado el patrón de expresión de Pax6 mediante IHC e ISH, obteniendo resultados comparables con ambas técnicas. Sin embargo la IHC nos ha proporcionado una mayor resolución histológica, y además nos ha permitido combinar fácilmente desde un punto de vista metodológico Pax6 con otros marcadores.

En este estudio sobre la morfogénesis de la retina de tiburones hemos definido tres periodos de desarrollo, que no se corresponden con los descritos en el cerebro puesto que el desarrollo de la retina es más tardío:

- Primer periodo (estadios 26 a 29), caracterizado por el aspecto neuroepitelial de la retina y la ausencia de laminación. Abundantes células neuroepiteliales Pax6-inmunoreactivas (Pax6-ir) intensas se observan en la retina neural, pero también en el RPE y en el cristalino.

- Segundo periodo (estadios 30 a 32), se caracteriza por la progresiva formación de capas (laminación) que comienza en la parte más central de la retina y se extiende del interior (vitreal) al exterior (escleral) y del centro a la periferia; por la organización de una zona

neuroepitelial denominada zona marginal ciliar (CMZ) adyacente al epitelio ciliar; y por la presencia de una zona de transición (TZ), entre la CMZ y la retina central laminada. La TZ presenta una parte interna laminada (donde la IPL separa la GCL de la parte interna de la INL) y una parte externa neuroepitelial. Al comienzo del segundo periodo (estadio 30) observamos cambios en la distribución de células Pax6-ir en la retina central (donde se ha formado la IPL) con respecto a la retina no laminada (incluyendo la CMZ y la región que bordea al nervio óptico): en la retina central observamos células Pax6-ir intensas formando una densa banda en la región mas interna (futura GCL), más dispersas en la parte más interna de la INL y en la parte externa neuroepitelial; sin embargo en la retina externa no laminada observamos células Pax6-ir pálidas. En el estadio 32 temprano la laminación de la retina central se completa con la aparición de la OPL en la retina central, y la distribución de células Pax6 permanece sin cambios. Al final de este segundo periodo la mayoría de células Pax6-ir intensas se encuentran en la GCL y en la parte interna de la INL, la densidad de células Pax6-ir intensas disminuye en la parte externa de la INL, y observamos células Pax6 en la HCL.

- Tercer periodo (estadios 33 a 34): se caracteriza por la progresiva laminación de la retina que se extiende formando un gradiente del centro a la periferia. Las dos capas plexiformes se distinguen en toda la retina, salvo en la retina temporoventral (donde solo se aprecian IPL). Durante el tercer periodo, la retina central presenta células Pax6-ir intensas en la GCL, IPL, parte interna de la INL y en la HCL. La CMZ, cuya extensión se ha reducido mucho, presenta células débilmente Pax6-ir. La zona de transición consta de una parte interna laminada con la misma distribución de células Pax6 descrita en la retina más central al comienzo del segundo periodo (estadio 30). La retina adyacente a la TZ presenta la misma distribución de células Pax6-ir que la retina central al final del segundo periodo (estadio 32 tardío).

Por lo tanto, la morfogénesis de la retina neural de los tiburones se caracteriza por la progresiva aparición de capas (laminación) desde la superficie interna (vitreal) a la externa (escleral), y por un gradiente de diferenciación que va del centro a la periferia, puesto que en cada estadio observamos áreas centrales mas maduras que las periféricas. Así pues, los patrones de inmunoreactividad a Pax6 observados desde la retina más periférica a la central recapitulan lo observado en la retina central desde etapas tempranas a etapas tardías del desarrollo.

El patrón espaciotemporal de expresión de Pax6 en la GCL e INL observado en tiburones es bastante similar al descrito en la retina neuroepitelial/madura de otros vertebrados (incluyendo peces óseos, anfibios, pollo, ratón e incluso humanos). La presencia de Pax6 en la capa de células horizontales de *S. canicula* coincide con lo observado en la retina de pez cebra.

La distribución espaciotemporal de Pax6 durante el desarrollo de la retina de elasmobranquios, junto con las evidencias proporcionadas por estudios funcionales en otras especies [revisado en Osumi et al., *Stem Cells* 26(2008):1663] sugieren que Pax6 ejerce una doble función en los procesos de proliferación y de diferenciación celular. La disminución de la intensidad de Pax6-ir en la retina no laminada (incluyendo la CMZ) al comienzo del segundo período, contrasta con la intensa inmunoreactividad a Pax6 observada en la mayoría de las células neuroepiteliales durante el primer periodo podría. Esta disminución podría deberse a cambios en la forma y tamaño de los núcleos de las células en diferenciación, o bien a variaciones en la cantidad de proteína relacionadas con una regulación negativa de Pax6 durante el ciclo celular neurogénico tal como han descrito en pollo [Hsieh y Yang, *Neural Dev*, 4(2009):32].

La presencia de Pax6-ir en células de las capas ganglionar, nuclear interna y horizontal (células ganglionares, amacrinas y horizontales) pero no en fotorreceptores, células bipolares o de Müller, en la retina madura de tiburones sugiere algún papel para Pax6 en las neuronas maduras.

CAPÍTULO 6. Patrones de proliferación en la retina de elasmobranquios.

El análisis del patrón de proliferación en la retina de tiburones ha evidenciado que durante el primer periodo, la mayoría de células neuroepiteliales de la retina son células proliferativas PCNA-inmunoreactivas (PCNA-ir), al final del periodo (estadio 29) algunas células PCNA-negativas se observan en la región interna de la retina central, pero aun no se aprecian signos de laminación. Al principio del segundo periodo, la retina central presenta abundantes células PCNA negativas en la GCL primordial y algunas en la parte interna de la INL. En el estadio 32 la laminación en la retina más central es clara, y se observan muy pocas células PCNA-ir. La densidad de células PCNA-ir en las capas externas aumenta hacia la TZ, donde la capa plexiforme externa aun no es evidente. Durante el tercer periodo, la retina central contiene

muy pocas células PCNA-ir dispersas por la INL y la ONL, y aun más escasas en la GCL y en la IPL. También se observa alguna célula PCNA-ir en el epitelio pigmentario retiniano. Las regiones no laminadas (incluyendo la región que bordea al nervio óptico, la CMZ, y la parte neuroepitelial de la TZ) presentan células PCNA-ir durante todo el desarrollo. Los patrones de proliferación observados desde la CMZ a la retina central recapitulan los cambios que se producen en la retina central durante el desarrollo.

El estudio de doble marcajes ha evidenciado colocalización de células débilmente immunoreactivas a Pax6 y PCNA en la retina no laminada a partir del segundo período, lo que sugiere que Pax6 puede desempeñar un papel en el mantenimiento de la proliferación de los progenitores de la retina. Nuestros resultados muestran que la mayoría de células con inmunoreactividad intensa a Pax6-ir en la retina laminada son PCNA-negativas, sugiriendo que en la retina madura Pax6 interviene en funciones distintas al mantenimiento de la proliferación. A diferencia de lo observado en teleósteos, la aparición progresiva de células PCNA-inmunonegativas en la retina de tiburones ocurre una vez que se completa la laminación.

CAPÍTULO 7. Organización espaciotemporal de la inmunoreactividad a GABA/GAD en la retina de tiburones

Nuestros resultados indican que GABA y GAD evidencian el mismo patrón de inmunoreactividad, y que la organización de elementos GABAérgicos es similar en las dos especies estudiadas. Las primeras células GABAérgicas se observaron en la retina neuroepitelial en el estadio 26. A partir del estadio 30, las células GABAérgicas aparecen organizadas principalmente en la retina externa e interna, mientras que los procesos y fibras GABAérgicos se organizan en la IPL primordial, la capa de fibras ópticas y en el tallo óptico. En el estadio 32 se observan cuerpos celulares GABAergicos en la HCL, INL, y GCL, así como numerosos procesos que cursan en la IPL, capa de fibras del nervio óptico y en el nervio óptico. A partir del estadio 32 y hasta la eclosión, la laminación de la retina se extiende desde el centro a la periferia, recapitulando lo observado en la retina central en estadios más tempranos. En adultos, solo observamos inmunoreactividad a GABA/GAD en la HCL en la retina marginal. La síntesis de GABA previamente a laminación de la retina sugiere que el GABA podría desempeñar, además de su papel clásico como neurotransmisor, un papel en el desarrollo.

La comparación con el patrón de expresión de Pax6 ha evidenciado la presencia de colocalización de GAD y Pax6 tanto en regiones neuroepiteliales (PCNA-positivas) como en células amacrinas y horizontales tan pronto como se diferencian en la retina laminada, pero se desconoce cuál puede ser el papel de Pax6 en el desarrollo del sistema GABAérgico en la retina.

CAPÍTULO 8. Organización espaciotemporal de la inmunoreactividad a calretinina en la retina de tiburones

Hemos observado células CR-inmunoreactivas (CR-ir) a partir del estadio 32 (segundo periodo) en la retina de ambas especies. Las primeras células CR-ir se observan en la retina central principalmente en la GCL, y en la parte interna de la INL, y algunas en la IPL. También observamos fibras CR-ir en la IPL, y en la cabeza del nervio óptico. No observamos células CR-ir en la retina periférica. Al avanzar el desarrollo, las células y fibras CR-ir se extienden del centro a la periferia, excepto en la retina temporoventral (no laminada). En el tercer periodo se observan: células grandes CR-ir en la GCL, extendiendo procesos que cursan por la capa de fibras del nervio óptico y que hemos identificado como células ganglionares; células CR-ir con morfología bipolar en la IPL; abundantes fibras CR-ir en la IPL; y células CR-ir en la parte interna de la INL, que por su morfología pueden corresponder a dos tipos celulares: (1) células grandes, redondeadas, intensamente marcadas similares a las observadas en la GCL, que pueden corresponder con células ganglionares desplazadas, y (2) células mas pequeñas y más débilmente marcadas que pueden representar células amacrinas.

Los dobles marcajes inmunofluorescentes han evidenciado colocalización entre Pax6 y CR en la capa de células ganglionares (GCL), que dada su morfología, podrían representar células amacrinas desplazadas.

CAPÍTULO 9. Organización espaciotemporal de la inmunoreactividad a TH y 5-HT en la retina de tiburones.

Mediante la aplicación de técnicas inmunohistoquímicas hemos evidenciado células TH-ir, y células 5HT-ir en la retina de embriones de *S. canicula* y *H. fuscus* a partir del estadio 32 (tercer periodo de desarrollo) que parecen corresponder con células amacrinas. Además en *H. fuscus* hemos observado células horizontales TH-ir de forma transitoria en el estadio 32.

Hemos observado colocalización de Pax6 y 5-HT en la parte interna de la INL, pero sólo en células que presentan in intenso inmunomarcaje anti-5-HT. No hemos observado colocalización entre Pax6 y TH, aunque codistribuyen en la INL. Observaciones similares en el cerebro de pez cebra han llevado a sugierir que las células Pax6 podrían inducir la diferenciación de neuronas catecolaminérgicas.

CAPÍTULO 10. Organización espaciotemporal de las células inmunoreactivas a opsina en la retina de tiburones.

De los diferentes anticuerpos anti-opsinas utilizados en este estudio, solamente el anticuerpo anti-rodopsina (CERN-922 opsin) ha evidenciado células inmunoreactivas al comienzo del estadio 32 en *S. canicula* y en el estadio 32 medio en *H. fuscus*. En ambas especies los primeros fotorreceptores rodopsina-inmunoreactivos (rodopsina-ir) se observaron en la región centrodorsal de la ONL. En el tercer periodo observamos fotorreceptores rodopsina-ir en toda la retina excepto en la CMZ. El anticuerpo utilizado marca células antes de que puedan observarse los segmentos externos e internos de la mayoría de los fotorreceptores, indicando que es un buen marcador para el estudio de las etapas tempranas de diferenciación de los fotorreceptores, los cuales expresan opsinas antes de que se diferencien morfológicamente por la presencia de los característicos segmentos externos e internos retina de tiburones. Además hemos observado células rodopsina-ir en la parte externa de la capa nuclear interna en la retina central embrionaria. En juveniles y adultos se observa el mismo patrón de inmunoreactividad a rodopsina que en embriones en estadios pre-eclosión.

Nuestros resultados indican que la mayor parte de los fotorreceptores en la retina de *S. canicula* y *H fuscus* son bastones porque: 1) la mayor parte de los núcleos de la ONL presentan inmunoreactividad a rodopsina y 2) la retina de estos tiburones presenta células ganglionares CR-ir y ratios TH/5-HT bajas, características típicas de especies con retinas en las que predominan los bastones.

En definitiva, nuestros resultados ponen de manifiesto la importancia de los estudios de desarrollo en peces cartilaginosos, para investigar la evolución del desarrollo del SNC de vertebrados mandibulados. Y también evidencian la idoneidad de tiburones para el estudio de la dinámica del desarrollo del cerebro y la retina, porque su crecimiento lento y el tamaño del cerebro embrionario permiten analizar detalladamente los procesos morfogenéticos.